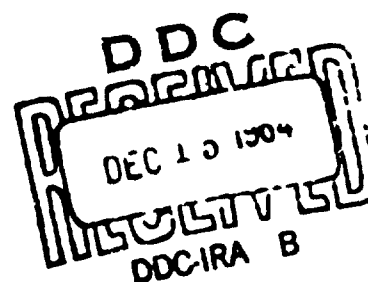## TECHNICAL REPORT

ADS-4

ENGINEERING SUMMARY OF AIRFRAME

ICING TECHNICAL DATA

by

D. T. Bowden, A. E. Gensemer, and C. A. Skeen

General Dynamics/Convair, San Diego, California

Under Contract FA-WA-4250

for

FEDERAL AVIATION AGENCY

WASHINGTON, D.C.   ARCHIVE COPY   MARCH 1964

ENGINEERING SUMMARY OF AIRFRAME ICING TECHNICAL DATA

Contract FA-WA-4250

Technical Report ADS-4

by

D. T. Bowden, A. E. Gensemer, and C. A. Skeen
General Dynamics/Convair, San Diego, California

March 1964

Federal Aviation Agency
Washington, D. C.

CONTENTS

4. APPLICATIONS TO AIRCRAFT

5. ICE DETECTORS AND ICE PROTECTION
SYSTEM INSTRUMENTS AND CONTROLS

6. TESTING AIRCRAFT AND ICE PROTECTION SYSTEMS

Abstract Cards

SUMMARY

This report provides, in a single reference document, an engineering summary of selected technical data on airframe icing conditions, methods of detecting, preventing, and removing ice from airframes in flight, and methods of testing ice protection systems to ensure their adequacy. An aircraft engineer can use this report to design adequate ice protection systems for any type aircraft for any flight mission profile.

The work done in preparing this report covered a survey, study, analysis, and summary of the vast amount of technical literature on airframe icing available in the world today. Key technical data on airframe icing was selected and summarized for the report. Results of the work provide a design engineer with the following:

a. Complete statistical data on the earth's icing weather conditions that can be used as design criteria for airframe ice protection systems.

b. An explanation of the physics of airframe ice collection.

c. A discussion of known methods of airframe ice protection, an' formulas and data to be used in their design.

d. Selected specific applications of ice protection systems to conventional aircraft airframes.

e. Data on known methods and systems for detection of airframe icing.

f. Various methods of testing ice protection systems and aircraft for adequacy.

INTRODUCTION

Increased use of light and heavy aircraft of fixed- and rotary-wing types in private and business transportation has extended their operation into all weather conditions. But to date only civil aircraft certificated by the Federal Aviation Agency to Civil Air Regulation Part 4b (CAR 4b) have ice protection systems designed, manufactured, installed, and proved adequate in natural icing conditions.

The cost of providing aircraft with proved adequate ice protection is high. Cost of adequate ice protection systems for airline transport aircraft carrying passengers and cargo has been considered a necessary expense in the production of these aircraft — to provide an acceptable level of flight safety in icing conditions. But, until this report, the specialized engineering data and technology available in the organizations of CAR 4b aircraft manufacturers has not existed in a consolidated form readily available to all aeronautical design engineers.

The Federal Aviation Agency contracted with General Dynamics/Convair for the preparation of a summary engineering report on airframe icing data that can be used by airframe design engineers in providing aircraft with adequate ice protection systems and proving the adequacy of systems. The report is divided into six sections:

Section 1 discusses statistical icing data to be used as design criteria for ice protection systems.

Section 2, concerned with the physics of ice collection, presents formulas and charts for determining the rate, size, and shape of ice formations on aircraft.

ix

Section 3 discusses the known methods of ice protection and presents formulas and data to be used in designing ice protection systems.

Section 4 shows specific applications of ice protection systems to light aircraft, transports, and rotorcraft.

Section 5 presents data on detection of icing and on ice protection system instruments and controls.

Section 6 discusses methods of testing ice protection systems and aircraft for adequacy. Included are data on icing tunnel testing, dry-air flight testing, flight testing in natural icing, and flight in simulated icing.

The symbols used to denote various parameters are defined in each section, and are consistent throughout the section. They are not, however, consistent from one section to another. In using the equations presented here, special care must be taken to use the definition appropriate for the particular section.

This technical report is an adequate single reference document for airframe design engineers to use in designing airframe ice protection systems. New and different airframe protection systems, methods, and test procedures that are as good or better than those given here may exist and certainly will exist in the future.

The adequacy of the ice protection system on each type of aircraft must be proved in the mission icing environment the design engineer established for the aircraft.

Protection of aircraft power plants is not covered in this report. The power plant ice protection system is designed as an integral part of the power plant and tested for adequacy by the power plant manufacturer. Ice protection for power plant air induction systems is included; this protection is designed and tested by the airframe manufacturer.

1 | ICING DATA STATISTICS FOR DESIGN CRITERIA

CONTENTS

ICING DATA STATISTICS FOR DESIGN CRITERIA

LIST OF FIGURES

1-3

TABLES

SYMBOLS

CAR	Civil Air Regulation
FAA	Federal Aviation Agency
F	Dimensionless liquid water content factor (F for standard distance = 1.0)
gm/m^3	grams of liquid water per cubic meter of air
IFR	Instrument Flight Rules
LWC	liquid water content
micron	one millionth of a meter (one thousandth of a millimeter)
NACA	National Advisory Committee for Aeronautics
NASA	National Aeronautics and Space Administration (formerly NACA)
P_e	exceedance probability

1.1 SUMMARY

This section of the report presents statistical icing data for use in designing ice protection equipment. Ice forms on the forward-facing surfaces of an aircraft when it flies through clouds of supercooled water droplets. The droplets freeze almost instantaneously upon impact with the aircraft, resulting in formation of ice. The rate and extent of ice formation are important factors in the design of ice prevention and removal equipment. For a given flight speed and altitude, and a particular aircraft configuration, the rate of formation is dependent on the liquid water content of the cloud, water droplet diameter and ambient temperature.

Icing conditions are generally encountered in the altitude range from 3,000 to 24,000 ft. Icing may also be experienced at altitudes from sea level to 3,000 ft., and occasionally at altitudes from 24,000 to as high as 44,000 ft. or more. High-altitude icing encounters are rare, and normally result in very little ice formation because the liquid water content is low.

Icing clouds fall into two general categories: stratus and cumulus. Continuous icing for distances up to 200 mi. is found with stratus clouds (however, maximum cloud depth is 6,500 ft.). Liquid water contents are moderate (0.1 to 0.9 gm/m^3) and the water droplet mean diameter will be in the 5 to 50-micron range (one micron is one millionth of a meter). Ambient temperature can vary from -22° to 32° F, with values above 0° F being most common.

Intermittent icing results from flight through cumulus clouds which have a horizontal extent of about three to six mi. Liquid water contents normally vary from 0.1 to 1.7 gm/m^3, with occasional peak values as high as 3.9 gm/m^3 or more for very short distances (at the core of ascending currents in an actively growing cumulus cloud). Temperature, altitude and droplet diameter ranges are similar to those for stratus clouds; however, the most likely altitude for cumulus clouds is 10,000 ft. compared with 5,000 ft. for stratus.

Typical values from CAR 4b for use in design of evaporative anti-icing systems would be:

0.43 gm/m^3 liquid water content

+15° F ambient temperature

20 microns mean droplet diameter

For de-icing systems or "running wet" anti-icing systems, typical design values from CAR 4b would be:

0.23 gm/m^3 liquid water content

0° F ambient temperature

20 microns mean droplet diameter

For turbine engine and engine inlets, typical intermittent icing values from CAR 4b to be considered for the design of running wet anti-icing systems are:

1.7 gm/m^3 liquid water content

-4° F ambient temperature

20 microns mean droplet diameter

3 mi. per encounter

Freezing rain must also be considered for possible effects on static ports, exposed control cables, etc. Values to be considered are:

0.15 gm/m^3 liquid water content

25° to 32° F ambient temperature

1,000 microns - water drop size

100 mi. - horizontal extent

The maximum ice accretion on an unheated component is also shown. Thicknesses of 2.3 to 5 in. are possible (for a 1 per cent probability) for an 1/8-in. diameter cylinder. For larger bodies or components the maximum thickness would be correspondingly smaller.

Methods for calculating ice accretion rate for specific flight icing conditions (and airframe geometry) are shown in Section 2 of this report.

The presence of ice crystals or ice crystals plus liquid water can be a problem for turbine engines. Current test criteria are shown, and involve concentrations of 1 to 8 gm/m^3 for time durations of 30 minutes to 30 seconds, respectively.

1.2 INTRODUCTION

The formation of ice on aircraft has been a problem since the early days of aviation. Aircraft carrying U.S. mail were often forced down by ice accretion on wings, tail and propellers. If the aircraft was undamaged, ice was removed from the canvas-covered surfaces and propeller, and the flight was continued. Later, pneumatic-boot wing and tail de-icers were developed, followed by fluid and thermal anti-icing systems, and by cyclic electric and hot gas de-icing. Design of these systems, however, is dependent on a knowledge of the icing cloud characteristics. This section of the report is concerned with definition of icing cloud parameters, specifically directed toward the values commonly used for design of systems for ice prevention and removal. Because of the great variability of cloud systems, these design standards have been established by considering statistical icing data. This data was, of course, influenced by the methods of gathering the data; therefore, care and judgement must be exercised in its use.

Formation of ice on aircraft surfaces results from flight through clouds of supercooled water droplets; i.e., very small water drops suspended in the air at temperatures below freezing. The supercooled droplets freeze on contact with the forward-facing aircraft surfaces (such as the wing, tail and propeller leading edges, windshields, air inlets and nose of the fuselage). The supercooling process is influenced by a large number of factors such as drop size, ambient temperature, presence of nucleating agents (dust) etc. For this reason, any approach to the problem of defining icing cloud physics must

consider statistical data.

The amount of ice accumulated and its shape are functions of the airfoil or body shape, flight speed, and properties of the icing cloud in terms of liquid water content, drop size, temperature, horizontal and/or vertical extent and altitude. Design of systems to remove or prevent ice formation is dependent upon knowledge of these factors, as well as tolerance to ice buildup on unprotected surfaces. A summary of available data on the characteristics of icing clouds and probability of encountering icing is presented in this section. Most of the data is obtained from the NACA statistical icing reports, which include icing encounters by commercial, military and icing research aircraft. Some foreign data is also included. For additional guidance, the various design standards currently in use by the FAA, the military, and by foreign designers are presented. All these design standards have met the test of usefulness; that is, systems designed and tested to these requirements have been found adequate for routine flights through icing. Specific recommendations for design icing values are not made, as this is a function of the particular aircraft, its operating characteristics or mission, operational techniques, the needs of the specific customer or aircraft operator, and the risk level considered appropriate. However, the report does present the necessary information for selection of icing design criteria once the aircraft and operational factors are defined.

The terminology used in the succeeding portions of the report may be unfamiliar, and deserves some explanation. The cloud liquid water content is expressed in grams of liquid water per cubic meter of air, and includes only the water in supercooled droplet form (it does not include the water in vapor form). Typical ranges of values are 0.1 to 0.8 gm/m^3 for layer type clouds, and 0.2 to 2.5 gm/m^3 for cumulus clouds. Droplet size is expressed in microns. Typical icing cloud droplet diameters are 10 to 40 microns. (Freezing rain may involve droplets as large as 1,000 microns, or one millimeter.) Cloud

temperature may vary from -40° F to 32° F (below -40° F, supercooled water droplets rarely exist). Horizontal extent used for design purposes may vary from 20 to 200 mi. for layer type clouds (stratiform), whereas two to six mi. is often used for cumuliform clouds. Specific relationships of these variables and the probabilities of occurence are presented.

Ice crystals and snow usually do not present a hazard to an aircraft, since the particles are dry and do not adhere to the surfaces. In certain cases involving engine inlet ducting of considerable length or with abrupt turns, flow reversals, partly heated areas, etc., concentrations of ice crystals can be a problem. Mixed conditions (ice crystals plus liquid water) may be a problem for airframe surfaces. Data is presented on frequency of encounter with ice crystals, and on current standards in use for testing engines in both ice crystal and mixed ice crystal/liquid water conditions.

Additional data has been solicited and is presented for icing at both very low and very high altitudes to supplement the NACA data that is confined, for the most part, to altitudes of 3,000 to 22,000 ft.

The droplet diameters quoted herein and in other sections of this report are volume median diameters; i.e., half the volume of water in a given sample is contained in drops larger than the quoted value, and half in drops smaller.

Data is also presented on the frequency and severity of encounters with freezing rain. Although the water drops associated with freezing rain are quite large (as compared to icing clouds), the liquid water content is usually quite low. Aircraft capable of operating in normal icing conditions usually will experience no difficulty with flight through freezing rain. Freezing rain should be considered in the design and location of air inlets and vents, control surface horns and linkage, antenna masts, etc., that may build up ice under these conditions.

1.3 STATISTICAL ICING DATA

1.3.1   NACA STATISTICAL ICING DATA — The National Advisory Committee for Aeronautics (now NASA) and cooperating groups conducted research on natural icing conditions for a period of many years. Early work was performed by specially equipped research aircraft using a rotating multicylinder to measure icing intensity. Later data was obtained by mounting icing rate meters on commercial and military aircraft; thus, obtaining icing data related to routine flight operations. This data (Ref. 1-1 to 1-16) forms the major part of icing statistical data, and is the basis for most U.S., Canadian and British commercial and military design criteria. For this reason, the significant results of the various reports are presented in this section as Figures 1-1 to 1-20 and in Tables 1-1 to 1-5. Discussion of these figures and tables follows.

As mentioned in the Introduction, icing cloud types can be placed in two broad classifications: layer type clouds (stratiform) and cumuliform clouds. Stratiform clouds are characterized by moderate liquid water content (0.1 to 0.8 gm/m^3), maximum probable cloud depth of 6,500 ft., mean effective droplet diameters of 10 to 40 microns, temperatures of 32° to -22° F, altitudes of 3,000 to 22,000 ft., and horizontal extent of 20 to 200 mi. Variation of cloud properties with altitude for a specific stratus cloud is shown in Figure 1-1, as obtained from Ref. 1-1. Within the cloud, free air temperature decreases with altitude, but liquid water content (LWC) increases, reaching a maximum at or near the top of the cloud. This is in agreement with adiabatic lifting theory (Figure 1-2), which predicts an increase in LWC as cloud temperature (and capacity to hold water in vapor form) decreases. Droplet diameter also increases (in the statistical sense) with increasing altitude. Flight in layer clouds can result in icing conditions of long duration, and form the criteria most often used for design of ice protection systems for such airframe components as wings, empennage, propellers, windshields, etc.

Flight through cumuliform clouds can result in short-duration exposure to high liquid water contents. This represents a condition of special interest for turbine engines and engine inlets. Typical isolated cumuliform clouds may vary from two to six miles in horizontal extent, with LWC of 0.2 to 2.5 gm/m^3 or more, and mean droplet diameters of 15 to 50 microns or larger. The maximum water content of a cloud containing only a single cell is likely to be at the cloud center at a height above the freezing level as shown in Figure 1-3a (From Ref. 1-17). Droplet size and LWC tend to increase with cloud height as shown in Figure 1-3b. The drop sizes quoted are volume mean values, as defined previously. Measurements shown in Figure 1-3a and 1-3b are for two separate typical cumulus clouds; other cumulus clouds may have greater or smaller LWC and drop size values, or may be composed of multiple cells rather than single cells.

Statistical data indicates that maximum values of drop size and LWC are not likely to occur simultaneously. This is shown in Figure 1-4a and 1-4b. In Figure 1-4a, the maximum LWC of 0.9 gm/m^3 for stratiform clouds occurs at a drop size of 10.5 microns, whereas the maximum drop size of 50 microns involves only 0.18 gm/m^3. A somewhat similar trend can be seen for cumuliform clouds in Figure 1-4b. The rate of ice accretion is quite similar for these two extreme combinations of LWC and drop size, although the shape of the ice accretion would vary somewhat.

Liquid water content also tends to decrease with decreasing ambient temperature, as shown in Figure 1-5. Note that for stratiform clouds the maximum LWC compares favorably with a theoretical limit based on two-thirds the LWC of a 3,000-ft. cloud, calculated by adiabatic lifting theory (Figure 1-2). (For a detailed discussion and equations on adiabatic lifting theory, see Ref. 1-1.) The data for cumulus clouds shows less correlation between LWC and temperature. In both cases, however, no icing was found below -15°F. The minimum temperature established by laboratory tests for existence of supercooled water droplets is -40°F. At extreme low temperatures, virtually all water is con-

verted to ice crystals, and icing is not likely to be a problem. (Ice crystals and snow can be a problem, however, for air inlet systems having extreme bends or flow reversal curves.)

Droplet diameter does not show a definite correlation with temperature (Figure 1-6). For design purposes, a diameter of 20 microns is most often used to calculate water catch with LWC and temperature appropriate to the specific flight operation. A diameter of 40 microns is often used to calculate the maximum droplet impingement limits.

The probability of exceeding specific values of LWC, drop size and temperature (depression below freezing) is shown in Figures 1-7 through 1-9. The plots are in terms of exceedance probability; i.e., the probability that the given parameter will be equalled or exceeded. A probability of 10 per cent, for example, means that the given parameter will be exceeded in one out of 10 icing encounters. For layer type clouds, the liquid water content for 10 per cent exceedance is 0.5 to 0.6 gm/m^3, whereas it is 1.18 gm/m^3 for cumuliform clouds. For the same probability, the mean effective drop diameter is 18 to 21 microns, and the maximum 23 to 27 microns. The temperature for this same probability level is 5° to -4°F, depending on the particular data source.

Because of the horizontal variations of cloud structure, the average LWC for a long-duration encounter is substantially lower than the average for short-duration encounters. This is shown in Figure 1-10, where the maximum value for a 40-mi. encounter is 0.8 gm/m^3, whereas for 200 mi. it is 0.3 gm/m^3. This variation is also shown in Figure 1-11 in dimensionless form. For cumuliform clouds, the LWC for a six-mi. cloud is 0.85 of the water content for a three-mi. cloud. For layer clouds, the LWC for a 40-mi. distance is 0.64 of that for 10 mi., and at 150 mi. is only 0.32 of the 10-mi. value. The probability of encountering icing conditions in excess of specific distances is shown in Figure 1-12. From this data, it can be seen that 90 per cent of all encounters are for a distance of less than 53 mi., and 99 per cent are less than 123 mi.

These variations of LWC with distance are of interest primarily for predicting the amount of ice accumulation on unprotected components for various flight plans.

The altitude range in which icing can be expected is also of interest, as many current aircraft cruise above the icing level and encounter icing only during climb, descent and low-level hold. As shown in Figure 1-13a, low-level icing rarely occurs below 0° F. At higher levels (up to 22,000 ft.), the minimum icing temperature is -22° F. Icing encounters above 22,000 ft. are rare. The icing envelope for cumuliform clouds is somewhat more narrow than for stratiform clouds, as shown in Figure 1-13b. The minimum altitude for cumuliform clouds is 4,000 ft., and the maximum (for this data) is 24,000 ft. The temperature range is more restricted for cumuliform clouds at a given altitude than for stratiform clouds. The icing envelopes shown here have been used as a basis for the CAR 4b transport category airworthiness requirement, as will be shown later. Some additional data on low-level and extreme high-level icing has been obtained and is presented in succeeding sections of this report. The frequency of encounter versus altitude can be seen in Figure 1-14 (which is a crossplot of previous data). Stratiform icing encounters are most likely at low altitudes (3,000 to 6,000 ft.), whereas cumuliform cloud encounters are more prevalent at 8,000 to 12,000 ft. The maximum cloud depth for layer type clouds is 6,500 ft. (Figure 1-15) and would be found where there is a double layer of clouds. Maximum single layer cloud depth is likely to be less than 3,500 ft. Maximum cloud depth is of particular interest for climbout and descent, where the icing cloud cannot be avoided (whereas for level flight it is often possible to fly over or under the cloud).

For some types of icing studies, it may be convenient to define an average or most probable icing temperature versus altitude (Figure 1-16). At sea level, the most probable icing temperature is 26° F decreasing to -11° F at 20,000 ft. At the higher altitudes (16,000 to 24,000 ft.) the probable icing temperature is very close to the NACA standard day temperature.

The probability of encountering icing when flying IFR (instrument flight rules) is of particular interest. It may be seen in Figure 1-17 that at ambient

temperatures of 14° to 32° F (where icing is encountered most frequently) about 40 per cent of the flights through clouds will result in ice accumulation. At lower temperatures, the frequency of icing in clouds is much lower: about six per cent at -22° F.

The probability of accumulating a specific amount of ice is of special interest for parts of an aircraft that do not have icing protection. The data of Figure 1-18 shows that a maximum accretion during climbout and descent is 0.4 in., whereas for continuous icing the maximum amounts are 3.5 to 5 in., depending on the data source. (The 0.4-in. maximum during climb and descent was based on data from jet fighter aircraft. For aircraft with lower rates of climb and descent, the maximum value may be higher. Values of ice accretion for specific rates of climb and probabilities are shown in NACA TN 4314, Ref. 1-16.) These values are based on the rate of accretion on a 1/8-in. diameter probe (icing rate meter) which would have a collection efficiency of nearly 100 per cent regardless of airspeed or drop size. For bodies of larger size with a greater leading edge radius, the collection efficiency at stagnation and, thus, the maximum thickness may be substantially less.

Rate of ice formation and ice shape are affected by many factors, including LWC, drop size, air speed, temperature, body size and shape. Nevertheless, the data of Figure 1-18 does indicate the order of magnitude that might be anticipated for various levels of probabilities. Methods of predicting ice size and shape are reported in detail in Section 2.

At a combination of higher speed, ambient temperature and LWC, there is a limiting temperature above which the water will not freeze completely, but will run off. This is shown in Figure 1-19. As the ambient temperature exceeds the give   urves, water will freeze only partly or not at all, and calculations of ice accretion must consider this factor. (Further discussion of this subject is contained in Section 2.)

1.3.2 LOW-ALTITUDE ICING DATA — Most of the data presented in the previous section is based on altitudes in the range of approximately 3,000 to 24,000 ft. Concern has been expressed as to the severity of low-altitude icing, particularly with respect to light aircraft that might operate in the low-altitude regime. Data was obtained from William Lewis of the NASA Lewis Research Center on low-altitude icing (Ref. 1-18). This data (Figure 1-20) and adiabatic lifting theory show that the liquid water content is reduced at low altitude. In terms of height above the ground, maximum values for 1,000, 3,000, and 5,000 ft. are 0.24, 0.65, and 0.8 gm/m^3 respectively. Thus, design use of the liquid water contents for normal operational altitudes will produce systems that are more than adequate for very low altitude operation.

Freezing rain at low altitudes can be a problem also, and is discussed separately in Paragraph 1.3.5.

1.3.3 HIGH-ALTITUDE ICING — The data presented in Paragraph 1.3.1 covers several hundred icing encounters, but is obtained primarily from aircraft having operational ceilings of about 22,000 ft. The advent of turbine powered aircraft with high-altitude capabilities has raised the question of whether the temperature - altitude icing envelopes established previously are adequate. Data was solicited from various sources; however, the only response was from the Boeing Company (Ref. 1-19). A considerable number of reports of icing encounters were collected by Boeing from operation of B-52 type bombers, KC-135 tanker aircraft, and 707 commercial jet transports. These are plotted in Figure 1-21. Also included in Figure 1-21 are the icing envelopes based on the NACA data of Ref. 1-1 through 1-15 (and used for the FAA commercial transport criteria). Data from NACA TN 4314 (Ref. 1-16) which was obtained from icing encounters during climb and descent by a jet interceptor squadron, is also included.

From the data presented, it may be seen that icing encounters above 24,000 ft. are rare, as are icing encounters below -22° F. It does appear that the

temperature range of the icing envelopes could be increased by about 10° F at the higher altitudes.

With one exception, the high-altitude icing encounters are reported as "light" icing; this is in agreement with previous data showing reduced LWC with lower temperature.

Two data points are found at temperatures well below -40° F; however, the notation with the Boeing data states that the temperatures were probably measured in dry air after the icing encounter. (Temperature in clouds may be several degrees warmer than the adjacent air.) Existence of water in supercooled droplet form at temperatures below -40° F is very unlikely.

Based on the data available, it appears that high-altitude icing is infrequent and when encountered is not likely to be of a severe nature. An aircraft having ice protection systems designed to cope with the icing conditions defined in Paragraph 1.3.1 will probably have no difficulties when icing is encountered at high altitudes. Exceptions to this statement may occur where extreme conditions are deliberately sought, as in the USAF "Project Rough Rider." For routine commercial and military operation, the statements are considered applicable.

1.3.4 FOREIGN DATA -- Search of foreign literature has not produced a large amount of statistical icing data (of the type published in the NACA reports). Some recent data has been summarized in a report by R. F. Jones, published by the World Meteorological Organization (Ref. 1-20). The maximum and mean liquid water contents reported by the USSR are of interest, as representing a different area of the Northern hemisphere than the NACA data. In Figure 1-22, the mean liquid water contents for stratiform clouds are shown to range from 0.1 to 0.34 gm/m^3, decreasing slightly with decreasing ambient temperatures (0 to -25° C). The maximum values range from 0.15 to 1.1 gm m^3, with a sharp reduction in water content as temperature decreases.

For cumuliform clouds, the mean liquid water contents shown (Figure 1-23) are surprisingly small, ranging from less than 0.3 gm/m^3 at 0° C to as little as 0.1 gm/m^3 at -25° C (-12° F). Maximum values, however, vary from less than 0.1 gm/m^3 to 1.55 gm/m^3.

Little data is available on the statistical frequency of icing encounters for areas other than the continental USA and certain areas of the North Atlantic and Pacific Oceans. One approach to the problem is outlined in a report by R. W. Jailer in which icing probabilities for the northern hemisphere are predicted by means of frequency data on low pressure areas and freezing level altitudes (Ref. 1-21). The assumption is made that the frequency of clouds and below freezing temperature is proportional to the icing frequency. In the chart for January, (Figure 1-24) it may be seen that the frequency varies from 0.01 (southeast USA) to 0.05 (Great Lakes area) for the continental USA. Values up to 0.07 are seen in the Aleutian Islands area.

Consideration of both References 1-20 and 1-21 supports a conclusion that the data presented previously (in NACA reports) should be adequate for design of ice protection for aircraft flying in any region.

1.3.5 FREEZING RAIN — Flight through freezing rain can have adverse effects on aircraft performance and on function of its instruments. Quantitative data on freezing rain encounters in flight are virtually non-existent; however, reports from aircraft that have encountered freezing rain are not at all rare. According to NACA TN 1855 (Ref. 1-2, Table 1-5) freezing rain is characterized by large droplet size (1,000 microns), temperatures of 25 to 32° F, altitudes of 0 to 5,000 ft., and liquid water content of 0.15 gm/m^3 (which corresponds to a rainfall rate of 0.1 in./hr.). Horizontal extent may be as much as 100 mi.

The large droplet sizes found in flight through freezing rain can result in ice accumulations on parts of aircraft that might normally be ice-free.

Static vents (air speed, fuel, etc.) can ice over in freezing rain. On light aircraft, exposed control cables and mass balances could accumulate ice. In any new aircraft design, the effects of freezing rain should be considered in addition to the current design procedures for normal (small droplet) icing conditions.

The frequency of freezing rain must be deduced from ground level observations reported in Ref. 1-22 (since no flight data other than those of Table 1-2 can be found). The time frequency of rainfall rate is shown in Figure 1-25 for rain and freezing rain/snow, plotted against the parameter of annual precipitation/number of days with precipitation. For rain and freezing rain and snow combined, the maximum frequency is 3.15 per cent for 0.06 in./hr. and 1.8 per cent for 0.12 in./hr. The corresponding maximum frequencies for freezing rain and snow (combined) are 0.47 per cent (for 0.06 in./hr.) and 0.015 per cent (for 0.12 in./hr.). From this data it can be seen that the suggested data of NACA TN 1855 (based on 0.1 in./hr.) represents a realistic value for design purposes.

1.4 CURRENT DESIGN STANDARDS

1.4.1 DESIGN CRITERIA FOR COMMERCIAL TRANSPORTS — Civil Aeronautics Regulation, Part 4b (Ref. 1-23) has icing envelopes defined for use in the design and certification of commercial transport aircraft. This data is based on the NACA reports presented previously (TN 1855, 2569 and 2738, Ref. 1-2, 1-8, and 1-10, respectively). Current experience with aircraft designed and certified to these standards indicates that the standards are adequate.

The data is presented in terms of LWC, drop size, temperature, horizontal extent and altitude. Icing is divided into two classes: continuous maximum (layer type clouds) and intermittent maximum (cumulus clouds).

Liquid water content is plotted versus mean effective drop diameter in Figure 1-26 for ambient temperatures of 32° to -22° F. These values are to be considered for sea level to 22,000 ft., with a maximum vertical extent of

6,500 ft. The data is for a standard distance of 20 mi. (horizontal extent of up to 200 mi. are possible - the effect of distance on LWC is shown in a later figure). The usual practice has been to design airframe anti-icing systems for a droplet diameter of 20 microns, with consideration of 40-micron droplet impingement limits for determination of maximum area to be protected. Choice of ambient temperature depends on the type of system being designed. Typical choices might be 25° F for an evaporative anti-icing system for low flight speeds, 15° F for evaporative anti-icing at higher speeds, 0° F for running wet anti-icing or cyclic de-icing (avoiding icing flight at lower temperatures), and -22° F for running wet anti-icing or cyclic de-icing where limitations on operation at low temperature are not acceptable.

An envelope of ambient temperature and altitude for continuous icing is shown in Figure 1-27 and is intended for use with Figure 1-26 to establish operating conditions for design purposes. This figure was derived from NACA TN 2569 (Ref. 1-8), and the data has been presented previously in Figure 1-13a.

The average LWC decreases with increasing distance, as shown in Figure 1-28, in terms of a liquid water content factor, F, (which has a value of 1.0 at 20 miles) versus distance. Most designs are based on LWC associated with the 20-mi. distance; however, where components are not protected, the maximum amount of ice that could accumulate is of interest. The relative amount of ice collected versus distance can be derived from Figure 1-28, and is shown in Figure 1-29 versus distance. The maximum amount of ice accumulation is seen to be more than three times that for a 20-mi. encounter. From a probability viewpoint, encounters of more than 150 to 175 mi. are unlikely (see Figure 1-12); for this distance the ice accumulation is three times that for the standard 20-mi. distance.

Liquid water content, drop size, temperature and distance are defined for maximum intermittent icing in Figures 1-30 through 1-32. Intermittent icing

1-21

is found in flight through cumulus clouds and is characterized by high liquid water contents (up to 3.9 gm/m^3) for short distances (0.3 to 6 miles). The primary use for this data is in design of turbine engine inlets (or other critical air inlets) where a sudden exposure to high liquid water content might overwhelm the anti-icing system and cause engine operating problems. Normal anti-icing design practice is to provide at least running wet (surface temperature of 35°F) protection for intermittent conditions if the ice formed during such an encounter would otherwise present a significant hazard to safe flight. The amount of runback icing will normally be small and acceptable because of the short duration; however an evaluation should be made for each new airframe and engine inlet application.

1.4.2 MILITARY AIRFRAME ANTI-ICING DESIGN SPECIFICATION — Airframe thermal anti-icing systems for military aircraft have in recent years been designed to meet the requirements of USAF specification MIL-A-9482 (Ref. 1-24). The meteorological conditions of this document for evaporative anti-icing are ambient temperature, + 15°F; liquid water content, 0.5 gm/m^3; and mean effective droplet diameter of 20 microns. Duration or horizontal extent of icing conditions are not specified. These values are to be used in the design of evaporative thermal anti-icing systems and are similar to the maximum continuous conditions of the FAA regulations. If the operational speed of the aircraft is in the order of 450 kt. or more (see Figure 1-33), anti-icing systems usually have been deleted, as icing would ordinarily occur only during loiter and descent. Loiter and descent times are usually of very short duration and, therefore, may not be considered for design purposes. (This is not true for commercial aircraft, however, where holding times of 30 min. are not uncommon.) Also, a military aircraft capable of high speeds has a large excess of power available at low speeds, so that the drag associated with wing and tail icing is not a significant problem.

Additional data contained in MIL-A-9482 is relative to system design details and is discussed separately in Section 3.

1.4.3 MILITARY ENGINE DESIGN SPECIFICATION, MIL-E-5007B — The meteorological criteria used for design of engine inlet guide vane anti-icing

1-22

systems for military turbine engines are found in MIL-E-5007B (Ref. 1-25).
Two specific conditions are called out: Condition I has a liquid water content
of 1.0 gm/m^3 at -4° F with a 15-micron drop size. For Condition II, the
values are 2.0 gm/m^3, +23° F and 25 microns. These conditions are normally
used for design and static testing of running wet anti-icing systems for inlet
guide vanes and compressor nose cones. No specific time duration is called
out; however, the conditions are quite similar to those of the "maximum inter-
mittent" conditions of the FAA regulations.

A comparison of the various design standards is shown in Paragraph 1.4.4

1.4.4 BRITISH CIVIL TRANSPORT DESIGN CRITERIA — The British Civil
Airworthiness Requirements (Ref. 1-26) contain standards for liquid water
content similar to those shown previously for the FAA transport regulation.
The liquid water content (Figure 1-34) for maximum continuous icing is identi-
cal to that of the FAA regulation values for 15-micron drops except that the
drop size is 20 microns rather than 15. In this respect, the British require-
ments are slightly more severe than the FAA standard. The U.S. military
standard (0.5 gm, 15° F and 20 microns) is also shown for comparison, and
falls between the FAA and British standards.

The maximum intermittent condition of the British CAR is identical to the
FAA regulation for the standard distance of three miles (Figure 1-35). The
U.S. military engine specification values are also shown for comparison. In
the British regulation, the intermittent condition is considered to exist for
three miles with "continuous maximum" icing gaps of three miles up to 30,000
ft. Above 30,000 ft., the gaps are considered to be 20 miles of clear air (see
Table 1-5).

The similarity between British and U.S. civil air regulations is not coin-
cidental; both are based on NACA icing data, with slightly different interpreta-
tions of the data.

1.4.5 USSR STANDARDS — The design standards used for Soviet aircraft (Ref. 1-27) may be of interest for aircraft operating in various areas of Europe and Asia. The only data found is summarized in Figure 1-34 in terms of LWC versus temperature for a 16-micron mean drop size and 15-minute duration (flight speed is not specified). At 14° F the LWC is identical to the British requirement (but 20-micron droplet diameter) and the FAA requirement (at 15-micron drop diameter). At higher and lower temperatures, the USSR standards for LWC are higher than the corresponding U.S. and British standards. Anti-icing systems designed to U.S. and British standards would at most show a small amount of runback under the Soviet design conditions.

1.4.6 FREEZING RAIN DESIGN CONSIDERATIONS — Search through various literature sources (see Table 1-1 and Figure 1-25) indicated that the proposed values of NACA TN 1855 would rarely be exceeded. These are shown in Table 1-1, as 0.15 gm/m^3, 25 to 32° F, 1,000-micron drop diameter, and altitude range of sea level to 5,000 ft. Horizontal extent (maximum) is 100 mi. The possible effects of freezing rain should be considered for components not usually protected — such as air speed static vents, fuel tank vents, exposed control horns, cables, etc.

1.4.7 ICE CRYSTALS — Flight through clouds of ice crystals, snow or mixtures of ice crystals and liquid water is not uncommon, as shown by Table 1-2. During one year of operation, 23.6 per cent of the total time in visible moisture was in ".mixed" snow and liquid water, and 32.5 per cent was in snow; more than half of the encounters involved ice crystals or snow to some degree. Dry snow or or ice crystals are not usually a problem. The exceptions have been in the case of turbine engine inlets of great length and curvature. Concentrations of ice crystals at bends or flow reversal points can result in intermittent shedding into the engine, resulting in engine flameout. This problem may be aggravated by areas of ducting that may be warm from contact with hot sections of the engine.

Little quantitative data can be found on ice crystal concentrations, as the subject has not received intensive flight research comparable to the icing field. Most of the flight and laboratory testing in ice crystal environments has been conducted in the United Kingdom. Standards in use for turbine engine design and testing are shown in Table 1-6. The engine must operate satisfactorily in ice crystals of 1.0 gm/m^3 for thirty minutes and for shorter times at concentrations up to 8.0 gm/m^3. A second "mixed" condition is also used, which includes 0.5 to 1.0 gm/m^3 liquid water with a corresponding decrease in ice crystal content. Tests are usually conducted at 0° to -5° C, because this represents the highest concentration of ice crystals.

Flight through clouds of ice crystals calls for careful exercise of good judgment by the aircraft pilot. Normally, the ice protection systems should not be turned on, as the airframe and engine surfaces will remain clean. In a "mixed" cloud, ice may accumulate and require use of the ice protection equipment. The capacity of thermal systems may be exceeded, however, and it may be necessary to escape the icing condition as rapidly as possible.

It has been speculated that reports of excessive icing (e.g., Ref. 1-20) might be the result of flight in mixed clouds with anti-icing systems overtaxed by the increased heat needed first to melt the ice crystals, then to warm and evaporate the water. Documented evidence of severe airframe icing problems in clouds of ice crystals or mixed clouds is lacking, however. As long as the engine continues to deliver the required thrust, operation in ice crystals is not likely to present severe problems.

REFERENCES

1-1   NACA TN 1391 "Icing Properties of Non-Cyclonic Winter Stratus
        Clouds," William Lewis, 1947.

1-2   NACA TN 1855 "Recommended Values of Meteorological Factors to be
        Considered in the Design of Aircraft Ice-Prevention Equipment,"
        A. R. Jones and William Lewis, March 1949.

1-3   NACA TN 1392 "Icing Zones in a Warm Front System with General
        Precipitation," William Lewis, 1947.

1-4   NACA TN 1393 "A Flight Investigation of the Meteorological Conditions
        Conducive to the Formation of Ice on Airplanes," William Lewis, 1947.

1-5   NACA TN 1424 "A Further Investigation of the Meteorological Conditions
        Conducive to Aircraft Icing," William Lewis, D. B. Kline, and C. P.
        Steinmetz, 1947.

1-6   NACA TN 1793 "Investigation of Meteorological Conditions Associated
        with Aircraft Icing in Layer-Type Clouds for 1947-48 Winter," Dwight
        B. Kline, 1949.

1-7   NACA TN 1904 "Observations of Icing Conditions Encountered in Flight
        During 1948," William Lewis and W. H. Hoecker, Jr., 1949.

1-8   NACA TN 2569 "A Summary of Meteorological Conditions Associated
        with Aircraft Icing and a Proposed Method of Selecting Design
        Criterions for Ice-Protection Equipment," P. T. Hacker and R. G.
        Dorsch, 1951.

1-9   NACA TN 2306 "Meteorological Analysis of Icing Conditions Encountered
        in Low Altitude Stratiform Clouds," Dwight B. Kline and Joseph A.
        Walker, 1951.

1-10   NACA TN 2738 "A Probability Analysis of the Meteorological Factors
        Conducive to Aircraft Icing in the United States," William Lewis and
        Norman R. Bergrun, 1952.

1-11   NACA TN 3984 "Statistical Study of Aircraft Icing Probabilities at the
        700 and 500 Millibar Levels Over Ocean Area in the Northern Hemi-
        sphere," P. J. Perkins, William Lewis, and D. R. Mulholland, 1957.

1-12   NACA RM E52J06 "Preliminary Survey of Icing Conditions Measured
       During Routine Transcontinental Airline Operation," Porter J. Perkins,
       1952.

1-13   NACA RM E55F28a "Statistical Survey of Icing Data Measured in
       Scheduled Airline Flights over the United States and Canada from
       November 1951 to June 1952," Porter J. Perkins, 1955.

1-14   NACA RM A54I23 "A Heated-Wire, Liquid-Water Content Instrument
       and Results of Initial Flight Tests in Icing Conditions," Carr B. Neel,
       1955.

1-15   NASA Memo 1-19-59E "Summary of Statistical Icing Cloud Data
       Measured Over United States and North Atlantic, Pacific, and Arctic
       Oceans During Routine Aircraft Operations," Porter J. Perkins, 1959.

1-16   NACA TN 4314 "Icing Frequencies Experienced During Climb and
       Descent by Fighter-Interceptor Aircraft," Porter J. Perkins, July
       1958.

1-17   "Liquid Water Content and Distribution of Drops in Cumulus Clouds,"
       V. A. Zaitsev, National Research Council of Canada, Technical
       Translation TT-395, Ottawa, 1953.

1-18   Letter from William Lewis, NASA Lewis Research Center, dated
       April 14, 1963 (Unpublished).

1-19   Letter No. 6-7731-69, dated April 29, 1963, from E. A. Rock, Staff
       Engineer, the Boeing Company, Renton, Washington.

1-20   "Ice Formation on Aircraft," R. F. Jones, Technical Note No. 39,
       World Meteorological Organization Report WMO-No. 109.TP.47.

1-21   WADC TN 55-225 "Evaluation of Northern Hemisphere Icing Probabilities,"
       Robert W. Jailer.

1-22   "Handbook of Geophysics," U.S. Air Force, the Macmillan Co., New
       York, 1960 (Chapter 6).

1-23   Civil Aeronautics Regulation, Part 4b, Airplane Airworthiness: Trans-
       port Categories, Federal Aviation Agency.

1-24   MIL-A-9482 "Military Specification - Anti-Icing Equipment for Aircraft,
        Heated Surface Type, General Specification," Amendment 1, dated 10
        June 1955.

1-25   MIL-E-5007B "Military Specification - Engine, Aircraft, Turbojet,
        General Specification," dated 27 July 1951.

1-26   British Civil Airworthiness Requirements, "Subsections D 4-7 and
        D 5-5," dated 16 March 1959.

1-27   "Some Results of Experimental Flights in Natural Icing Conditions and
        Operation of Aircraft Thermal Ice Protection," by O.K. Trunov (paper
        presented at 1960 Aircraft Ice Protection Conference, D. Napier and
        Son, Ltd.).

1-28   "Vaguard Icing Encounter," G. Hinton Lever and M. R. Chick (paper
        presented at 1962 Aircraft Ice Protection Conference, D. Napier and
        Son Ltd.).

1-29   "Aviation Publication 970" (Leaflets 714/2 and 714/3, last revised
        December 1958 and July 1961 respectively) United Kingdom Ministry
        of Aviation (British Crown Copyright reserved, reproduced by permission
        of the Controller, Her Britannic Majesty's Stationery Office).

Table 1-1

Recommended Values of Meteorological Factors for Consideration in the Design of Aircraft Ice Prevention Equipment.

(Based on NACA TN 1855; Maximum Instantaneous Class Deleted)

Class	Air Temp. (°F)	Liquid Water Content (gm/m³)	Drop Diameter (Microns)	Pressure Altitude (1,000 Ft.)	Remarks
II-M Intermittent, Maximum	32	2.5		10-15	
	14	2.2		10-20	Horizontal extent -
	- 4	1.7		12-30	3 miles
	-22	1.0	20	15-30	Characteristic - High
	-40	0.2		15-30	liquid water content
	32	1.3		8-15	Applicable to: Any
	14	1.0		8-20	critical component of
	- 4	0.8	30	10-30	the airplane where ice
	-22	0.5		15-30	accretion, even though
	-40	0.1		15-30	slight and of short duration, could not be tolerated
	32	0.4		8-15	Example: Induction
	14	0.3		8-20	system (particularly
	- 4	0.2	50	10-30	turbine engine inlets)
	-22	0.1		15-30	
	-40	0.1		15-30	
II-N Intermittent, Normal	32	0.8	20	8-12	
	14	0.6	20	8-15	
	- 4	0.4	18	12-20	
	-22	0.1	15	15-25	
	-40	0.1	13	15-25	

Table 1-1
(Cont'd.)

Class	Air Temp. (°F)	Liquid Water Content (gm/m³)	Drop Diameter (microns)	Pressure Altitude (1.000 Ft.)	Remarks
III-M Continuous Maximum	32 14 - 4 -22 -40	0.8 0.6 0.3 0.2 0.05	15	3-22	<u>Horizontal extent</u> - Continuous <u>Characteristic</u>: Moderate to low liquid water content for an indefinite period
	32 14 - 4 -22 -40	0.5 0.3 0.15 0.10 0.03	25	3-22	<u>Applicable to</u>: All components of the airplane; i.e., every part of the airplane should be examined with the question - "Will this part be affected seriously by accretions during continuous flight in icing conditions?"
	32 14 - 4 -22 -40	0.15 0.10 0.06 0.04 0.01	40	3-22	<u>Example</u>: Wing and tail surfaces
III-N Continuous Normal	32 14 - 4 -22	0.3 0.2 0.1 0.1	15	3-22	
IV-M Freezing Rain	25- 32	0.15	1.000	0-5	<u>Horizontal extent</u>. 100 ml. <u>Characteristic</u>. Very large drops at near-freezing temperatures and low values of liquid water content <u>Applicable to</u>. Components of the airplane for which no protection would be supplied <u>Example</u>. Fuselage static pressure airspeed vents

Note: Based on 0.10 in. hr. rainfall rate

Table 1-2

Frequency of Encounter With Various Types of Meteorological Conditions During The 1948 Operation

Condition	No. of min. condition	Per cent of total flight time	Per cent of total time in continuous or intermittent visible moisture
Clear Air	6,523	61.1	----
Liquid cloud			
Continuous	209	2.0	5.0
Intermittent			
Clear air predominant	504	4.7	12.1
About one-half clear	368	3.5	8.9
Cloud predominant	325	3.0	7.8
Subtotal, liquid	1,406	13.2	33.8
Mixed snow and liquid cloud			
Liquid predominant			
Continuous	180	1.7	4.3
Intermittent	384	3.6	9.2
Snow predominant			
Continuous	310	2.9	7.5
Intermittent	108	1.0	2.6
Subtotal, mixed	982	9.2	23.6
Snow			
Continuous	1,122	10.5	27.0
Intermittent	226	2.1	5.5
Subtotal, snow	1,350	12.6	32.5
Rain	335	3.1	8.1
Rain and snow	30	0.3	0.7
Freezing rain	13	0.1	0.3
Freezing rain and liquid cloud	41	0.4	1.0
Subtotal, rain	419	3.9	10.1
Total	10,680	100.0	100.0

Source: NACA TN 1904 (Ref. 1-7)

Table 1-3

Comparison of Values of Liquid Water Content for Pacific Coast Cumulus Clouds, $P_e = 0.001$, With Corresponding Values for Intermittent Maximum Conditions Listed in NACA TN 1855

Temperature °F	Drop Diameter Microns	Liquid Water Content (gm/m^3)	
		TN 1855 - Recommended Design Values	TN 2738 - Probability Analysis
32	20	2.5	2.46
32	30	1.3	1.50
32	50	0.4	0.42
14	20	2.2	2.30
14	30	1.0	1.35
14	50	0.3	0.37
- 4	20	1.7	1.45
- 4	30	0.8	0.70
- 4	50	0.2	0.15
-22	20	1.0	0.37
-22	30	0.5	0.15
-22	50	0.1	0
-40	20	0.2	0
-40	30	0.1	0
-40	50	0.1	0

Table 1-4

Comparison of Weighted Average Values of Liquid Water Content for
Layer Clouds, $P_e = 0.001$, With Corresponding Values for Con-
tinuous Maximum Conditions Listed in NACA TN 1855

Temperature °F	Drop Diameter Microns	Liquid Water Content (gm/m^3)	
		TN 1855 - Recommended Design Values	TN 2738 - Probability Analysis
32	15	0.80	0.77
32	25	0.50	0.49
32	40	0.15	0.20
14	15	0.60	0.50
14	25	0.30	0.28
14	40	0.10	0.08
- 4	15	0.30	0.17
- 4	25	0.15	0.09
- 4	40	0.06	0.02
-22	15	0.20	0.02
-22	25	0.10	0.01
-22	40	0.04	0.003
-40	15	0.05	0
-40	25	0.03	0
-40	40	0.01	0

Table 1-5
British Civil Airworthiness Requirements
(Reference 1-29)
Continuous Maximum (D 4-7 & D 5-5)

Temperature °C	LWC - gm/m^3	Drop Size, Microns	Altitude - Ft.
0	0.8	20	SL - 20,000
-10	0.6	20	3,000 - 27,500
-20	0.3	20	3,000 - 30,000
-30	0.2	20	3,000 - 30,000

Icing layer thickness is 6,500 ft. maximum

(Note: Continuous maximum values are identical to Table 1-1, Class III-M, except that droplet size is 20 microns instead of 15)

Intermittent Maximum (D 5-5)

Temperature °C	LWC - gm/m^3	Drop Size, Microns	Altitude - Ft.
0	2.5	20	10,000 - 20,000
-10	2.2	20	10,000 - 27,500
-20	1.7	20	15,000 - 30,000
-30	1.0	20	15,000 - 35,000
-40	0.2	20	15,000 - 40,000

Up to 30,000 ft. - three mi. duration, with three-mi. gaps of "continuous maximum" condition. Between 30,000 and 40,000 ft. the gaps are 20 mi. of clear air. (Note: Intermittent maximum values are identical to Table 1-1, Class II-M values)

For powerplant, 30 min. of operation is required in a combination of "intermittent" and "continuous" maximum icing, with one-half mile at approximately double the LWC of the "intermittent" condition (see following tabulation).

Instantaneous Maximum

Temperature °C	LWC - gm/m^3	Drop Diameter Microns	Altitude Feet	Horizontal Extent Miles
0	5.0	20	10,000 - 20,000	
-10	4.0	20	10,000 - 27,500	Continuous
-20	3.0	20	15,000 - 30,000	for
-30	2.0	20	15,000 - 35,000	1/2 mile
-40	0.5	20	15,000 - 40,000	

Table 1-6

Ice Crystal Concentration Standards

(Supplied by the National Research Council of Canada.)

Ambient Temperature °C	Altitude 1,000 Ft.	Maximum Total Concentration (ice crystals plus LWC) gm/m^3	Maximum Concentration in Liquid Form gm/m^3	Extent Mi.
0 to -20	10 to 30	8	1	0.5
		5	1	3
		2	1	50
		1	0.5	Indef.
-20 to -40	15 to 40	5	0	3
		2	0	10
		1	0	50
		0.5	0	Indef.
-40 to -60	20 to 45	2	0	3
		1	0	10
		0.25	0	Indef.
-60 to -80	30 to 60	1	0	3
		0.50	0	10
		0.10	0	Indef.

Thirty minutes exposure is considered for the "indefinite" extent.

NOTES (Ref 1-29)
1. In the present state of knowledge, it is not possible to say how much of the "total free water contents" tabulated exist in the form of water and how much as ice crystals, because supercooled water has been shown to exist at temperatures down to -40°C. Furthermore the percentage of ice crystals and water may vary considerably in any one cloud.
2. From present information it appears that the worst condition for engine and intake icing in mixed water/ice crystals occurs when there is a small quantity of water present.
3. The following assumptions may reasonably be made for design purposes:
   a. Below -20°C all the water present may be assumed to be in the form of ice crystals.
   b. Of the total free water shown in the 0°C to -20°C range, not more than 1 gm/m^3 should be taken as water and the remainder as ice crystals, except where the total water content is shown as 1 gm/m^3, when half should be considered as water and half ice crystals.
   c. When the extent of the condition is shown as "indefinite," it is acceptable to show that the airplane functions satisfactorily during 30 minutes continuous exposure to the conditions.
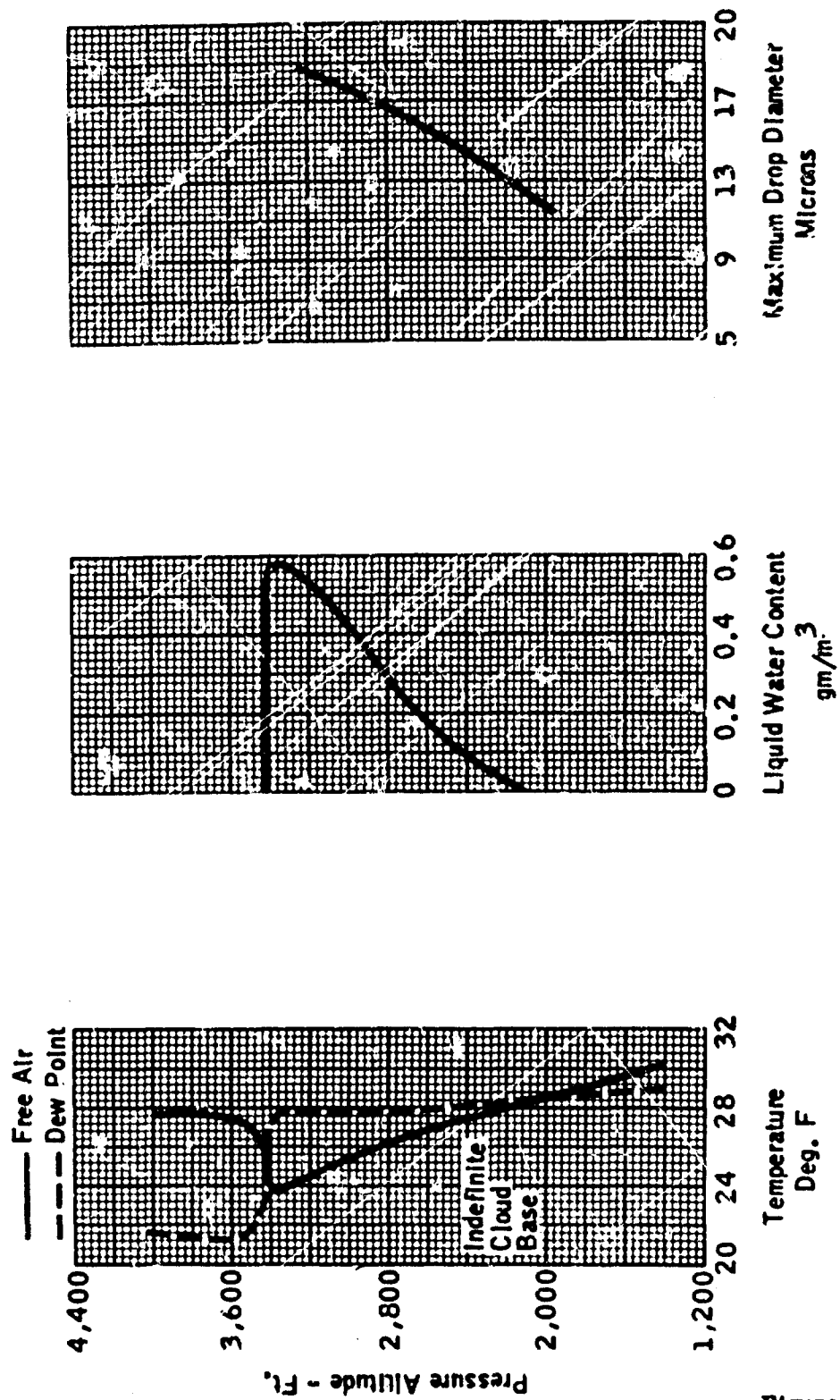
Properties of a Typical Non-Cyclonic Stratus Cloud (From Figure 3a, NACA TN 1391, Ref. 1-1)

Figure 1-1
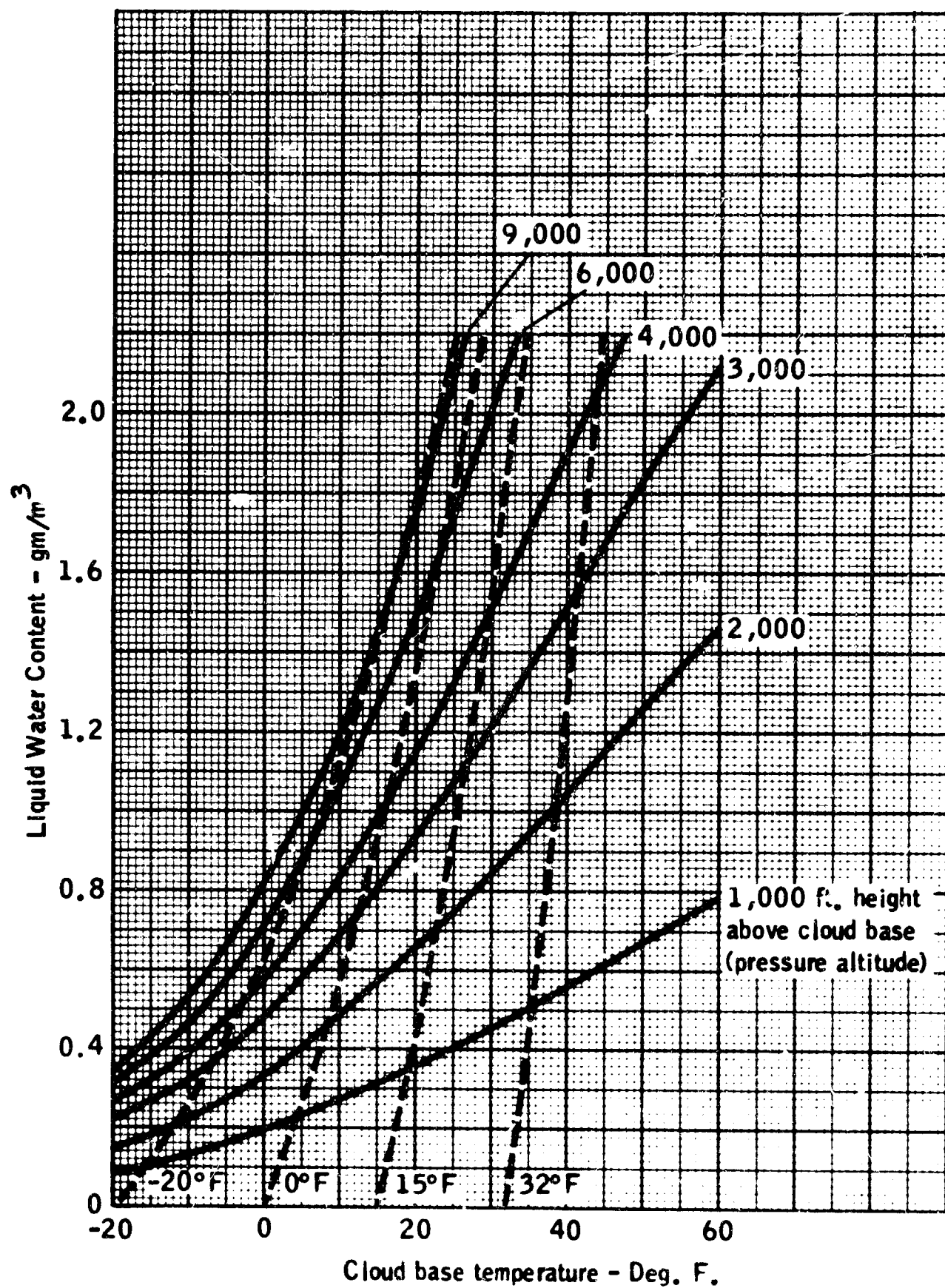
Figure 1-2. Theoretical Liquid Water Concentration in Clouds Formed
by Adiabatic Lifting (Cloud Base at 948 ft. Pressure
Altitude). Data From NACA TN 1391, Ref. 1-1.

1-37
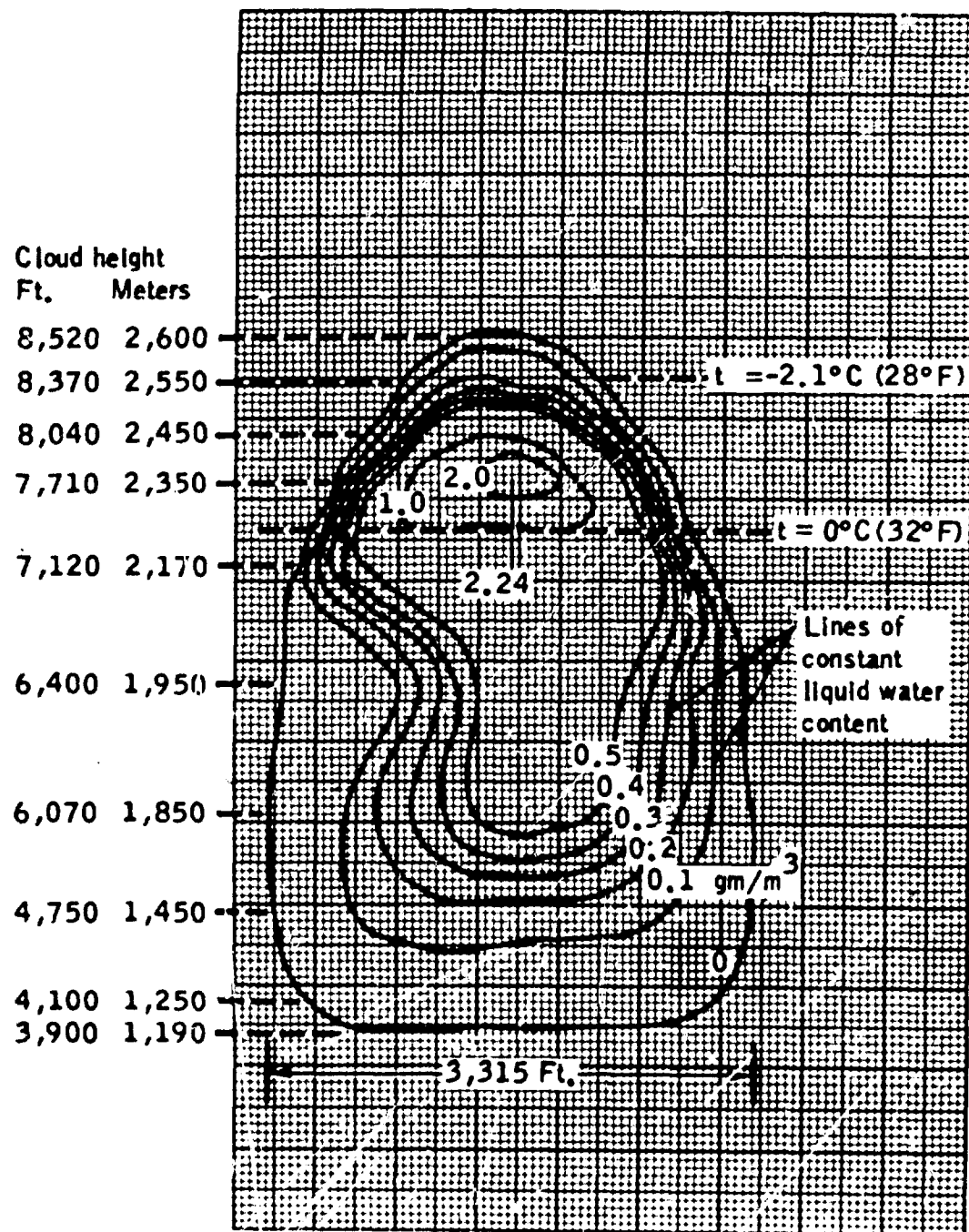
Figure 1-3a. Properties of Typical Cumulus Congestus Clouds — LWC, Drop Size, Temperature, Vertical and Horizontal Dimensions (From NRC-TT-395, Fig. 4 and 7, Ref. 1-17).
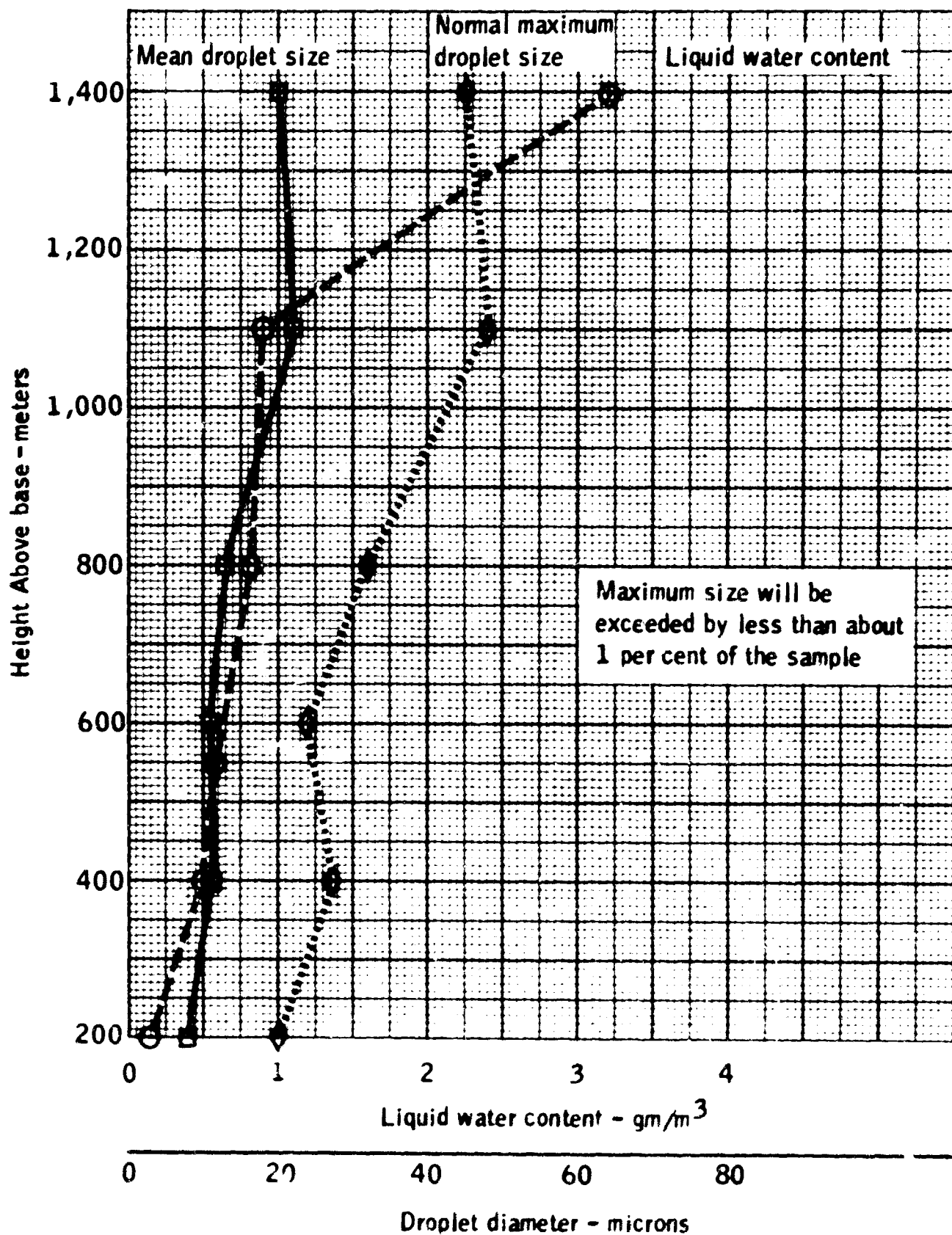
DROPLET SIZE AND LIQUID WATER CONTENT

Figure 1-3b. Properties of Typical Cumulus Congestus Clouds — LWC.
Drop Size. Temperature. Vertical and Horizontal Dimen-
sions (From NRC-TT-395. Fig. 4 and 7. Ref. 1-17)
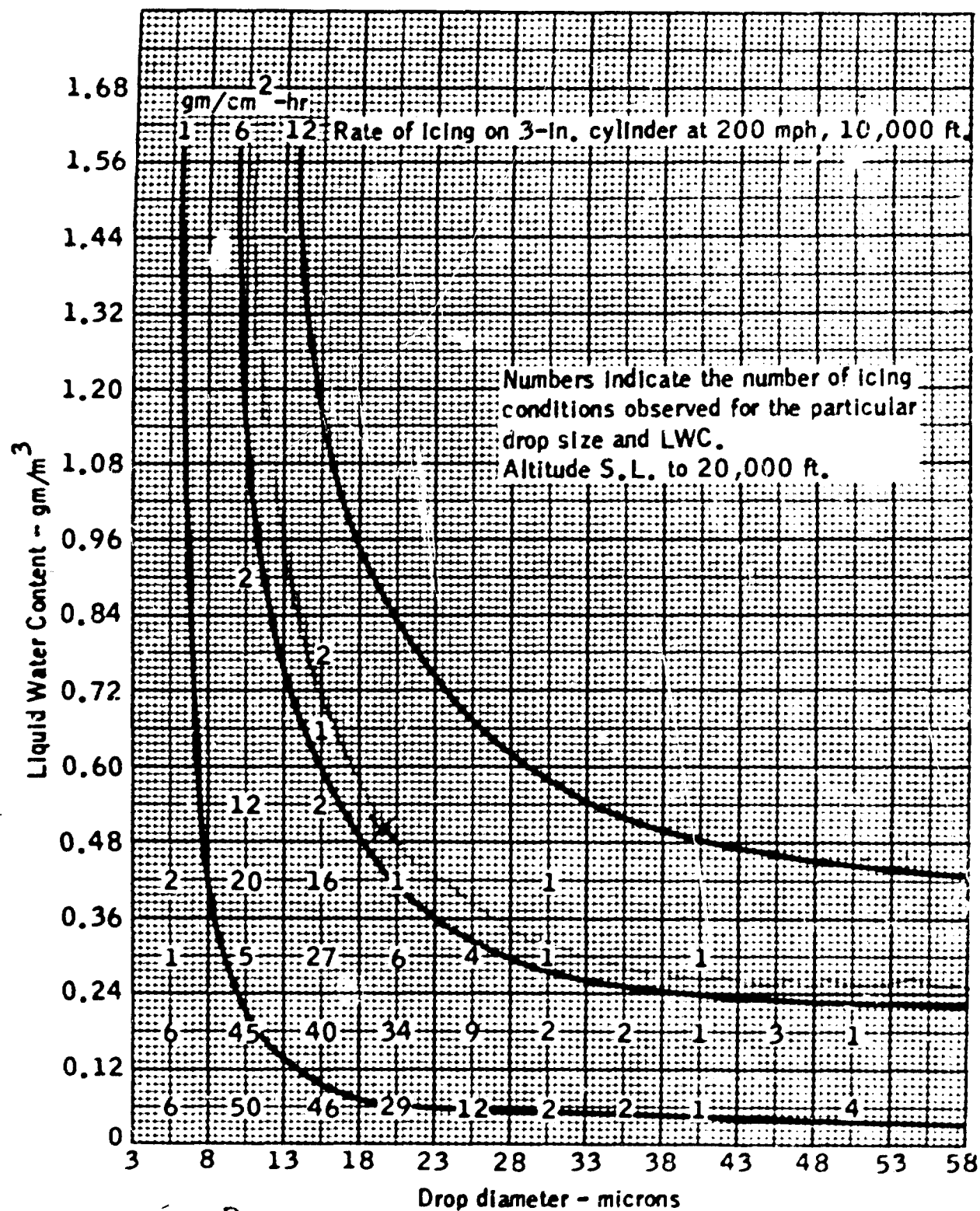
Figure 1-4a. Stratiform Clouds — Layer Type. LWC Versus Drop Diameter (From NACA TN 2569, Ref. 1-8).
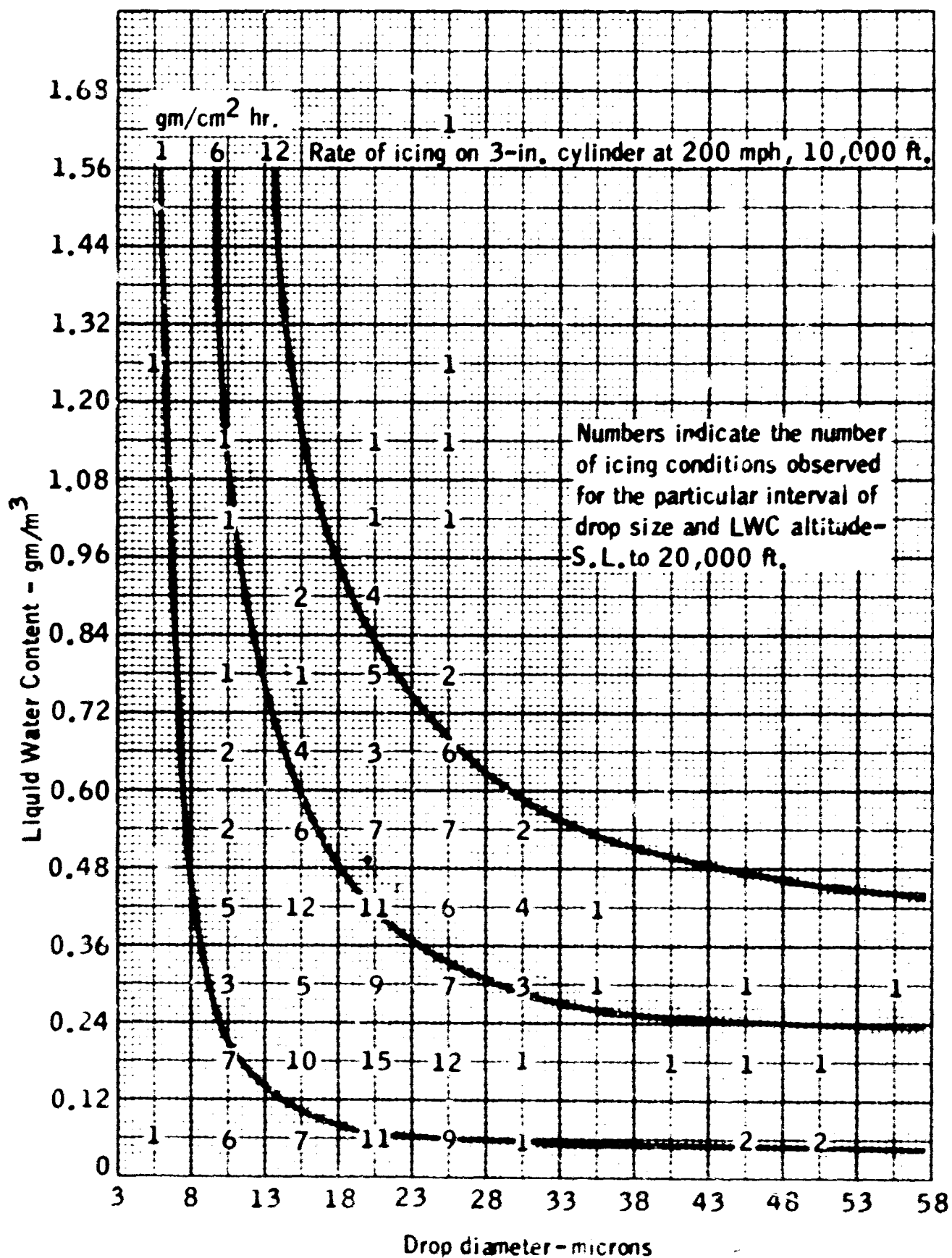
Figure 1-4b. Cumuliform Clouds — LWC Versus Drop Diameter (From NACA TN 2569, Ref. 1-8).
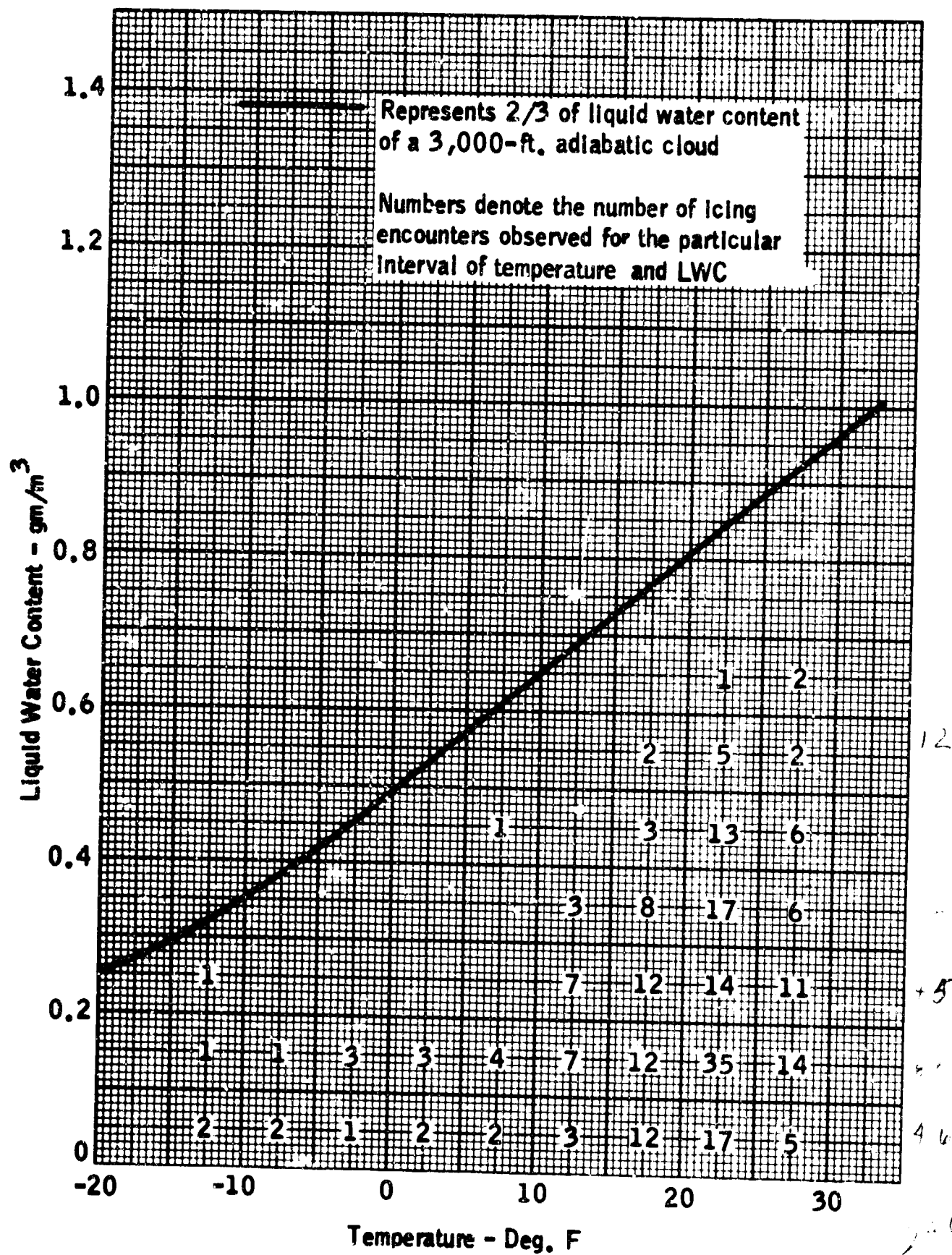
Figure 1-5a.   LWC Versus Temperature — Stratus Clouds (From
NACA TN 1393 and 1424, Ref. 1-4 and 1-5).
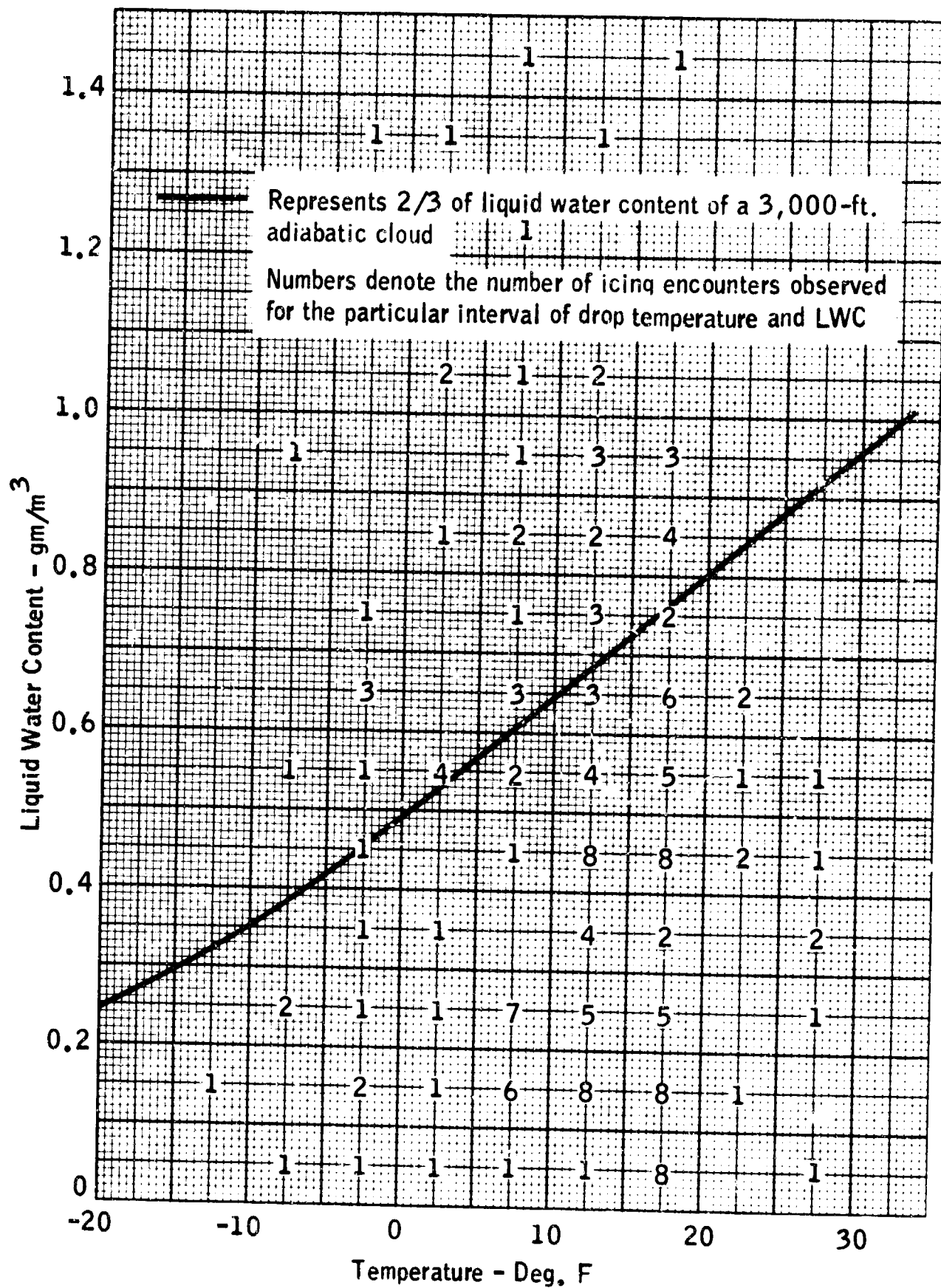
Figure 1-5b. LWC Versus Temperature — Cumulus Clouds (From NACA TN 1393 and 1424. Ref. 1-4 and 1-5).
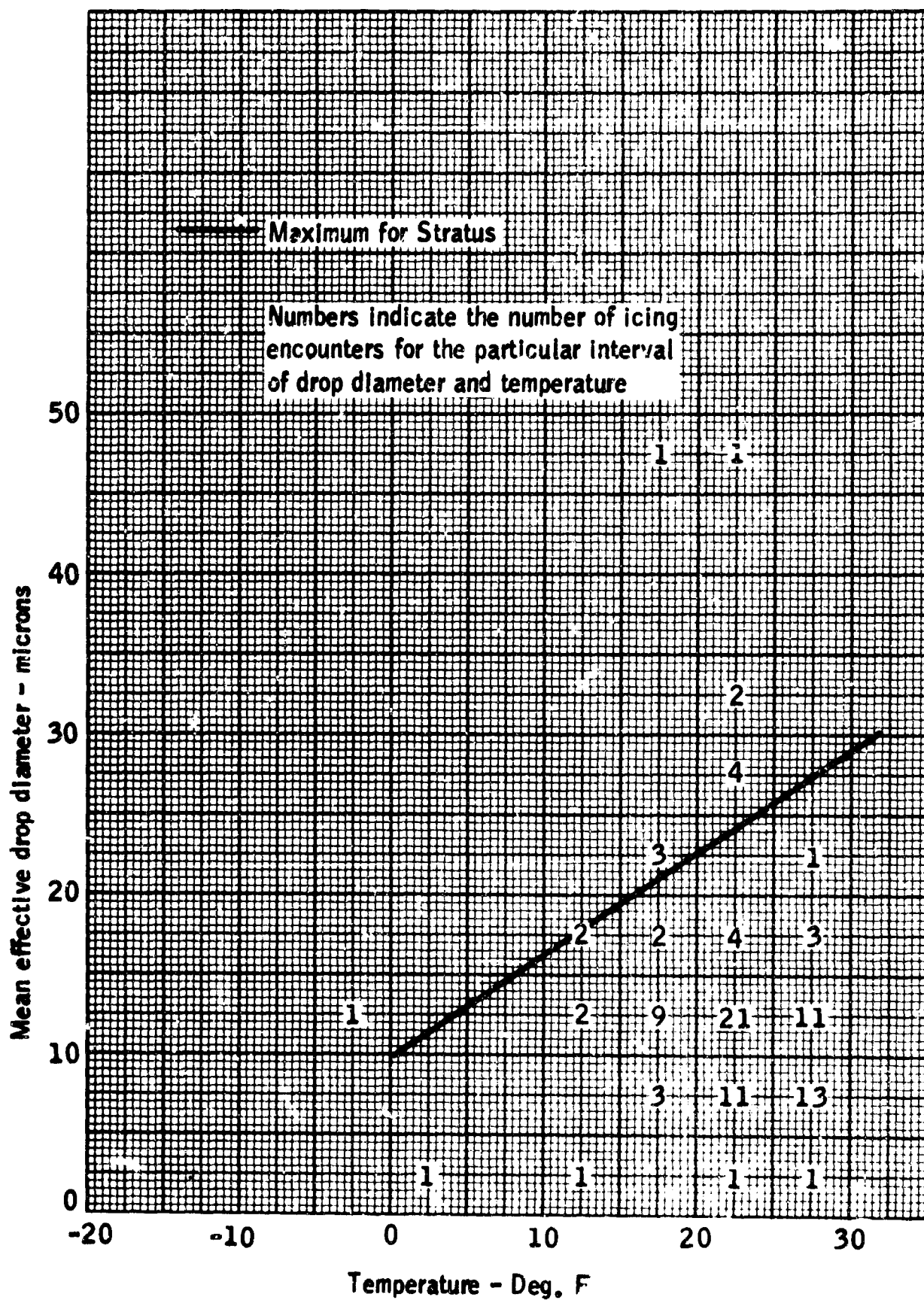
Figure 1-6a. Droplet Diameter Versus Temperature – Stratus Clouds (From NACA TN 1393, Ref. 1-4).

1-44
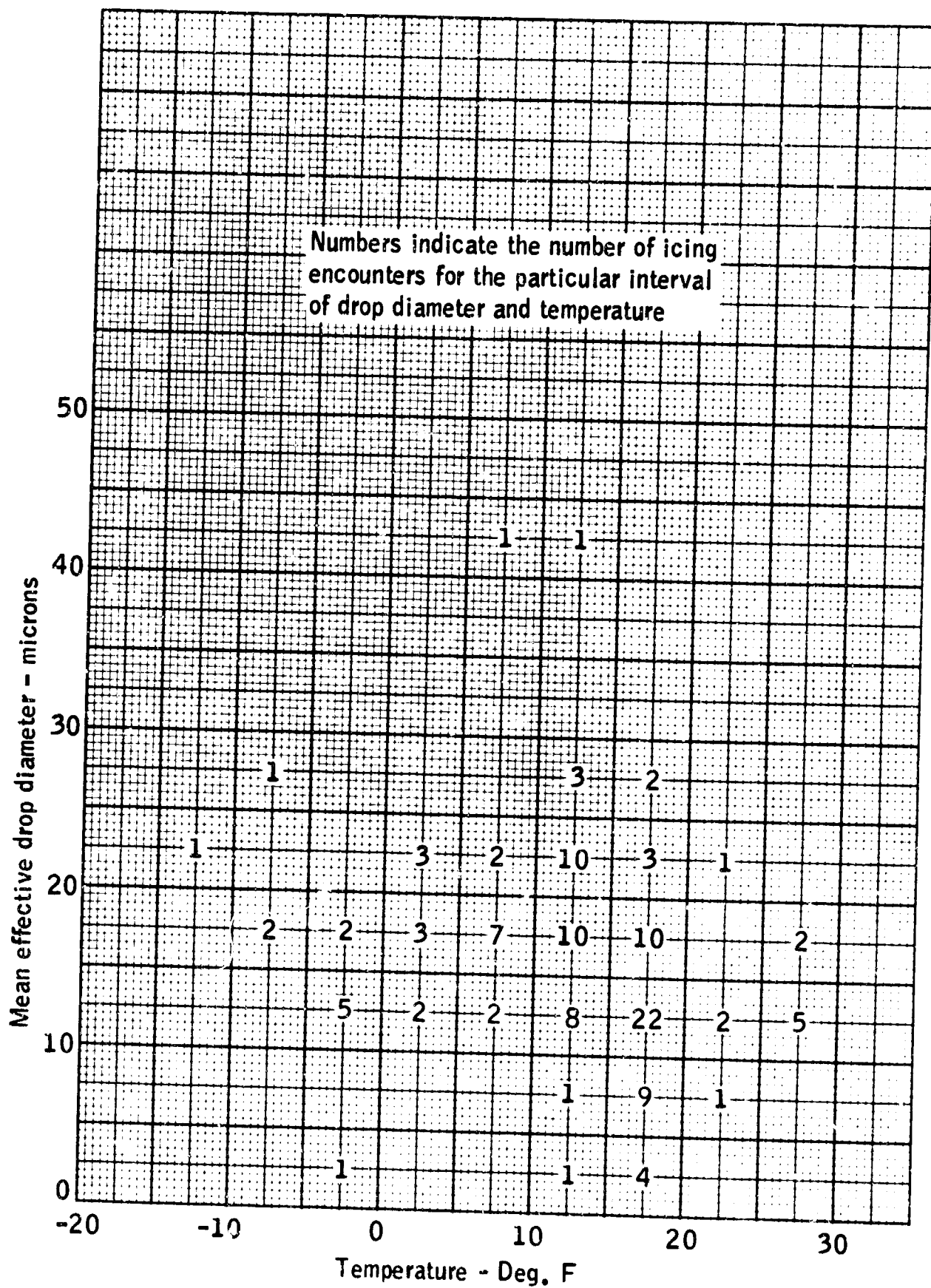
Figure 1-6b. Droplet Diameter Versus Temperature – Cumulus Clouds
(From NACA TN 1393, Ref. 1-4).

1-45
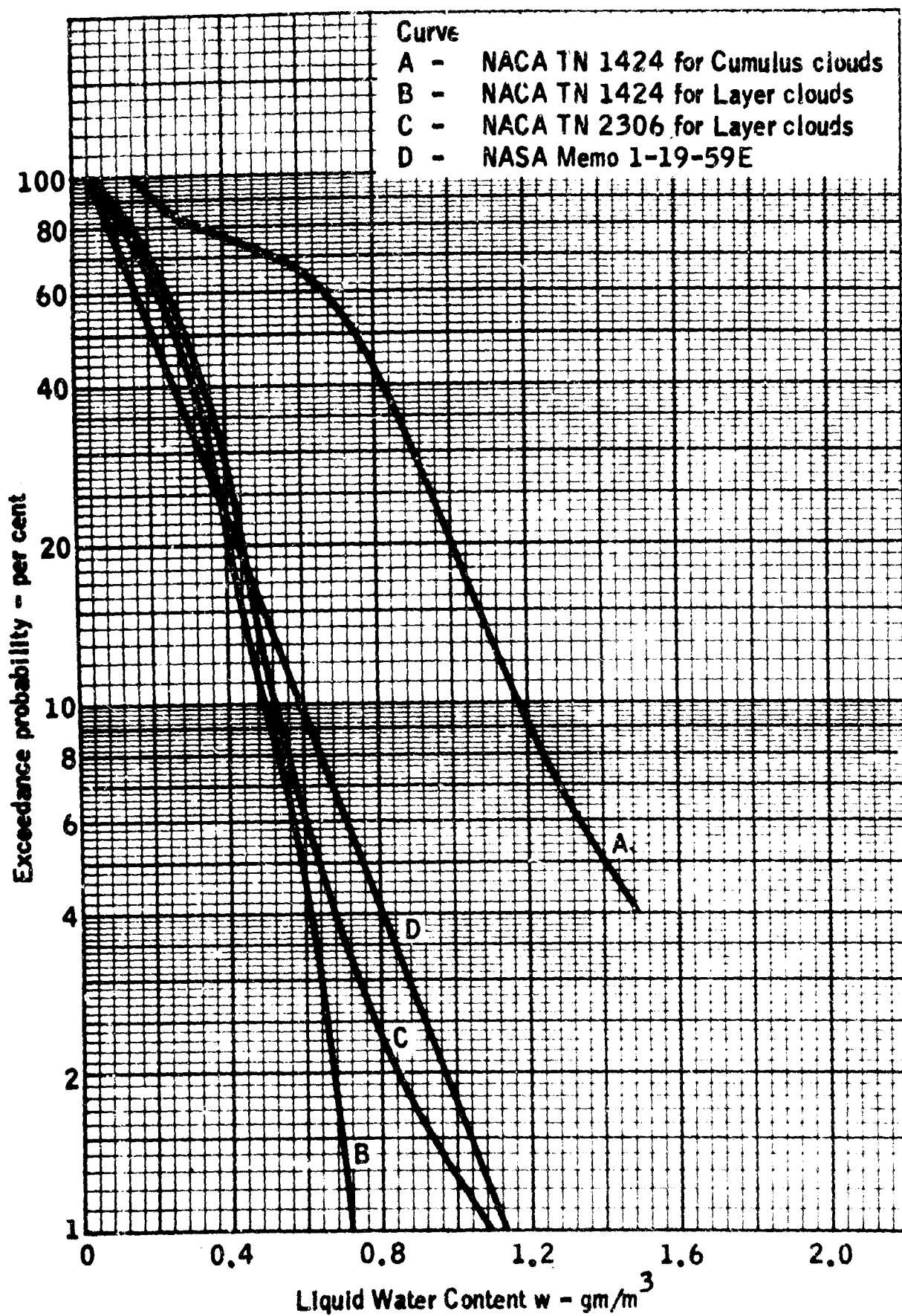
Figure 1-7. Exceedance Probability for LWC (From NACA TN 1424 nd 2306, and NASA 1-19-59E; Ref. 1-5, 1-9 and 1-15).
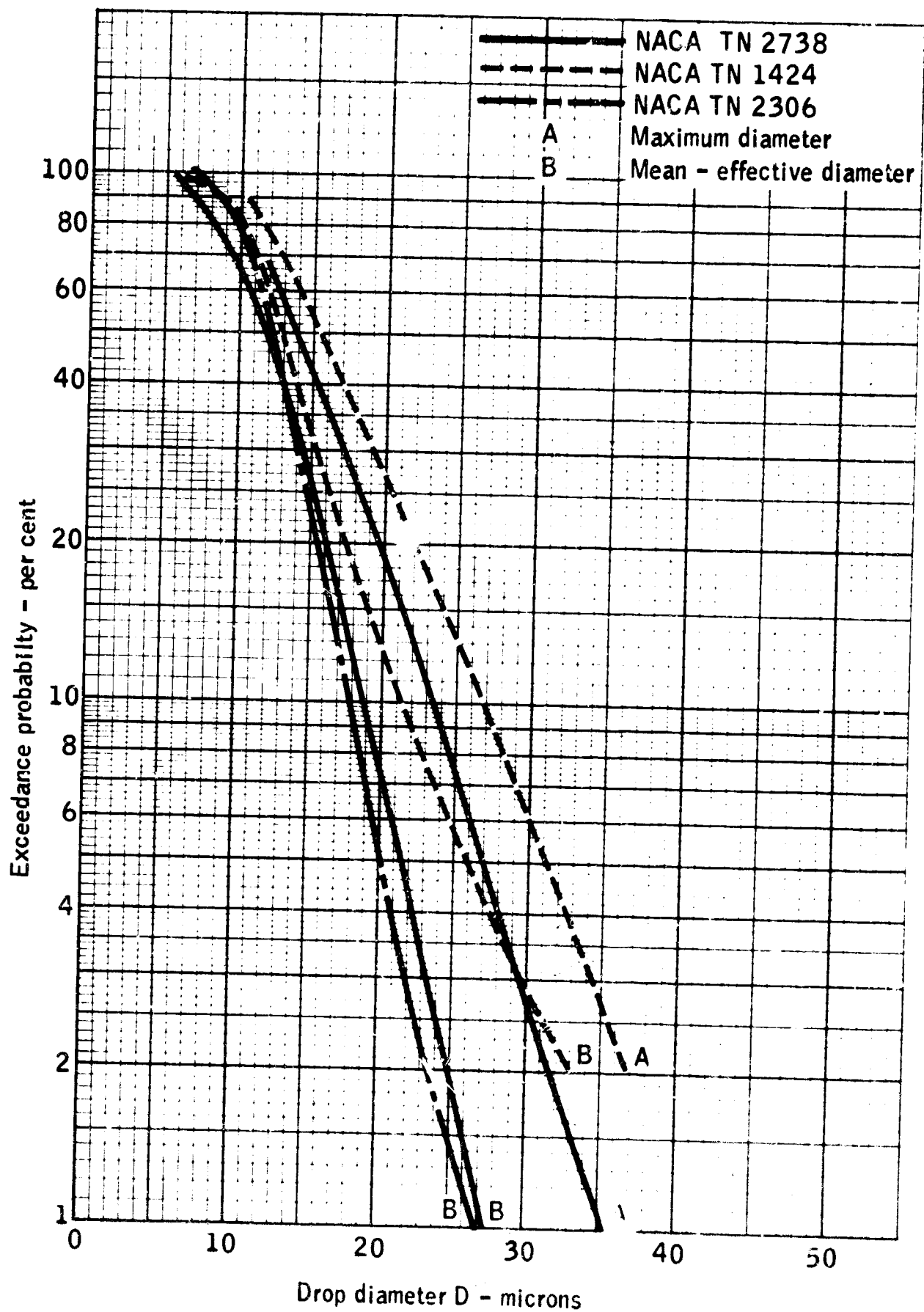
Figure 1-8. Exceedance Probability for Drop Diameter (From NACA TN 1424, 2306 and 2738; Ref. 1-5, 1-9 and 1-10).
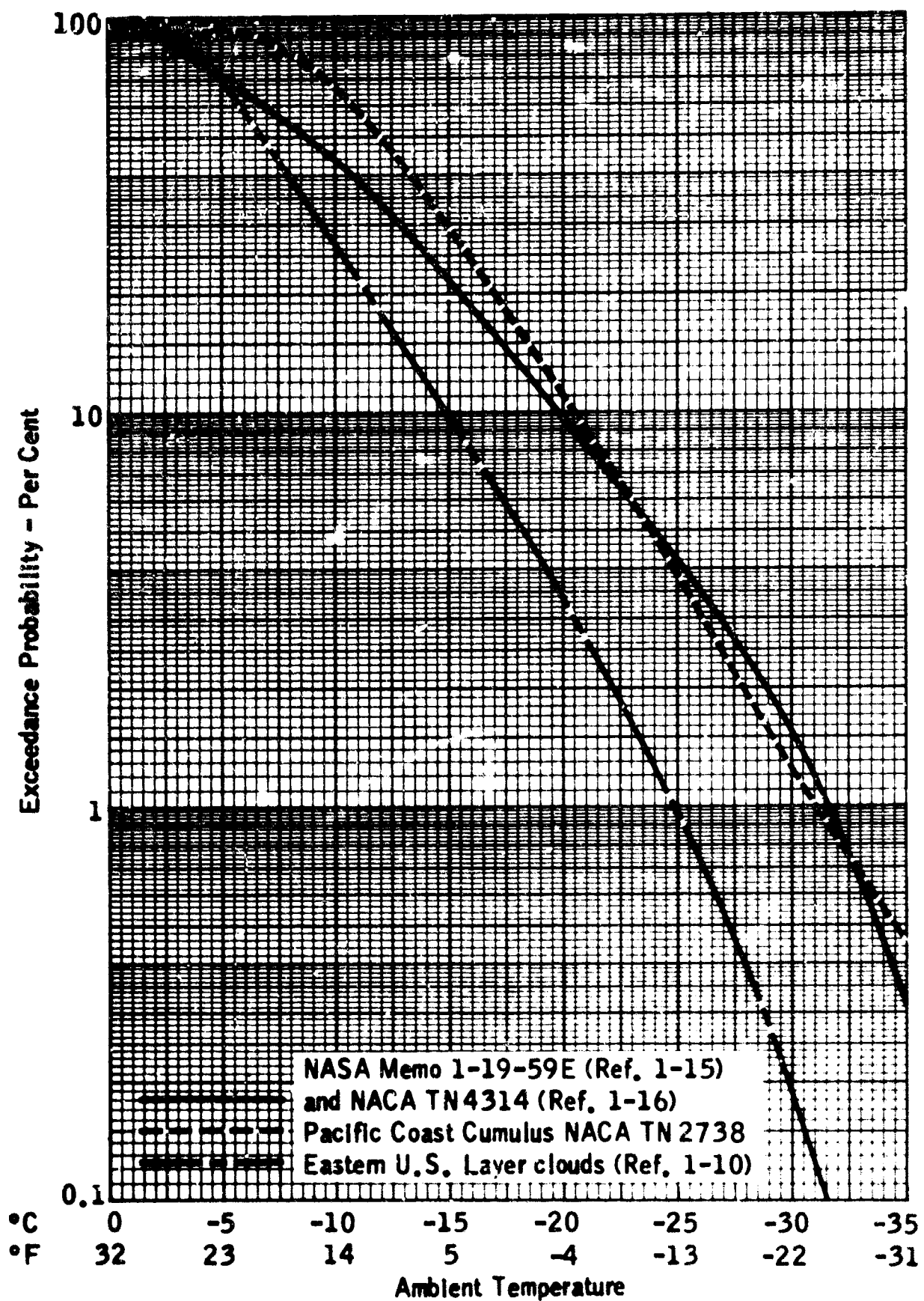
Figure 1-9.   Probability of Cloud Icing Temperature
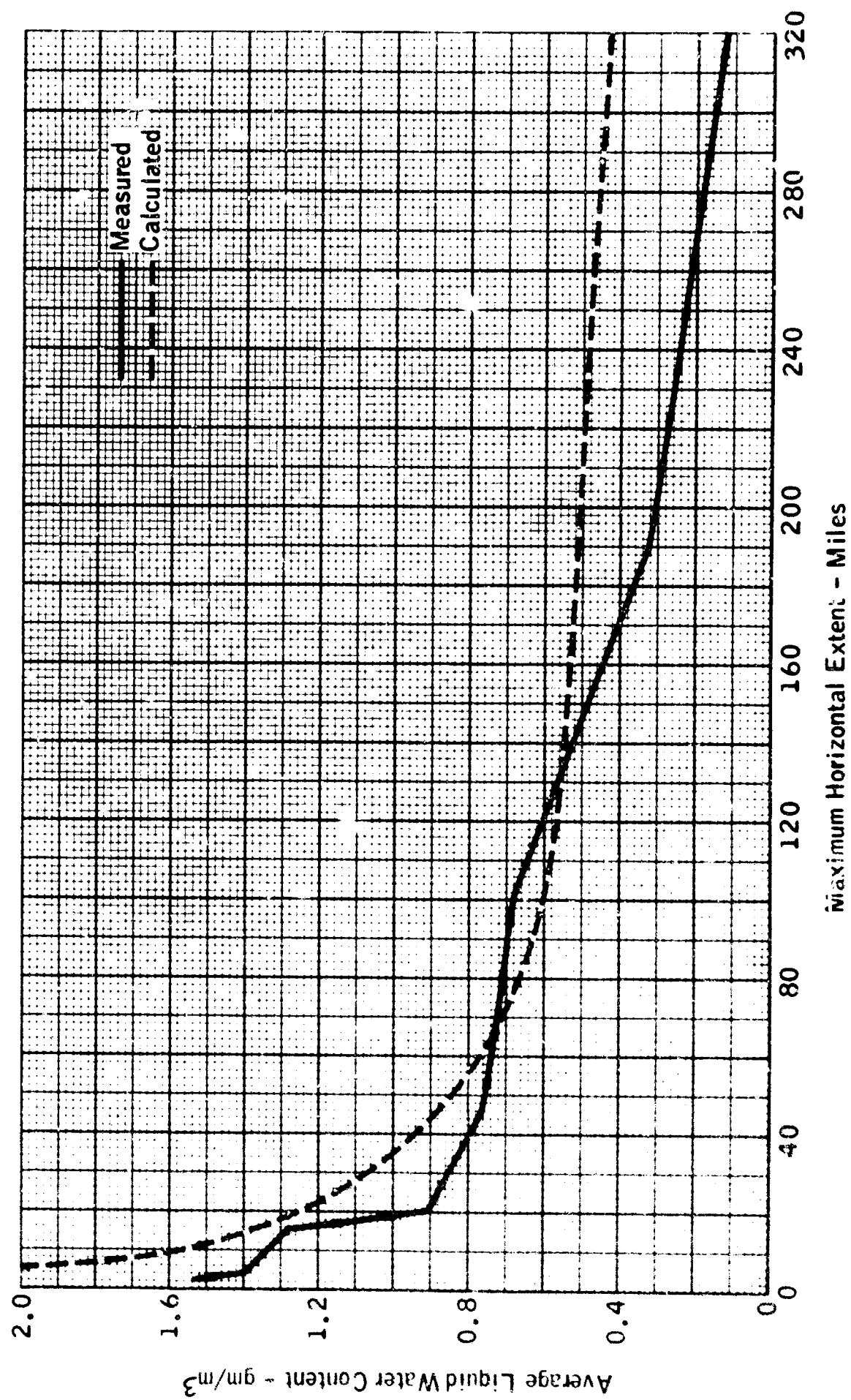
LWC Versus Horizontal Extent (From NACA TN 2569, Ref. 1-8)

Figure 1-10
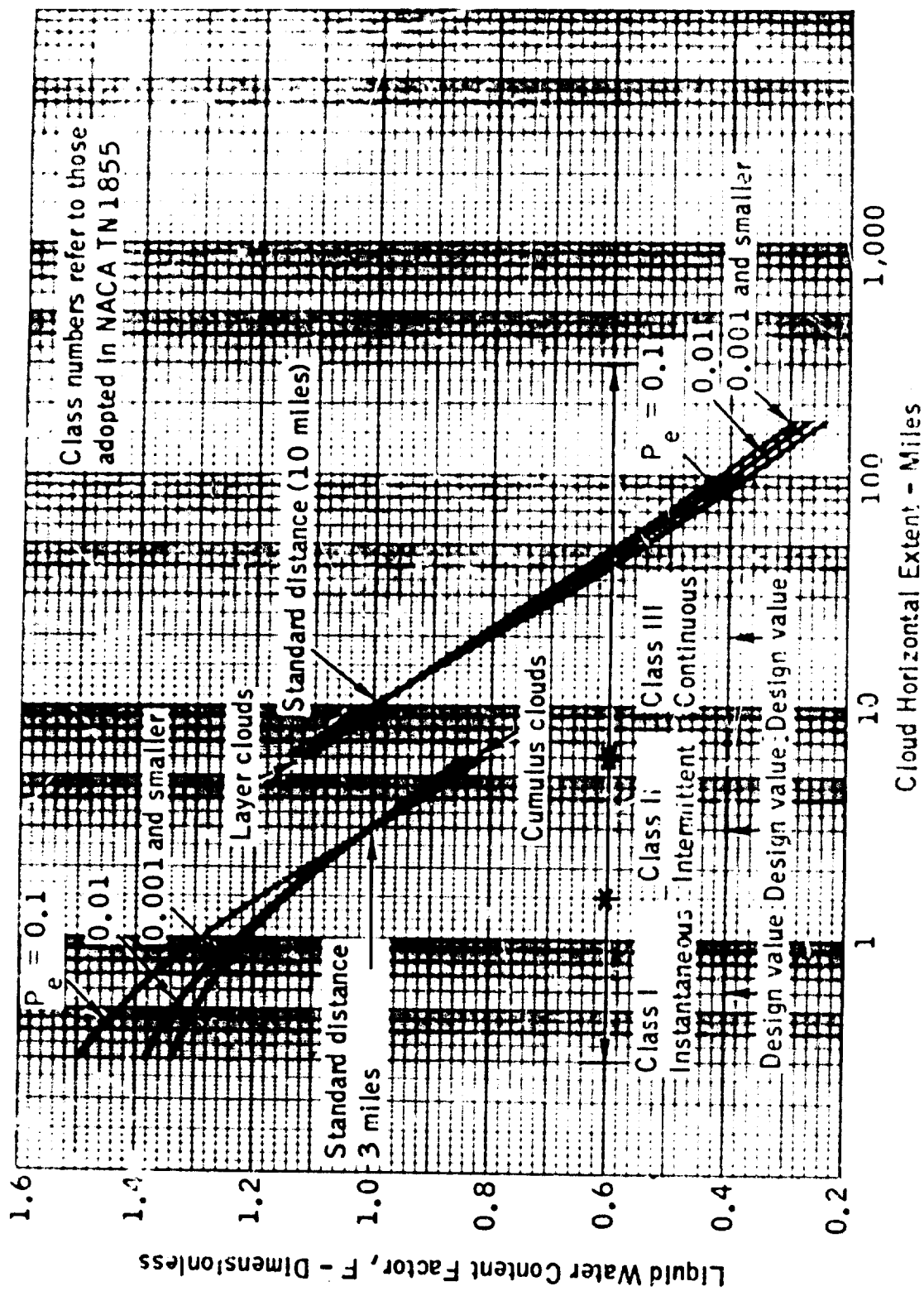
Variation of LWC Factor, F, With Cloud Horizontal Extent for Various Exceedance Probabilities (From NACA TN 2738, Ref. 1-10).

Figure 1-11
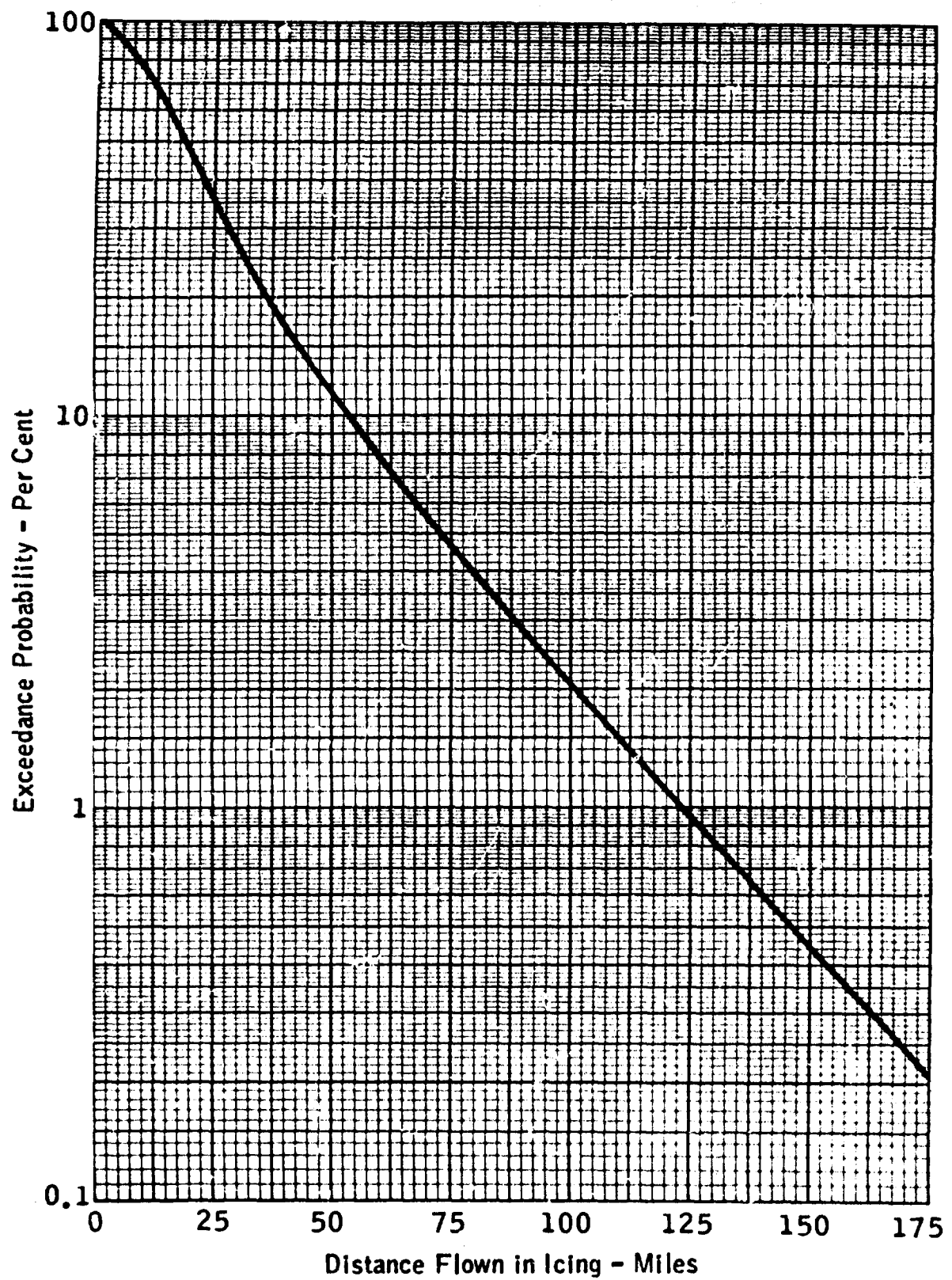
Figure 1-12. Probability Curve of Distance Flown in Icing (From NASA Memo 1-19-59E, Ref. 1-15).

Ambient temperature – Deg. F

32
26
20
14
8
2
-4
-10
-16
-22
-28
-34
-40

1
7 2   1
1 32 30 10 3 17
   21 32 7 8 5 2
   7 30 9 8 10 4 2
   8 2 2 2 10 4 1   Envelope of Icing conditions
   7 2 7 9 15 4
   4 3 10 6 4 5   1
   1   2 1 6
      1 5   1 5   2 4
      2   1   1 3 2
                  1 1 3 4 1   Average Icing temperature
                     3 1 2
      3
      1   2 1 3 1
                  2 1 2
                  3
                                NACA standard atmosphere
                     1

0   4   8   12   16   20   24   28 x 10³

Pressure altitude – Ft.
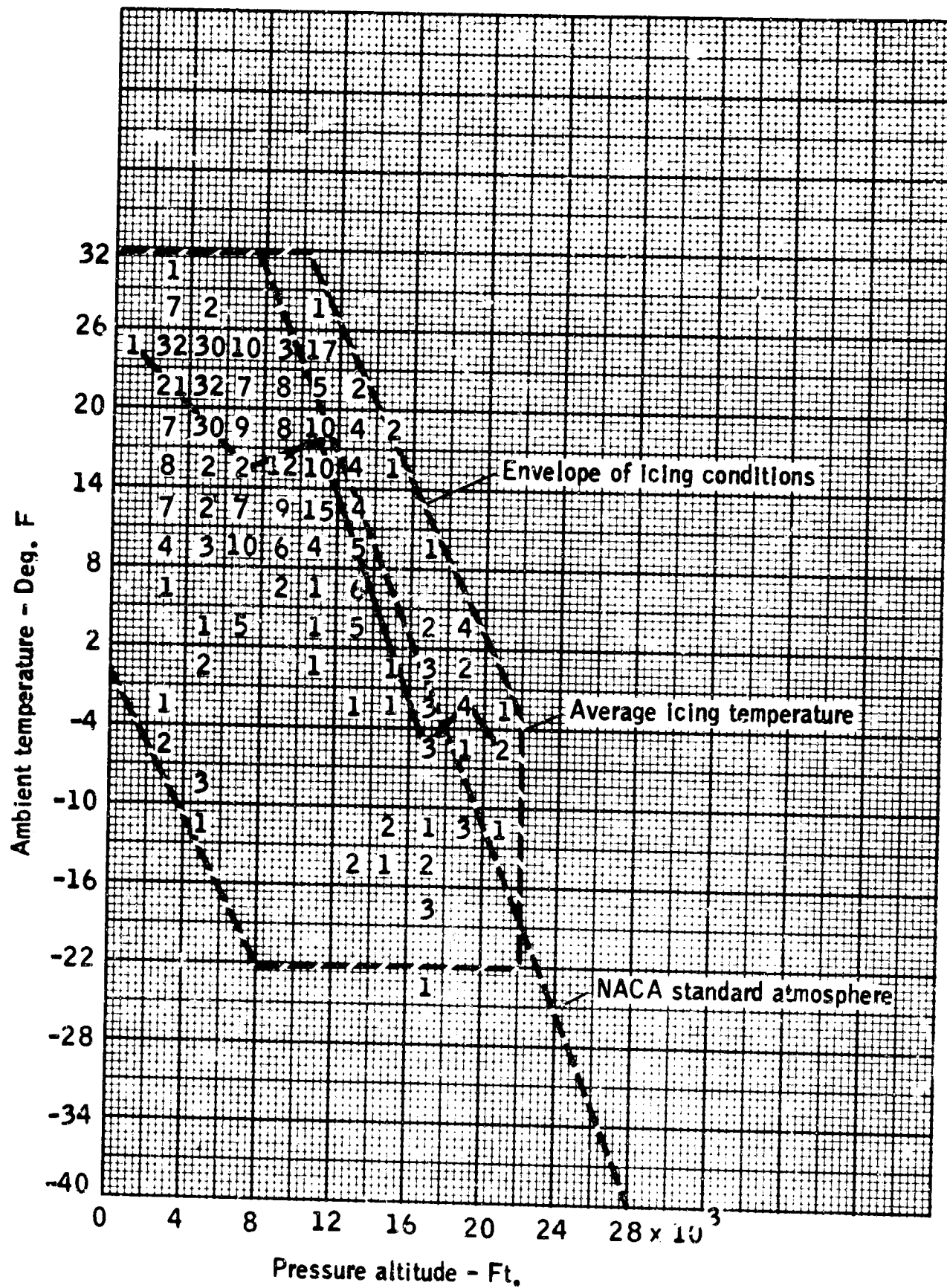
Figure 1-13a.   Frequency Distribution of Icing Encounters in Stratiform
Clouds for Increments of Temperature and Altitude (From
NACA TN 2569, Ref. 1-8).

1-52
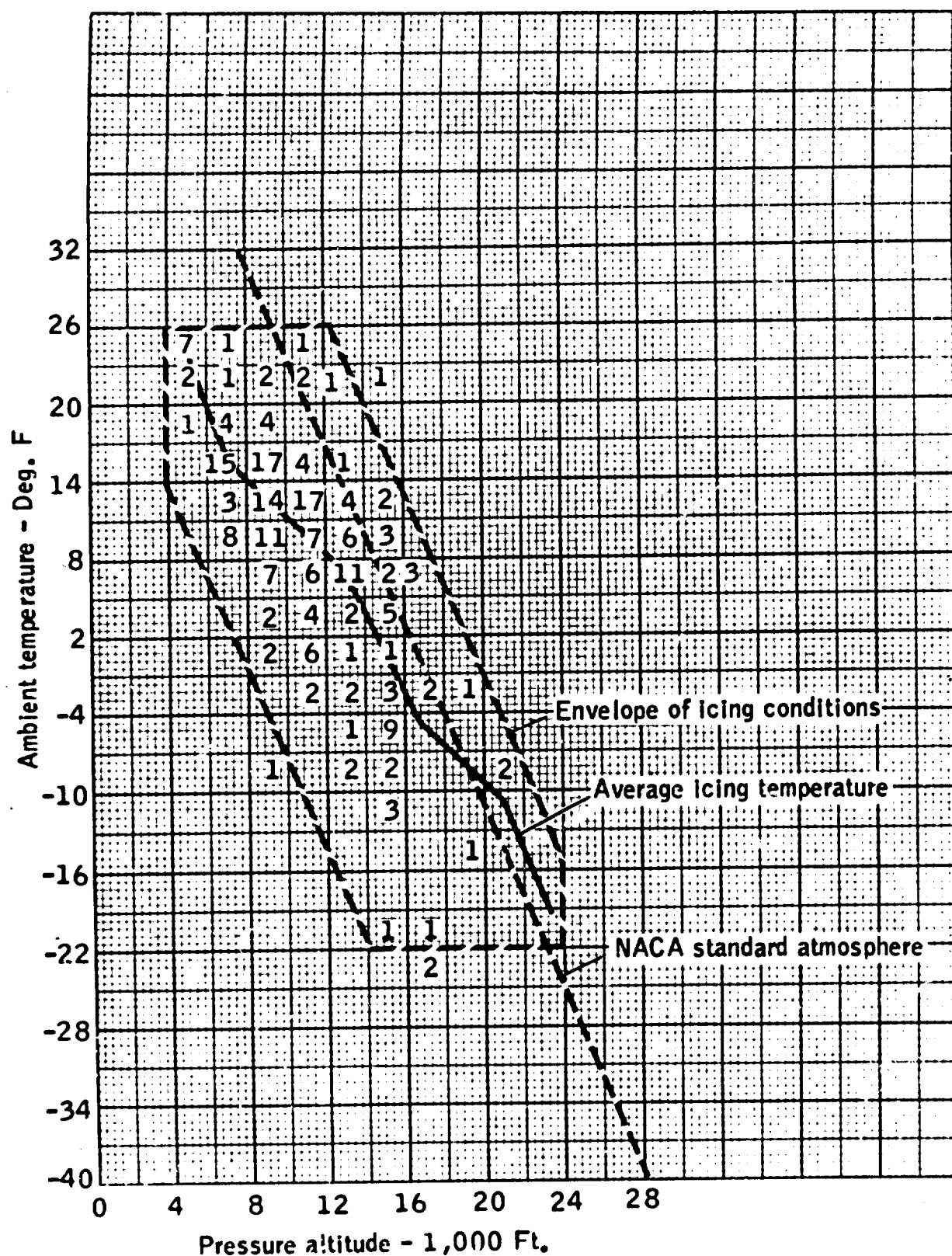
Figure 1-13b. Frequency Distribution of Icing Encounters in Cumuliform Clouds for Increments of Temperature and Altitude (From NACA TN 2569, Ref. 1-8).

1-53
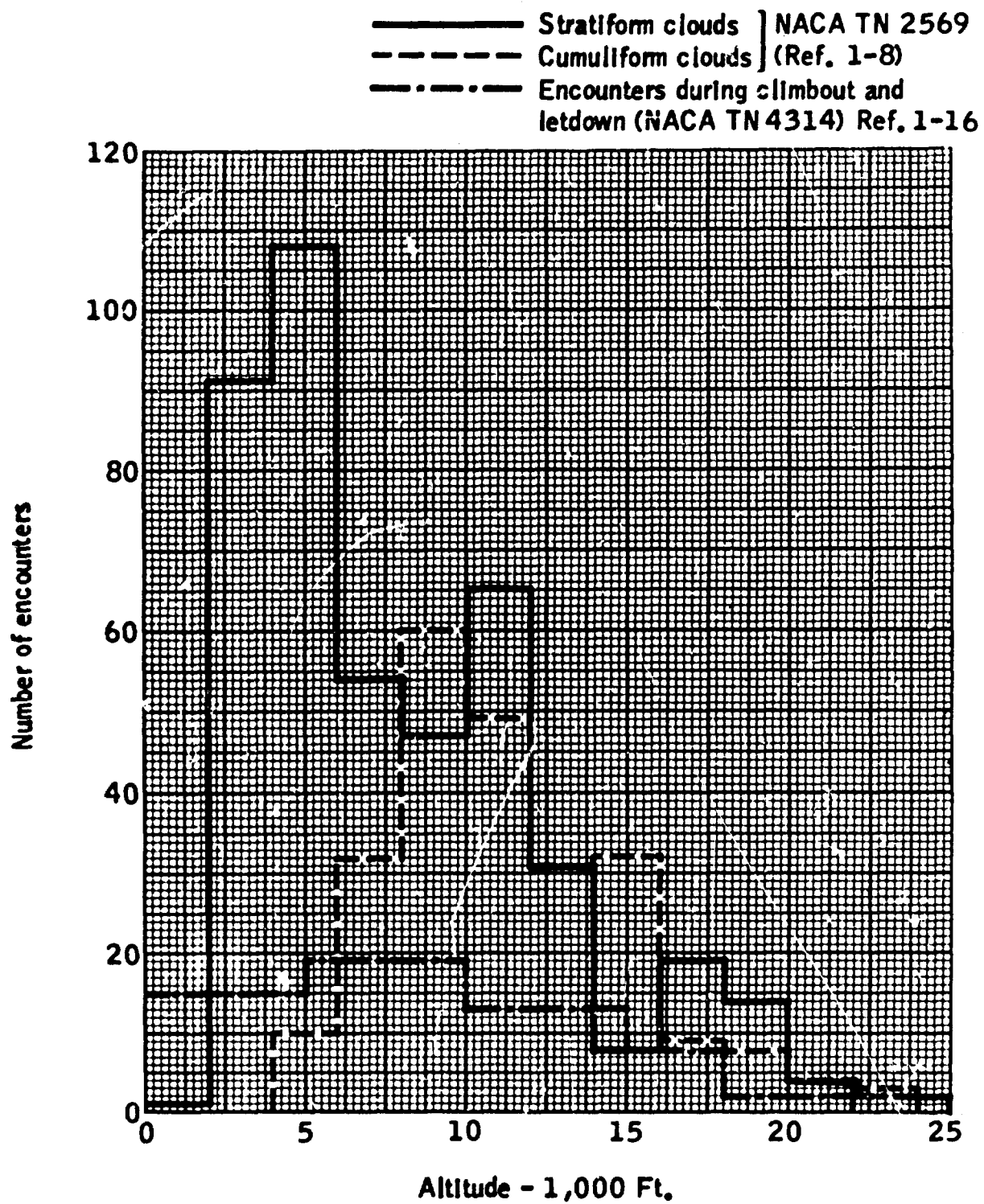
Figure 1-14.   Icing Encounter Frequency Versus Altitude
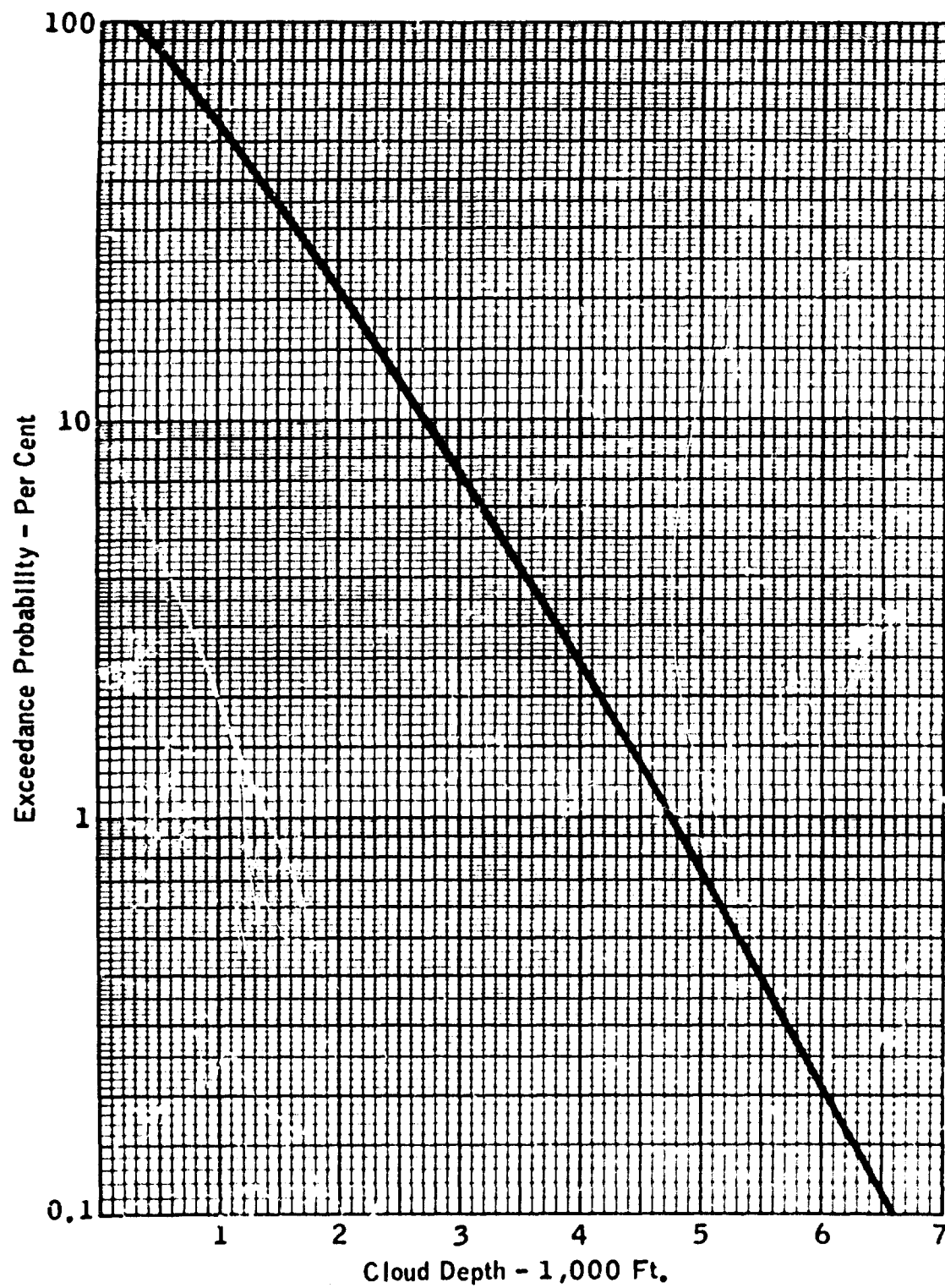
Figure 1-15.   Cloud Depth Probability for Layer Type Clouds (From
NASA Memo 1-19-59E , Ref. 1-15).
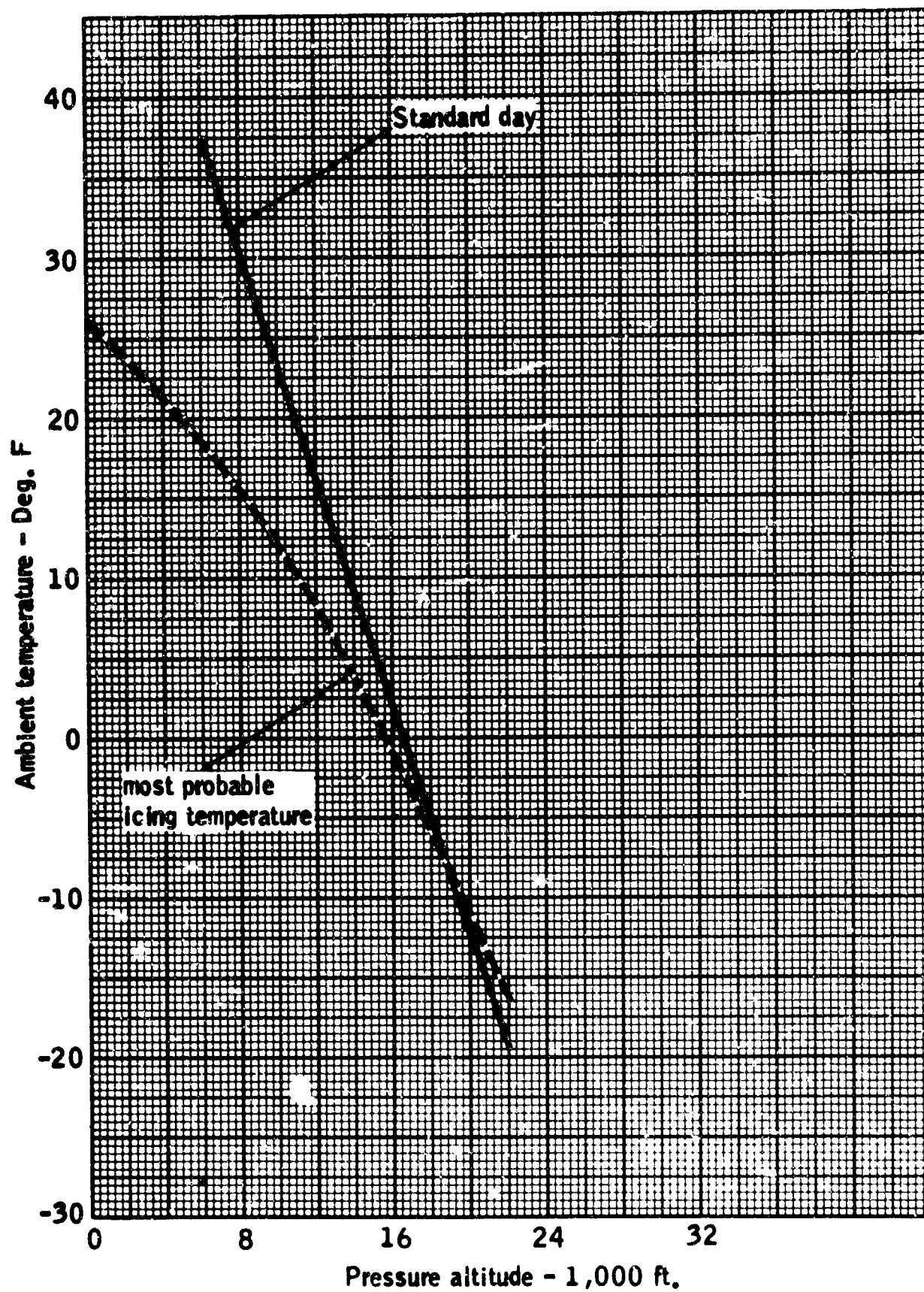
Figure 1-16.   Most Probable Icing Temperature Versus Altitude
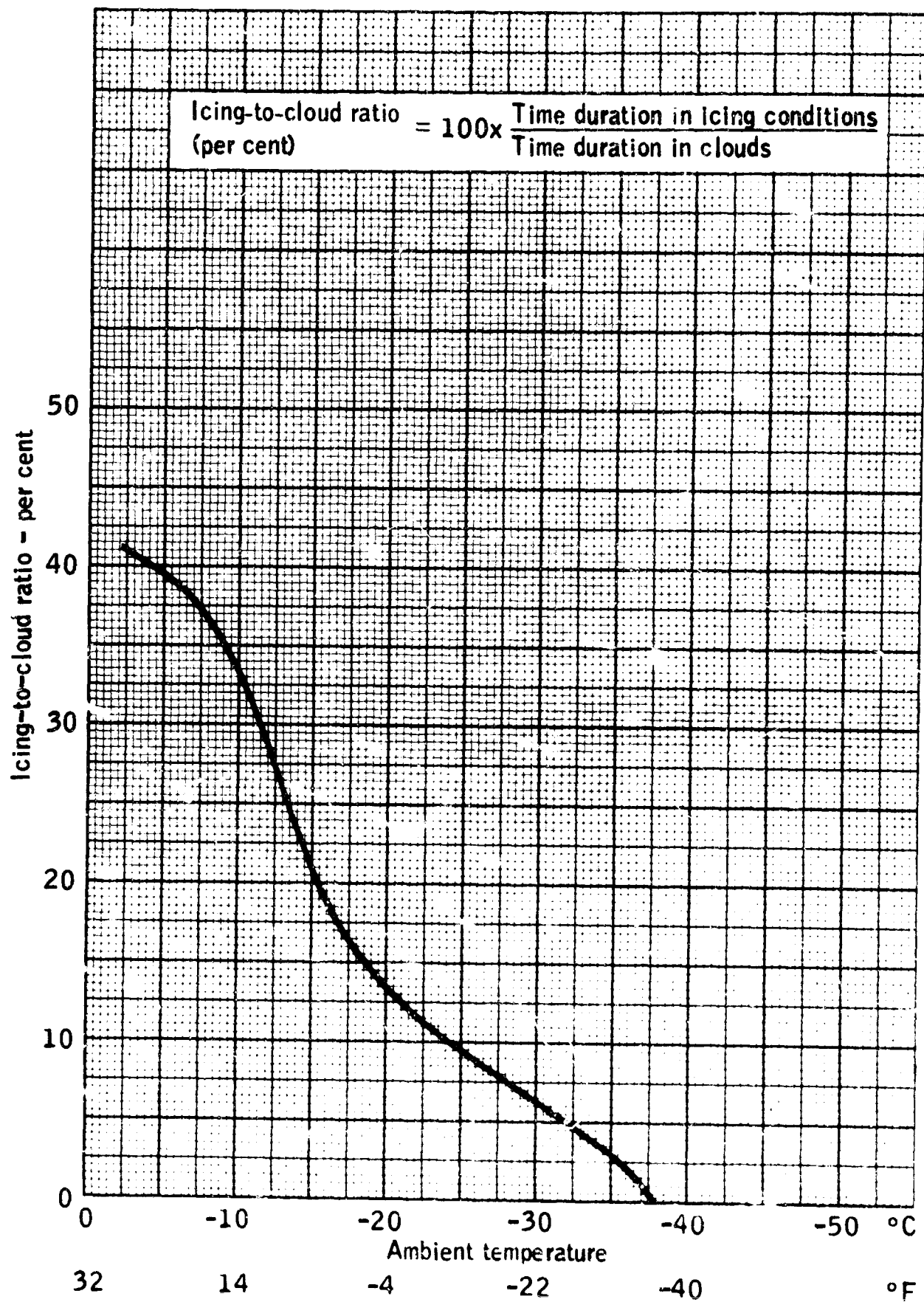   (From NACA TN 2569, Ref. 1-8).

1-56

Figure 1-17. Average Relation of Icing-To-Cloud Ratio to Ambient Temperature (From NACA TN 3984, Ref. 1-11).
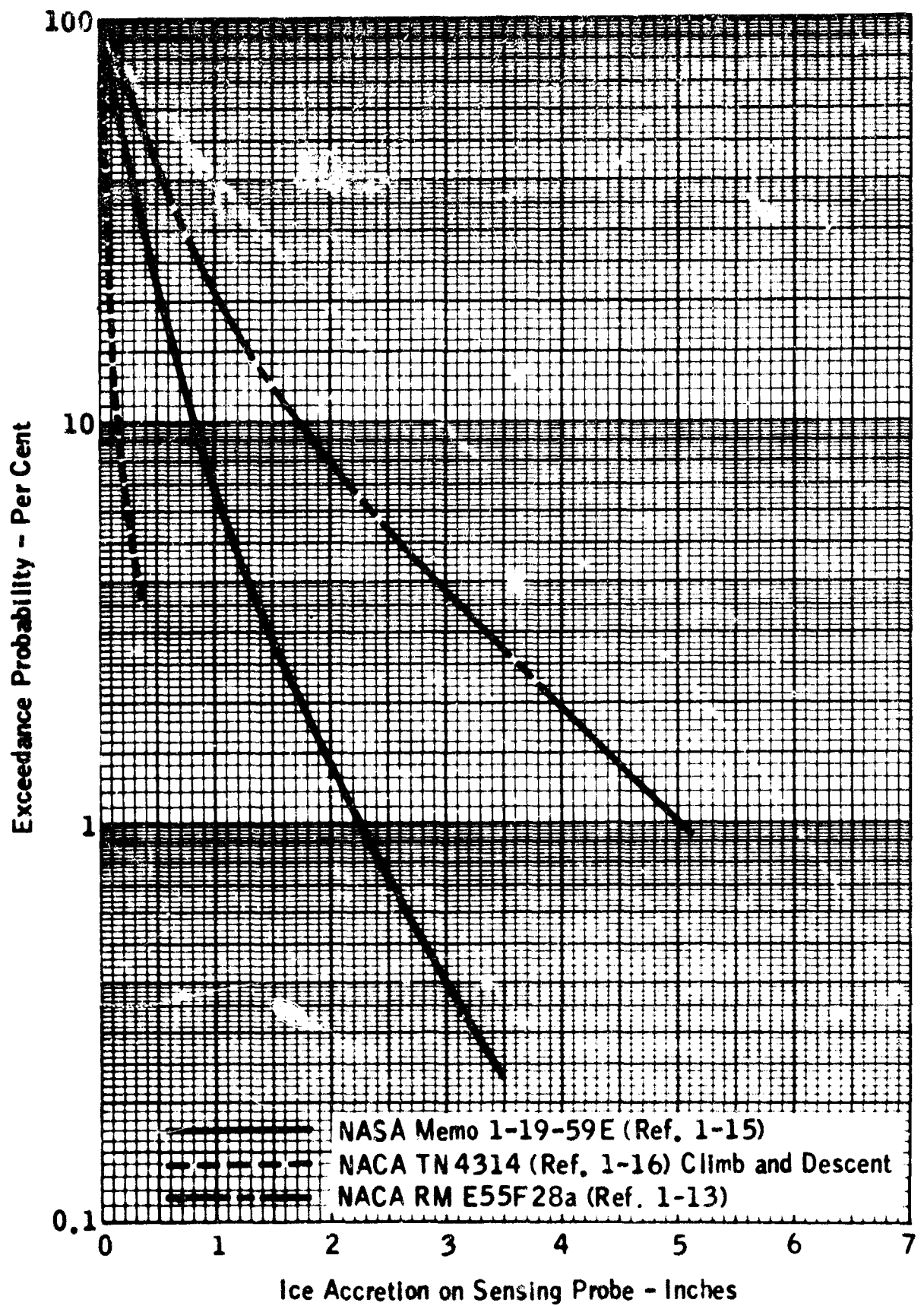
Figure 1-1b.   Ice Accretion Probabilities (Based Upon 1/8-in. Diameter Probe).
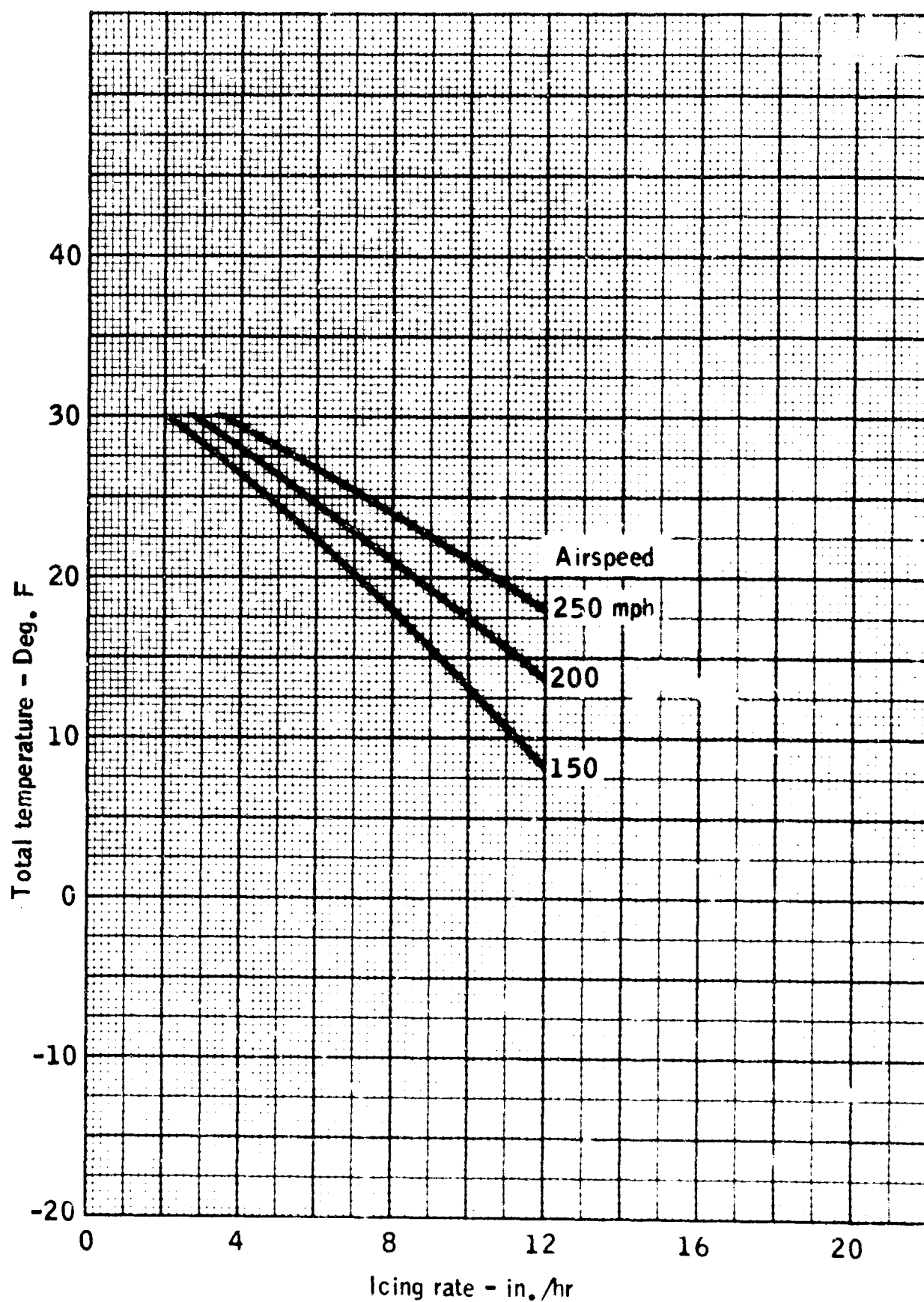
Figure 1-19. Limiting Curves for Onset of Water Runoff (for 1 8-in. Probe) — Based Upon NASA Memo 1-19-59E, Ref. 1-15.
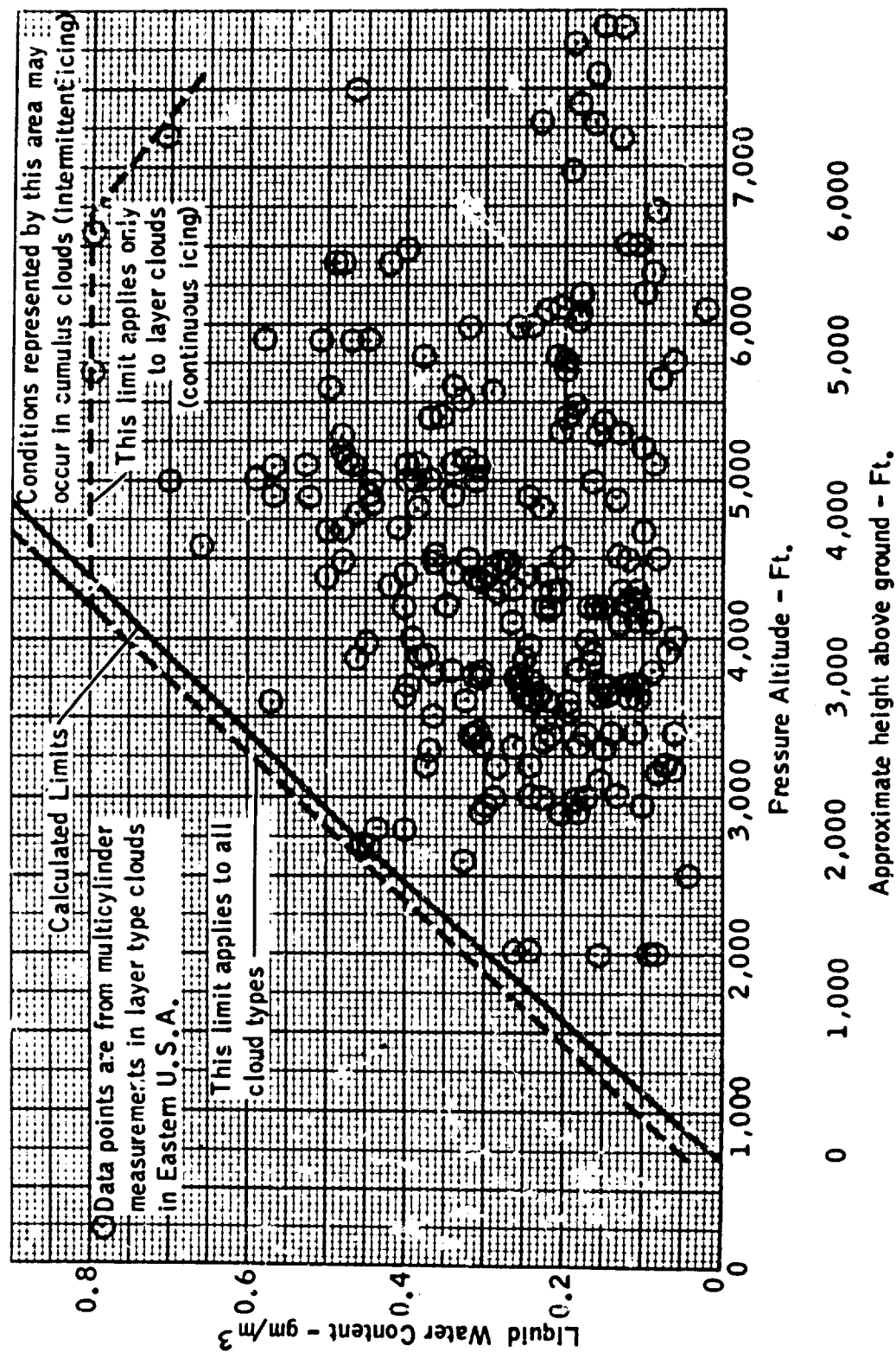
Cloud LWC Limits at Low Altitudes (From Ref. 1-18).
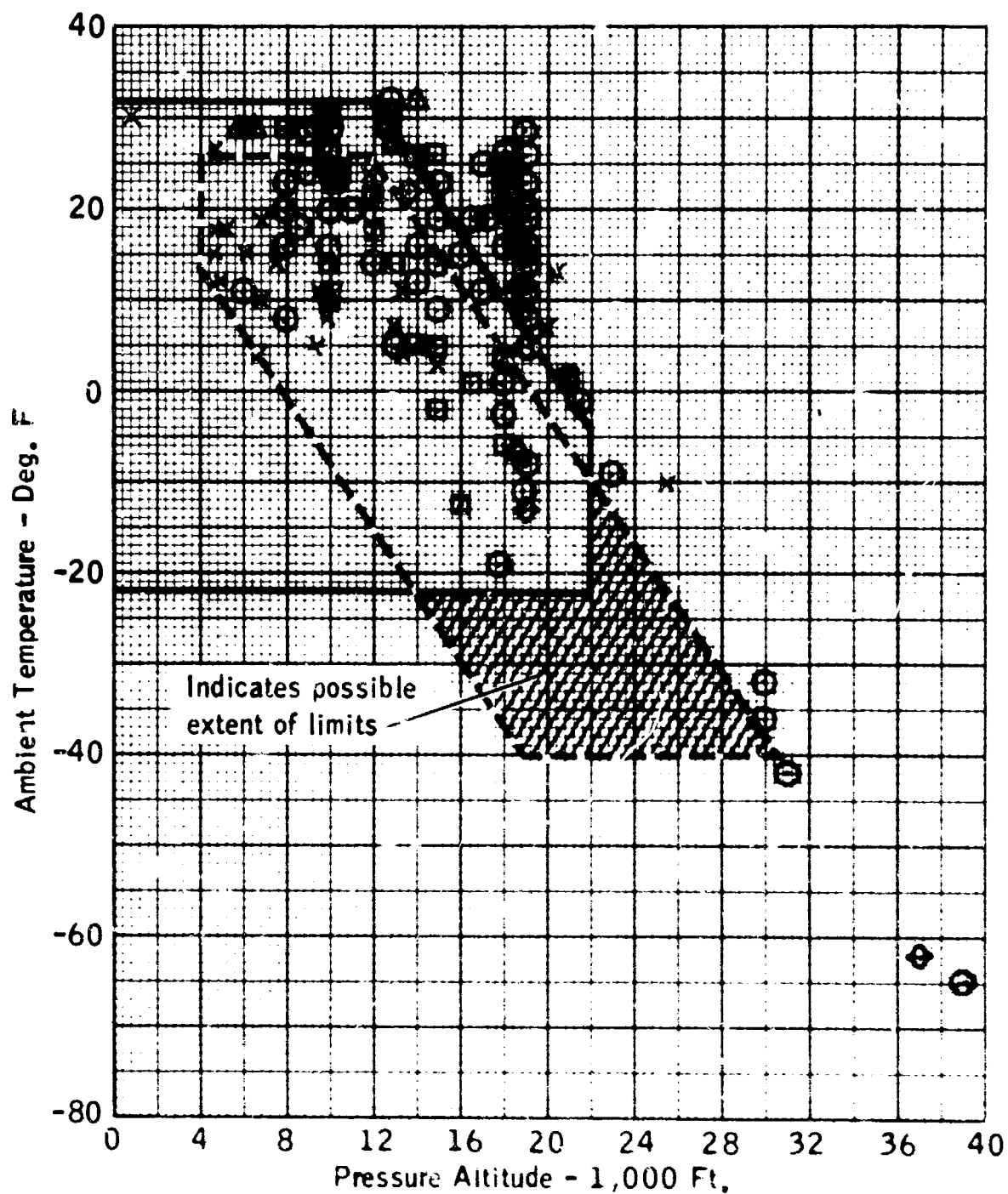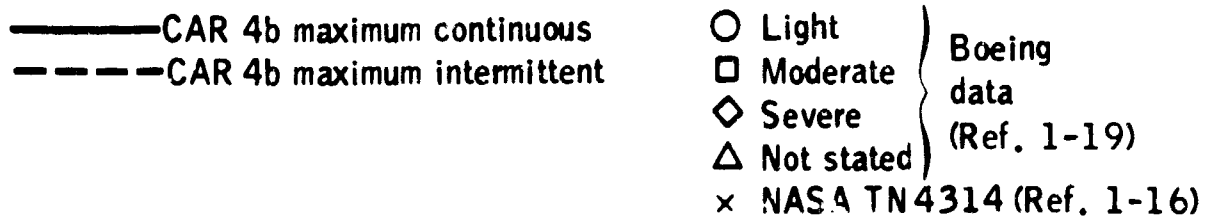
Figure 1-20

Figure 1-21. Comparison of CAR 4b Icing Envelopes With Reported Icing Encounters (From Boeing Co. Data. Ref. 1-19).
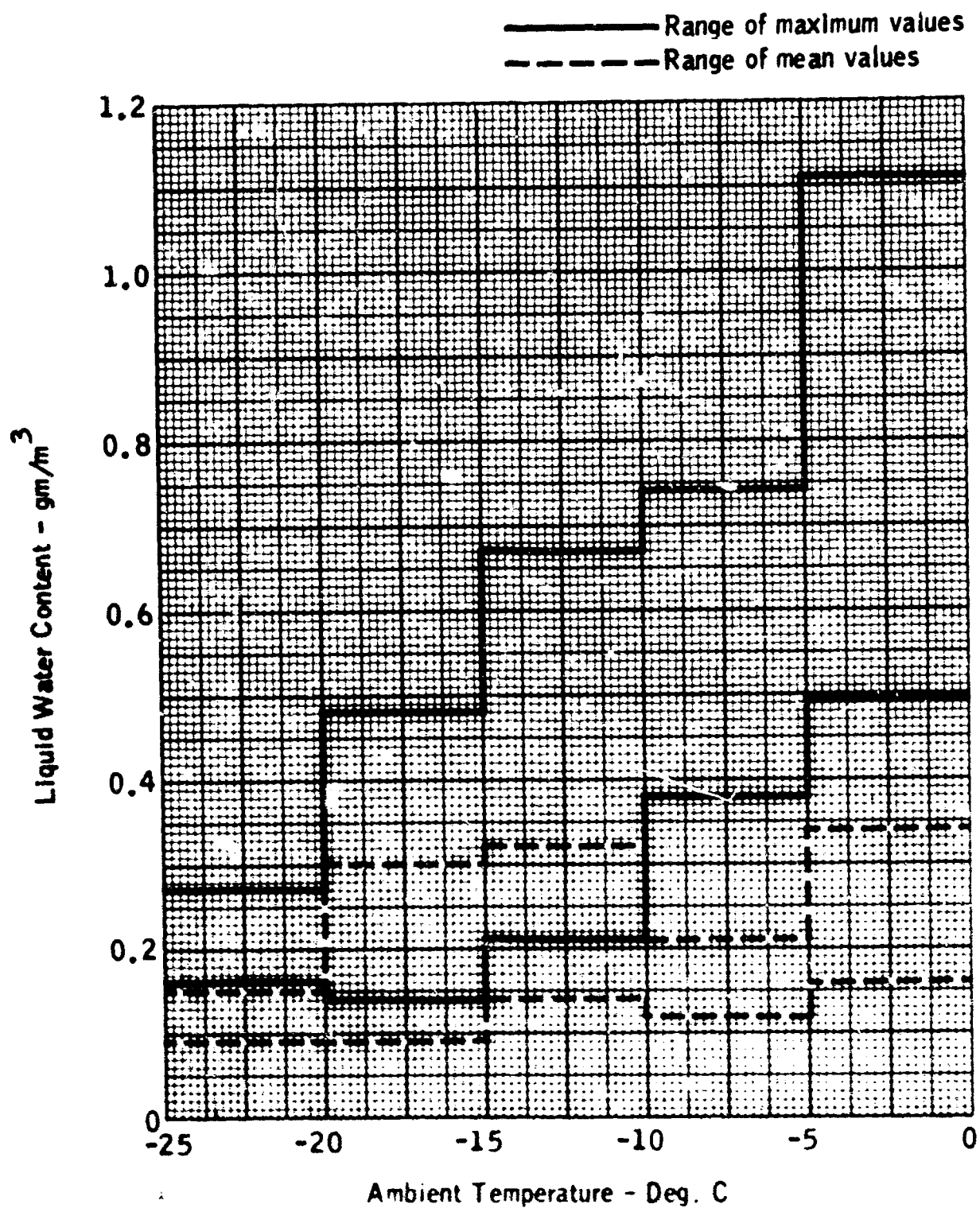
Figure 1-22.   Maximum and Mean LWC Measured in the USSR for Layer
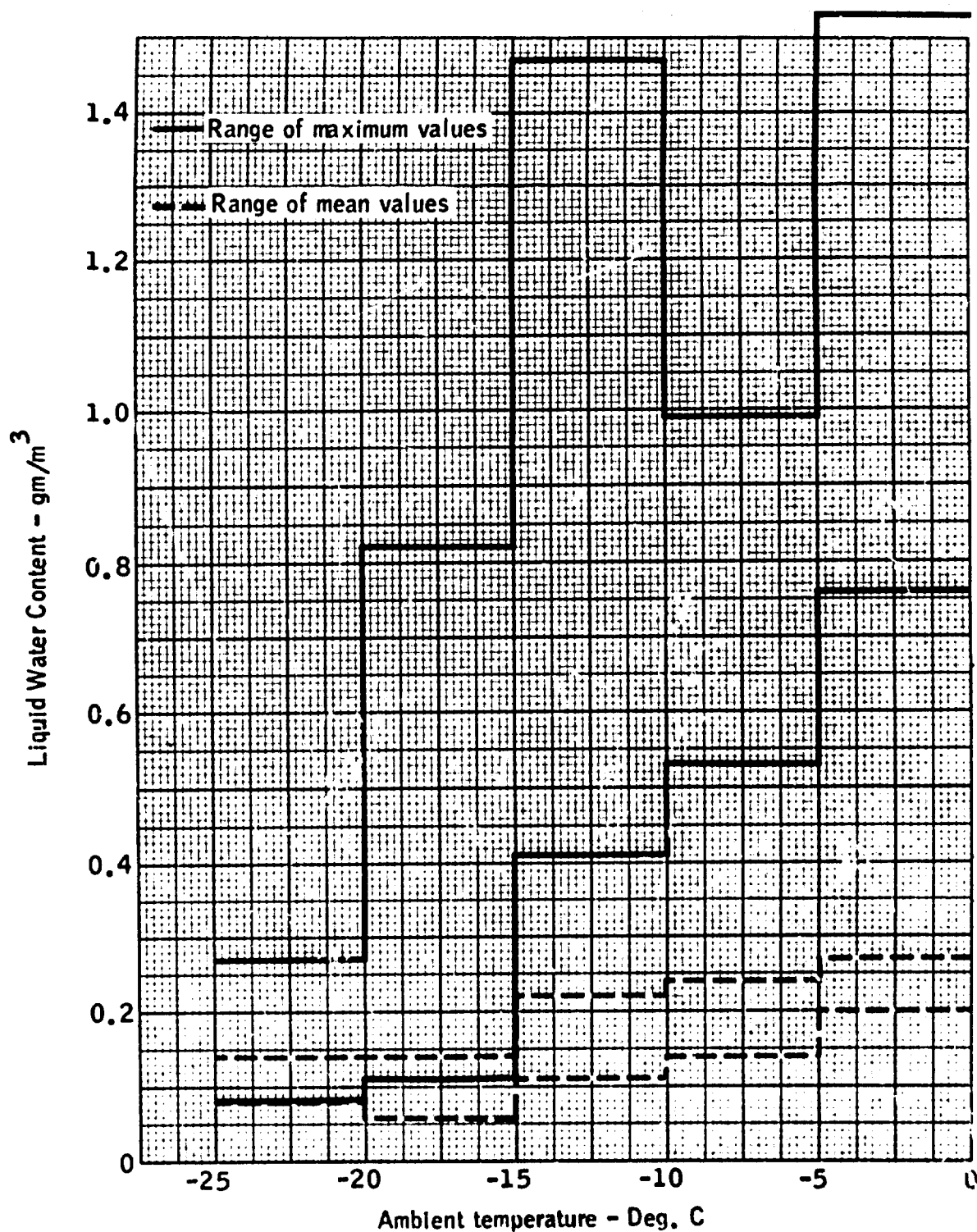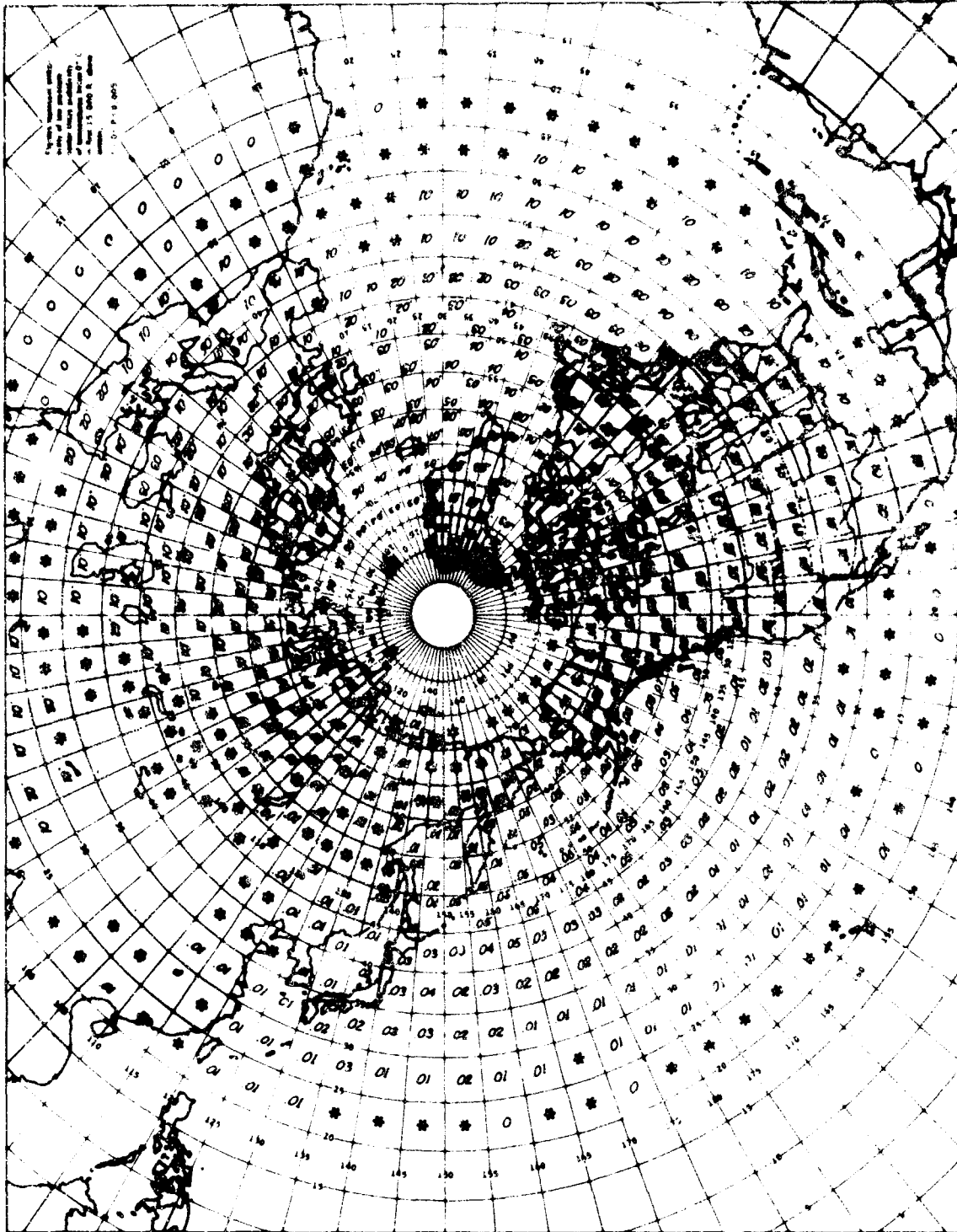Type Clouds (From WMO TN No. 39, Ref. 1-20).

1-62

Figure 1-23.   Maximum and Mean LWC Measured in the USSR for
Cumulus Type Clouds (From WMO TN No. 39, Ref. 1-20).

Low Altitude Icing Probabilities for the Northern Hemisphere — January
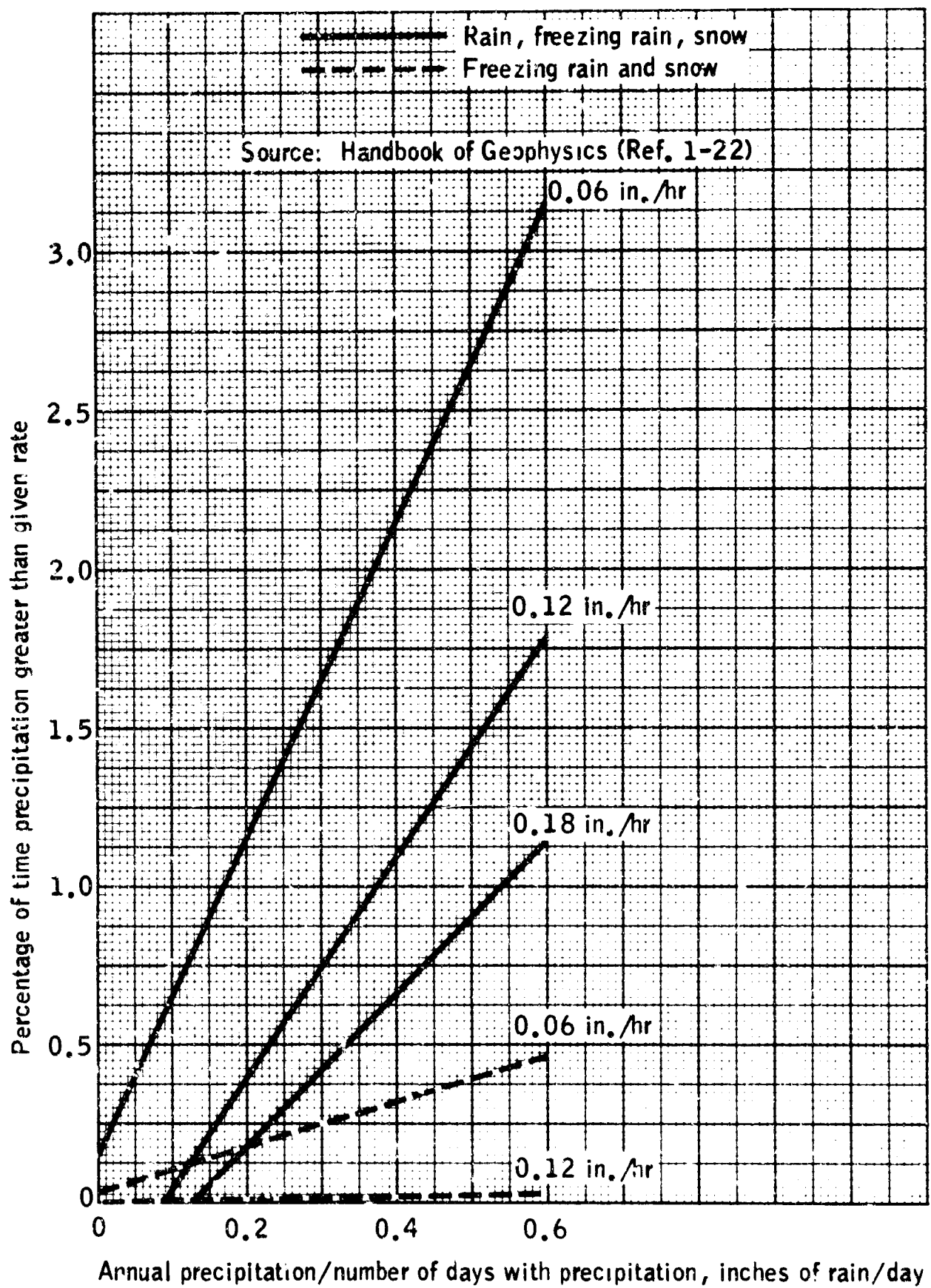(From WADC TN-55-225. Ref. 1-21).

Figure 1-24

Figure 1-25. Frequency Rates for Rain, Freezing Rain and Snow
(From Ref. 1-22).

1-65

Pressure altitude range S.L. to 22,000 Ft.
Maximum vertical extent 6,500 ft.
Horizontal extent, standard distance of 20 mi.

Source: NACA TN 1855
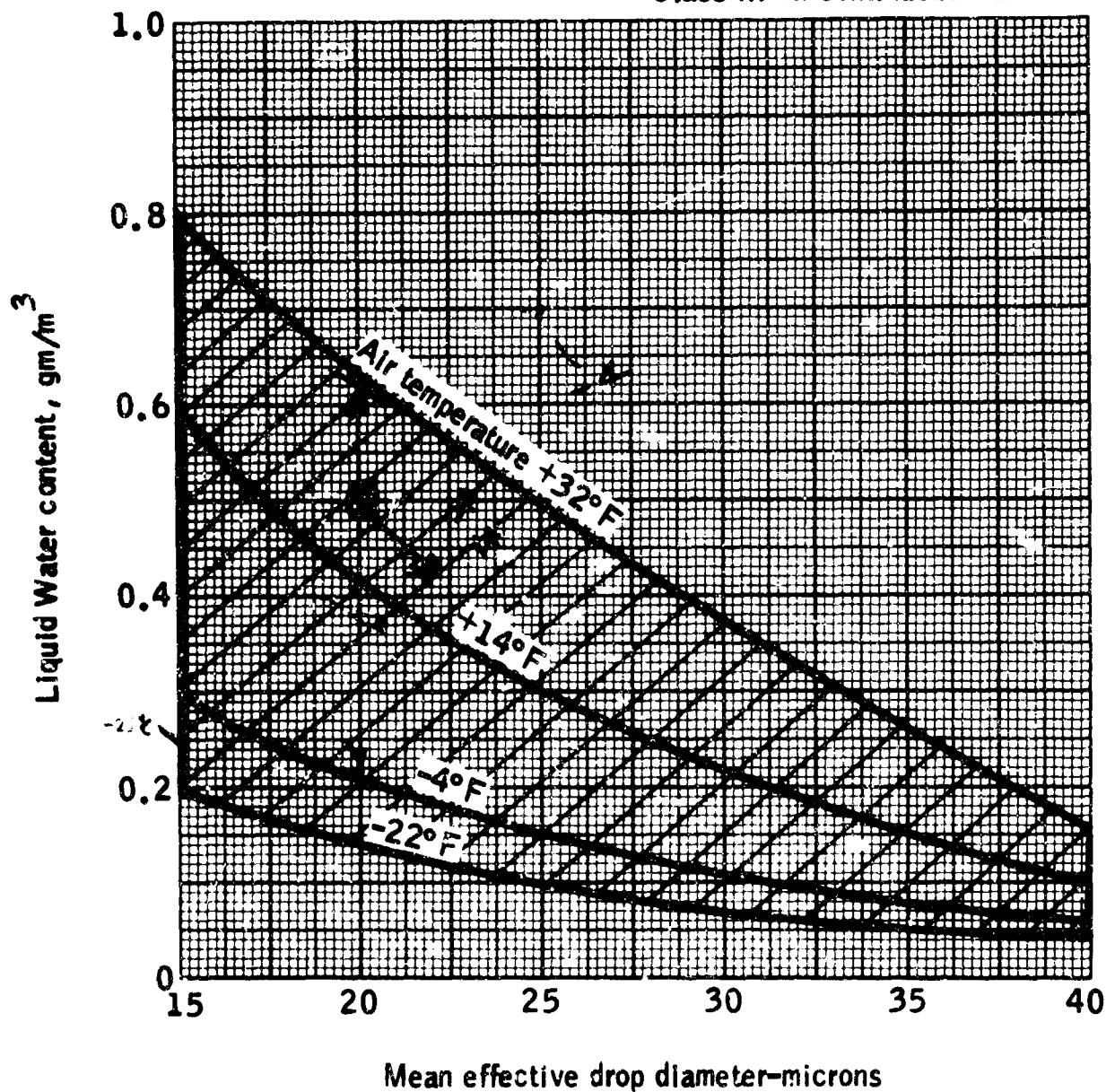Class III-M continuous maximum

Figure 1-26. Continuous Maximum Atmospheric Icing Conditions —
Stratiform Clouds. LWC Versus Mean Effective Drop
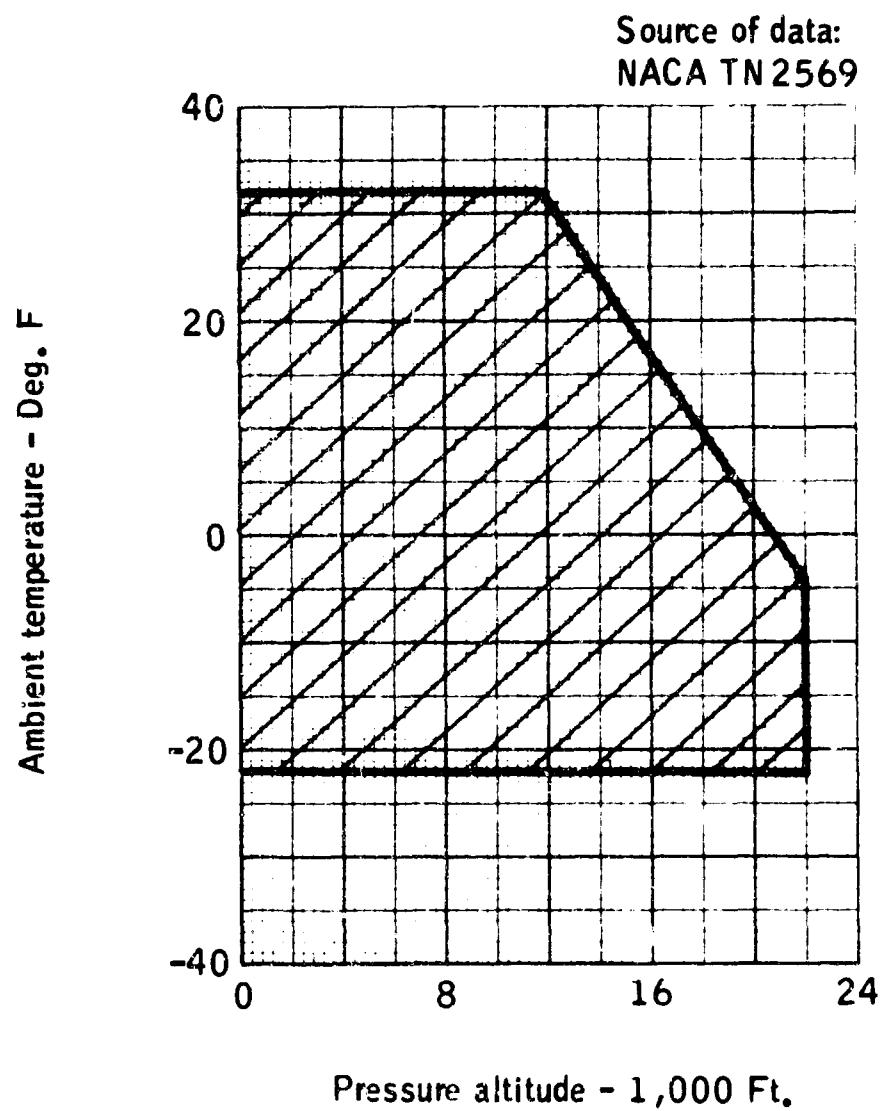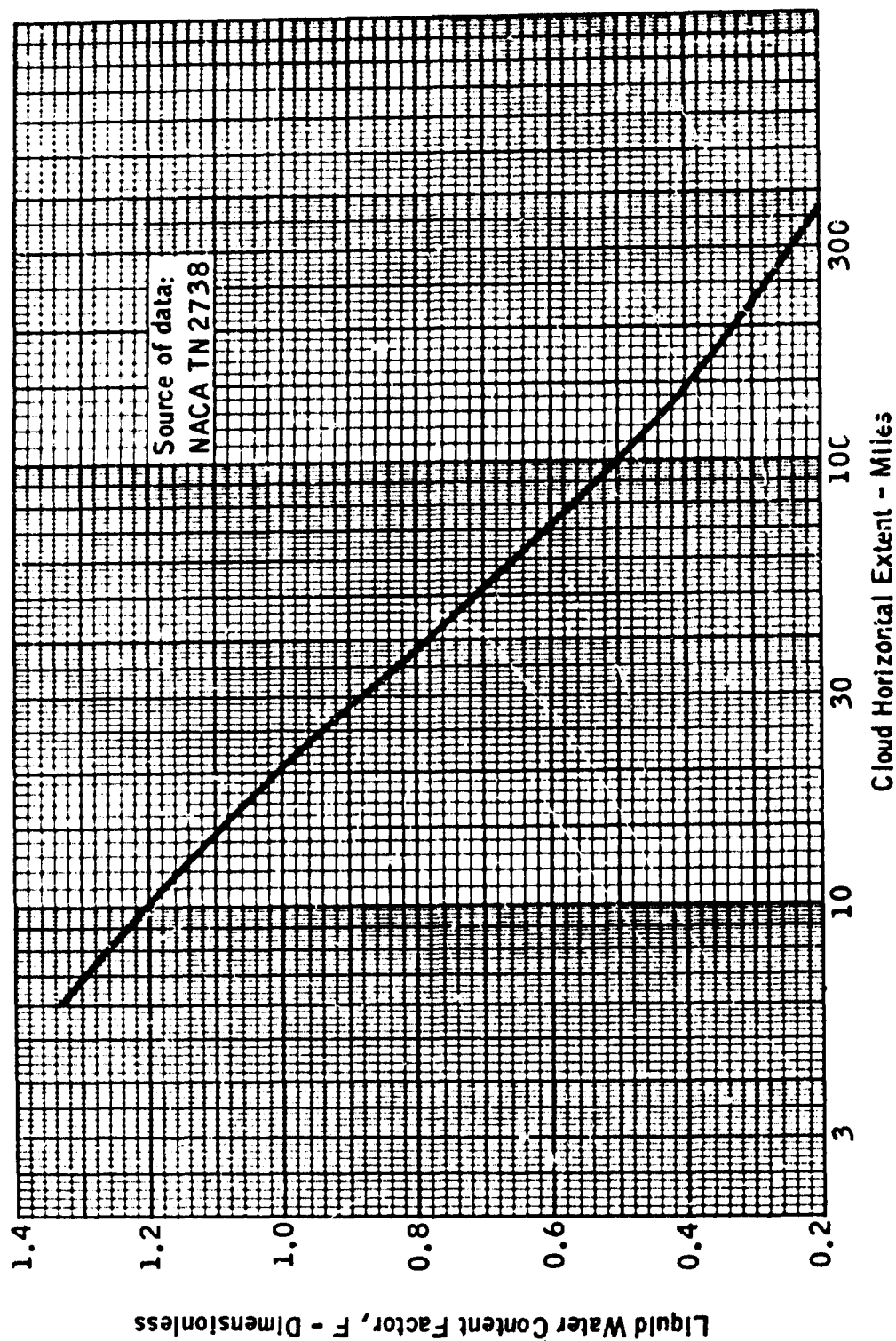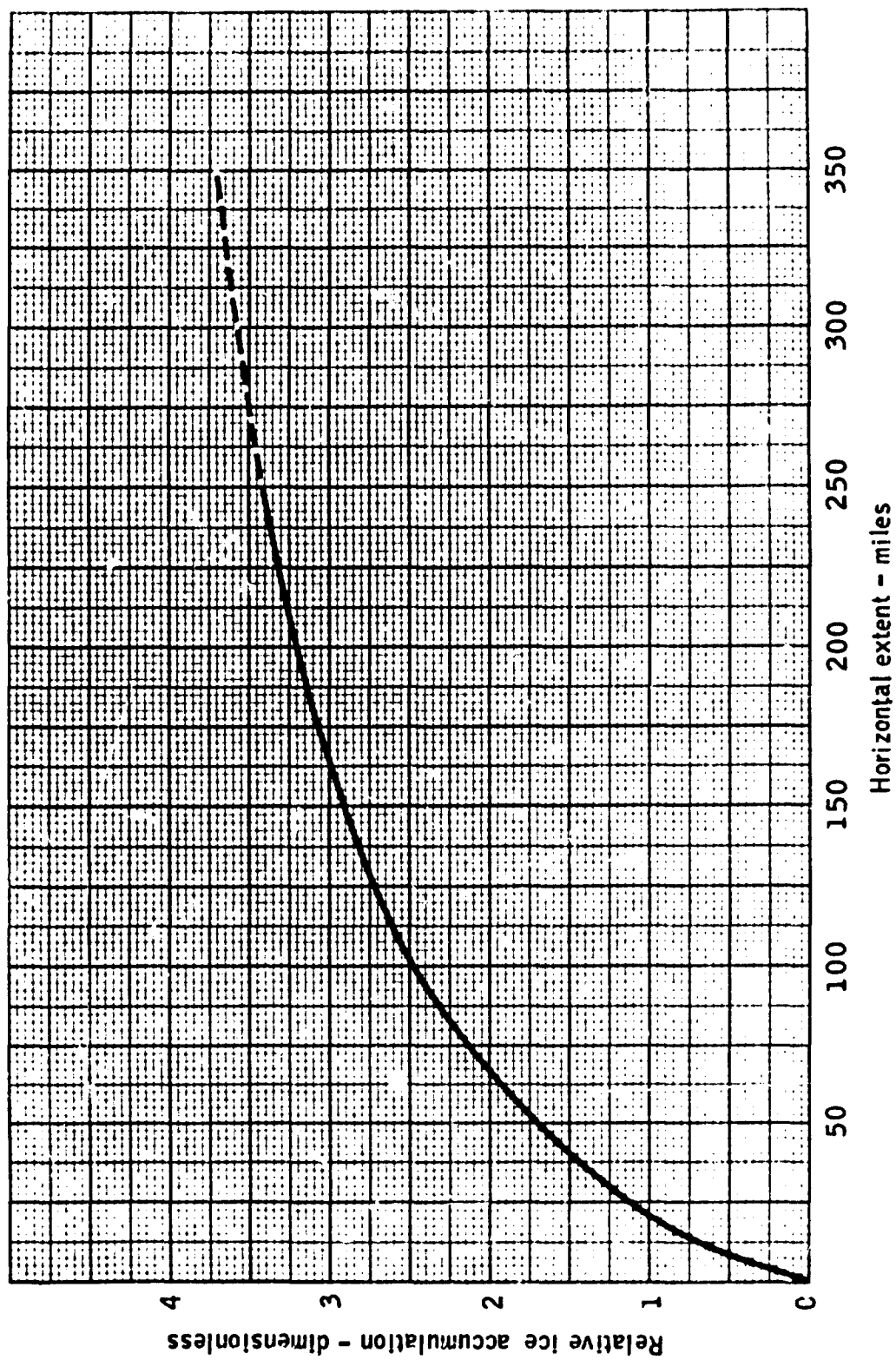Diameter (From CAR 4b).

Source of data:
NACA TN 2569

Figure 1-27. Continuous Maximum Atmospheric Icing Condition —
Stratiform Clouds. Ambient Temperature Versus
Pressure Altitude (From CAR 4b).

1-67

Continuous Maximum Atmospheric Icing Conditions — Stratiform Clouds. LWC Factor Versus Cloud Horizontal Distance (From CAR 4b).

Figure 1-28

Plot of Relative Amount of Ice Accumulation for Various Flight Distances in Continuous Maximum Icing (Based Upon a 20-mile Standard Distance and the Data of Ref. 1-28).

Figure 1-29

Figure 1-30.   Intermittent Maximum Atmospheric Icing Conditions —
Cumuliform Clouds. LWC Versus Mean Effective Drop
Diameter (From CAR 4b).
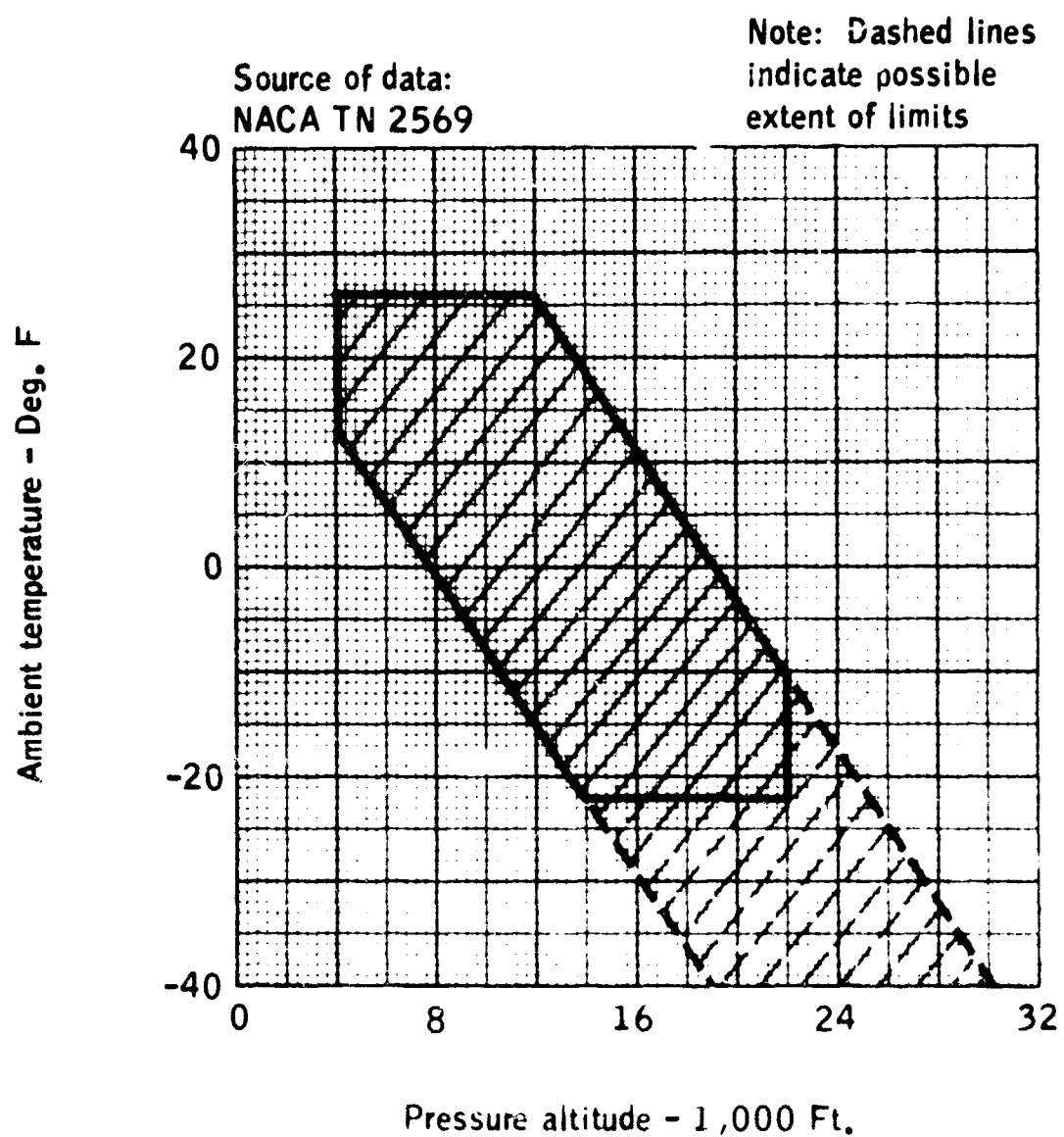
Figure 1-31. Intermittent Maximum Atmospheric Icing Conditions –
Cumuliform Clouds. Ambient Temperature Versus
Pressure Altitude (From CAR 4b).

1-71
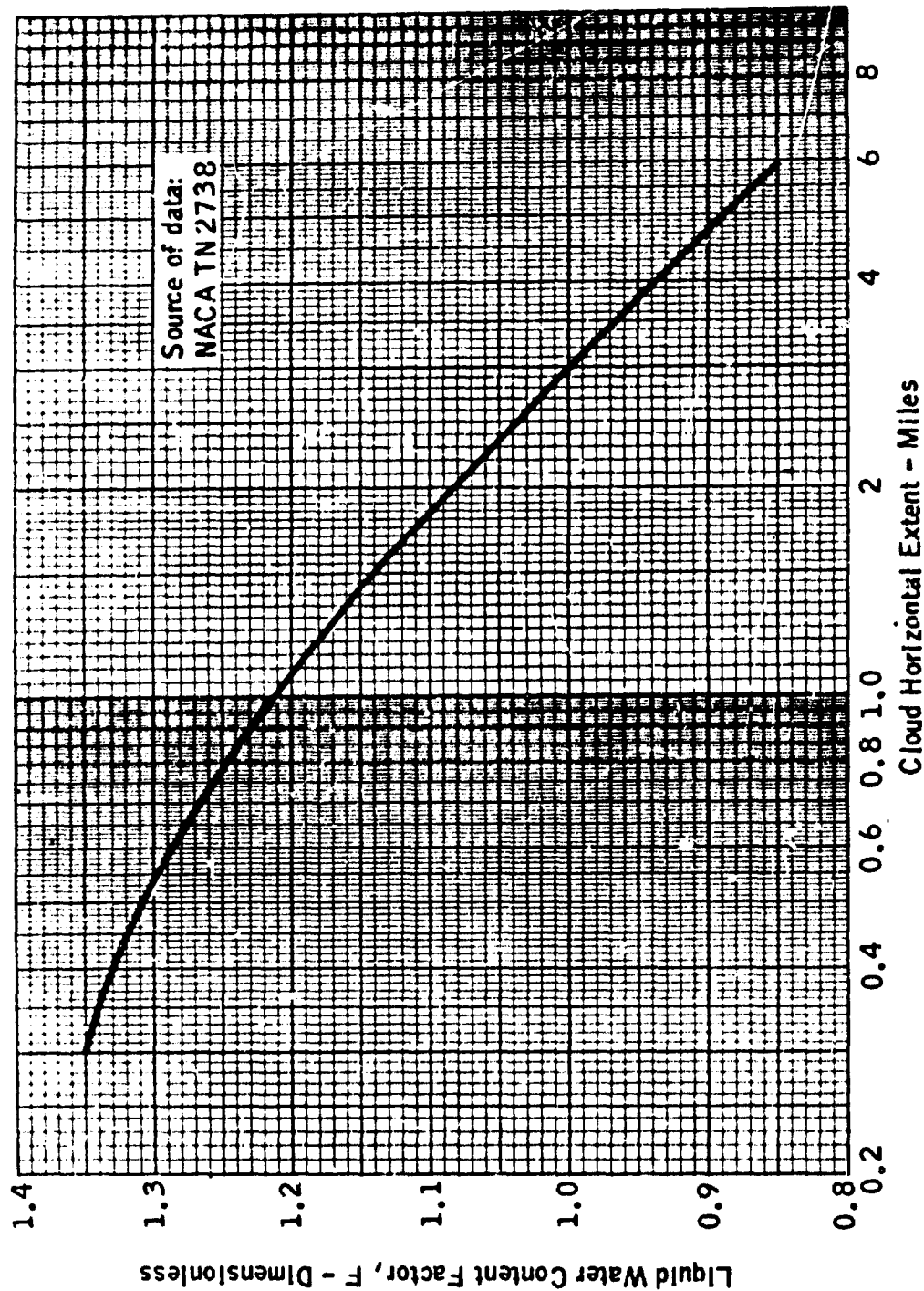
Intermittent Maximum Atmospheric Icing Conditions — Cumuliform Clouds. Variation of LWC Factor With Cloud Horizontal Extent (From CAP. 4b).

Figure 1-32
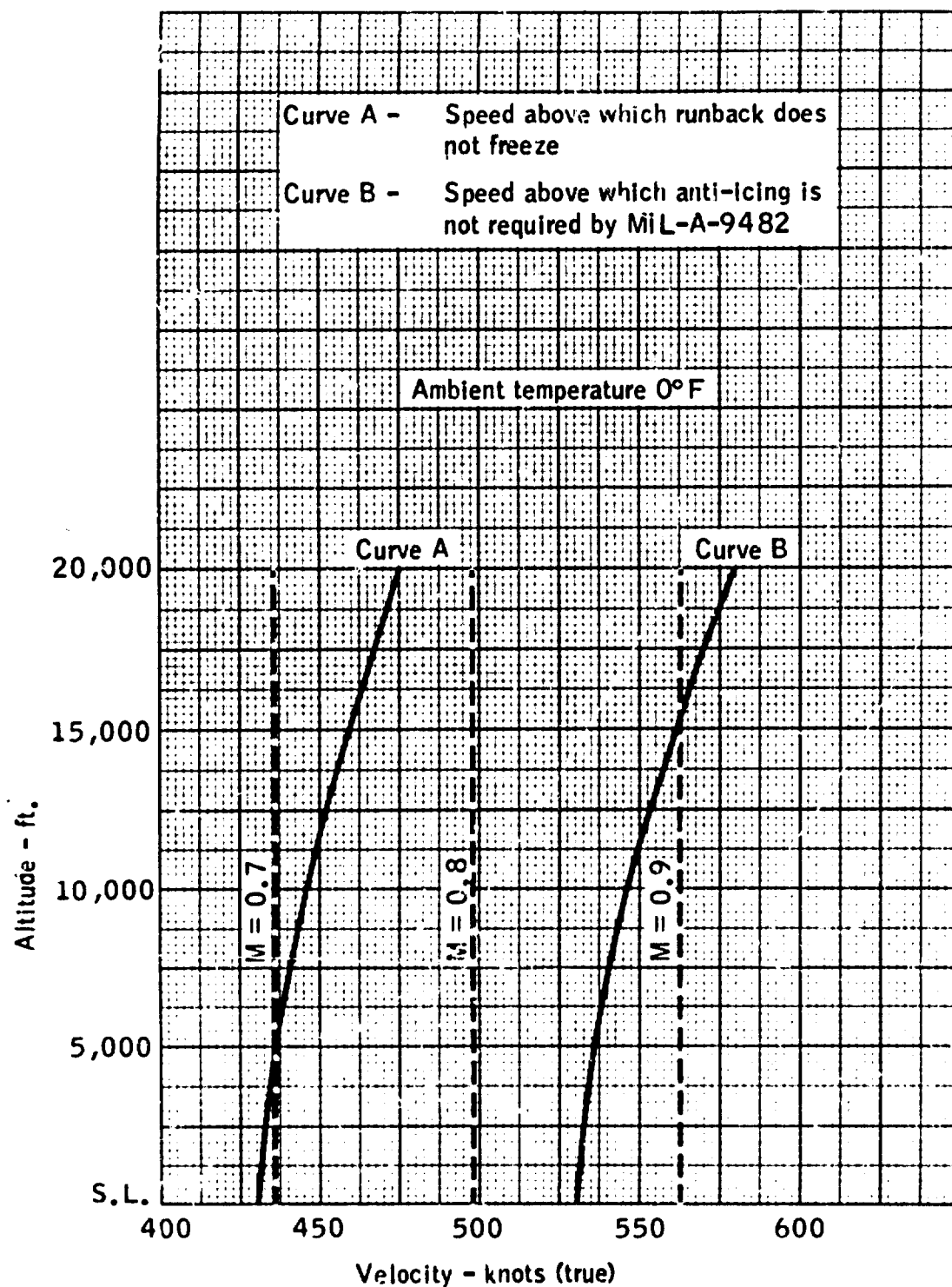
Figure 1-33.   Effect of Speed Upon Requirements for Anti-Icing
               (From MIL-A-9482 USAF, Ref. 1-24).
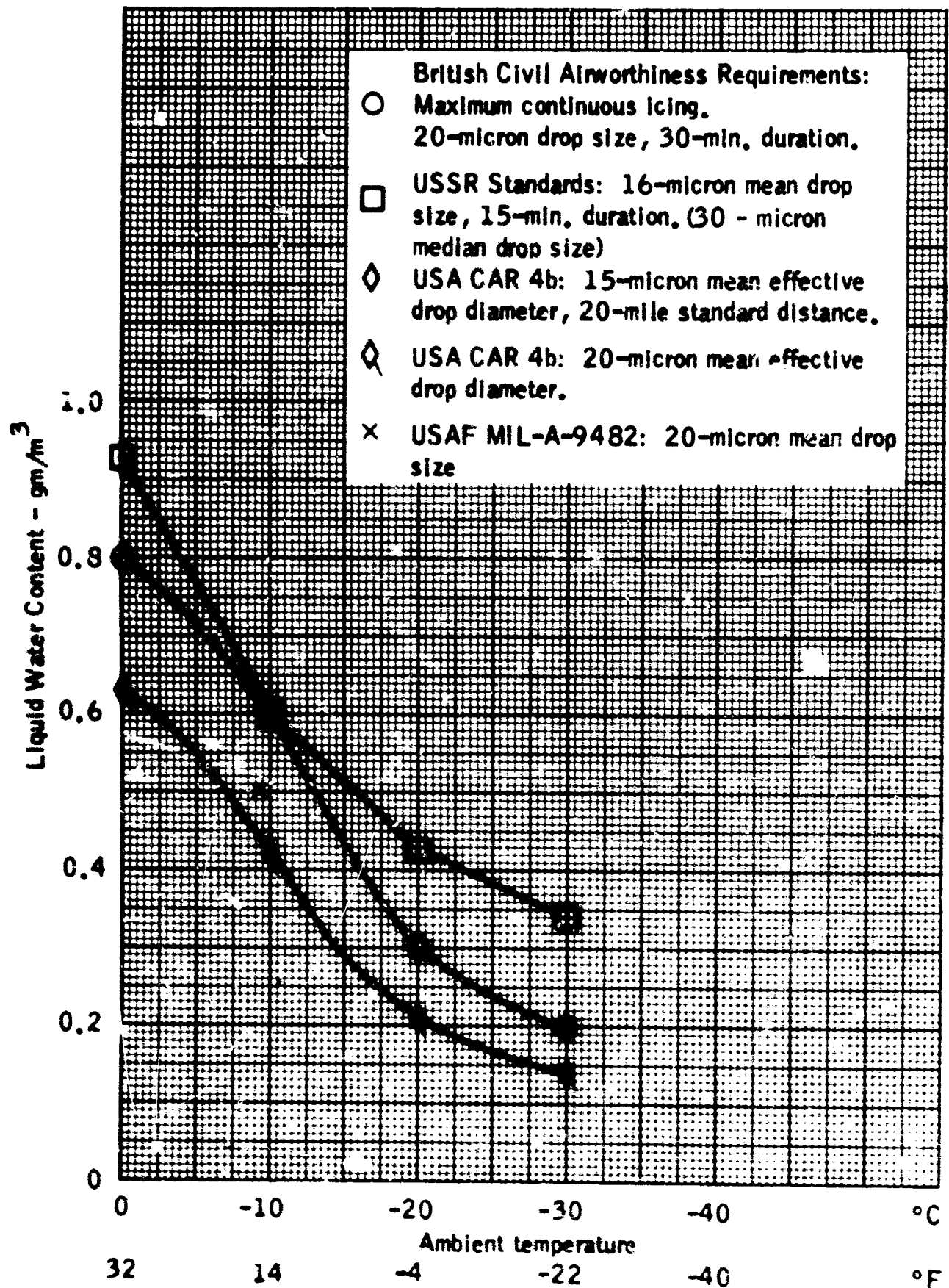
Figure 1-34. Comparison of U. S., British and USSR Civil Transport Standards for Continuous Icing.
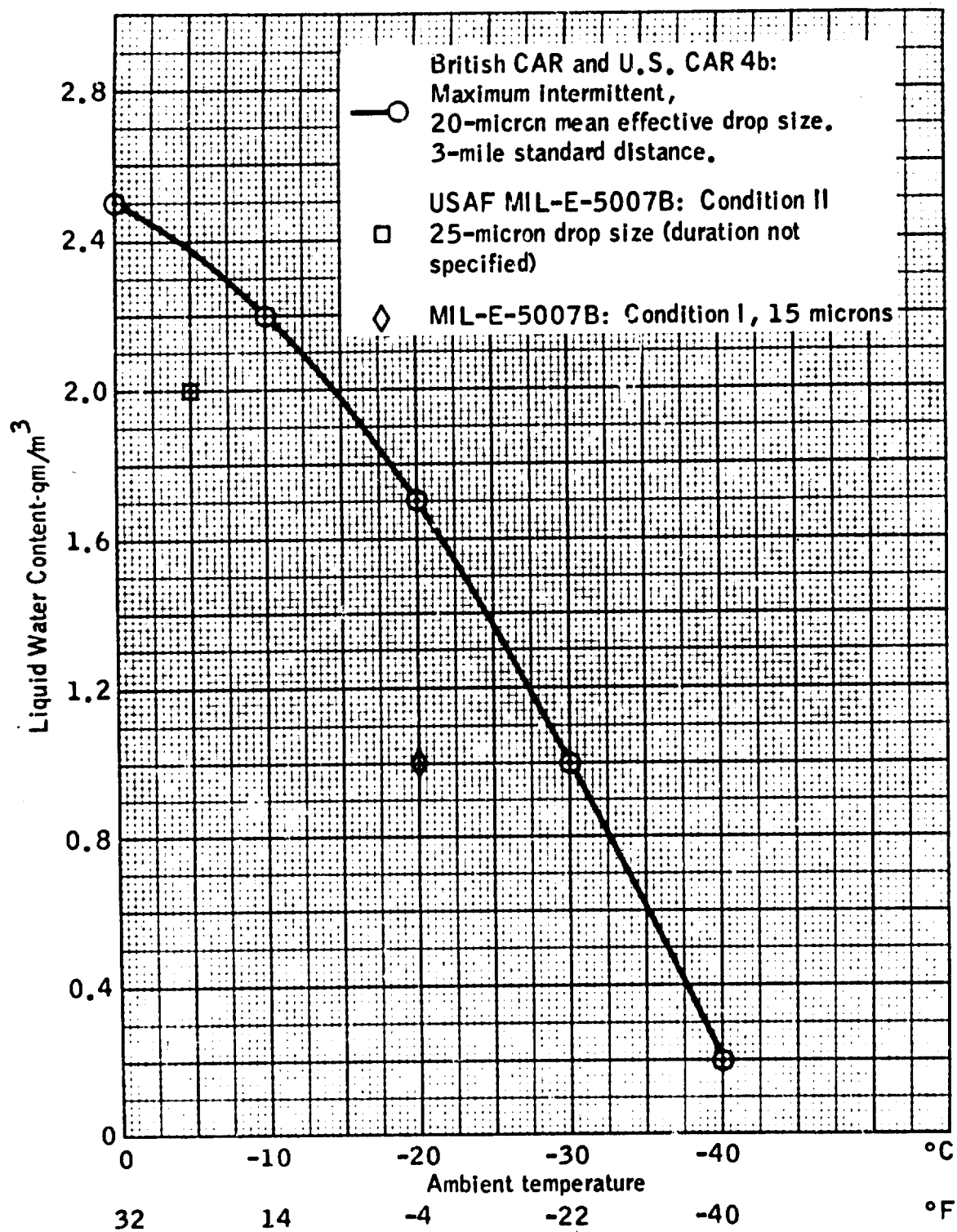
Figure 1-35. British and U. S. Standards for Intermittent Icing.

2 | PHYSICS OF ICE COLLECTION

CONTENTS

PHYSICS OF ICE COLLECTION

LIST OF FIGURES

LIST OF TABLES

LIST OF SYMBOLS

a   Droplet radius, ft.

A/B   Semi-length/maximum radius ratio of ellipsoid, dimensionless

A_F Frontal area, projected length along line of flight, sq. ft.

b   Ribbon width, ft.

b_1 Relative heat factor, dimensionless (see Figure 2-32)

C   Airfoil chord length, ft.

C_D Drag coefficient, dimensionless

c_p Specific heat, BTU/lb. - °F

C_p Pressure coefficient. $\dfrac{p_\ell - p_o}{q_o}$. dimensionless

D   Cylinder or sphere diameter, ft.

d   Droplet diameter, microns

d_{med} Volume median droplet diameter. microns

d_{max} Maximum droplet diameter. microns

e_1 Vapor pressure of saturated air at edge of boundary layer, in. Hg

e_{ok} Vapor pressure of air at surface of airfoil, in. Hg

E_M Total collection efficiency based upon frontal area projected along the line of flight, dimensionless

g   Gravitational constant, 32.2 ft./sec.^{2}

h   Airfoil projected height along line of flight, ft.

J   Mechanical equivalent of heat, 778 ft.-lb./BTU

k   Thermal conductivity, BTU/hr. ft. °F

K   Impingement parameter, dimensionless: $K = 2/9 \dfrac{a^2 v_o \rho_w}{C \mu_a g}$

K_o Inertia parameter, dimensionless: $K_o = (\lambda/\lambda_s) K$

$K_{o_{med}}$ K_o based upon mean effective drop diameter

$K_{o_{max}}$ K_o based upon maximum drop diameter

L_{eb} Arbitrary length dimension for elbow, ft.

L_{el} Ellipsoid body length. ft.

L_s Latent heat of evaporation of water, BTU/lb.

m^3 Cubic meter (of air)

M   Free stream Mach number, dimensionless

n   Freezing fraction, dimensionless

p   Pressure just outside the boundary layer, in. Hg

P_o Free stream static pressure, psf

2-5

p_ℓ — Surface pressure, psf

Pr — Prandtl number (for air) $3{,}600\, c_p\, \mu / k$

q_o — Incompressible free stream dynamic pressure, psf; $q_o = 1/2\, \rho_o v_o^2$

Re,d — Free stream droplet Reynolds number, dimensionless; $Re,d = \rho_a v_o d / \mu_a$

S — Surface distance, measured from foremost point of body, ft.

S_U — Impingement limit on upper surface, ratio to chord length, dimensionless

S_L — Impingement limit on lower surface, ratio to chord length, dimensionless

t_o — Ambient temperature, °F

t_{ok} — Datum temperature or wet air boundary layer temperature, °F

U_o — Flight speed, kt.

v — Local velocity along the surface, fps

v_o — Free stream velocity, fps

y_o — Starting ordinate for droplet trajectory, ft.

y_{o_u} — Starting ordinate for upper surface tangent trajectory, ft.

y_{o_ℓ} — Starting ordinate for lower surface tangent trajectory, ft.

W_t — Liquid water content, gm/m^3

W_M — Rate of water catch on airfoil, lb./hr.-ft. span

W_β — Rate of water catch at point on airfoil surface, lb./hr.-sq. ft.

W_z — Rate of water catch on body, lb./hr.

λ — Droplet range when projected into still air

λ_s — Droplet range when projected into still air according to Stokes law

α — Angle of attack, deg.

μ — Viscosity, lb. sec./sq. ft.

μ_a — Air viscosity, lb. sec./sq. ft.

γ_a — Density of air, lb./cu. ft.

β	Collection efficiency at any point on airfoil or body, dimensionless
β_o	Collection efficiency at stagnation, dimensionless
γ	Ratio of specific heats
ρ_a	Air density, slugs/cu. ft.
ρ_o	Free stream air density, slugs/cu. ft.
ρ_w	Density of water droplet, slugs/cu. ft.
γ_w	Specific weight of water, lb./cu. ft.

β_o

2.1 SUMMARY

Ice can form on aircraft forward surfaces during flight through clouds at temperatures below freezing. For a given icing condition (as defined in Section 1), the rate and extent of ice accumulation is a function of flight speed and airfoil or body geometry. This section of the report presents the formulas and tabulations of impingement data that will allow calculation of ice accretion rate and extent for a large number of airfoils and geometric bodies. The ice collection rate for nearly any object can be approximated from the data presented. These values are needed for the design of the various types of ice protection systems, or to consider the effects of ice accretion if the surface is not protected.

Typical ice accretion rate for a six-foot chord, 65_1-212 airfoil at 200 kt., 10,000-ft. altitude, 15° F, 0.5 gm/m^3 liquid water content. 20-micron droplet diameter and 4 deg. angle of attack is 5.82 lb./hr.-ft. span. The ice extent is 1.5 in. on the upper surface and 9.2 in. on the lower surface.

Equations of motion are also presented so that droplet trajectories could be calculated for the unique and/or critical application that may not be covered by the general data.

Graphs are also presented that will help determine whether a particular flight and icing situation will result in accretion of ice. For example, at 20° F ambient a flight speed of more than 300 kt. is required to prevent the formation of ice; whereas, at 0° F ambient a speed of more than 485 kt. is required.

If ice does form, the type of ice is of interest as aerodynamic effects vary widely, dependent on ice shape. At moderate airspeeds (less than 250 kt.)and high total air temperatures (25 to 32° F), glaze ice ("double horn" shape) is most common, and can produce severe aerodynamic effects in terms of increased drag and decreased maximum lift coefficient. At moderate airspeeds and total air temperatures below 10° F, rime ice is most common and has a relatively streamlined shape. Lift and drag effects are much less serious (about one-third

as great) for rime ice than for glaze ice. At total air temperatures between 10° and 25° F, a mixed glaze-rime ice accretion is usually found.

Photographs and sketches of ice shapes on typical airfoils are also presented.

2.2 INTRODUCTION

Ice may form on the unheated forward facing surfaces of an aircraft flying through clouds of supercooled water droplets. At low temperature, the water droplets freeze immediately on impact with airfoil leading edges, forming rime ice (Figure 2-1 from Ref. 2-1). At higher temperatures, the water droplets may flow over the surface for a short distance before freezing, resulting in glaze ice (Figure 2-1). The size, shape and extent of ice formation depends on the cloud liquid water content, the drop size and temperature, the flight speed and angle of attack, airfoil or body geometry, and duration of the icing encounter.

Design of ice protection systems require a knowledge of rate of water catch, impingement limits and — in certain cases — impingement distribution. Fortunately, a large body of impingement data exists, covering a wide range of airfoils and geometric bodies. This section of the report presents a summary of all available data (of known accuracy) on droplet impingement (Ref. 2-2 through 2-25). The data may be used in conjunction with the icing cloud data of the previous section to determine rates of water catch and impingement limits for specific flight conditions.

The data is presented in correlated form to reduce the amount of information to a manageable level. Collection efficiency — defined as the ratio of water collected to the maximum possible water catch — is correlated with a dimensionless inertia parameter, K_o. Impingement limits (the distance from stagnation to the end of the water impingement region on both upper and lower surfaces) are also correlated with the K_o parameter. Collection efficiency at

the stagnation point is shown for several bodies. Typical variation of water catch efficiency versus surface distance is also shown for typical airfoils.

Equations and a method for calculating droplet impingement from the equations of motion are also presented. Although impingement can be approximated for most bodies from the correlated data, new problems may arise that would call for calculation of droplet trajectories. The equations are based on the assumption that pressure distribution around the body of interest is known (from theory or wind tunnel tests).

Equations and methods of determining ice shapes on unprotected airframe components are shown. The flight speeds above which icing will not occur are shown versus ambient temperature. Typical ice shapes are also shown, as well as plots to define the three basic types of ice accretion in terms of flight speed, ambient temperature, liquid water content and droplet size.

The terms used in this report to describe the three types of ice are glaze, intermediate and rime. The terms are in common use in icing literature and by icing research and design engineers. The terminology commonly used by aircraft pilots in reporting ice may differ; the following tabulation may help clarify the discrepancies:

Ice Designation		Ice Description
Icing Literature	Pilots	
—	Glaze	Smooth film of ice covering leading edge at temperatures just below freezing.
Glaze	Mushroom	Double-horn ice formations, hard clear ice with rapid growth rate.
Intermediate	—	Combination of glaze and rime ice; glaze in forward areas, rime in aft areas.
Rime	Spearhead	Milky white appearance, lower density ice with a relatively streamlined shape.

2-11

2.3 SUMMARY OF AVAILABLE DATA

2.3.1 IMPINGEMENT COLLECTION EFFICIENCY VERSUS K_c — The rate of water droplet impingement for an airfoil is usually expressed in pounds per hour per foot of span and may be calculated from the general equation

$$W_M = 0.379 \, U_o \, W_t \, C \, (h/C) \, E_M$$

For any given flight condition and body geometry, the above factors will be known except collection efficiency, E_M. For small objects at high speeds and large droplet size, E_M will have a value of nearly 1.0, because the water droplet trajectories are straight lines. For most cases, however, E_M will have a value less than 1.0, and must be determined from known data on airfoils.

Collection efficiency is a function of flight speed, droplet size, body geometry, ambient temperature and pressure. In the literature, E_M is presented versus various dimensionless parameters — the method of presentation varies widely among authors. In this report, E_M is correlated with the dimensionless inertia parameter K_o. Use of this parameter results in essentially a single-valued curve of E_M versus K_o for bodies of the same geometrical shape. The error involved in use of the K_o parameter for correlation of E_M is less than ± 10 per cent for most airfoils and bodies, for the normal range of flight conditions.

In this report, E_M is based upon the projected height (h), or upon the projected area of the airfoil or body involved. As shown in Figure 2-2, E_M is equal to $(y_{o_u} - y_{o_\ell})/h$, where $y_{o_u} - y_{o_\ell}$ is the part of the cloud swept out by the airfoil, and h is the projected height of the airfoil at the angle of attack involved. In this definition, E_M cannot exceed 1.0. (In some parts of the literature, E_M is based on maximum thickness at 0 deg. angle of attack, resulting in collection efficiencies of more than 100 per cent in many cases.) A plot of projected height versus angle of attack for various airfoils is shown in Figure 2-3, for angles of attack of 0 to 12 deg. A flat plate is also shown for comparison. At angles of attack greater than 2 deg., the thin airfoils approach

very closely the flat plate projected height.

The parameter K_o may be obtained graphically from Figures 2-4, 2-5 and 2-6, or by use of the approximate equation

$$K_o = 1.87 \times 10^{-7} \left(\frac{1.15\, U_o}{\mu_a g} \right)^{0.6} \left(\frac{d_{med}^{1.6}}{12 \gamma_a^{0.4} C} \right)$$

This equation yields a value of K_o that is correct within ±5 per cent for droplet Reynolds numbers (Re_d) from 25 to 1,000.

Graphically, K_o may be determined by obtaining the droplet Reynolds number from Figure 2-4, inertia parameter K from Figure 2-5, and the ratio λ/λ_s from Figure 2-5. K_o is then found from the equation

$$K_o = (\lambda/\lambda_s)(K)$$

A typical example of the calculation of K_o, E_M and rate of ice accretion follows:

Given the following data:

Airfoil. six-foot chord NACA 65_1-212 (C = 6 ft.) — Airfoil designations
 are NACA airfoil sections. The characteristics of various NACA
 airfoils are defined in "Theory of Wing Sections," I. H. Abbott
 and A. E. von Doenhoff. Dover Publications, Inc., New York, 1959.

Flight speed, U_o. 200 kt.

Altitude, 10,000 ft.

Ambient temperature, t_o. 15° F

Droplet size. d_{med}. 20 microns (mean effective diameter)

Liquid water content. W_t, 0.5 gm/m^3

Angle of Attack, α. 4 deg.

The solution is as follows:

Projected height, h/C = 0.128 is found from Figure 2-3

$U_o (d_{med}) = 200 (20) = 4,000$ (kt. x microns)

$Re, d = 114$ is found from Figure 2-4 and $U_o(d_{med}) = 4,000$

$C/U_o = 6/200 = 0.030$ ft./kt.

$K = 0.077$ from Figure 2-5 and $C/U_o = 0.030$

$\lambda/\lambda_s = 0.332$ from Figure 2-6 and $Re, d = 114$

$K_o = (\lambda/\lambda_s)(K) = 0.332 (0.077)$

$K_o = 0.0256$

Collection efficiency, E_M, may be found from the plots of Figures 2-7 through 2-14. For the 65_1-212 airfoil at $K_o = 0.0256$, the theoretical E_M at a 4-deg. angle of attack (Figure 2-10) is

$E_M = 0.200$

The water catch is

$W_M = 0.379 \, U_o W_t \, C(h/C)E_M$

$= 0.379 \, (200)(0.5)(6)(0.128)(0.200)$

$= 5.82$ lb./hr.-ft. span

Some comment must be made concerning the data on collection efficiency presented in Figures 2-7 through 2-14. The airfoil data is plotted as E_M versus K_o for angles of attack of 0, 2, 4, and 8-deg. (Some data at 5 deg. is included on the 4 deg. plot, and some 10 and 12-deg. data is included on the 8 deg. plot.) Most of the data is theoretical, obtained from analysis of droplet trajectories. Some data is experimental — obtained by the dye-spray techniques described in Ref. 2-2.

For some airfoils, both experimental and theoretical data are shown. In most cases there is good agreement; however, one exception is the 65_1-212 airfoil. The experimental data shows a lower collection efficiency than the theoretical over a large part of the K_o range. In this case, the theoretical data may be used if a conservative answer is desired, although experience has shown that the experimental data is more representative of actual flight in

natural icing. Also, experimental data for the 65_2-015 airfoil is 10 to 20 per cent lower than theoretical.

The accuracy of the data shown is compromised to a small degree by the use of the K_o parameter; however, plots shown are generally within ±10 per cent of the original data for the practical range of Reynolds numbers from 100 to 250. For extremely critical cases — where better accuracy is considered essential — the original data sources can be consulted (Ref. 2-2 through 2-25). Use of the K_o correlation is considered justified by the small loss in accuracy versus the large condensation in data presentation made possible by its use. No theoretical proof of the validity of the K_o correlation is available, but extensive use has been made of it in recent years for both theoretical studies and actual design work. It was originally proposed by Dr. Langmuir, (Ref. 2-3) and has subsequently been used by various investigators.

In using the K_o parameter for geometric bodies, great care must be taken in selecting the body length value used for obtaining the impingement parameter, K, — an intermediate step to determine K_o. For airfoils, the characteristic length is the airfoil chord, C, in feet. For other bodies, the characteristic dimension may be the diameter; but in some cases body length, half body length or radius have been used. Tables have been prepared showing the water catch equation (Table 2-1) and characteristic body length (Table 2-2) for the various shapes.

It should be noted that all the theoretical data is based upon uniform drop size. A volume mean droplet size is normally used in design work, rather than calculating the water catch for each of the several size ranges that make up an icing cloud.

Use of a single mean drop size gives an adequate approximation of water catch for most airfoils; however, for blunt bodies such as ellipsoids and cones, serious error can result from use of uniform drop size. For critical applications involving blunt bodies or cones, water catch should be determined for the

various drop sizes making up an icing cloud, and the results added to obtain the total. Table 2-3 shows several typical droplet distributions. The experimental data is based upon a water spray cloud having approximately a "D" distribution (see Table 2-3). The parameter K_o is noted as $K_{o_{med}}$ for the experimental data, and is evaluated at the volume median droplet diameter.

The mean droplet size (often called the mean effective drop size) as used in this report and nearly all icing literature is a volume median drop size. It is defined as that diameter (for a given sample or cloud) for which half the total volume of liquid water is contained in drops larger than the volume median and half in drops smaller than the volume median.

2.3.2 IMPINGEMENT LIMITS VERSUS K_o — Impingement limits are plotted for most of the airfoils and bodies in Figures 2-15 through 2-25. The K_o parameter is the same as that used for collection efficiency. S_U and S_L are the impingement limits, expressed as a ratio to airfoil chord length (or geometric body length).

Impingement limits are determined by the maximum droplet size in the cloud. Thus, for design purposes, 40 microns is often used to determine impingement limits, whereas 20 microns is often used to calculate water catch. For the experimental data, which was obtained from actual dyed water spray, the mean effective drop size is used for water catch, and the maximum drop size is used for determining impingement limits. K_o is evaluated using the mean effective drop diameter for E_M, but using maximum drop diameter for S_U and S_L.

For example — using the case shown previously of a 65_1-212 airfoil with a six-foot chord at 200 kt. and 20-micron drop size:

K_o = 0.0256

S_U = 0.021 (1.5 in.) from Figure 2-15

S_L = 0.128 (9.2 in.) from Figure 2-16

For 40-micron drops,

Re, d = 228, from Figure 2-4

K = 0.300

λ/λ_s ≈ 0.254

K_o = 0.254 (0.300) = 0.0762

S_U = 0.042 (3.0 in.)

S_L = 0.230 (16.6 in.)

Note that this example is based upon arbitrarily selected values, for the purpose of illustration only. For specific results applicable to aircraft, refer to Section 4 - Aircraft Applications. In a practical case (e.g., a cloud with a 20-micron volume mean diameter and a maximum diameter of 40 to 45 microns) most of the ice will be found within the 20-micron impingement limits. The amount of ice catch on the surface between the 20 and 40-micron limits is small and may or may not be ignored, depending upon the nature of the specific problem, and the criticality of a small amount of ice on the area aft of the leading edge.

2.3.3 IMPINGEMENT DISTRIBUTION FOR TYPICAL AIRFOILS — The collection efficiency at stagnation is occasionally of interest, as it is the point of maximum collection efficiency. A plot of β_o versus K_o is shown in Figure 2-26 for several bodies. Values for bodies other than those shown in Figure 2-26 may be found in the literature (Ref. 2-2 through 2-23).

Some design problems may require a general or specific knowledge of impingement distribution over the collecting surface. Typical values are shown in Figures 2-27 through 2-29 for three airfoils at 4 deg. angle of attack.

For other airfoils and bodies, distribution curves are available in the literature. Space limitations do not allow inclusion of additional data in this report.

The impingement distribution for any body can be approximated to a satis-factory level for most uses, if E_M, S_U, and S_L are known, from a knowledge of

the typical distribution shape (Figures 2-27 through 2-29) and the fact that:

$$E_M = \frac{1}{h} \int_{S_L}^{S_U} \beta \, dS/C$$

Knowing S_U and S_L, a curve of β versus S/C can be estimated, and the area under the curves tested against E_M; re-fairing the curve until the area under the curve is equal to E_M. Local water catch rates may then be calculated from the equation

$$W_\beta = 0.379 \, \beta \, U_o W_t$$

2.3.4 AIRFOIL MATCHING PROCEDURES — In many cases, the contour of the airfoil or body under consideration will not match exactly those designated in the plots already presented. Where this is the case, either of two methods (or a combination) may be used to obtain an engineering approximation of the impingement characteristics of an airfoil or body.

One method is to approximate the contour of the forward portion of the airfoil in question by that of an airfoil with known impingement characteristics. The second is to match the pressure (or velocity) distribution of the airfoil of interest with the pressure (or velocity) distribution of an airfoil having known impingement characteristics.

The first method — that of matching the airfoil contour with airfoils of known impingement characteristics — needs little explanation. The contour match is most important in the region from stagnation to about 20 per cent chord. The aft areas have less effect on impingement, and contour matching is less critical for the regions beyond 30 per cent chord. The underlying theory is that for a given set of flight parameters similar contours should yield similar pressure distributions and, thus, similar droplet impingement.

In some cases, contour matching may not be adequate — as in the case of an engine inlet or a highly swept and/or tapered wing. In these cases a better

approximation can be obtained by matching experimental pressure distributions for the body in question against pressure distribution for the bodies of known impingement characteristics. This, of course, is a tedious process, but may be necessary in the cases mentioned (inlets and swept and/or tapered wings) where simple two-dimensional airfoil data may yield an overly conservative or incorrect value of water catch and impingement limits. Typical velocity distribution for an airfoil is illustrated in Figure 2-30.

The pressure distribution may be calculated in terms of pressure coefficient from known velocity distribution by using the equation

$$C_p = 1 - (v/v_o)^2 \quad \text{(incompressible)}$$

$$C_p = \frac{p_i - p_o}{q_o} \quad \text{, the pressure coefficient (incompressible), where}$$

v is the surface velocity

p_i is the surface pressure

v_o is the free stream velocity

p_o is the free stream pressure

q_o is the free stream dynamic pressure

In compressible flow, the pressure coefficient should be modified by the Prandtl-Glauert equation (Ref. 2-24, pg. 180)

$$C_{p_{(comp.)}} = \frac{C_{p_{(incomp.)}}}{\sqrt{1 - M^2}}$$

This correction becomes significant at Mach numbers in excess of 0.25.

Wing sweep can have a significant effect upon water catch rates. A method of converting straight-wing data to swept-wing data is shown in Ref. 2-25. Unfortunately, this method requires that the swept-wing airfoil be designated on a plane perpendicular to the leading edge, whereas, it is common aircraft design practice to define the airfoil in the streamwise plane. Consequently, the

usefulness of the report is rather limited. The best approach then would be to match the swept-wing pressure distribution with pressure data on non-swept airfoils of known impingement characteristics.

2.4 CALCULATION OF DROPLET TRAJECTORIES AND IMPINGEMENT FOR BODY OF KNOWN PRESSURE DISTRIBUTION

The impingement characteristics of most airfoils, bodies of revolution and geometric shapes can be approximated to a satisfactory level for engineering design use from the data presented in the previous section. For critical and/or unique applications, it could be desirable in some cases to calculate the impingement for a body from the equations of motion for a body traversing a cloud of water droplets. This section presents these equations in a form that would allow computation of droplet trajectories for a body of known pressure distribution. Pressure data is easily obtained for a body by theoretical or simple experimental means (wind tunnel testing). The calculation of droplet trajectories can be extremely tedious and time consuming; however, the problem can be set up and solved using modern high-speed electronic computers.

2.4.1 CALCULATION OF THE FLOW FIELD — The flow field ahead of the body moving through an airstream must be known before droplet trajectory calculations can be made. The surface pressure distribution of a body can be obtained experimentally by wind tunnel or flight tests, or by theoretical means. Once the pressure distribution is known, the flow field can be calculated by the vortex distribution method. This consists of placing a sheet of vortices on the airfoil surface of such strength that the velocities on the surface caused by the vortices are the same as the velocities obtained from wind tunnel or theoretical studies. The principles of the method are presented in Ref. 2-26. Further equations and methods of calculating the flow field may be found in Ref. 2-4. The method and equations are not given in this report, as the referenced reports are readily available and the subject is rather complex.

2.4.2 DROPLET TRAJECTORY EQUATIONS — With a known flow field ahead
of and around the airfoil, as determined above, the droplet trajectories may be
calculated from the equations relating the inertia and drag forces on the water
droplets. These equations are presented below and were obtained from NACA
TN 2904 (Ref. 2-5).

For convenience in referring to NACA TN 2904, the nomenclature used in
the following equations and listed below is the same as that used in TN 2904.

a   Droplet radius, ft. (1 ft. $= 3.048 \times 10^5$ microns)

D   Drag force, lb.

C_D Drag coefficient for droplet in air, dimensionless

$\bar{v}$ Local vector difference between velocity of droplet and velocity of
air, fps

Re   Local Reynolds number with respect to droplet $\dfrac{2a\rho_a \bar{v}}{\mu}$,
dimensionless

μ Viscosity of air, slugs/ft. -sec.

ρ_a Density of air, slugs/cu. ft.

ρ_w Density of water, slugs/cu. ft.

Prime superscript — Applied where velocity terms are in fps

x subscript — Horizontal component

y subscript — Vertical component

u   Local air velocity, ratio of the actual local air velocity to the free
stream velocity, dimensionless

v   Local droplet velocity. ratio of the actual droplet velocity to the
free stream velocity, dimensionless

L   Characteristic body length or dimension, ft.

t   Time, sec.

U   Free stream velocity, fps

τ Time scale, tU/L, dimensionless

K   Inertia parameter, $\dfrac{2}{9} \dfrac{\rho_w a^2 U}{\mu L}$, dimensionless

Re_o Free stream Reynolds number with respect to droplet $\dfrac{2a\,\rho_a\,U}{\mu}$, dimensionless

These definitions are not to be used in other parts of this section of the report.

The drag force on a body (i.e., a droplet) in a fluid is

$$D = C_D \, 1/2 \, \rho_a \, \pi a^2 \bar{v}^2$$

The Reynolds number of the body (droplet) is $Re = \dfrac{2a\rho_a \bar{v}}{\mu}$

Combining, the equation $D = \dfrac{C_D Re}{4} \, \pi a \mu \bar{v}$

is obtained for a sphere (droplet) having a relative velocity, $\bar{v}$, with respect to the fluid.

The equation of motion of a water droplet in terms of its x component is:

$$4/3 \, \pi a^3 \rho_w \, \frac{dv'_x}{dt} = \frac{C_D Re}{4} \, \pi a \mu \, (u'_x - v'_x)$$

$$\frac{2}{9}\left(\frac{a^2 \rho_w U}{\mu L}\right) \frac{dv'_x}{dt} \, \frac{L}{U^2} = \frac{C_D Re}{24} \, \frac{(u'_x - v'_x)}{U}$$

In dimensionless terms, the equation of motion for the x component is:

$$\frac{dv_x}{d\tau} = \frac{C_D Re}{24} \, \frac{1}{K} \, (u_x - v_x)$$

and for the y component

$$\frac{dv_y}{d\tau} = \frac{C_D Re}{24} \, \frac{1}{K} \, (u_y - v_y)$$

where $K \equiv \dfrac{2}{9} \, \dfrac{\rho_w a^2 U}{\mu L}$ (K is the inertia parameter)

The Reynolds number, Re, can be obtained in terms of the freestream Reynolds number

$$\bar{R}e_o = \frac{2a \, \rho_a U}{\mu}$$

2-22

such that

$$\left(\frac{Re}{Re_o}\right)^2 = (u_x - v_x)^2 + (u_y - v_y)^2$$

The term C_D Re/24 which defines the drag coefficient for a sphere is shown in Table 2-4 from Ref. 2-6.

The path or trajectory of a water droplet approaching the body or airfoil can be calculated using the preceding equations and the known flow field. As can be seen in Figure 2-2, the droplet paths diverge near the airfoil. Trajectories must be calculated to determine the upper and lower limiting trajectories. Above and below these limits, the water drops will not impinge on the airfoil.

Calculation of droplet trajectories can be made for various values of the inertia parameter and droplet Reynolds number. From these trajectories, the collection efficiency and impingement limits can be determined, as well as local distribution of water catch over the surface. Equations for defining these values are shown in succeeding sections.

2.4.3 OVERALL COLLECTION EFFICIENCY — The collection efficiency is defined as the ratio of actual water impingement to the maximum value that could occur (straight-line trajectories).

In equation form for an airfoil (Figure 2-2):

$$E_M = \frac{y_{o_u} - y_{o_\ell}}{h}$$

where y_{o_u} is the starting ordinate of the upper tangent trajectory, and y_{o_ℓ} is the starting ordinate for the lower tangent trajectory. In this equation, h is the projected height of the airfoil. Note that in some early impingement reports, collection efficiency may be based on maximum airfoil thickness rather than on projected height. In this case, collection efficiencies of more than 100 per cent are possible.

For bodies of more complex shape, collection efficiency can be defined as the frontal area defined by the starting ordinates of the tangent trajectories,

divided by the projected area of the body (along the line of flight).

2.4.4 LOCAL COLLECTION EFFICIENCY -- The collection efficiency at any point on the surface may be determined if the corresponding intermediate droplet trajectories are known. The equation is:

$$\beta = \frac{dy_0}{dS}$$

It may be noted that

$$y_{0_u} - y_{0_\ell} = \int_{S_L}^{S_U} \beta \, dS$$

and that the overall collection efficiency

$$E_M = 1/h \int_{S_L}^{S_U} \beta \, dS$$

Curves of impingement efficiency versus surface distance can be plotted, using the equation $\beta = \frac{dy_0}{dS}$. As a final check on the fairing of the curves, the area under the curve can be obtained to determine the overall collection efficiency and minor re-fairing made as necessary to obtain agreement with E_M as defined by $\frac{y_{0_u} - y_{0_\ell}}{h}$.

2.4.5 IMPINGEMENT LIMITS — The limits of impingement on the upper and lower surface are obtained from the upper and lower tangent trajectories. These values may be correlated as shown in previous sections in terms of K and Re,d or in terms of K_0. In many cases, better accuracy can be obtained by expanding the x ordinate of the trajectory plots to obtain a more accurate definition of the point of tangency. The lower surface limit on airfoils at an angle of attack can be particularly difficult to define.

2.5 ICE SHAPES ON UNPROTECTED SURFACES

Ice shapes on airfoils and bodies are classified in icing literature as "glaze"

and "rime"; however, many ice shapes will be a mixture of the two. See Paragraph 2.2 for discussion of ice classifications. Rime ice is found at combinations of low temperature and low water catch rates and has a milky-white appearance resulting from inclusion of air in the ice during the freezing process. The water droplets freeze at the point of impact; therefore, the ice shape can be predicted quite readily from the impingement data presented previously in terms of catch rate, impingement limits and distribution. The drag and other aerodynamic effects of rime ice are much less severe than glaze ice, because of the relatively streamlined form of the ice, and the low rates of water catch associated with this type of ice.

Glaze ice forms at combinations of high water catch rate and temperatures near freezing. Characteristically, the water droplets run some small distance before freezing, resulting in a typical "double horn" ice shape (Figure 2-1). The ice is usually clear except at the aft regions. Glaze ice can cause severe aerodynamic effects in terms of increased drag and decreased maximum lift coefficient. The upper "horn" acts as a spoiler, increasing drag and decreasing lift. The lower surface "horn" usually has only a minor effect, because of the low local air velocities. If angle of attack is varied, however, it may have a significant effect. Detailed data on effects of ice on unprotected aircraft are presented later under "Methods of Protection" (Section 3).

2.5.1 ICING LIMIT AND TYPES OF ICE AS A FUNCTION OF FLIGHT CONDITIONS — The following discussion presents information on characteristic ice shapes and means of determining the type of ice shape associated with various combinations of airspeed and icing conditions.

The temperature of an airfoil exposed to icing conditions is a complex function of airspeed, liquid water content, ambient temperature and altitude. The shape and type of ice (if any) that forms is dependent on the surface temperature. In this section of the report, equations for calculating surface temperature are presented, as well as typical results. Types of ice and shape are also

shown and are related to flight and meteorological conditions.

The "datum temperature" has been widely used to represent the temperature of an unheated surface in icing. (This usage is not entirely accurate, as will be discussed later.) It has also been described as "wet adiabatic" and "wet air boundary layer" temperature. It may be calculated from the equation:

$$t_{ok} = t_o + \frac{(1.688 \, U_o)^2}{2gJc_p} \left[1 - \left(\frac{V}{V_o}\right)^2 (1 - Pr^{1/2}) \right] - 0.622 \, \frac{L_s}{c_p} \left(\frac{e_{ok} - e_1}{p}\right)$$

Solution of this equation is shown in Figure 2-31 for flight speeds up to 800 kt., ambient temperatures of -20 to 30° F, and an altitude of 10,000 ft. Curves for sea level and 20,000 ft. are shown in Section 3 (Figure 3-8). It may be seen that a flight speed of 300 kt. will produce a 32° F datum temperature at 20° F ambient, but that at 0° F a speed of 485 knots is needed. This graph may be used as a guide in determining whether a particular combination of flight speed and ambient temperature is likely to represent a potential icing problem.

An exact account of the heat balance on an unheated, insulated icing surface may be found in Ref. 2-27. Typical curves of surface temperature versus free stream velocity are shown in Figure 2-32, and are compared with the temperatures in clear air and those calculated by the "datum temperature" equation. At the lower speeds, release of heat of fusion (as the water freezes) can result in temperatures in excess of dry air total temperature. At 32° F, a region exists where the water catch is completely frozen (n = 1), partly frozen, or all in liquid form (n = 0). (The freezing fraction, n, is defined in Ref. 2-27 as that part of the water catch that freezes in the region where it impinges.) At the higher speeds, the equilibrium surface temperature is not greatly different from the "datum" temperature.

It should be noted that the method of Ref. 2-27 is based upon an insulated surface (no chordwise heat flow). This is true for a plastic radome or fiberglass leading edge as well as for a titanium or steel leading edge. However, an aluminum-skinned airfoil will transfer heat chordwise and the surface

temperature at the lower speeds may be fairly close to the "datum" temperature.

It may be seen from the preceding data that relatively high speeds are needed to preclude the formation of ice, and that aircraft with low operating speeds will experience icing much more frequently than higher speed aircraft.

The type of ice that forms and its shape are a function of speed, liquid water content and temperature. Ice shapes are generally classified as glaze, intermediate and rime. A correlation of ice shape is shown in Figures 2-33 through 2-35 in terms of liquid water content. ambient temperature and flight speed.

This correlation was obtained from an analysis by Dickey (Ref. 2-28), using the "freezing fraction" concept developed by Messinger (Ref. 2-27). The specific values shown are based on the stagnation line of a two-inch cylinder (insulated) with a drop size of 15 microns. An aluminum-skinned airfoil would tend to accumulate rime and intermediate glaze-rime ice at slightly higher temperatures than shown, because of the conduction of heat away from the area of high water catch (and release of heat of fusion). The plots of Figures 2-33 through 2-35 can be used as a guide in determining the probable type of ice formed for various flight and icing conditions. These curves have not been validated by experiment over the complete range of parameters shown; therefore, caution and judgment must be exercised in their use.

In general terms, it can be stated that rime ice is likely to occur at total air temperatures of about 10° F and below, while glaze ice usually occurs at total temperatures of 25 to 32° F. Between 10 and 25° F, a glaze-rime formation will usually occur, with clear glaze ice at the stagnation region, and milky-white rime ice in the aft regions.

2.5.2 GLAZE AND RIME ICE SHAPES FOR VARIOUS AIRFOILS AND BODIES OF REVOLUTION — The shape of ice formation is of particular interest in the case of unprotected airframe components. Flight tests are often made

with simulated ice shapes on developmental aircraft to determine the need for protecting these components. In this case, the ice shape must be determined by a combination of analysis and reference to existing data on ice shapes from both wind tunnel and flight tests.

Although a large number of photographs are available of ice shapes on unheated bodies, very few actually show cross-sections of the ice, or give critical dimensions (maximum thickness, extent, etc). Several photographs and sketches from Ref. 2-29 and 2-30 are shown in Figures 2-36 through 2-40 to illustrate glaze, intermediate and rime ice deposits. Cross-sections of ice on a four per cent airfoil are shown in Figure 2-36. Rime ice forms in a manner that is easily predictable; that is, the drops freeze on impact and the resulting ice shape has the same form as would be predicted by the droplet impingement data shown previously. The rate of growth is generally linear for rime ice, because the ice shape does not alter the flow field significantly. The glaze ice exhibits the typical "double horn" shape, that results from water flow in the stagnation region. As the ice increases in size, the aft regions are sheltered from impingement so that virtually all the water is deposited in the stagnation region. The exact shape of glaze ice is difficult to predict; however, most glaze ice shapes will be similar to those of Figures 2-36 and 2-37. Rate of growth for glaze ice may be nonlinear (increasing with time in icing) because the ice affects the flow field. This is particularly true for thin airfoils at low angle of attack (See Ref. 2-29). This factor should be considered in predicting ice shapes on unheated airfoils.

On highly swept airfoils, glaze ice tends to form as a series of discontinuous cup shapes. A comparison of ice shapes for various sweep angles is shown in Figure 2-40.

The ice shapes shown are based upon maintaining angle of attack (as well as other parameters) constant throughout the icing encounter. This is a reasonable assumption for current turbine aircraft which have a large power reserve at the lower speeds where icing is most likely to occur. Aircraft powered by piston engines may not have adequate power to maintain airspeed as drag

increases in icing. In this case, speed is reduced and the angle of attack is increased. Analysis of ice shapes on unprotected surfaces should consider this change in angle of attack when it is applicable.

A correlation of ice shape and drag effects with impingement parameters has been published as an SAE paper (Ref. 2-31). The report contains significant and useful data; however, the correlations shown are entirely empirical. It is believed that the correlations should be further qualified before they are used for design purposes.

REFERENCES

2-1   "The Icing Problem: Current Status of NACA Techniques and Research," Uwe H. von Glahn, NACA, presented at Ottawa AGARD Conference, 10-17 June 1955.

2-2   NACA TN 3338, "A Dye-Tracer Technique for Experimentally Obtaining Impingement Characteristics of Arbitrary Bodies and a Method for Determining Droplet Size Distribution," U. von Glahn, T. F. Gelder, W. H. Smyers, Jr., 1955.

2-3   AAFTR 5418, "A Mathematical Investigation of Water Droplet Trajectories," I. Langmuir and K. Blodgett, 19 February 1946.

2-4   NACA TN 2952, "Impingement of Water Droplets on NACA 65_1-208 and 65_1-212 Airfoils at $4°$ Angle of Attack," R. J. Brun, H. M. Gallagher and D. E. Vogt, May 1953.

2-5   NACA TN 2904 "Impingement of Water Droplets on a Cylinder in an Incompressible Flow Field and Evaluation of Rotating Multicylinder Method for Measurement of Droplet Size Distribution. Volume Median Droplet Size and Liquid Water Content." R. J. Brun and H. W. Meagler.

2-6   WADC TR 54-313. "A Design Manual for Thermal Anti-Icing Systems," H. H. Sogin. December 1954.

2-7   NACA RM 9A05. "Determination of Rate, Area and Distribution of Impingement of Waterdrops on Various Airfoils from Trajectories Obtained on the Differential Analyzer," A. G. Guibert, E. Janssen, and W. M. Robbins, 16 February 1949. Also Addendum I, University of California (unpublished), April 1949.

2-8   NACA TN 1397, "A Method for Numerically Calculating the Area and Distribution of Water Impingement on the Leading Edge of an Airfoil in a Cloud," N. R. Bergrun, August 1947.

2-9   NACA TN 3155, "Impingement of Water Droplets on NACA 65A004 Air-
       foil at 8-degree Angle of Attack," R. J. Brun, H. M. Gallagher, and
       D. E. Vogt, July 1954.

2-10   NACA Report 1215, (supersedes NACA TN 2903, TN 2904 and
       RME53D23). "Impingement of Cloud Droplets on a Cylinder and Pro-
       cedure for Measuring Liquid-Water Content and Droplet Sizes in
       Supercooled Clouds by Rotating Multicylinder Method," R. J. Brun,
       W. Lewis, P. J. Perkins, and J. S. Serafini.

2-11   WADC TR 53-284, "A Study of Heat Requirements for Anti-Icing Radome
       Shapes with Dry and Wet Surfaces," W. L. Torgeson and A. E. Abramson,
       September 1953.

2-12   NACA TN 3047, "Impingement of Water Droplets on NACA 65A004 Air-
       foil and Effect of Change in Airfoil Thickness from 12 to 4 Percent at
       4-degree Angle of Attack," R. J. Brun, H. M. Gallagher, and D. E.
       Vogt, November 1953.

2-13   NACA TN 3839, "Experimental Droplet Impingement on Several Two-
       Dimensional Airfoils with Thickness Ratios of 6 to 16 Percent," T. F.
       Gelder, W. H. Smyers, Jr., and U. von Glahn, December 1956.

2-14   NACA TN 4092, "Experimental Droplet Impingement on Four Bodies of
       Revolution," by J. P. Lewis, R. S. Ruggeri, December 1957.

2-15   NACA TN 4035, "Impingement of Cloud Droplets on 36.5 Percent Thick
       Joukowski Airfoil at Zero Angle of Attack and Discussion of Use as
       Cloud Measuring Instrument in Dye-Tracer Technique," R. J. Brun,
       D. E. Vogt, September 1957.

2-16   NACA TN 3658, "Impingement of Water Droplets on a Rectangular Half
       Body in a Two-dimensional Incompressible Flow Field," W. Lewis and
       R. J. Brun, February 1956.

2-17   NACA TN 3770, "Impingement of Droplets in 60° Elbows with Potential
       Flow," P. T. Hacker, P. G. Saper, and C. F. Kadow, October 1956.

2-18   NACA TN 3586, "Impingement of Water Droplets on NACA 65A004 Air-
       foil at Zero-degrees Angle of Attack," R. J. Brun and D. E. Vogt,
       November 1955.

2-19   NACA TN 2999, "Impingement of Droplets in 90-degree Elbows with
       Potential Flow." P. T. Hacker, R. J. Brun, and B. Boyd, September
       1953.

2-20   NACA TN 3099, "Impingement of Water Droplets on an Ellipsoid with
        Fineness Ratio 5 in Axisymmetric Flow," R. G. Dorsch, R. J. Brun,
        and J. L. Gregg, March 1954.

2-21   NACA TN 3587, "Impingement of Water Droplets on a Sphere," R. G.
        Dorsch, P. G. Saper, and C. F. Kadow, November 1955.

2-22   NACA TN 3147, "Impingement of Water Droplets on an Ellipsoid with
        Fineness Ratio 10 in Axisymmetric Flow," R. J. Brun and R. G. Dorsch,
        May 1954.

2-23   NA-63-303, "Use of the K_0 Correlation in Preliminary Design and Scale
        Model Icing," Frederick R. Weiner, North American Aviation, Inc.
        (Presented at Spring Meeting of Aircraft Air-Conditioning Forum, Los
        Angeles, California, March 21, 1963).

2-24   "Principles of Aerodynamics," J. H. Dewinnell, McGraw-Hill, 1949.

2-25   NACA TN 2931, "A Method for Determining Cloud-Droplet Impingement
        on Swept Wings," R. G. Dorsch and R. J. Brun, April 1953.

2-26   "Theory of Flight," R. von Mises. McGraw-Hill, 1945.

2-27   "Equilibrium Temperature of an Unheated Surface as a Function of
        Airspeed," b. L Messinger, Journal of Aeronautical Sciences,
        January 1953 (Vol. 20, No. 1).

2-28   AEL 1206, "An Analysis of the Effects of Certain Variables in Deter-
        mining the Form of an Ice Accretion," T. A. Dickey (presented at Mt.
        Washington Spring Planning Conference, April 1952, Aeronautical
        Engineering Laboratory, Naval Air Experimental Station, 29 May 1952).

2-29   NACA TN 4151, "Correlations Among Ice Measurements, Impingement
        Rates, Icing Conditions and Drag Coefficients for Unswept NACA
        65A004 Airfoil," V. H. Gray, February 1958.

2-30   NACA TN 3564, "Effects of Pneumatic De-Icer and Ice Formations on
        Aerodynamic Characteristics of an Airfoil," D. T. Bowden, February
        1956.

2-31   "Correlation of Airfoil Ice Formations and Their Aerodynamic Effects
        With Impingement and Flight Conditions," V. H. Gray, (paper presented
        at SAE National Aeronautics Meeting, October 1957.

Table 2-1. Rate of Water Catch Formulas

		Water Catch Rate
Airfoil	$W_M = 0.379\, U_o\, W_t\, C(\frac{h}{C})\, E_M$	lb./hr.-ft.-span
Cylinder	$W_M = 0.379\, U_o\, W_t\, D\, E_M$	lb./hr.-ft.-span
Ribbon	$W_M = 0.379\, U_o\, W_t\, b\, E_M$	lb./hr.-ft.-span
Semi-infinite rectangle	$W_M = 0.379\, U_o\, W_t\, b\, E_M$	lb./hr.-ft. span
Ellipsoids (10%, 20%)	$W_Z = 0.379\, U_o\, W_t\, A_F\, E_M$	lb./hr.
Ellipsoids (A/B = 2, 3, 5)	$W_Z = 0.379\, U_o\, W_t\, A_F\, E_M$ *	lb./hr.
Sphere	$W_Z = 0.379\, U_o\, W_t\, A_F\, E_M$	lb./hr.
Cone	$W_Z = 0.379\, U_o\, W_t\, A_F\, E_M$	lb./hr.
Elbow	$W_Z = 0.379\, U_o\, W_t\, A_F\, E_M$ **	lb./hr.

* $A_F = \dfrac{\pi\, \text{radius}^2}{4}$ ($\alpha = 0°$)

** $A_F = \dfrac{\pi\, L_{eb} \times \text{depth}}{4}$ (width $= \dfrac{\pi\, L_{eb}}{4}$)

Table 2-2. Characteristic Length (in feet) for K_o

		Data Source
Airfoil	Chord, C	All airfoil data
Cylinder	Radius, D/2	NACA Rpt. 121$\overline{0}$
Ribbons	Half width, b/2	AAFTR 5418
Semi-infinite rectangle	Half width	NACA TN 36$\overline{0}$8
Ellipsoids (10%, 20%) A/B = 10, 5	Body length. L_{el}	NACA TN 3099, 3147
Ellipsoids (A/B = 2, 3, 5)	Half body length, $L_{el}/2$	WADC TR 53-284
Cones	Cone length, ft.	WADC TR 53-284
Elbow	Arbitrary length, L_{eb} proportional to elbow size *	NACA TN 2999, 3770

* Elbow entrance width is $\dfrac{\pi L_{eb}}{4}$, so that $L_{eb} = \dfrac{4 \times \text{entrance width}}{\pi}$

2-$\overline{0}$3

Table 2-3. Langmuir Droplet Size Distributions

Liquid Water Content Per Cent	TYPE	A	B	C	D	E
5		1.0	0.56	0.42	0.31	0.23
10		1.0	0.72	0.61	0.52	0.44
20		1.0	0.84	0.77	0.71	0.65
30		1.0	1.00	1.00	1.00	1.00
20		1.0	1.17	1.26	1.37	1.48
10		1.0	1.32	1.51	1.74	2.00
5		1.0	1.49	1.81	2.22	2.71

From Reference 2-3.

Table 2-4.   Values of $C_D \text{Re},d/24$ and λ/λ_s as Functions of Re,d

Re,d	$C_D \text{Re},d/24$	λ/λ_s	Re,d	$C_D \text{Re},d/24$	λ/λ_s
0.00	1.00	1.00	200	6.52	0.2668
0.05	1.009	0.9956	250	7.38	0.2424
0.1	1.018	0.9911	300	8.26	0.2234
0.2	1.037	0.9832	350	9.00	0.2080
0.4	1.073	0.9652	400	9.82	0.1953
0.6	1.103	0.9493	500	11.46	0.1752
0.8	1.142	0.9342	600	12.97	0.1597
1.0	1.176	0.9200	800	15.81	0.1375
1.2	1.201	0.9068	1000	18.62	0.1215
1.4	1.225	0.8950	1200	21.3	0.1097
1.6	1.248	0.8842	1400	24.0	0.1003
1.8	1.267	0.8744	1600	26.9	0.0927
2.0	1.285	0.8653	1800	29.8	0.0863
2.5	1.332	0.8452	2000	32.7	0.0809
3.0	1.374	0.8273	2500	40.4	0.0703
3.5	1.412	0.8120	3000	47.8	0.0624
4.0	1.447	0.7978	3500	55.6	0.0562
5.0	1.513	0.7734	4000	63.7	0.0513
6.0	1.572	0.7527	5000	80.0	0.0439
8.0	1.678	0.7185	6000	96.8	0.0385
10	1.782	0.6905	8000	130.6	0.0311
12	1.901	0.660	10000	166.3	0.0262
14	2.009	0.6440	12000	204	
16	2.109	0.6242	14000	243	
18	2.198	0.6065	16000	285	
20	2.291	0.5904	18000	325	
25	2.489	0.5562	20000	365	
30	2.673	0.5261	25000	470	
35	2.851	0.5045	30000	574	
40	3.013	0.4840	35000	674	
50	3.327	0.4505	40000	778	
60	3.60	0.4237	50000	980	
80	4.11	0.3829	60000	1175	
100	4.59	0.3524	80000	1552	
120	5.01	0.3285	$1.0 \cdot 10^5$	1905	
140	5.40	0.3090	$1.2 \cdot 10^5$	2234	
160	5.76	0.2928	$1.4 \cdot 10^5$	2549	
180	6.16	0.2789	$1.6 \cdot 10^5$	2851	

WADC TR 54-313
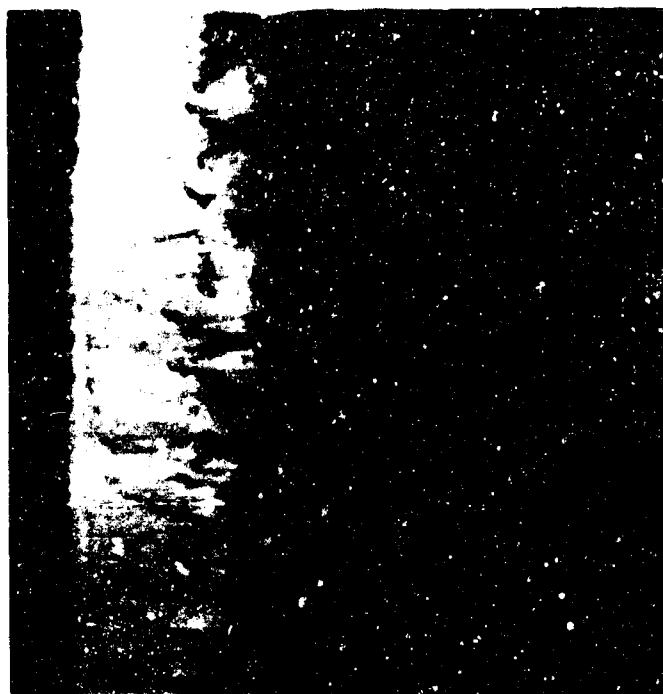
↑ LeadingEdge

a. Rime Ice, datum air temperature, 0° F
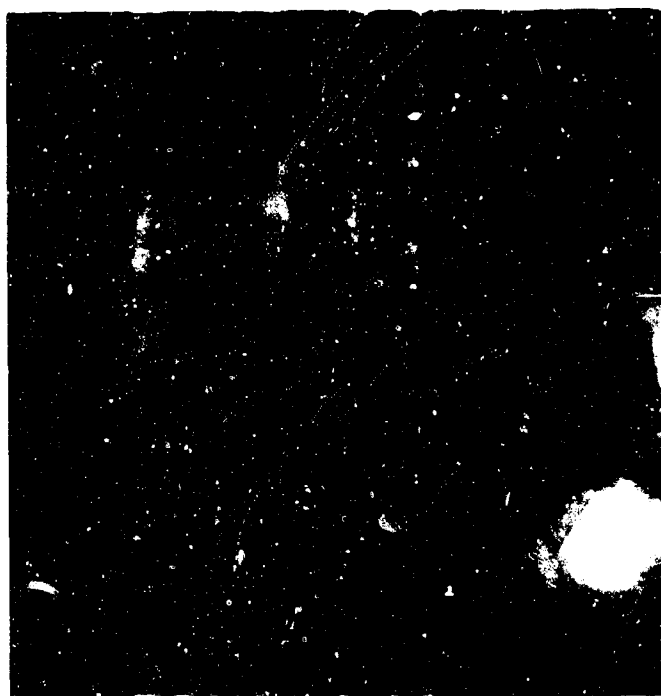
↑ Leading edge

b. Double-peak glaze ice, datum air temperature, 30° F; High rate of water catch

Figure 2-1.   Typical Ice Formations on an Airfoil

S_U = Upper Surface Impingement Limit
S_L = Lower Surface Impingement Limit
$E_m = (y_{o_u} - y_{o_\ell})/h$
h = Projected Height of Airfoil
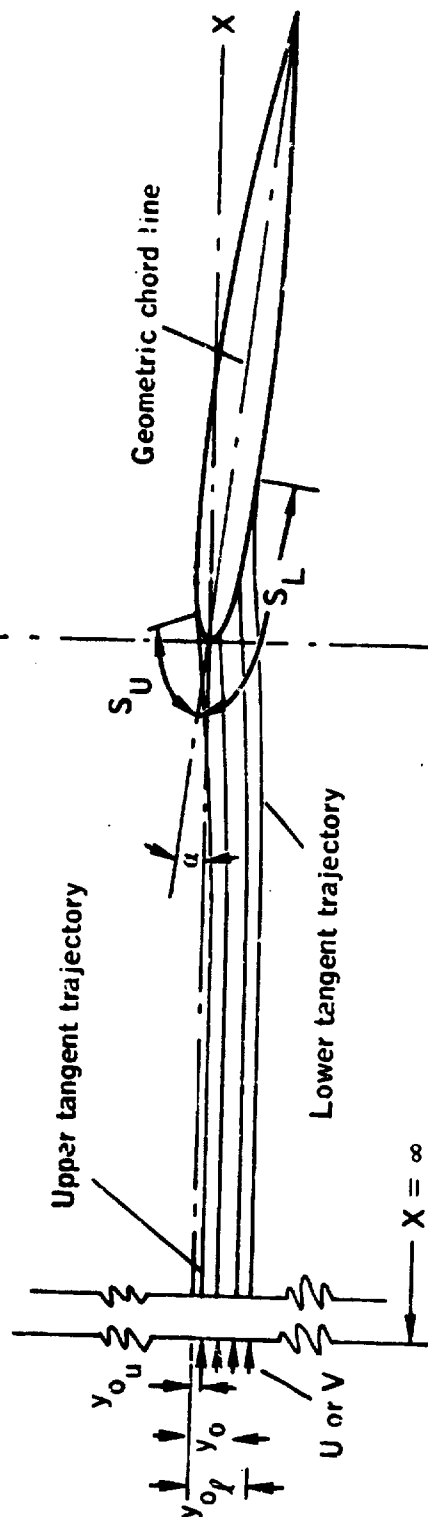
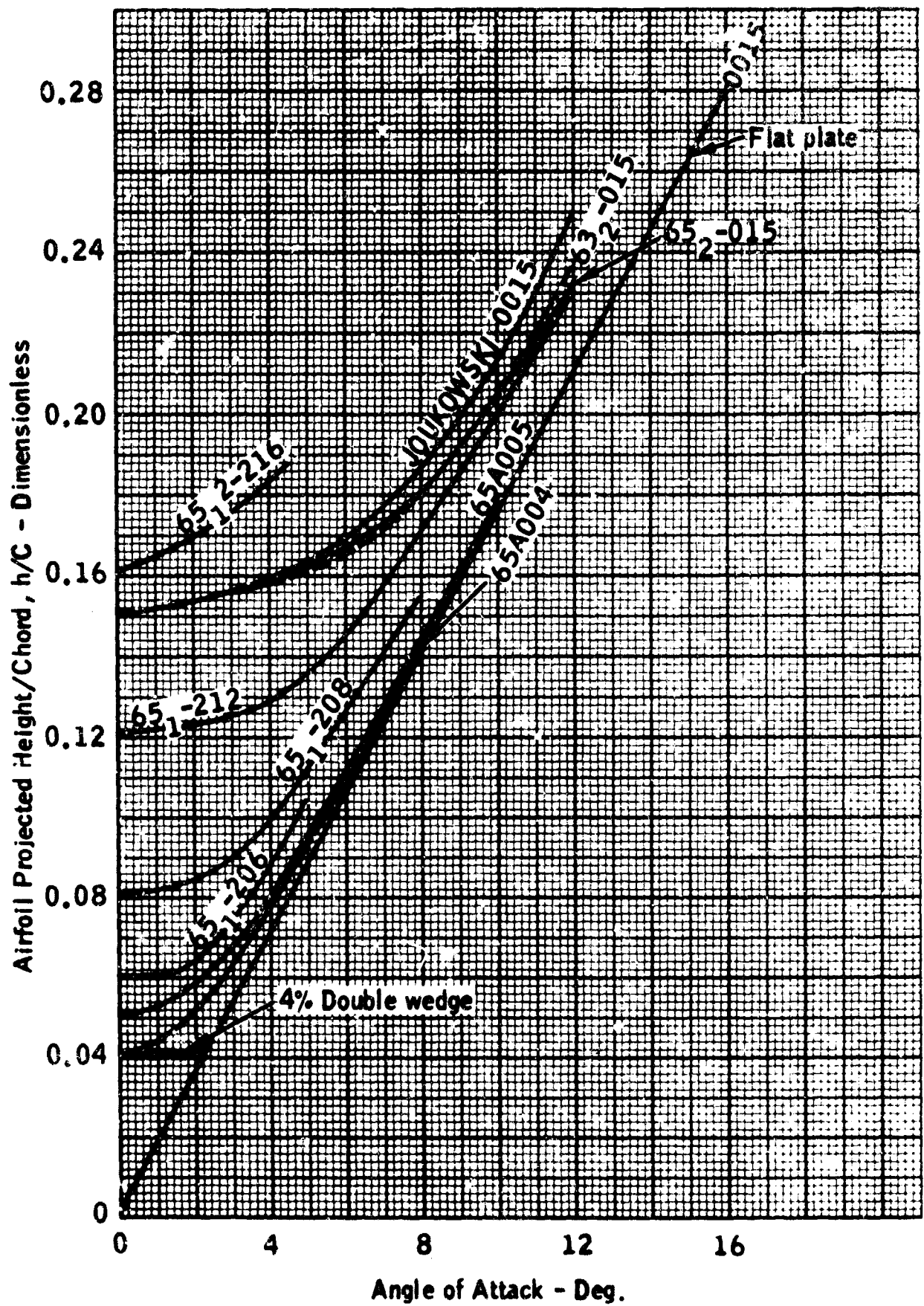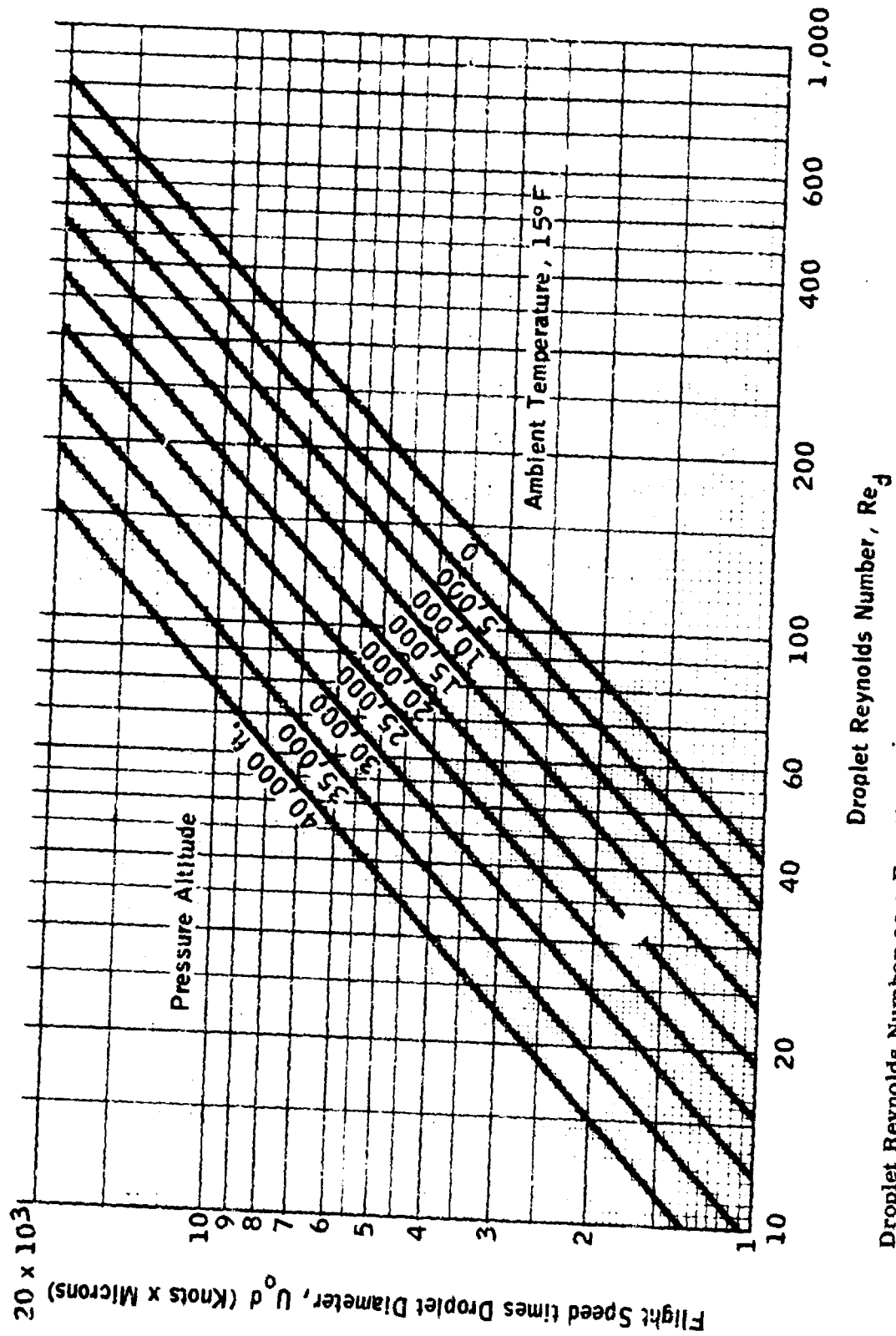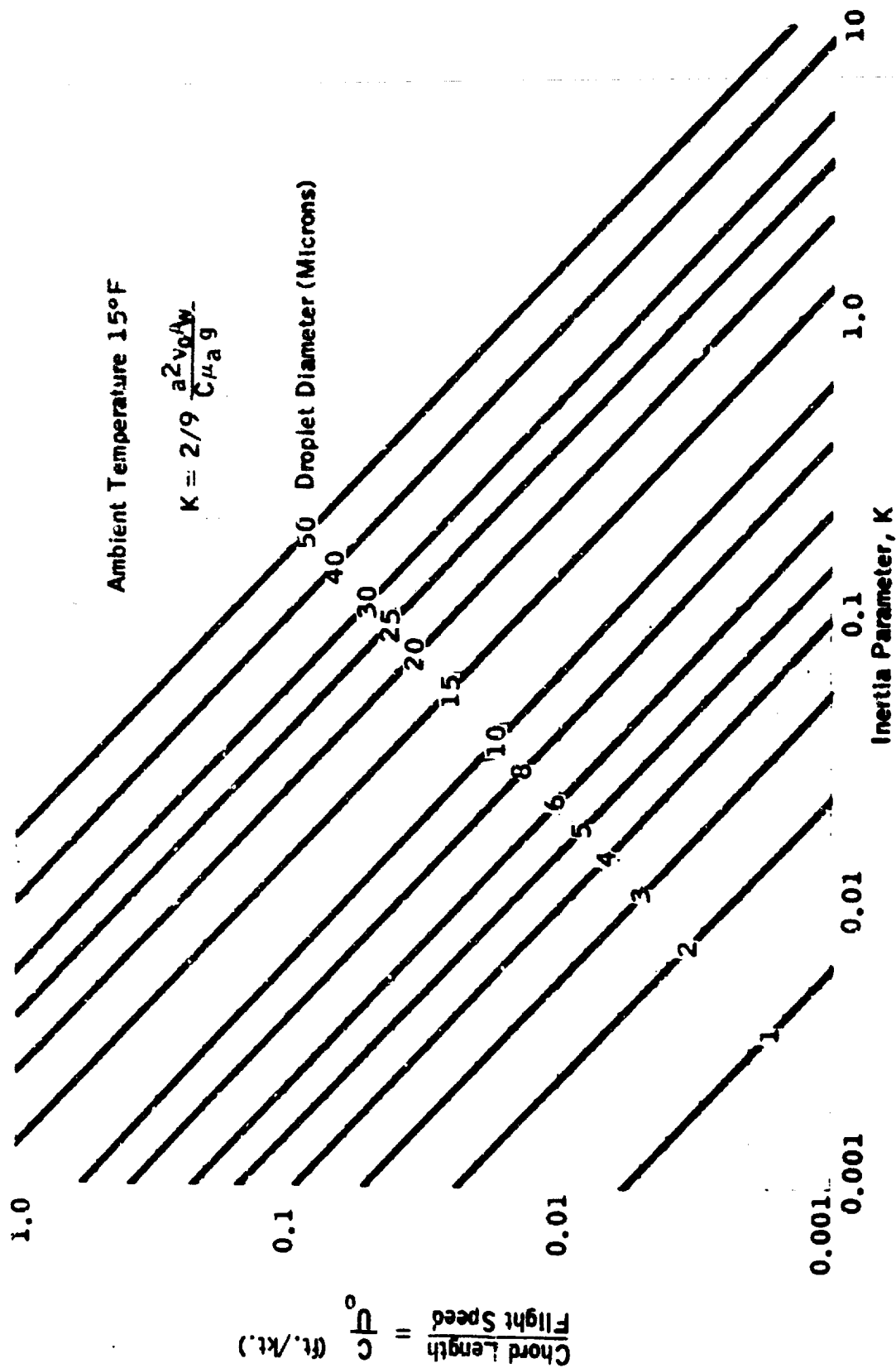Water Droplet Trajectory in an Airfoil Flow Field and Illustration of Impingement Terminology (From NACA TN 2952, Ref. 2-4).

Figure 2-2

Figure 2-3. Projected Height of Several Airfoils Plotted Versus Angle of Attack.

2-38

Droplet Reynolds Number as a Function of Flight Speed. Droplet Diameter and Altitude.

Figure 2-4

2-39

Figure 2-5

2-40
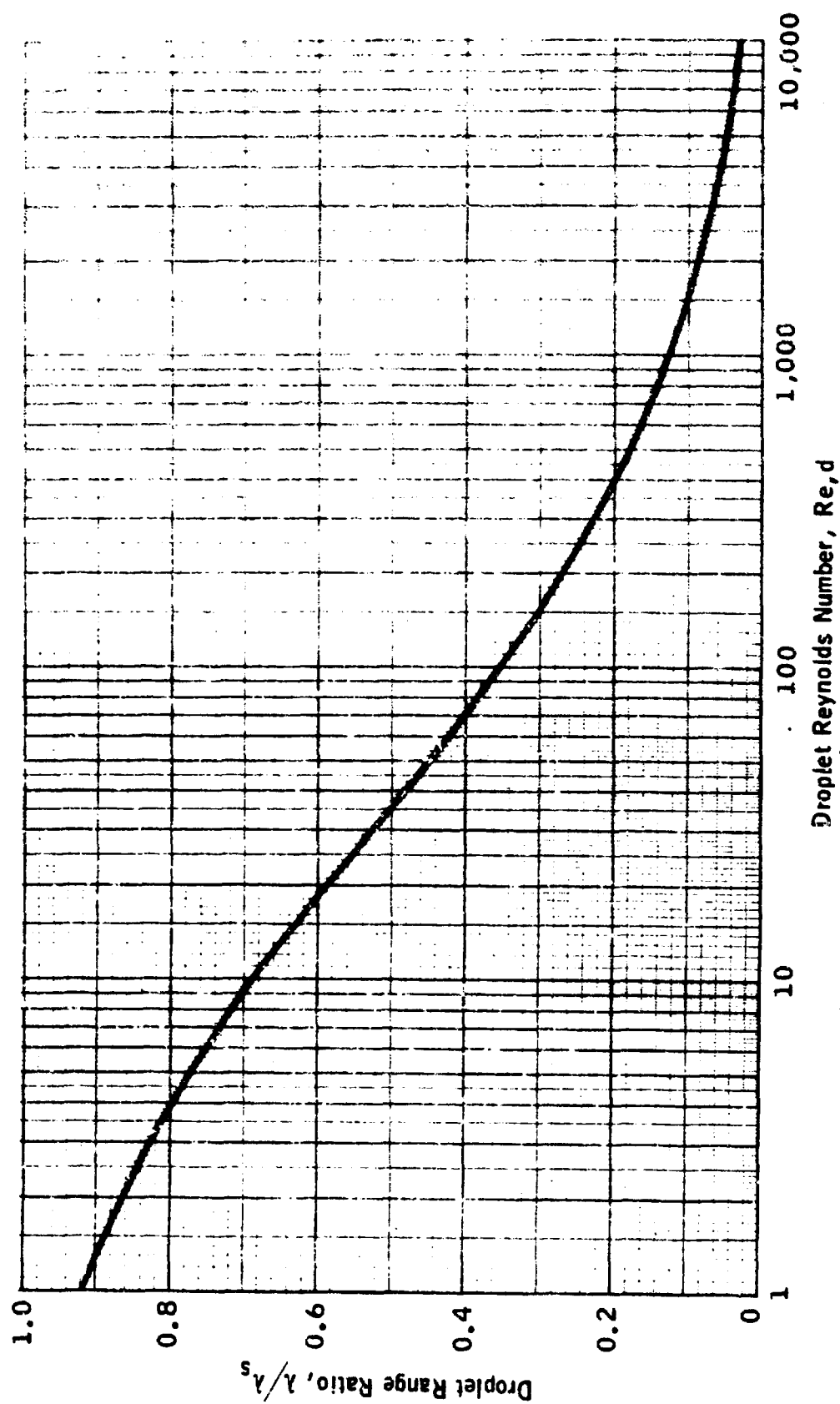
Droplet Range Ratio, λ/λ_B, as a Function of Droplet Reynolds Number.

Figure 2-6

2-41
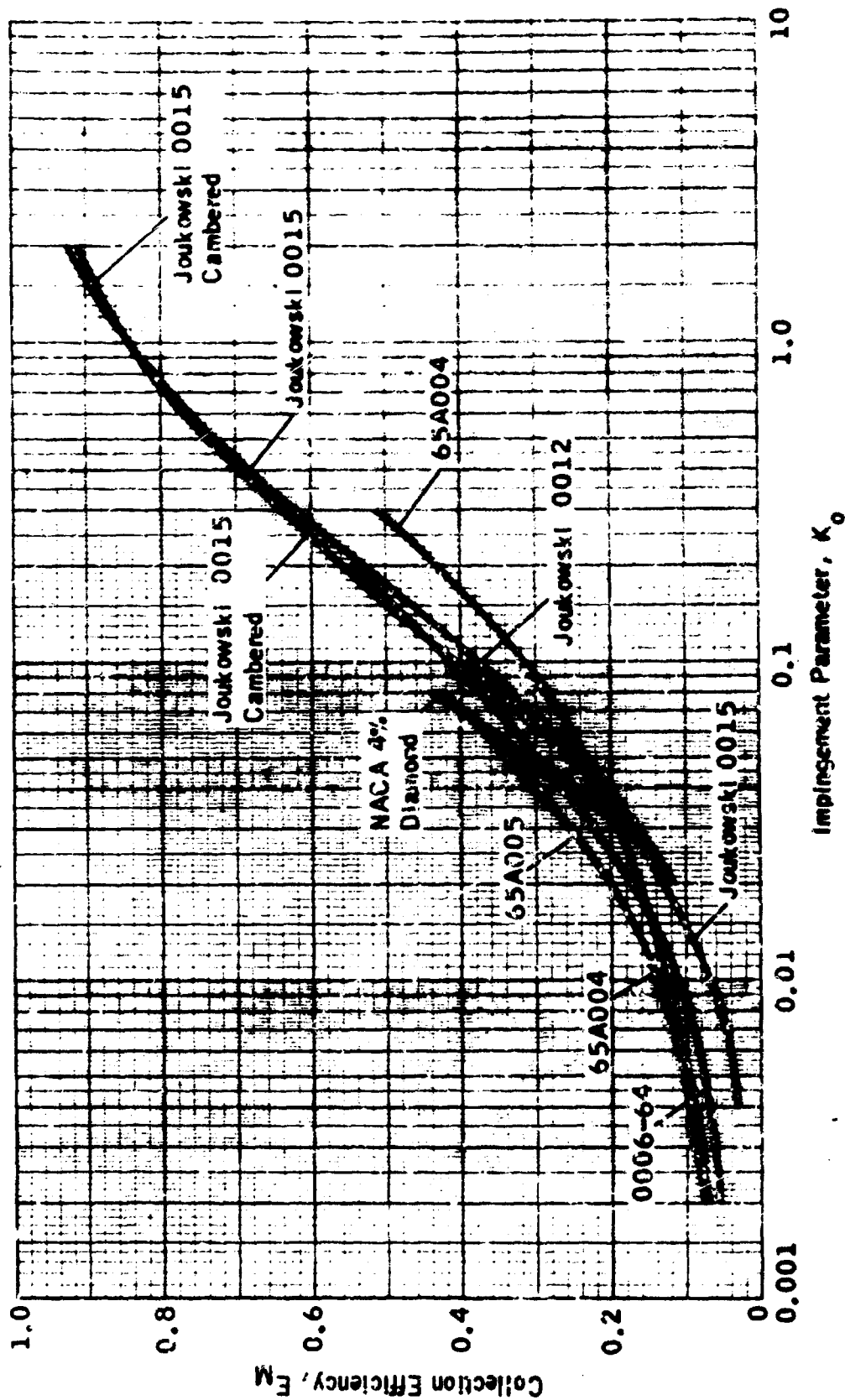
Collection Efficiency Versus K_o for Airfoils — Theoretical Data at 0° Angle of Attack.

Figure 2-7

2-42
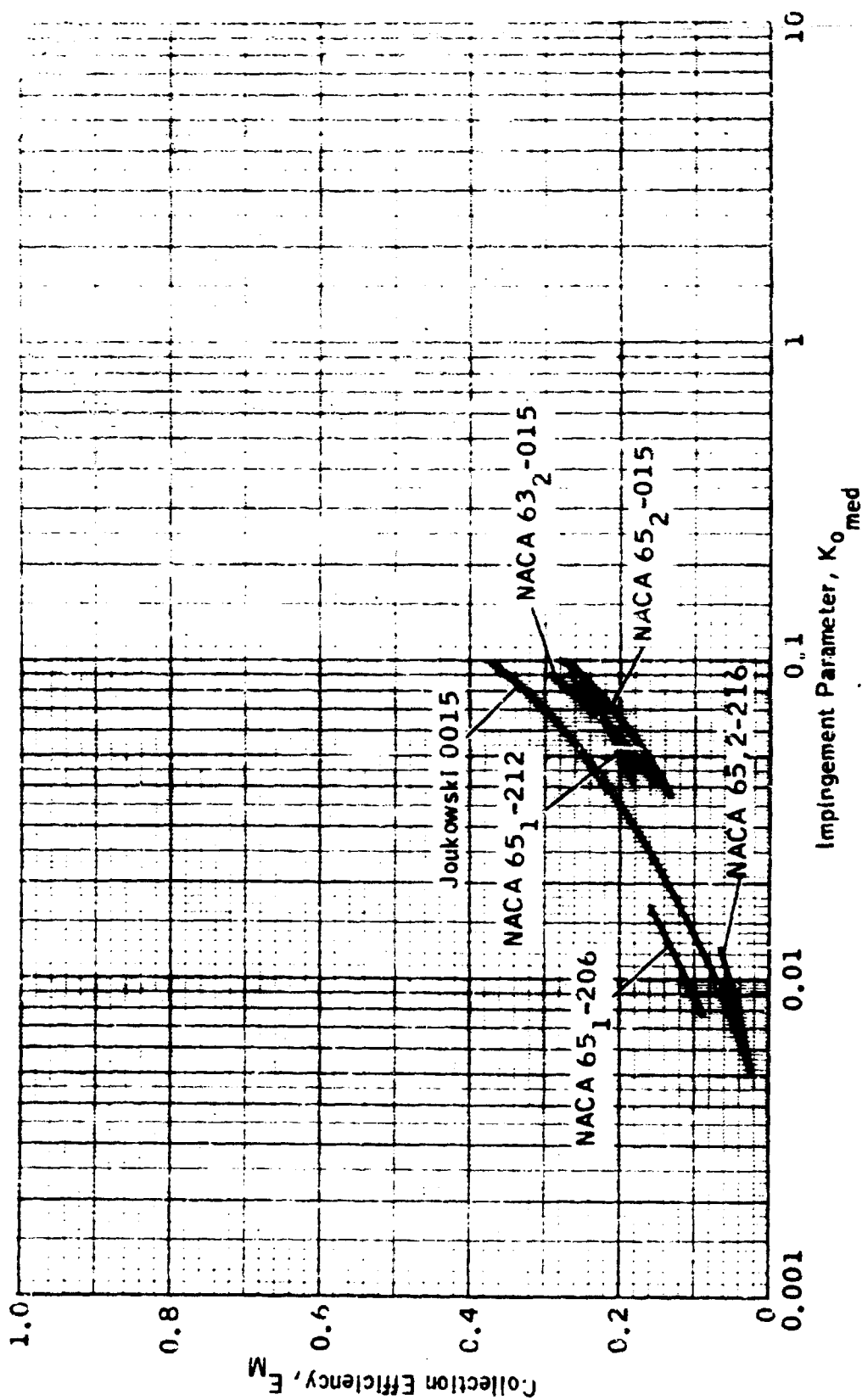
Collection Efficiency versus $K_{o_{med}}$ for Airfoils — Experimental Data at 0° Angle of Attack.

Figure 2-8

2-43

Collection Efficiency Versus K_o for Airfoils — Theoretical and Experimental Data for 2° Angle of Attack.
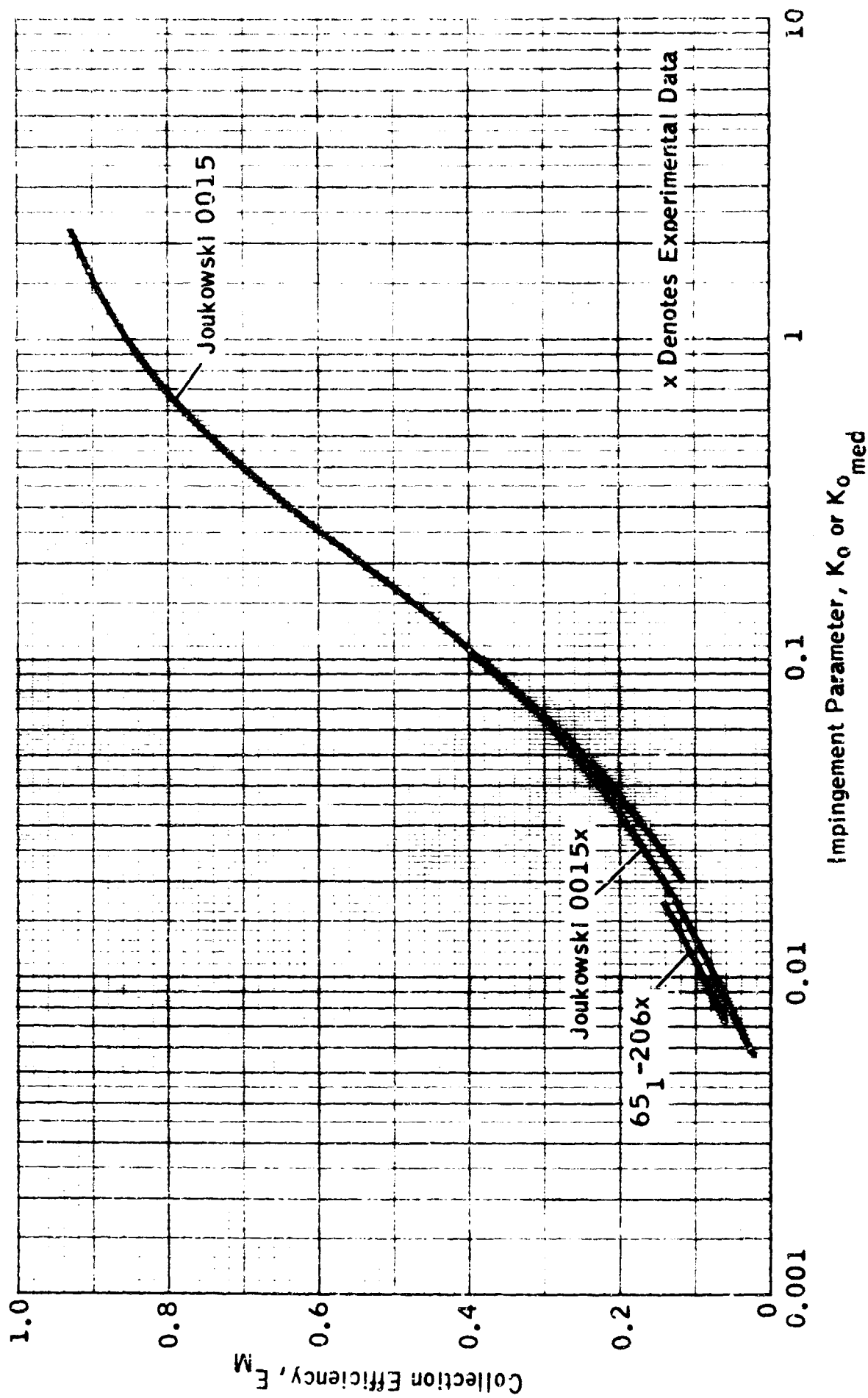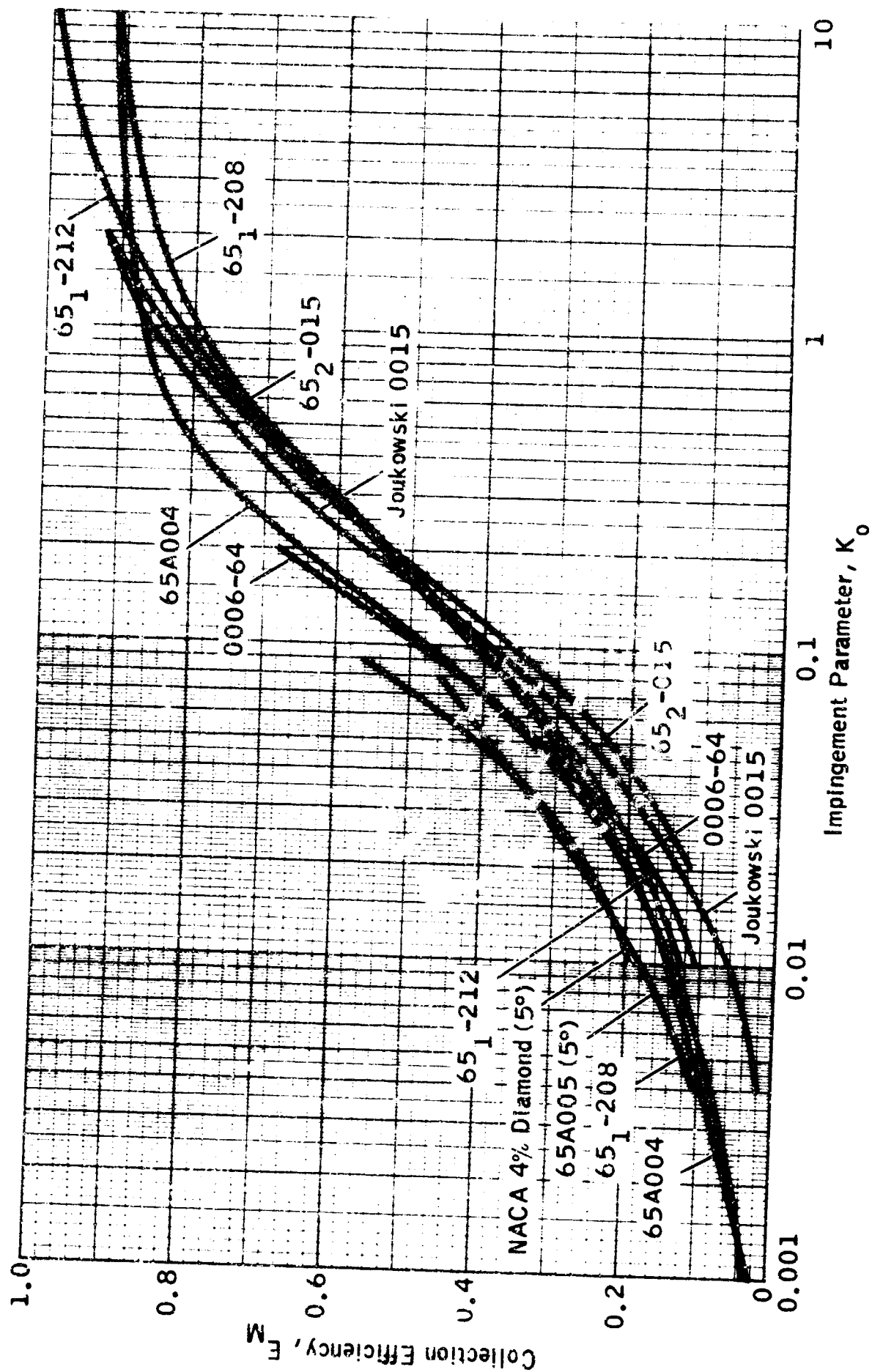
Figure 2-9

Collection Efficiency Versus K_O for Airfoils — Theoretical Data for 4° Angle of Attack (and 5°, Where Noted).

Figure 2-10

Collection Efficiency Versus $K_{O_{med}}$ for Airfolls — Experimental Data for 4° Angle of Attack.
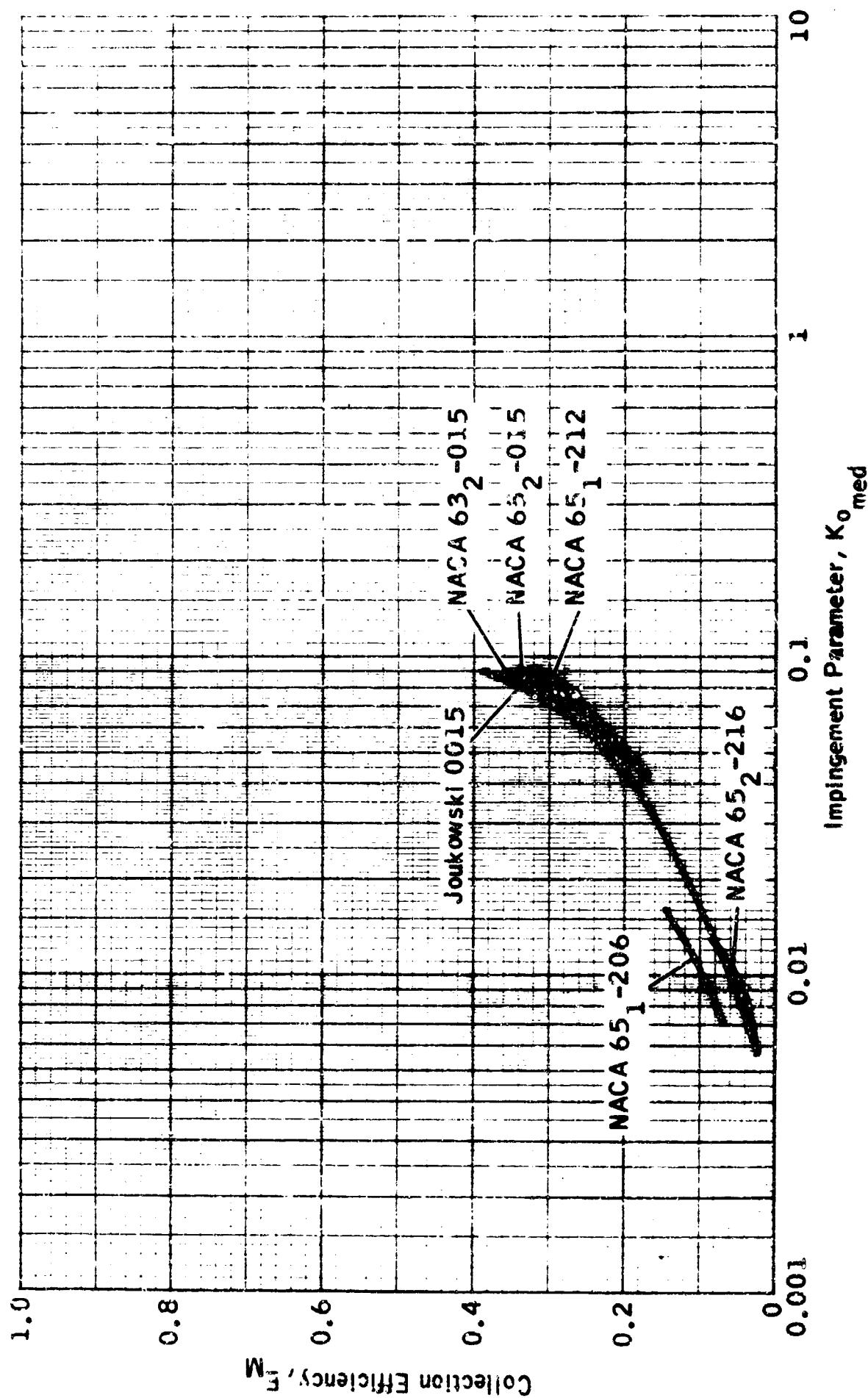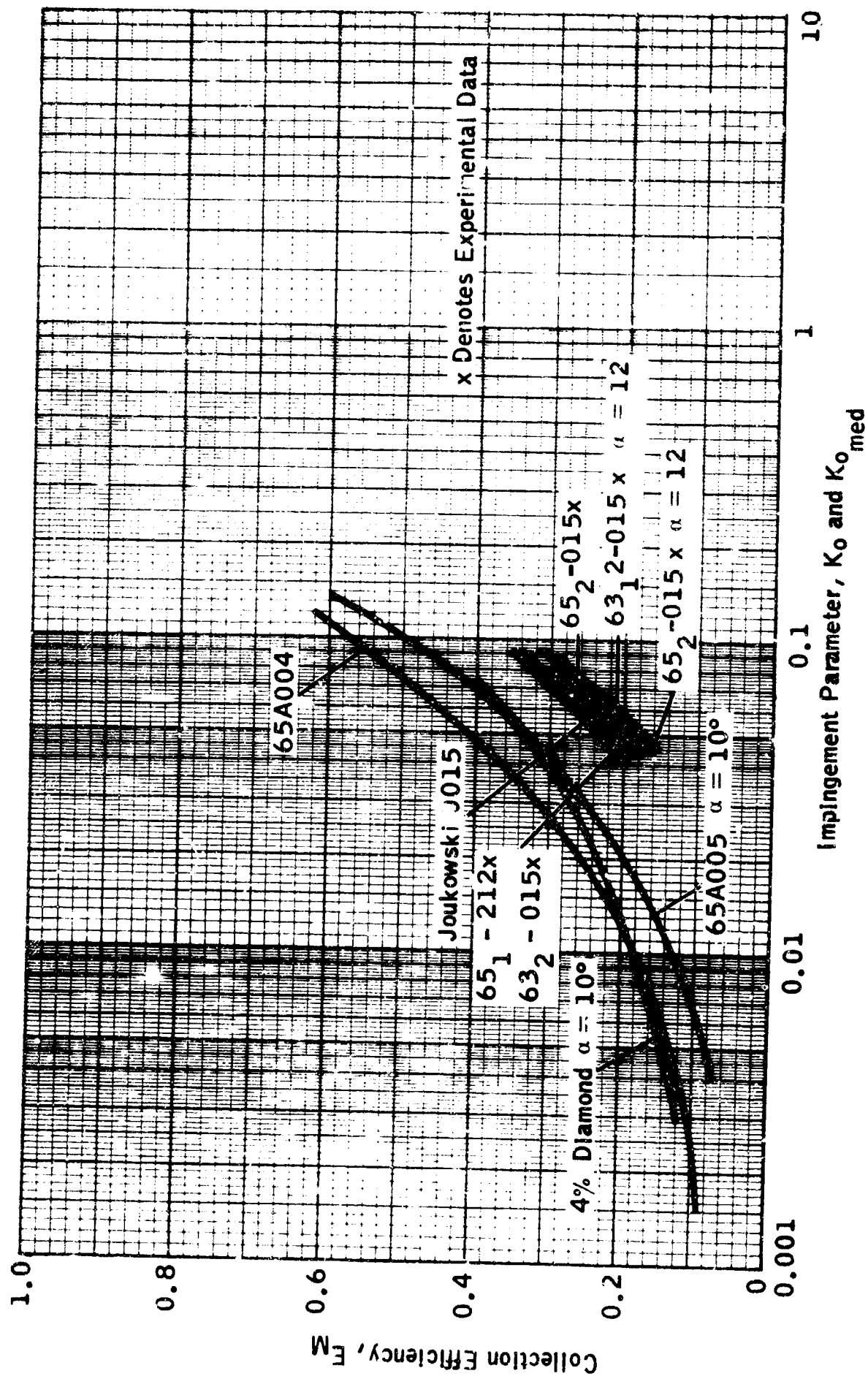
Figure 2-11

Collection Efficiency Versus K_o for Airfoils — Theoretical and Experimental Data for 8° Angle of Attack (and 10°, Where Noted)

Figure 2-12

Collection Efficiency Versus K_o for Geometric Bodies — Theoretical Data for 0° Angle of Attack.
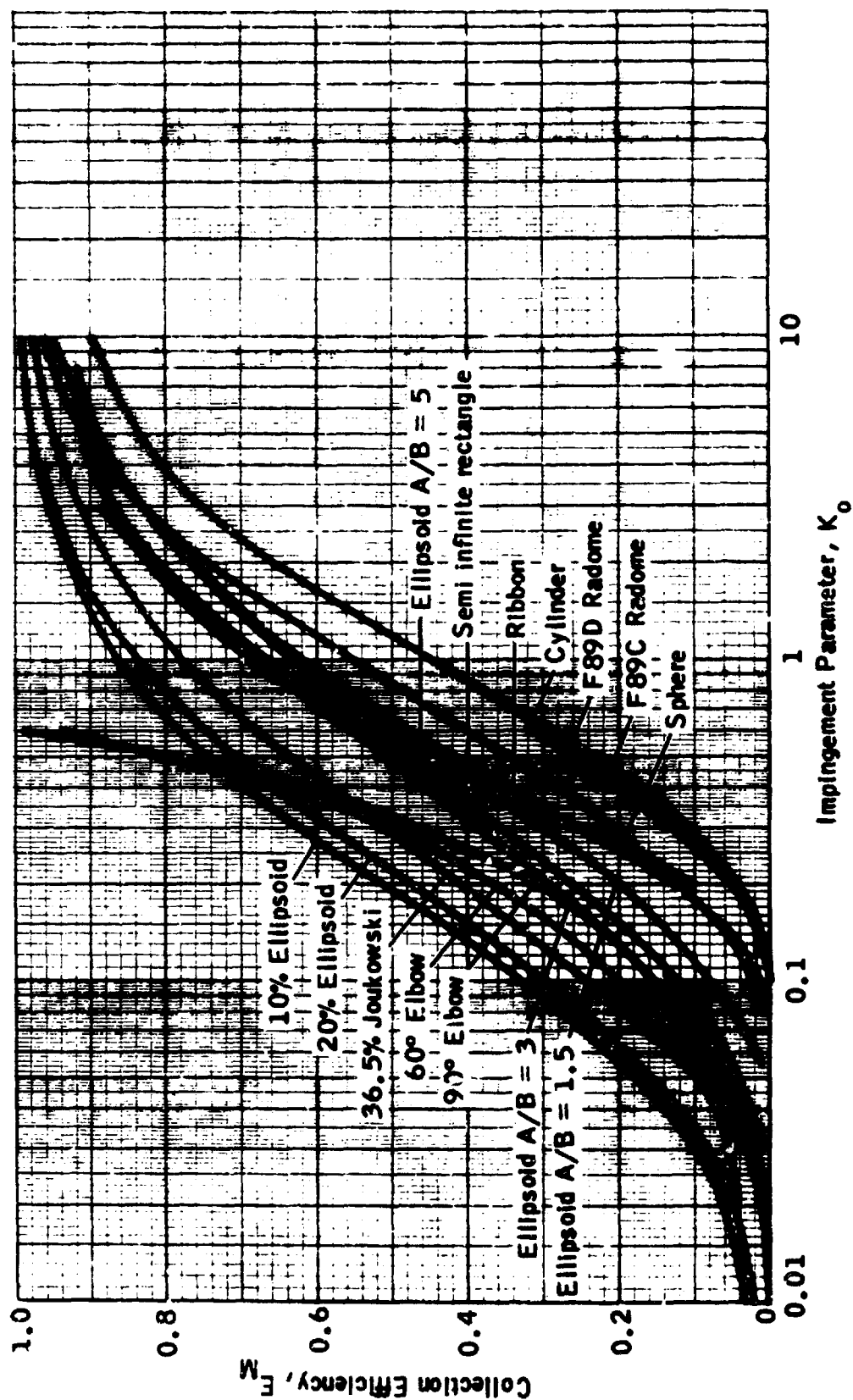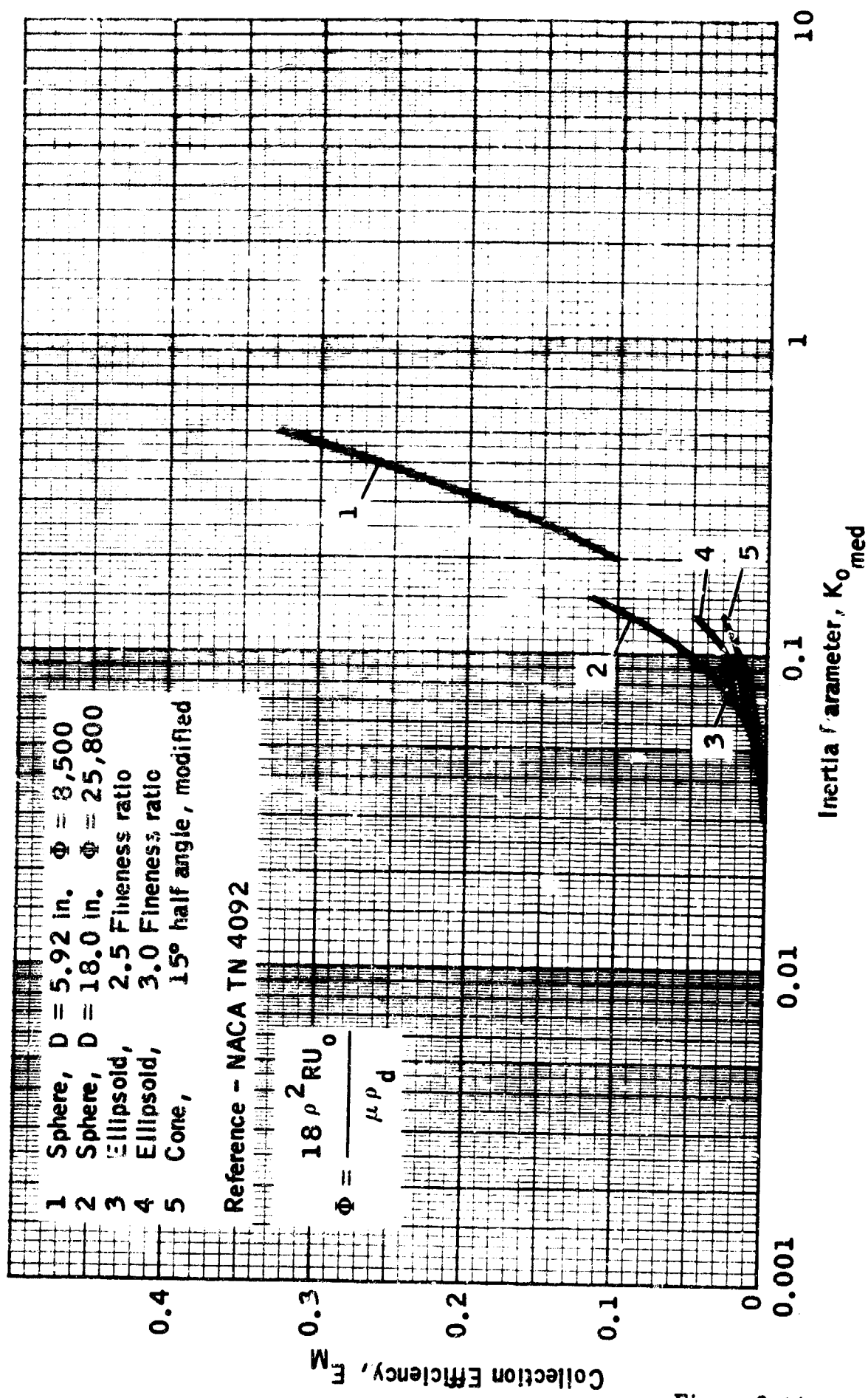
Figure 2-13

Collection Efficiency Versus $K_{o_{med}}$ for Geometric Bodies — Experimental Data for 0° Angle of Attack.

Figure 2-14

2-49
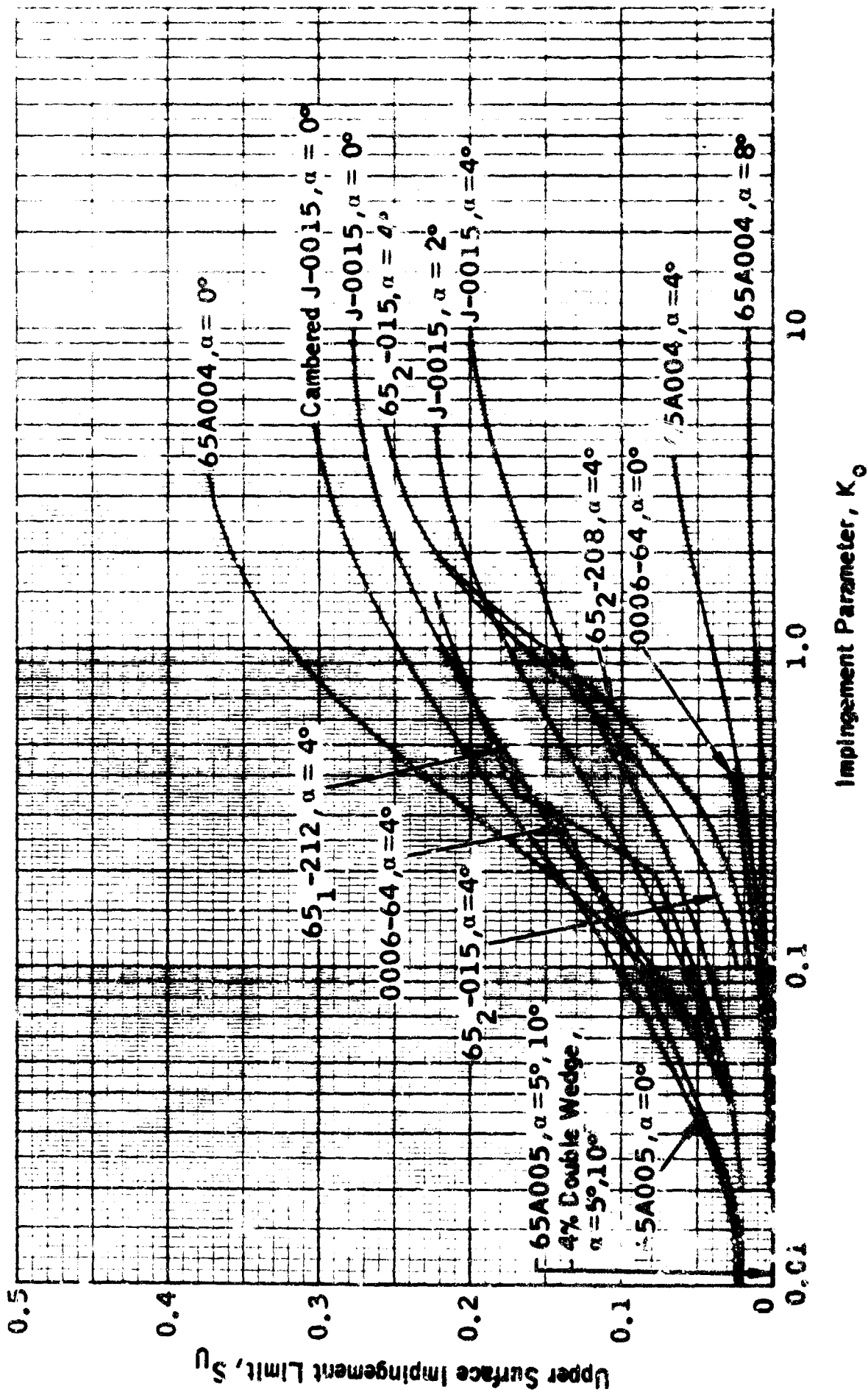
Impingement Limit on the Upper Surface of Several Airfoils Versus K_o for 0, 2, 4, 5, 8 and 10°
Angle of Attack (Theoretical Data).

Figure 2-15
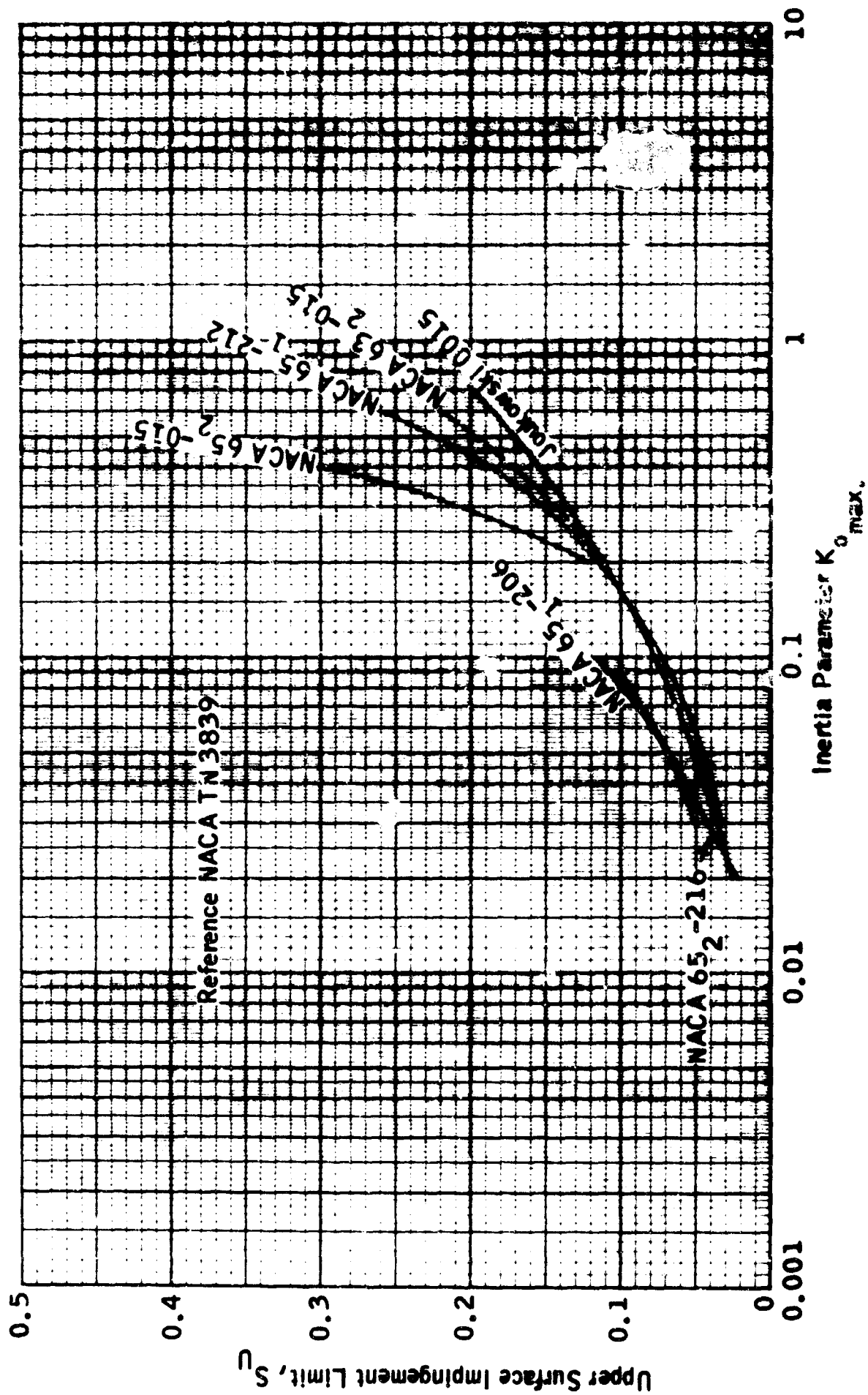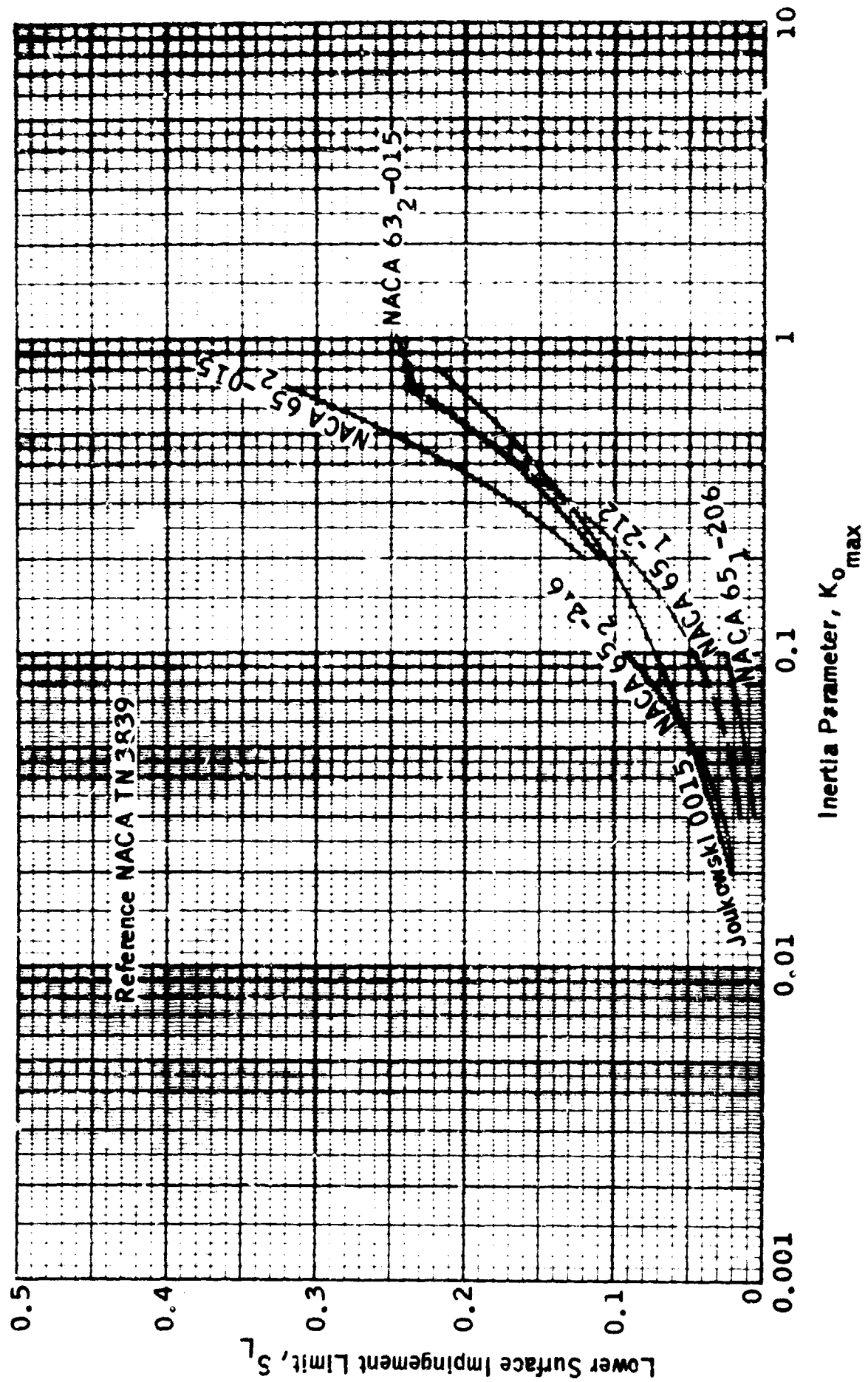
Impingement Limit on the Lower Surfaces of Several Airfoils Versus K_o for 0, 2, 4, 5, 8 and 10°
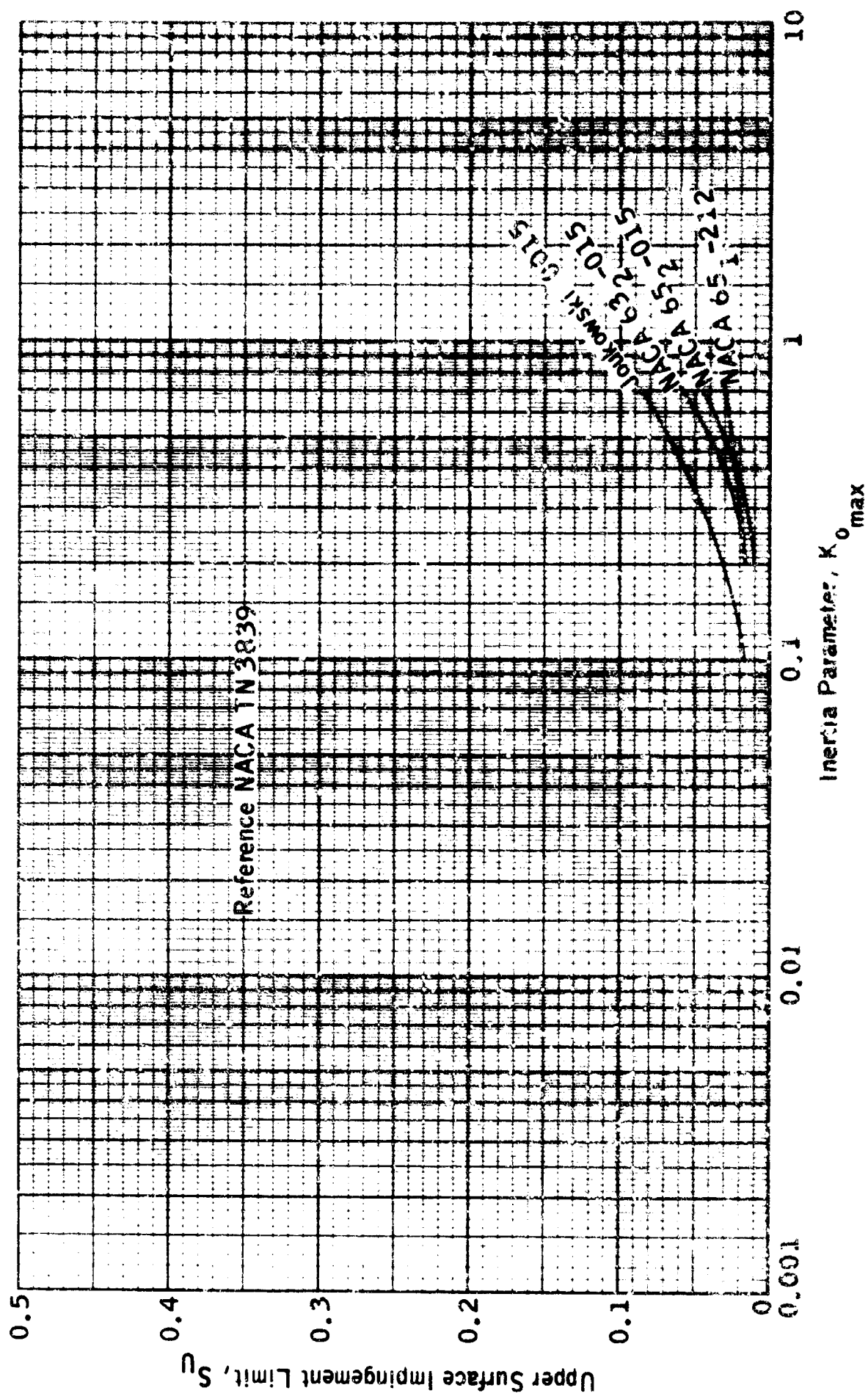Angle of Attack (Theoretical Data).

Figure 2-16

Figure 2-17

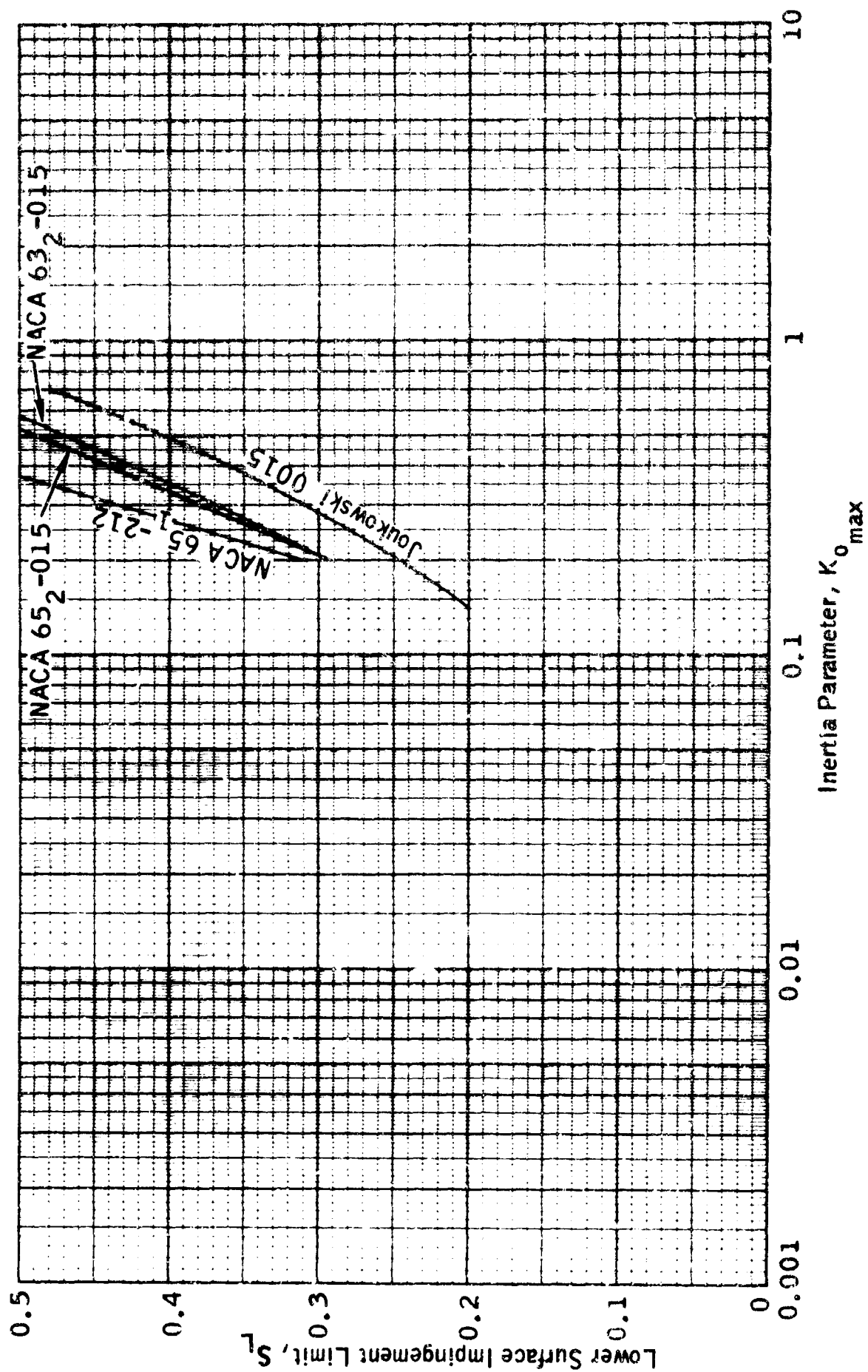Upper Surface Impingement Limits for Several Airfoils at 0° Angle of Attack (Experimental Data).

Lower Surface Impingement Limits for Several Airfoils at $0°$ Angle of Attack. (Experimental Data).
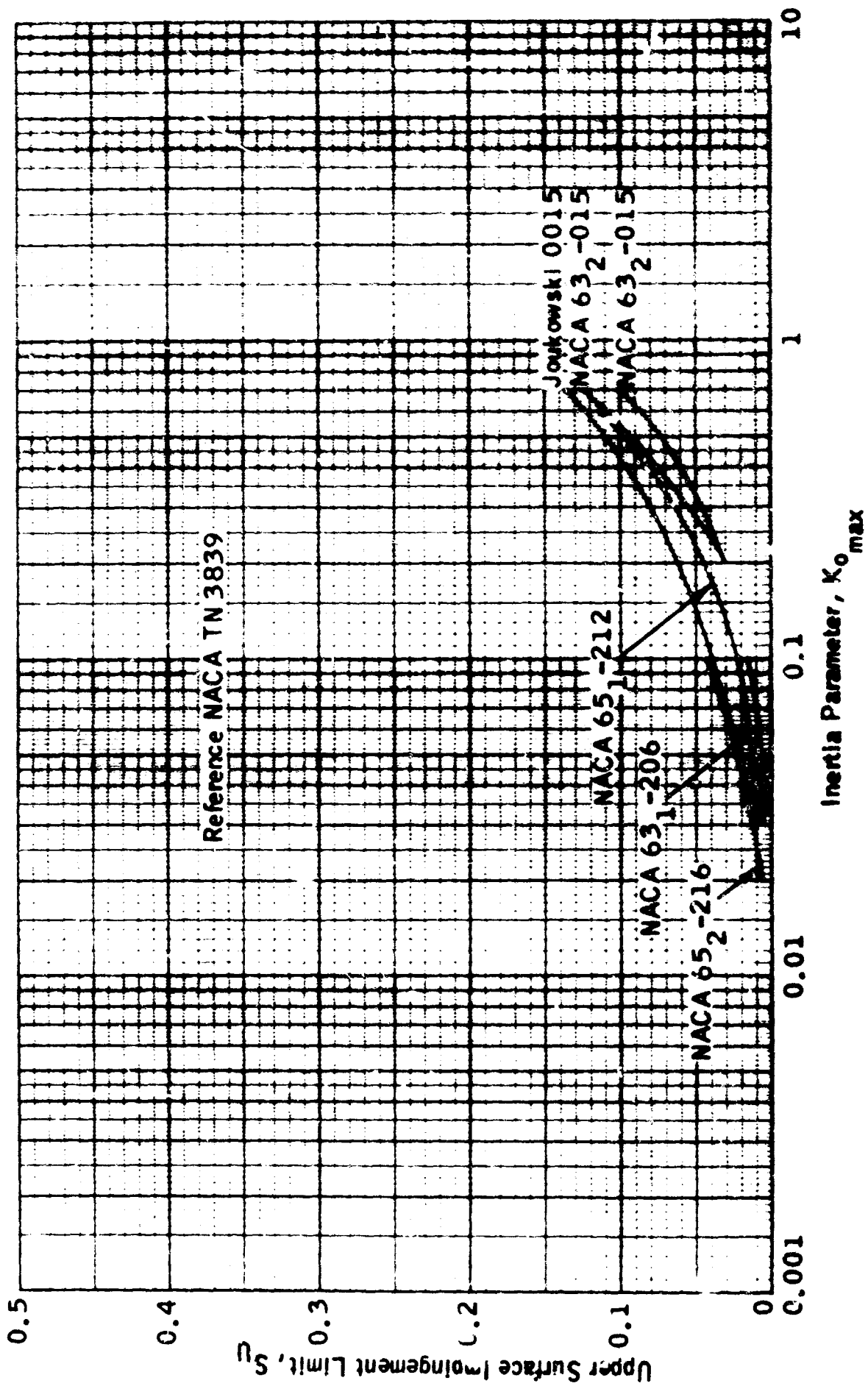
Figure 2-18

Figure 2-19. Upper Surface Impingement Limits for Several Airfoils at 4° Angle of Attack (Experimental Data).
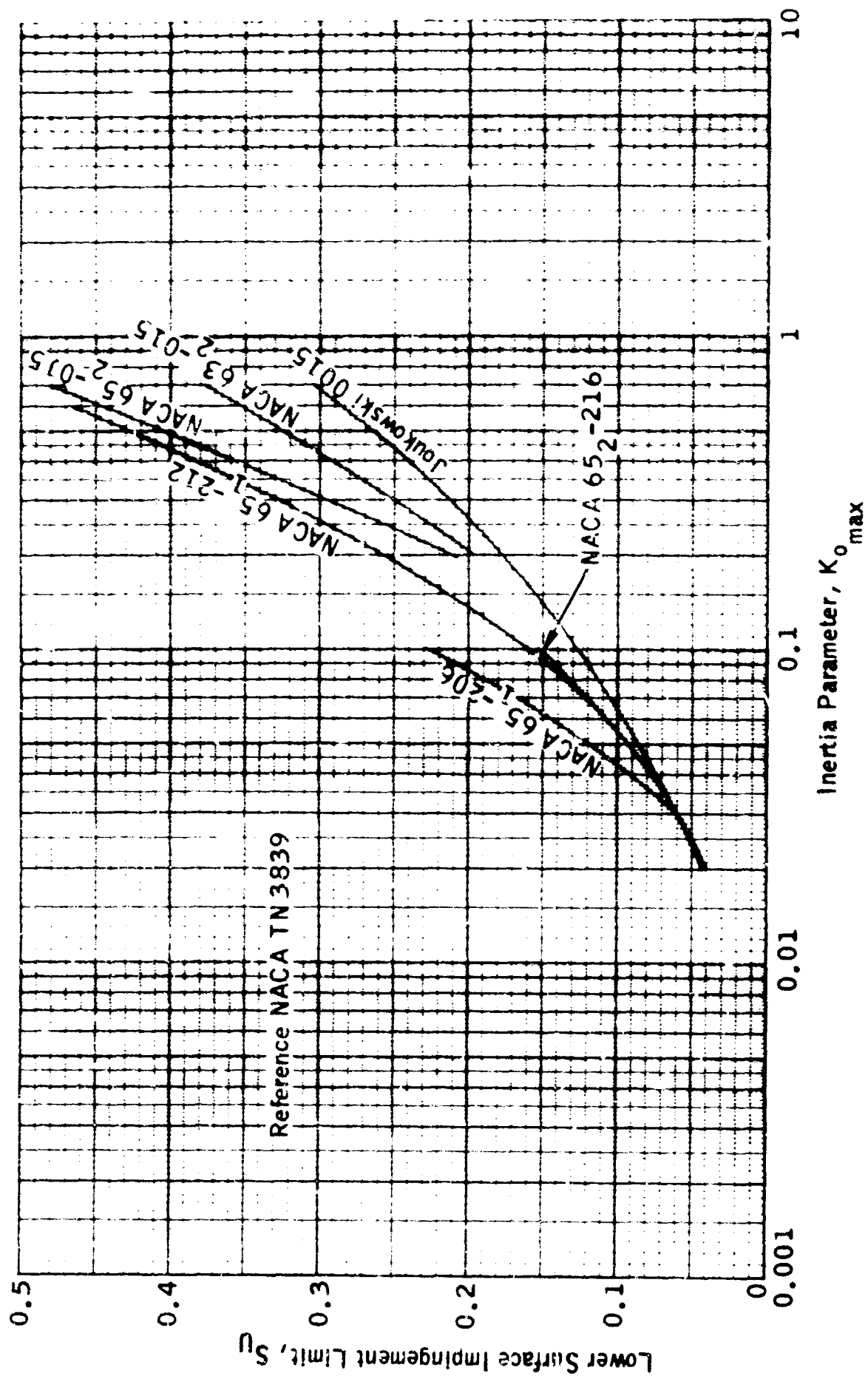
Lower Surface Impingement Limits for Several Airfoils at 4° Angle of Attack (Experimental Data).
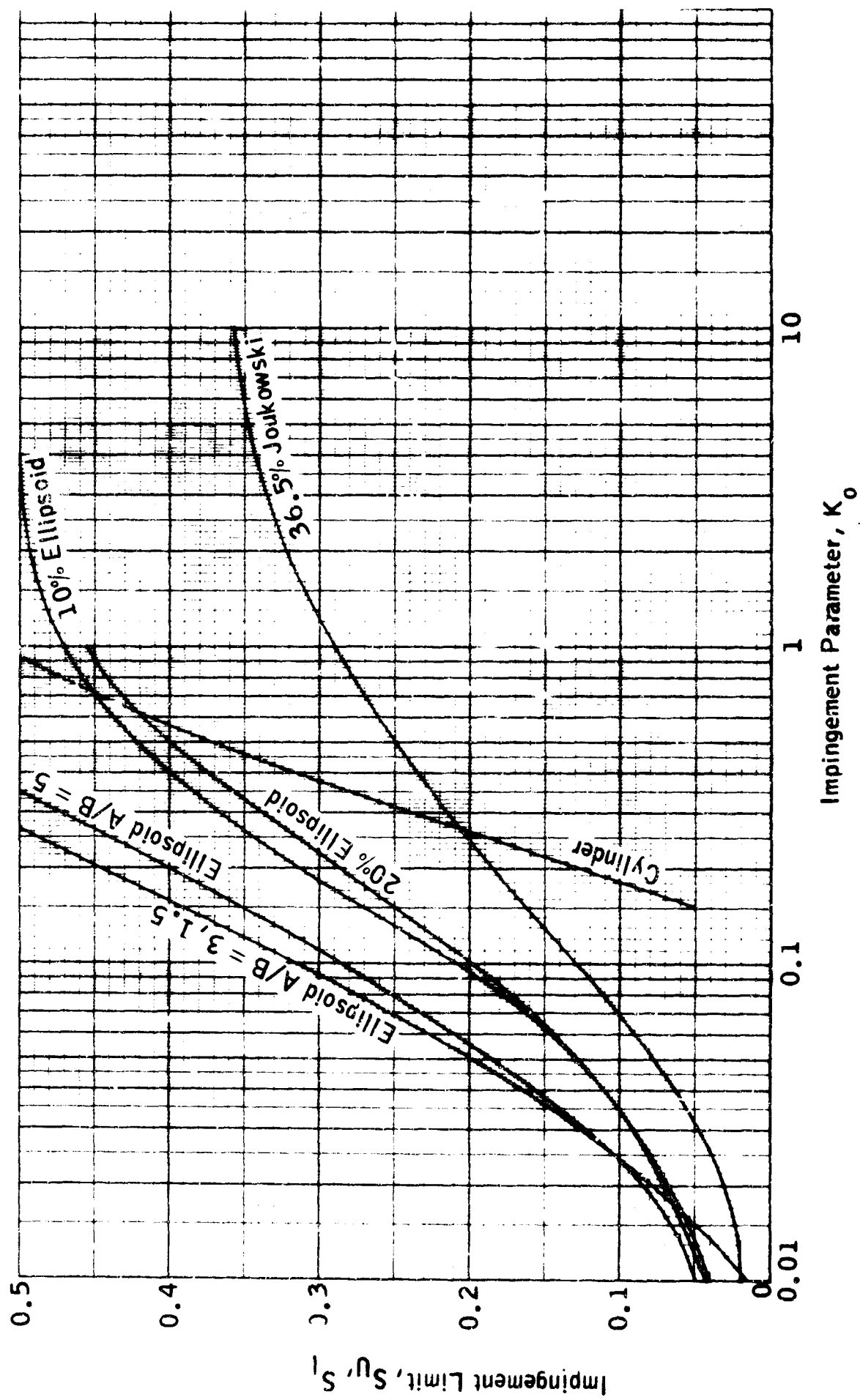
Figure 2-20

Upper Surface Impingement Limits for Several Airfoils at 8° Angle of Attack (Experimental Data).
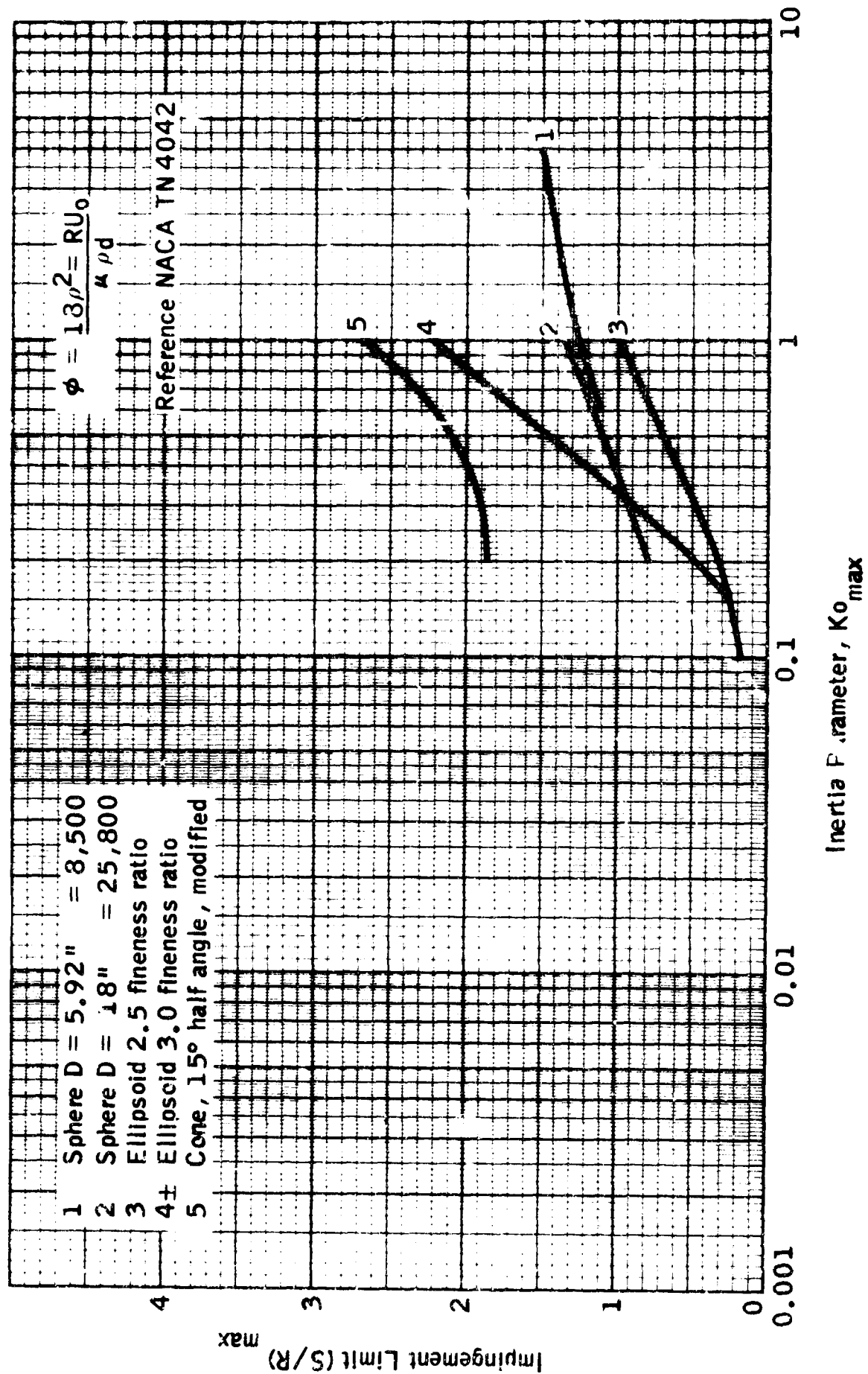
Figure 2-21

Lower Surface Impingement Limits for Several Airfoils at 8° Angle of Attack (Experimental Data).
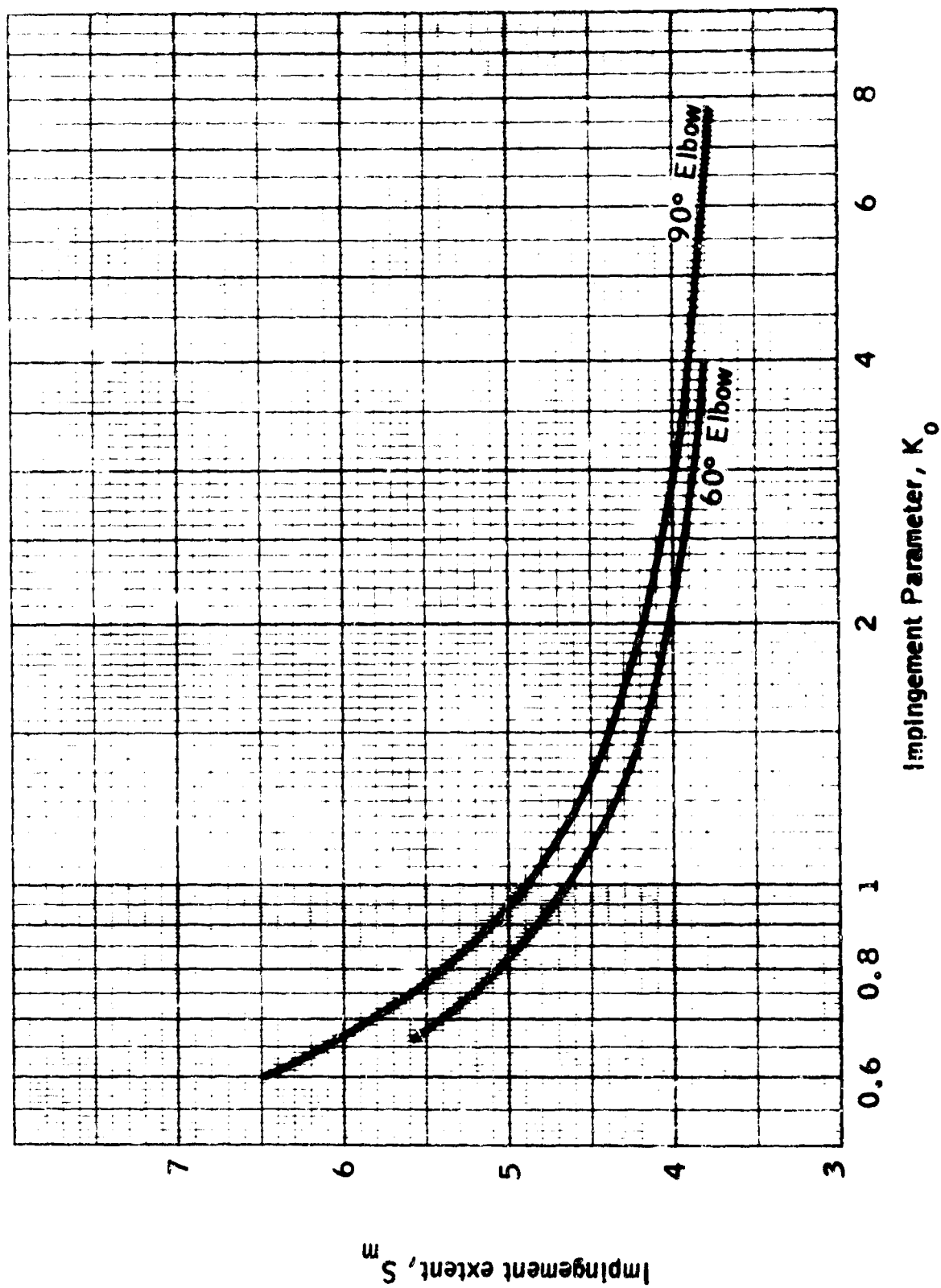
Figure 2-22

Impingement Limits on Several Geometric Shapes at 0° Angle of Attack (Theoretical Data).

Figure 2-23

Figure 2-24

Impingement Limits for Several Bodies of Revolution at 0° Angle of Attack (Experimental Data).

$$\phi = \frac{13\rho^2}{\mu\rho d} = \frac{RU_0}{}$$

Reference NACA TN 4042

1 Sphere D = 5.92" = 8,500
2 Sphere D = 18" = 25,800
3 Ellipsoid 2.5 fineness ratio
4 Ellipsoid 3.0 fineness ratio
5 Cone, 15° half angle, modified

Inertia Parameter, Ko_{max}

Impingement Limit $(S/R)_{max}$

Maximum Extent of Droplet Impingement Inside 60° and 90° Elbows (From NACA TN 2999 and 3770).
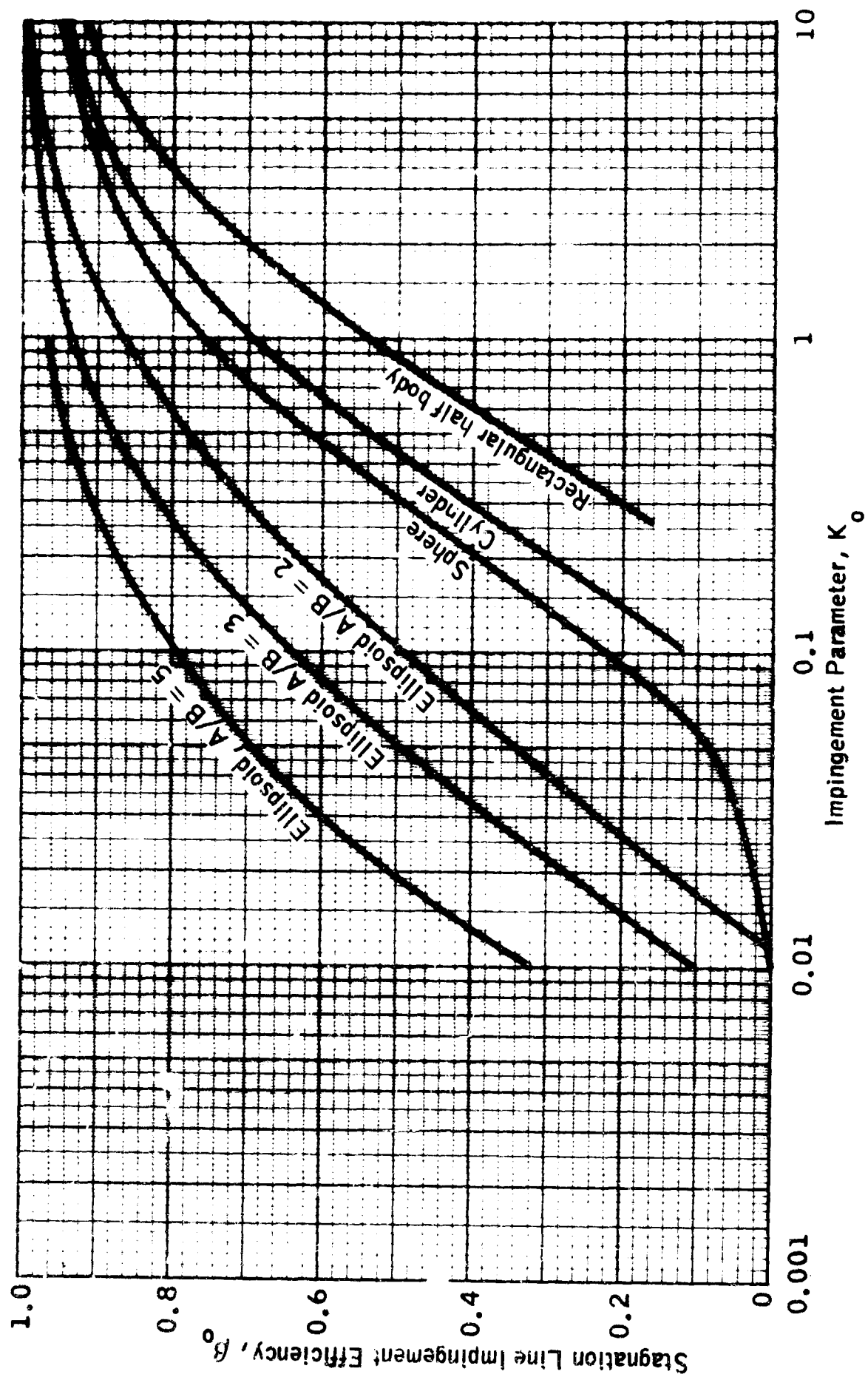
Figure 2-25

Impingement Efficiency at the Stagnation Line for Several Bodies.
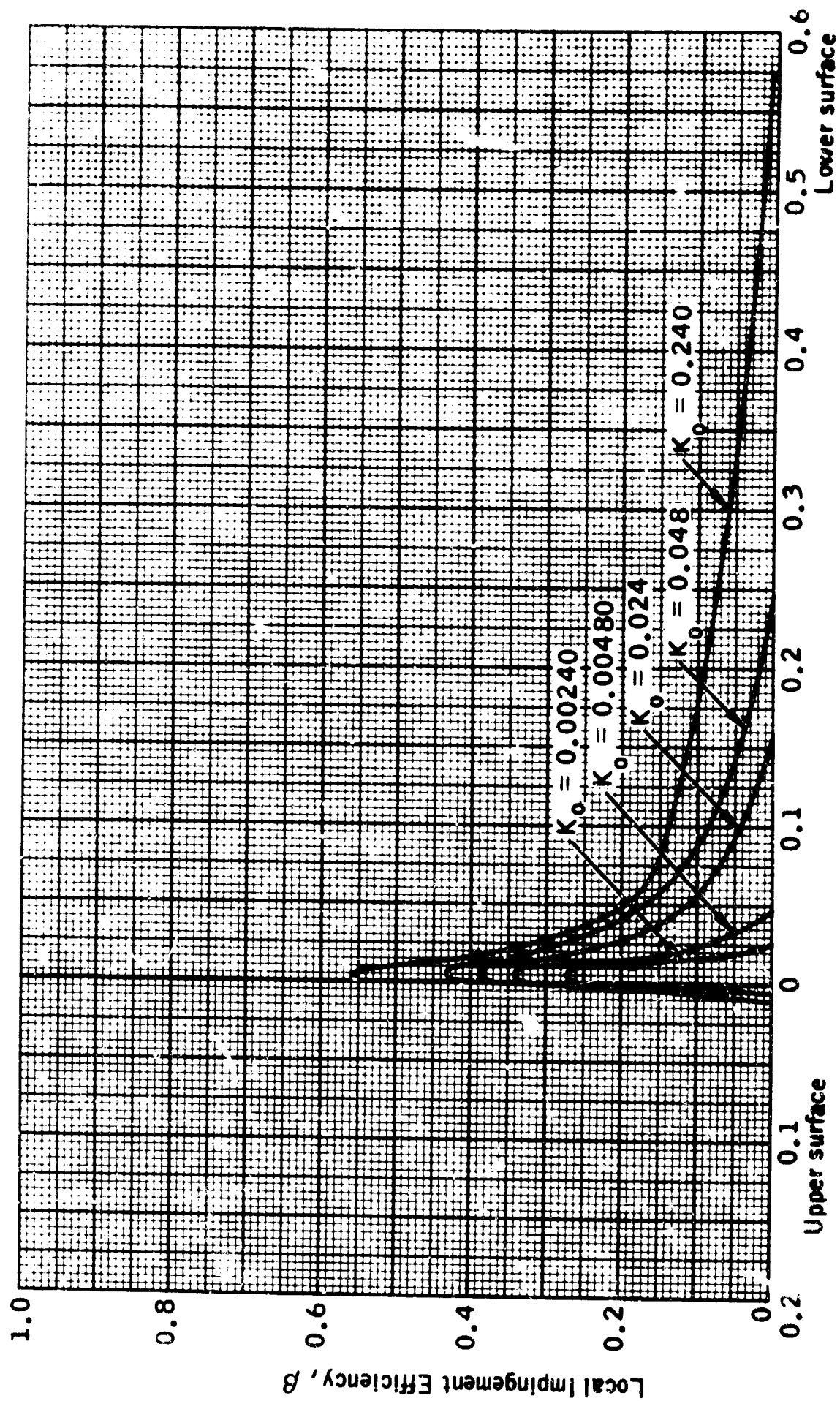
Figure 2-26
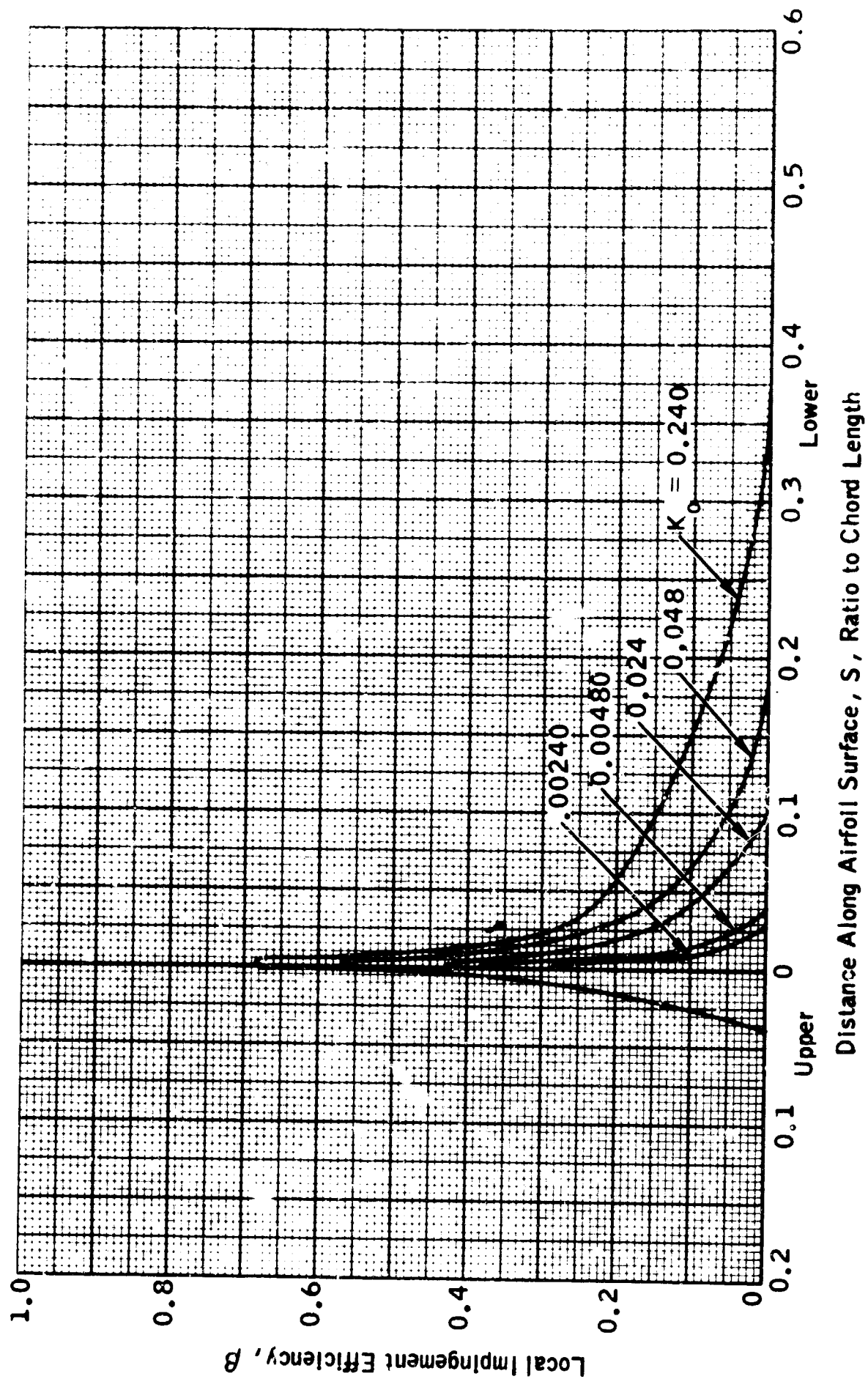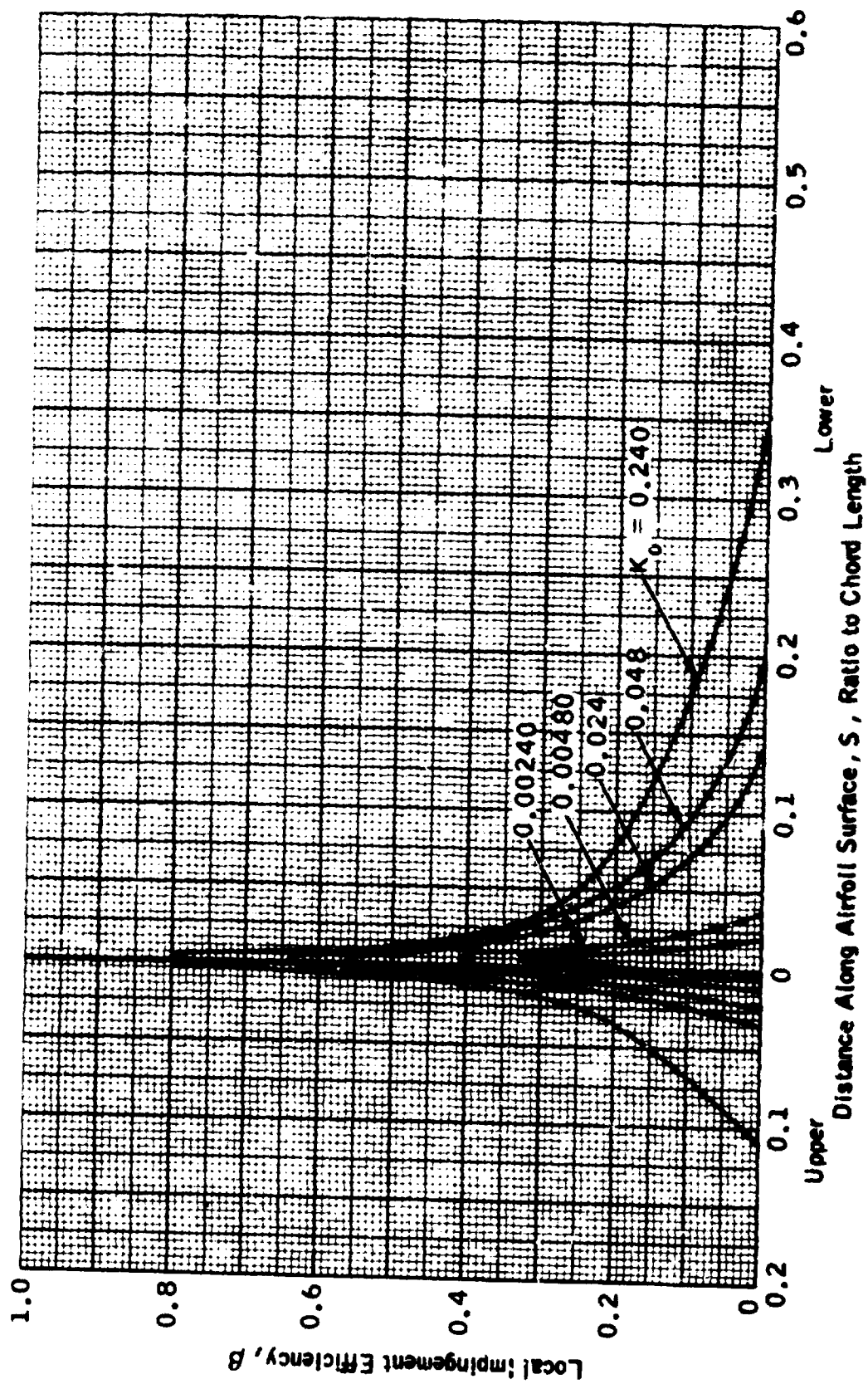
Local Impingement Efficiencies for 65A004 Airfoil at 4° Angle of Attack (From NACA TN 3047, Ref. 2-12).
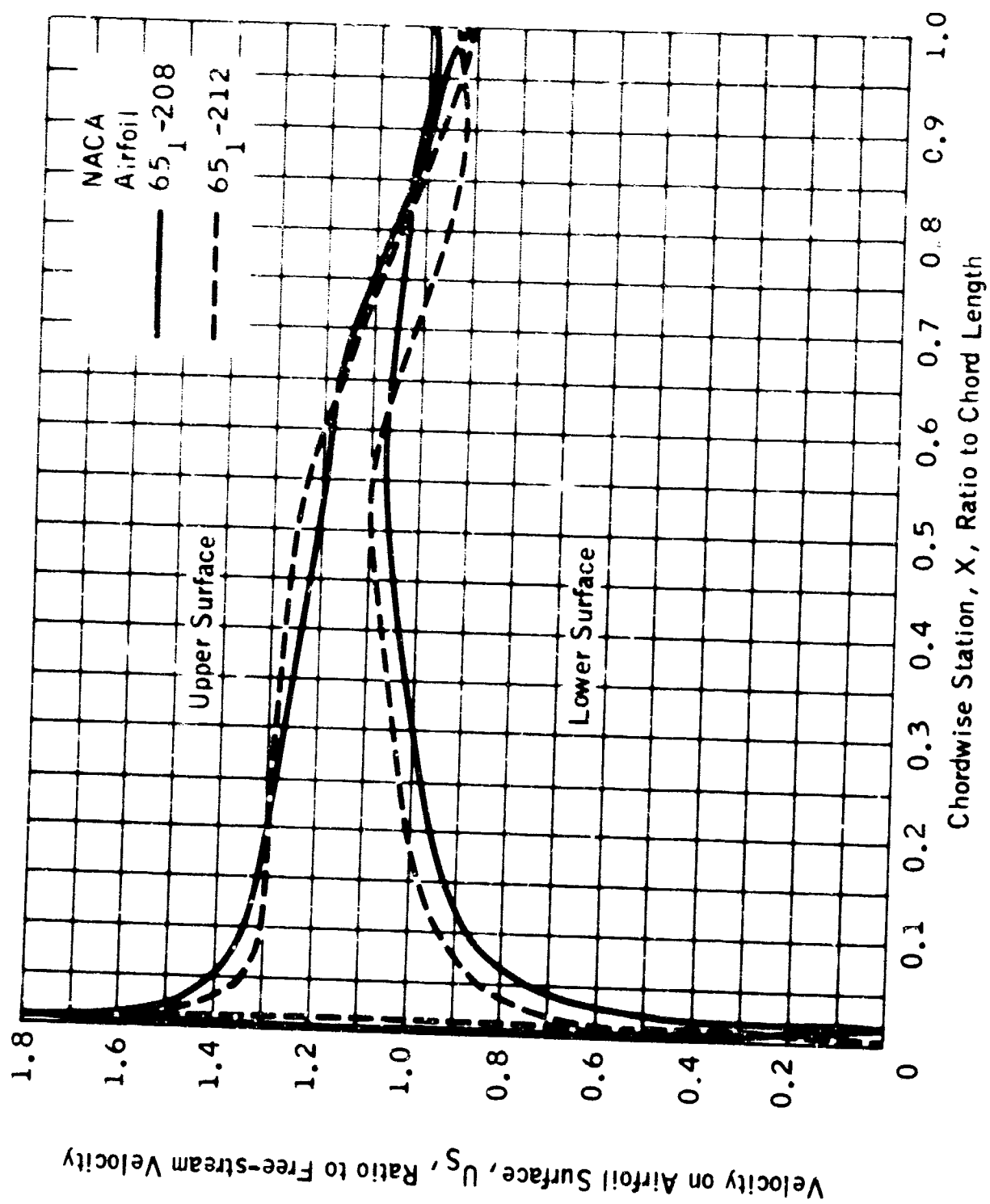
Figure 2-27

2-82

Local Impingement Efficiencies for 65_1-208 Airfoil at 4° Angle of Attack (From NACA TN 2952, Ref. 2-4).

Figure 2-28

Local Impingement Efficiencies for 65_1-212 Airfoil at 4° Angle of Attack (From NACA TN 1952, Ref. 2-4).

Figure 2-29

2-84

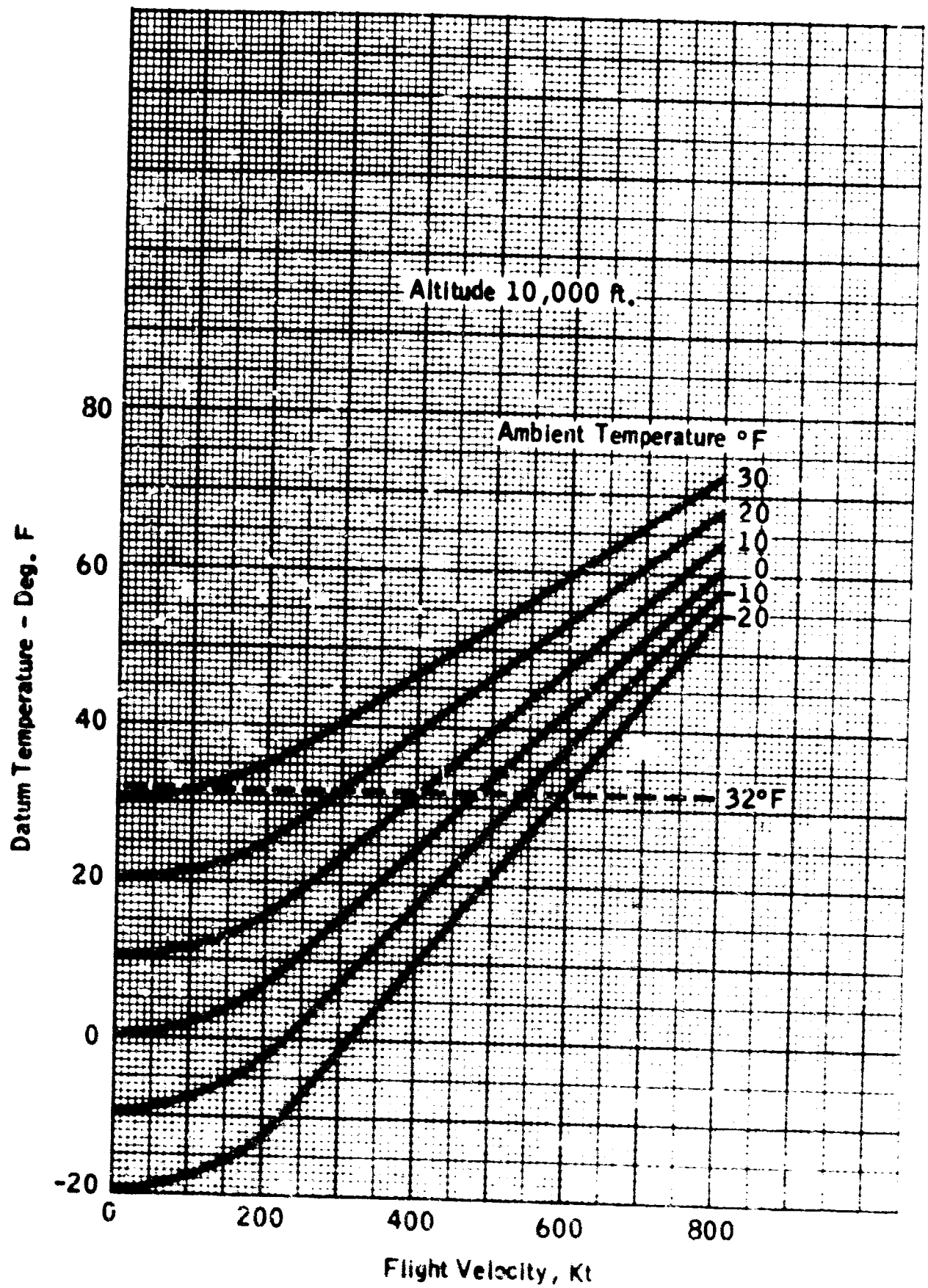Typical Airfoil Velocity Distributions

Figure 2-36

Figure 2-31. Datum Temperature as a Function of Flight Speed and Ambient Temperature.

2-66
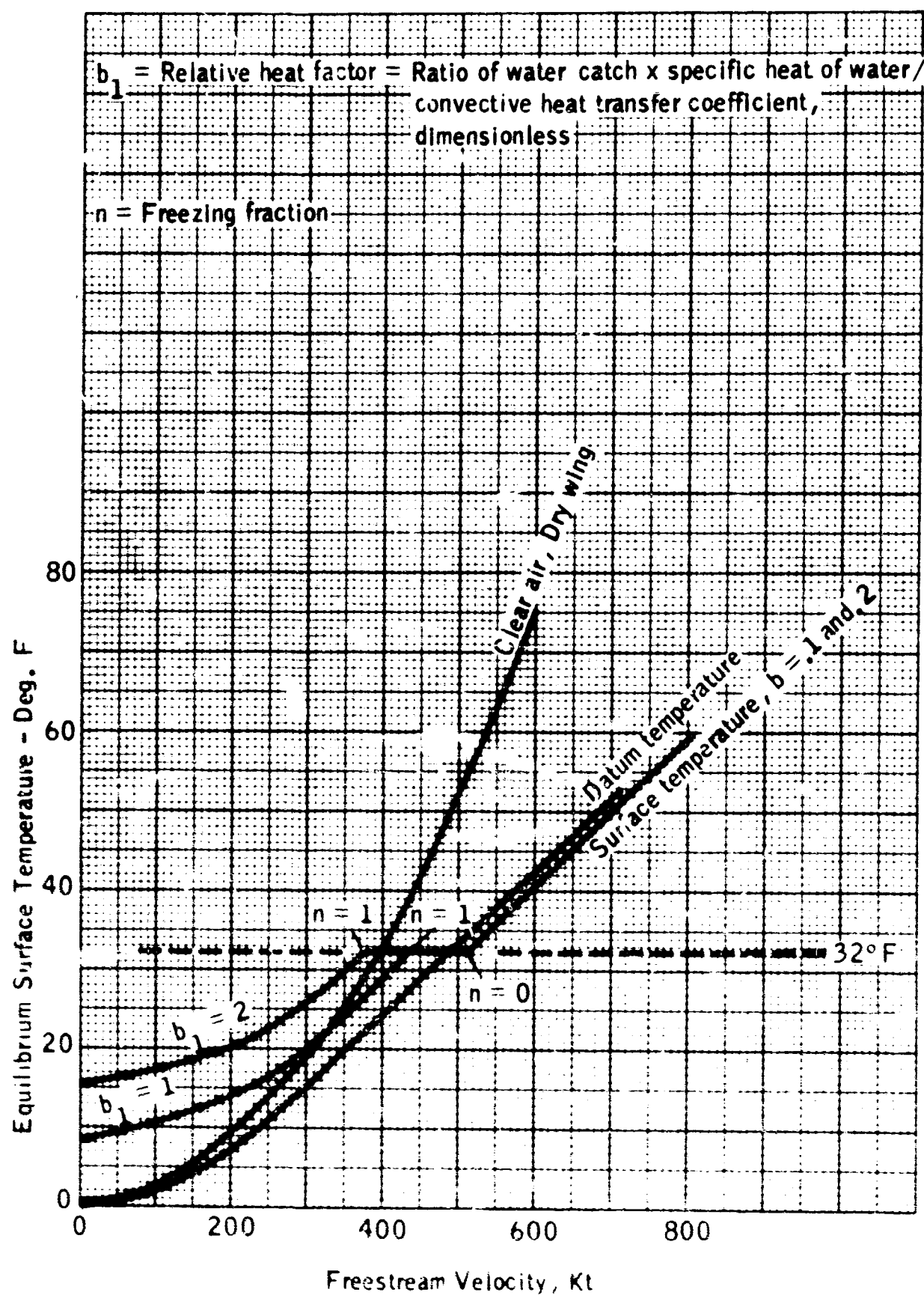
Figure 2-32. Equilibrium Surface Temperature Versus Free Stream Velocity for 10,000-ft. Altitude (Ref. 2-27).

Figure 2-33. Ice Shape Types as a Function of Speed and Ambient Temperature for a Liquid Water Content of 0.2 gm/m^3.

Figure 2-34. Ice Shape Types as a Function of Speed and Ambient Temperature for a Liquid Water Content of 0.5 gm/m³.
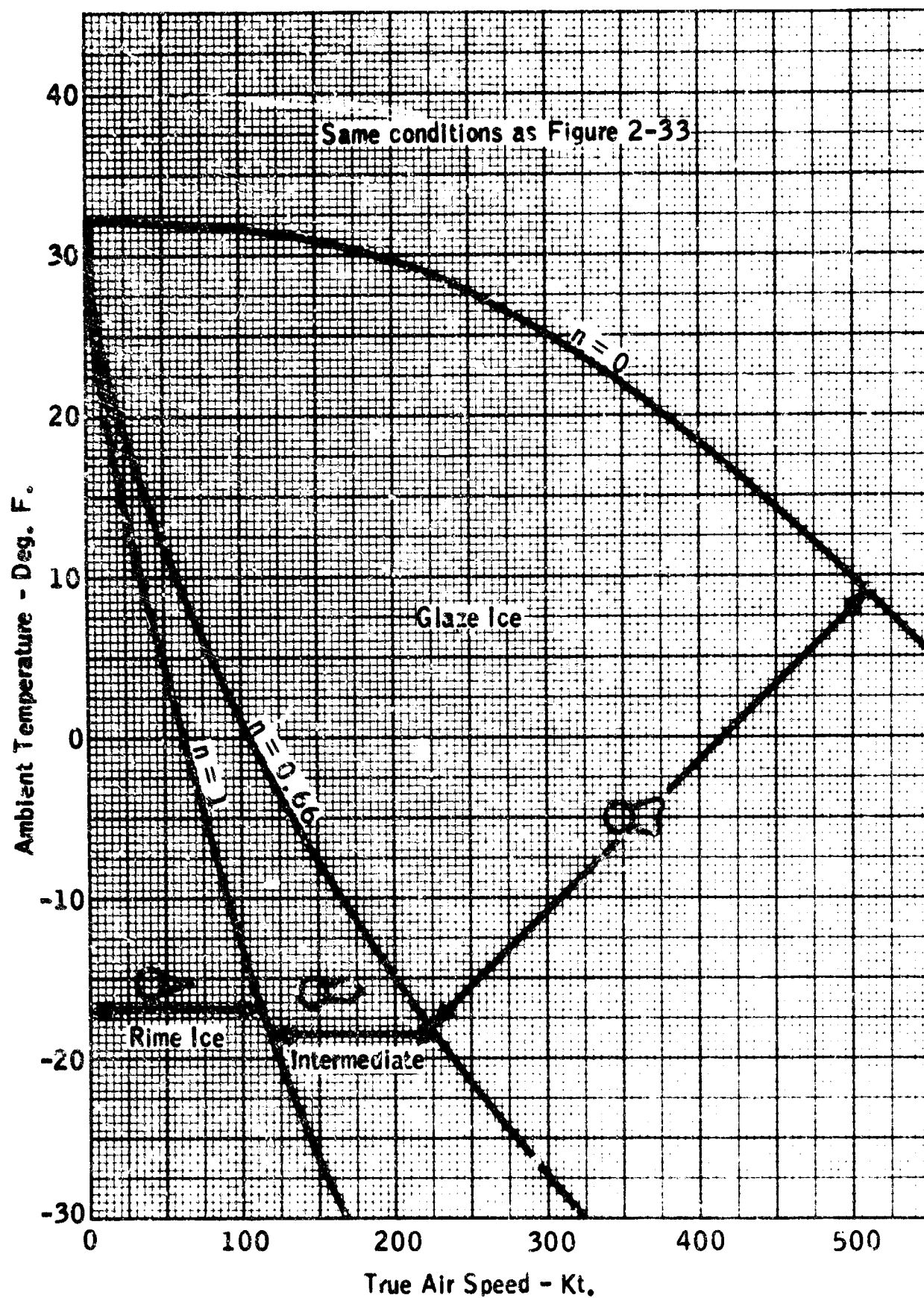
Figure 2-35.   Ice Shape Types as a Function of Speed and Ambient Temperature for a Liquid Water Content of 1.0 gm/m³

Rime Ice

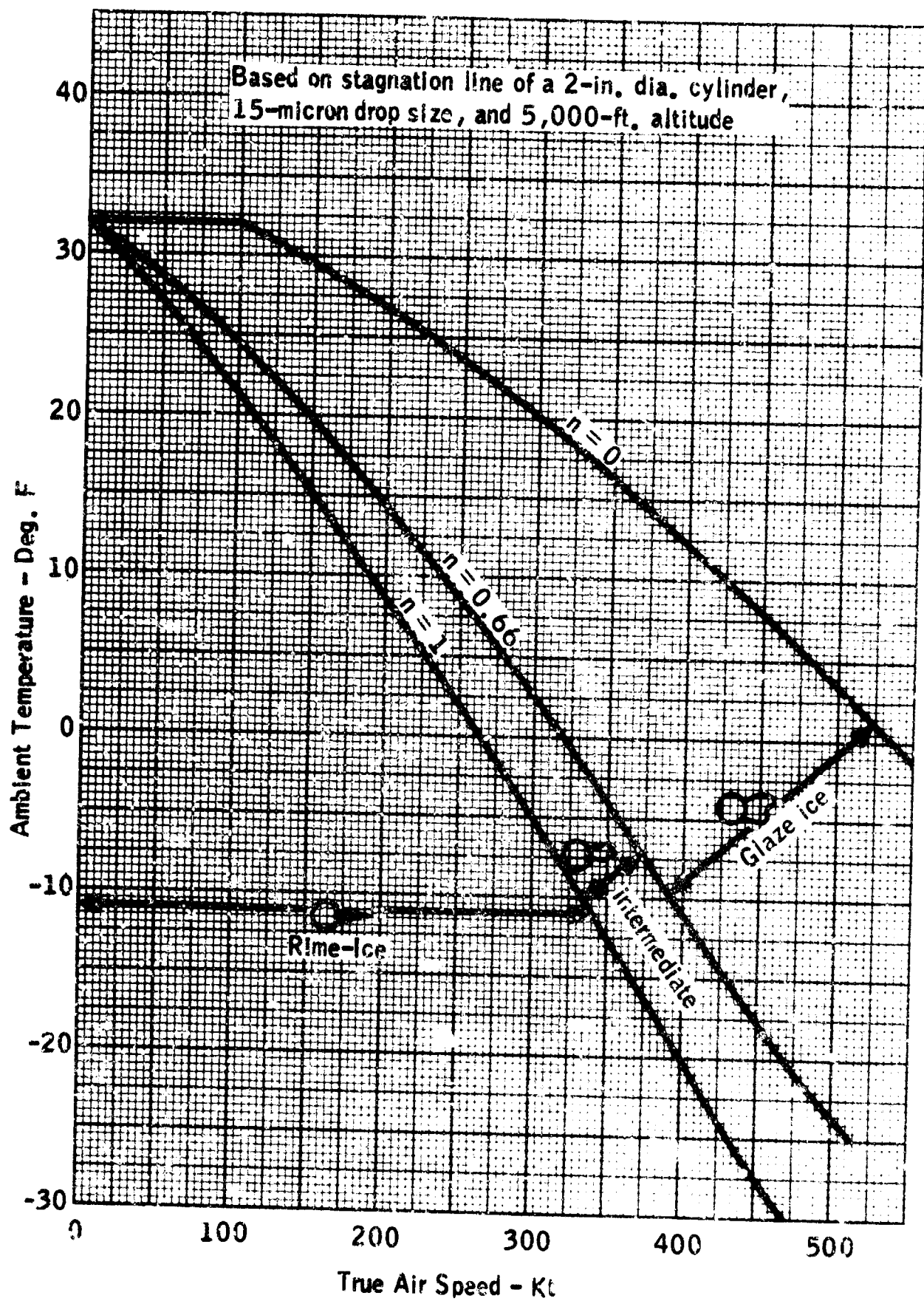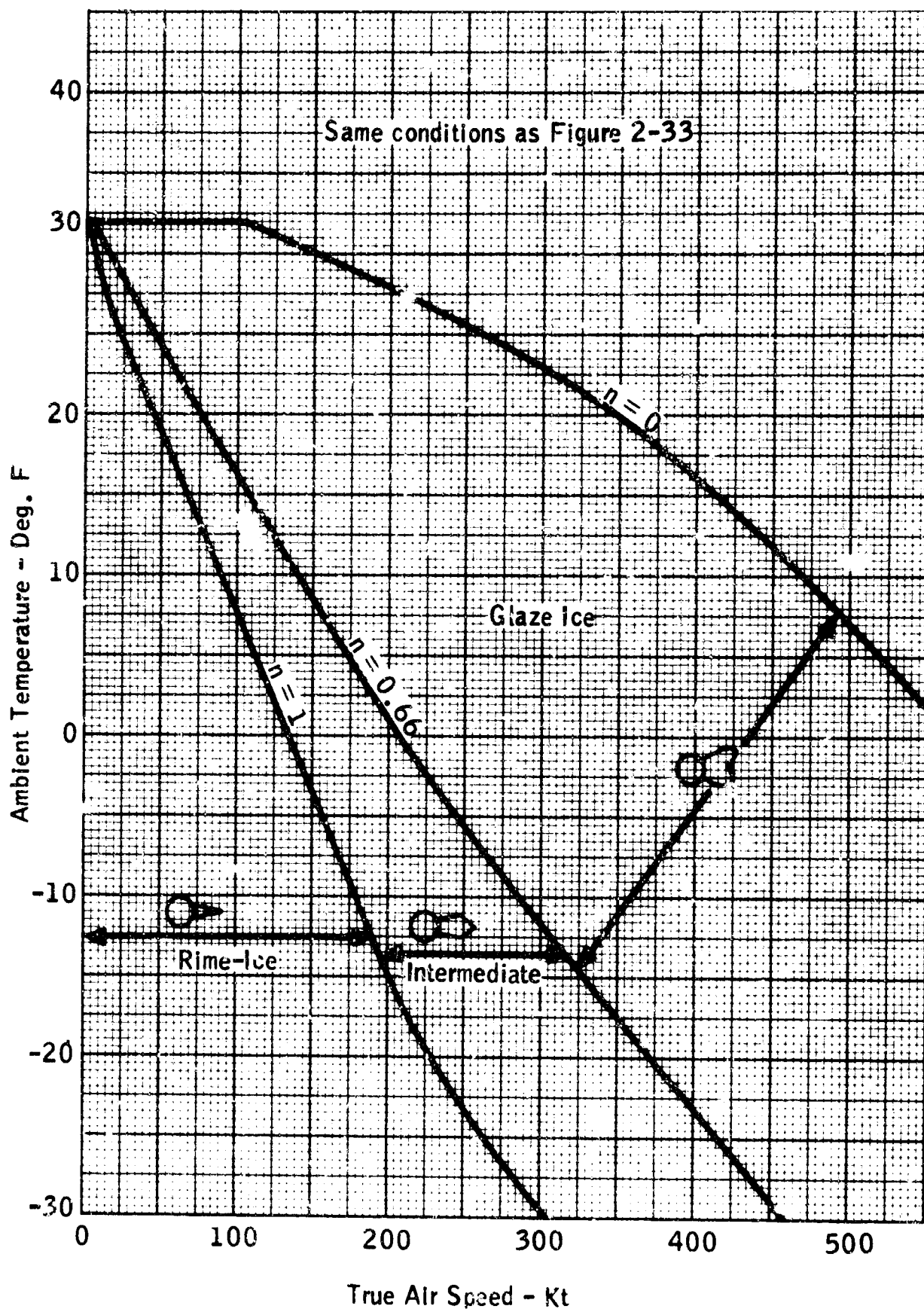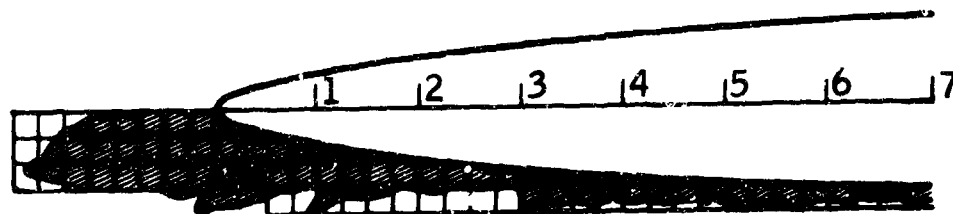Air speed 275 mph, air total temperature 0°F, LWC
0.90gm/m^3, 15-micron droplet diameter, icing
time 7 min., weight of ice 0.555 lb./ft. span, change
in drag (ΔC_D) = 0.0061
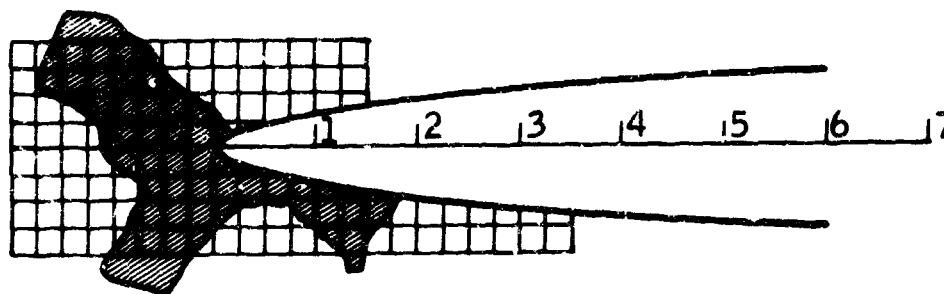
Glaze Ice

Air speed 275 mph, air total temperature 25°F, LWC
0.90gm/m^3, 15-micron droplet diameter, icing time
12 min., weight of ice 0.60 lb./ft. span, change in
drag (ΔC_D) = 0.0370

Chord = 6 ft.
Scale = 1/2

Figure 2-36. Typical Rime and Glaze Ice Deposits on a 65A004 Airfoil
at 2° Angle of Attack (From NACA TN 4151. Ref. 2-29).

Upper surface | Lower surface

Leading edge ↓ | ↓ Leading edge

a. Angle of Attack 2.3°, 0.5 gm/m^3, 18 minutes, 0.31 lb./ft. span

Upper surface | Lower surface

Leading edge ↓ | ↓ Leading edge
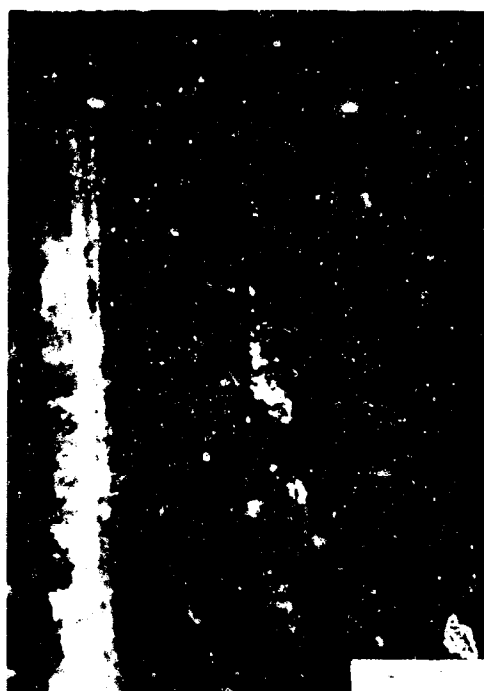
b. Angle of attack 7.0, 1.0 gm/m^3, 10 minutes, 0.75 lb./ft. span

Figure 2-37. Typical Glaze Ice Formations on an 87-in. Chord 11 per cent Airfoil at 25° F Total Air Temperature.

Upper surface   Lower surface
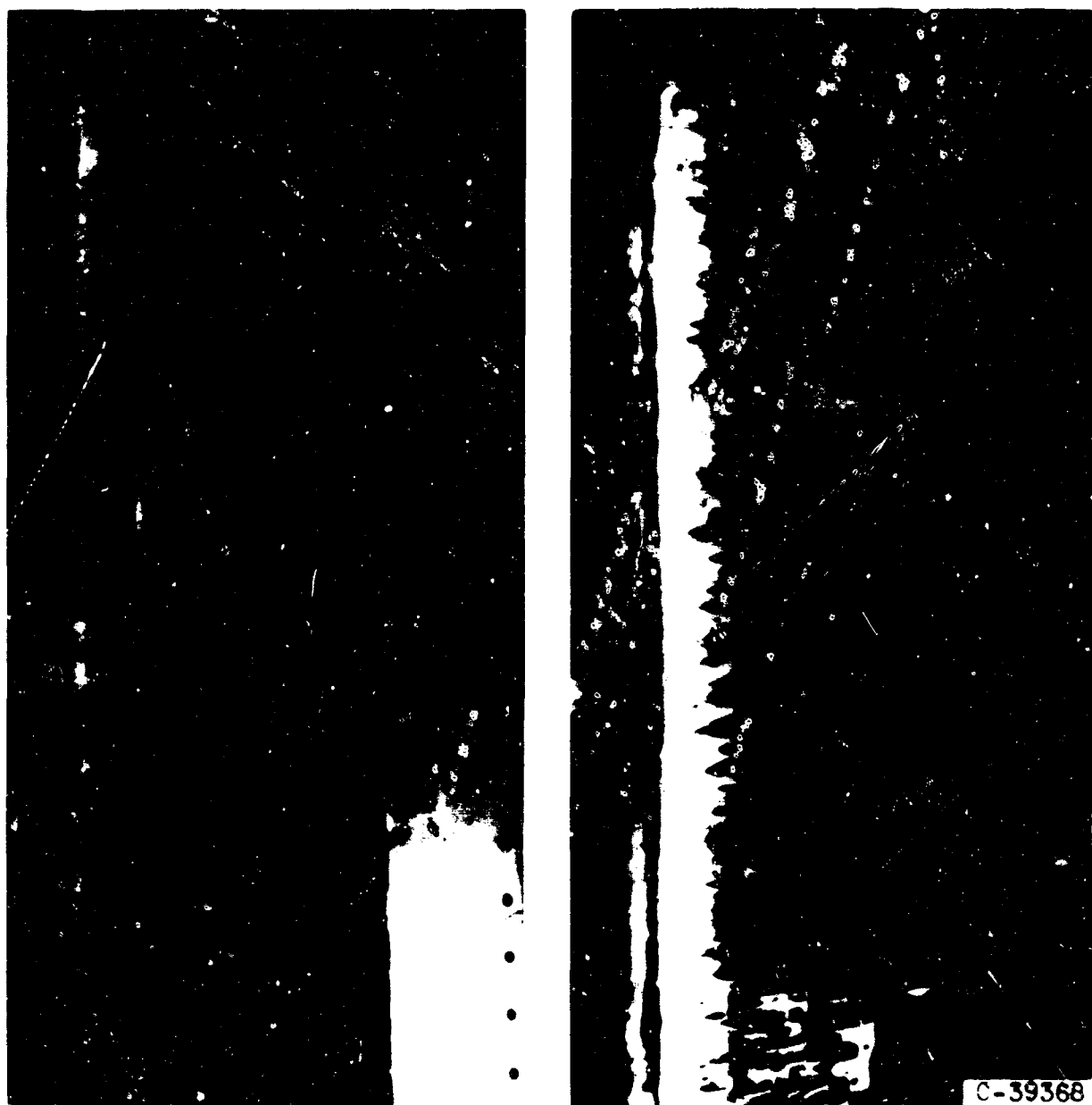
c.   Angle of att ck 7.0°, 0.5 gm/m^3, 26 minutes, 0.45 lb./ft. span

Figure 2-37.   Typical Glaze Ice Formations on an 87.4-in. Chord 11 per cent
                Airfoil at 25° Total Air Temperature.

↓ Leading edge   ↓ Leading edge
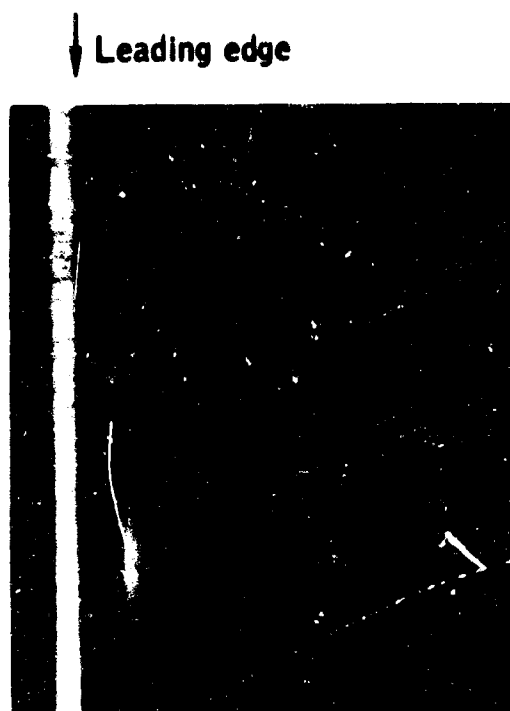
a. Angle of attack $0°$, 0.5 gm/m^3,   b. Angle of attack $0°$, 0.5 gm/m^3,
    11 minutes, 0.16 lb./ft. span   12 minutes, 0.52 lb./ft. span

Upper surface   Lower surface

↓ Leading edge   ↓ Leading edge

c. Angle of attack $2.3°$, 0.5 gm/m^3, 15 minutes, 0.22 lb./ft. span

Figure 2-38.   Typical Rime Ice Formations on an 87.4-in. Chord
11½ Airfoil at $10°$ F Total Air Temperature.

Leading edge ↓   ↓ Leading edge

Upper Surface   Lower Surface
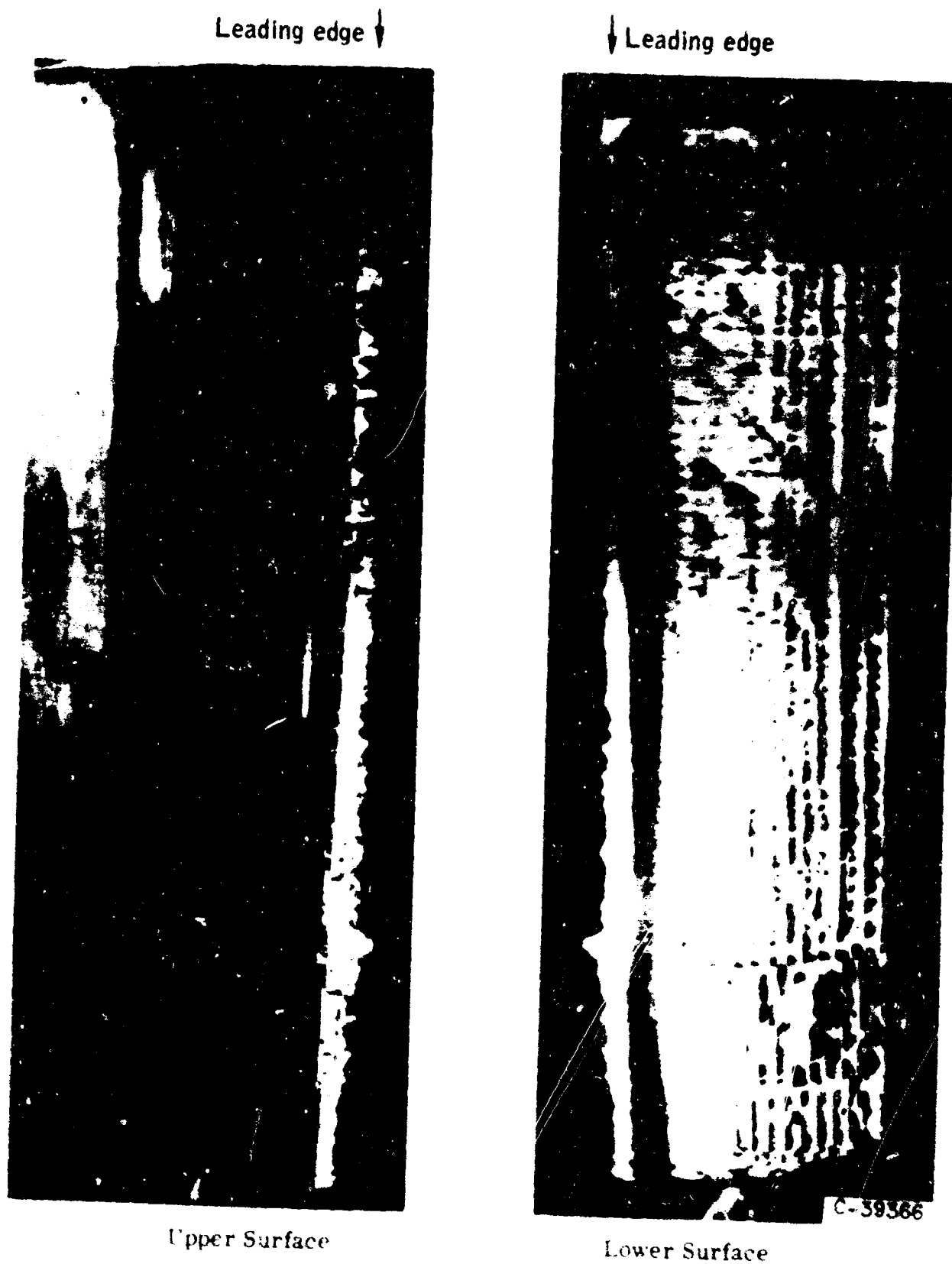
Figure 2-39.   Typical Glaze-Rime Ice Formation on an 57.4-in. Chord
11 per cent Airfoil — Angle of Attack, 9.3 , Total Air
Temperature, 10° F. LWC, 1.0 gm m³. Ten min.,
1.55 lb. ft. span

a.   Sweep angle 0°

b.   Sweep angle 36°   c.   Sweep angle 60°

Figure 2-40.   Glaze Ice Formations on Airfoils for Three Sweep Angles.

3 | METHODS OF PROTECTION

CONTENTS

METHODS OF PROTECTION

LIST OF FIGURES

NOMENCLATURE

A   Area, sq. ft.

C_D Coefficient of drag, dimensionless

C_h Rate of climb, feet per min.

D   Cylinder diameter, ft.

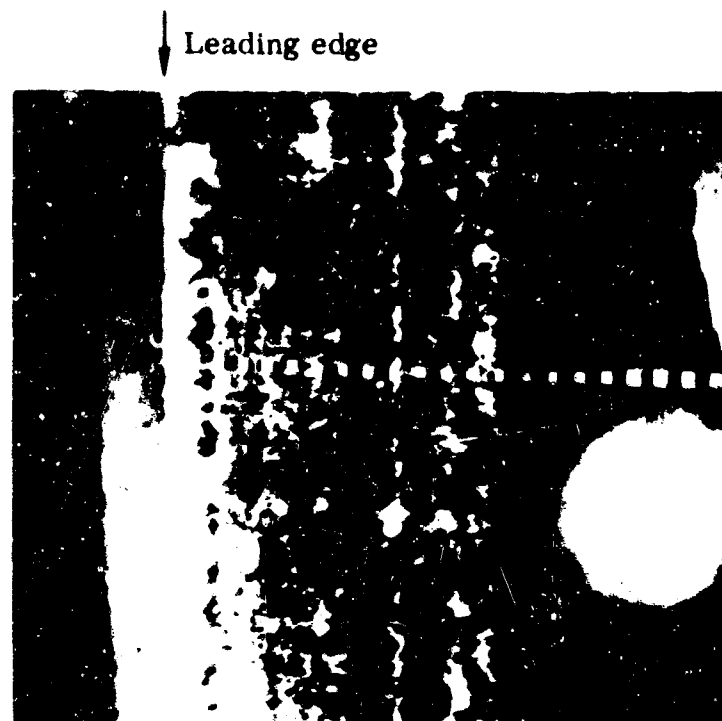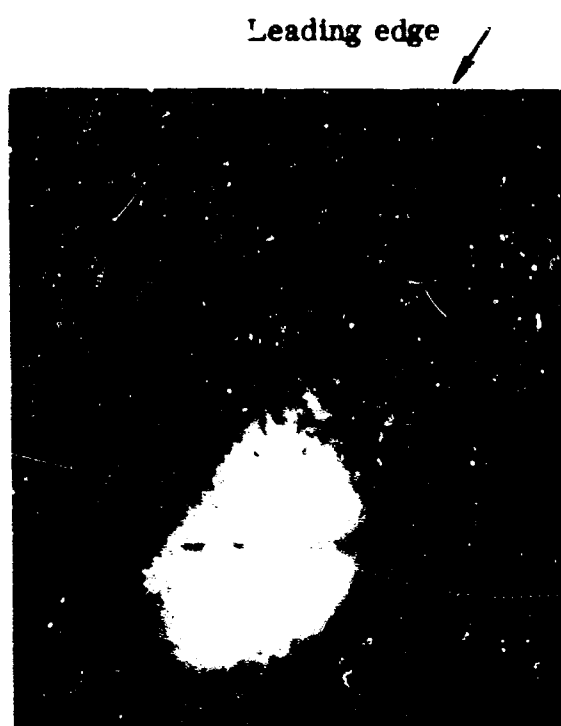G   Per cent freezing point depressant in final mixture

h_{cy} Heat transfer coefficient for a cylinder, BTU/hr.-ft.^{2} °F

h_{lp} Heat transfer coefficient for a flat plate in laminar flow, BTU/hr.-ft.^{2} °F

h_{tp} Heat transfer coefficient for a flat plate in turbulent flow, BTU/hr.-ft.^{2} °F

h_a Average external dry air convective heat transfer coefficient, BTU/hr.-ft.^{2} °F

HP_a Available horsepower

HP_r Rated horsepower

k   Thermal conductivity of air, BTU/hr.-ft.^{2} °F ft.

K   Surface wetness fraction, dimensionless

M_{ev} Rate of evaporation of water, lb./hr.-ft.^{2}

M_w Water catch rate, lb./hr. ft.^{2}

p_0 Undisturbed ambient absolute static pressure, in Hg

p_1 Local absolute static pressure, in Hg

Pr   Prandtl number

q   Heat transfer rate, BTU/hr.-ft.^{2}

q   Dynamic pressure, psf

r   Aircraft range with full military load, hr.

Re_d Reynolds number for a cylinder

Re_s Reynolds number over a flat plate

S   Surface distance from stagnation point in stream direction, ft.

t_{ok} Datum temperature, °F

t_s Surface temperature, °F

V   Velocity, fps

W   Weight, lb.

W_f Required weight flow of freezing point depressant mixture, lb./hr.

W_m Water catch, lb./hr.-ft. span

W_p Pump capacity for windshield protection, qt./hr.

W_t Tank capacity for windshield protection, U.S. gal.

X   Per cent by weight of freezing point depressant in the fluid mixture.

θ Angle in degrees from air stagnation point to point of interest

τ_1 through τ_5 temperature terms defined by Eq. 11 through 15 of Reference 3-2, °F.

Subscript

ice   With ice accretion

3.1 SUMMARY

If a need for ice protection has been established for an airframe, then the depth or degree of protection that is desired or can be provided must be established. Areas that may require ice protection are presented in Figure 3-1. Several degrees of ice protection are possible. First is de-icing, in which ice accretion is permitted on the protected surface and then removed periodically. Second is running wet anti-icing, in which moisture is prevented by some means from freezing on the surface. This moisture may run back beyond the protected surface and freeze (commonly called runback ice). Third is evaporative or dry anti-icing, in which all moisture impinging upon the surface is evaporated with no runback.

These various degrees of ice protection may be provided by pneumatic de-icers, fluid freezing point depressants, and thermal-hot gas and thermal-electric systems.

This section of the report will describe the various ice protection systems and will present methods of determining the requirements placed on the systems to provide a particular degree of ice protection.

3.2 INTRODUCTION

The purpose of this section is to describe the most commonly used techniques of providing aircraft ice protection and to assist in the determination of the most suitable type of protection for a particular airframe. Many other ice protection systems have been devised and applied to aircraft but have not received widespread acceptance. These systems have not been included, as in most instances they employ the same principles as the more common systems. A few unique systems are in the process of development and testing, but, since details as to effectiveness and application are lacking, they have not been included.

3.3 MECHANICAL DE-ICING SYSTEMS

3.3.1 DESCRIPTION — In a mechanical de-icing system, ice is permitted to accumulate on the surface to be protected and is removed periodically by mechanical means. Many such systems have been devised, but only one has received widespread acceptance. This system consists of inflatable tubes made of fabric covered with synthetic rubber. The tubes are fabricated into a thin pad which is wrapped around and bonded to the leading edge of the surface to be protected. These tubes may be oriented spanwise or chordwise. The tubes are manifolded together and connected to a 15 to 22 psig air pressure source. Inflation of the tubes under accreted ice breaks the ice into particles and destroys the ice bond to the surface. Aerodynamic forces then remove the ice. The tubes may be manifolded and supplied in such a manner as to permit alternate or simultaneous inflation of the tubes. Figures 3-2 and 3-3 show the spanwise and chordwise inflatable tube de-icing boots on an airfoil leading edge.

3.3.2 REQUIREMENTS — Components required for the installation and operation of the inflatable tube de-icing system are: the pneumatic de-icers of either spanwise or chordwise orientation; a pressurizing air source of from 15 to 22 psig for tube inflation; a vacuum source for tube deflation; solenoid-actuated valves to permit pressurization, venting and evacuating the tubes; a timer for sequencing the operation; and the air distribution system. Miscellaneous components such as filters, check valves, relief valves and regulators may also be required. A schematic of such a system is presented as Figure 3-4. Installation of this equipment is normally directed by the manufacturer. Before installing such a system, it is desirable to know what effects the system will have upon aircraft performance.

The weight of a pneumatic boot system for a CAR 3 type aircraft is approximately 40 lb. The distribution of the weight is such that it should not affect the aircraft balance, and the total weight should not cause an appreciable performance

loss. The power extracted for air pump operation of the boot in a piston-driven aircraft is negligible in relation to total power. The bleed air extracted from a turbine engine for boot inflation should not affect turbine performance. Aerodynamically, a performance loss may or may not be experienced by an increase in airfoil section drag, depending upon the condition of the airfoil prior to installation and the method of installation.

NACA has conducted wind tunnel icing tests on pneumatic boots and their de-icing effectiveness. Results of a series of these tests appear in Ref. 3-1. One result reported in Ref. 3-1 is that boot installation has no appreciable effect upon airfoil lift.

After a de-icing cycle, small particles of ice may still adhere to the surface. This is residual ice and may be used as a measure of de-icing system effectiveness. Residual ice may be minimized by permitting from one quarter to three eighths of an inch of ice to accrete before actuating the de-icers. Unless removed, the residual ice may cause an airfoil section drag increase of from five to fifteen per cent and is independent of the number of de-icing cycles.

Spanwise tubes and chordwise tubes were found to be equally effective in removing ice down to a leading edge radius of 0.75 in.; at that radius and smaller, the chordwise tubes were less effective.

Military specifications for pneumatic de-icers are contained in Ref. 3-2.

3.3.3 FEASIBILITY — Pneumatic boot de-icing system installation requires only minor airframe modifications — e.g., holes in the leading edge for air connections and installation of the air and vacuum sources. Power requirements for mechanical de-icing are considerably less than for thermal de-icing systems.

Residual ice on a mechanical system may be reduced on a temporary basis by applying an ice bond depressant. This depressant does wear off with each

de-icing cycle and during flights through rain or for extended periods in clear air; consequently, it should be replenished before flights through predicted icing conditions. Continued improvements in de-icing boot design should reduce any installation drag increase as well as the drag caused by tube inflation.

3.4 FLUID ICE PROTECTION SYSTEM

3.4.1 DESCRIPTION — A fluid ice protection system uses a fluid (miscible with water) which — when mixed with water — lowers the freezing point. If the freezing point depressant is on the surface prior to ice accretion, the impinging water droplets mix with the depressant, resulting in a solution with a freezing point lower than the surface temperature; consequently, no ice will form. This is an anti-icing system. For a de-icing system, ice accretion is permitted before actuating the system. The freezing point depressant then mixes with the ice to form a slush which is swept away by aerodynamic forces. Among the fluids used for this purpose are ethylene glycol, isopropyl alchohol, ethyl alcohol and methyl alcohol. Other proprietary fluids are available, and their properties may be compared to those listed when considering them for design purposes.

One method of applying the depressant to airfoils is through a porous metal strip located along the stagnation point. Figure 3-5 is a schematic of a porous metal strip. The depressant, after reaching the surface of the airfoil, flows chordwise over the upper and lower surfaces. For airfoils where the stagnation point shifts appreciably, a porous metal panel covering the entire stagnation point has been developed (see Figure 3-6). The porous metal system of ice protection may be used for either anti-icing or de-icing. Fluid usage for de-icing should be appreciably less than for anti-icing in that only the bonding surface need be wetted by the depressant to break the bond and have the ice swept away by aerodynamic forces.

Another method of applying the freezing point depressant is through a spray nozzle. This method normally would be used on surfaces where the installation

of a porous strip would be impractical or uneconomical. Sharply curved surfaces, debris screens, engine inlets, windshields and radomes are examples which have had spray nozzle installations. The military requirements for windshield fluid protection appear in Ref. 3-3. There are several designs of spray nozzles; Figure 3-7 is one example. The spray nozzle normally faces into the airstream, and the fine mist of freezing point depressant is swept back over the surface to be protected.

Propeller freezing point depression systems use centrifugal force to distribute the fluid. The fluid is pumped into a slinger ring at the back of the propeller hub. The ring is divided to afford equal distribution to each blade. From the slinger ring, the fluid flows by centrifugal force into cups at the propeller blade root. From the cups, the fluid is discharged onto the leading edge of the propeller and is directed down the blade by grooves molded into the rubber boot which extends down the blade. Beyond the boot centrifugal force will normally keep the blade clear, or at least prevent any large accumulation of ice.

3.4.2 REQUIREMENTS — Calculations to determine the required amounts of freezing point depressant are begun by solving an equation for datum temperature (t_{ok}) found in Section 2, Paragraph 2.7.1 (see also Ref. 3-4).

Figures 3-8a through 3-8c are solutions to the equations for specific altitudes. The rate of water catch (M_w) is also calculated as shown previously in Section 2. Having selected a freezing point depressant (e.g., 50 per cent ethylene glycol in water), determine the percentage required from the freezing point plot of Figure 3-9 which will satisfy the calculated t_{ok}. For example, find the required flow rate of freezing point depressant (50 ethylene glycol in water) for the following condition.

Flight speed   250 KTAS

Altitude   20,000 ft.

Ambient temperature	$t = -10° F$
Water catch rate, M_w	1.13 lb./hr.-ft.^{2}
Area	15 ft.^{2}
Total water catch	17 lb./hr.

First, solving the equation for t_{ok} or determining t_{ok} from Figure 3-8c, we get $t_{ok} = 0° F$. Figure 3-9 indicates 35.5 per cent ethylene glycol is needed to maintain a 0° F freezing point. Next, solving Eq. 3.4.1 or 3.4.2 shows 41.6 lb./hr. of the 50 per cent ethylene glycol in water is theoretically required to prevent freezing at this condition

$$W_f = \frac{G M_w}{X - G} \tag{3.4.1}$$

Note, of course, that this amount would be satisfactory to prevent freezing only if the impinged area is completely covered with the freezing point depressant solution. In general, because of distribution efficiency, the actual amounts will be from 1.2 to 1.5 times greater, even for a well-designed system. For engine inlets, a factor up to twice theoretical is often used, depending upon inlet geometry and protection required. Tests conducted by NACA on fluid ice protection of radomes show a good correlation of theoretical and experimental fluid ice-protection requirements. The results were reported in NACA RM E52J31 (Ref. 3-5). Cirves from this report are presented as Figures 3-11 through 3-14.

Calculation of the required fluid flow for de-icing using the porous metal system is almost impossible. A laboratory example of the decrease in ice bond strength with addition of a glycol-based fluid is listed below for a datum temperature of + 14° F (Ref. 3-6).

Per Cent Fluid Added	Shear Strength Ice to Light Alloy
0	104 psi
1	7 psi
2	1 psi
3	0 psi

Twenty four per cent (by weight) of ethylene glycol must be added to water to lower the freezing point to 14° F. As an ice formation grows the aerodynamic forces on it increase. The point at which these forces overcome the bond strength is impossible to predict.

After considerable study and several tests the British Air Registration Board has arrived at a fluid flow rate of 1/3 Imperial pint of ethylene glycol per hour (0.46 lb./hr.) per square foot of airfoil projected frontal area for the porous metal panel distributor. What this would mean for a light aircraft with a 33-ft. wingspan and 0.67-ft. chord thickness would be a supply on board of 7.35 pt. per hour (10.25 lb./hr.) of flight in icing conditions. This flow would allow anti-icing at temperatures near 32° F, and intermittent removal (de-icing) at lower temperatures.

Anti-icing this aircraft under the following typical conditions: water catch rate 2.84 lb./hr.-ft. of span, airspeed 200 kt., altitude 10,000 ft. and temperature -10° F, would require a fluid flow rate of 35 lb./hr. of ethylene glycol. Additional fluid would be required for propeller and other areas to be protected. The rate of fluid flow laid down for propeller de-icing by the British Air Registration Board is 0.83 Imperial pt. (1.16 lb.) per foot run of blade per hour.

Other formulas to be used for determining system requirements are as follows:

For 50 50 glycol water only,

$$W_f = \frac{2 \, G \, M_w}{100 - 2G} \tag{3.4.2}$$

The following equations are taken from Ref. 3-3, a military specification, and are for the most severe conditions. They may be overly conservative for many applications.

Pump capacity for windshield protection:

$$W_p = (2 \, 3 \, A) \, (2 \text{ qt. hr.} - \text{ft.}^2)$$

Tank capacity for windshield protection:

$$W = 0.7 \frac{A \, r}{12}$$

3.4.3 FEASIBILITY — The theoretical required flow rate of freezing point depressant calculated in Eq. 3.4.1 must be modified for practical use. For an anti-icing system, the distribution efficiency must be considered. Porous metal panel or strip efficiency may be affected by variations in local static pressure or by variations in porosity caused by dirt or damage. The efficiency of a spray nozzle will be affected by the degree of atomization, local air patterns and the spray patterns. Test programs usually can overcome most of the difficulties and keep the fluid requirements within tolerable limits. Excess weight may be a limiting factor for missions requiring long flight duration in icing. For radomes the anti-icing fluid may cause transmission losses as great as moderate ice accretions.

As indicated in Figures 3-5 and 3-6, the porous strips and panels must be designed into the airfoil leading edge. Installation on an existing aircraft would probably require fabrication of a new leading edge with the system incorporated. Installation weights are nominal; the distribution system requires but little space. Figure 3-10 is a schematic of a typical distribution system.

A spray nozzle system may be installed on an existing airfoil with a minimum of modification. The distribution system would be similar to that shown in Figure 3-10 with spray nozzles in place of the porous panels. This type of installation probably should be used as an anti-icing system, because a spray nozzle de-icing system requires considerably more fluid.

Advantages of the porous metal fluid distribution system are low fluid flow requirements, smooth contour to leading edge, and better efficiency when used an an anti-icing or de-icing system. Disadvantages are: (1) the porous strip must be designed into an aircraft; (2) the fine holes in the porous panel are subject to plugging by dirt from the outside or by impurities from the inside; (3) the installed weight when compared to the spray nozzle system is greater; (4) the system is not easily adaptable to complex shapes without considerable design and fabrication; and (5) the system is time-limited by tank capacity.

Advantages of a spray nozzle system are: (1) it is applicable to almost any surface; (2) it can be installed in most existing aircraft; and (3) it can be easily maintained. Disadvantages are: (1) excessive fluid is required due to system inefficiency; (2) the system is not adjustable to changing angles of attack; and (3) The system is not very suitable for de-icing.

Installation of a freezing point depressant system would be practical on an aircraft which lacked sufficient hot air for thermal ice protection. Installation weight of the fluid system is comparable to several other ice-protection systems. Weight of fluid may be several times the installation weight, however, if long periods of protection are required.

Any of the fluids shown in Figure 3-9 are suitable for use in anti-icing or de-icing systems. Ethylene glycol in a common choice. Although it is not as effective a freeze-point depressant as the alcohols, it has several advantages: it is commercially available in large quantities, has low volatility, and does not represent a fire hazard.

3.5 THERMAL ANTI-ICING

3.5.1 DESCRIPTION — Thermal anti-icing systems use heat to maintain the temperature of the surface to be protected above freezing throughout an icing encounter. Thermal anti-icing systems are classified as evaporative and running wet. Evaporative systems, as the name implies, supply sufficient heat to evaporate all water droplets impinging upon the heated surface. The running wet systems, however, provide only enough heat to prevent freezing upon the heated surface. Beyond the heated surface of a running wet system, the water could freeze (generally called runback ice). For this reason, running wet systems must be used carefully so as not to permit runback ice buildup in critical locations. For example, the heated surface of a running wet system on a turboprop or turbojet inlet should extend into the inlet to the compressor face so that the water runoff will combine with the intake air and not strike cold surfaces where it could refreeze, break off, and possibly damage the engine.

Basically, two sources of heat for thermal anti-icing are used in aircraft: electrical heaters and hot air. For anti-icing, the heat source must remain on throughout the icing encounter. Areas of an aircraft that may be afforded thermal ice protection are included in Figure 3-1. Of these areas, the windshield is always given anti-ice protection while the remainder of the areas may be given anti-icing or de-icing protection, depending on the power available for ice protection and the effects of ice accretion on the aircraft.

3.5.1.1 Electrical System Description — The power requirements for completely anti-icing an airplane using an electrical powered heat source are prohibitive; therefore, the areas generally anti-iced electrically are the windshield, small air inlets and areas remote from any hot air source. For windshields, three basic systems of electrical heating are used. One, a thin, transparent, metallic oxide film fired on to the inner surface of the outer glass ply. Second, a thin, transparent, metallic film deposited on the inner surface of the outer glass or plastic ply. Third, a wire grid system placed adjacent to the inner surface of the outer glass or plastic ply. Figure 3-15 shows typical windshield construction for light aircraft. Typical construction for heavy aircraft is shown later in Section 4.2, figure 4.2-26. The thickness of the conducting medium can be varied to accommodate variation in heating requirements or to heat irregular shaped. High power density heating is usually limited to nearly rectangular areas, however. Small inlets and other areas to be given electrical anti-ice protection will have the heating element (foil, resistance wires, flame-sprayed metal, expanded metal, etc.) imbedded in a flexible pad bonded to the surface to be protected, or the heating element may be imbedded in a plastic, fiberglass or metal part which is the basic structure.

3.5.1.2 Hot Air System Description — Several sources of hot air for anti-icing are available, depending on the aircraft type. In turbojet and turboprop aircraft, engine bleed air may be available. For piston engine aircraft, combustion heaters or exhaust gas heat exchangers may be used.

Areas usually protected by a hot air system are engine inlets, wing leading edges, and occasionally empennage leading edges. Basically, the hot air is manifolded to the various portions of the aircraft to be protected and finally distributed in any one of several methods, as shown in Figures 3-16 and 3-17. The hot air is introduced as close as possible to the stagnation point of the surface to be protected and permitted to flow chordwise toward an exit point through gas passages. The exhaust gas is generally dumped overboard at a non-critical location.

3.5.2 REQUIREMENTS — Equations expressing heat transfer and evaporation from wetted surfaces during icing encounters have been used to develop a graphical solution for the determination of heat required for anti-icing (Ref. 3-4). Figures 3-18a and 3-18b are presented for this purpose. Preparatory to using these figures, the local heat transfer coefficient and rate of water catch (M_w) must be determined.

To determine the local heat transfer on an airfoil, the following three equations may be used:

a. Heat transfer coefficient for a cylinder (h_{cy}) of the same radius as the leading edge of the airfoil.

$$h_{cy} = \frac{1.14 \, Pr^{0.4} \, Re_D^{0.5} k}{D} \left| 1 - (\frac{\theta}{90})^3 \right| \qquad \text{(Ref. 3-7)}$$

b. Heat transfer coefficient for laminar flow over a flat plate (h_{lp}) to the chordwise extent of the heated surface.

$$h_{lp} = \frac{0.332 \, Pr^{1/3} \, Re_S^{0.5} k}{S} \qquad \text{(Ref. 3-7)}$$

c. Heat transfer coefficient for turbulent flow over a flat plate to the chordwise extent of the heated surface

$$h_{tp} = \frac{0.0296 \, (Pr)^{1/3} \, Re_S^{0.8} k}{S} \qquad \text{(Ref. 3-7)}$$

A typical plot of these heat transfer coefficients is presented in Figure 3-19 for a specific altitude and airspeed. The transitions from flat plate laminar to flat plat turbulent are only estimates, as the location of the transition region will vary with surface roughness, airfoil shape and angle of attack. Transition will usually start at a Reynolds Number of .5 to 2×10^6 and the flow will be fully turbulent at a Reynolds Number of 2 to 4×10^6.

These equations may be used to determine the heat required per unit area along the chord. On tapered and swept-back airfoil, these calculations, performed at several span stations, can become unnecessarily tedious. In practice, the heat transfer coefficients for a span station are plotted as in Figure 3-19 and an average value assumed for that station. This average value (h_a) is then used to enter Figures 3-18a and 3-18b to determine the anti-icing heat requirements. This assumption of an average value of heat transfer coefficient has a percentage of error in the same order of magnitude as the assumptions made in the meteorological variables.

The water catch rate (M_w) is obtained by dividing the water catch (W_m) by the heated area per foot of span for each spanwise position (see Section 2 and the example in Section 4). For a completely evaporative system, the rate of evaporation of water (M_{ev}) must equal the rate of water catch (M_w). With this knowledge, the following equation may be solved for τ_3.

$$\tau_3 = \frac{1066 \; M_{ev}}{h_a K} + \tau_4$$

(3.5.1)

(Ref. 3-4)

where K is the surface wettness fraction which is assumed to be 1.0 in the impingement region and 0.20 to 0.25 beyond the impingement region. With τ_3, Figure 3-18b is entered with p_o to find t_s.

If designing for a running wet system, the surface temperature (t_s) is assumed to be some value above freezing (such as 35° F, and τ_3 is found graph-

3-18

ically. The next steps are the graphical solution for τ_1 through τ_5 using Figures 3-18a and 3-18b and the solution of Equation 3.5.2 for the heat transfer rate at each spanwise position.

$$q/h_a = \tau_1 - \tau_2 + K(\tau_3 - \tau_4) + \tau_5 \qquad (3.5.2)$$
$$(\text{Ref. } 3\text{-}4)$$

The heat transfer rate (q) may then be plotted versus spanwise position to obtain heating distribution requirements. Typical values for a wing are from 2,5000 to 5,5000 BTU/hr.-ft. span.

Military requirements for thermal anti-icing systems may be found in Ref. 3-8.

Windshield anti-icing, defrosting and de-fogging requirements for military aircraft are specified in Ref. 3-9. Figure 3-20 is a curve of heat requirements from Ref. 3-9 to be met during all conditions up to normal cruising speed of the airplane with an exterior windshield surface temperature of 35° F. Although not stated in the specification, it is believed that the values shown are based on an ambient temperature of ° F. Reference 3-23 requires that the windshield anti-icing system shall be capable of operation during engine warm-up, taxi, takeoff and touchdown, as well as during normal flight. The specification values are based on the most severe condition of a windshield normal to the airstream. Less heat will be needed for windshields that are inclined.

3.5.3 FEASIBILITY

3.5.3.1 Electrical System Feasibility — The use of continuously heated electrical ice protection systems for relatively large areas, (e.g., leading edges of wing or tail surfaces) is not feasible for any aircraft because of the great amount of power required and the associated weights of the power generating equipment. Icing protection for windshields and other small components will usually be the running wet system unless runback ice would create a hazardous condition. An example of a hazardous condition would be windshield runback

ice breaking off and entering a rear-mounted engine. The power required for windshield protection of CAR 3 aircraft will usually be between 2.0 to 4.0 watts per sq. in. depending on airspeed, windshield configuration, and design ambient temperature. Power requirements for the other components will depend upon their shape or icing potential.

3.5.3.2 Hot Air System Feasibility — In determining the feasibility of a hot air system, the heat required for anti-icing (as determined in Paragraph 3.5.2) must be translated into terms of bleed air flow requirements. In some cases, the amount of bleed air available at certain operating conditions may be inadequate, or may have excessive effects on engine performance. Also to be considered are the pressure and temperature losses throughout the distribution system. The suggested procedure is for the designer, either by experience or by preliminary calculations, to arrive at a double-skin heat exchanger and supply system. This system is then analyzed, adjusting the inlet temperature and rate of flow until effective operation is obtained. If this condition cannot be met within the limits of available flow, permissible temperatures and allowable expenditure of energy, the design must be altered until a satisfactory solution is obtained. An excellent design manual for thermal anti-icing systems is WADC Technical Report 54-313, "A Design Manual for Thermal Anti-Icing Systems" (Ref. 3-10).

Military specifications state that exhaust gases from either turboprop or turbojet engines shall not come into contact with any portion of the aircraft other than the exhaust ducts; consequently, if the energy of the exhaust gases is to be used, a heat exchanger must be incorporated. This is necessary because of the toxic and corrosive nature of the exhaust gases (Ref. 3-8).

3.6 THERMAL DE-ICING

3.6.1 SYSTEM DESCRIPTION — In a de-icing system, ice accretion is permitted on the surfaces to be protected and is removed periodically. Thermal de-icing systems function by applying sufficient heat to the ice interface to melt

the bonding layer of ice; aerodynamic or centrifugal forces then remove the bulk of the ice. The areas that may be protected by a de-icing system are shown in Figure 3-1.

Large areas to be protected will normally be divided into small shedding sections by continuously heated (anti-icing) chordwise and spanwise parting strips. Figure 3-21 is a schematic of such a division showing the spanwise parting strip located along the stagnation line of the airfoil and the chordwise parting strips running chordwise. Cyclic de-icing is usually reserved for the larger areas as the weight and complexity of controls does not justify its use on small areas.

3.6.1.1 Electrical System Description — Electrical thermal de-icing systems contain electrical resistance heaters (foil, film, wire network, mesh, etc.) imbedded in Fiberglas, plastic, rubber or metal that is either the basic structure to be protected or can be attached to the basic structure (Ref. 3-11). Figure 3-22 shows cross-sections of typical electric heaters. Anti-icing parting strips are used in the electrical de-icing system to divide the total protected area into smaller, sequentially heated areas. This reduces the total instantaneous power requirement and maintains a stable load on the electrical system. The size of the cycled shedding sections will depend upon the total wattage available and the wattage density required for efficient de-icing.

Electric thermal de-icing of propellers may be accomplished by applying heating pads to the external surface of the blade or by heating the blade internally (Ref. 3-12 and 3-13). An example of the construction of an external electric heater for a propeller is shown in Figure 3-23. The outer ply of the propeller heater must be of a material which is rain erosion resistant and not too vulnerable to hail damage. All blades of a propeller should be de-iced at the same time, to avoid the vibration problems of non-uniform shedding.

3.6.1.2 Hot Air System Description — Hot air thermal de-icing systems are similar to electrical thermal systems in that heat is applied intermittently to each shedding section. In lieu of an electrical controller, the hot air system contains valves at each shedding section. Sources of hot air vary depending upon the type of powerplant. In turbojet and turboprop engines, hot air may be obtained directly from compressor bleed or from a heat exchanger located in the exhaust system. Combustion heaters may be used with either piston or turbine engines. The hot air is distributed from its sources to the shedding section by lightweight ducts. Figure 3-24 shows an NACA air-heated cyclic de-icing wing section with a continuously heated parting strip, and valving for cyclicly heating the shedding sections (Ref. 3-14). The air is then discharged overboard at some convenient location.

3.6.2 REQUIREMENTS — Heat used for de-icing must be used as economically as possible. It is thus necessary to ensure that as much of the heat as possible is used for melting ice and that no more ice is melted than necessary, or runback ice may occur on unheated surfaces. It has been found desirable to have the following characteristics in the cyclicly heated shedding zones:

a. A high specific heat input applied over a short period. This generally requires less total energy than a lower specific heat over a longer period of time. The high specific heat input reduces the convective heat losses from the exposed ice surface and conductive losses to the ice and structure.

b. Immediate cessation of heating and rapid cooling of the surface after shedding occurs. (This is to avoid runback ice.)

c. The heated area should be the minimum necessary so that heat is applied only under the ice and not dissipated to the airstream.

d. Good insulation between the heater and the supporting structure is required to direct the heat outwards to the exposed surface.

e.   To produce clean shedding and to avoid runback icing, the proper distribution of heat is required. It is desirable that melting of the ice bond should occur uniformly over the surface; this may require some chordwise gradient to the heat input.

f.   The spanwise and chordwise parting strips must prevent any bridging from one shedding zone to another. A small strip of anchorage may prevent large pieces of ice from shedding.

g.   The cycle "off time" should be controlled to permit adequate ice accretion for the best shedding characteristics. Runback ice formations can be minimized by decreasing the number of cyclic operations (using longer heat off times).

This "off time" will depend upon the thermal capacity of the shedding zone and the rate at which the surface cools to 32° F. It should also depend upon the icing rate so that the ice thickness accumulated is the best for shedding when de-icing occurs. If an icing rate meter is available, then coupling it to the de-icing system would assist in optimizing the system. For an electric system, the "off time" may be from three to four minutes; the "off time" for a hot gas system may be from four to six minutes. The longer "off" period for the hot gas system is a result of its greater thermal inertia.

System requirements for de-icing must be considered in two parts. first, the parting strips and dividing strips, and second, the cycled shedding area. Requirements for parting strips are calculated as shown in Paragraph 3.5.2 The heat input to the strips must provide at least running wet anti-icing to prevent ice from bridging. Control of the temperature of the strips is desirable both for economy and to prevent over-heating. Over-heating the parting strip encourages runback icing and detracts from shedding performance. Severe overheating may cause a burnout of the heating elements. Parting strip widths must be sufficient to accommodate the change in stagnation point with changes in angle of attack. A parting strip width of from 1 to 1.25 in. should be adequate for most installations.

Power requirements for the parting strips are essentially a single valued function of the surface datum temperature with no significant variations resulting from angle of attack, water content, droplet size or cycle times. Figure 3-25 is a reproduction of Figure 6 of NACA RM E51J30 (Ref. 3-11) showing parting strip electrical power requirements versus datum temperature. The difference between the input power and the measured net power to the outer surface is a measure of the efficiency of the system.

Aircraft wings with 30-deg. sweep-back or more will normally use only chordwise parting strips, since aerodynamic forces will remove the ice from the shedding zones without the aid of stagnation line parting strips.

Heat for the hot gas de-icing system parting strips may be obtained through a conductive fin from the hot gas duct to the stagnation point (see Figure 3-24), or a parting strip may be created during cycling of the shedding section by very high heat transfer occurring along the stagnation point. The power requirements at the outer surface for a parting strip would be the same for either a hot gas or electric system. However, the hot gas input power will be higher to compensate for the inefficiency of the hot gas system.

Shedding zone power requirements are difficult to determine. Heat transfer rates, aerodynamic forces and bonding characteristics of the ice (to the surface material) are some of the factors affecting the power requirements. Experimental values of shedding zone electrical power density on an airfoil for various heat-on times are shown in Figure 3-26 (Reference 3-11). From these curves it can be seen that the most desirable heat-on times would be between 10 and 30 seconds. Heat-on times less than 10 seconds would require heaters capable of withstanding very high power densities and a large number of cycled areas. Heat-on times longer than 40 seconds would not result in an appreciable reduction in power density. Shedding zone power density requirements are not

appreciably affected by variations in heat-off times or liquid water content. To achieve an even melting of ice throughout the shedding zone, it was found desirable to have a uniform power distribution in the region of direct water impingement and a decreasing power requirement downstream.

Hot gas shedding zone power requirement calculations have to account for the decreased efficiency of this system compared to an electric system. Tests conducted by NACA on a cyclic hot-gas de-icing system installed in an NACA 65_1-212 airfoil of eight-foot chord are reported in Ref. 3-14. Test results show that the required heating rate increases rapidly with a decrease of heat-on period and is particularly marked for heat-on periods less than 10 seconds as with the cyclic electric system. The heating rate required is affected largely by the air temperature. Curves showing heating rate required for marginal de-icing performance versus datum air temperature for various heat-on times is shown in Figure 3-27. A comparison of the heat requirements for de-icing versus anti-icing for the same airfoil are shown in Figure 3-28. In this figure, a cycle ratio of 1.0 denotes continuous heating or anti-icing heat requirements. The equivalent continuous heating requirements of a de-icing system drops rapidly up to a cycle ratio of "off-time" to "on-time" of approximately 5. By using a cycle ratio greater than 5, very little increase in economy can be realized. In addition, a long cycle time may permit heavy ice accretions. As shown in this figure, a de-icing system with a cycle ratio of 5 requires from one third to one fourth the power of an equivalent anti-icing system.

Over-heat protection devices may be required for both electrical and hot air de-icing systems. Inadvertent actuation of the electrical de-icing system during a period where little cooling takes place would cause burnout of the high wattage density heating pads. Inadvertent operation of the hot gas system might cause structural members to exceed safe temperature limits. The over heat protection device should be temperature sensing so that the systems may be used during ground operation to remove accumulated ice and during takeoff to prevent excessive ice formation.

Propeller thermal de-icing requirements will vary depending upon propeller diameter, rotational speed and aircraft forward velocity. Results from an NACA wind tunnel test of an external electric propeller de-icing system indicate a power requirement of from 4.5 to 10 watts per square inch for an ambient temperature range from 21 to 2° F (Ref. 3-12). Other conclusions reached during this investigation were: the radial extent of heating will depend upon the kinetic temperature rise of the propeller, and the chordwise distribution of heat input should approach uniformity. Tests have also been conducted on an internal electric de-icing system (Ref. 3-13). These tests indicate that a maximum of 1,500 watts per blade for a 5.5-ft. blade (11 ft. dia.) may be required for temperature conditions from 0° to 17° F. A heat-on time of approximately 60 seconds with a total cycle time of four minutes was used.

Shedding of ice from propellers should be uniform from each blade to prevent unbalance. Also, the frequency of shedding should be scheduled to prevent large pieces of ice from forming, as they may cause damage to the aircraft when they are shed. Structural protection from ice shed by propellers is specified in CAR 4b.

3.6.3 FEASIBILITY

3.6.3.1 Electrical System Feasibility — An electric thermal de-icing system may be installed on any existing aircraft by attaching flexible wrap-around heating pads to the structure with an adhesive. The heating pads are fairly thin and may not appreciably affect the aircraft performance. Another method of providing thermal-electric ice protection is to mold the heating elements into the leading edge structural member as shown in Figure 3-22. No aerodynamic performance loss may be experienced by this construction method. Early fabrication techniques using wire heating elements had the disadvantage that damage to a small section required replacement of the complete unit. One of the latest methods uses expanded metal which may be repaired, thereby making large structural sections both practical and economical.

The electrical wiring supplying power for the heating pads requires little space and can normally be routed through existing passages within the structure. Generating equipment may be either engine-driven or driven by an auxiliary power source. The required capacity of the power generator will depend upon several factors: the efficiency of the heating pads, the wattage of the shedding sections and the number required to be on at any one time. The cycling of the shedding sections may be scheduled to maintain an even power load upon the generating equipment.

In higher speed aircraft, the rubber heating pads are subject to rain erosion and hail damage. A metal overshoe will protect the pads and at the same time will even out the heat distribution and prevent cold spots on the surface. Detracting from the overshoe installation is the loss in heater efficiency and the added weight to the aircraft.

Electrical thermal de-icing may be installed on the external surface of a propeller without appreciably affecting its performance. Coverage should be approximately 15 per cent of the chord on the camber side and approximately 30 per cent of the thrust face. The power to the heating pads is supplied through slip-rings at the propeller hub. Installation of the heating element on the interior of the propeller would protect the heating elements from damage, but the loss of efficiency and the difficulty of repair make the external system more feasible.

3.6.3.2 Hot Air System Feasibility — Several hot air sources are available for de-icing, depending upon the aircraft type and power extraction limitations. The hot air sources on a piston engine aircraft may be an exhaust gas heat exchanger or a combustion heater. A combustion heater burns fuel and, by means of a heat exchanger, heats ram air for the de-icing system. On turboprop and turbojet aircraft, the hot air source may be compressor bleed air, a combustion heater, or an exhaust gas heat exchanger.

Another system requirement is a method of distributing this heat to the surfaces to be de-iced. The more efficient method is to use a narrow-passage, thin, double-walled heat exchanger (Figure 3-24). The hot air is transferred to the heat exchanger by lightweight ducts. This type of system must normally be designed into the aircraft at its beginning. Installation of a hot air de-icing system in an existing aircraft would require major modifications to the first 10 to 15 per cent of chord. In making a choice between electrical or hot gas de-icing systems, the greater ease of installation of the electrical system must be weighed against the better serviceability and lower maintenance requirements of the hot air system. The final choice must depend upon the available sources of heat and the type and location of components requiring protection. The final selection may be a combination of the two systems. Because of the large air mass flows and heat transfer requirements, the cyclic hot gas system will probably have application only to large turbine engine aircraft.

3.7 RESERVE POWER

3.7.1 DESCRIPTION — Reserve power may be considered a method of overcoming icing conditions because the drag effects of ice accretion may be compensated for by the aircraft powerplant Ice accretion affects thrust, lift, drag and weight of an airplane. What these effects will be depends upon the type and amount of ice. Effects on range, stall speed, flutter and controllability must also be considered. Thes section will present methods for estimating and evaluating aircraft performance with ice accretion in tems of rate of climb.

3.7.2 REQUIREMENTS — The horsepower required for level flight of a clean airplane is expressed as:

$$HP_r = C_D \, q A V \div 550, \text{ horsepower} \qquad (3.7.1)$$

A similar expression for an aircraft with ice accretion is

$$HP_{r_{ice}} = C_{D_{ice}} \, q A V \div 550, \text{ horsepower} \qquad (3.7.2)$$

where the subscript "ice" denotes iced conditions. Figures 3-29 and 3-30 show the lift and drag effects of rime and glaze ice accretion on a particular aircraft. The "standard indicator" noted in these figures is a small diameter fixed rod, unheated, with calibration markings to show the amount of ice accumulated at any given time.

Dividing Eq. 3.7.1 by 3.7.2 results in

$$HP_r/HP_{r_{ice}} = C_D/C_{D_{ice}}$$

The ability of an aircraft to maintain level flight or to climb with ice accretion is expressed as:

$$C_{h_{ice}} = \frac{HP_a - HP_{r_{ice}}}{W} \; 550$$

where $C_{h_{ice}}$ is the rate of climb with ice accretion in ft./min.

By substitution

$$C_{h_{ice}} = \frac{HP_a - \left(\frac{C_{D_{ice}}}{C_D}\right) HP_r}{W} \; 550 \tag{3.7.3}$$

To solve Eq. 3.7.3, it will be necessary to determine the drag coefficient with ice ($C_{D_{ice}}$). First approximations of this value can be made from icing tunnel tests or by comparison with icing flight tests of similar type aircraft. Effects of icing on rate of climb for a particular aircraft are presented in Figures 3-31 and 3-32. Another curve of interest is Figure 3-33, which presents velocity versus available horsepower and required horsepower for this same aircraft. This curve shows that without ice protection on this aircraft, single-engine flight is not possible, and that even with ice protection a limited speed range is available during one-engine operation. The icing condition referred to in this curve is the more severe glaze ice.

3.7.3 SYSTEM FEASIBILITY -- To determine an aircraft's capabilities accurately during an icing encounter, icing wind tunnel tests and icing flight

tests should be performed. An estimate of the effects of ice accretion can also be made from evaluating icing data from a similar type aircraft. A polar curve for the airplane should then be determined with the lift and drag decrements caused by ice. Aircraft performance can then be calculated. The effects on flutter, controllability and stall speed cannot be predicted and must be obtained by actual experience. As icing encounters and severity of icing are difficult to forecast, an operator should not depend upon marginal reserve power for ice protection and fly into an area where icing is predicted. If icing is inadvertently encountered, it is advisable to know the aircraft capabilities and performance characteristics with ice.

3.8 MISCELLANEOUS METHODS OF PROTECTION

Several methods of protection have been devised — and in some cases tested and used — but have not attained widespread use for one reason or another. Some of these systems are described in this paragraph and the limitations discussed. Additional systems are discussed in Ref. 3-15.

3.8.1 LIMITED PROTECTION SYSTEMS — One limited protection system consists of applying ice adhesion depressant to the surface to be protected. The chemical does not mix with the moisture to lower its freezing point, rather it decreases the ice bond strength to the surface so that centrifugal or aerodynamic forces can remove ice accumulations. The chemicals, primarily silicone based, must be renewed periodically whether ice has been encountered or not. The physical manner in which they shed ice is by delamination of the silicone. One such product has been approved as being equivalent to an electrical propeller de-icer under the following conditions: It must be renewed after 48 hours of elapsed time, provided no precipitation has been encountered, or after eight hours of flying time during which no more than three hours of precipitation is encountered. The chemicals also can be used effectively on pneumatic boot systems to assist in removing ice and to reduce residual ice. (See Figure 3-34, obtained from Reference 3-1).

Several test programs have been conducted on other chemicals to test their ice bond depressant properties. One such program (Ref. 3-16) tested organic polar chemicals and although several of the chemicals did reduce the ice bond appreciably, none reduced the ice adhesion sufficiently to indicate that practical ice-repellant compounds could be developed using these organic polar chemicals as the major active ingredients.

Another chemical action tested as an ice protection method is an exothermic reaction. This method appears possible, but it has an extremely short protection duration and at present has found no practical application.

In addition to chemicals, many water-repellant materials have been tested with but limited success; these include the fluorocarbon compounds and others.

3.8.2 VAPOR CYCLE PROTECTION SYSTEM — A vapor cycle protection system circulates a hot vapor through a ducting pattern in the protected surface and uses the high latent heat of condensation of the vapor to maintain the protected surface above the freezing point. The heat source for boiling the liquid and forming the hot vapor is an exhaust gas heat exchanger. The vapor circulates through the ducts, condenses and is returned by gravity flow to the heat exchanger. The system is a closed system depending upon a leak-tight network to continue functioning. The pressure in the system is the saturated vapor pressure at the lowest temperature in any part of the system. This pressure may go as high as 250 psig during takeoff on a hot day. A line diagram of such a system is presented in Figure 3-35.

Some of the salient disadvantages are its initial cost of installation, its weight and its maintenance difficulties, which have so far ruled out any practical application.

REFERENCES

3-1   NACA TN 3564, "Effect of Pneumatic De-Icers and Ice Formations on
      Aerodynamic Characteristics of an Airfoil," Dean T. Bowden, Feb. 1956.

3-2   Mil Spec. MIL-D-8804A, "De-Icing System, Pneumatic Boot, Aircraft,
      General Specification for," 14 June 1956.

3-3   Mil Spec. MIL-S-6625A, "Spray Equipment, Aircraft Windshield, Anti-
      Icing," Oct. 1951

3-4   NACA TN 2799, "Simple Graphical Solution of Heat Transfer and Evapora-
      tion from Surface Heated to Prevent Icing," Vernon H. Gray, Oct. 1952.

3-5   NACA RM E521J31, "Experimental Investigations of Radome Icing and
      Icing Protection," J. P. Lewis and R. J. Blade, Jan. 1953.

3-6   "Fluid De-Icing," D. C. Tanner, (paper presented at 1961 Aircraft Ice
      Protection Conference, D. Napier & Son, Ltd.).

3-7   NACA TN 2866, "Icing Protection for a Turbojet Transport Airplane.
      Heating Requirements, Methods of Protection, and Performance
      Penalties," T. F. Gelder, J. P. Lewis and S. L. Koutz, Jan. 1953.

3-8   Mil Spec. MIL-A-9482, "Anti-Icing Equipment for Aircraft, Heated
      Surface Type, General Specification for," 15 Dec. 1947, amended
      10 June 1955.

3-9   Mil Spec. MIL-T-5842A, "Transparent Areas, Anti-Icing Defrosting
      and Defogging Systems, General Specifications for," 1 Sept. 1950.

3-10 WADC Technical Report 54-313, "A Design Manual for Thermal Anit-
      Icing Systems," H. H. Sogin of Illinois Institute of Technology, Dec. 1954.

3-11 NACA RM E521J30, "Experimental Investigations of Cyclic De-Icing of
      an Airfoil Using External Electric Heater," J. P. Lewis and Dean T.
      Bowden, June 1953.

3-12 NACA TN 1520, "De-Icing Effectiveness of External Electric Heaters
      for propeller Blades," J. P. Lewis, Feb. 1948.

3-13 NACA TN 1691, "Icing and De-Icing of a Propeller with Internal Electric
      Blade Heaters," J. P. Lewis and Foward C. Stevens, Jr., Aug. 1948.

3-14 NACA RM E53C27, "Comparison of Several Methods of Cyclic De-Icing
      of a Gas Heated Airfoil," V. H. Gray and Dean T. Bowden, June 1953.

3-15 WADC Technical Report 55-262, "Study of Limited Type Ice Removal and Prevention Systems (Mechanical Phase)," H. C. Johnson and E. G. Johnson of Research Inc., April 1955.

3-16 WADC Technical Report 56-591, "Ice Adhesion Tests on Films of Organic Polar Materials," W. R. Meyer, Phd, and E. F. Foley, Jr., March 1957.

3-17 "Results of Experimental Flights in Natural Icing Conditions and Operation of Aircraft Thermal Ice Protection Systems," O. K. Trunov and M. S. Egorov (paper presented at 1960 Aircraft Ice Protection Conference, D. Napier & Son, Ltd.).

EMPENNAGE
LEADING EDGES

WING LEADING
EDGES

PROPELLERS

WIND SHIELD

RADOME

ESSENTIAL INSTRUMENTS

AUXILIARY AIR
INLETS

ENGINE AIR
INLETS
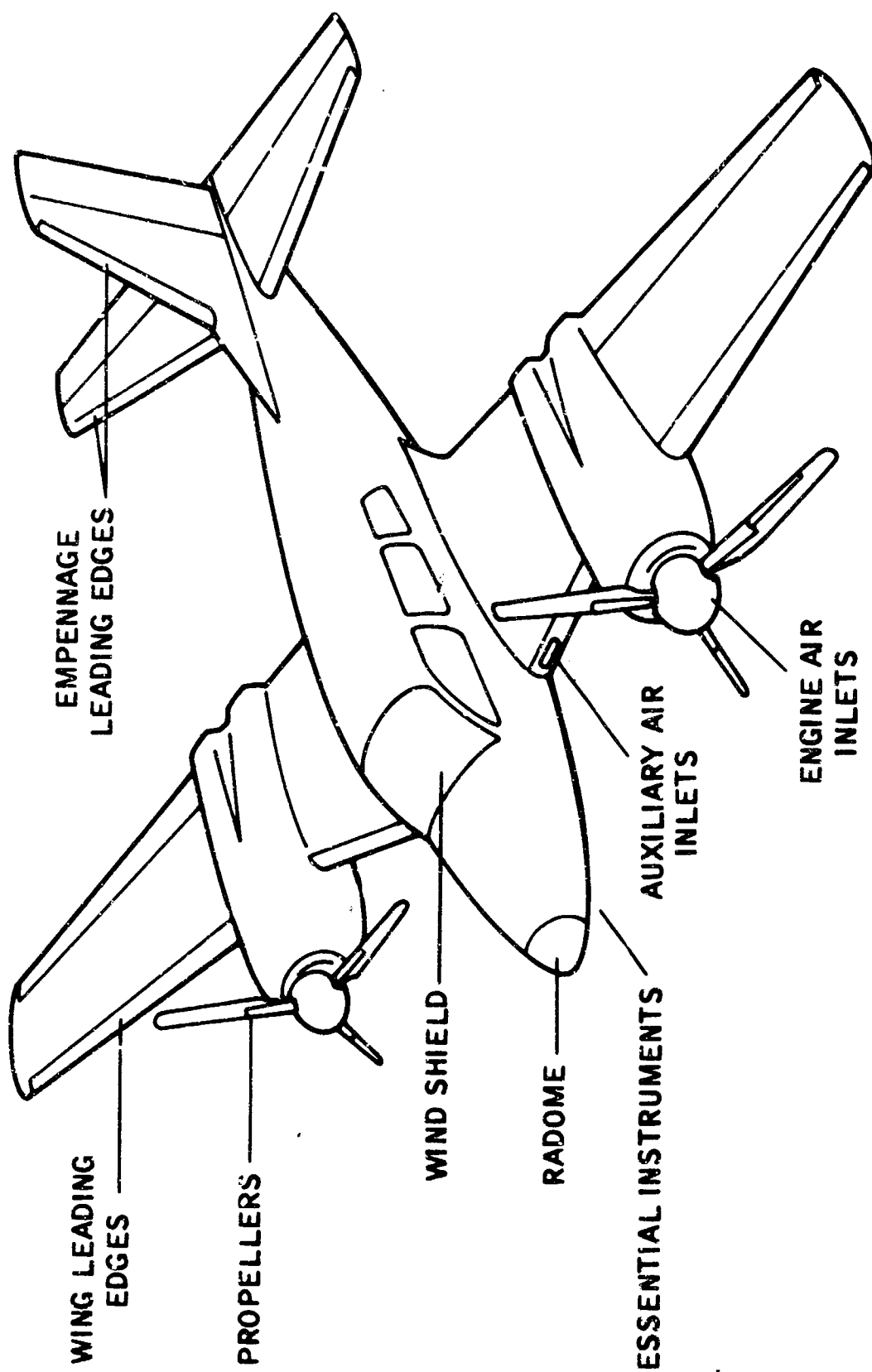
Areas of Airframe That May Require Ice Protection.

Figure 3-1
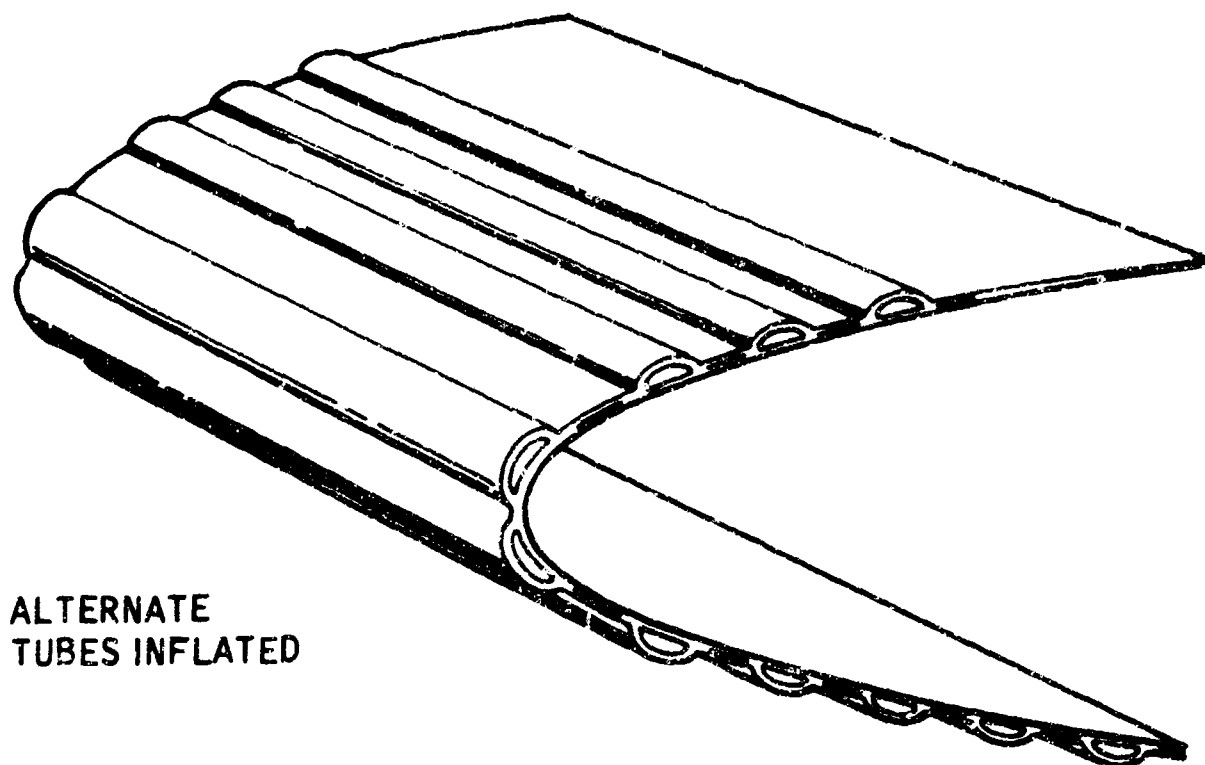
ALTERNATE
TUBES INFLATED
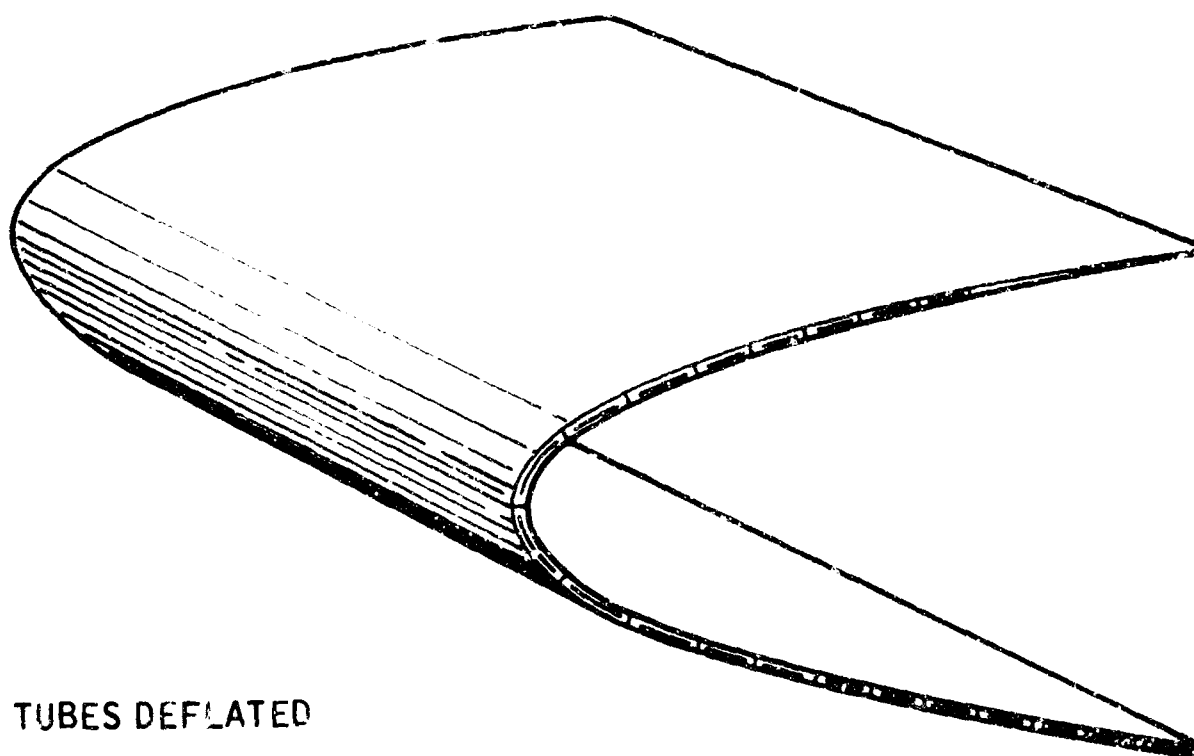
TUBES DEFLATED

Figure 3-2.   Spanwise Inflatable De-Icing Tubes
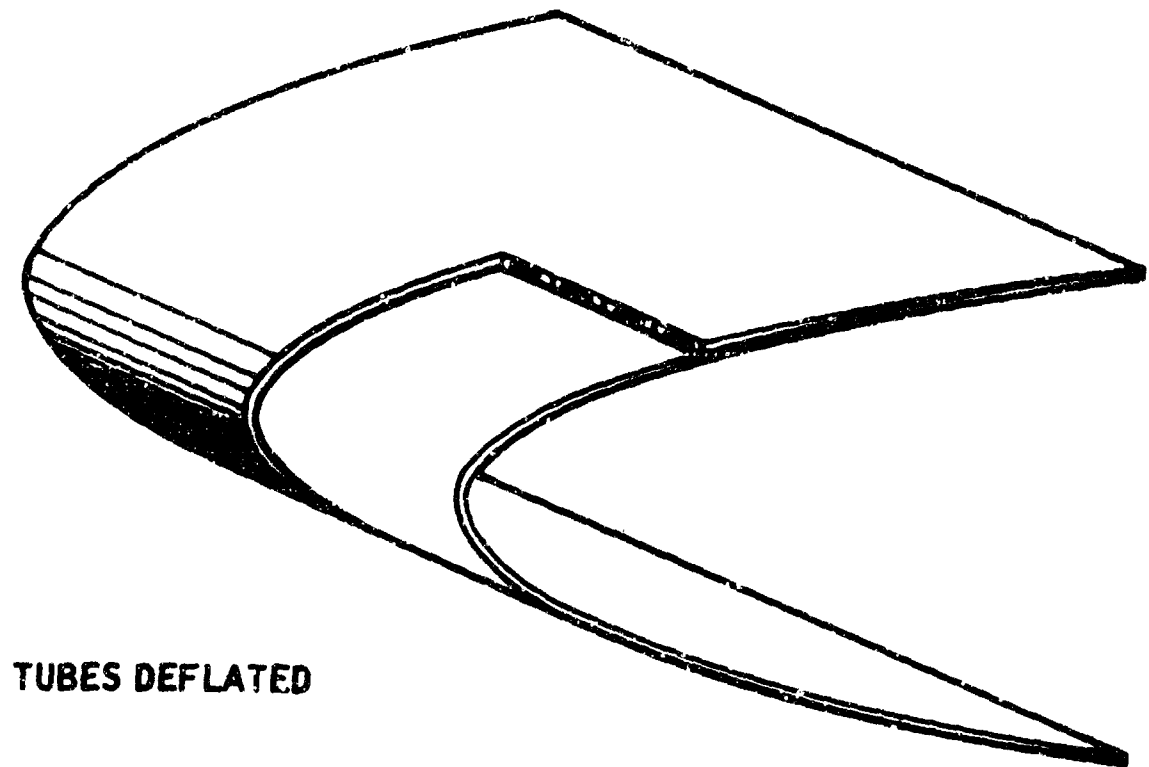
TUBES DEFLATED
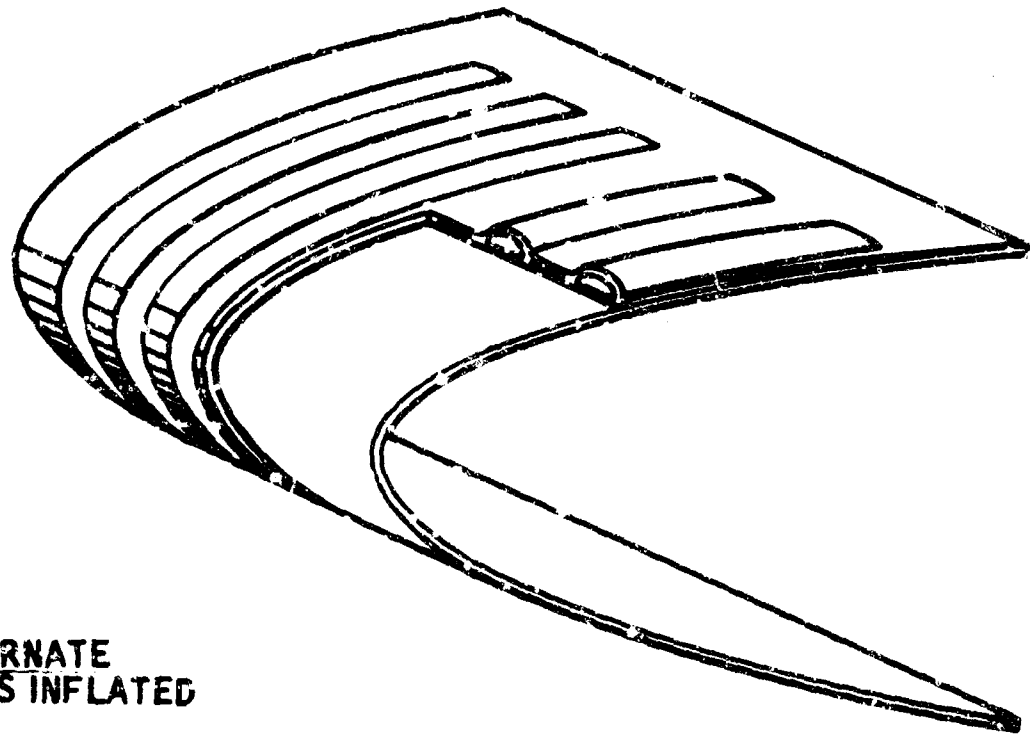
ALTERNATE
TUBES INFLATED

Figure 3-3. Chordwise Inflatable De-Icing Tubes

3-36

1. AIR PUMP
2. PRIMARY OIL SEPARATOR
3. CONTROL VALVE
4. FILTER ASSEMBLY
5. SHUTTLE VALVE
6. VACUUM RELIEF VALVE
7. VACUUM SYSTEM CHECK VALVE
8. PRESSURE SWITCH ASSEMBLY
9. NACELLE TO TIP L.H. DE-ICER
10. NACELLE TO TIP R.H. DE-ICER
11. HORIZONTAL STABILIZER DE-ICER
12. FIN DE-ICER
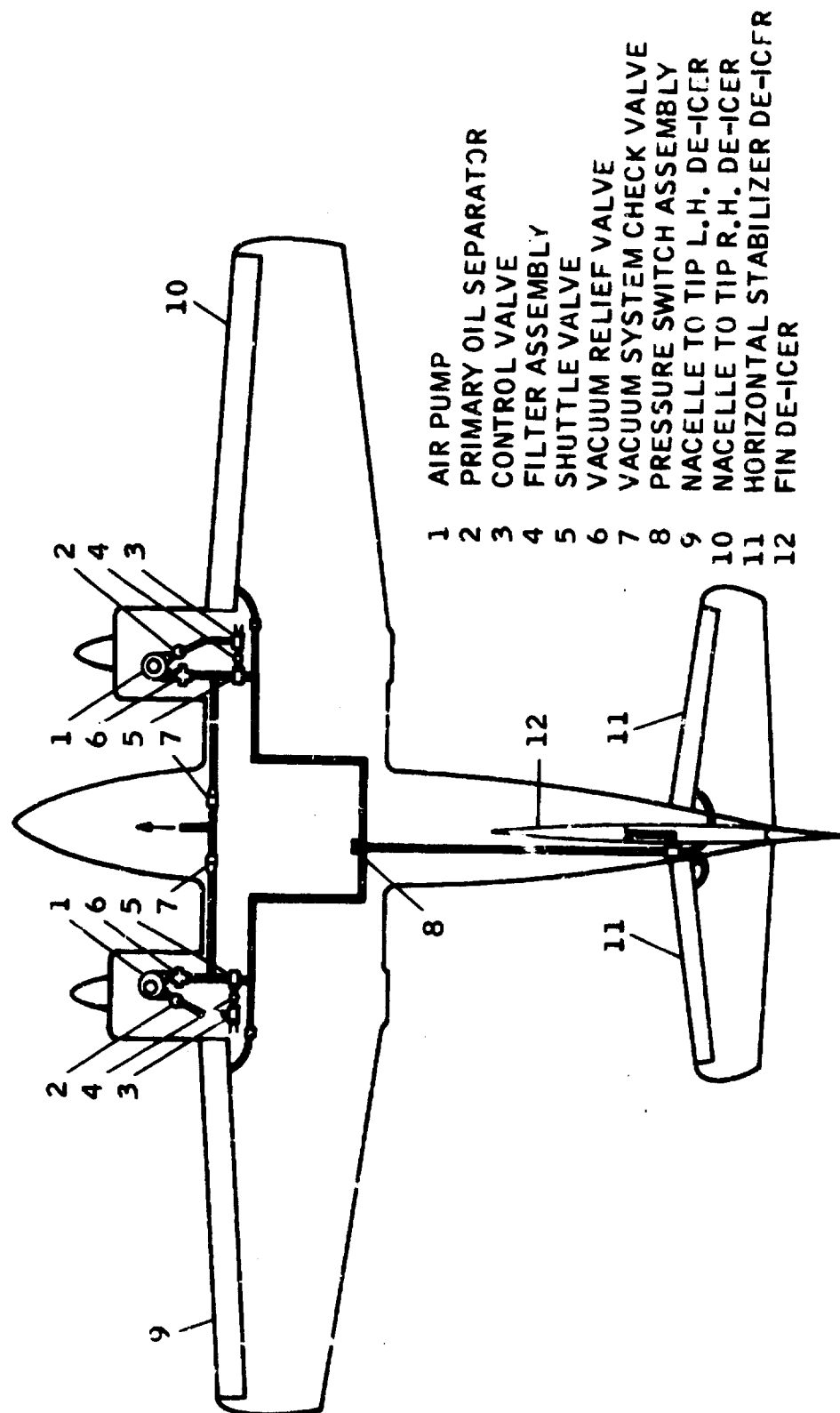
Inflatable Tube De-Icing System — Schematic

Figure 3-4

Flow Control Tubes

Dam

Porous Metal Spreader

Bushing For Attaching Bolt

Secondary Feed Channel

Primary Feed Channel

Central Web

Double-Strip Installation - Compensate for Change in Stagnation Line with Angle of Attack
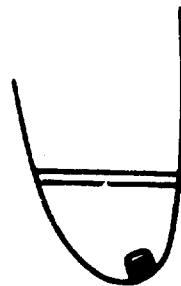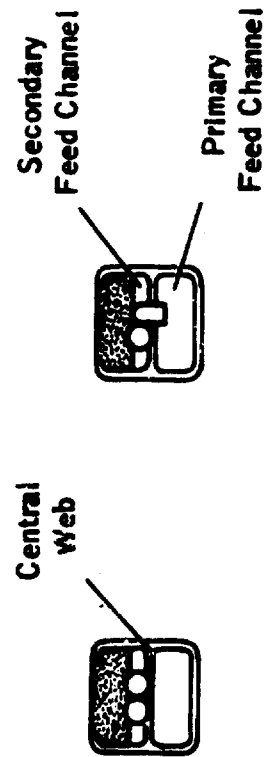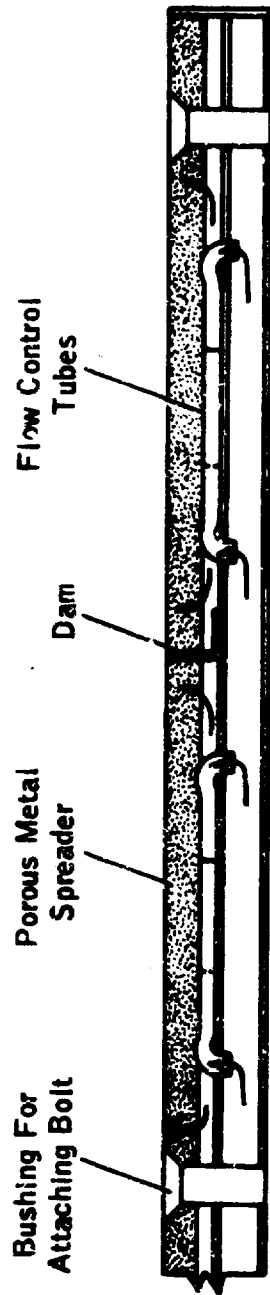
Single-Strip Installation Along Stagnation Line

Fluid De-Icing Strip Distributor Construction Details (Ref. 3-6).

Figure 3-5

3-38

STAINLESS POROUS PANEL

BACK PLATE

FLEXIBLE POROUS SHEET

DE-ICING FLUID METERING TUBE
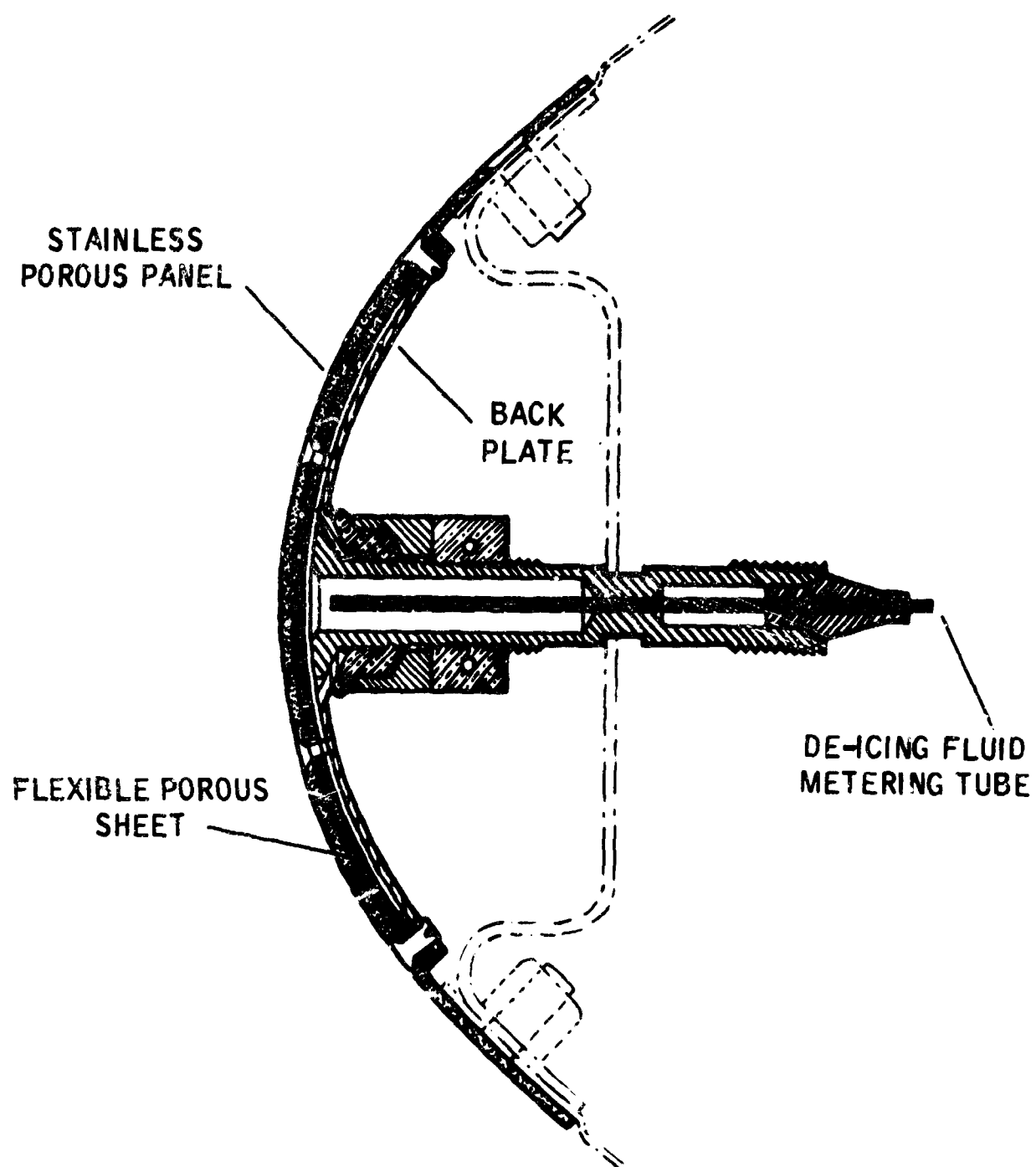
Figure 3-6. De-Icing Fluid Distribution Panel.

FLUID DISCHARGE ORIFICE

AIR

FLUID

AIR SWIRL TUBE

FLUID INLET

AIR INLET

SURFACE TO BE ICE PROTECTED
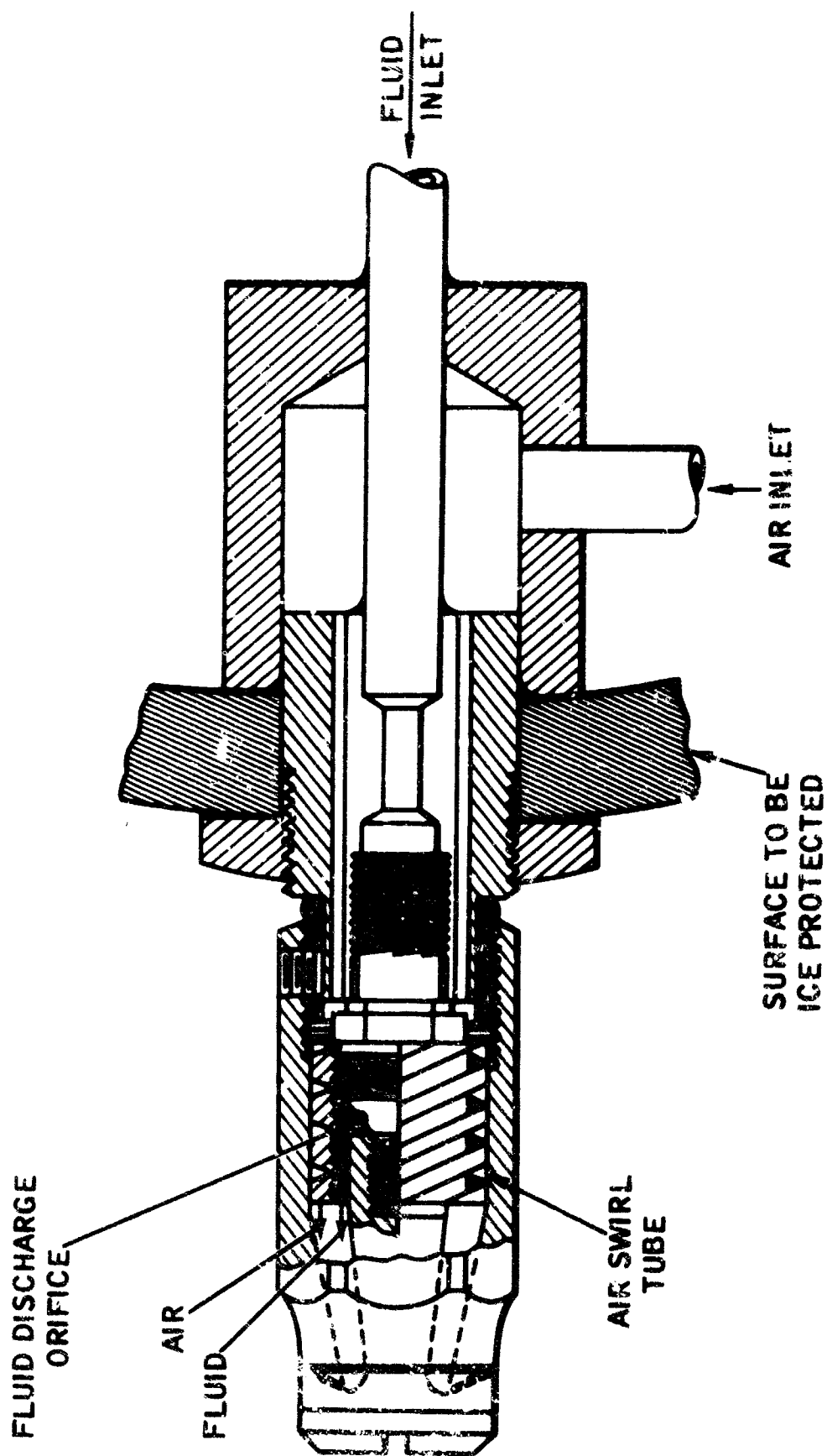
Fluid Spray (Air Atomizing) Nozzle (Ref. 3-5).

Figure 3-7
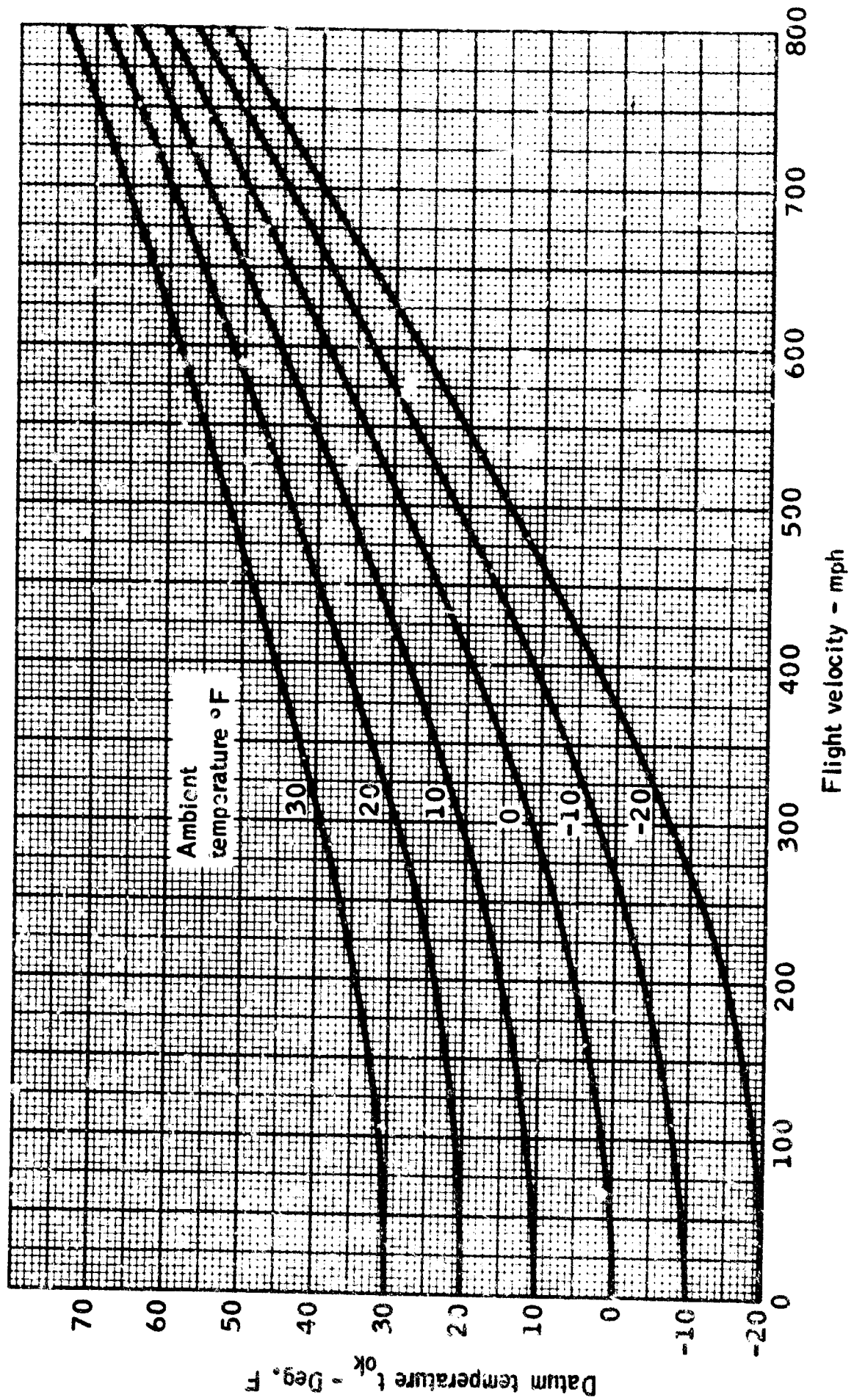
Datum Temperature at Sea Level -- Temperature Versus Airspeed.

Figure 3-8a
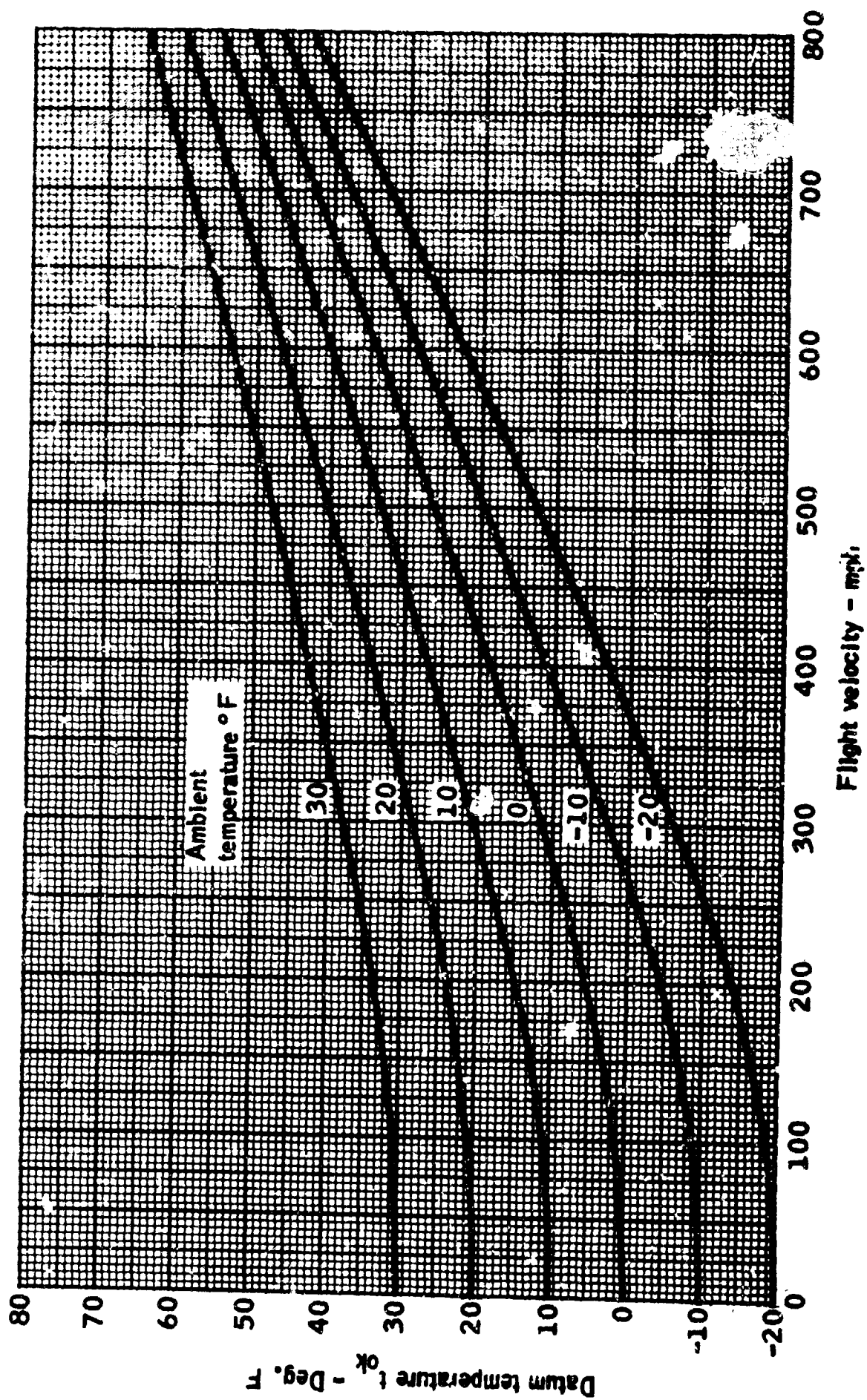
Datum Temperature at 10,000 ft. — Temperature Versus Airspeed

Figure 3-8b
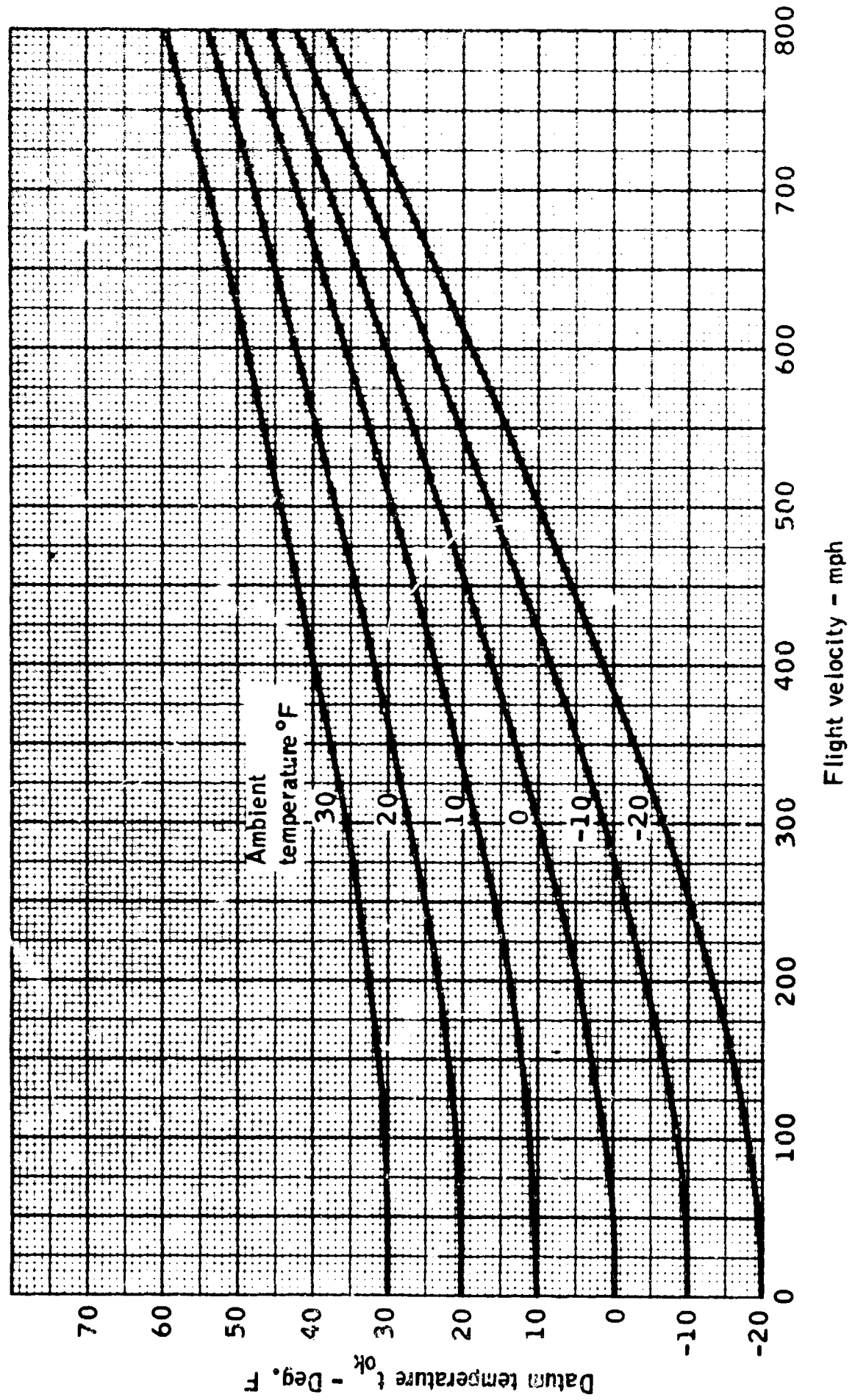
Figure 3-8c

Datum Temperature at 20,000 ft. — Temperature Versus Airspeed
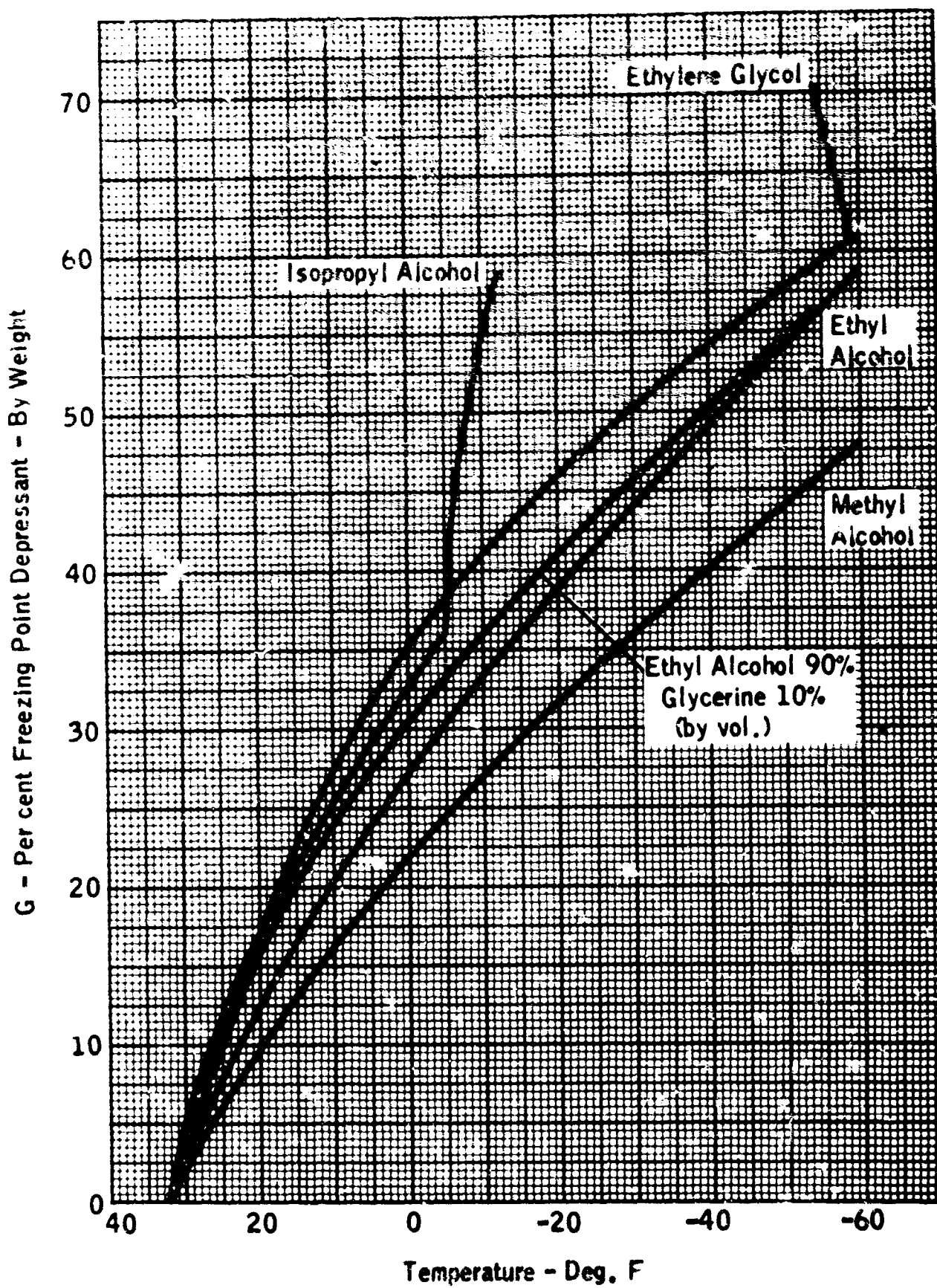
Figure 3-9.   Freezing Point Plots for Aqueous Solutions of Several
Freezing Point Depressant Fluids.

PANEL DISTRIBUTORS

ON-OFF SWITCH

PUMP

SUPPLY TANK

STRIP OF PANEL DISTRIBUTORS
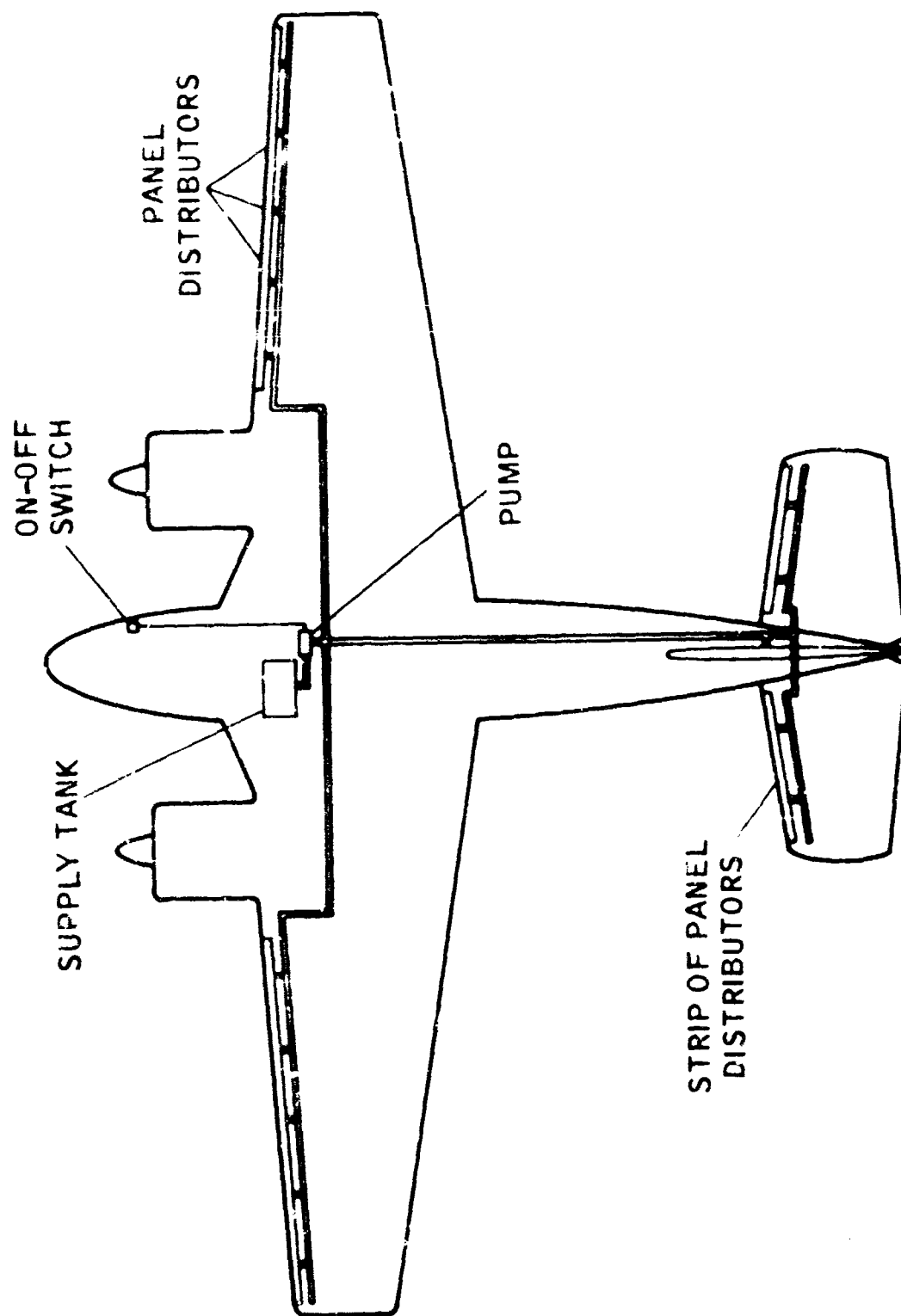
Diagrammatic Layout of Fluid Ice Protection System

Figure 3-10

3-45
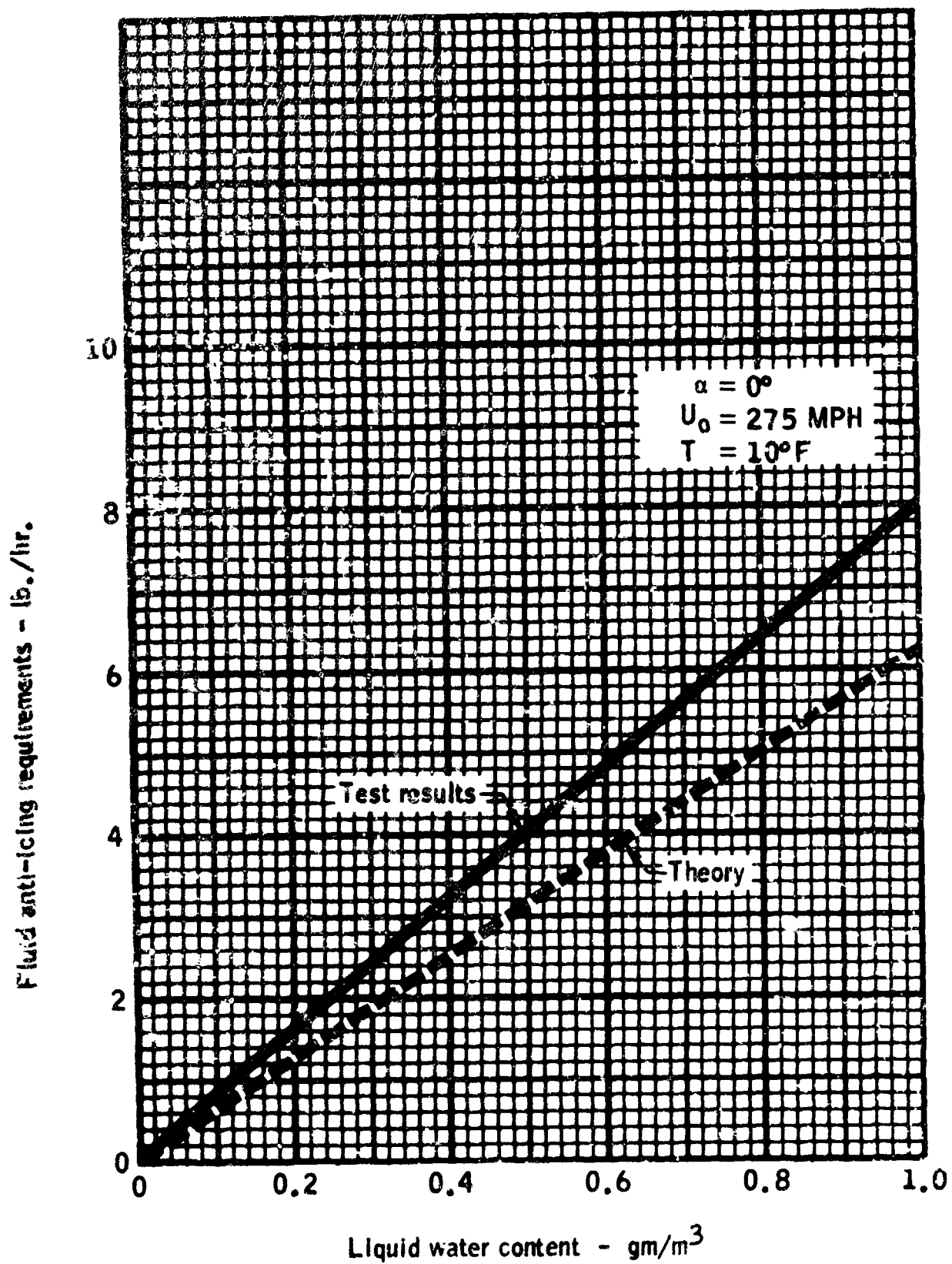
Figure 3-11. Variation of Fluid Anti-Icing Requirement With LWC (Ref. 3-5)
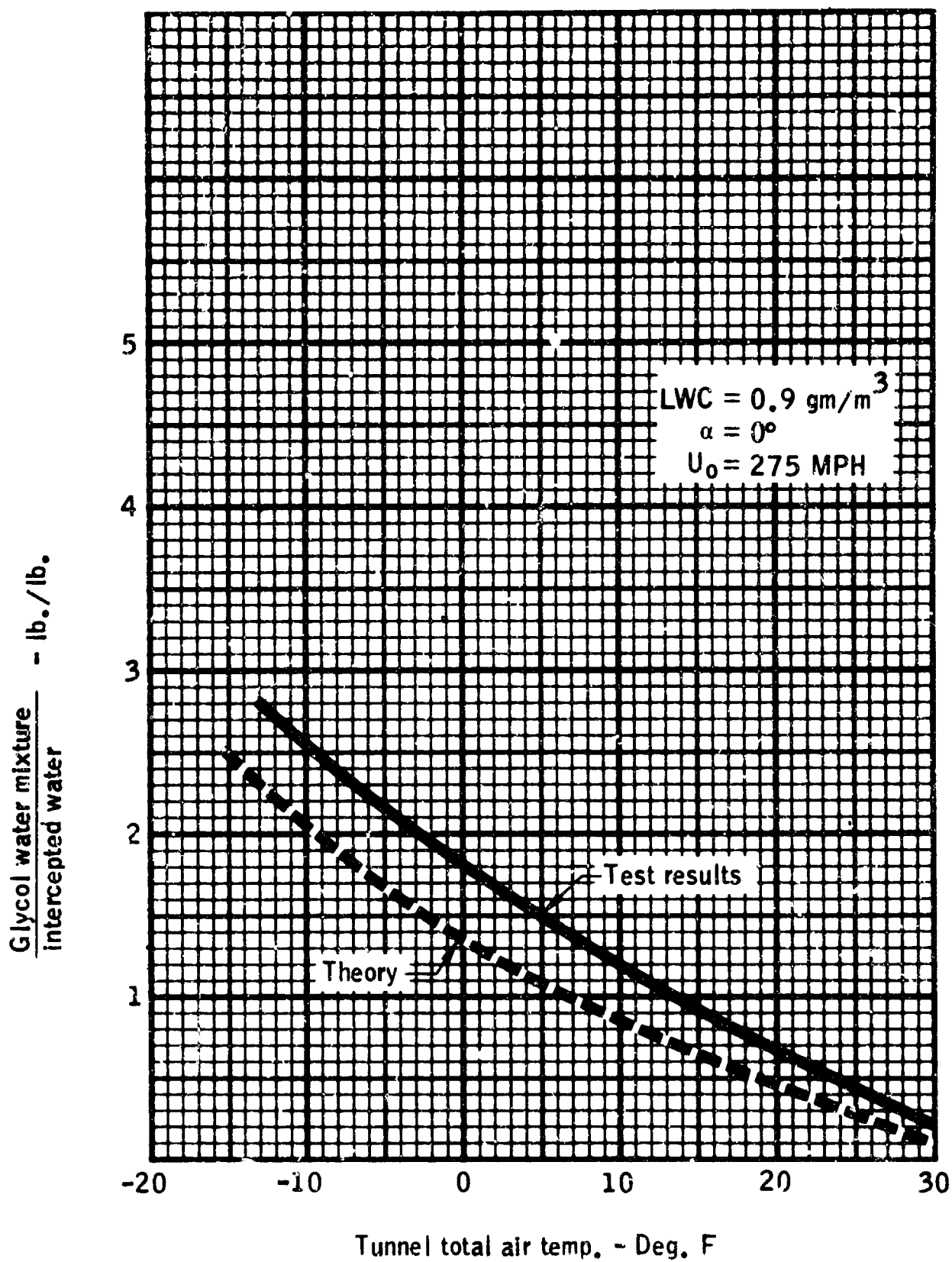
Figure 3-12. Variation of Fluid Anti-Icing Requirement With Air Temperature (Ref. 3-5)
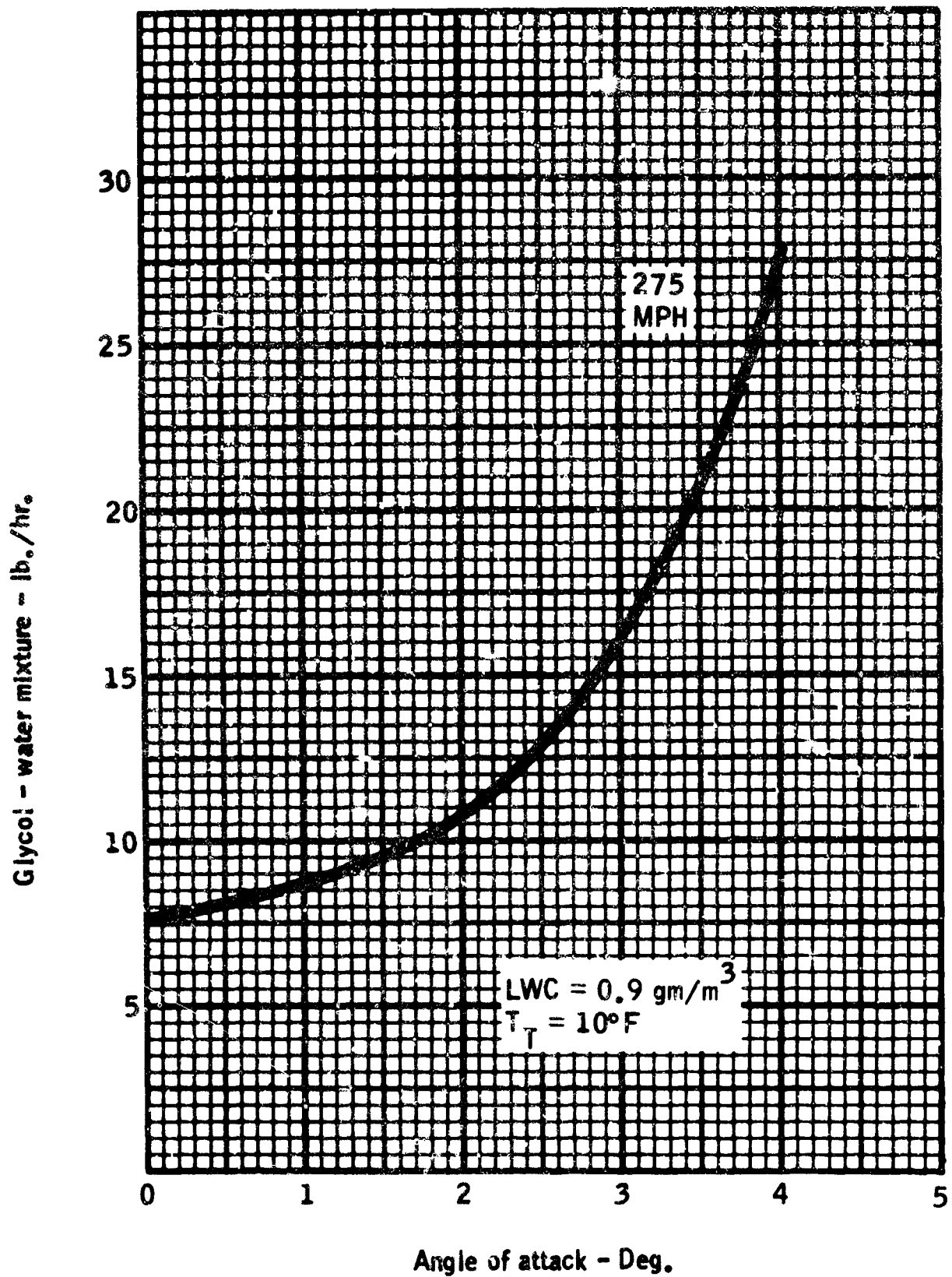
Figure 3-13. Variation of Fluid Anti-Icing Requirement
With Angle of Attack (Ref. 3-5)
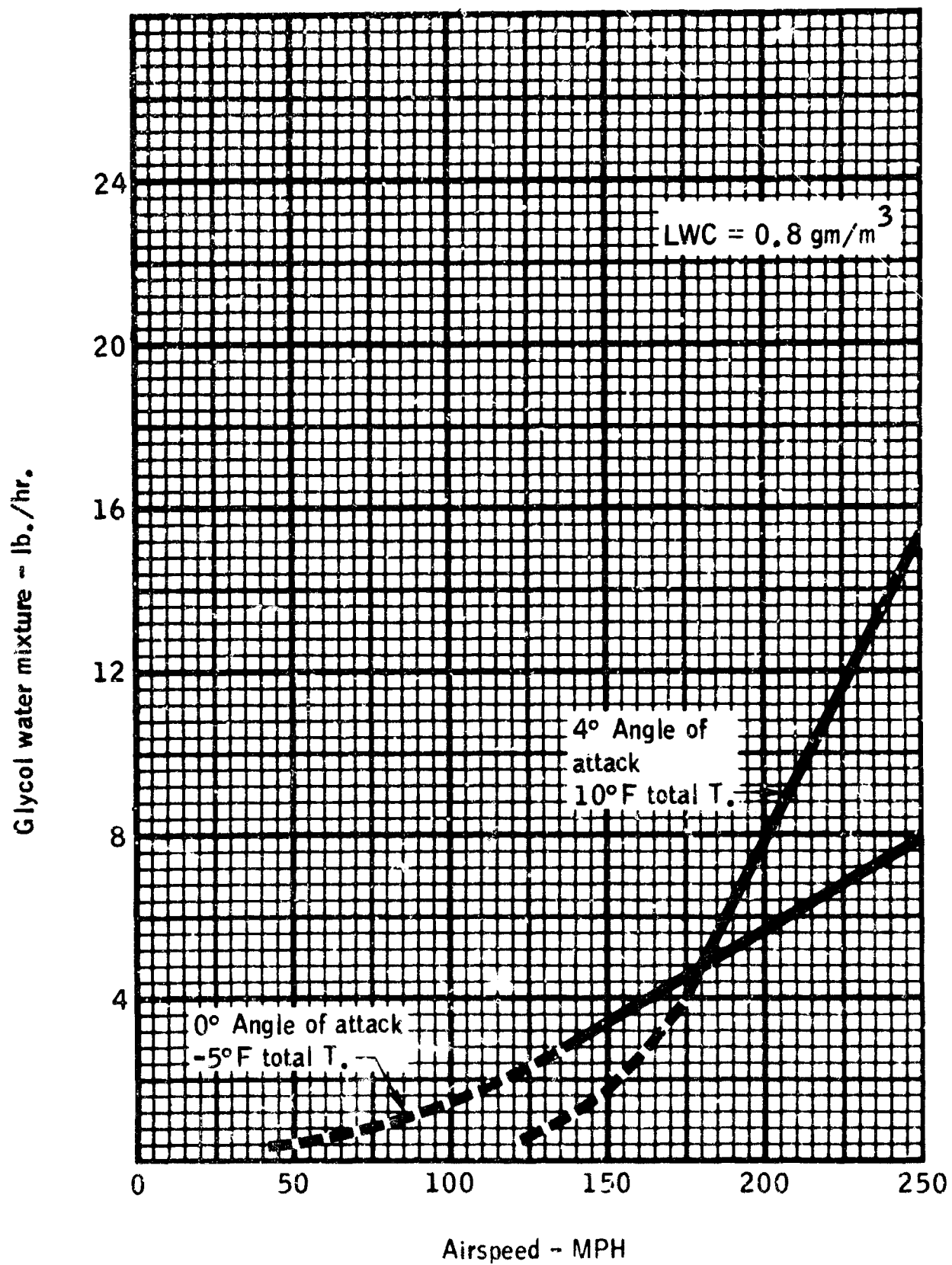
Figure 3-14. Variation of Fluid Anti-Icing Requirement
With Airspeed (Ref. 3-5)

HEATED AREA

OUTER PLY

CONDUCTIVE FILM

PLASTIC INTER-
LAYER

PLEXIGLASS

BUS BARS

EDGE SEALANT

TEMPERATURE
SENSING ELEMENT

CABIN
SIDE

EDGE
REINFORCEMENT
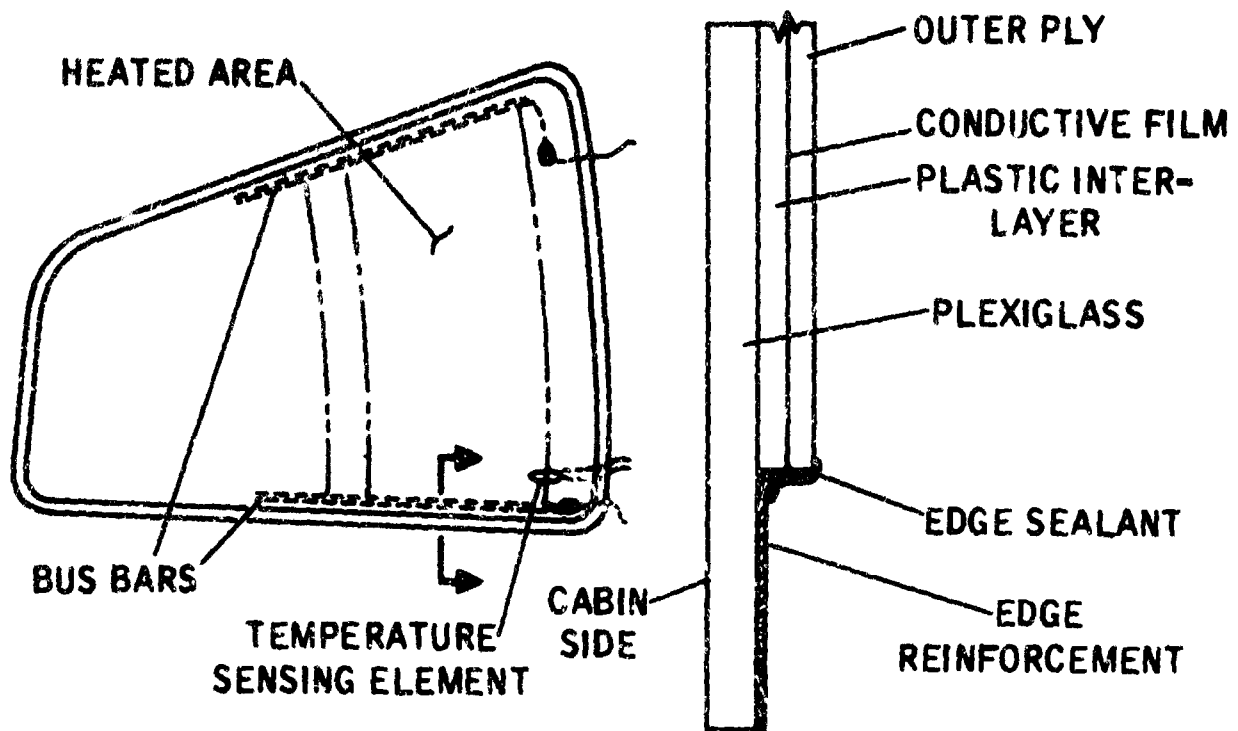
TYPICAL ELECTRICALLY HEATED PLASTIC WINDSHIELD

SENSING
ELEMENT

HEATING
SURFACE

ELECTRICALLY
HEATED AREA

GLASS

VINYL

GLASS

METAL
INSERT

INNER
SURFACE

BUS
BARS
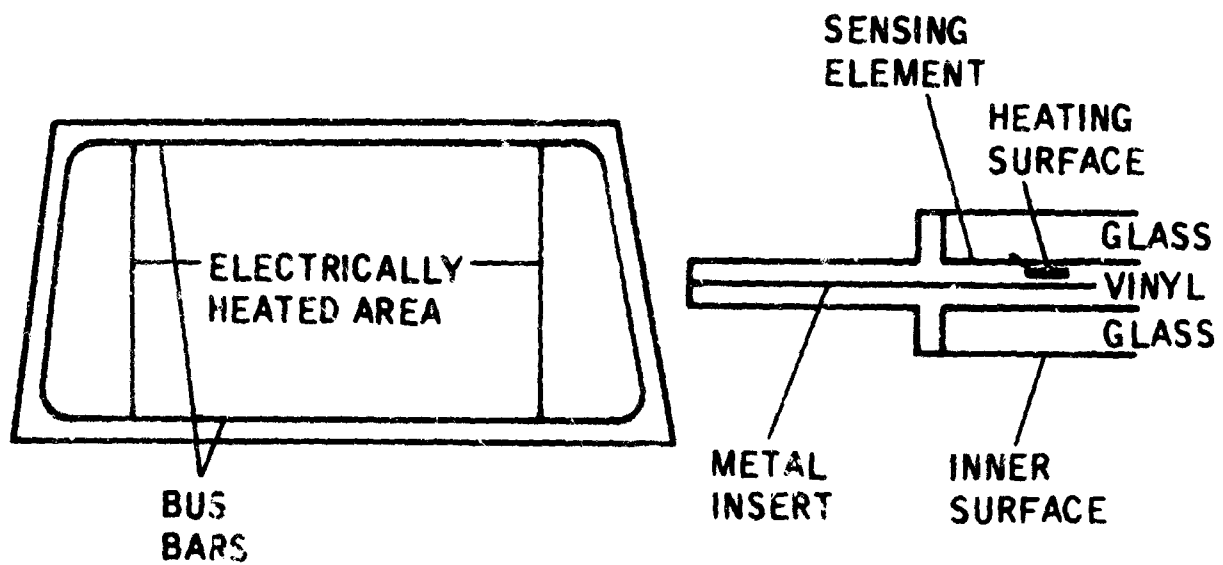
TYPICAL ELECTRICALLY HEATED GLASS WINDSHIELD

Figure 3-15. Typical Electrically Heated Windshield Construction .
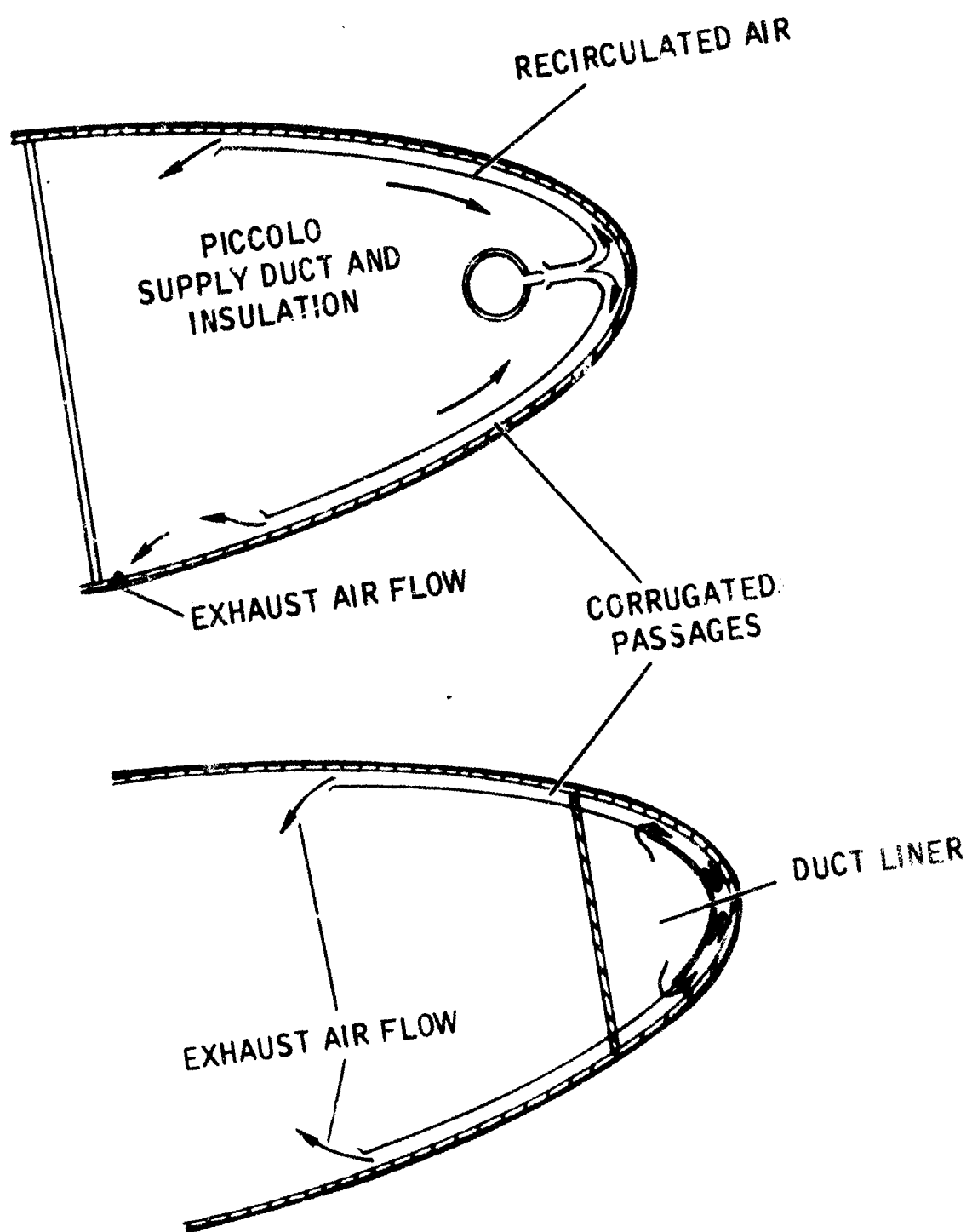
Figure 3-16. Air Flow in Typical Leading Edges of Heated Wings (Ref. 3-10).
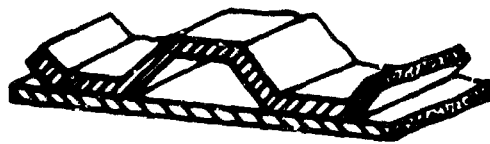
CORRUGATED CHANNEL
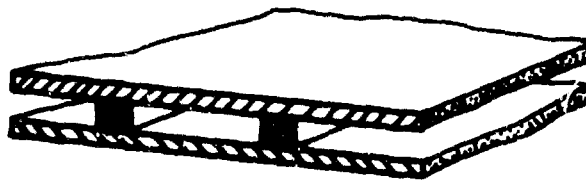
SPACER STRIPS
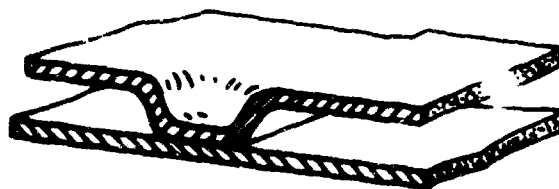
DIMPLE EMBOSS
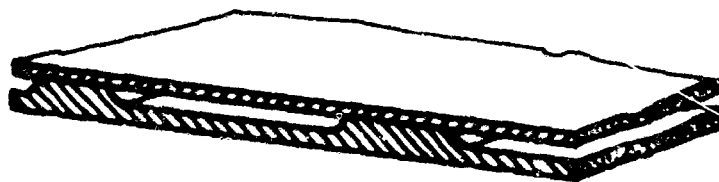
ETCHED CHANNEL

Typical Cross-Sections of Double-Skin Gas Passages (Ref. 3-10).
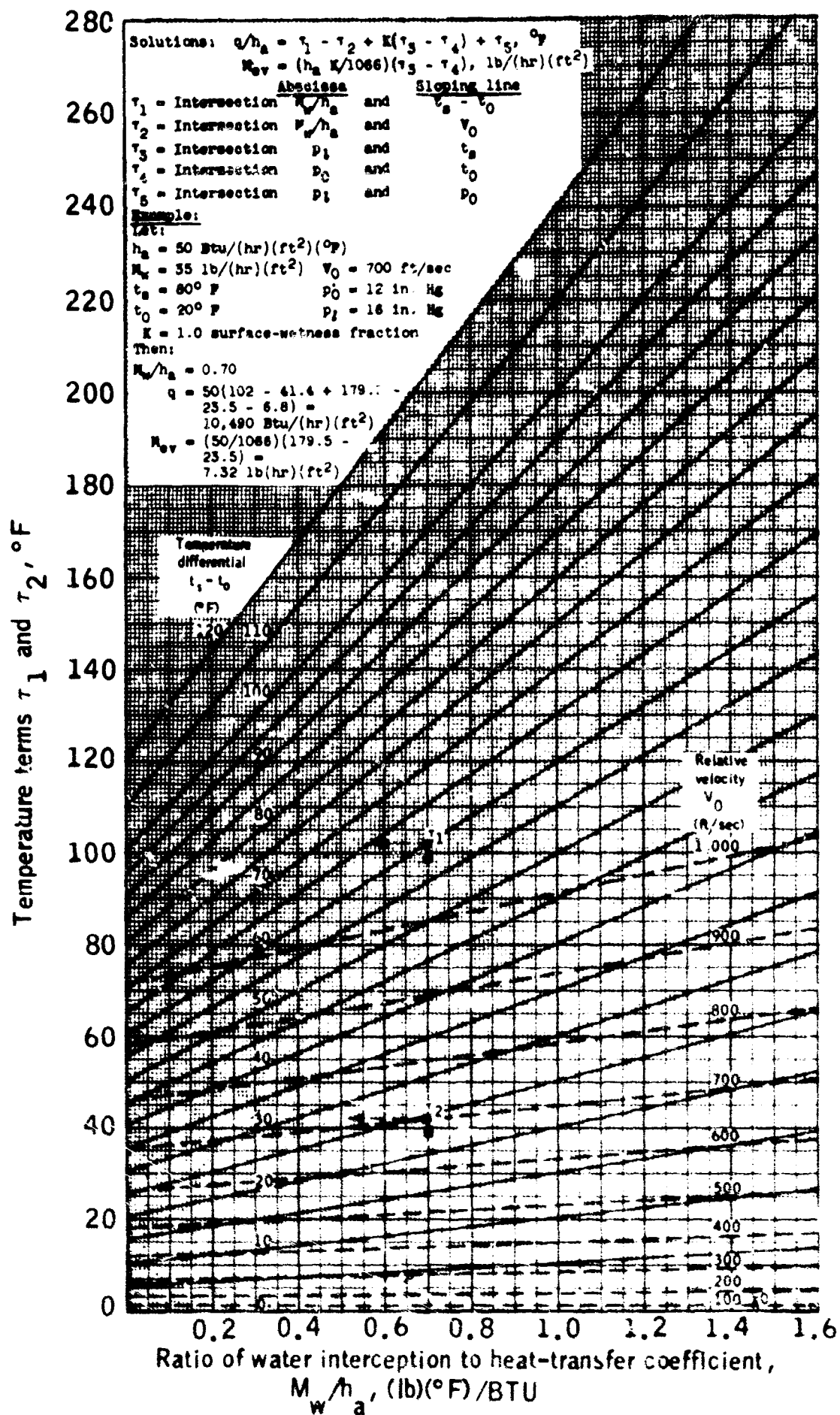
Figure 3-17

Figure 3-13a. Graphical Solutions of Anti-icing Heat and Mass Transfer From a Surface Subject to Impingement and Heated Above Freezing (Ref. 3-4)
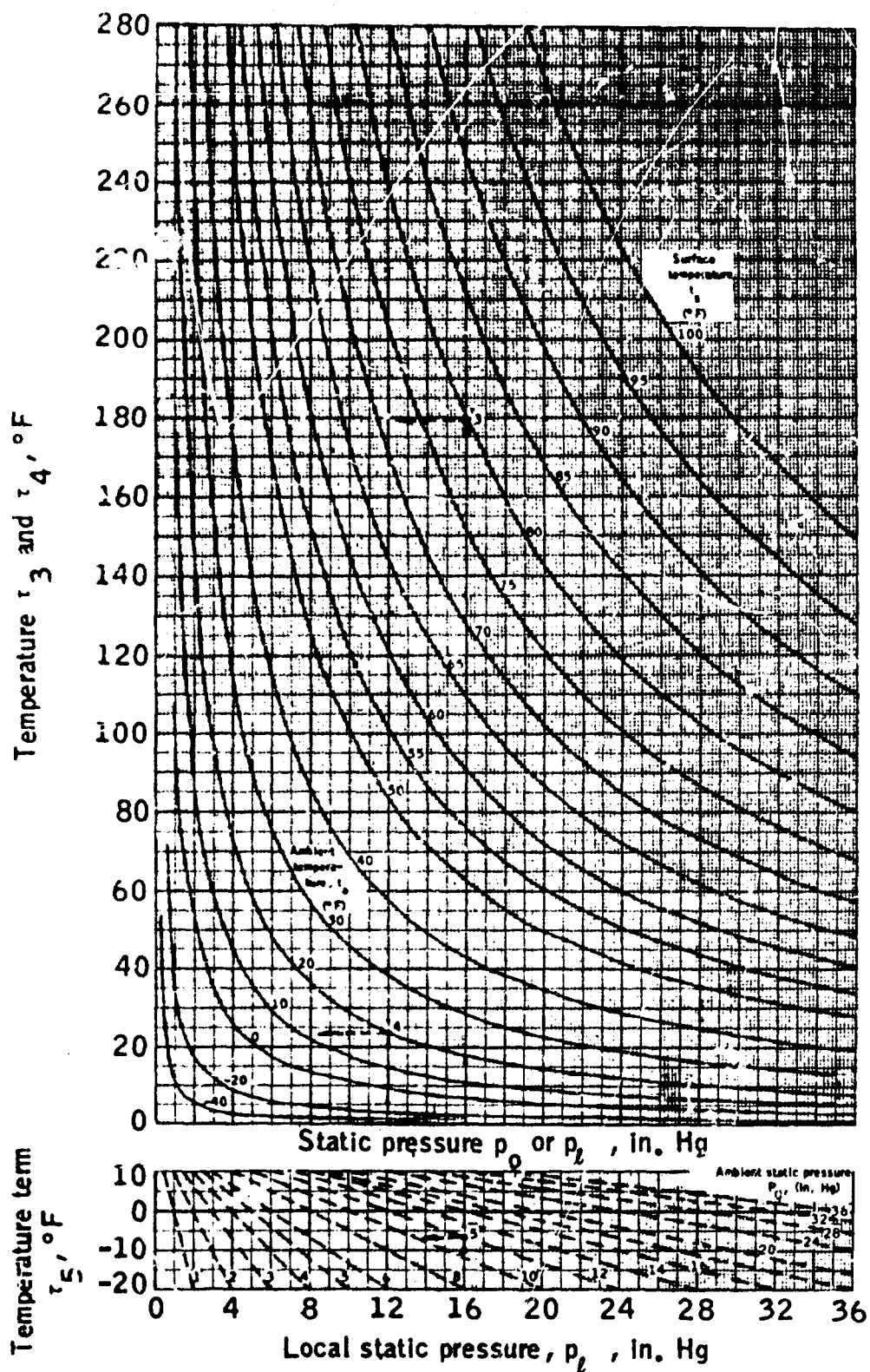
Figure 3-18b. Graphical Solutions of Anti-Icing Heat and Mass Transfer From a Surface Subject to Impingement and Heated Above Freezing (Ref. 3-4).
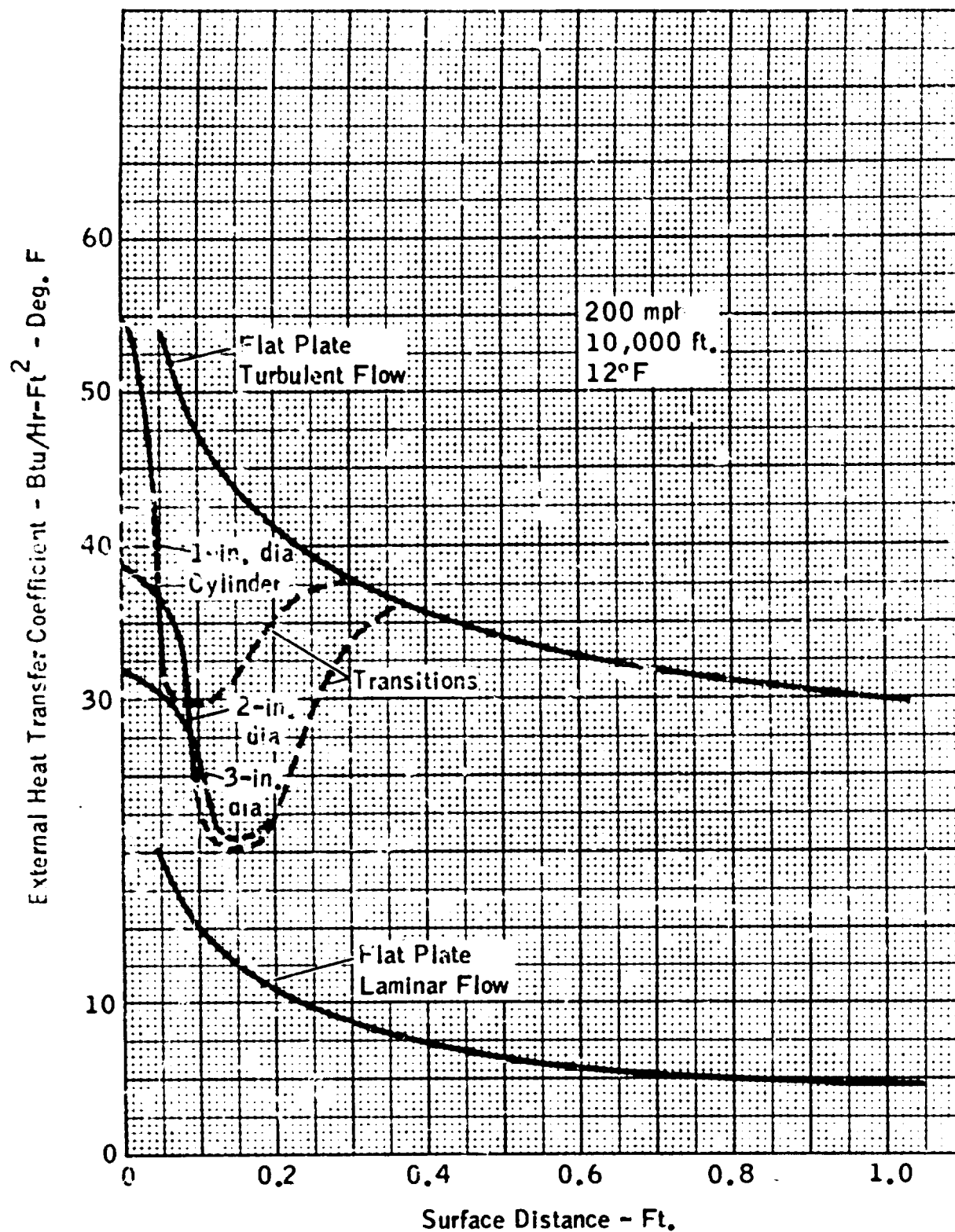
Figure 3-19. Typical External Heat Transfer Coefficients for Cylinder and Flat Plate
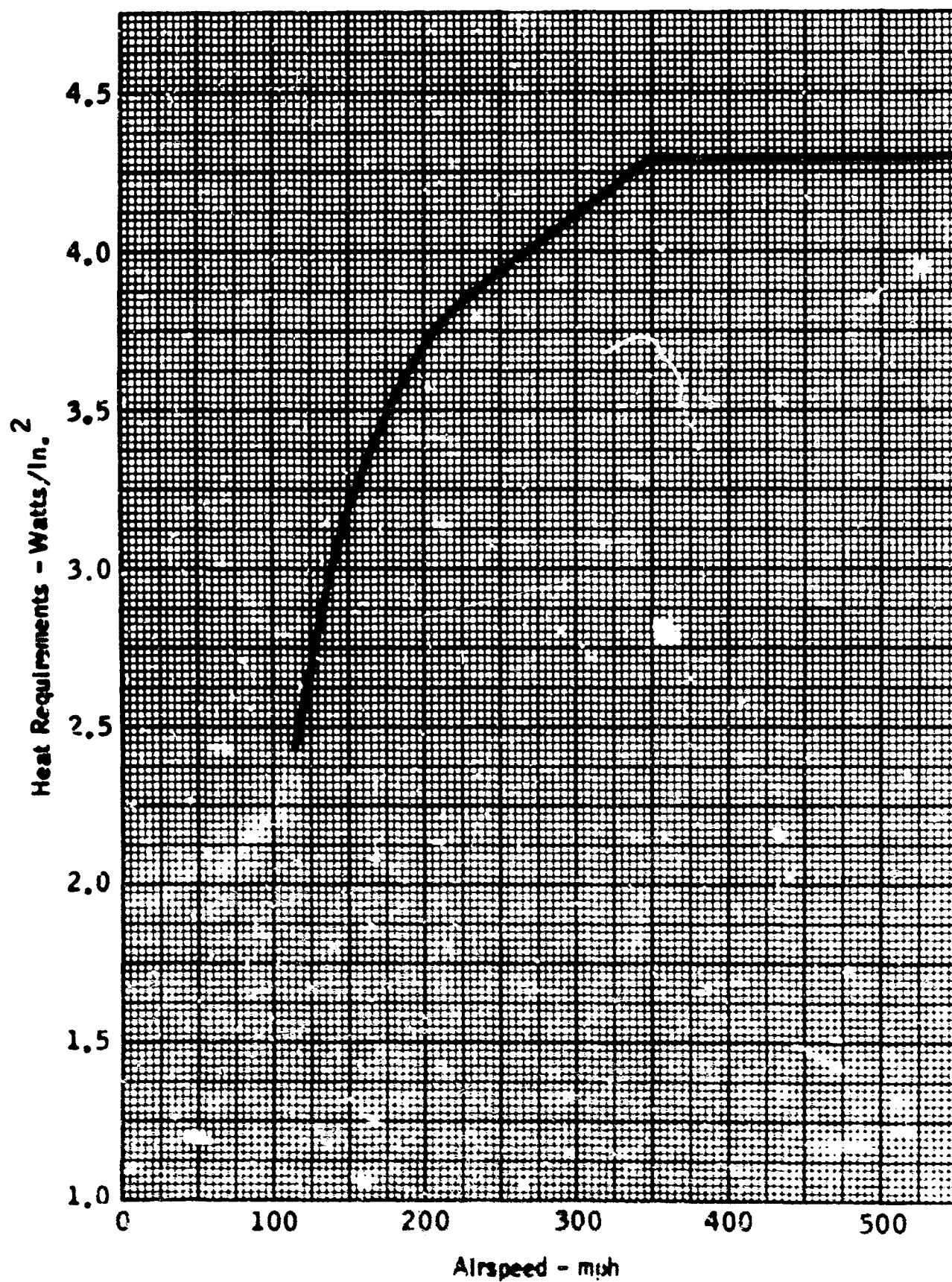
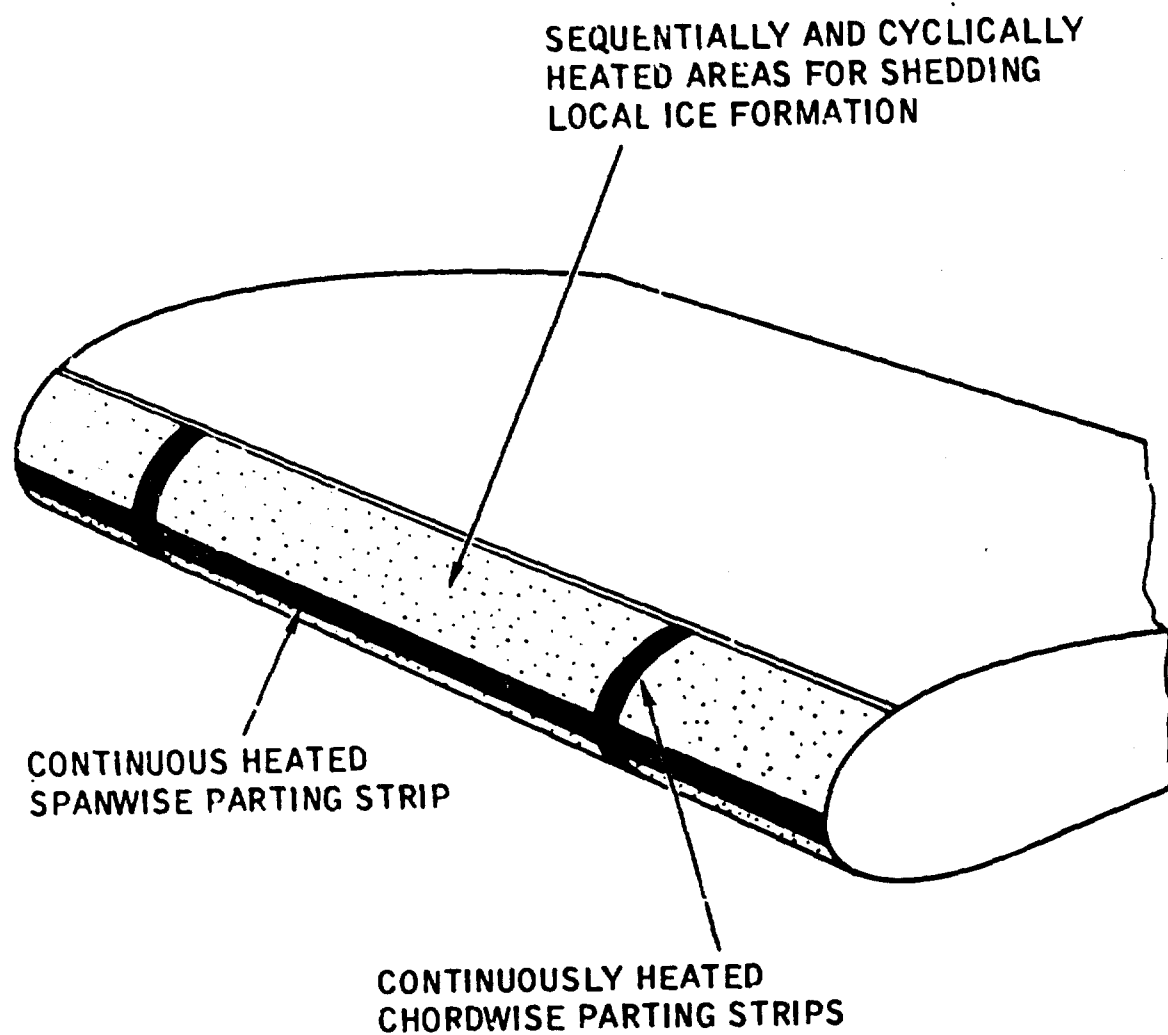Figure 3-20. Windshield Anti-Icing Heat Requirements (Ref. MIL-T-5842A)

SEQUENTIALLY AND CYCLICALLY
HEATED AREAS FOR SHEDDING
LOCAL ICE FORMATION

CONTINUOUS HEATED
SPANWISE PARTING STRIP

CONTINUOUSLY HEATED
CHORDWISE PARTING STRIPS

Figure 3-21.   Arrangement for Cyclic Thermal De-Icing.

0.012 Neoprene Outer Layer
0.003 Glass Cloth
0.001 Heating Elements
0.003 Glass Cloth
0.125 Synthetic Rubber Inner Layer
Aluminum Skin

NACA Heater Construction (RM E51J30) Maximum 22 watts/sq. in., Bonded to surface

0.005 Stainless Steel
0.012 Insulation
0.003 Ribbon Heater
0.012 Insulation
0.025 Aluminum Skin

Typical Heater Construction with Metal Overshoe - 18-22 watts/sq. in. - Laminated to structure

0.005 Stainless Steel
0.008 Outer Layer (Two 0.004 Layers) Epoxy Impregnated Glass Cloth
0.002 Expanded Metal Heating Element
0.010 Epoxy Impregnated Glass Cloth

Typical Heater Construction Molded as a Structural Member - 16-20 watts/sq. in.
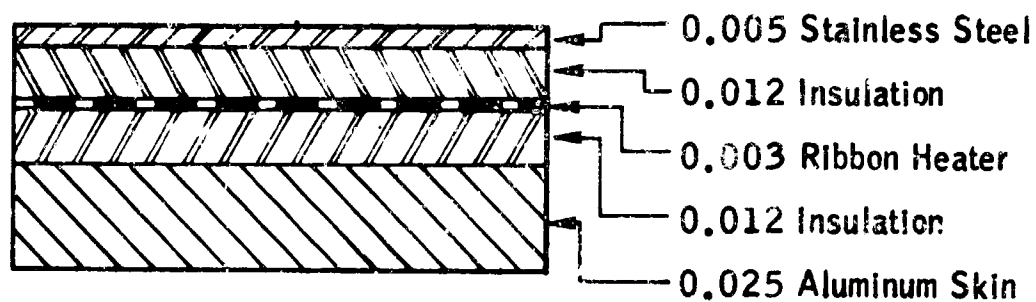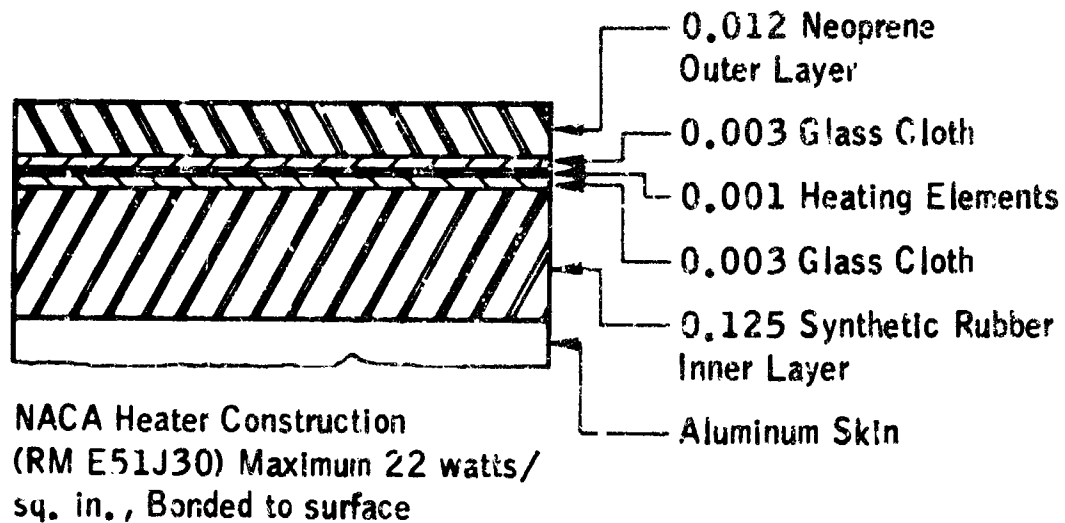
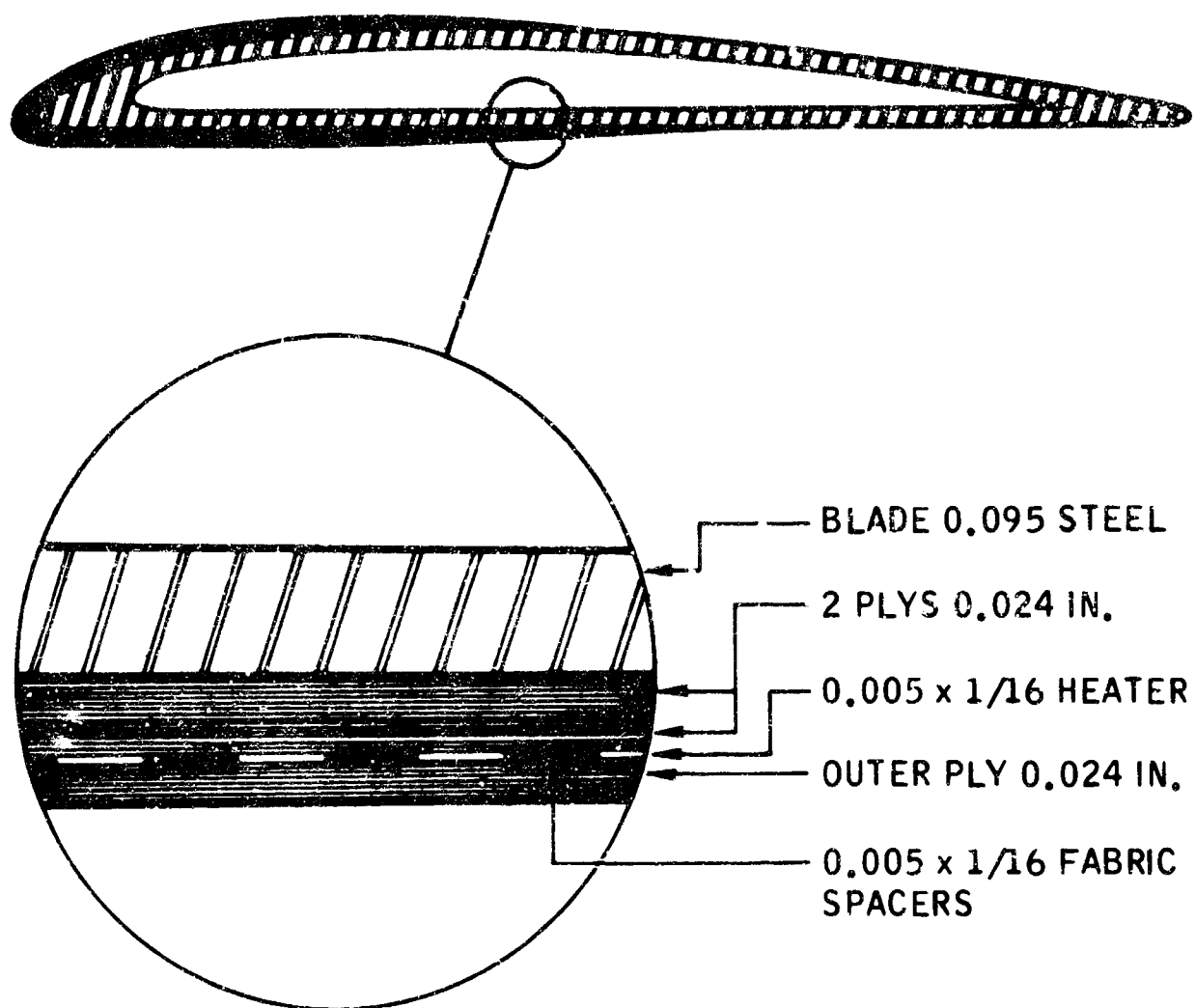Figure 3-22.   Cross-Sections of Typical Electric Heaters.

Figure 3-23.   Details of Construction of Electrical External, Rubber-
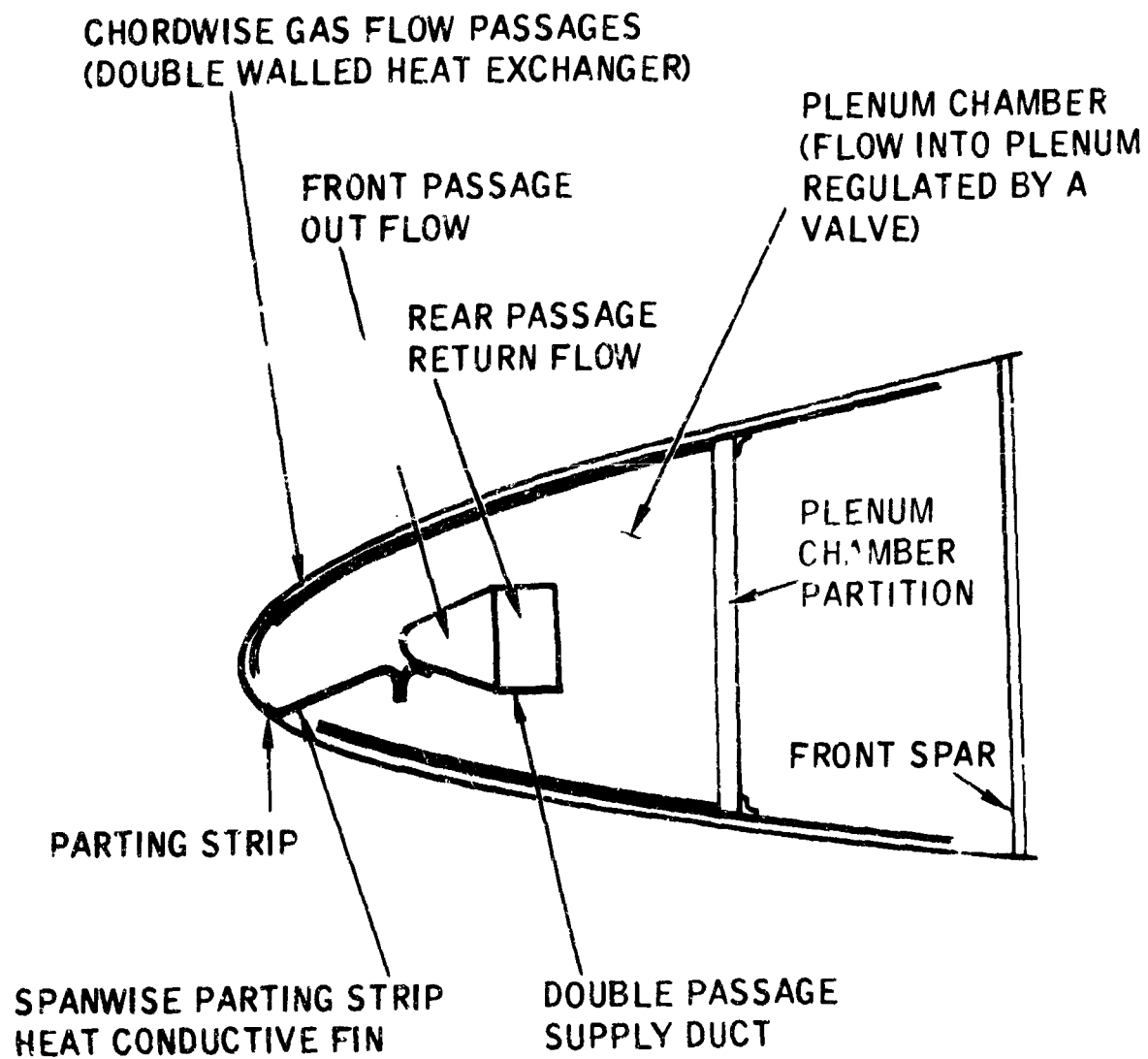Clad, Propeller Blade Heaters (Ref. 3-12).

Figure 3-24.   Construction Details of Gas-Heated Airfoil for Cyclic
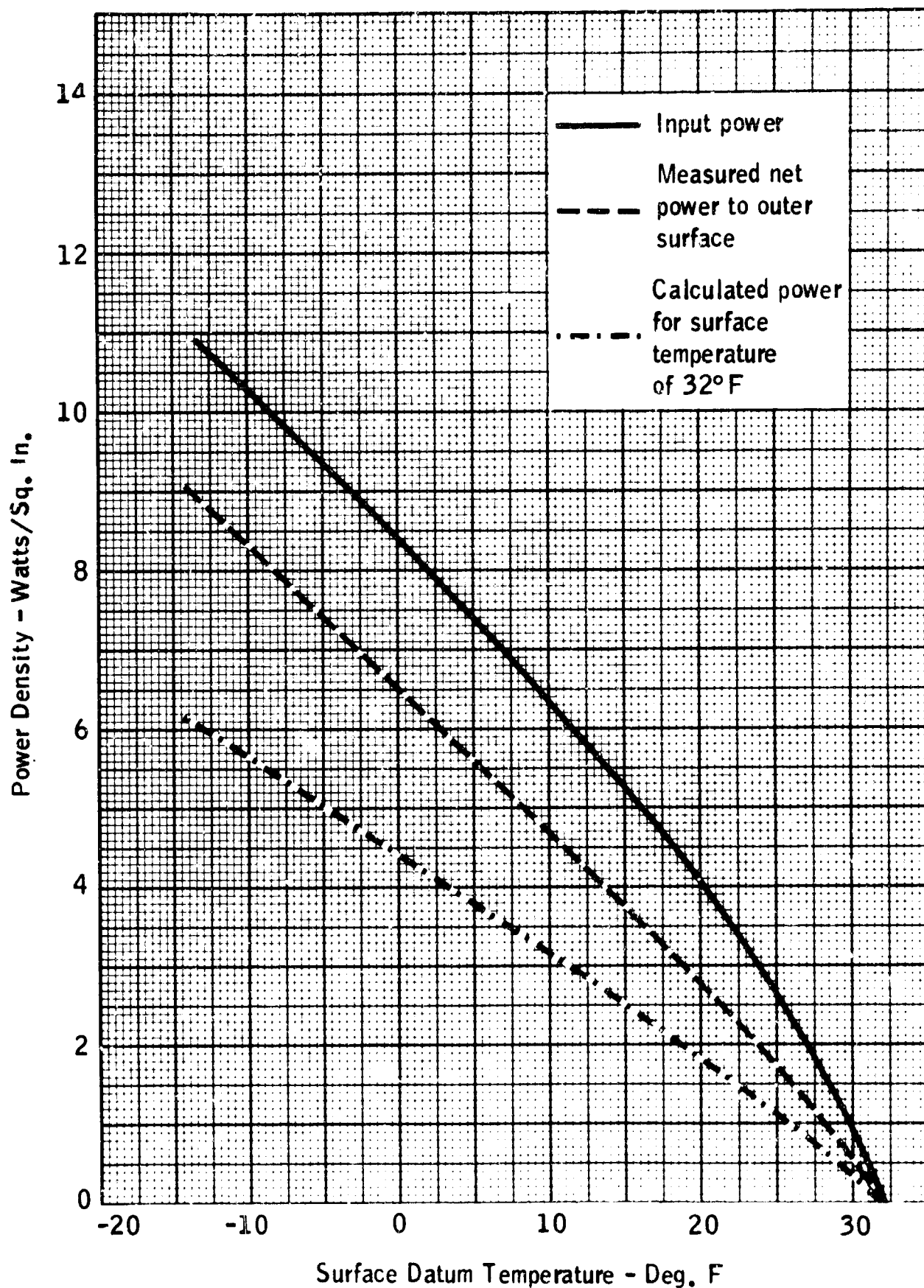De-Icing (Ref. 3-14).

Figure 3-25. Power Requirements for Parting Strip (Airspeed: 175 mph,
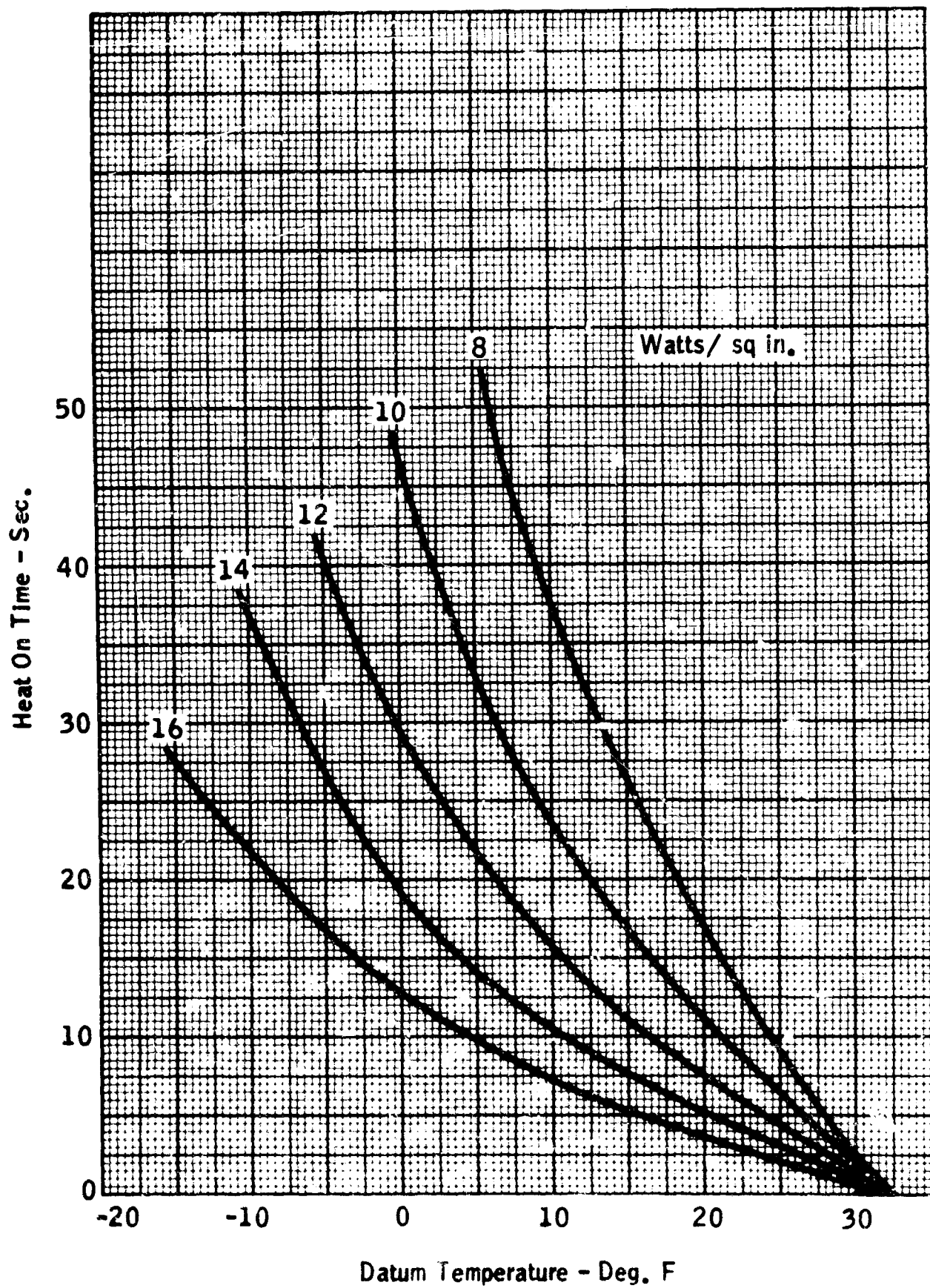Angle of Attack: 2 Deg.) — Ref. 3-11.

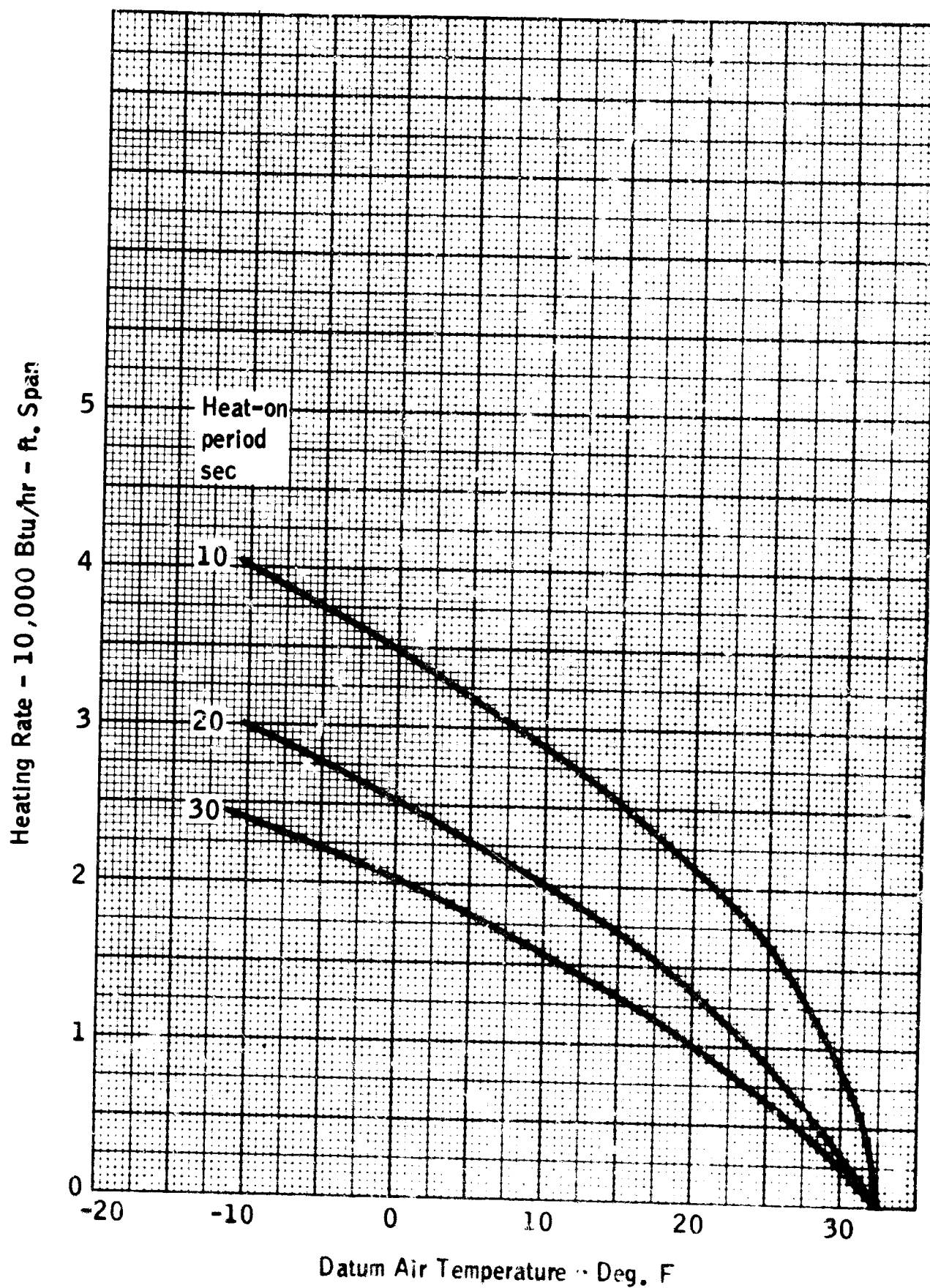Figure 3-26.   Heat-On Time Versus Datum Temperature for Various
Power Densities.

Figure 3-27. Variation of Heating Rate With Datum Air Temperature (Airspeed: 200 mph. Heat-Off Period 4 min. Nominal LWC) — Ref. 3-14.
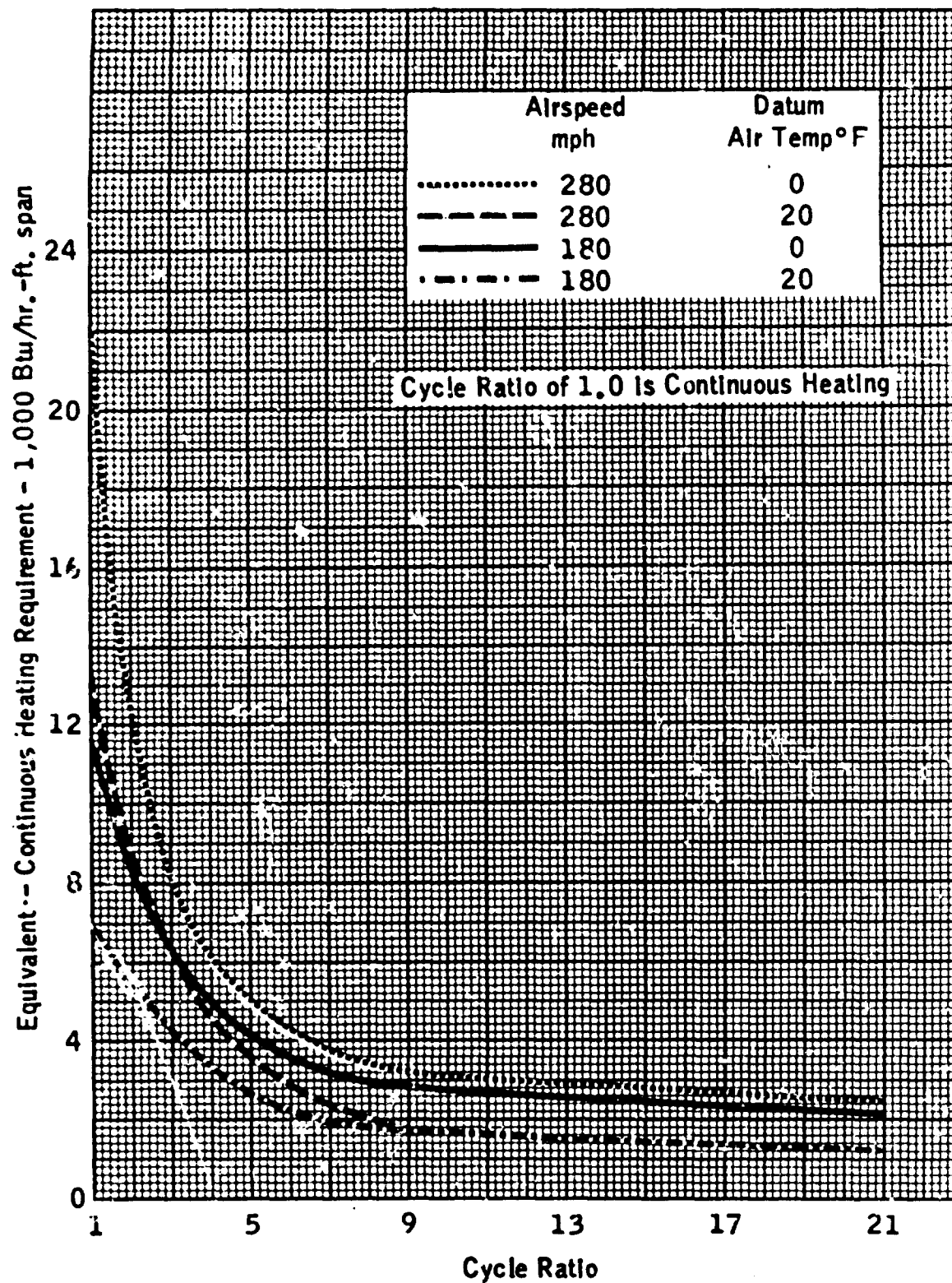
Figure 3-28. Comparison of Cyclic System With Continuous Anti-Icing
Systems (Thermal — Hot Gas) — Ref. 3-14.
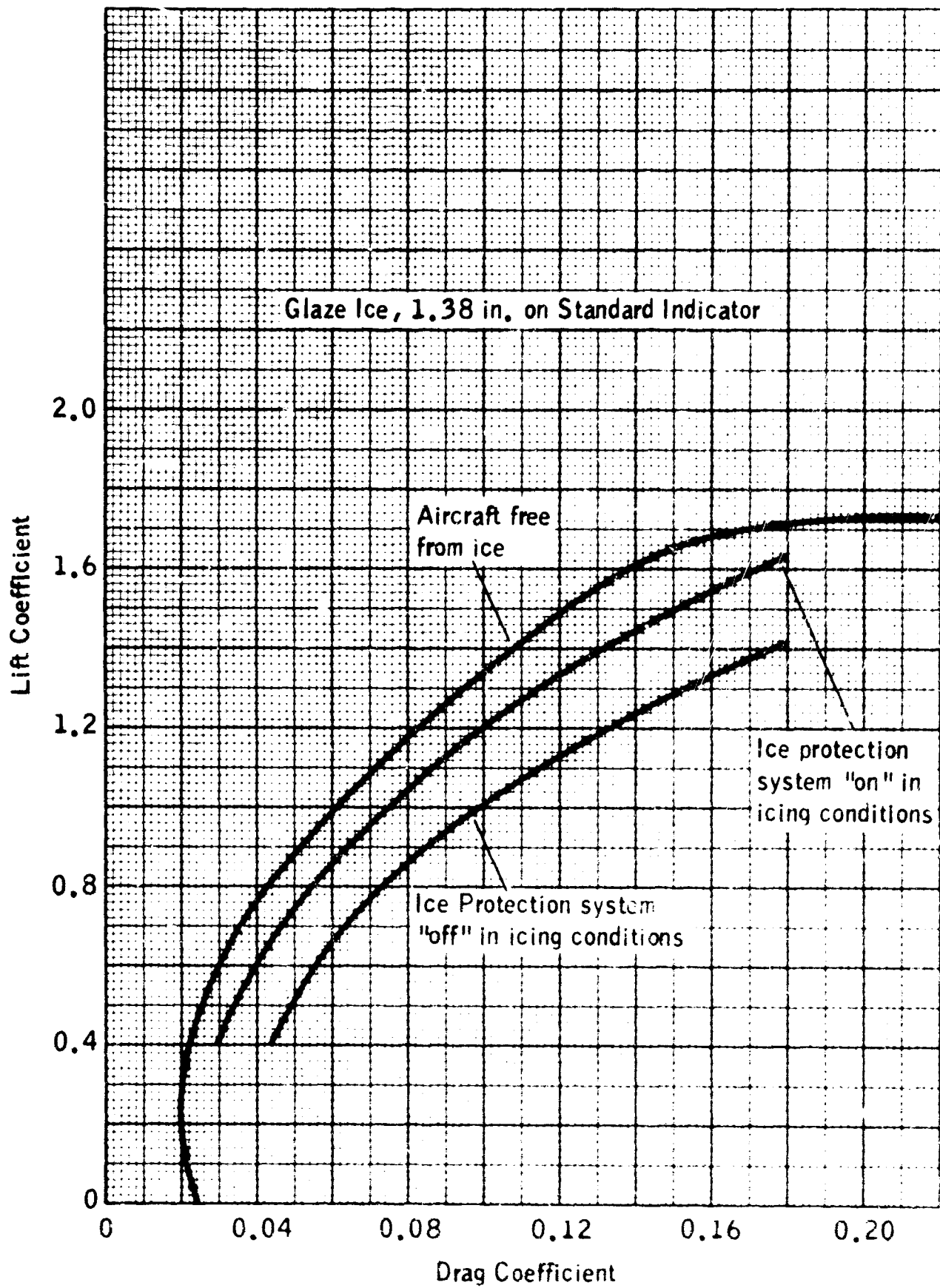
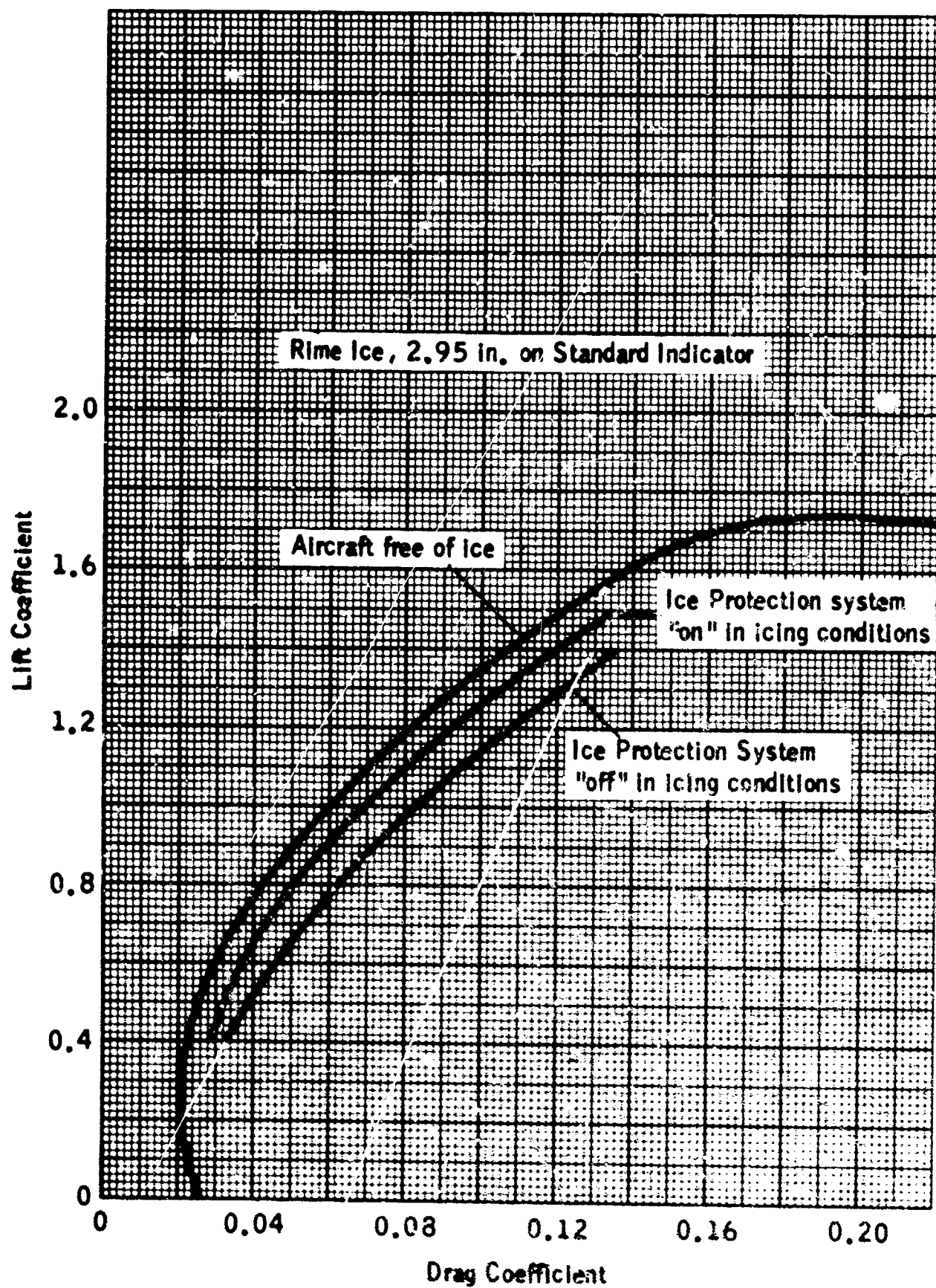Figure 3-29. Drag Polars of USSR IL-14 During Glaze Ice Encounter (Ref. 3-17).

Figure 3-30.   Drag Polars of USSR IL-14 During Rime Ice Encounter (Ref. 3-17).
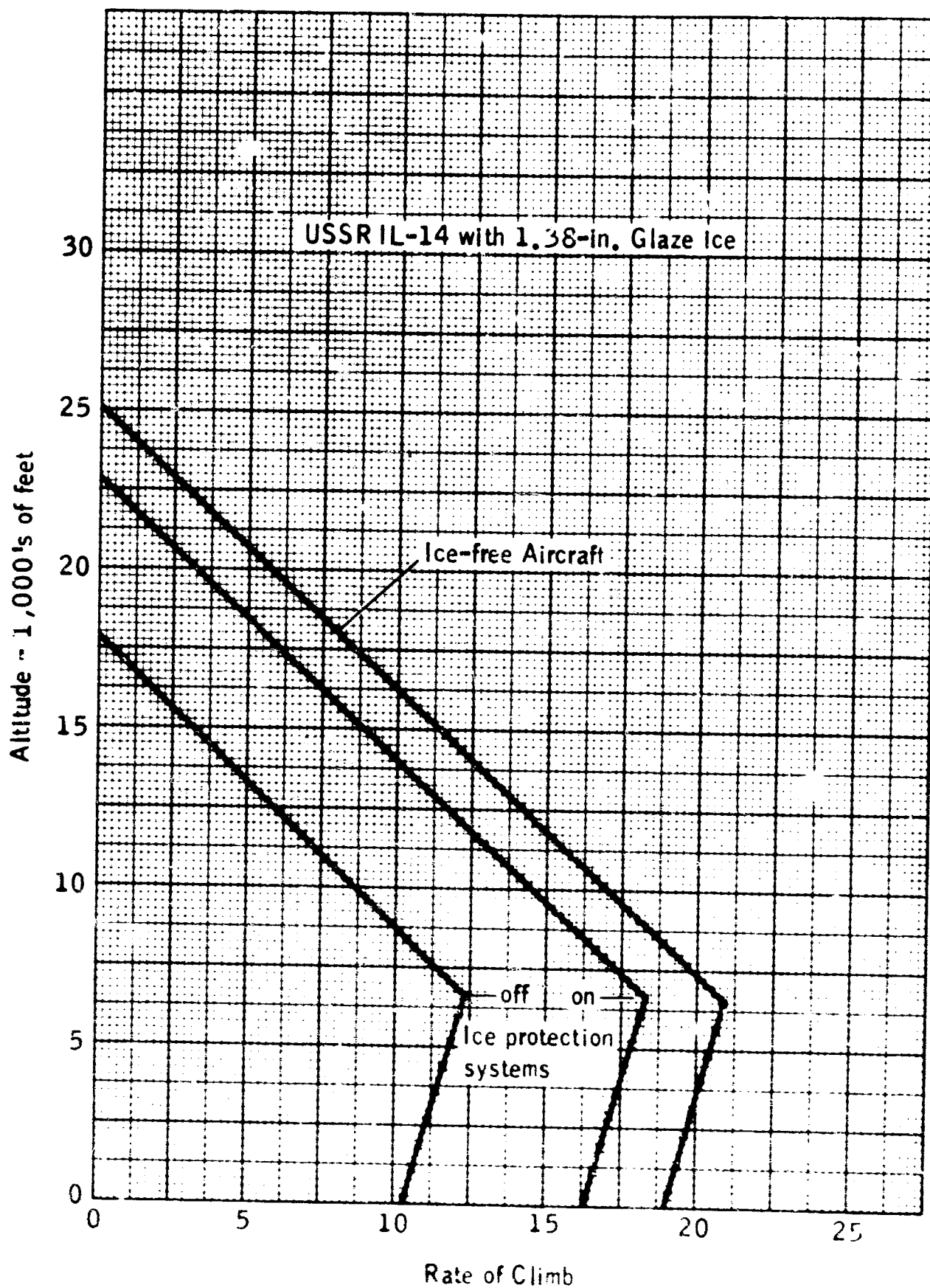
Figure 3-31.   Effect of Glaze Ice Encounter on Rate of Climb (Ref. 3-17).
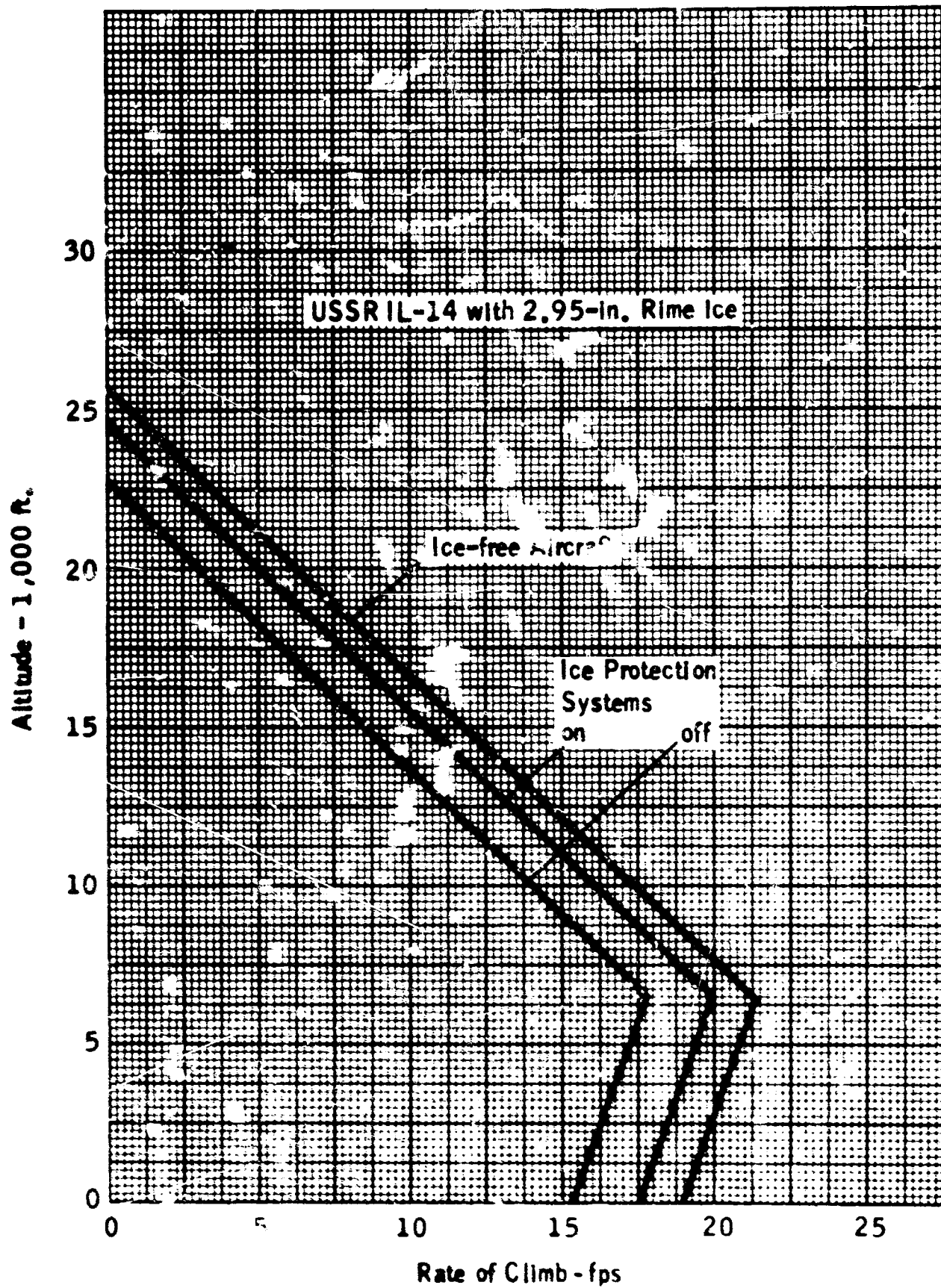
Figure 3-32. Effect of Rime Ice Encounter on Rate of Climb (Ref. 3-17).
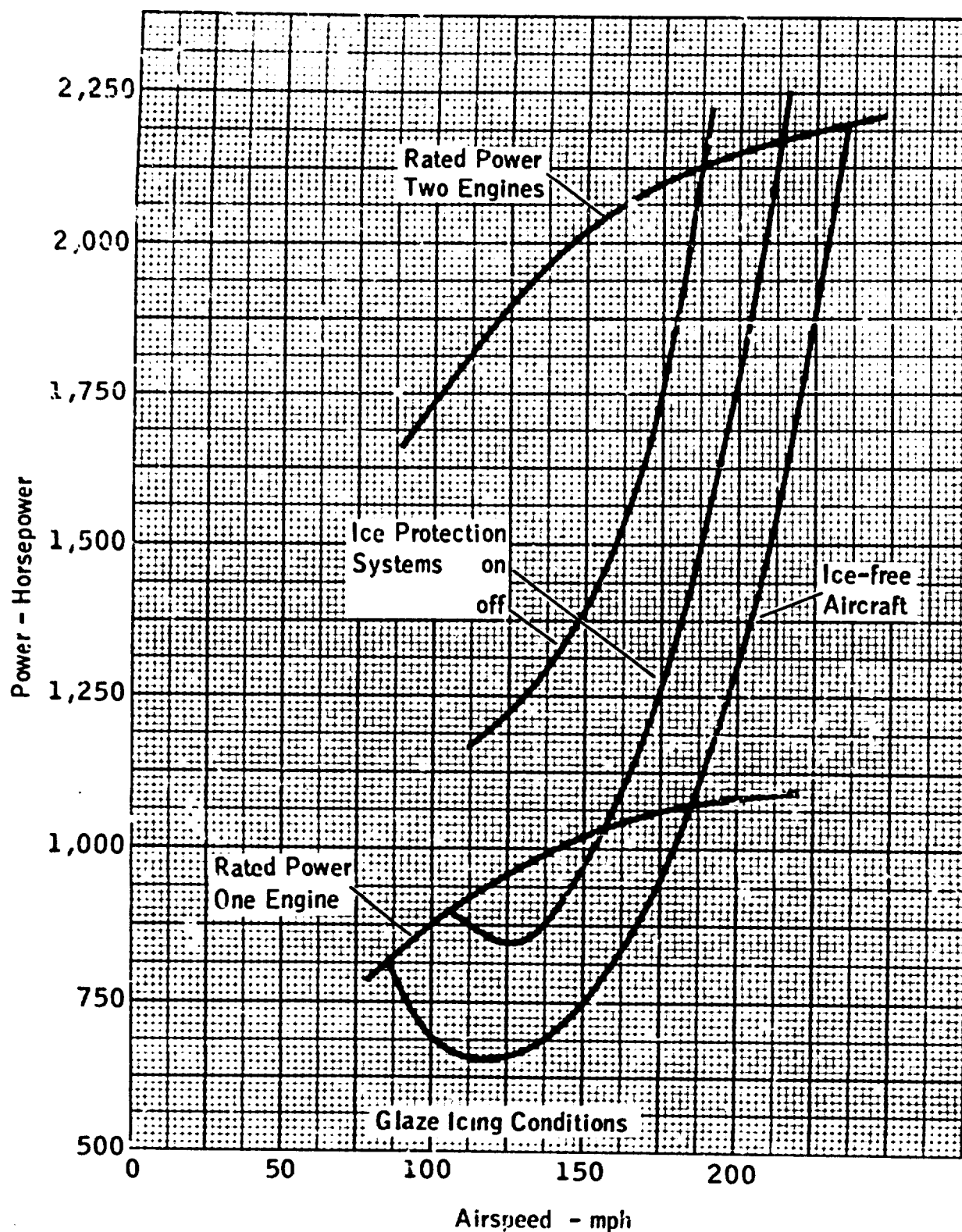
Figure 3-33. Airspeed Versus Horsepower Available and Required for
IL-14 (Ref. 3-17).
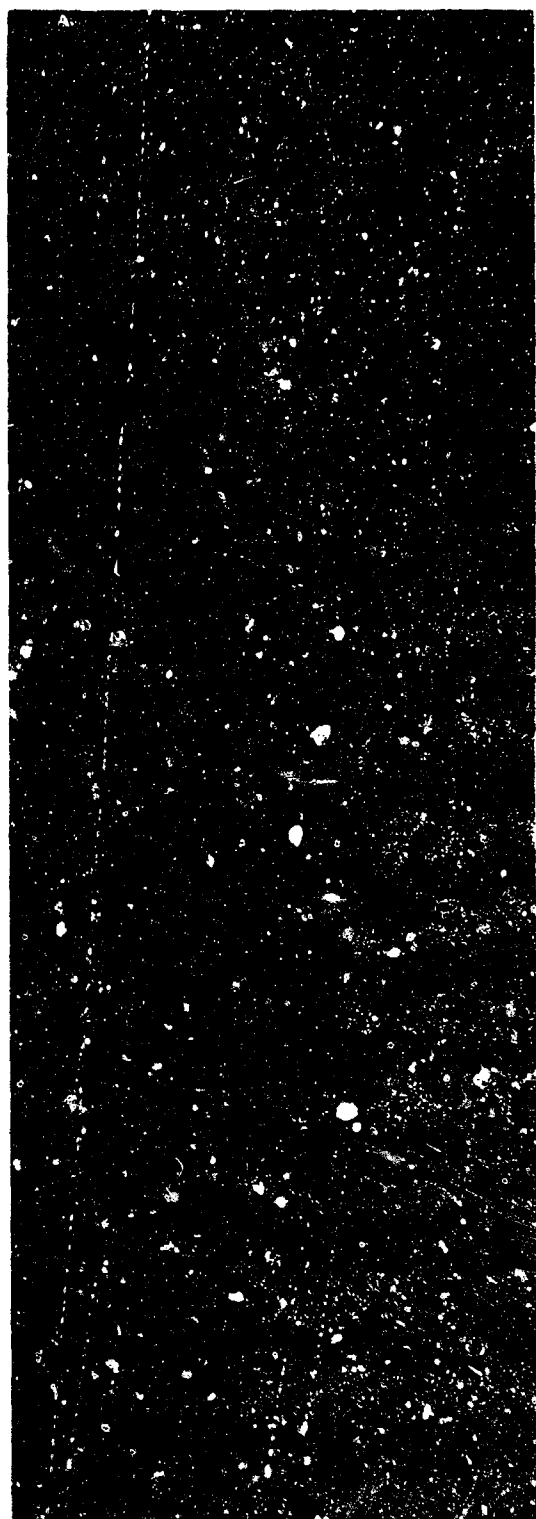
a. Lower surface before ice removal   b. Lower surface after ice removal

Note: Lower half of boot coated; air speed 275 mph; angle of attack, 4.6°; total air temperature, 10°F; icing period, 234 sec.

Figure 3-34. Effect of Coating to Reduce Ice Adhesion on Ice Removal Characteristics of Spanwise Tube De-Icers (Ref. 3 1).
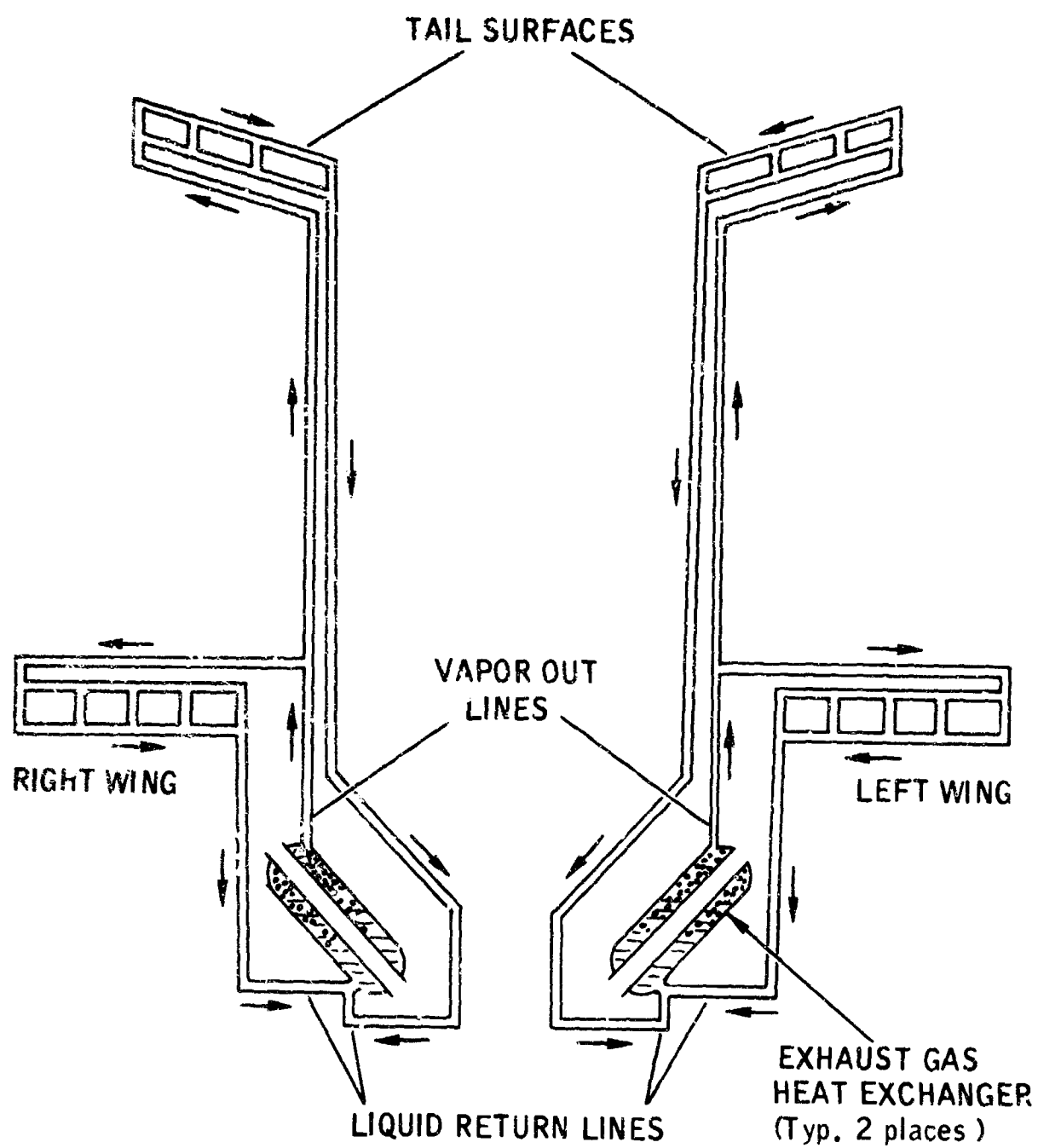
Figure 3-35. Vapor Cycle Ice Protection System.

4 | APPLICATIONS TO AIRCRAFT

4.1 APPLICATION TO LIGHT AIRCRAFT (CAR-3)

CONTENTS

LIST OF FIGURES

NOMENCLATURE

a   Droplet Radius, ft.

A   Wing Area, sq. ft.

A_p Projected windshield area, sq. ft.

A_w Total windshield area, sq. ft.

C   Chord length, ft.

C_D Drag coefficient, dimensionless

ΔC_D Change in drag coefficient, dimensionless

C_L Lift coefficient, dimensionless

$C_{L_{max.}}$ Maximum lift coefficient, dimensionless

C_p Specific Heat, BTU/lb. ° F

d   Propeller diameter, ft.

$d_{cyl.}$ Cylinder diameter, ft.

D   Drag, lb.

D_d Droplet diameter, microns

E_M Collection efficiency, dimensionless

F   Distance factor, dimensionless

G   Per cent glycol in water-glycol mixture

n_a Average external heat transfer coefficient, BTU hr. -ft.^{2}-° F

h_c Convective heat transfer coefficient, BTU hr. -ft.^{2}-° F

h/C   Ratio of projected airfoil height to chord, dimensionless

K	Inertia parameter, dimensionless
K_o	Modified inertia parameter, dimensionless
l	Windshield height, ft.
L	Lift, lb.
LWC	Liquid water content, gm/m^3
M_W	Water collection rate, lb./hr.-sq. ft.
n	Revolutions per second
p	Ambient pressure, in. Hg
hp	Power, horsepower
q	Dynamic pressure, psf
Q	Surface heat requirements, BTU/hr.-sq. ft.
Re,d	Droplet Reynolds number, dimensionless
S_L	Impingement limit on lower surface, ratio to chord length
S_U	Impingement limit on upper surface, ratio to chord length
s_L	Impingement limit (distance from zero chord) on lower surface, in.
s_U	Impingement limit (distance from zero chord) on upper surface, in.
t_f	Boundary layer temperature, °R
t_g	Gas temperature, °F
t_o	Ambient temperature, °F
t_{ok}	Datum temperature, °F
t_s	Surface temperature, °F
T	Thrust, lb.
U_o	Velocity, mph

4.1-4

v_r	True helical speed (at some point on propeller), fps
V	Velocity, fps
w	Anti-icing airflow, lb./sec.
W	Rate of water interception, lb./hr.
W_F	Flow rate of anti-icing fluid, lb./hr. - sq. ft.
W_M	Water catch, lb./hr.-ft. span
W_β	Local water collection rate, lb./hr. - sq. ft.
x	Surface distance from stagnation, ft.
X	Range, hr.
α	Angle of attack, deg.
β	Local collection efficiency, dimensionless
β_{max}	Local collection efficiency at stagnation, dimensionless
γ	Air density (at t_f), lb./cu. ft.
η	Propeller efficiency, dimensionless
η_c	Anti-icing channel efficiency, dimensionless
λ	True range of droplet as projectile injected into still air, ft.
λ_s	Range of droplet as a projectile following Stokes' law. ft.
μ	Viscosity, slugs/ft.-sec.
π	3.1416
ρ	Air density, slugs/cu. ft.
ρ_w	Water density, slugs/cu. ft.
τ_1 to τ_5	Temperature terms (NACA TN 2799 - Ref. 4.1-5), °F

4.1.1 SUMMARY

The different methods of affording ice protection to light aircraft are illustrated in this section for typical single- and twin-engine piston aircraft and for a typical light jet aircraft. Calculations are presented to show the effect of ice upon unprotected airframe components. Other calculations are presented to illustrate a method for determining the requirements for several different types of ice protection systems for the wings, empennage, windshield, propeller and pitot tube.

The calculation of requirements for pneumatic boot de-icing, hot gas anti-icing, cyclic electric de-icing, and fluid anti-icing systems are illustrated for the wings and empennage. Requirements for both electrical and fluid protection systems are determined for the windshield and propeller. Requirements for electrical protection of the pitot tube are also determined.

The effect of complete installed ice protection systems on aircraft weight and performance is also illustrated in this section. Ice protection system weights and power extraction are tabulated in Paragraph 4.1.7 for different combinations of systems for each of the three typical aircraft.

4.1.2 INTRODUCTION

This section illustrates the various means of affording ice protection to light aircraft and the calculation of the different protection system requirements. Specific light aircraft chosen for study are a typical twin-engine aircraft ("A"), a typical single-engine aircraft ("B"), and a typical light jet aircraft ("C").

The effect of ice upon unprotected airframe components will be illustrated first for the typical light twin shown in Figure 4.1-1. The increase in drag due to ice (and, therefore, loss of airspeed or necessary increase in power) can be estimated using any one of several different sources in the literature. Flight testing would be necessary, however, to demonstrate the effect of ice on handling characteristics before it could be determined whether ice protection is necessary.

Ice protection systems will be selected in this section for the wings, empennage, air inlets, windshield, propeller and pitot tube for the typical aircraft. Requirements for alternative systems will also be shown for the different components. A comparison of system weights and power extraction will be made for different combinations of systems to illustrate the effect of the complete installed ice protection system on aircraft weight and performance.

4.1.3 EFFECT OF ICE UPON UNPROTECTED AIRFRAME COMPONENTS

To assist in determining whether ice protection is necessary for various airframe components, calculations can be made of the effect of ice upon unprotected airframe components - as illustrated below for a typical twin-engine light plane. The estimates made of the increase in drag due to ice are representative only of the order of magnitude. The method shown may be conservative because it is based upon icing tunnel test results in which special care was taken to prevent the partial shedding of ice that may occur during actual flight. Nevertheless, these calculations will provide an indication of whether an iced airplane can maintain airspeed and altitude. But, before it can be determined whether ice protection is necessary, the effect of ice on stall speed, handling characteristics, and other must be determined by actual flight tests.

There is a definite decrease in the maximum lift coefficient and a consequent increase in the stall speed due to ice. Therefore, although an iced airplane can maintain cruising airspeed and altitude, there may be danger of stall during certain maneuvers such as the approach for a landing when the airplane is at a higher angle of attack. The change in the lift curve near stall ($C_{L_{max.}}$) due to ice is illustrated in Figure 4.1-2. This effect of ice has been a source of accidents.

The following sample calculations illustrate a method of estimating the effect of ice on unprotected airframe components (assuming glaze ice) for aircraft "A" shown in Figure 4.1-1.

4.1-8

Twin-Engine Aircraft "A" (250 hp per engine)

Maximum gross weight, 4,800 lb.

Wing Area A, 207 sq. ft.

USA 35-B Airfoil (12 per cent thick)

205 mph cruise at 7,000 ft. altitude (75 per cent power)

Ambient temperature, t_o = 17° F (most probable icing temperature from
Figure 1-16)

Dynamic pressure

$$q = 1/2 \, \rho \, V^2$$
$$= 1/2 \, (1.996 \times 10^{-3} \text{slugs/ft.}^3)(205 \times 1.467 \text{ fps})^2$$
$$= 90.2 \text{ psf}$$

Aircraft thrust at 75 per cent power

$$T = \frac{550 \text{(hp)} \, \eta}{V}$$
$$= \frac{550(0.75)(500 \text{ hp})(1)}{(205)(1.467) \text{ fps}}$$
$$= 686 \text{ lb.}$$

Aircraft drag coefficient

$$C_D = \frac{D}{q \, A} \qquad \text{(D = T for steady state level flight)}$$
$$= \frac{686 \text{ lb.}}{(90.2 \text{ psf})(207 \text{ sq. ft.})}$$
$$= 0.0367$$

Aircraft lift coefficient

$$C_L = \frac{L}{q \, A}$$
$$= \frac{4,800 \text{ lb.}}{(90.2 \text{ psf})(207 \text{ sq. ft.})}$$
$$= 0.257$$

Using the water catch calculated in Paragraph 4.1.4 for a 20-mi. encounter, the weight of ice per foot of span that will accumulate on the wing can be

determined for a 200-mi. distance. (An icing condition in excess of 200 miles is unlikely, based on the data of Section 1, Figure 1-12)

$$\text{lb./ft. span} = W_M \; (F) \; (\text{no. hours})$$

$$= 2.95 \; \text{lb./hr.-ft. span} \; (0.32)\left(\frac{200 \; \text{mi.}}{205 \; \text{mph}}\right)$$

$$= 0.92 \; \text{lb./ft. span}$$

The distance factor, F, was obtained from Figure 1-28. Similarly, the weight of ice per foot of span can be determined for the horizontal stabilizer and vertical fin.

The increase in drag coefficient, ΔC_D, can then be estimated using NACA TN 3564 (Ref. 4.1-1 and shown in Figure 4.1-5) which was based on an NACA 0011 airfoil with chord length of 87.4 in. (Other sources could be used such as a Soviet report, Reference 4.1-2; NACA TN 1598, Reference 4.1-3; and various other NACA publications.)

The following table summarizes the calculation of the total drag increase.

Aircraft Component	Lb./ft. span (200-mi. dist.)	ΔC_D from Fig. 4.1-5	Avg. Chord in.	Surface Area ft.^{2}	ΔC_D Correction
Wings	0.92	0.0185	67	207	$\frac{87.4}{67}(0.0185) = 0.0241$
Horiz. Stab.	0.621	0.0130	37	37	$\frac{87.4}{37}\left(\frac{37}{207}\right)(0.0130) = 0.0055$
Vert. Fin	0.702	0.0144	56	25	$\frac{87.4}{56}\left(\frac{25}{207}\right)(0.0144) = 0.0027$

Misc. (engine cowls, nose, antennas, etc.)   (Assumed equal to empennage)

	0.0082
Total	0.0405

The values of ΔC_D taken from Figure 4.1-5 are corrected for chord length and (for the empennage) multiplied by the ratio of surface areas as shown above.

Adding the total ΔC_D to the clean aircraft drag coefficient gives the drag

coefficient of the iced airplane:

$$C_{D_{iced}} = 0.037 + 0.040 = 0.077$$

Aircraft drag is then:

$$D = C_D q A$$
$$= 0.077 (90.2 \text{ psf})(207 \text{ sq. ft.})$$
$$= 1,440 \text{ lb.}$$

And since thrust equals drag, the power necessary to maintain cruise speed assuming 10 per cent propeller efficiency loss is:

$$hp = \frac{TV}{550\eta}$$
$$= \frac{(1440 \text{ lb.}) \left|(205)(1.467) \text{ fps}\right|}{550(0.9)}$$
$$= 874 \text{ hp} \quad (175 \text{ per cent power})$$

Since 175 per cent power is not available, of course, airspeed would be reduced under the above icing conditions. The resultant airspeed at a cruise power setting can be determined by trial and error. Assuming V = 150 mph; the new dynamic pressure

$$q = \left(\frac{150}{205}\right)^2 90.2 = 48.3 \text{ psf}$$

The new lift coefficient

$$C_L = \left(\frac{205}{150}\right)^2 (0.257) = 0.480$$

The ice-free aircraft drag coefficient is $C_D = 0.045$, from Figure 4.1-3. (This figure is based on an assumed ice-free aircraft drag polar.) The iced aircraft drag coefficient is then:

$$C_D = 0.045 + 0.040 = 0.085$$

The new value of aircraft drag is

$$D = C_D \, q \, A$$

$$= 0.085 \ (48.3 \text{ psf})(207 \text{ sq. ft.})$$

$$= 848 \text{ lb.}$$

Assuming 10 per cent propeller efficiency loss due to ice, the equivalent power

$$hp = \frac{TV}{550 \, \eta_i}$$

$$= \frac{848 \text{ lb.} \left| (150)(1.467) \text{ fps} \right|}{550 \ (0.9)}$$

$$= 377 \text{ hp}$$

Since this is approximately equal to the cruise power setting of 375 hp, the correct airspeed has been chosen. The loss of airspeed at the cruise power setting then is 55 mph under the given icing conditions.

The cross-sectional area of ice formed on the wings can be found using the 20-mile water catch (Paragraph 4.1.4.1), the ice density, and the distance factor, F, from Figure 1-28.

$$\text{Ice cross-sectional area} = W_M(F)(\text{hr.})\left(\frac{1}{\rho_{ice}}\right)$$

$$= 2.95 \text{ lb./hr.-ft. span} \ (0.32)\left(\frac{200 \text{ mi.}}{205 \text{ mph}}\right)\left(\frac{\text{ft.}^3}{56 \text{ lb.}}\right)$$

$$\left(144 \ \frac{\text{in.}^2}{\text{ft.}^2}\right)$$

$$= 2.36 \text{ sq. in.}$$

(This answer tends to be slightly conservative because the airspeed will decrease as ice forms.)

Ice cross-sectional area calculations for the wing and tail are summarized in the following table:

Component	W_M(20-mi.) lb./hr.-ft. span	W_M(200-mi.) lb./hr.-ft. span	Ice Accretion lb./ft.-span	Ice Cross-Sectional Area sq. in.
Wing	2.95	0.94	0.92	2.36
Horiz. Stab.	1.94	0.637	0.621	1.60
Vert. Tail	2.25	0.720	0.702	1.81

Knowing the cross-sectional area and the impingement limits (Paragraph 4.1.4.1), the shape of the ice formation can be estimated as shown in Figure 4.1-4.

The following calculations will illustrate the effect of ice on the same airplane for a hold condition, which may also be a critical flight condition.

125 mph hold at 2,000 ft. altitude (for 30 min.)

Ambient temperature, t_0 = 23.5° F (most probable icing temperature, from Figure 1-16)

Droplet diameter, D_d = 20 microns

Liquid water content, LWC = 0.54 gm/m^3 (from Figure 1-26)

Air density, ρ = 0.00237 slugs/cu. ft.

Air viscosity, μ = 0.37 x 10^{-6} slugs/ft.-sec.

Wing angle of attack = 3 deg.

Calculations of drag increases due to ice at hold conditions for the wings and empennage are summarized in the following table. (Detailed calculations of water catch are shown in Paragraph 4.1.4.1.)

	Wing	Horiz. Stab.	Vert. Fin
Droplet Re_d	77	77	77
λ/λ_s (Figure 2-6)	0.39	0.39	0.39
Average chord, ft.	5.58	3.08	4.37
Inertia Parameter, K	0.0414	0.0749	0.0528
Modified Inertia Parameter, K_0	0.0161	0.0292	0.0206
Collection Efficiency, E_M (Fig. 2-7)	0.10	0.17	0.135

	Wing	Horiz. Stab.	Vert. Fin
Water Catch W_M, lb./hr.-ft. span	1.52	1.045	1.18
Lb. ice/ft.-span	0.76	0.522	0.59
Ice cross-sectional area, sq. ft.	1.96	1.35	1.52
ΔC_D from Figure 4.1-5	0 0155	0.011	0.0125
Corrected ΔC_D (see Cruise calculations, p. 4.1-10)	0.0202	0.00465	0.0025

Then assuming ΔC_D for miscellaneous components is equal to ΔC_D for the empennage,

$$\Delta C_{D_{total}} = 0.0202 + 2(0.00465 + 0.0025)$$
$$= 0.0345$$

The power necessary to maintain the 125-mph speed can now be determined knowing the ΔC_D. First, the dynamic pressure at 125 mph,

$$q = 1/2 \, \rho \, V^2$$
$$= 1/2 \, (2.37 \times 10^{-3} \text{ slugs/ft.}^3) \left[(125)(1.467) \text{ fps} \right]^2$$
$$\approx 39.7 \text{ psf}$$

The coefficient of lift

$$C_L = \frac{L}{q \, A}$$
$$= \frac{4,800 \text{ lb.}}{(39.7 \text{ psf})(207 \text{ sq. ft.})}$$
$$= 0.584$$

Therefore, from Figure 4.1-3, the ice-free airplane drag coefficient $C_D = 0.051$ and the iced airplane drag coefficient

$$C_{D_{iced}} = 0.051 + 0.0345$$
$$= 0.0855$$

The iced airplane drag is then

$$D = C_D \, q \, A$$

$$= 0.0855 \, (39.7 \text{ psf})(207 \text{ sq. ft.})$$

$$= 702 \text{ lb.}$$

Since thrust equals drag, the power necessary to maintain 125 mph (assuming 10 per cent propeller efficiency loss) is

$$hp = \frac{TV}{550\eta}$$

$$= \frac{702 \text{ lb. } \left[(125)(1.467) \text{ fps}\right]}{550 \, (0.9)}$$

$$= 260 \text{ hp } (52 \text{ per cent})$$

Knowing the cross-sectional area of ice formed and the impingement limits, an estimation of the ice shape at hold conditions can be made as shown in Figure 4.1-4.

4.1.4 STUDY OF VARIOUS ICE PROTECTION SYSTEMS FOR A TYPICAL TWIN-ENGINE LIGHT PLANE

4.1.4.1 SELECTION OF ICE PROTECTION FOR WING AND EMPENNAGE — In selection of ice protection for light airplanes, the wings and empennage will be treated together since they would have the same type system. The water catch and impingement limits are calculated first to determine the extent protection is necessary. This is illustrated by the following sample calculations for the wing of twin-engine aircraft "A" shown in Figure 4.1-1:

Calculation of Impingement Limits and Water Catch

Wing - twin-engine aircraft "A"

Gross weight, 4,800 lb.

USA 35-B airfoil (12 per cent thick)

Wing area, A = 207 sq. ft.

Chord length, C = 67 in.

205 mph cruise at 7,000 ft. altitude (75 per cent power)

Ambient temperature, t_o = 17° F (most probable icing temperature from Figure 1-16)

Droplet diameter, D_d = 20 microns

Liquid water content, LWC = 0.46 gm/m^3 (Figure 1-26)

Air density, ρ = 0.001996 slugs/cu. ft.

Air viscosity, μ = 0.36 x 10^{-6} slugs/ft.-sec.

Dynamic pressure, q = 90.2 psf (from page 4.1-9)

Lift coefficient, C_L = 0.257 (from page 4.1-9)

The angle of attack can then be estimated from a C_L versus α curve (Figure 4.1-2) for the given airfoil:

α = -1.7°

Droplet Reynolds Number

$$Re_d = \frac{4.81(D_d)(\rho)(U_o)(10^{-6})}{\mu}$$

$$= \frac{4.81\ (20\ \text{microns})(0.00199\ \text{slugs/ft.}^3)(205\ \text{mph})(10^{-6})}{(0.36 \times 10^{-6}\ \text{slugs/ft.-sec.})}$$

$$= 109$$

λ/λ_s = 0.342 (From Figure 2-6)

Inertia parameter

$$K = \frac{1.705\ (D_d^2)(U_o)(10^{-12})}{\mu\,(C)} \qquad \text{(This formula is equivalent to that of Section 2.)}$$

$$= \frac{1.705\ (20\ \text{microns})^2(205\ \text{mph})(10^{-12})}{(0.36 \times 10^{-6}\ \text{slugs/ft.-sec.})(5.584\ \text{ft.})}$$

$$= 0.0695$$

Modified inertia parameter

$$K_o = K(\lambda/\lambda_g)$$

$$= 0.0695\ (0.342)$$

$$= 0.0238$$

The ratio of projected airfoil height to chord

$h/C = 0.1225$ (at $\alpha = -1.7°$), based on measured values for USA 35-B airfoil

Collection efficiency can be obtained from Figure 2-7 for a 12 per cent Joukowski airfoil at a zero-deg. angle of attack

$$E_M = 0.135$$

Water catch

$$W_M = 0.329\ (U_o)(LWC)(h/C)(C)(E_M)$$

$$= 0.329\ (205\ \text{mph})(0.46\ \text{gm}/\text{m}^3)(0.1225)(5.584\ \text{ft.})(0.135)$$

$$= 2.95\ \text{lb.}/\text{hr.-ft. span}$$

The limits of impingement can be found from Figures 2-15 and 2-16 using a 15 per cent Joukowski airfoil at $\alpha = 2$ deg. to represent the USA 35-B airfoil a $\alpha = -1.6$ deg. The Joukowski airfoil was used because of the profile similarity to the USA 35-B airfoil for which no data was available. See Paragraph 2.3.4 for an explanation of airfoil matching procedures.

$S_U = 0.04$ $\qquad$ $S_L = 0.02$

$s_U = 2.7$ in. $\qquad$ $s_L = 1.3$ in.

(These values are not typical of other classes of airfoils; more commonly, impingement limits are greater on the lower surface.)

Figure 4.1-6 shows impingement limits versus span for the wing at both 20 and 40-micron drop sizes. Similar calculations of water catch and impingement limits can be made for the horizontal stabilizer and vertical fin. Results of these calculations for the same airplane are shown in Figures 4.1-7 and 4.1-8.

The determination of local water collection rate, W_β, is illustrated for the wing of the same airplane by the following calculations:

Calculation of Local Water Collection Rate

205 mph cruise at 7,000 ft. altitude

Droplet diameter, $D_d = 20$ microns

Liquid water content, $LWC = 0.46 \text{ gm}/m^3$ (from Figure 1-26)

Modified inertia parameter, $K_o = 0.0238$ (from above)

At the stagnation point, the local collection efficiency

$\beta = 0.46$ (from NACA TN 3839, Ref. 4.1-4)

using the 15 per cent Joukowski airfoil at 2-deg. angle of attack to approximate the USA 35-B airfoil at -1.6 deg.

Local water collection rate, therefore, is:

$W_\beta = 0.329\beta$ (U_o)(LWC)

$= 0.329 \ (0.46)(205 \text{ mph})(0.46 \text{ gm}/m^3)$

$= 14.57$ lb./hr.-sq. ft.

Values of local collection rate can also be found for different chordwise locations on the airfoil and, therefore, the local water collection rate can be found and plotted versus distance from zero chord as shown in Figure 4.1-9 for the wing. Curves for both 20 and 40-micron drop sizes are shown. Figures 4.1-10 and 4.1-11 present the results of similar calculations made for the horizontal stabilizer and vertical fin.

The 40-micron curves shown in these figures are normally used to determine the necessary chordwise extent of ice protection. Although it is not necessary to protect entirely the 40-micron limits of impingement, protection usually is extended to between the 20 and 40-micron limits, where only a small amount of ice would remain beyond the protected area.

For example, for this typical twin-engine aircraft, it appears that ice protection should extend about six inches from zero chord on the upper surface and four inches on the lower surface of the wings, and about 2.o inches from zero chord on both surfaces of the horizontal stabilizer and vertical fin. The final choice of area protected is, of course, the prerogative of the designer and may depend on spar location and/or various other factors.

Requirements for Pneumatic De-Icing

Based on the above impingement calculations, the coverage required for a pneumatic de-icing system can be determined for aircraft "A." For each wing an area nine ft. from the engine nacelle to the wing tip can be covered, and the chordwise extent should be six in. (wrap-around) from zero chord on the upper surface and four inches on the lower surface. (For many aircraft, the coverage needed will be greater on the lower surface than the upper, because the wing flies at a positive angle of attack. An analysis should be made for any new aircraft to determine the appropriate coverage.) Protection is probably not necessary on the inboard portion of the wings. Ice accretion in this area usually does not affect stall speeds, although it does increase aircraft drag. The horizontal stabilizer can be covered with two 5.5-ft. sections having a chordwise extent of 2.5 in. (wrap-around) from zero chord on both upper and lower surfaces. The vertical fin can be protected with a six-ft. long area with a chordwise extent of 2.5 in. on both surfaces.

The nine-ft. length covered on each wing could be divided into two separate de-icers, making a total of seven different de-icers. The inflatable tubes in these boots should be spanwise, rather than chordwise. From a cost and installation viewpoint, spanwise tubes have been found to be more desirable than chordwise tubes when the wrap-around distance is less than 12 in. The tubes should be inflated to 15 to 18 psig by an engine-driven pressure pump. A slight suction (approximately 4 in. Hg) is normally applied to deflate the tubes when not in use.

Pneumatic de-icers may be cycled manually by the pilot or automatically with a timing device. Inflation times are normally from three to five seconds; the de-icers can be inflated either alternately or simultaneously. Each individual de-icer should be inflated once every one to three minutes.

An estimate of the pneumatic de-icing system weight for the typical twin-engine aircraft can be made as follows:

De-icers $(0.7$ lb./ft.$^2)(28$ ft.$^2)$ ≈ 20 lb.

Mechanical equipment (pumps, valves, lines, etc.) ≈ 20 lb.

Total 40 lb.

(The de-icer area shown includes a tapered edge extending beyond the protected area.)

A line diagram of this typical pneumatic de-icing system is shown in Figure 4.1-12. See Paragraph 3.3 for a further description of this method of protection.

Requirements for Hot Gas Anti-Icing

Hot gas anti-icing systems use several sources of hot gas. Direct exhaust-gas heat exchanger, combustion heater, and vapor cycle systems have been used (see Paragraph 3.5). However, hot gas systems are not generally suitable for light aircraft and are not likely to be used because of their high weights and costly installation. "Add-on" type systems are more desirable for light aircraft because they are less costly to install.

Nevertheless, for completeness of this report, calculations of hot gas system heat and airflow requirements are illustrated below for the wing and tail of aircraft "A." Results are shown for both evaporative and running-wet systems; however, small aircraft anti-icing systems are seldom designed to be completely evaporative.

Wing of typical light twin (Aircraft "A")
205 mph cruise at 7,000 ft. altitude

Ambient temperature, t_o = 20° F (conventional design point)

Ambient pressure, p = 23.1 in. Hg

Average surface heat transfer coefficient, h_a = 27.5 BTU/hr.-ft.^{2}-° F
(determined graphically as described in Paragraph 3.5 and Figure 3-19)

Water catch, W_M = 2.95 lb./hr.-ft. span (calculated above)

Average wrap-around distance = 15 in. (heated area extends to front
spar - 10 per cent chord)

Heated area/ft. span = 1.25 sq. ft.

Water impingement rate, $M_W = \dfrac{2.95 \text{ lb./hr. ft. span}}{1.25 \text{ ft.}^2/\text{ft. span}}$

$$= 2.36 \text{ lb./hr. ft.}^2$$

Using the method of NACA TN 2799 (Ref. 4.1-5) described in Paragraph 3.5,
for an evaporative system

$$M_W/h_a = \frac{2.36 \text{ lb./hr. ft.}^2}{27.5 \text{ BTU/hr.-ft.}^2\text{-° F}}$$

$$= 0.0858$$

τ_4 = 11.3° F (from Figure 3-18)

$\tau_3 = 1{,}066 \,(M_W/h_a) + \tau_4$

$\quad = 1{,}066 \,(0.0858) + 11.3$

$\quad = 102.7°\,F$

Therefore, t_s = 74.5° F (from Figure 3-18)

$t_s - t_o$ = 54.5° F

τ_1 = 59.5° F (from Figure 3-18)

τ_2 = 7° F (from Figure 3-18)

τ_5 = 0° F (assuming local static pressure equal to freestream pressure –
Figure 3-18)

Surface heat requirements

$$Q = h_a(\tau_1 - \tau_2 + \tau_3 - \tau_4 + \tau_5)$$

$$= (27.5 \text{ BTU/hr.-ft.}^2\text{-}°\text{F})(59.5 - 7 + 102.7 - 11.3 + 0)°\text{F}$$

$$= 27.5 \ (143.9)$$

$$= 3,960 \text{ BTU/hr.-ft.}^2 \text{ (see Figure 4.1-13)}$$

or 4,950 BTU/hr.-ft. span

or 89,000 BTU/hr. (for 18 ft. of span)

The required anti-icing airflow can be estimated using the equation:

$$w = Q/C_p (t_g - t_s) \, \eta_c$$

in which the channel efficiency, η_c, will normally be from 0.5 to 0.8 depending upon the chordwise channel length and on whether the system is a high or low-pressure system. A method for calculating the channel efficiency can be found in Appendix E of NACA TN 2866 (Ref. 4.1-6).

Assume gas temperature, $t_g = 350°\text{F}$

Specific heat of air at 350° F, $C_p = 0.244 \text{ BTU/lb.-}°\text{F}$

The required anti-icing airflow for a low pressure system with a relatively short channel length (assuming $\eta_c = 0.5$) would be:

$$w = \frac{89,000 \text{ BTU/hr.}}{(0.244 \text{ BTU/lb.-}°\text{F})(350-74.5°\text{F})(0.5)(3,600 \text{ sec./hr.})}$$

$$= 0.73 \text{ lb./sec.}$$

If the system were a high pressure system, the channel efficiency would more likely be 0.8 and the anti-icing airflow required would be:

$$w = \frac{89,000}{(0.244)(350-74.5)(0.8)(3,600)}$$

$$= 0.46 \text{ lb./sec.}$$

(A channel efficiency of $\eta_c = 0.5$ is probably the better assumption for light aircraft.)

The foregoing calculations of heat and airflow requirements are for an entirely evaporative system. To determine the requirements for a "running-wet" system, the ambient temperature, t_o, should be taken as $0°$ F and the surface temperature, t_s, should be assumed equal to about $35°$ F. (The run-back can be tolerated at this surface temperature for a relatively short duration of icing.) The τ_3 for the running-wet system then should be found using Figure 3-18 rather than solving for it as described above:

$$\tau_3 = 24.5° \text{F}$$

$$\tau_4 = 4.5° \text{F}$$

$$\tau_1 = 38.3° \text{F}$$

$$\tau_2 = 7° \text{F}$$

$$\tau_5 = 0° \text{F}$$

Therefore, the surface heat requirements for a running-wet system,

$$Q = h_a (\tau_1 - \tau_2 + \tau_3 - \tau_4 + \tau_5)$$

$$= (27.5 \text{ BTU/hr.-ft.}^2 \text{-}° \text{F}) (38.3 - 7 + 24.5 - 4.5 + 0) ° \text{F}$$

$$= 1,410 \text{ BTU/hr.-ft.}^2$$

$$\text{or } 1,765 \text{ BTU/hr.-ft. span}$$

$$\text{or } 31,800 \text{ BTU/hr. (for 18 ft. of span)}$$

The anti-icing airflow requirements then are:

$$w = Q/C_p (t_g - t_s) \eta_c$$

$$= \frac{31,800 \text{ BTU/hr.}}{(0.244 \text{ BTU/lb.-}° \text{F})(350-35° \text{F})(0.5)(3,600 \text{ sec./hr.})}$$

$$= 0.23 \text{ lb./sec.}$$

Results of both evaporative and running wet surface heat requirement calculations made for the wing, horizontal stabilizer and vertical fin of aircraft "A" are shown in Figures 4.1-13, 4.1-14, and 4.1-15.

Requirements for Cyclic Electrical De-Icing

With cyclic electrical de-icing systems, continuously heated parting strips divide the ice buildup into portions which will shed more easily (with the help of aerodynamic forces) when power is applied to the cycled areas. Parting strips, which are normally one inch wide, should be laid out in a spanwise direction on the leading edge (at stagnation) when the sweep angle is less than 30 deg. Chordwise parting strips are used when the sweep angle is more than 30 deg. The protected area is divided into a number of smaller (cycled) areas which receive power alternately to minimize the total power required. A normal total cycled time is about three minutes. That is, each cycled area receives power once every three minutes. (See Paragraph 3.6.1.1 for more details on cyclic electrical de-icing systems.)

Cycled area power requirements:

Assuming a heat-on time of 20 sec. and t_o = 0° F, the datum temperature, t_{ok}, is about 5° F (from Figure 3-8). The input power density then is approximately 12 watts/sq. in. from Figure 3-26, which was taken from NACA RM E51J30 (Ref. 4.1-7). An ambient temperature of 0° F was chosen as representative of the probable minimum icing temperature that would be encountered by a light aircraft operating at low altitude. Power requirements for a cyclic electric system are at a maximum at minimum ambient temperature (for a given airspeed).

Parting strip power requirements for the wing of Aircraft "A":

205-mph cruise at 7,000 ft. altitude

Ambient temperature, t_o = 0° F (normal design point)

Liquid water content, LWC = 0.25 gm/m^3 (from Figure 1-26)

Modified inertia parameter, K_o = 0.0238 (calculated previously)

Local collection efficiency at stagnation, β_{max} = 0.46 (calculated previously)

Local collection rate at stagnation therefore is:

$$W_\beta = 0.329 \, (U_o)(LWC)\beta_{max}$$

$$= 0.329 \, (205 \text{ mph})(0.25 \text{ gm/m}^3)(0.46)$$

$$= 7.75 \text{ lb./hr.-sq. ft.}$$

Average surface heat transfer coefficient,

$$h_a = 28.3 \text{ BTU/hr.-ft.}^2\text{-}^\circ F \quad \text{(determined graphically as described in Paragraph 3.5)}$$

Using the method of NACA TN 2799 (Ref. 4.1-5):

$$W_\beta/h_a = \frac{7.75 \text{ lb./hr.-ft.}^2}{28.3 \text{ BTU/hr.-ft.}^2\text{-}^\circ F} = 0.274$$

Assuming the surface temperature, $t_s = 35^\circ F$, τ_1 through τ_5 can be found from Figure 3-18:

$$\tau_1 = 45^\circ F$$

$$\tau_2 = 7^\circ F$$

$$\tau_3 = 24.5^\circ F$$

$$\tau_4 = 4.5^\circ F$$

$$\tau_5 = 0^\circ F \quad \text{(assuming local static pressure equal to freestream pressure)}$$

Surface heat requirements

$$Q = h_a(\tau_1 - \tau_2 + \tau_3 - \tau_4 + \tau_5)$$

$$= (28.3 \text{ BTU/hr.-ft.}^2\text{-}^\circ F)(45 - 7.0 + 24.5 - 4.5 + 0)^\circ F$$

$$= 1,640 \text{ BTU/hr.-ft.}^2$$

$$\text{or } 3.33 \text{ watts/sq. in.}$$

Actual heater input power requirements will be approximately Q/0.6 or 5.5 watts/sq. in. assuming 60 per cent of the input heat would be transferred to the outer surface. The 60 per cent efficiency appears to be a good number based on previous experience (see NACA RM E51J30 - Ref. 4.1-7).

Parting strip power requirements calculated for the wing, horizontal stabilizer, and vertical fin are shown versus span in Figures 4.1-16, 4.1-17, and 4.1-18. An 8-watts/sq. in. power density should be used for the parting strips on both wing and tail because of the larger requirements for the empennage (if it is desirable to maintain all parting strips at uniform power density for simplicity in manufacturing).

Total power for the nine sections shown in Figure 4.1-19 for a 20-second heat-on time is determined as follows:

$$\text{Cycled area power} = \frac{(300 \text{ sq. in.})(12 \text{ watts/ sq. in.})}{1,000} = 3.6 \text{ kw}$$

$$\text{Parting strip power} = \frac{(404 \text{ sq in.})(8 \text{ watts/sq. in.})}{1,000} = \underline{3.2 \text{ kw}}$$

$$\text{Total Power} = 6.8 \text{ kw}$$

For 18 sections at a 10-sec. heat-on time, the total power would be:

$$\text{Cycled area power} = \frac{(144 \text{ sq. in.})(16 \text{ watts/sq. in.})}{1,000} = 2.3 \text{ kw}$$

$$\text{Parting strip power} = \frac{(404 \text{ sq. in.})(8 \text{ watts/sq. in.})}{1,000} = \underline{3.2 \text{ kw}}$$

$$\text{Total Power} = 5.5 \text{ kw}$$

The largest cycled area was used in finding the cycled area power. The total power required is plotted in Figure 4.1-20 versus ambient temperature for both nine and eighteen sections. Although the power requirements are less for the eighteen sections, the weight and cost of the system would be greater because of more individual sections, more wiring, relays, etc.

The weight of a cyclic electric system for the wing and tail of a typical light twin would be about 60 lb.

Requirements for Fluid Anti-Icing

Using an anti-icing fluid made up of 50 per cent ethylene glycol and 50 per cent water, the mixture of impinging water and anti-icing fluid that will depress the freezing point to 0° F is 35 per cent glycol by weight according to Figure 3-9. (Fluid systems are normally designed to 0° F.)

4.1-26

The amount of anti-icing fluid necessary can be found from the equation:

$$W_F = \frac{2 \, G \, M_W}{100 - 2G}$$

where G is the percentage by weight of glycol. For the wings of aircraft "A," the water catch based on a 200-mi. icing encounter is $W_M = 0.94$ lb./hr.-ft. span as calculated in Paragraph 4.1.3. For a 10-in. wrap-around extent of protection, the water collection rate would then be:

$$M_W = \frac{0.94 \text{ lb./hr.-ft. span}}{(10/12) \text{ sq. ft./ft. span}}$$

$$= 1.13 \text{ lb./hr.-sq. ft}$$

Therefore, the amount of anti-icing fluid necessary for the wings would be

$$W_F = \frac{2(35)(1.13 \text{ lb./hr.-sq. ft.})}{100 - 2(35)}$$

$$= 2.63 \text{ lb./hr.-sq. ft.}$$

For 15 sq. ft. of wing surface (two nine-ft. sections), the total fluid required would be

$$(2.63 \text{ lb./hr.-sq. ft.})(15 \text{ sq. ft.}) = 39.5 \text{ lb./hr.}$$

and for a one-hour icing encounter (200 mi.), the tank capacity necessary would be $(39.5 \text{ lb./hr.})(1 \text{ hr.}) = 39.5$ lb.

Fluid anti-icing system requirements for the wings and empennage of aircraft "A" are summarized in the following table:

	W_M (200 mi.), lb. / hr. ft. span	sq. ft. ft. span	M_W, lb. hr. sq. ft.	W_F, lb. hr. sq. ft.	Protected Area, sq. ft.	Total Fluid lb./hr.	Tank Capacity, lb.
Wings	0.94	0.862	1.13	2.63	15	39.5	39.5
Horiz. Stab.	0.637	0.417	1.57	3.57	4.6	16	16
Vert. Fin	0.720	0.417	1.73	4.03	2.5	10	10

These amounts of fluids should be increased by a factor based on experience or specific test results to account for non-uniform distribution (as discussed in Paragraph 3.4.2 and shown in Figures 3-11 and 3-12).

Fluid de-icing systems have been put into use (see Paragraph 3.4). This type of system would require a considerably smaller amount of fluid — possibly one-fifth of that required for anti-icing.

4.1.4.2 SELECTION OF ICE PROTECTION FOR WINDSHIELD

Requirements for Electrical Anti-Icing

The following calculations illustrate a method of determining water catch and anti-icing heat requirements for an inclined windshield. Water catch can be found by treating the windshield as a "rectangular half body" using the method of NACA TN 3658 (Ref. 4.1-8).

Twin-engine aircraft "A"

205-mph cruise at 7,000 ft. altitude (300 fps)

Droplet radius, $a = 10$ microns (3.28×10^{-6} ft./micron)

Ambient temperature, $t_o = 0°$ F (conventional design point)

Liquid water content, LWC = 0.25 gm/m^3

Air density, $\rho = 0.00207$ slugs/cu. ft.

Air viscosity, $\mu = 0.36 \times 10^{-6}$ slugs/cu. ft.

Windshield area = 7.5 sq. ft.

Windshield height, $\ell = 0.875$ ft.

Projected windshield area, $A_p = 3.6$ sq. ft.

Droplet Reynolds number

$$Re_d = \frac{2 a \rho V}{\mu}$$

$$= \frac{2(10 \text{ microns})(3.28 \times 10^{-6} \text{ ft./micron})(0.00207 \text{ slugs/cu. ft.})(300 \text{ fps})}{(0.36 \times 10^{-6} \text{ slugs/ft.-sec.})}$$

$$= 113$$

Inertia parameter

$$K = \frac{2\rho_w a^2 V}{9\mu \, l}$$

$$= \frac{2(1.935 \text{ slugs/cu. ft.})(10 \text{ microns})^2 (3.28 \times 10^{-6} \text{ ft./micron})^2 (300 \text{ fps})}{9(0.36 \times 10^{-6} \text{ slugs/ft.-sec.})(0.875 \text{ ft.})}$$

$$= 0.44$$

Then from Figure 5 of NACA TN 3658 (Ref. 4.1-3) the collection efficiency, $E_M = 0.07$. (This could also be found by the K_o method illustrated in Paragraph 4.1.4.1 for the wings and tail. Collection efficiency can be found versus K_o for a semi-infinite rectangle in Figure 2-13.)

Rate of water interception

$$W = 0.33 \, E_M \, (A_p)(LWC)(U_o)$$

$$= 0.33 \, (0.07)(3.6 \text{ sq. ft.})(0.25 \text{ gm/m}^3)(205 \text{ mph})$$

$$= 4.26 \text{ lb./hr.}$$

Water collection rate

$$M_W = \frac{4.26 \text{ lb./hr.}}{7.5 \text{ sq. ft.}}$$

$$= 0.57 \text{ lb./hr. sq. ft.}$$

The convective heat transfer coefficient, assuming a flat plate, can be found from this equation extracted from SAE 24 (Ref. 4.1-9):

$$h_c = 0.51 \frac{t_f^{0.3} (V\gamma)^{0.8}}{x^{0.2}}$$

where t_f is the boundary layer temperature in deg. R; where x, in this case, is the distance in feet from the airplane nose (this would be the case for an inclined windshield); and γ is density of air in lb./cu. ft.

$$h_c = \frac{0.51(465° \text{ R})^{0.3} (300 \text{ fps})(0.667 \text{ lb./cu. ft.})^{0.8}}{(8 \text{ ft.})^{0.2}}$$

$$= 23.4 \text{ BTU/hr.-sq. ft.-° F}$$

Then using the method of NACA TN 2799 (Ref. 4.1-5):

$$M_W/h_c = \frac{0.57\ \text{lb./hr.-sq. ft.}}{23.4\ \text{BTU/hr.-sq. ft.-}^\circ F}$$

$$= 0.0243$$

From Figure 3-18 assuming the surface temperature $t_s = 35^\circ F$,

$$\tau_1 = 36.3\ ^\circ F$$

$$\tau_2 = 7^\circ F$$

$$\tau_3 = 24.5^\circ F$$

$$\tau_4 = 4.5^\circ F$$

$$\tau_5 = 0^\circ F$$

The surface heat requirement

$$Q = h_c\ (\tau_1 - \tau_2 + \tau_3 - \tau_4 + \tau_5)$$

$$= (23.4\ \text{BTU/hr.-sq. ft.-}^\circ F)(36.3 - 7 + 24.5 - 4.5 + 0)^\circ F$$

$$= 1,154\ \text{BTU/hr.-sq. ft.}$$

$$\text{or } 2.34\ \text{watts/sq. in.}$$

Values of power required are shown plotted versus ambient temperature in Figure 4.1.21. For comparison, results are also shown for a nearly vertical windshield, where heat transfer coefficient is based on the distance, x, from the base of the windshield. Using the distance from the windshield base is more correct when the windshield is near vertical (because of development of a new boundary layer), while the distance from the airplane nose is normally used for windshields slanted back at a greater angle. Power requirements for most windshields will lie between the two curves of Figure 4.1-21.

The total power required to protect two 18-in. square sections of the windshield of aircraft "A" at $t_o = 0^\circ F$, then, would be

$$\frac{(2.34\ \text{watts/sq. in.})(648\ \text{sq. in.})}{1,000} = 1.52\ \text{kw}$$

Requirements for Fluid Anti-Icing

The mixture of impinging water and 50 per cent ethylene glycol anti-icing fluid that will depress the freezing point to $0°$ F is 35 per cent glycol by weight, according to Figure 3-9.

The flow rate of anti-icing fluid necessary can be found from this equation:

$$W_F = \frac{2G\ M_W}{100 - 2G}$$

$$= \frac{2(35)(0.57\ lb./hr.-sq.\ ft.)}{100 - 2(35)}$$

$$= 1.33\ lb./hr.-sq.\ ft.$$

For two 18-in. square sections of windshield, the total fluid required is

$$(1.33\ lb./hr.-sq.\ ft.)(4.5\ sq.\ ft.) = 6.0\ lb./hr.$$

And for a one-hour duration, the tank capacity required would be:

$$(6\ lb./hr.)(1\ hr.) = 6\ lb.\ of\ fluid$$

The windshield fluid system flow rate and tank capacity required by military specifications (MIL-S-662?A - Ref. 4.1-10) are presented below. These values are not necessarily applicable to light aircraft unless, of course, they are to be used as military aircraft.

The military specification requirements for tank capacity would be:

$$gal = \frac{0.7\ A_W\ X}{12}$$

$$= \frac{0.7(7.5\ sq.\ ft.)(5\ hr.)}{12}$$

$$= 2.19$$

$$or \sim 18\ lb.$$

The military specification also requires a flow rate of two quarts of fluid per square foot of two-thirds the windshield area per hour:

$$(2 \text{ qt./sq. ft.-hr.})(7.5 \text{ ft.})(2/3) = 10 \text{ qt./hr.}$$

$$= 2.5 \text{ gal./hr.}$$

$$\text{or} \sim 21 \text{ lb./hr.}$$

4.1.4.3 SELECTION OF ICE PROTECTION FOR PROPELLERS

Requirements for Electrical Protection

Electrical protection for propellers is normally cyclic de-icing. For twin-engine aircraft, power could be applied to either one or both propellers at one time. If the power to the propeller de-icers is cycled with electrical de-icers on the wings and empennage, no power would be required in addition to that used for the wing and tail.

Calculation of the requirements for electrical propeller de-icing is illustrated by the following:

Twin-engine aircraft "A" (4,800 lb. gross weight)

205 mph cruise at 7,000 ft., (2,400 rpm)

Propeller diameter, 74 in. (31-in. blades)

Propeller chord $C = 6$ in. (12 per cent thick)

Ambient temperature, $t_o = 17°$ F (most probable icing temperature, from Figure 1-16)

Wing area, $A = 207$ sq. ft.

Dynamic pressure, $q = 90.2$ psf (from page 4.1-9)

Wing coefficient of lift, $C_L = 0.257$ (from page 4.1-9)

$L/D = 21$ from Figure 29 of NACA TR 669 (Ref. 4.1-11).

Total drag therefore is

$$D = \frac{4,800 \text{ lb.}}{21} = 230 \text{ lb.}$$

Propeller lift coefficient

$$C_{L_{prop}} = \frac{L}{q A}$$

$$= \frac{230 \text{ lb.}}{(90.2 \text{ psf})(4.3 \text{ sq. ft.})}$$

$$= 0.593$$

If the total propeller area is 4.3 sq. ft. and the propeller lift is equal to airplane drag.

Therefore, the propeller angle of attack is approximately 8 deg. according to the C_L vs. α curve for an NACA 0012 airfoil (NACA TR 669, Ref. 4.1-11).

The true helical speed of the propeller at the midpoint of the blade (21.5-in. radius),

$$v_r = \sqrt{V^2 + (\pi dn)^2}$$

$$= \sqrt{\left[(205)(1.467) \text{ fps}\right]^2 + \left[(\pi)(43/12 \text{ ft.})(40 \text{ rps})\right]^2}$$

$$= \sqrt{90,300 + 202,500}$$

$$= 541 \text{ fps}$$

or 369 mph

Droplet Reynolds number

$$Re,d = \frac{4.81 (D_d)(\rho)(v_r)(10^{-6})}{\mu}$$

$$= \frac{4.81(20 \text{ microns})(0.00199 \text{ slugs/cu. ft.})(369 \text{ mph})(10^{-6})}{(0.36 \times 10^{-6} \text{ slugs/ft.-sec.})}$$

$$= 196$$

$\lambda/\lambda_s = 0.27$ (from Figure 2-6)

Inertia Parameter

$$K = \frac{1.705 \ (D_d)^2 (v_r)(10^{-12})}{\mu \ (C)}$$

$$= \frac{1.705 \ (20 \ \text{microns})^2 (369 \ \text{mph})(10^{-12})}{(0.36 \times 10^{-6} \ \text{slugs/ft.-sec.})(0.5 \ \text{ft.})}$$

$$= 1.395$$

Modified inertia parameter

$$K_0 = K \ (\lambda/\lambda_s)$$

$$= 1.395 \ (0.27)$$

$$= 0.376$$

Then from Figures 2-21 and 2-22 (assuming a 15 per cent Joukowski airfoil at $\alpha = 8$), the chordwise limits of impingement are:

$$S_L \ = 0.35 \qquad\qquad S_U \ = 0.055$$

$$s_L \ = 2.1 \ \text{inch} \qquad\qquad s_U = 0.33 \ \text{inch}$$

Limits of impingement using a 40-micron drop diameter were found to be 3.5 inches on the lower surface and 0.6 in. on the upper surface. The desirable chordwise coverage then would be about 4 in. (wrap around) if the system were to be designed to 40-micron drops.

To find the radial extent of icing on the propeller blade, the velocity (565 fps) at which the datum temperature will be above freezing is first obtained from Figure 3-8. The equation

$$v_r = \sqrt{v^2 + (\pi d \ n)^2}$$

for local helical blade velocity can then be solved for the diameter, d, beyond which no ice will form.

$$565 \ \text{fps} = \sqrt{\left|(205)(1.187 \ \text{fps}\right|^2 + \left|\pi(d)(40 \ \text{rps})\right|^2}$$

then

$d = 3.8$ ft. $= 45.7$ in. diameter

Therefore, if the spinner is 12 in. in diameter, the extent of icing on the
propeller blade is 16.85 in. at $t_0 = 17°$ F (the most probable icing temperature).
The desirable heater area then would be about four in. (wrap-around) by 17 in.
long. Figure 4.1-22 shows the extent of protection and a flat layout of the
heater area.

For a 20-sec. heat-on time, the power density would be about six watts/
sq. in. as indicated by Figure 4.1-23, which is taken from NACA TN 1520
(Ref. 4.1-12).

The total power required to de-ice two blades at one time would be

$$\frac{(68 \text{ sq. in.})(2)(6 \text{ watts/sq. in.})}{1,000} = 0.8 \text{ kw}$$

To protect to 0° F, the necessary coverage would be about four by 30 in.
on each blade, and the total power required to de-ice two blades at one time
is 1.2 kw as shown in Figure 4.1-24, the variation in propeller power require-
ments with ambient temperature.

In practice, shorter propeller de-icers (13 in. outboard of the spinner)
have been used for CAR-3 aircraft because of the effect of centrifugal force.
Wrap-around coverage used has been about 2.5 in. (which corresponds to the
20-micron limits determined above). Also, a power density closer to eight
watts/sq. in. has been used for propellers of CAR-3 aircraft because of ie-
icer efficiencies existing in practice.

Requirements for Fluid Protection

The requirements for a fluid protection system for the propeller are deter-
mined as illustrated by the following for aircraft "A":

Modified Inertia Parameter, $K_o = 0.376$ (from above)

Collection efficiency, $E_M = 0.67$ (from Figure 2-13 for a 15% Joukowski airfoil at $\alpha = 6°$)

Water catch (20 mile)

$$W_M = 0.329 \, (v_r)(LWC)(h/C)(C)(E_M)$$

$$= 0.329(369 \text{ mph})(0.46 \text{ gm/m}^3)(0.185)(0.5 \text{ ft.})(0.67)$$

$$= 3.46 \text{ lb./hr.-ft. span}$$

For a 200-mi. icing encounter, the distance factor $F = 0.32$ from Figure 1-28, and the water catch is

$$(3.46 \text{ lb./hr.-ft. span})(0.32) = 1.14 \text{ lb./hr.-ft. span}$$

If the protected area is 0.333 sq. ft./ft. span of propeller, the water collection rate

$$M_W = \frac{1.14 \text{ lb./hr.-ft. span}}{0.333 \text{ sq. ft./ft. span}}$$

$$= 3.42 \text{ lb./hr.-sq. ft.}$$

Using the same 35 per cent by weight glycol described above for wings, empennage, and the windshield, the amount of de-icing fluid necessary is

$$W_f = \frac{2G \, M_W}{100 - 2G}$$

$$= \frac{2(35)(3.42 \text{ lb./hr.-sq. ft.})}{100 - 2(35)}$$

$$= 7.98 \text{ lb./hr.-sq. ft.}$$

For a 17-in. protected area on each of the four blades (two per engine), the total fluid required is

$$(7.98 \text{ lb./hr.-sq. ft.})(4) \, (0.472 \text{ sq. ft.}) = 15 \text{ lb./hr.}$$

The tank capacity required then for a one-hour icing encounter would be

$$(15 \text{ lb./hr.})(1 \text{ hr.}) = 15 \text{ lb.}$$

4.1.4.4 SELECTION OF ICE PROTECTION FOR THE PITOT TUBE

Requirements for Electro-Thermal Protection

The following sample calculations will illustrate a method for determining the power requirements for an electrically heated pitot tube:

Twin-engine aircraft "A"

205-mph cruise at 7,000 ft. altitude

Assume ambient temperature, $t_o = 0°$ F

The convective heat transfer coefficient can be obtained at the stagnation point by assuming that the tip of the pitot is equivalent to a 1/4-in. diameter cylinder:

$$h_c = 0.194 \, t_f^{0.49} \left(\frac{V\gamma}{d_{cyl}} \right)^{0.5} \quad \text{(from Ref. 4.1-9)}$$

$$= 0.194 (465° \, R)^{0.49} \left[\frac{(300 \text{ fps})(0.0667 \text{ lb./cu.ft.})(12 \text{ in./ft.})}{0.25 \text{ in.}} \right]^{0.5}$$

$$= 123 \text{ BTU/hr.-sq. ft.-° F}$$

Assuming $M_W/h_c = 0.1$ (because the running wet requirements are not sensitive to M_W), the surface heat requirements may be found by the method of NACA TN 2799 (Ref. 4.1-5). For a running wet system, $t_s = 35°$ F and (from Figure 3-18):

$$\tau_1 = 39° \text{ F}$$
$$\tau_2 = 7° \text{ F}$$
$$\tau_3 = 24.5° \text{ F}$$
$$\tau_4 = 4.5° \text{ F}$$
$$\tau_5 = 0° \text{ F}$$

Power requirements at the tip of the pitot tube then are:

$$Q = h_a (\tau_1 - \tau_2 + \tau_3 - \tau_4 + \tau_5)$$

$$= (123 \text{ BTU/hr.-sq. ft.}^\circ\text{F})(39\text{-}7 + 24.5 - 4.5 + 0)^\circ\text{F}$$

$$= 6,400 \text{ BTU/hr.-sq. ft.}$$

or 13 watts/ sq. in.

The heat transfer coefficient aft of the tip can be obtained assuming a flat plate (turbulent flow):

$$h_c = 0.51 \, t_f^{0.3} \, \frac{(V \, \gamma)^{0.8}}{x^{0.2}} \quad \text{(from Ref. 4.1-9)}$$

The anti-icing power requirements can then be obtained versus distance from stagnation as shown in Figure 4.1-25.

Figure 4.1-26 shows icing tunnel test results of total power requirements versus ambient temperature for a typical heated pitot tube. From this Figure, a typical value of anti-icing power required to protect to 0° F is approximately 103 watts.

4.1.5 SELECTION OF ICE PROTECTION FOR SINGLE-ENGINE AIRCRAFT

For the typical single-engine light plane shown in Figure 4.1-27 (aircraft "B"), calculations of the different ice protection system requirements were made in the same manner described in Paragraph 4.1.4 for a typical light twin-engine aircraft. Since the results for the single-engine airplane were nearly identical to those for the twin, little value could be seen in presenting the single-engine calculations in this report.

However, a summary of complete ice protection system weights and power extraction for the typical single-engine aircraft are presented in Paragraph 4.1.7. Values are shown for several different combinations of systems considered to be the most desirable for this type aircraft.

4.1.6 SELECTION OF ICE PROTECTION FOR LIGHT JET AIRCRAFT

In the selection of ice protection for the wings, empennage, windshield and pitot tube of a typical light jet (Figure 4.1-28), the requirements for the different systems were found in the same manner described in Paragraph 4.1.4 for the reciprocating twin-engine lightplane. Since the results for the jet were

quite similar to those for the reciprocating twin, presenting the detailed calculations and results for the jet would be of no value to this report. However, a summary of weight and power extraction for several different combinations of ice protection systems is presented in Paragraph 4.1.7 for this type aircraft.

The most desirable systems for the reciprocating twin will not necessarily be the most desirable for the jet. More consideration may be given to hot gas anti-icing systems for the wing and tail of the jet because of the availability of engine bleed air. Also, the jet aircraft may have more power available for electrical protection systems. Special consideration must be made of the potential problem of ice shedding from the inboard wing into the engine inlet, if aft-mounted engines are used.

For the light jet aircraft, requirements must also be determined for ice protection of the engine inlet. The calculations below illustrate this for typical light jet aircraft "C" shown in Figure 4.1-28. For purposes of illustration, the requirements are determined at a 20,000 ft. cruise condition. However, calculations are ordinarily made at a number of different flight conditions to determine the design condition.

Calculation of Impingement Limits and Water Catch for Engine Inlet Lip

Twin jet aircraft "C" (12,500 lb. gross weight)

500-mph cruise at 20,000 ft. altitude

Ambient temperature, t_o = -11° F (most probable icing temperature, from Figure 1-16)

Droplet diameter, D_d = 20 microns

Liquid water content, LWC = 0.17 gm/m^3 (from Figure 1-26)

Air density, ρ = 0.001262 slugs/cu. ft.

Air viscosity, μ = 0.332 x 10^{-6} slugs/ft.-sec.

4.1-39

Droplet Reynolds number

$$Re_d = 4.81 \frac{D_d \, (\rho)(U_o)(10^{-6})}{\mu}$$

$$= \frac{4.81(20 \text{ microns})(0.001262 \text{ slugs/cu. ft.})(500 \text{ mph})(10^{-6})}{0.332 \times 10^{-6} \text{ slugs/ft. -sec.}}$$

$$= 183$$

Therefore, $\lambda/\lambda_s = 0.278$ (from Figure 2-6)

Assume chord length, $C = 1.5$ ft. (based on inlet lip thickness and pressure distribution)

The inlet is assumed to be circular.

Inertia parameter

$$K = \frac{(1.705 \times 10^{-12})(D_d)^2(U_o)}{\mu (C)}$$

$$= \frac{(1.705 \times 10^{-12})(20 \text{ microns})^2(500 \text{ mph})}{(0.332 \times 10^{-6} \text{ slugs/ft. -sec.})(1.5 \text{ ft.})}$$

$$= 0.682$$

Modified inertia parameter

$$K_o = K(\lambda/\lambda_s)$$

$$= 0.682 \, (0.278)$$

$$= 0.190$$

Therefore, using 14.5 per cent Joukowski airfoil at a 2-deg. angle of attack, the collection efficiency from Figure 2-9 is $E_M = 0.54$.

(The inlet lip contour and pressure distribution are approximately equal to a 14.5 per cent Joukowski airfoil at $\alpha = 2$ deg. For an explanation of airfoil matching procedures, see Paragraph 2.3.4.)

Ratio of projected height to chord, $h/C = 0.15$ (from Figure 2-3)

Water catch

$$W_M = 0.329 \, (U_o)(LWC)(h/C)(C)(E_M)$$

$$= 0.329 \, (500 \text{ mph})(0.17 \text{ gm/m}^3)(0.15)(1.5 \text{ ft.})(0.54)$$

$$= 3.4 \text{ lb./hr.-ft. span}$$

Therefore, the impingement limits from Figures 2-15 and 2-16 are:

$$S_L/C = 0.17 \qquad\qquad S_U/C = 0.09$$

$$s_L = 3.1 \text{ in.} \qquad\qquad s_U = 1.6 \text{ in.}$$

(The larger value, s_L, refers to the inside surface of the inlet lip.)

Similar calculations using a 40-micron drop size would result in impingement limits of 4.3 in. on the inside surface and 2.6 in. on the outside surface. The minimum coverage required to protect for 40-micron drops then would be about seven inches total wrap-around distance.

Requirements for Anti-Icing of Engine Inlet Lip

For axial flow engines, which can be damaged by ice ingestion, it is desirable to anti-ice the engine inlet lip. Requirements are determined below for both evaporative and running-wet hot gas anti-icing systems for the engine inlet lip of typical light jet aircraft "C." Requirements are also shown for running-wet electrical anti-icing for the engine inlet lip. (Evaporative electrical anti-icing is usually impractical because of excessive power requirements).

    Twin-jet aircraft "C"

    500-mph cruise at 20,000 ft. altitude

    Ambient temperature, $t_o = -11°$ F (most probable icing temperature from Figure 1-16)

For an eight-inch wrap-around coverage, the protected area per foot of circumference would be 0.667 sq. ft.

Water collection rate

$$M_W = \frac{3.4 \text{ lb./hr.-ft. circumference}}{0.667 \text{ ft.}^2/\text{ft. circumference}}$$

$$= 5.1 \text{ lb./hr.-sq. ft.}$$

The average heat transfer coefficient obtained by the method described in Paragraph 3.5 is

$$h_a = 45 \text{ BTU/hr.-sq. ft.-}^\circ F$$

The surface heat requirements for an evaporative system can be found by the method of NACA TN 2799 (Ref. 4.1-5):

$$M_W/h_a = \frac{5.1 \text{ lb./hr.-sq. ft.}}{45 \text{ BTU/hr.-sq. ft.}^\circ F}$$

$$= 0.111$$

From Figure 3-18

$$\tau_4 = 5^\circ F$$

$$\tau_3 = (1066 \frac{M_W}{h_c}) + \tau_4 = 118.3 + 5 = 123.3^\circ F$$

$$t_s = 64^\circ F$$

$$\tau_1 = 84^\circ F$$

$$\tau_2 = 40^\circ F$$

$$\tau_5 = 0^\circ F$$

Surface heat requirements

$$Q = h_a(\tau_1 - \tau_2 + \tau_3 - \tau_4 + \tau_5)$$

$$= (45 \text{ BTU/hr.-sq. ft.-}^\circ F)(84 - 40 + 123.3 - 5 + 0)^\circ F$$

$$= 45 (162.3)$$

$$= 7,300 \text{ BTU/hr.-sq. ft.}$$

or 21,500 BTU/hr. (per engine)

if the engine inlet circumference is 53 in. and the heated area is 2.94 sq. ft. per engine.

For a hot gas anti-icing system, assuming a gas temperature of $t_g = 350°$ F and a channel efficiency of $\eta_c = 0.8$, the airflow requirements are:

$$w = \frac{Q}{C_p(t_g - t_s)(\eta_c)}$$

$$= \frac{21,500 \text{ BTU/hr.}}{(0.24 \text{ BTU/lb.° F})(350 - 64° \text{F})(0.8)(3,600 \text{ sec./hr.})}$$

$$= 0.109 \text{ lb./sec. (per engine)}$$

(The exact gas temperature would have to be determined by an engine bleed analysis based on data from the engine manufacturer.)

Evaporative electrical anti-icing of the engine inlet lip is usually impractical because of the excessive power requirements. (Total power requirements for the engine inlet lip of typical light jet aircraft "C" are on the order of 7 kw per engine.)

A running-wet anti-icing system for the engine inlet lip may require less heat input than for an evaporative system. Runback is not a problem as long as the heated area is extended to the compressor face. This is quite feasible for the engine of aircraft "C" because the engine face is only about 18 in. from the leading edge of the engine inlet. However, for engines in which the compressor face is 3 to 4 ft. or more from the leading edge, it may not be practical to heat entirely to the compressor face, and a hot air evaporative system may be the logical choice.

The calculation of requirements for running-wet anti-icing of the engine inlet are illustrated by the following: Taking the surface temperature, $t_s = 35°$ F,

$$\tau_1 = 51.5°\,F$$

$$\tau_2 = 40°\,F$$

$$\tau_3 = 41°\,F$$

$$\tau_4 = 5°\,F$$

$$\tau_5 = 0°\,F$$

from Figure 3-18.

The average convective heat transfer coefficient obtained by the method described in Paragraph 3.5 is

$$h_a = 37\ BTU/hr.-sq.\ ft.$$

Therefore, the surface heat requirements for a running-wet system are

$$Q = h_a\ (\tau_1 - \tau_2 + \tau_3 - \tau_4 + \tau_5)$$

$$= (37\ BTU/hr.-sq.\ ft.°\,F)(51.5 - 40 + 41 - 5 + 0)°\,F$$

$$= 1,760\ BTU/hr.-sq.\ ft.$$

  or 13,500 BTU/hr. (per engine)

for a 7.67 sq. ft. heated area (per engine) extending to the compressor face.

Electrical anti-icing surface heat requirements for a running-wet system would also be

$$Q = 1,760\ BTU/hr.-sq.\ ft.$$

  or 3.6 watts/sq. in.

With a 90 per cent efficiency, the heater input requirement would be Q/0.9 or 4.0 watts/sq. in. Therefore, for a running-wet anti-icing system, the total power required would be:

$$\frac{(4.0\ watts/sq.\ in.)(1,100\ sq.\ in.)}{1,000} = 4.4\ kw\ (per\ engine)$$

Cyclic electric de-icing could be designed for an engine with a centrifugal compressor because this type is less susceptible to engine damage due to ice ingestion than the engine with an axial flow compressor.

For the purpose of illustration, assuming an engine with a centrifugal compressor with the inlet dimensions of the (axial flow compressor) engine of aircraft "C," an estimation can be made of the power requirements for cyclic electric de-icing of the engine inlet. For a 53-in. circumference inlet, a one-inch wide continuously heated parting strip is necessary at stagnation. If the parting strip power density required is 12 watts/sq. in., the total parting strip power required for two engines would be about 1.3 kw.

Dividing the 8-in. wide heated area into four different cycled areas per engine, each section could have a 10-sec. heat-on time with heat off for 70 sec. If the power density required for the cycled areas is 18 watts/sq. in., the cycled area power required would be about 1.7 kw. The total de-icing system power required, then, would be about 3.0 kw or 1.5 kw per engine.

4.1.7 EFFECT OF INSTALLED ICE PROTECTION SYSTEMS ON AIRCRAFT WEIGHT AND PERFORMANCE

The effect of installed ice protection systems on the weight and performance of light aircraft is illustrated by the table below. Ice protection system weights and energy or power requirements are tabulated for several different combinations of the most desirable systems for light aircraft. Values are shown for all three typical aircraft chosen for study.

From the type of information presented below, actual performance penalties can be predicted. The numbers shown, however, are representative only of the order of magnitude. A more detailed analysis would be necessary to determine these values more exactly for any particular airplane.

Certain weights and energy or power requirements shown below are higher for the single-engine aircraft than for the twin. The reason for this is the larger protected area taken for the wings of the single-engine airplane. Only the leading edge area outboard of the engine nacelles was protected on the twin.

Aircraft	Aircraft Component	System Type	Weight Lb.	Energy and Power Requirements			
				KW	BTU/Hr.	HP	Al·lb·Min.
"A" (Twin-Engine Recip.)	Wing & Tail	Pneumatic De-icing	40			0.5	
	Windshield	Elec. Anti-icing	10	1.5		2.0	
	Propeller	Elec. De-icing	10	0.8		1.1	
		Generator (a)	15			3.6	
	Total		75				
	Wing & Tail	Elec. De-icing	40	6.8		9.1	
	Windshield	Elec. Anti-icing	10	1.5		2.7	
	Propeller	Elec. De-icing	10	De-iced with wing & tail		0	
		Alternator (b)	20	8.3		11.1	
	Total		80				
	Wing & Tail	Fluid Anti-icing	111(45)				
	Windshield	Fluid Anti-icing	9(3)				
	Propeller	Fluid Anti-icing	17(2)	0.3		0.4	
	Total		137(50)				
	Wing & Tail	Fluid De-icing	53(40)				
	Windshield	Fluid Anti-icing	9(3)				
	Propeller	Fluid De-icing	7(2)	0.15		0.20	
	Total		68(45)				

Numbers in parenthesis are dry system weights.

(a) 15 lb. added for increase in generating capacity, (28-volt generator + transformer).

(b) 20 lb. added for increase in generating capacity (115-volt alternator substituted).

Aircraft	Aircraft Component	System Type	Weight Lb.	Energy and Power Requirements			
				KW	BTU/Hr.	HP	Air Lb./Min.
"B" (Single-Engine Recip.)	Wing & Tail	Pneumatic De-icing	40(a)			0.3	
	Windshield	Elec. Anti-icing	10	1.4		2.0	
	Propeller	Elec. De-icing	5	0.6		0.8	
	Generator (b)		15			3.1	
	Total		70				
	Wing & Tail	Elec. De-icing	45	3.3		12.5	
	Windshield	Elec. Anti-icing	10	1.4		1.9	
	Propeller	Elec. De-icing	5	De-iced with wing & tail		0	
	Alternator (c)		20			14.4	
	Total		80	10.7			
	Wing & Tail	Fluid Anti-icing	117(50)				
	Windshield	Fluid Anti-icing	6(3)				
	Propeller	Fluid Anti-icing	4(2)	0.3		0.4	
	Total		127(55)				
	Wing & Tail	Fluid De-icing	62(45)				
	Windshield	Fluid Anti-icing	5(3)				
	Propeller	Fluid De-icing	4(2)	0.15		0.20	
	Total		72(50)				

Numbers in parenthesis are dry system weights.

(a) New systems are currently available (with less chordwise coverage) which would reduce this weight to 25 - 30 lb.

(b) 15 lb. added for increase in generating capacity (28-volt generator + transformer).

(c) 20 lb. added for increase in generating capacity (115-volt alternator substituted).

Aircraft	Aircraft Component	System Type	Weight Lb.	Energy and Power Requirements			
				KW	BTU/Hr.	HP	Air/Lb./Min.
'C' (Light twin jet)	Wing & Tail	Pneumatic De-icing	45			0.5	
	Windshield	Elec. Anti-icing	10	1.5	43,000	2.0	13.1
	Engine Inlet	Hot Gas Anti-icing	10				
	Generator (a)		15				
	Total		80				
	Wing & Tail	Elec. De-icing	45	11.7		15.7	
	Windshield	Elec. Anti-icing	10	1.5		2.0	
	Engine Inlet	Elec. Anti-icing	10	8.8		11.8	
	Alternator (b)		20	22.0		29.5	
	Total		85				
	Wing & Tail	Fluid Anti-icing	91(50)				
	Windshield	Fluid Anti-icing	13(3)				
	Engine Inlet	Hot Gas Anti-icing	10	0.3	43,000	0.4	13.1
	Total		114(63)				
	Wing & Tail	Fluid De-icing	53(45)				
	Windshield	Fluid Anti-icing	13(3)				
	Engine Inlet	Hot Gas Anti-icing	10	0.15	43,000	0.20	13.1
	Total		76(58)				

Numbers in parenthesis are dry system weights.

(a) 15 lb. added for increase in generating capacity (28-volt generator + transformer).

(b) 20 lb. added for increase in generating capacity (115-volt alternator substituted).

REFERENCES

4.1-1   NACA TN 3564, "Effect of Pneumatic De-Icers and Ice Formations on Aerodynamic Characteristics of an Airfoil," D. T. Bowden, February 1956.

4.1-2   "Some Results of Experimental Flights in Natural Icing Conditions and Operation of Aircraft Thermal Ice Protection Systems," O. K. Trunov and M. S. Egorov (paper presented at Aircraft Ice Protection Conference, D. Napier & Son, Ltd.), May 1960.

4.1-3   NACA TN 1598, "Effects of Ice Formations on Airplane Performance in Level Cruising Flight," G. M. Preston and C. C. Blackman, May 1948.

4.1-4   NACA TN 3839, "Experimental Droplet Impingement on Several Two-Dimensional Airfoils with Thickness Ratios of 6 to 16 Percent," T. F. Gelder, W. H. Smyers, and U. von Glahn, December 1956.

4.1-5   NACA TN 2799, "Simple Graphical Solution of Heat Transfer and Evaporation From Surface Heated to Prevent Icing," V. H. Gray, October 1952.

4.1-6   NACA TN 2866, "Icing Protection for a Turbojet Transport Airplane: Heating Requirements, Methods of Protection and Performance Penalties," T. F. Gelder, J. P. Lewis, and S. L. Koutz, January 1953.

4.1-7   NACA RM E51J30, "Preliminary Investigation of Cyclic De-Icing of an Airfoil Using an External Electric Heater," J. P. Lewis and D. T. Bowden, February 1952.

4.1-8   NACA TN 3658, "Impingement of Water Drops on a Rectangular Half Body in a Two-Dimensional Incompressible Flow Field," W. Lewis and R. J. Brun, February 1956.

4.1-9   SAE Report No. 24, Airplane Air Conditioning Engineering Data – Heat Transfer, February 1, 1952.

4.1-10   MIL-S-6625A (ASG), Military Specification – Spray Equipment, Aircraft Windshield, Anti-Icing, 25 October 1951.

4.1-11   NACA TR 669, "Airfoil Section Data Obtained in the NACA Variable-Density Tunnel as Affected by Support Interference and Other Corrections." E. N. Jacobs and I. H. Abbott, 1939.

4.1-12 NACA TN 1520, "De-Icing Effectiveness of External Electric Heaters for Propeller Blades," J. P. Lewis, February 1948.
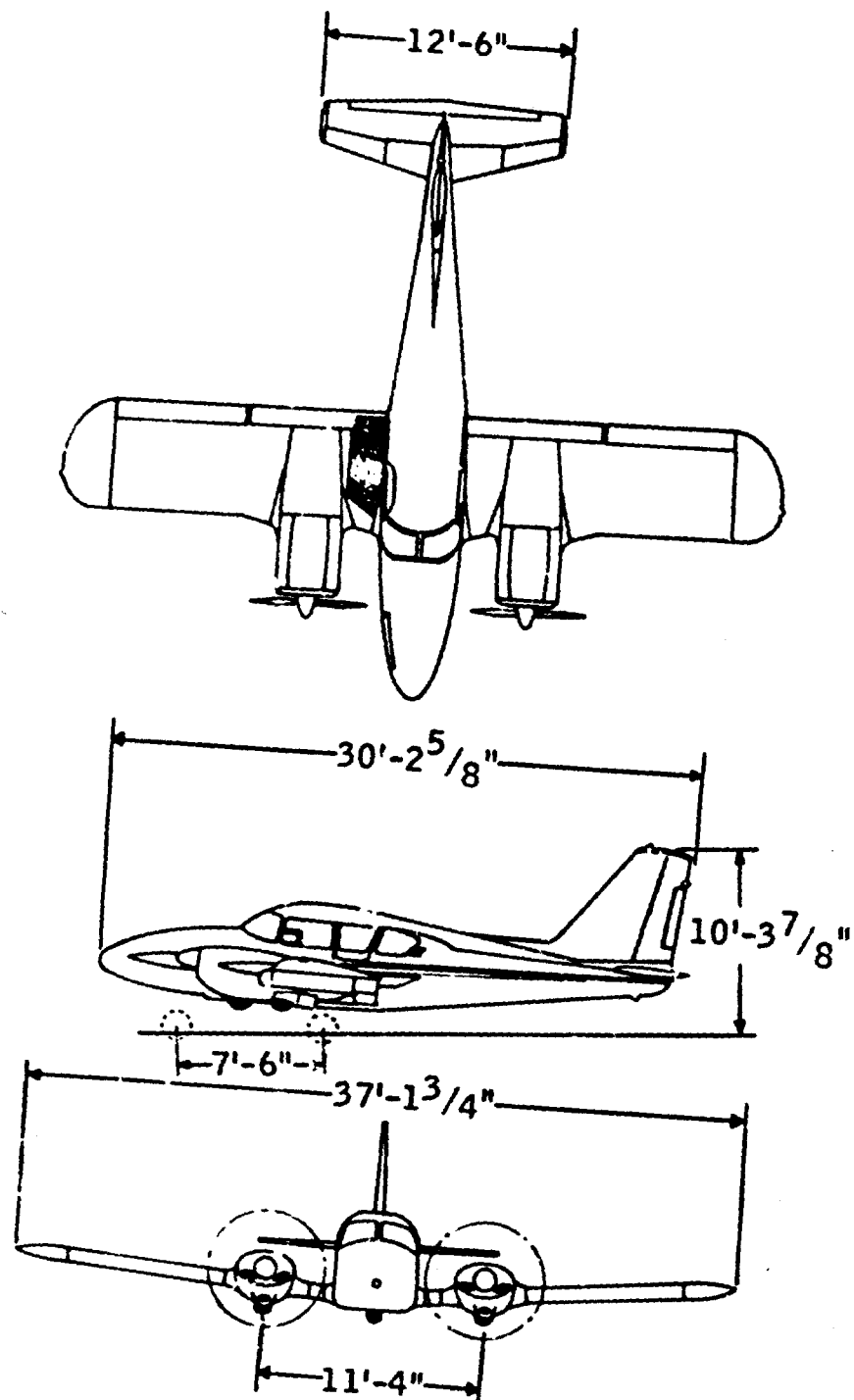
Figure 4.1-1. Typical Twin-Engine Aircraft "A."

4.1-51
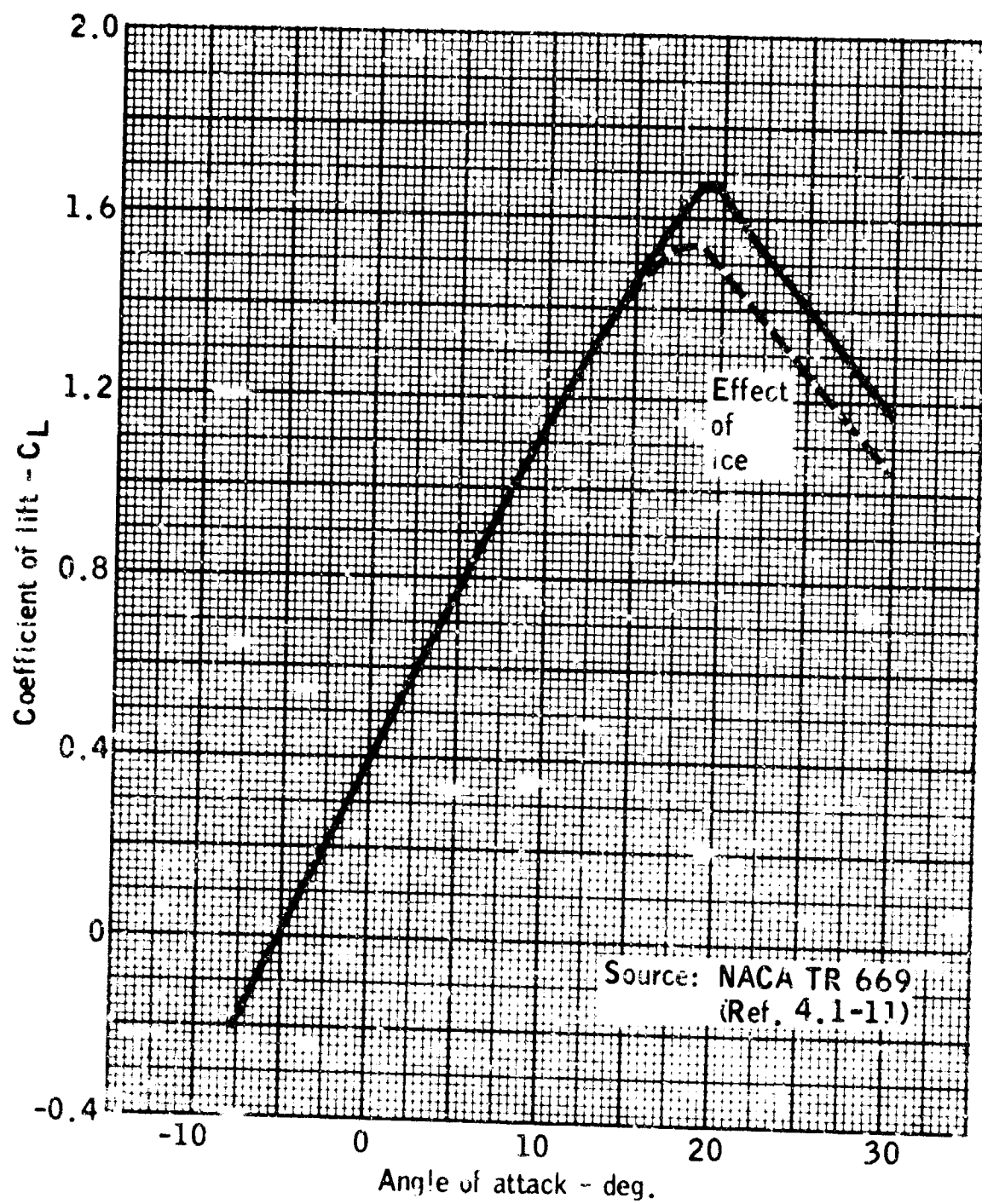
Figure 4.1-2.   USA 35-B Airfoil Lift Curve Showing Effect of Ice.
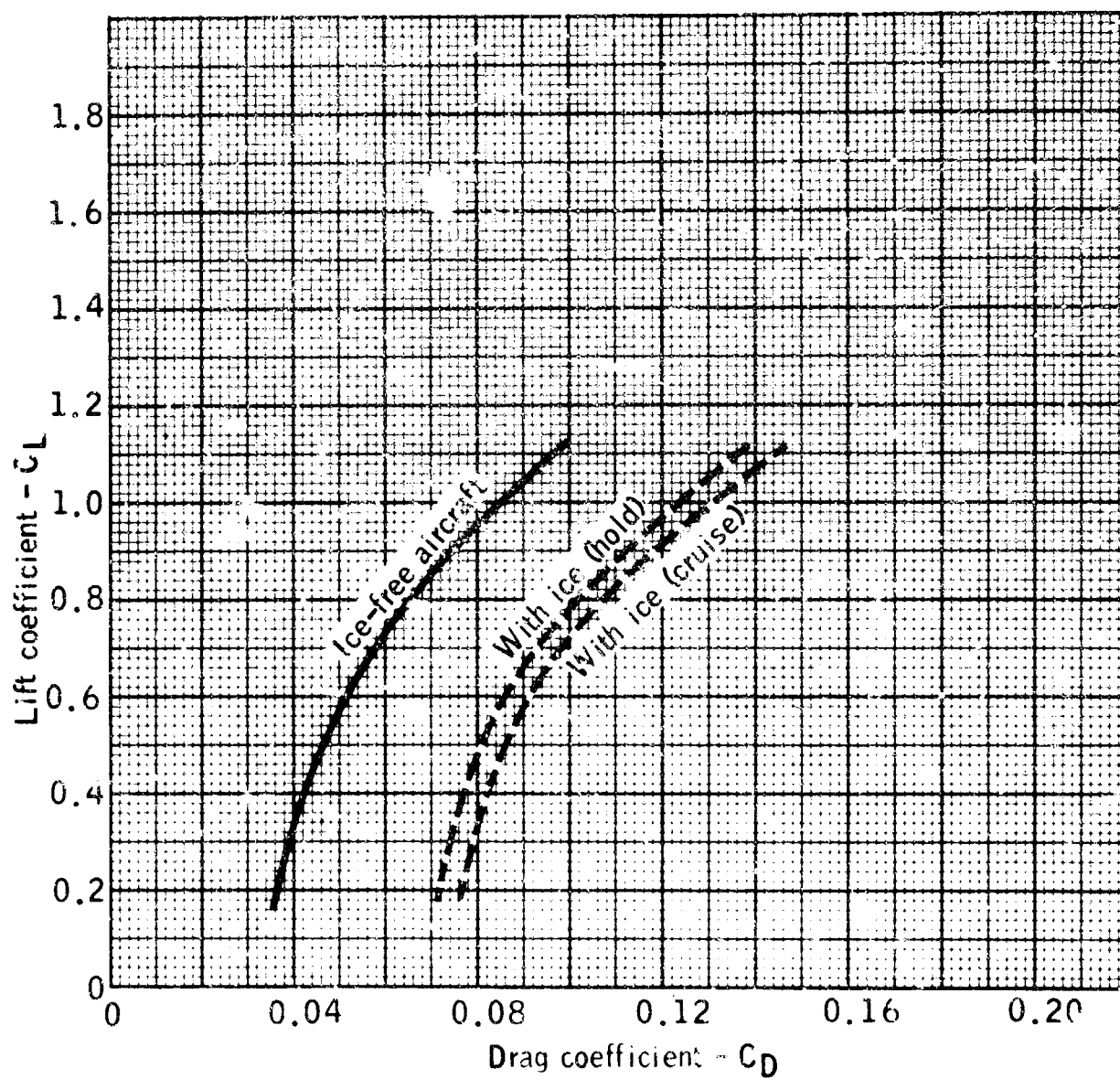
Figure 4.1-3. Drag Polars for Twin Engine Aircraft "A."
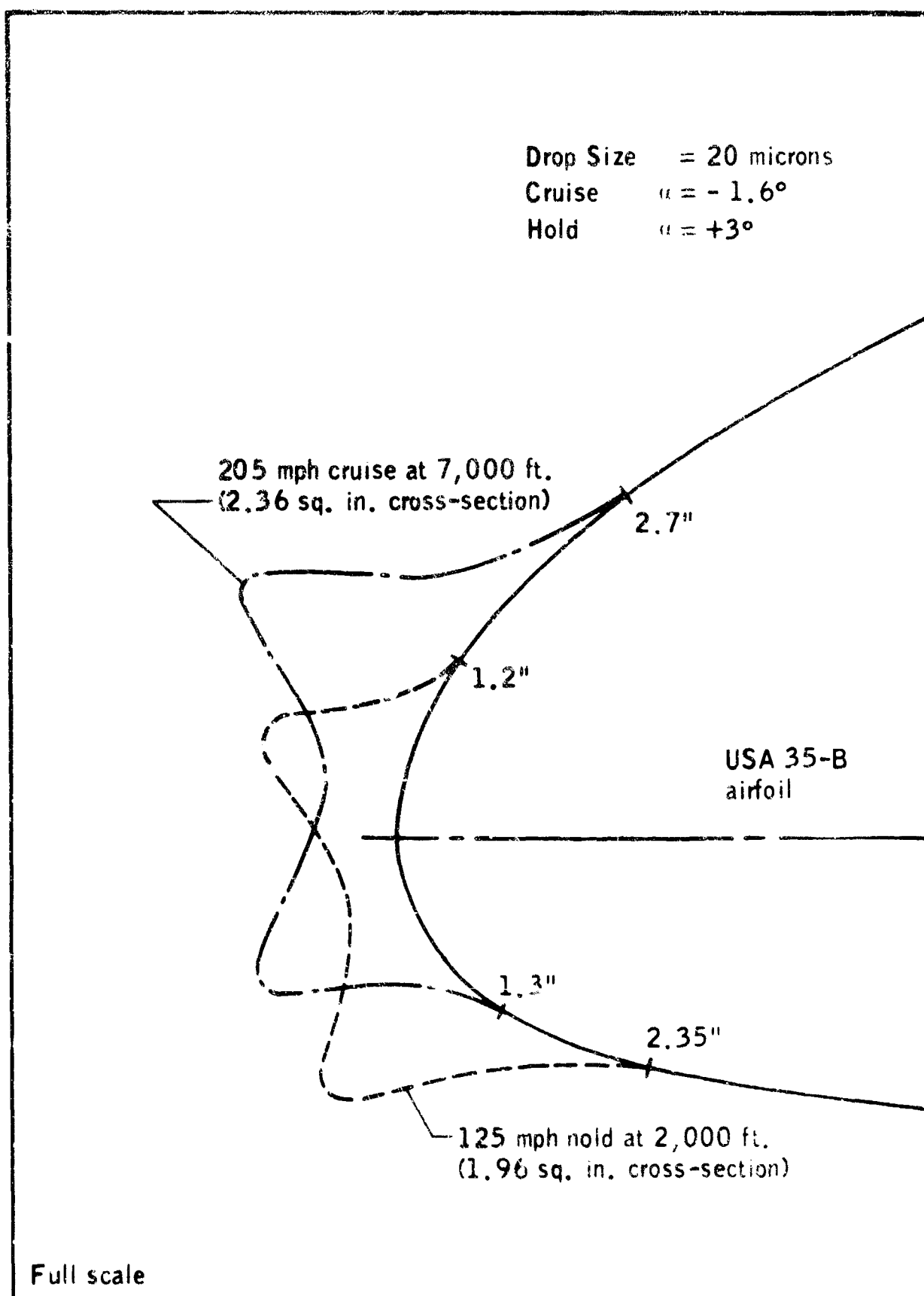
Figure 4.1-4.   Estimated Ice Shapes for Wing of Aircraft "A."
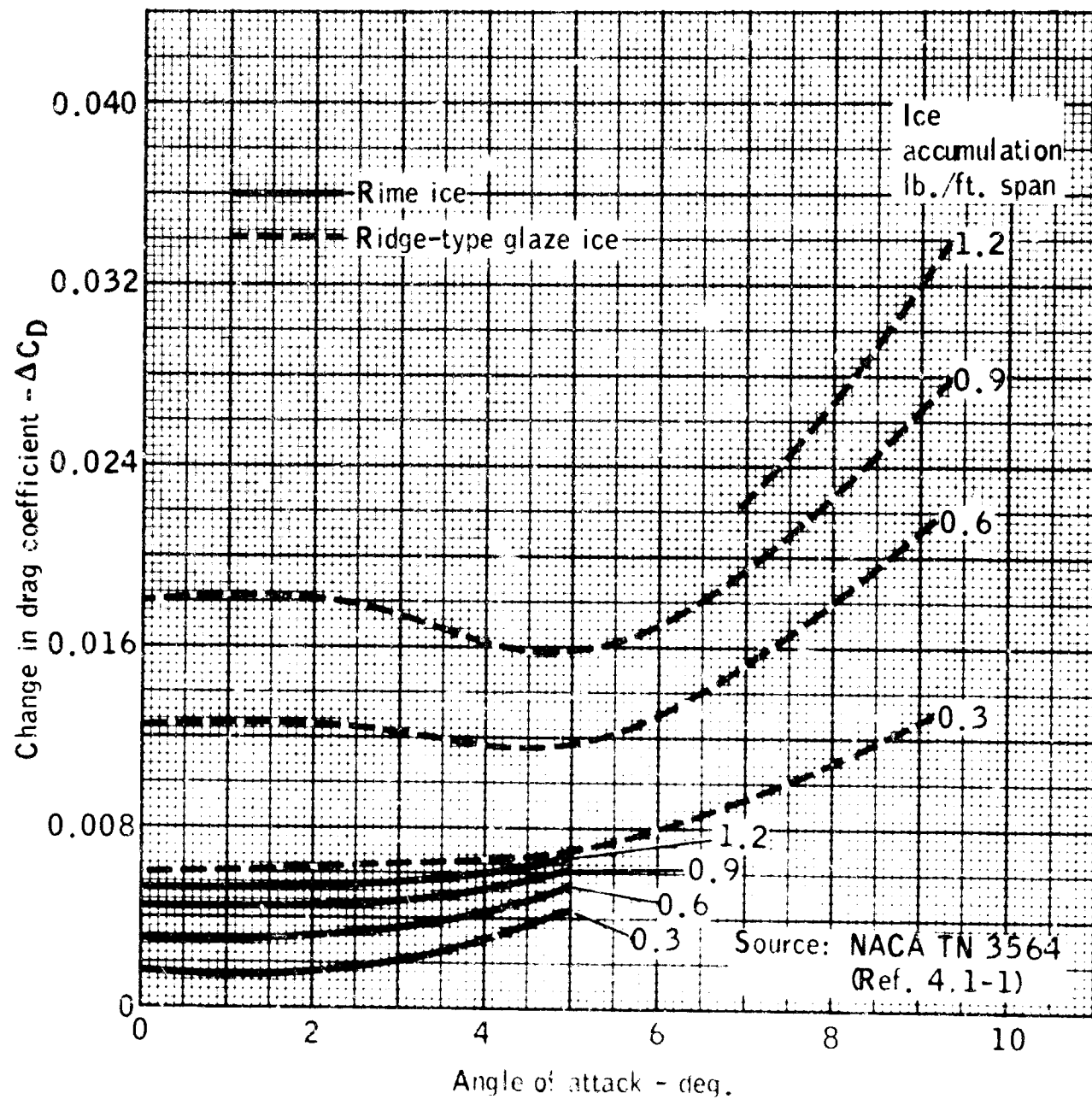
Figure 4.1-5.   Airfoil Section Drag Increase Versus Angle of Attack
for Rime Ice and Ridge-Type Glaze Ice.

4.1-55
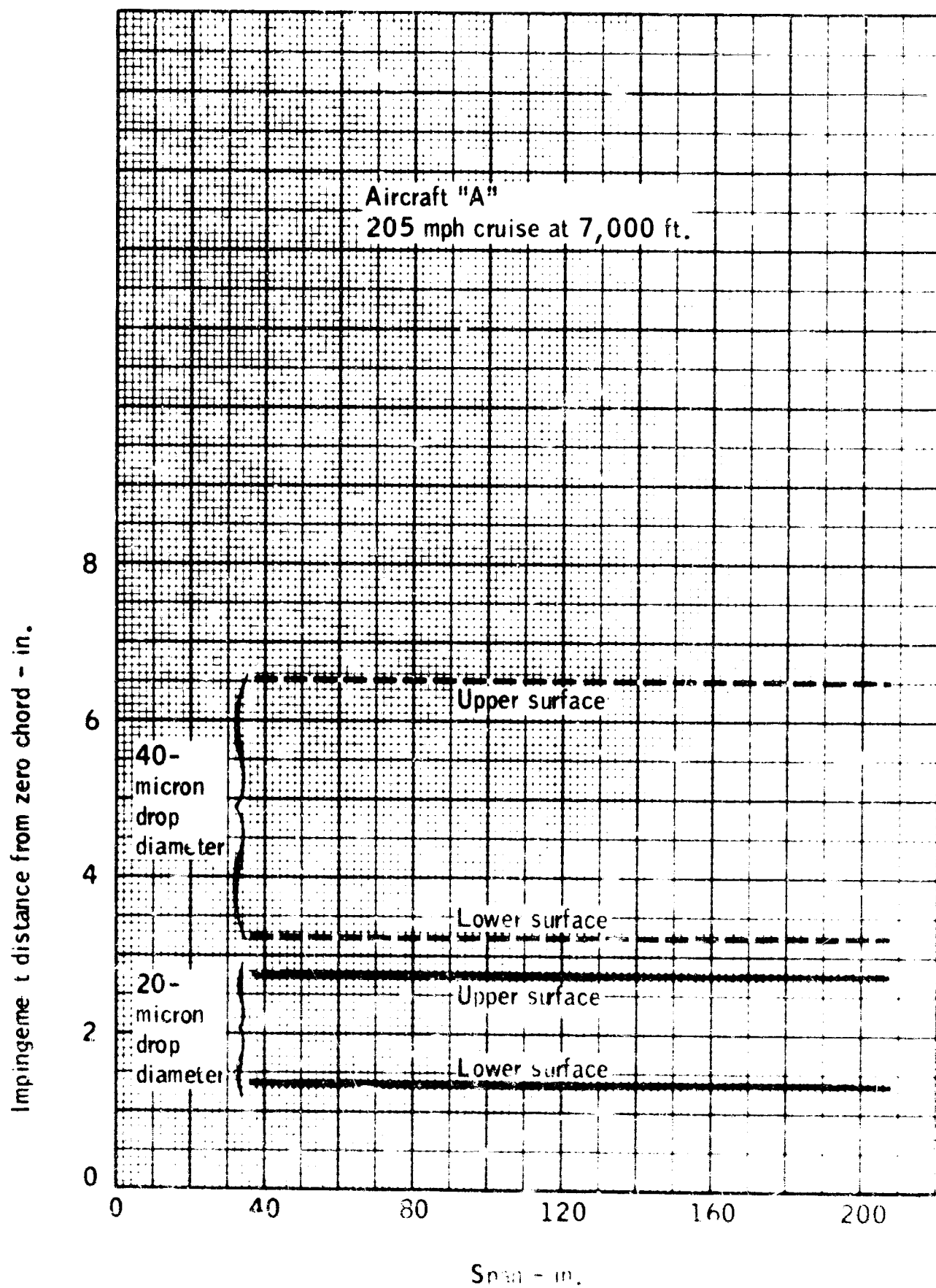
Figure 4.1-6. Wing Impingement Limits.
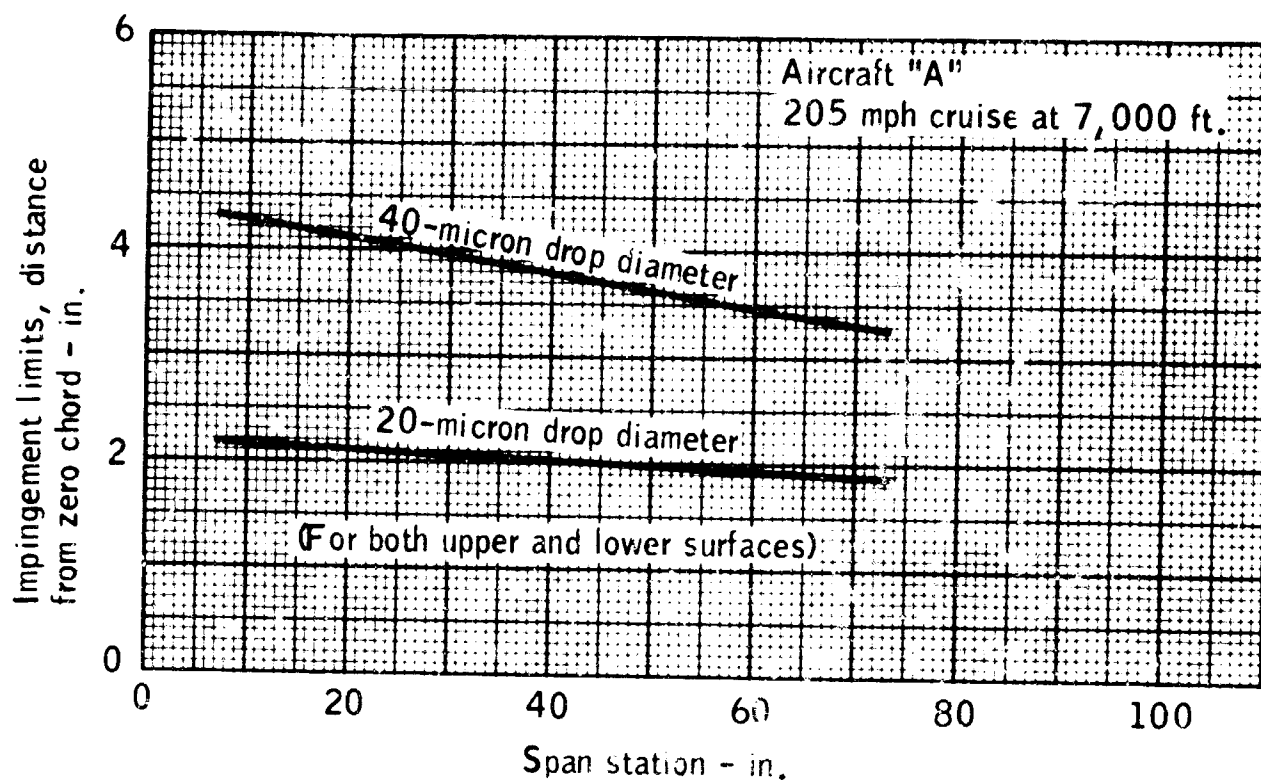
Figure 4.1-7. Horizontal Stabilizer Impingement Limits.
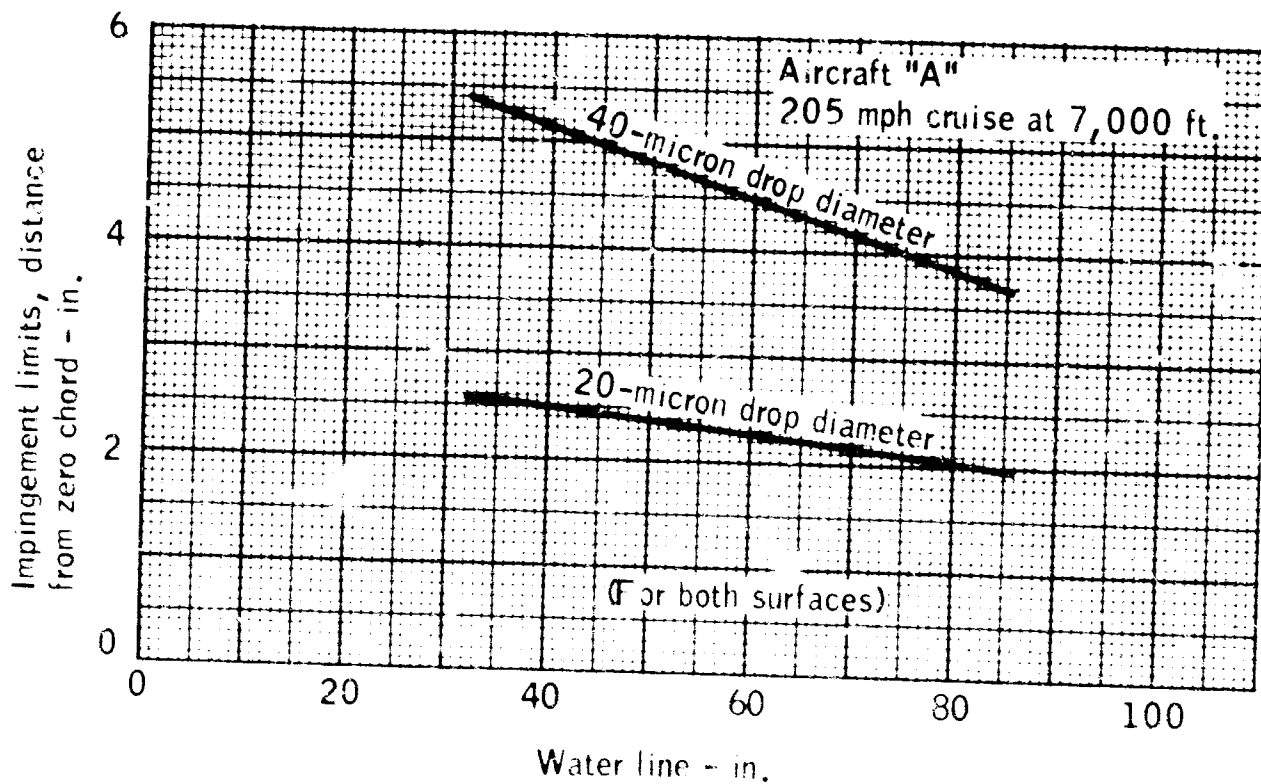
Figure 4.1-8. Vertical Fin Impingement Limits.
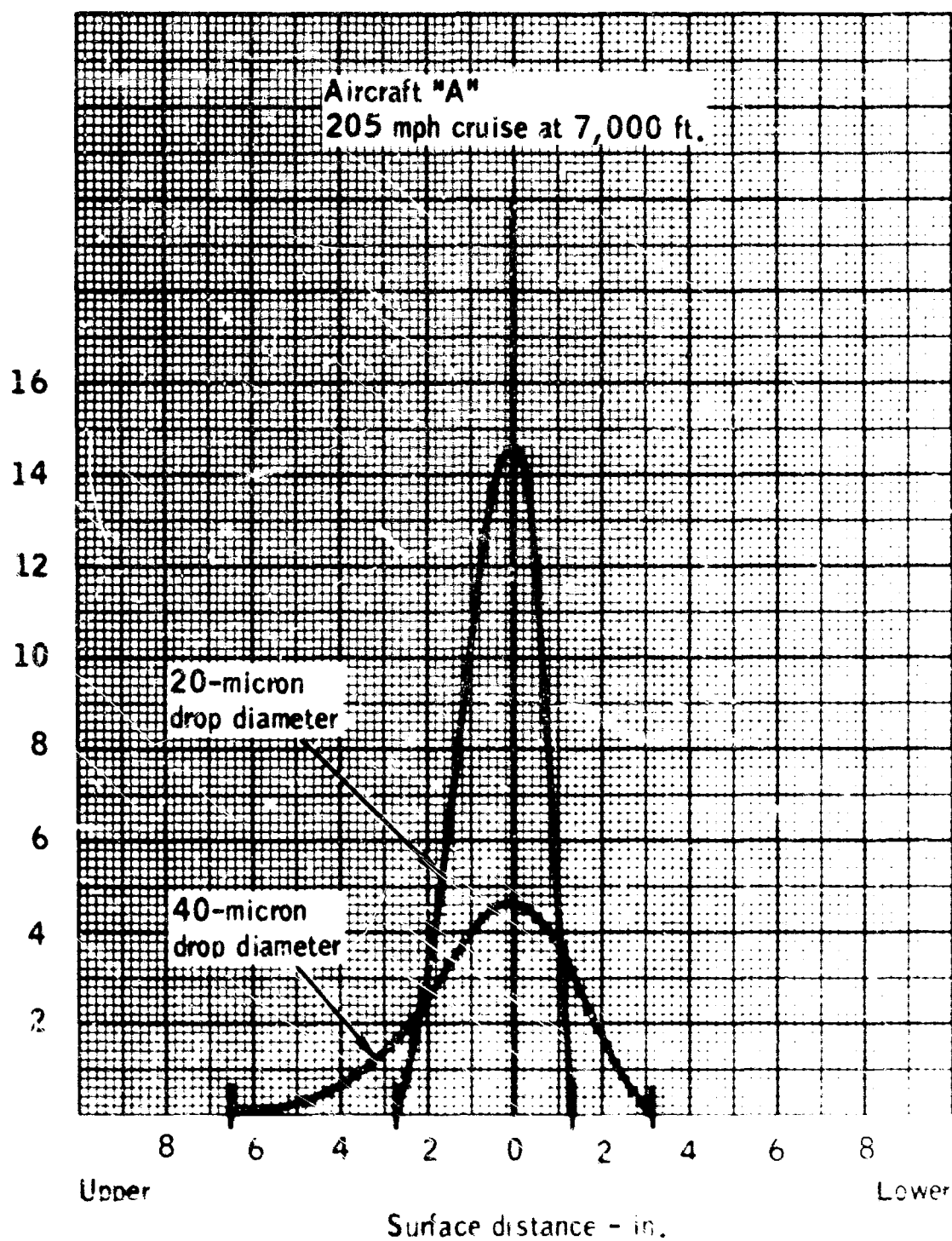
Figure 4.1-9. Wing Local Collection Rate.
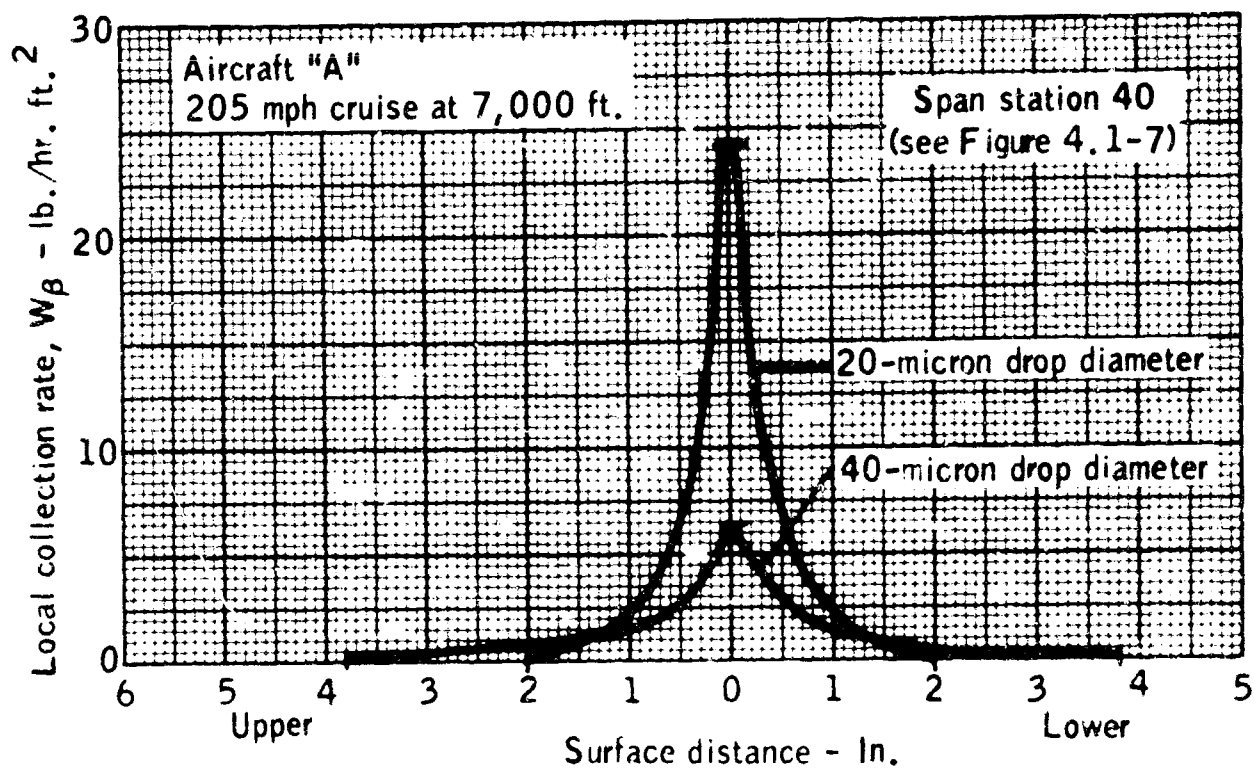
Figure 4.1-10. Horizontal Stabilizer Local Collection Rate.
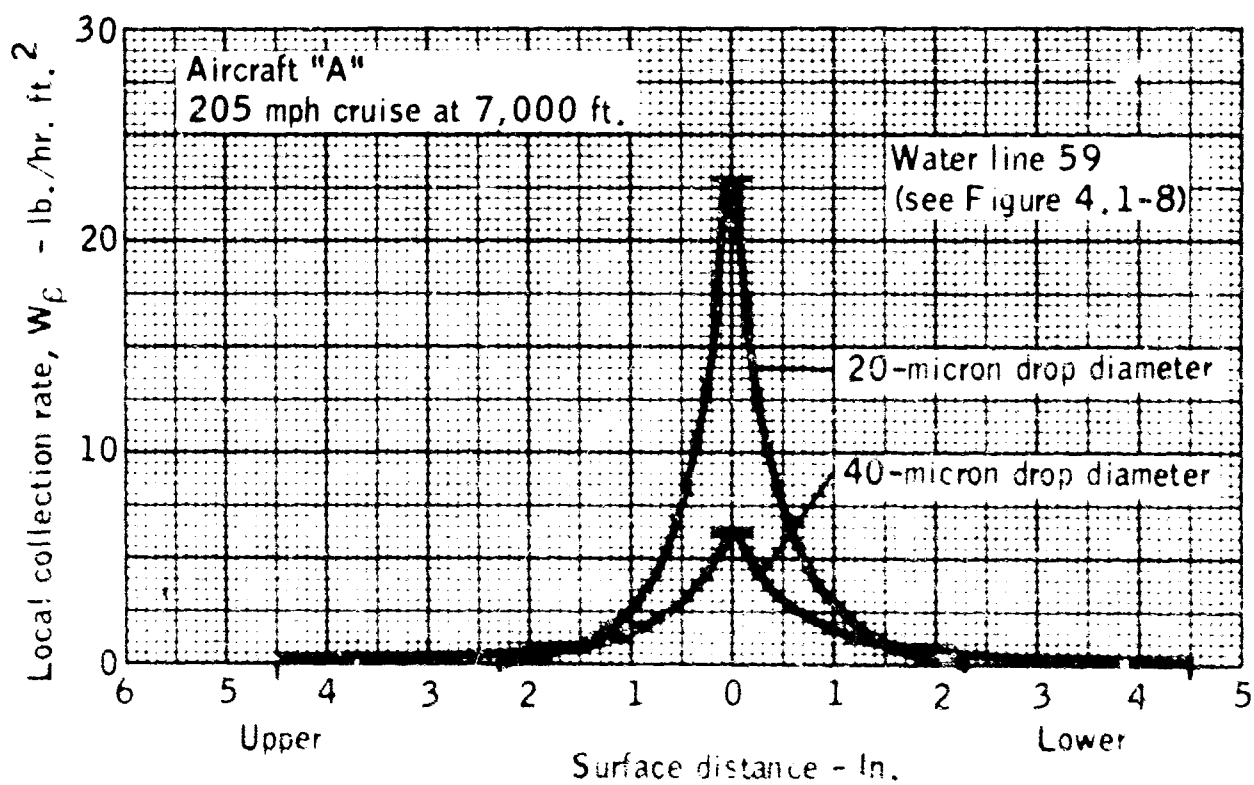
Figure 4.1-11. Vertical Fin Local Collection Rate.

5"

Vertical
fin

6'

5.5'   **5.5'**

5"   **5"**

Horizontal   stabilizer

Two separate de-icers

9'   **9'**

10"   **10"**

Wing   Wing
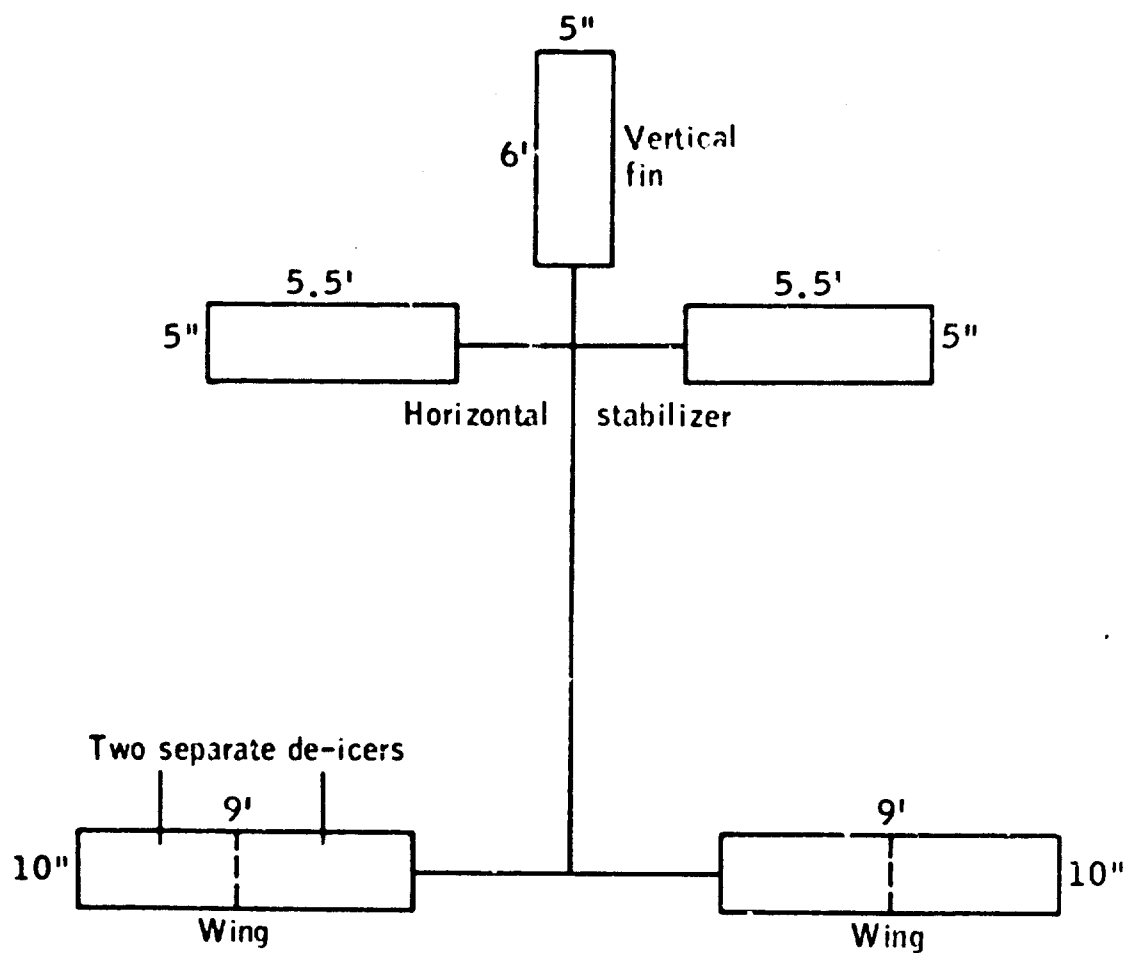
Total de-icer protected area   22.1 sq. ft.

Total area including tapered edge   28.0 sq. ft.

Figure 4.1-12.   Line Diagram of Pneumatic Boot De-Icing System for Wings
and Empennage of Aircraft "A."
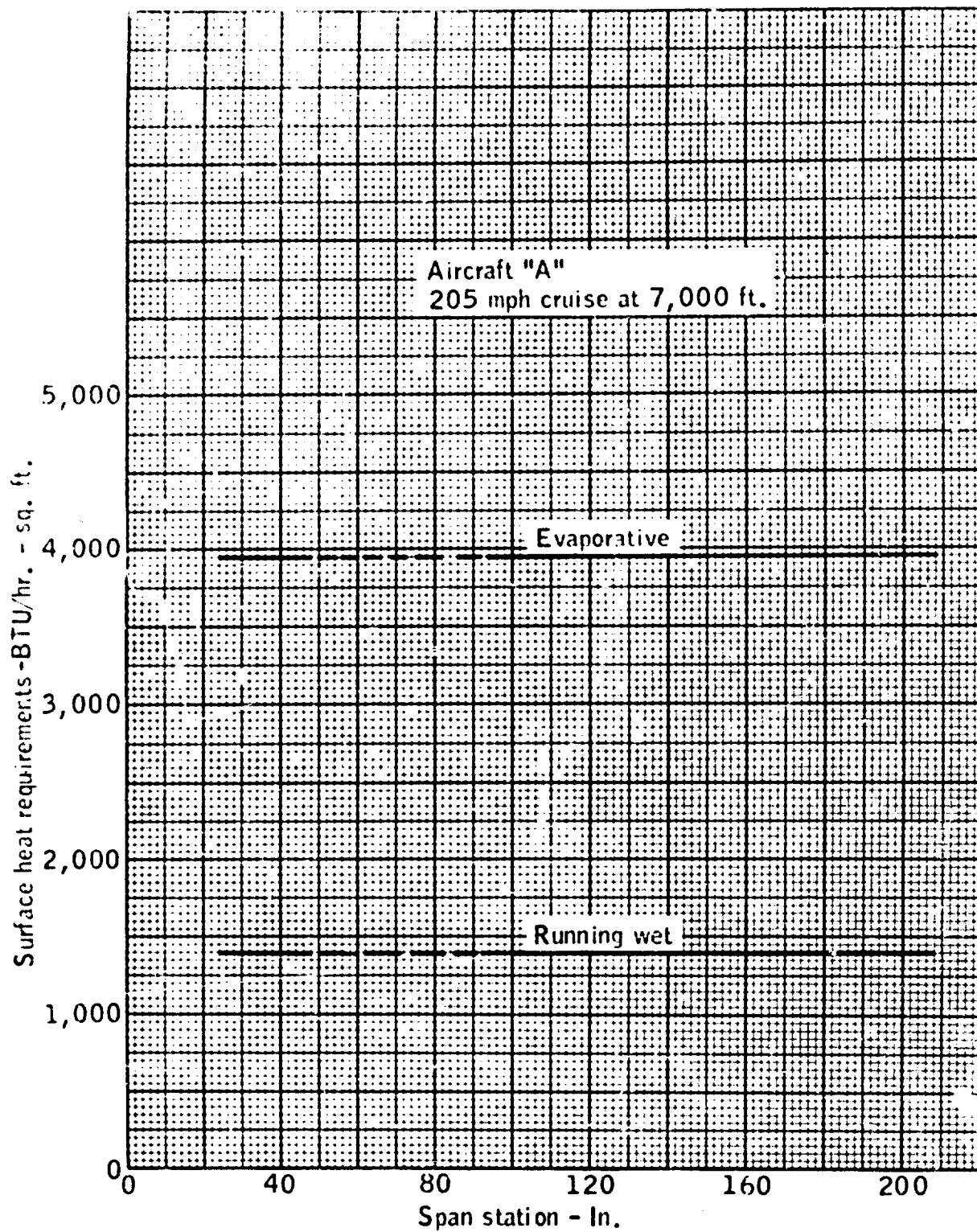
Figure 4.1-13.   Wing Surface Heat Requirements for Hot Gas Anti-Icing.
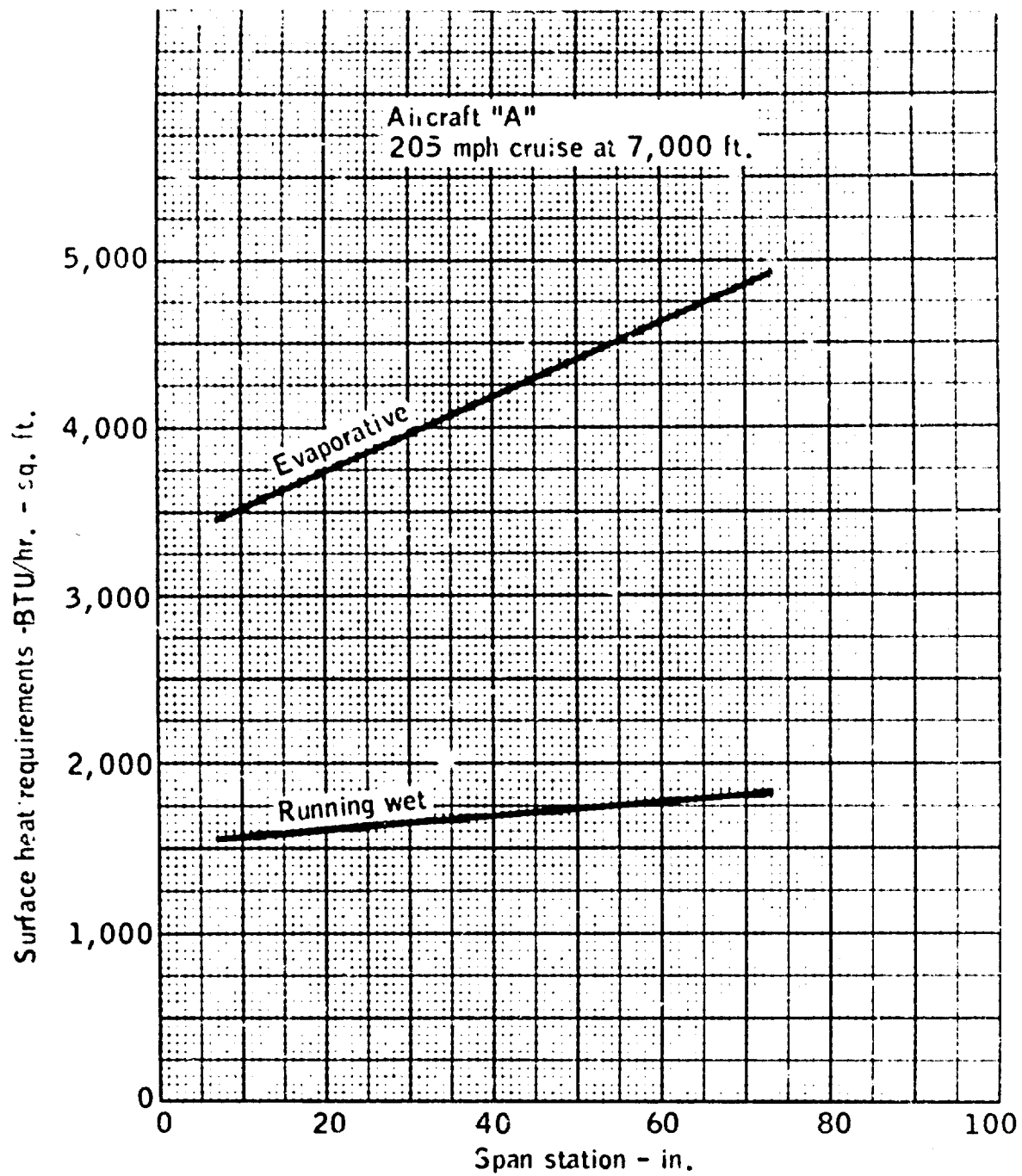
Figure 4.1-14.   Horizontal Stabilizer Surface Heat Requirements for Hot Gas Anti-Icing.
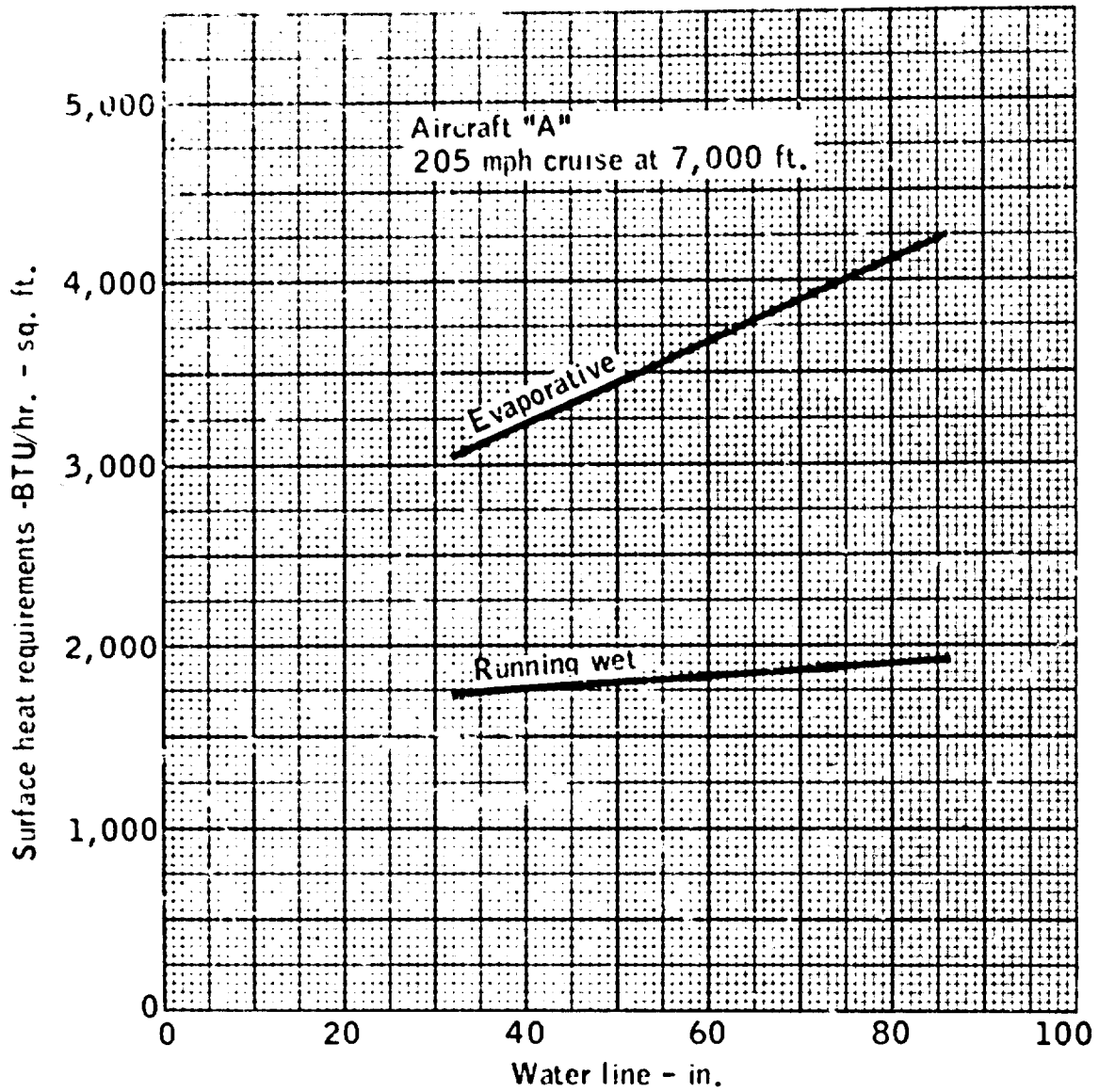
Figure 4.1-15. Vertical Fin Surface Heat Requirements for Hot Gas Anti-Icing.
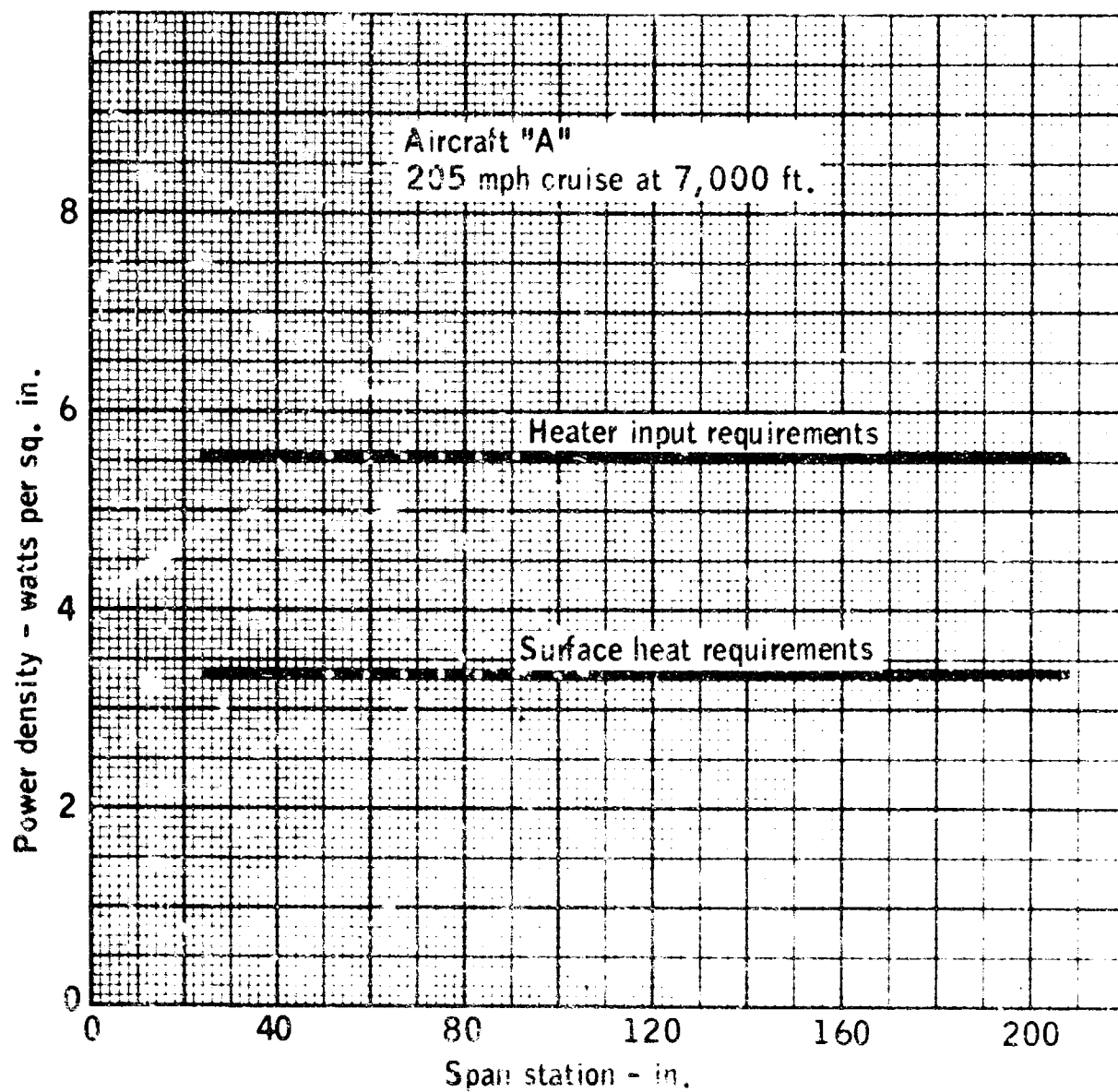
Figure 4.1-16. Parting Strip Power Requirements for Cyclic Electrical De-Icing of Wings.
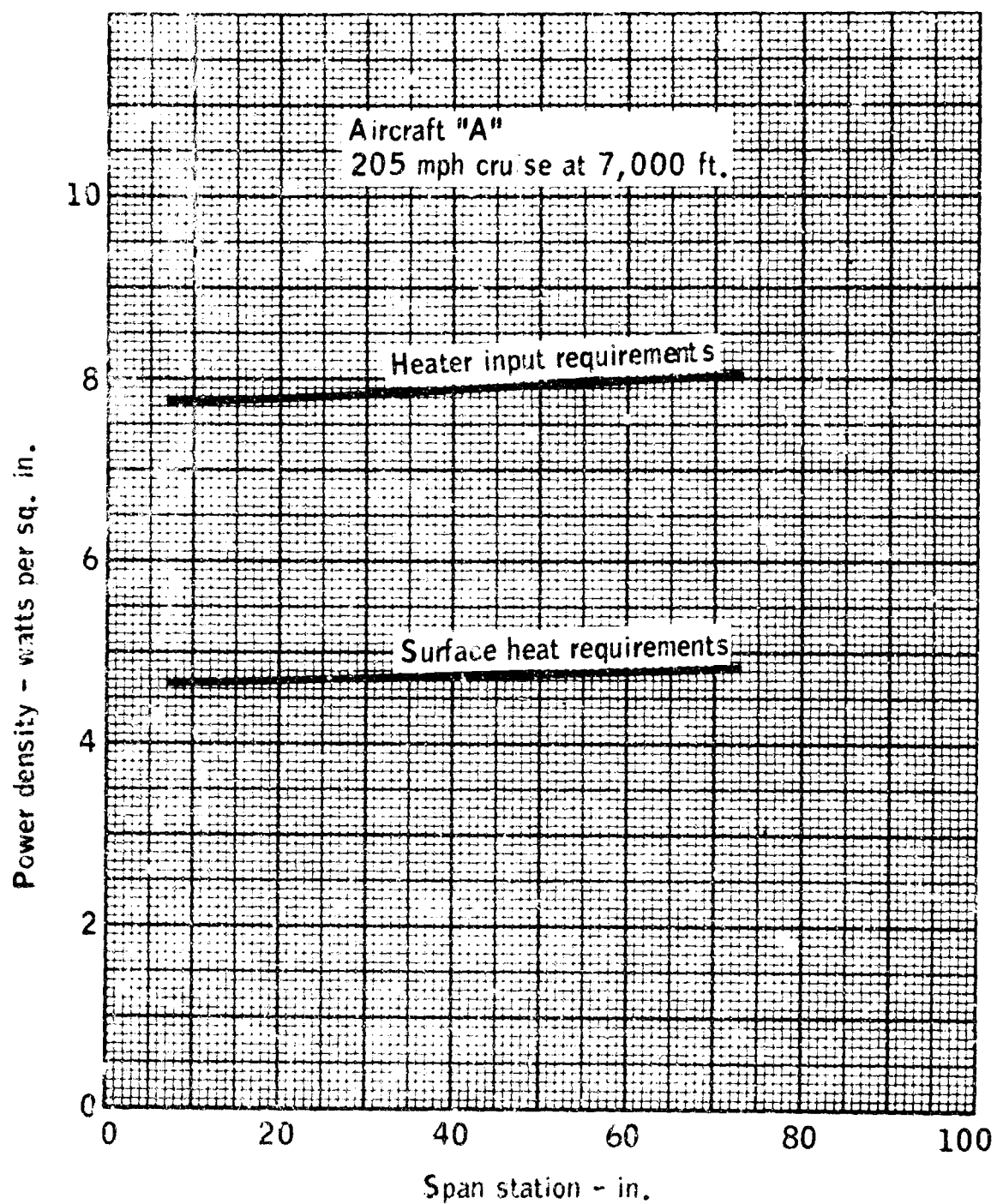
Figure 4.1-17. Parting Strip Power Requirements for Cyclic Electrical De-Icing of Horizontal Stabilizer.
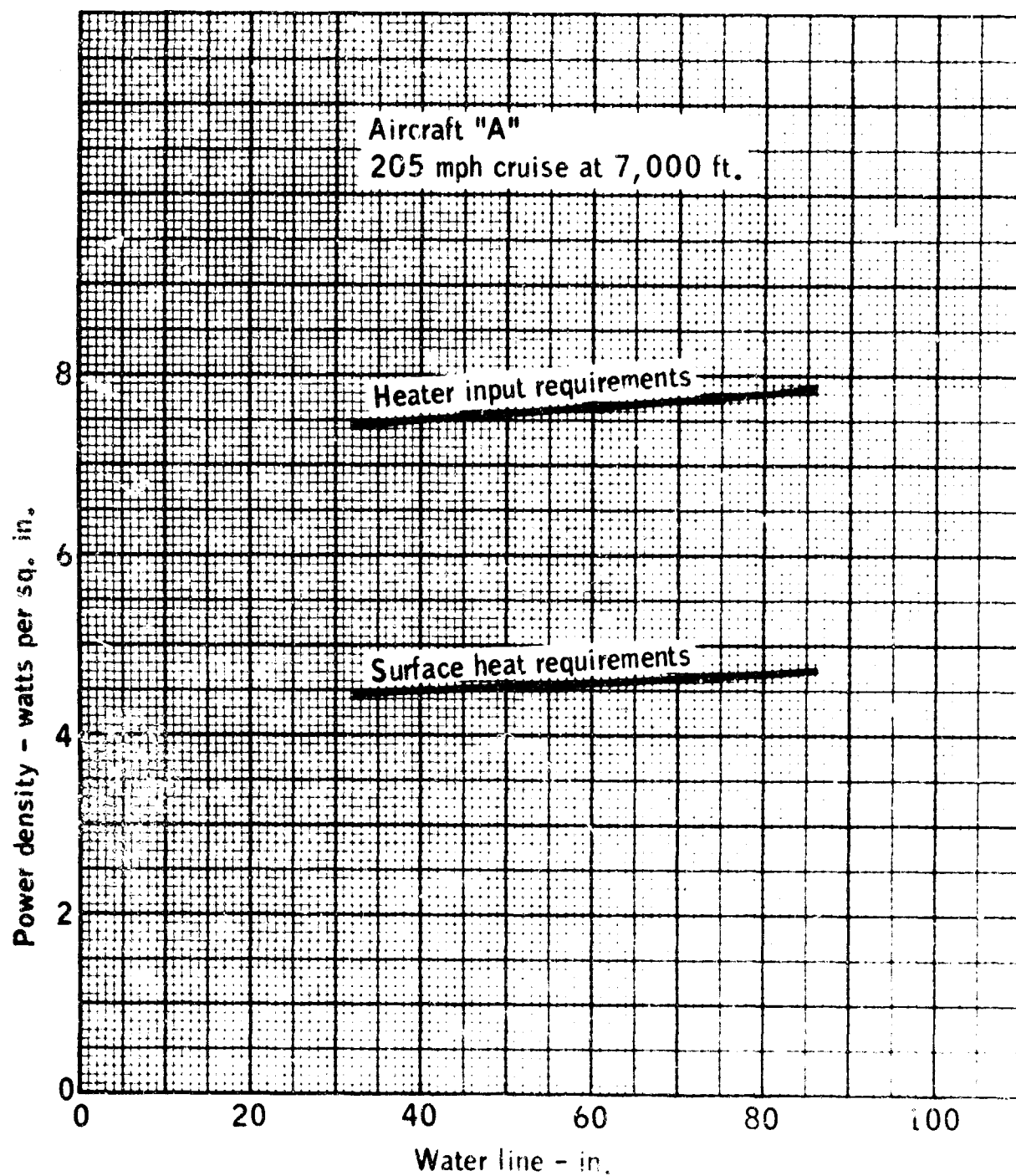
Figure 4.1-18. Parting Strip Power Requirements for Cyclic Electrical De-Icing of Vertical Fin.

5"

Vertical
fin

6'

2"

5'6"

5"

5'6"

5"

Horizontal stabilizer
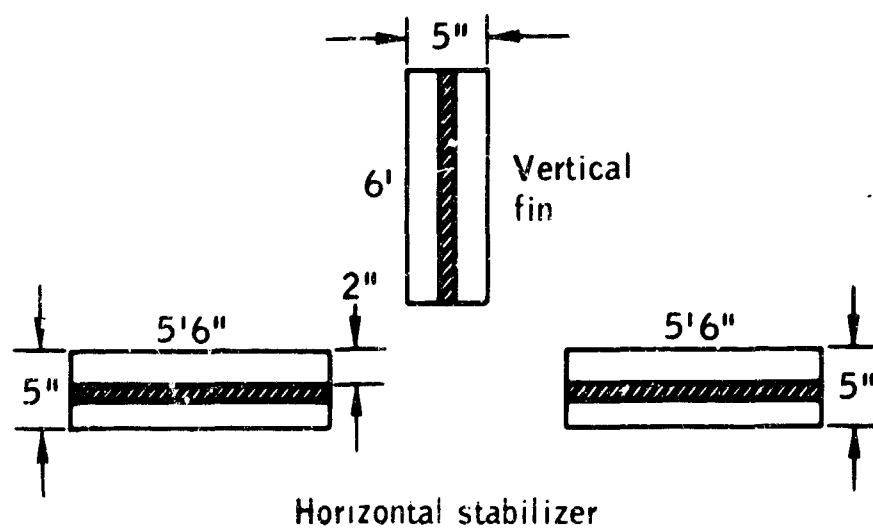
Spanwise
parting strips
are one inch wide

10"

5.5"

10"

8' 4"

8' 4"
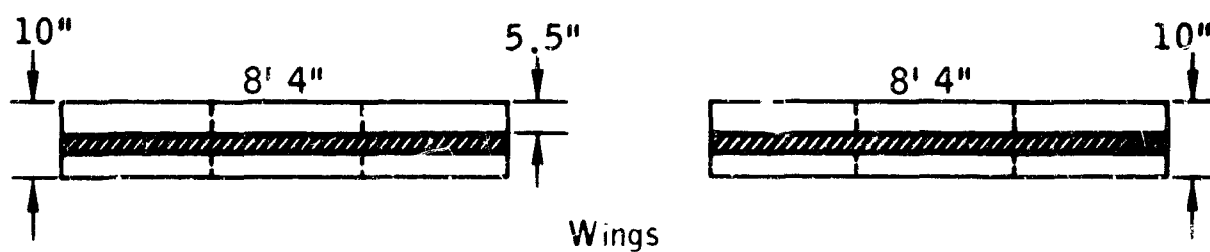
Wings

Wing heaters divided into
th.ee equal shedding areas

Figure 4.1-19.   Diagram of Cyclic Electrical De-Icing System for
Aircraft "A" Wings and Tail.
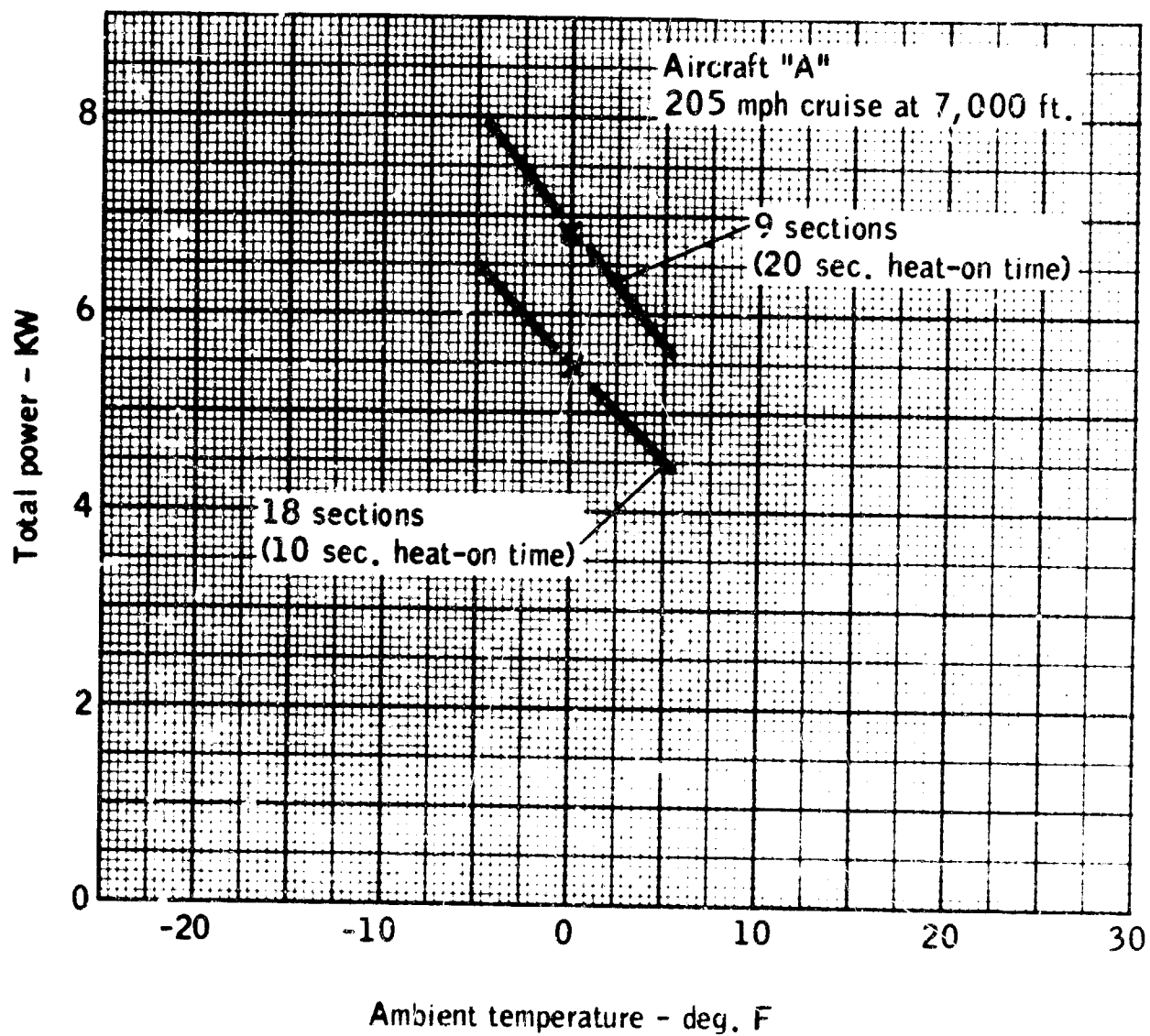
Figure 4.1-20.   Total Power Requirements for Cyclic Electrical
De-Icing of Wing and Tail.
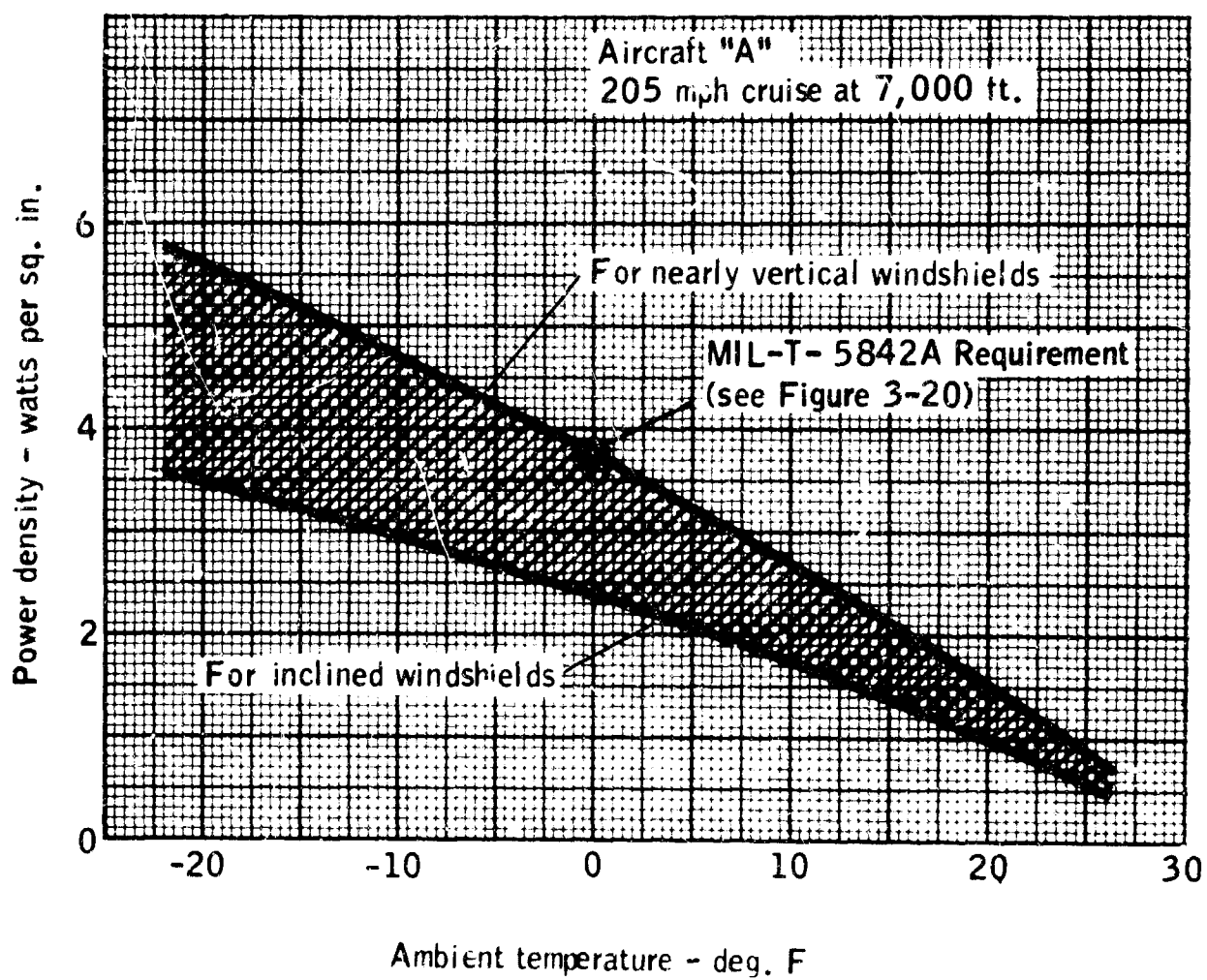
Figure 4.1-21.   Power Requirements for Electrical Protection of Windshield.
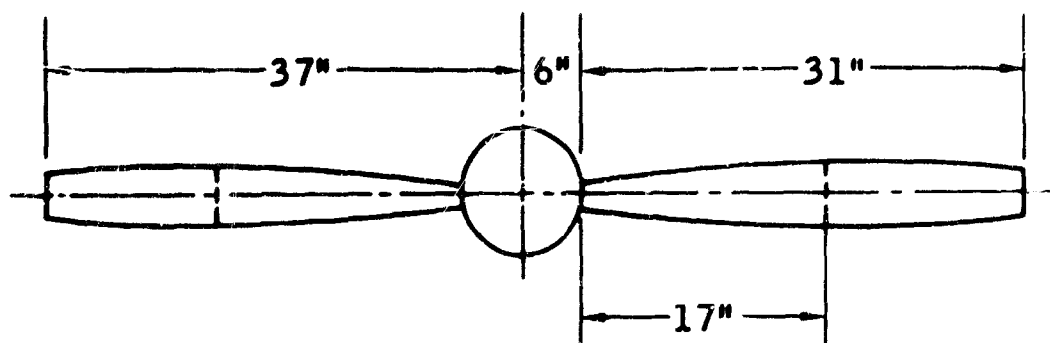
Extent of protection
(based on $t_0 = 17°F$)
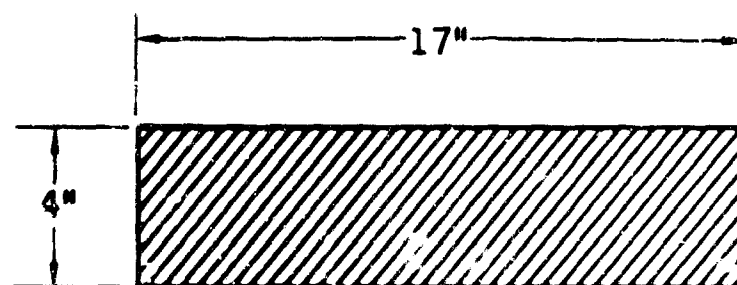
Flat layout of protected area

Figure 4.1-32. Propeller Protection Necessary for Aircraft "A."
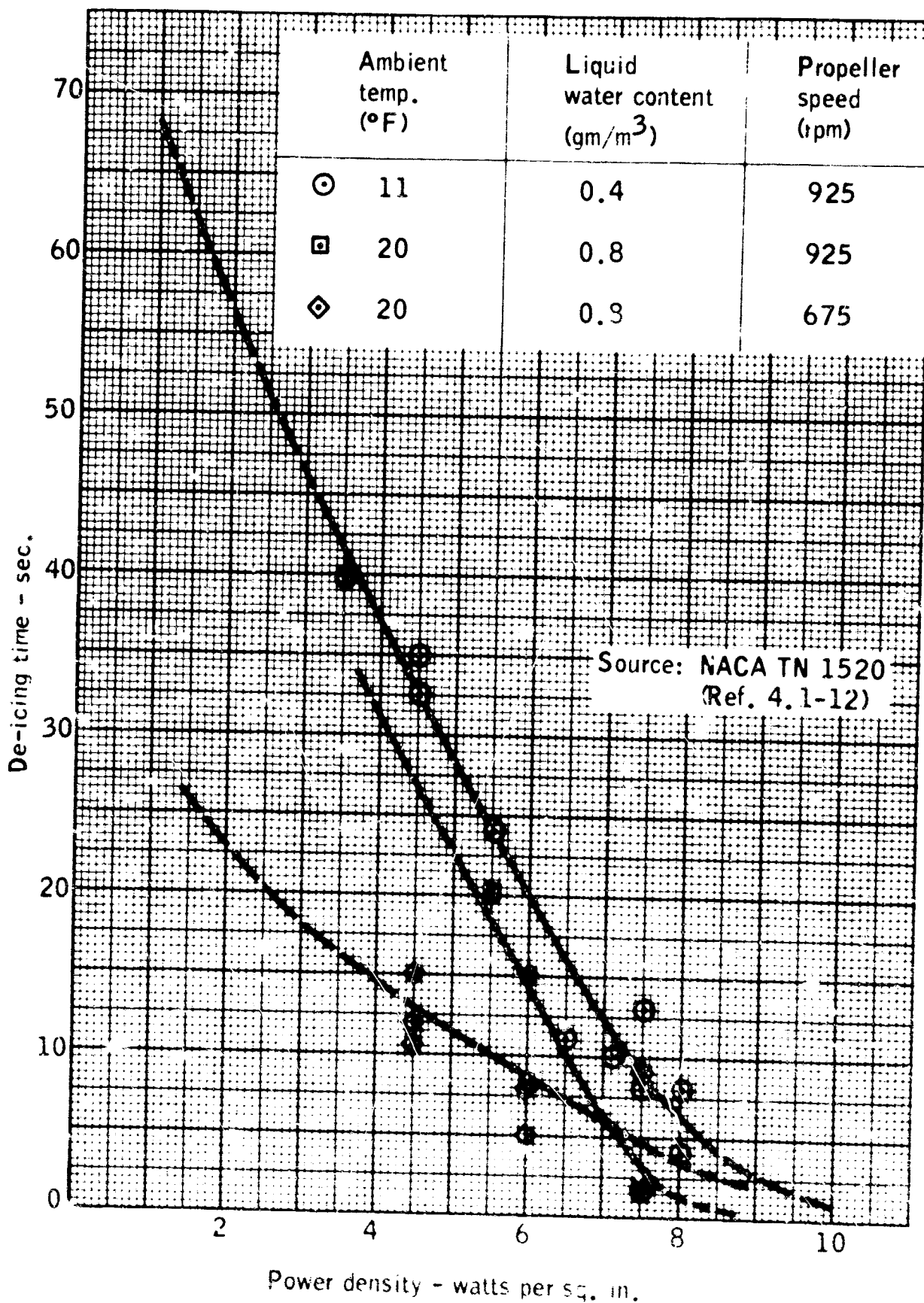
Figure 4.1-23.   Variation of De-Icing Time with Power Density at
Several Icing and Propeller Speed Conditions.
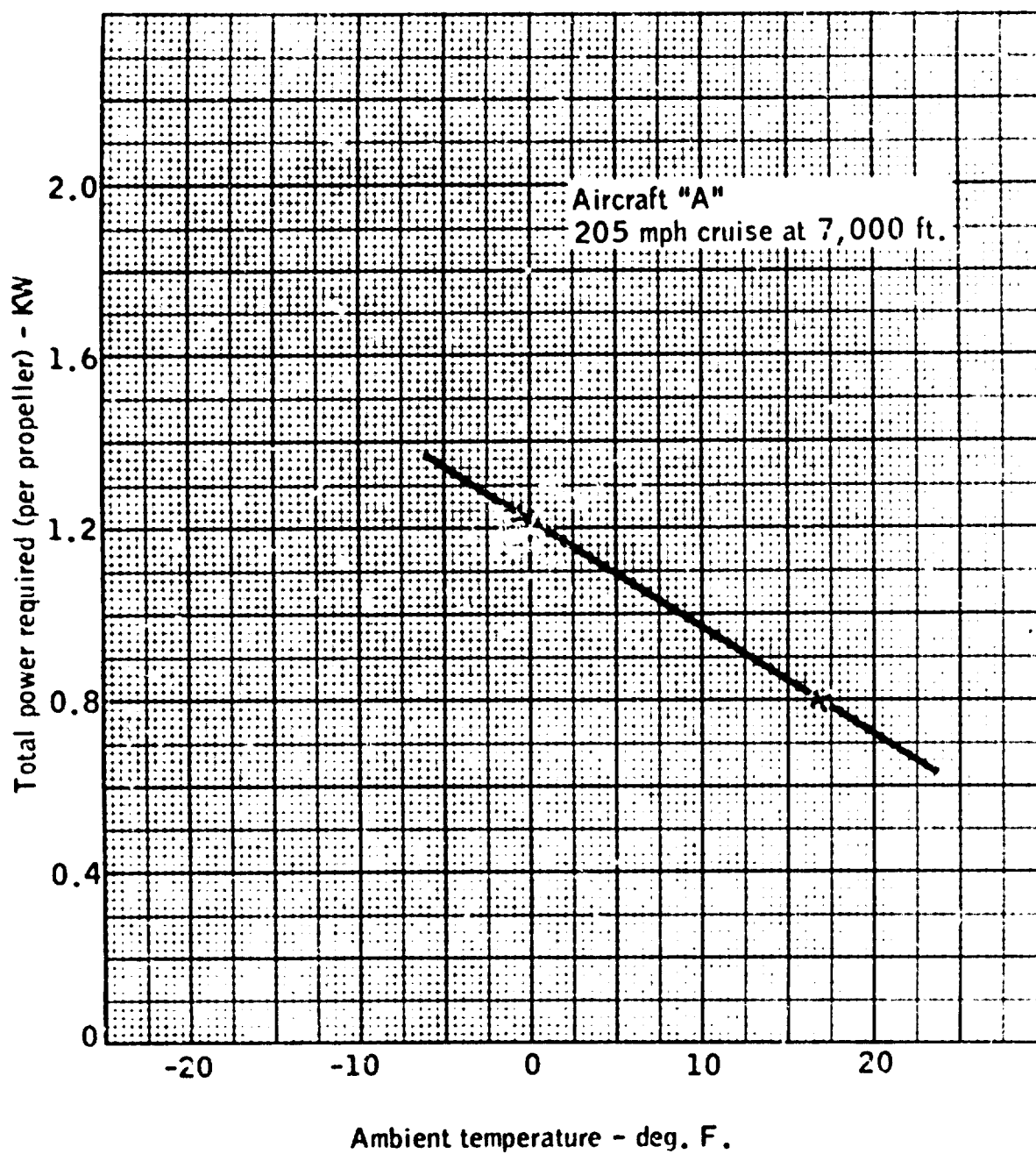
Figure 4.1-24. Variation of Propeller De-Icing Power Requirements with Ambient Temperature.
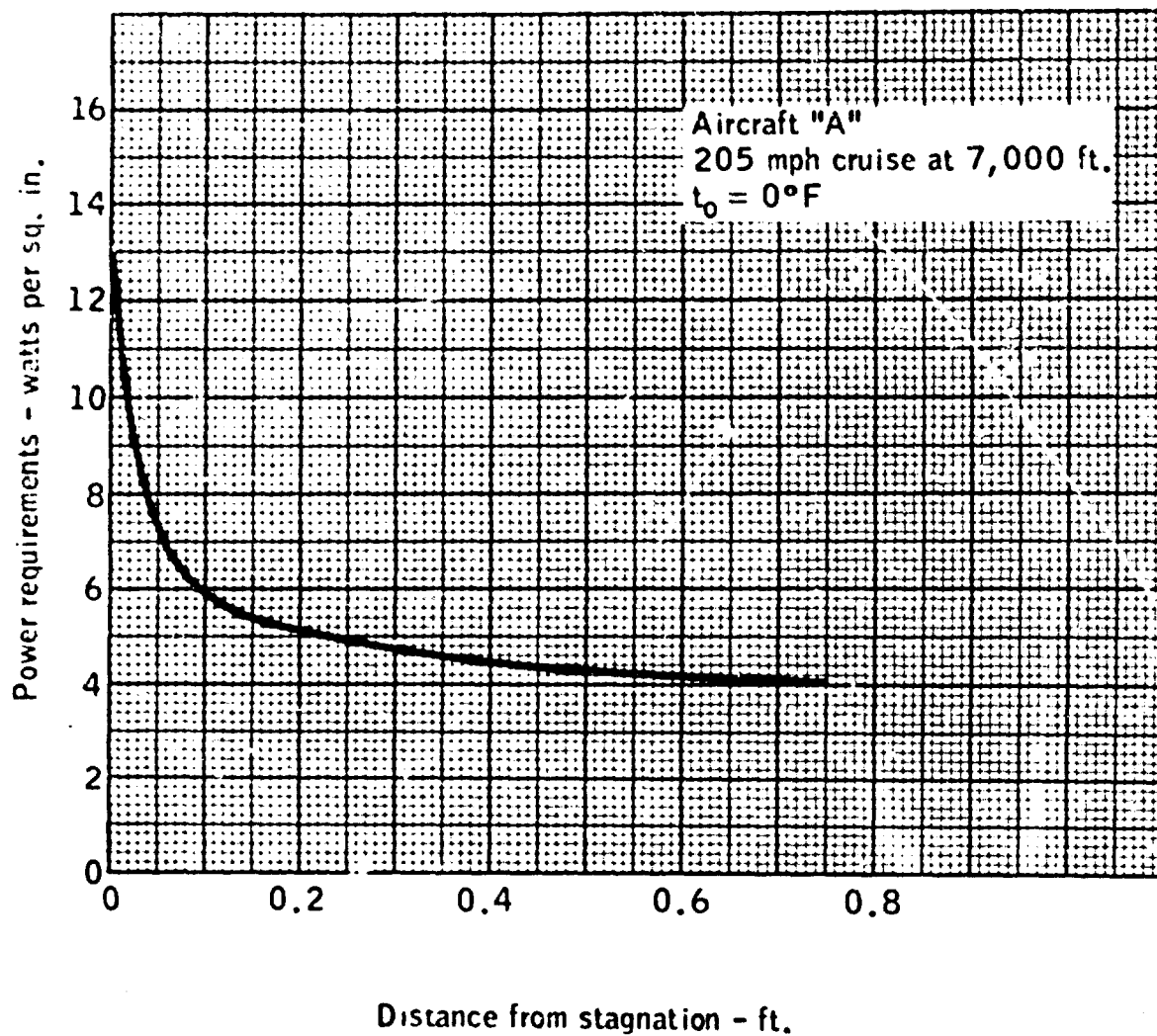
Figure 4.1-25. Pitot Tube Anti-Icing Power Requirements.

4.1-73
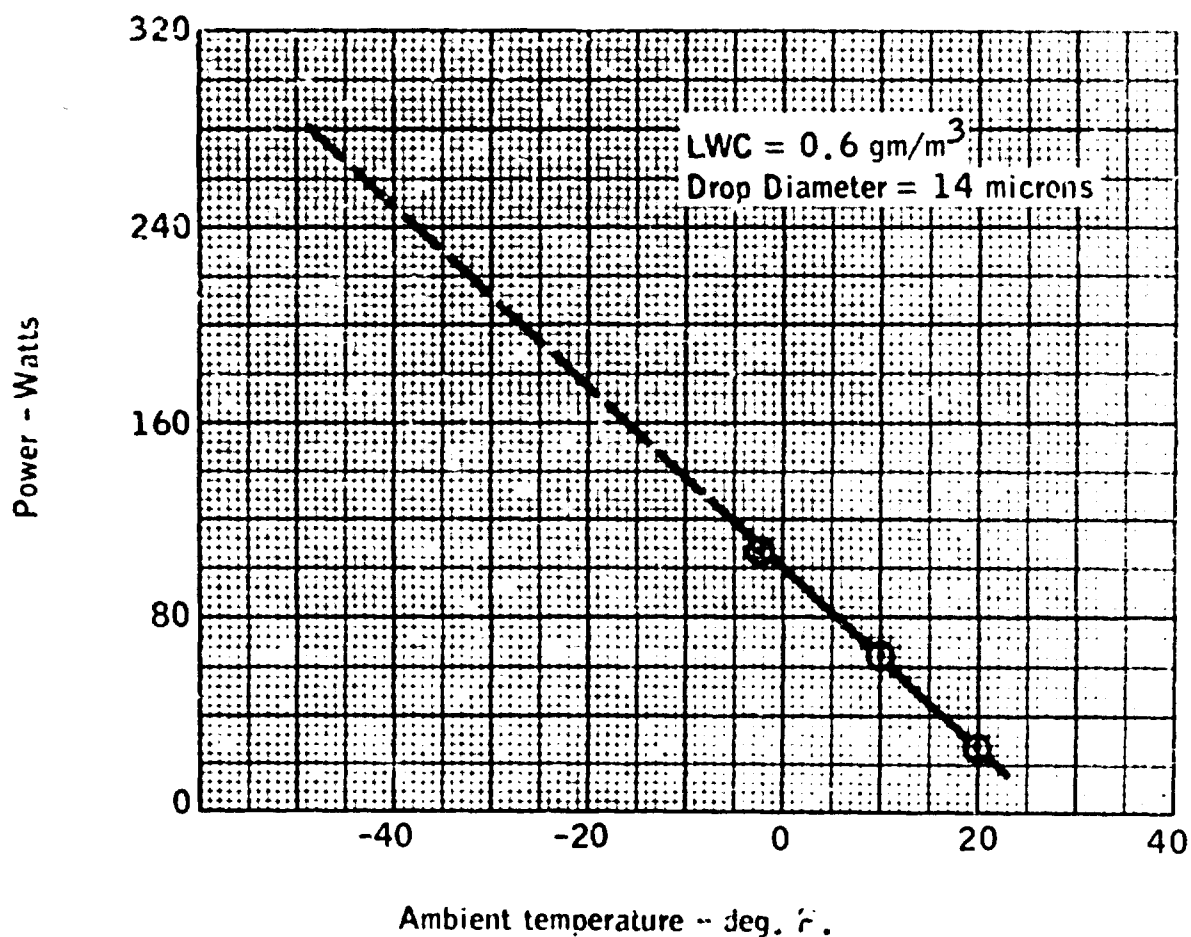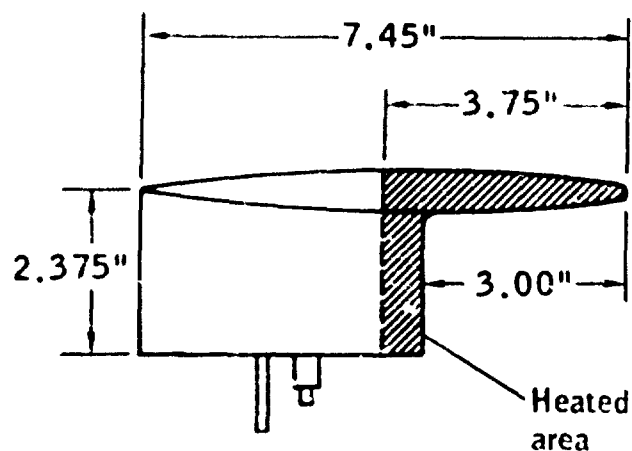
Figure 4.1-26. Total Anti-Icing Power Requirements for a Typical
Heated Pitot Tube.
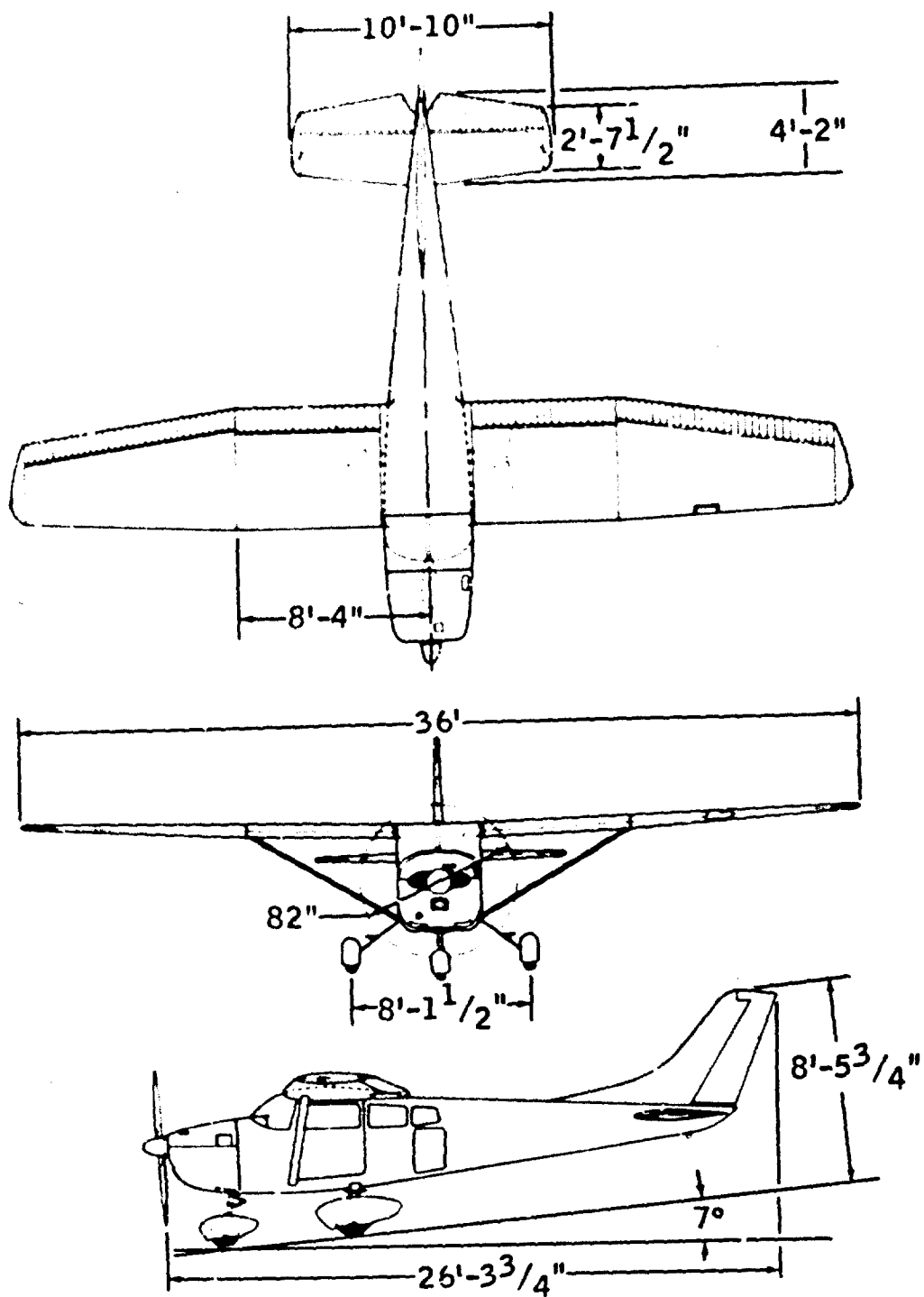
Figure 4.1-27.   Typical Single-Engine Aircraft "B."
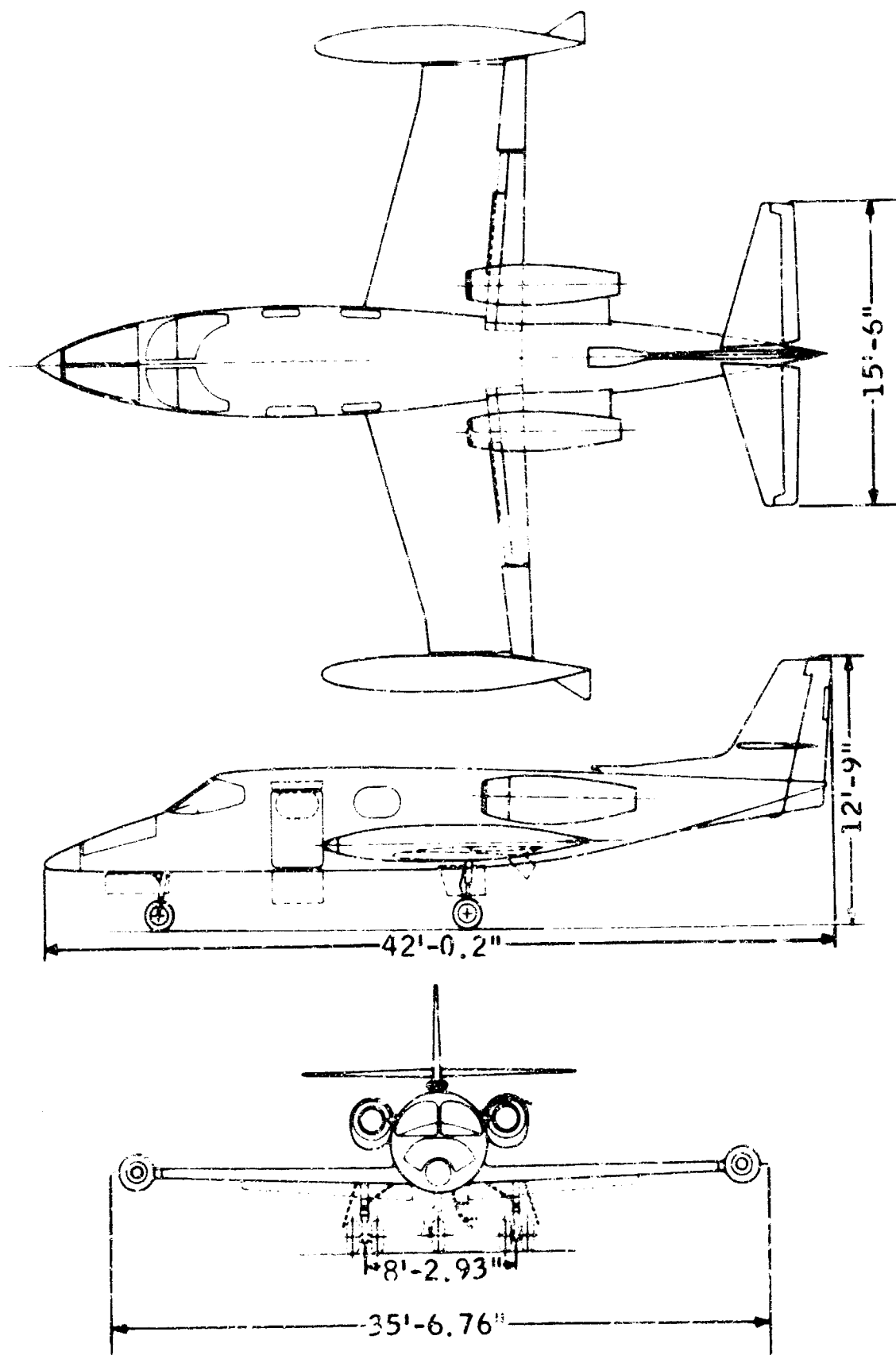
Figure 4.1-28. Typical Twin-Jet Aircraft "C."

Dimensions shown: 15'-5", 12'-9", 42'-0.2", 8'-2.93", 35'-6.76"

4.2 APPLICATION TO TRANSPORT AIRCRAFT (CAR-4b)

CONTENTS

LIST OF FIGURES

NOMENCLATURE

HR	Heating rate, BTU/hr.
Q	Heat input, BTU/hr.-ft. span
T_{ok}	Datum temperature, °F (see Section 2)
T_{gi}	Inlet gas temperature, °F
T_{∞}	Ambient temperature, °F
W_a	Gas flow rate, lb./hr.

4.2.1 SUMMARY

Various methods of providing ice protection to airframe components of a typical, four-engine CAR-4b transport are discussed in this section. Specific values of bleed air flow rates, electric power consumption, fluid flow rates, etc., are shown for the various systems; however, methods of calculation are not included. Section 3 contains data on specific methods of determining system requirements.

Methods illustrated for protection of wings and empennage are hot-gas anti-icing and de-icing, pneumatic boot de-icing, cyclic electric de-icing, and fluid anti-icing and de-icing. Typical anti-icing systems for wing leading edges having slats and/or Krueger flaps also are shown. Hot-gas and electrical anti-icing and electrical de-icing are illustrated for turbojet engine inlet lips. Hot-gas anti-icing of the turbojet engine compressor nose cone is described and electrical anti-icing requirements and configuration are shown for a typical windshield arrangement. Pneumatic boot de-icing and hot-gas anti-icing systems for radomes are presented. In addition, the effect of ice on radar transmission and the need for radome protection are discussed.

Methods are shown for protecting miscellaneous components, such as pitot tubes, antennas, and critical air inlets, while protection for propellers and spinners of a typical turboprop aircraft are described in a separate subsection.

4.2.2 INTRODUCTION

This section provides current data on ice protection systems that are adequate for use on CAR-4b transport aircraft. Practical aspects of the problem are emphasized and specific examples are shown for a particular turbo-engine aircraft (see Figure 4.2-1, Aircraft D).

This data is intended for use by design engineers in selecting ice protection systems for specific aircraft. For that reason, comments are included on advantages and disadvantages of the various systems.

4.2.3 ICE PROTECTION FOR WINGS AND EMPENNAGE

There are several methods of providing ice protection for the wings and empennage of a transport airplane. To illustrate these methods, a four-engine turbojet aircraft and its ice protection systems and the systems requirements are described. Alternate systems are discussed and several of the advantages and disadvantages of each are listed.

The general characteristics of the selected aircraft are illustrated in Figure 4.2-1. Its four engines are pod-mounted beneath the wings. Wing span is approximately 120 ft. with a fuselage length of 129 ft. The tail span and vertical fin length are 46 ft. and 21 ft. Maximum gross weight is approximately 185 000 lb.

4.2.3.1 HOT-GAS ANTI-ICING — The wing ice protection system selected for Aircraft D is hot-gas anti-icing. The source of the hot gas is the engine compressor bleed air. This high-pressure, high-temperature air is passed through regulating valves to each wing section (inboard, center, outboard) at 13 psig (see Figure 4.2-2). In each wing section are piccolo tubes which discharge the air to a plenum area at approximately 2 psig. The air then flows through narrow-gap, high-efficiency, chordwise gas passages which form the wing leading edge. The air then is discharged overboard through ports on the lower surface just forward of the front spar. This is illustrated in Figure 4.2-3. The chordwise gas passages are designed to use 85 to 90% of the initial heat energy before it is discharged. The extent of chordwise coverage needed depends on the airfoil, angle of attack, and other flight parameters, as well as on the effects of runback icing on airfoil drag.

To determine wing hot-gas ice protection system requirements, a specific design point is first established. For Aircraft D, the design point is the hold condition at 5,000-ft. altitude. This point was established by: (1) calculating the water catch and heat required for complete evaporation at several wing stations for various flight conditions, and (2) using the bleed air temperature schedule for these flight conditions to determine the condition requiring the

maximum flow. After the design point is established, the calculations proceed as demonstrated in Section 4.1.

Some illustrative values for these calculations (as applied to Aircraft D) taken at wing station 120 and at the "hold" design condition are:

a. Impingement limit upper surface $(S_U) = 1.32$ in. (20-micron droplet).

b. Impingement limit lower surface $(S_L) = 9.91$ in. (20-micron droplet).

c. Water catch rate $(W_M) = 10.1$ lb./hr.-ft. span.

(Note: The impingement limits for 40 micron drops are roughly twice the 20 micron limits; however, the bulk of the ice formation lies between the 20 micron limits).

The average heat-transfer coefficient at several wing stations is determined as described in Section 3. With these heat transfer coefficients, water catch rates, and design-point flight conditions, Figures 3.18a and 3.18b, are used to determine the heat requirements for evaporative anti-icing. A plot of these requirements vs. span station for the entire wing are presented in Figure 4.2-4.

This heat requirement must be converted into a hot-gas flow requirement to determine the feasibility of using hot gas. Information needed for calculating the hot-gas flow requirement is the piccolo tube gas temperature decay and the leading edge gas passage efficiency. Piccolo tube gas temperature decay and gas passage efficiency may be determined by analysis or laboratory tests. The required and actual hot air flow rates are presented vs. altitude in Figure 4.2-5. As shown, the system is marginal, but adequate, at the design point; performance is in excess of requirements for other flight conditions.

Typical weight flows for wing anti-ice protection at the design conditions are:

Inboard	0.76 lb./sec.
Center	0.82 lb./sec.
Outboard	0.66 lb./sec.
Total	2.24 lb./sec. (semi-span)
Grand Total	4.48 lb./sec. per airplane

4.2-6

Empennage hot-gas anti-icing may be accomplished using a system similar to the wing installation. On Aircraft D, this would require ducting the hot air from the engines the 90 ft. to the empennage through the pressurized fuselage. Aircraft with tail-mounted engines will not encounter these problems.

The design point for determining empennage anti-ice requirements will normally be the same as for the wings. The air-flow requirement calculations will have to account for the gas temperature losses experienced in the 90 ft. of ducting. An approximate value of the flow required to anti-ice the empennage at the design point is 2.0 lb./sec.

A system that reduces the bleed air temperature by recirculation of anti-icing discharge air also may be used for anti-icing protection. In this system, unregulated and uncooled bleed air is distributed to the wings (and empennage if hot-air protected) in lightweight stainless-steel ducts. At each protected section, a thermostatically regulated valve passes the air into piccolo tubes where the air is discharged through a large number of small ejector nozzles. The air from the ejectors mixes with plenum air, is cooled, and then passes through the leading edge double skin heat exchangers and back into the plenum. The excess air is dumped overboard. The thermostatic sensor used to control the regulating shutoff valves is located at the heat exchanger exit and controls the air to a discharge temperature of approximately 135° F. (Refer to Figure 3.16.) This system achieves high efficiency with relatively deep gas passages (1/8 to 3/16 inch) as opposed to the single pass system which requires narrow passages (in the order of 0.040 to 0.050 inch).

On turbojet engines having two compressor stages, bleed air from the low pressure compressor may also be used for anti-ice protection. To provide anti-ice protection with this lower energy air, larger mass flows will be required. To handle these larger mass flows, the ducting and leading edge heat exchanger passages will have to be larger, but in other ways the system will be generally the same as the high-pressure bleed air anti-ice protection system. Difficulty

may be experienced in obtaining adequate protection at low rpm, as in descent and hold. Use of low pressure bleed may allow elimination of pressure and/or temperature regulation, thus simplifying the system. Installed weights may be lower, because the reduced temperature and pressure will allow lighter ducting; this is offset to a large extent by the requirement for handling larger mass flows (for a given thermal requirement). Mixing systems may also be used that employ low pressure bleed air augmented by high pressure bleed as required to achieve a desired air temperature.

Hot-gas anti-icing systems have several advantages and disadvantages. On the positive side are: the availability of ice protection energy in the form of hot air at a reasonable penalty to aircraft performance; the ducting used for ice protection is often used for other purposes, thereby saving weight; the systems for hot-gas distribution are relatively simple, trouble-free and easy to maintain; and being anti-icing systems there is no decrement in aircraft performance because of ice accretion. The disadvantage of a hot-gas anti-ice protection system is primarily the potential high cost of installation which results from designing and fabricating the leading edge heat exchangers. The system must be designed into the original leading edge and cannot be "added on" at a later date without major retrofit problems.

There may be occasions when an anti-icing system may be used in a de-icing manner. Prior to such usage, the system should be tested for de-icing adequacy. Methods of testing are discussed in Section 6.

4.2.3.2 HOT-GAS DE-ICING — In a turbine-engine-powered aircraft, particularly one with turboprops, adequate bleed air may not be available under all flight conditions. In this case, a solution is the use of a hot-gas de-icing system. This system has been used on at least one military turboprop transport and one long-range commercial transport. Unfortunately, the advantage of reduced bleed-air requirements (typically 1/4 to 1/6 of anti-icing requirements) is offset by increased system complexity and, in some cases, increased weight. Thus.

the choice of hot-gas de-icing vs. hot-gas anti-icing must be made with due regard to all factors of a particular aircraft.

Actual analysis and design of a hot-gas de-icing system would require a major engineering effort because of the degree to which the system is integrated into the airplane. A full description of the results of such an effort is beyond the scope of this report. Instead, a de-icing system that would suit the needs of Aircraft D is described, with comments and suggestions on adaptations that would be required for other types of transport aircraft.

The operating principles of a hot-gas de-icing system are identical to those for a cyclic electric de-icing system. Only the mode of energy supply is changed. A sketch of a simple system for a swept-wing transport is shown in Figure 4.2-6. The bleed air from four engines is directed into a common spanwise manifold from which the de-icing ducts are led for the six wing systems and for the empennage. Only nine sections are shown in this arrangement, resulting in the de-icing of 18- to 20-foot-span sections at one time. Performance could be improved by supplying air at the center of each section rather than at each end as shown in the illustration. Further economies in air supply would be effected by using 18 ten-ft. sections rather than 9 twenty-ft. sections, but with increased system complexity.

The system shown in Figure 4.2-6 does not use or require spanwise parting strips because the sweep angle is greater than 30 degrees. In nonswept wings, the spanwise parting strips may be required as shown in Figure 4.2-7. (An alternate arrangement for parting strips is shown in Section 3.) Use of parting strips almost doubles system complexity and increases air flow requirements. Where parting strips are needed, the method most likely to produce uniform spanwise width is that shown in Figure 4.2-7(b). The duct is split to allow air to flow the length of the duct in one direction, reversing and flowing back in the opposite direction. Data on this system is available (in unpublished form) from NASA.

The gas passages shown in Figure 4.2-7 are the typical corrugated-skin type often used for anti-icing, although the passages may be tapered to allow equal heating of the surface. (The increased heat-transfer coefficient at the aft end of the gas passage compensates for the decreased gas temperature.)

Air supply ducts may or may not be used to carry air spanwise in the leading edge, depending on gas temperature, duct length, and strength/temperature characteristics of the aluminum alloy used for skins and baffles. Below 450° F gas temperature, ducts usually would not be required.

The de-icing cycle used for hot-gas systems will usually involve somewhat longer heat-on and heat-off times than for cyclic electric. This results from the thermal inertia of the inner and outer skins, baffles, etc., as compared to a cyclic electric that heats only a very thin layer of insulation and skin. For the system in Figure 4.2-6, 30 sec. on (maximum) and 240 sec. off would be a typical cycle. At higher datum temperatures than the minimum value, it is desirable to reduce heat-on time as a function of datum temperature (see Figure 4.2-8). This minimizes refreeze at the higher temperatures. Timers are available commercially to perform this function. The heat-off time may be fixed or may be made manually variable. Flight experience with one de-icing system has indicated that heat-off times of as much as six to eight minutes may be required to allow a system with high thermal inertia to cool down and collect sufficient ice before the next application of heat. Heat-off time may also be made variable by integrating ice detector signals and initiating de-icing action after a specific number of signals.

De-icing time vs. datum temperature is shown in Figure 4.2-8 for two typical de-icing systems. At 25° F, de-icing times are about 4 to 8 sec., whereas at -10° F, 28 to 29 sec. are required. The de-icing air flow is 1.16 to 1.74 lb./sec. based on 20-ft. sections, depending on the system used and gas temperature. Details are not shown on parting strip flow requirements. In most current applications (swept wing), parting strips are not needed. For nonswept

4.2-10

wings, data may be found in Reference 4.2-1; data on the configuration of Figure 4.2-7(b) may be obtained from the NASA Lewis Research Center (unpublished form).

Various combinations of anti-icing and de-icing also may be used, depending on the needs of a particular aircraft. For example, it might be desirable to anti-ice the more critical outboard wing areas and de-ice the inboard wing and empennage leading edges after leaving an icing condition. This procedure could be an acceptable compromise between available bleed air and excessive system complexity.

4.2.3.3 PNEUMATIC BOOTS — Pneumatic boots have been used extensively on piston-engine aircraft and smaller turbine-engine aircraft, but have not yet been used for larger four-engine turbine transports. Potential service-life problems, as well as availability of hot-gas for anti-icing on large turbine aircraft, have restricted the pneumatic boot application. Modern fabrication techniques and improved erosion resistance have made pneumatic boot systems feasible for high-speed aircraft. The design points for pneumatic boot coverage on Aircraft D would be based on droplet impingement limits. These limits determine the amount of chordwise boot coverage that is required for ice protection. The impingement limits on the lower surface of the wing are a maximum for the 20,000-ft. hold condition and are approximately 17 in. The impingement limits on the upper surface of the wing are a maximum for the cruise condition and are approximately 7 in. Impingement limits on the empennage surfaces will be about 10 in. on both surfaces (vertical and horizontal fins).

Pneumatic boots should inflate and deflate rapidly to function effectively. To accomplish this, the boot panels are of limited size. Aircraft D will require about five panels for each wing semi-span and about two for each empennage surface (see Figures 4.2-9 and 4.2-10). Inflation time for the panels is about 5 or 6 sec. During heavy icing, a 60-sec. cycle is suggested, while for light icing, longer accretion times of 3 to 4 min. should be permitted.

The approximate weight of a pneumatic boot system for Aircraft D would be 305 lb.; based on 238 lb. for the boots, 37 lb. for operating equipment, and 30 lb. for tubing and brackets.

4.2.3.4 CYCLIC ELECTRIC DE-ICING — Electro-thermal anti-icing is not considered for Aircraft D because of the prohibitive power requirements. Cyclic electric de-icing may be considered and would require about the same leading edge wraparound as the pneumatic boot. (Such applications have been limited to small aircraft having little or no available bleed.) Wraparound is based on consideration of impingement limits for 20- and 40-micron droplets. For practical reasons, the coverage extends only slightly beyond the 20-micron range. The amount of ice that accretes beyond this is negligible. Typical layouts for the cyclic electric system for the wing of Aircraft D are presented in Figure 4.2-11. The empennage layouts are shown in Figures 4.2-12 and 4.2-13. The impingement limits and heater limits are illustrated in Figure 4.2-14. The wing is divided into several shedding zones (12 zones per wing semi-span in this example). Based on calculated accretion rates, a shedding frequency is established. With the shedding frequency and the number of shedding zones, a heat-on time for each zone is established. These values then are used to determine the approximate power density for adequate shedding. For effective shedding, this power density should fall within the range of 10 to 25 watts/in^2; if not, the number of shedding zones should be readjusted. Each heating element design will have its own set of performance curves for this determination.

For purposes of this illustration, an accretion or cycling time of 4 min. will be assumed. The maximum heat-on time for each of the 24 shedding zones will be 10 sec., for which a wattage density of 18 watts/sq. in. should be adequate. At 18 watts/sq. in., each shedding zone will require approximately 27 kw. A larger number of segments with increased total cycle time could be used to reduce this requirement. The empennage is a more efficient collector of ice and

will require more frequent shedding. A three-minute accretion time is assumed for the empennage which results in a 10-sec. heat-on time for each of the 18 sections. At 18 watts/sq. in., each empennage shedding zone will require approximately 7.38 kw, plus 3.02 kw for parting strips. Combined with the wing cyclic system, the total power requirement for cycling is about 35 kw, plus 7.04 kw for parting strips.

To reduce this power requirement, a study should be made of the effect of cycle time, accretion rates, and parting strip power requirements.

With a power density of 18 watts/sq. in., the time for shedding at various operating conditions may vary from 1 to 10 sec.; therefore, a variable heat-on time may be desirable to prevent continued heating after shedding and the resultant runback ice formation. A method of controlling heat-on time could be by sensing surface temperature. De-icing is usually completed when the surface temperature reaches 45° F. The controller could be designed to switch zones when the surface temperature reaches 55 to 60° F or when maximum heat-on time is reached. For the shorter heat-on times, a dwell period should be incorporated at the end of cycling to permit accretion before resumption of shedding.

An alternate approach that is somewhat less complex is to schedule heat-on time as a function of datum temperature (which can be approximated by measuring the temperature of an unheated portion of the leading edge).

For practical reasons, the parting strip should be of uniform power density — that is, the density required to maintain the stagnation point (point of highest heat loss) above 32° F in all conditions. Methods of determining parting strip power requirements are described in Paragraph 4.1.4.1. A power density of 14 watts/ sq. in. is typical. Chordwise strips measuring 1 in. x 8 in. are used for sweep angles in excess of 30 degrees. For lower sweep angles, one inch wide spanwise parting strips would be used. Chordwise strips are sometimes used in conjunction with spanwise strips to insure reliable ice shedding; however, this causes an appreciable increase in total power requirements.

One advantage of a cyclic electric system is that it may be an "add-on" system, requiring little modification. Installed weight for the empennage would be less than for hot gas in the case of forward-mounted engines. Another advantage is availability of power independent of flight condition; also, the power requirements for a de-icing system are substantially less than for an anti-icing system. One disadvantage to the cyclic system is the airfoil performance loss during periods of ice accretion. The major disadvantage compared with hot-gas anti-icing is the increased frequency of repair, particularly after several thousand hours of flight.

4.2.3.5 FLUID ICE PROTECTION — Fluid ice protection has been applied to several smaller transport aircraft but at present has not been applied to any the size of Aircraft D. Most aircraft the size of "D" prefer to operate with anti-icing protection for the wings and possibly de-icing for the empennage and usually have adequate bleed air and electrical power to accomplish this. If energy for anti-icing is not available, then fluid de-icing may be considered. (Fluid anti-icing requirements may be prohibited for large surface areas and are not considered for this application.)

There are several methods of applying fluid for de-icing, such as spray nozzles, a series of discrete holes, porous metal strips, and porous metal panels. The latter two methods are the most economical in operation and their requirements as applied to Aircraft D will be presented. Schematics of these two distributor systems were shown in Figures 3-5 and 3-6.

The porous metal panels may be used on airfoils with straight leading edges, of either constant or tapered sections. Airfoils with curvature in plan and/or elevation must use the strip distributors. Two strip distributors are used where variations in stagnation line exceed the width of the strip. Width of the panel distributors will be based on the stagnation limits of the airfoil. This will ensure fluid distribution over both surfaces during all flight conditions.

Fluid flow rates for the panel and strip distributors for de-icing were established by a series of natural icing flight tests (see Ref. 4.2-2 and 4.2-3). The fluid flow rate from the strip distributor was set at 2/3 Imperial pt. per projected square foot of frontal area per hour (0.93 psf/hr.). The fluid flow rate from the panel distributor was set at 1/3 Imperial pt. per projected square foot per hour (0.46 psf/hr.). According to Ref. 4.2-2, these flow rates will give anti-icing performance at the higher icing temperatures and a continuous de-icing cycle at severe low icing temperatures. Based on these flow rates, the fluid required to protect Aircraft D using the panel distributors would be approximately 75 lb./hr.

The weight of a panel distributor system as applied to the wing of Aircraft D will depend upon the limits of stagnation variation. Assuming an arbitrary value of 4 in. for stagnation line variation and a wing leading edge length of 841 in., the weight of full span panels for both wings would be about 124 lb. The total weight of the wing system — pumps, filters, distribution lines, fluid, and panels — would be approximately 200 lb. Requirements for the empennage would be on the order of 1/3 of this value.

There are some recommended operating techniques to be used with the fluid system. For best performance, the protected surfaces should be wetted before encountering icing. This acts as an ice bond depressant and improves performance of the de-icer. This means the system should be actuated prior to entering a cloud or whenever icing conditions are anticipated and remain on throughout any icing encounter.

4.2.4 ICE PROTECTION FOR WING LEADING EDGES HAVING SLATS AND/OR KRUEGER FLAPS

The preceding descriptions of ice protection systems for the wing of Aircraft D assumed a fixed leading edge. Wings with leading edge devices will have the same ice protection requirements but methods of supplying these requirements will differ and will be more complex.

Leading edge devices may consist of slats, slots and flaps. A wing leading edge slat configuration is shown in Figure 4.2-15. This figure represents a hot-gas anti-icing system as applied to Aircraft D. The slat portion of the wing leading edge incorporates a piccolo tube which gives ice protection to the leading edge, upper surface of the leading edge, and to a small portion of the lower surface. The fixed portion of the wing leading edge also has a piccolo tube which supplies ice protection to the remainder of the airfoil's protected lower surface and to part of the fixed leading edge within the slot. The slat piccolo tube is supplied hot gas by means of a telescoping duct. The fixed wing behind the slot may or may not require protection, depending on geometry, ice accretion characteristics and time in icing. For each new aircraft, a study should be made of need for heating this area.

The anti-icing air flow must be divided between the slat and fixed leading edge in proportion to their requirements. This is accomplished by sizing the piccolo discharge holes using duct temperature and pressure losses and a discharge coefficient as parameters. At the design point (5,000-ft. altitude hold) the flow requirement of 0.8 lb./sec. for the center section is divided 60% for the slat and 40% for the fixed leading edge.

Alternate methods of wing ice protection such as pneumatic tube, electrothermal de-icing and fluid de-icing may also be applied to leading-edge slats. Difficulty in retraction of the slats may be experienced if ice accretes on the fixed leading edge or if residual ice or runback ice occurs within the slot.

Leading edge "Krueger" flaps may or may not be protected depending upon the effects of ice accretion on performance. Figure 4.2-16 illustrates an unprotected leading edge flap as might be installed on Aircraft D. Ice protection requirements for the wing leading edge will remain the same but because of the flap installation there will be a reduction in the heated area on the lower surface. Water may runback from the heated leading edge and freeze in the flap, if the

4.2-16

leading edge anti-icing system is not fully evaporative. Also, there will be a small amount of direct impingement. Evaluation of need for heating the flaps must be made by either an aerodynamic analysis or by flight test.

Ice accretion may occur when the flap is extended during takeoff and approach. Figure 4.2-17 illustrates the amount of ice that may accumulate, based on 30 minute hold in icing. No appreciable ice is accumulated during takeoff, as flaps are retracted about 1-1/2 minutes after brake release. If the flap is unprotected, flight tests should be conducted to determine the effects of this ice accretion. One flight-test method which may be employed is to simulate the predicted ice shapes and weight with wood and attach them to the flap. The airplane performance then may be evaluated in clear air.

Ice protection may be provided for the flap using hot gas by fabricating the flap as a double-skinned heat exchanger similar to the wing leading edge. The hot gas may be transmitted to the flap either through a telescoping duct or a swivel fitting and duct. Anti-icing heat requirements may be determined using the calculation methods described in Section 3.

De-icing requirements would be similar to the requirements of a fixed leading edge. Shedding characteristics will probably be different because of the airfoil shape and the aerodynamic forces the ice will encounter. An icing tunnel test program may be required, due to the difficulty in predicting shedding forces and impingement.

4.2.5 ICE PROTECTION FOR TURBOJET ENGINE INLET LIP

Ice protection is necessary for turbojet engine inlet lips to prevent engine damage due to ingestion of ice. Decrease of inlet area is not a significant factor, except for extremely small engines. The various methods of providing protection are hot-gas anti-icing, electrical anti-icing and de-icing, and fluid anti-icing and de-icing, which are discussed below.

4.2.5.1   HOT-GAS ANTI-ICING — A hot-gas anti-icing system for the engine inlet lip of typical CAR-4b transport is illustrated in Figure 4.2-18. The area of the nacelle requiring anti-icing extends aft from the leading edge along the inner and outer surface of the inlet lip, a horizontal distance of 6 in. The anti-icing air (engine compressor bleed air) is distributed around the lip by a modified "D" duct and passes through holes in the leading edge of the inner skin into 0.40-in. gas passages. The air flows aft through these passages into a plenum chamber between the "D" duct and a baffle and then is discharged tangentially into the inlet stream via six discharge ports. An alternate arrangement is also shown that eliminates the inner skin. Although it is less efficient thermally, the arrangement is particularly useful for thin leading edges (as on supersonic inlets) or flush scoops. Cost of manufacturing the single skin system may be lower for many applications.

Heat and air flow requirements for anti-icing the engine inlet of Aircraft D were determined at a number of different flight conditions, and the design condition was found to be a 15,000-ft. cruise condition. Since the calculations showed the greatest air flow demand at the 15,000-ft. cruise condition, the system was designed to meet the heat requirements at this condition. The system will provide complete evaporation of the impinging water droplets in maximum continuous icing for all flight conditions except descent (due to low bleed temperatures). The heated area will be maintained above 35' F (running wet) for descent. In maximum intermittent icing, the heated surface will be running wet for all flight conditions. The amount of refreeze is not significant for these encounters because of the short duration. Calculated values of both actual and required heat release are shown in Figure 4.2-19 for comparison. Figure 4.2-20 shows calculated values for both actual and required air flows.

The calculation of water catch, impingement limits, and heat release and air flow requirements for a turbojet engine inlet lip is described in Paragraph

4.1.6. Knowing the bleed air pressure available at the different flight conditions, the actual air flows can be calculated by performing a pressure drop analysis of the system. The actual heat release can then be found knowing the actual air flows.

For other aircraft with engines having a shorter distance from the inlet lip to the compressor face, it may be feasible to provide running wet protection for the entire area aft to the compressor face so that runback does not build up and shed into the engine. This would not be practical for Aircraft D, however, because the compressor face of its engines is on the order of 4 ft. from the inlet lip.

4.2.5.2 ELECTRICAL ANTI-ICING — A possible alternative method of ice protection for a turbojet engine inlet lip is electrical anti-icing. This type of protection makes use of electrical heating elements cemented to or integrated with the leading edge. A more detailed description is contained in Section 3. (Typical heater construction details are shown in Figure 3-22.)

Completely evaporative electrical anti-icing is usually impractical for protection of turbojet engine inlet lips because of the large amount of power required (about 28 kw per engine for Aircraft D to protect the same area protected by hot gas). Running wet electrical anti-icing is practical for engines having a relatively short distance from the inlet lip to the compressor face. Because this distance is approximately 4 ft. for Aircraft D, this type of protection would be impractical. Running wet electrical anti-icing may be practical, however, for engines having the engine face less than 2 ft. from the inlet lip. (Requirements for this type of protection were discussed in Section 4.1.)

4.2.5.3 ELECTRICAL DE-ICING — Electrical de-icing of the engine inlet lip usually is not practical for turbojet engines having axial flow compressors because of their susceptibility to damage from ice ingestion. However, electrical de-icing could be designed for many engines having centrifugal compressors because this type is less susceptible to ice ingestion damage.

This type of engine inlet protection would not be practical, then, for Aircraft D because its engines have axial flow compressors. For purposes of illustration, however, the determination of requirements for cyclic electrical de-icing of the engine inlet lip is discussed in Paragraph 4.1.6.

4.2.5.4 FLUID ICE PROTECTION — Another possible method of protection for engine inlets is fluid anti-icing, described in detail in Section 3.4. The amount of fluid required to protect the area described above for the engine inlet of Aircraft D is about 170 lb. per engine for a 1-hr. duration of icing using a 50% glycol-water solution. For such a high water catch condition, a solution with higher glycol content than the normal 50% could be used. In that case, the fluid requirements would be considerably smaller (as little as 40 lb. per engine using 100% glycol). Equation 3.4.2 in Paragraph 3.4.2 is used to determine fluid requirements at a given water catch rate.

Lower fluid flow rates may be possible using fluid de-icing, which is described in Ref. 4.2-2 and previously discussed in Section 3.4. With this type of protection, there is no attempt to prevent the formation of ice. Continuously supplying fluid at a somewhat lower flow rate will cause the ice formed to shed periodically, and a steady de-icing cycle will usually occur. A flow rate of 2/3 pint/hr./sq. ft. of projected frontal area has been reported to be satisfactory for de-icing purposes.

4.2.6 ICE PROTECTION FOR TURBOJET ENGINE COMPRESSOR NOSE CONE

Although engine manufacturers provide anti-icing for the engine inlet guide vanes and compressor front frame, the compressor nose cone usually is considered as part of the airframe. Nose cone geometry generally is unique for each installation of a particular engine. Once the external geometry is defined, the heat and air flow requirements may be determined by the methods described in Section 3. The only difference is that conditions within the air inlet duct must be used rather than free stream.

The nose cone usually is designed for "running wet" protection; that is, surface temperature of 35° or more under all conditions. The entire surface is heated so that residual ice cannot form and be taken into the engine. The "Intermittent Maximum" icing conditions of CAR-4b are usually used for design criteria.

Typical examples of nose cone geometry and heat requirements are shown in Figures 4.2-21 through 4.2-24. Two variations of nose cone anti-icing systems may be found in current turbojet engines.

In one case, compressor bleed is ducted through front frame support struts to a ring-shaped manifold. Air is taken from this manifold to anti-ice the variable-position inlet guide vanes, and also to anti-ice the compressor nose cone. A typical example is shown in Figure 4.2-21 and is called the direct bleed type. Air is diverted into the plenum through a supply tube containing a restricting orifice, and flows into tapered gas passages, discharging into the duct air stream at the aft end. Variable-depth gas passages are used to ensure adequate heat release at the aft end of the nose cone.

Typical flow requirements and actual flow are shown in Figure 4.2-22 for descent, climb, and hold flight conditions. Air flow is marginal (but adequate) for descent, and is more than adequate for the other conditions. The inlet gas temperatures are lower than compressor bleed temperature because of temperature losses in the supply ducting, support struts, and manifold.

For engines having fixed inlet guide vanes, the inlet anti-icing manifold usually supplies air at the outer periphery of the engine. The air then flows inward through the guide vanes and is discharged into the compressor nose cone. The entire discharge air flow is used to anti-ice the nose cone; the increased air flow (as compared to direct bleed) thus compensates for the reduced air temperature. Two flow arrangements that have been used on military aircraft are shown in Figure 4.2-23. Both systems gave satisfactory results; however, the arrangement shown in part (a) is somewhat simpler to fabricate.

Typical heating requirements and available heat are shown in Figure 4.2-24 for two values of duct air total temperature. At low rpm, the heat available is about equal to the required heat; but as rpm is increased, a substantial margin exists.

The design of an adequate nose cone anti-icing system usually has two opposing design points. At low rpm and air flow, adequate surface temperature must be maintained; however, at high rpm, the pressure drop through the nose cone must not be excessive as damage to the guide vanes would result. Engine manufacturers normally specify a maximum allowable back pressure in the guide vanes.

4.2.7 ICE PROTECTION FOR WINDSHIELDS

Although there are several possible methods of providing ice protection for transport windshields, the system currently in use is electrical anti-icing. The installation of such a system is relatively simple where adequate electric power is available. Double-paned windshields with hot air circulated between the panes have been used, but installation is difficult. Dirt between panes, noise, weight and cracking are other possible problems. Fluid anti-icing is not in current commercial use, possible because of the weight penalties and servicing problems. Further, a uniformly heated windshield may be necessary to meet bird-impact requirements, as discussed later. Although only the electrical anti-icing system is described here, design procedures for hot-air and fluid systems are contained in Sections 3 and 4.1.

The windshield arrangement of a typical multi-engine transport is shown in Figure 4.2-25. Ice protection is needed for the forward facing windshields (main and center), but not for the sliding and aft windows which are at minimum angle to the airstream and would not collect ice. An alternate arrangement often used deletes the center windshield and increases the size of the main windshields. In either case, the conductive anti-icing film or wire grid is applied to the inside

of the outer ply of glass, as shown in Figure 4.2-26. The film usually covers only a roughly rectangular area of the windshield, as non-uniformity of heating and actual "hot spots" become a serious problem with the high power density heating needed for anti-icing (3 to 4 watts/sq. in.).

Anti-fog films, in contrast, are often applied to non-rectangular areas. The low power densities (1/2 to 1 watt/sq. in.) used for anti-fog tend to reduce the problem of "hot spots" and attendant glass breakage problems. For this reason, the arrangement of Figure 4.2-26 has been used on at least one jet transport. The anti-fog film may be used to prevent fog and to maintain the vinyl at optimum temperature for resistance to bird strikes. Where the panel in question is nearly rectangular, a single anti-ice coating may meet the requirements for anti-icing, fog prevention, and maintenance of optimum vinyl temperature.

In the configuration of Figure 4.2-26, the anti-fog and anti-ice films are never used simultaneously.

Methods of calculating heat requirements were shown in Sections 3 and 4.1. Typical results for a jet transport center windshield are shown in Figure 4.2-27. For the flight profile studied, a maximum input of 1,800 BTU/hr.-ft.^{2} was found to be adequate. Inward heat losses have not been considered here as analysis shows them to be less than 5%. Calculations were based on buildup of the air boundary layer from the nose of the aircraft. For windshields that depart abruptly from the fuselage contour, a new boundary layer starts at the windshield's base and heat requirements will be higher (as described in Section 4.1).

One of the main problems associated with the use of electrically heated windshields is inflight breakage caused by thermal stress in the glass. Replacement rates for windshields often are several times as great in winter as in summer.

There are two effective approaches to this problem. One is to design the heat input to the minimum possible value. Clear vision is essential at low

altitude, but air temperatures associated with icing are not likely to be below
0° F (see Section 1). At higher altitudes where lower temperatures are found,
flight through icing would be made on instruments and partial obstruction of
vision might be acceptable. The non-uniformity of the conductive coating would
tend to prevent complete obscuring of the windshield even under marginal con-
ditions. Some transports equipped with high $(2,300$ BTU/hr. -ft.^{2}) and low
$(1,500$ BTU/hr. -ft^2) control settings have found no need for the higher setting.

A second approach (which can be used in conjunction with the first) is to
employ a power modulating control. Recent advances in static switching devices
have made this an attractive method of control. The alternate approach, (use of
a transformer, relay, and power contactor) may result in large transient cur-
rents and temperature differentials that adversely affect windshield service life.

4.2.8 ICE PROTECTION FOR RADOMES

Most transport aircraft now use radar to avoid severe weather conditions. The
radar commonly is housed in a nose radome made of reinforced fiberglass.
Since ice formation on the radome affects radar transmission, pneumatic boot
de-icing and hot-gas anti-icing systems were developed. Although experience
has shown that loss in radar range from ice on the radome is not critical (studies
show maximum values of about 10%) this section contains brief data on typical
pneumatic boot and hot-gas systems. Fluid systems could also be used as shown
in Section 3. Electrical systems are not applicable because of interference from
the heating element.

A schematic of a bleed-air inflated pneumatic boot system is shown in
Figure 4.2-28. The system inflates all tubes at the same time whereas some
wing de-icing boots inflate only half the tubes at a time. This simplifies the
plumbing and valve arrangement without decreasing de-icing effectiveness.
Suction is provided by a bleed-air ejector. An electronic timer is used to
allow inflation of the boot for about 6 sec., once every 3 min. In a piston-engine

aircraft, the system would be similar except that an engine-driven pump would provide pressure and suction.

Details of the de-icing boot are shown in Figure 4.2-29. The boot is about 0.1 in. thick, except in the supply manifold area where it is 0.2 in. thick. Greater thickness will give longer service life, but will cause further increases in transmission losses. The inflatable area extends aft 22 in., some 10 in. beyond the impingement limit for 20-micron droplets.

If a pneumatic boot is not used, it is advisable to use a rain erosion coating over the radome, plus a thin protective rubber-fabric erosion shoe in the nose cap region where rain erosion effects are most severe.

Another method that has been used on several specific kinds of aircraft is an air-heated radome. Gas passages are formed by a patented process of the "lost wax" type, as shown in Figure 4.2-30. Air is fed from a half-circle supply manifold at the rear of the radome, through the passages, and into a similar collector manifold, and is dumped overboard. An ejector system is used to mix compressor bleed air with ambient (or radome discharge air).

Analytical studies of such a system for Aircraft D showed that, with 1/2-in. deep gas passages, an air flow rate of 0.75 lb./sec. was required. Of this, 0.31 lb./sec. was bleed air, and 0.44 lb./sec. was obtained from the radome discharge. Mixed air temperatures varied from 175° F to 375° F. The system is designed for "running wet" protection in "continuous maximum" icing conditions of CAR-4b.

The major disadvantages of the air-heated radome are:

1.   Complex geometry, may be costly to build.

2.   Gas passage sizes may be compromised by radar transmission requirements.

3. Adequate heat transfer at stagnation required a thin skin, whereas rain erosion considerations demand a thick skin, plus erosion coating.

4. Radome strength may be adversely affected by heating.

At present, radome ice protection is not provided on commercial aircraft, because the transmission losses are small and do not represent an unacceptable effect on range. Changes in technology, work on reduced landing minimums, etc., could result in a need for ice protection, in which case the foregoing information will be of use.

4.2.9 ICE PROTECTION FOR MISCELLANEOUS COMPONENTS

Any large aircraft has small components that accumulate ice if not protected. Typical examples are pitot tubes, angle of attack indicators, antennas, auxiliary air intakes, stabilizer mass balances, etc. The need for ice protection of these components can be determined by answering the following questions:

1. Will ice accumulate on the object in question and in what amount?

2. Will this accumulation adversely affect the component's function?

3. If the components function is affected, will it have an effect on safe flight of the aircraft?

4. What is the effect of ice shedding on other components, such as engine inlets? Will ice shedding affect engine operation?

The methods of providing protection have been discussed in Section 3. The current practice for small, critical components is application of electrical heat applied to the critical area. In the case of engine inlet total pressure probes, engine bleed air also has been used successfully for anti-icing.

General practice has been to provide no protection for flush inlets and vents and for the small antennas located on the fuselage. Although detailed studies

must be made for each new application, it is usually found that the flush inlets will not close completely in icing, therefore, protection is not provided. Static ports located on the fuselage (if suitably far from the nose of the aircraft) usually have not been protected. Inlets for air conditioning systems may or may not be protected depending on whether ice formed on the inlet would shed into the heat exchangers or turbocompressors and cause damage. In any case, where ice protection is provided in small components, effect of a single failure should be considered. In the case of pitot tubes, for example, if the pilot's pitot tube fails, the copilot's may be used.

4.2.10 ICE PROTECTION FOR PROPELLERS AND SPINNERS OF TURBOJET AIRCRAFT

Propeller and spinner ice protection is necessary on turboprop aircraft for three reasons: (1) leading-edge ice formations may cause a propeller efficiency loss, (2) unsymmetrical shedding of ice may result in propeller unbalance, and (3) large pieces of ice shed from the propeller or spinner may be ingested by the engine.

Ice protection for propellers and spinners of turboprop aircraft is commonly provided by the electro-thermal method. A typical system of this type is illustrated in Figure 4.2-31 and is described in detail in Ref. 4.2-4. In this particular system, continuous (running wet) heating is provided for the forward portion of the spinner; cyclic heating is provided for the aft portion of the spinner, the spinner islands, and the propeller blade leading edges (to 30-per cent radius). These are the areas from which ice would have the greatest tendency to enter the engine. Propeller protection was extended only to the 30-per cent radius because ice formation was found to be negligible beyond that point (because of aerodynamic heating and centrifugal force effects).

For the system illustrated, the distribution of power to the forward (anti-ice) portion of the spinner is shown in Figure 4.2-31. Power to this area is varied in steps from 3.5 to 8 watts/sq. in. The watt densities supplied to the cycled

areas are 11 watts/sq. in. for the aft portion of the spinner and 13 watts/sq. in. for the spinner islands and propeller blade "cuffs." Heat-on time for these cycled areas is 20 sec. and the total cycle time is 160 sec. (Heat-off time is 140 sec.)

For other configurations, the same principles may be applied to obtain satisfactory protection. Other methods have been used in the past, such as fluid de-icing and hot-gas anti-icing, but have fallen into disuse because of installation difficulties, as compared to the electrical system.

4.2.11   EFFECT OF ICE ON UNPROTECTED AIRFRAME COMPONENTS

The effect of ice on unprotected airframe components can be estimated analytically as illustrated in Paragraph 4.1.3 for a typical light aircraft. An estimate of the drag increase due to icing (and, therefore, the effect on aircraft performance) can be obtained for the entire airplane or for any particular component for which it is desirable to consider elimination of protection.

However, before protection can be proved unnecessary, flight tests must be made to show that ice on the unprotected component will not adversely affect aircraft handling and flutter-free characteristics. This can be done in natural icing, behind an aerial tanker, or in dry air using simulated ice shapes made of wood or some other material. (See Section 6 for further discussion of testing.) Perhaps the most practical method of testing to determine the effect of ice on the unprotected component is the method of clear air tests using simulated ice.

Estimates of the shapes of simulated ice can be made knowing the impingement limits and ice cross-sectional area found by the methods illustrated in Paragraphs 4.1.3 and 4.1.4. For example, considering elimination of empennage protection for Aircraft D (Figure 4.2-1), impingement limits and ice cross-sectional areas were found and estimates were then made of the ice shapes. Typical examples of these shapes are shown in Figure 4.2-32 for the mid-span location on both the horizontal stabilizer and vertical fin. These shapes represent

the most severe icing expected for a hold condition of 45 min. duration (15 min. departure hold and 30 min. destination hold), the criterion for elimination of protection. The "mushroom" ice formation shown is typical of glaze ice and is a well-known phenomenon. It is desirable to simulate this kind of formation because it would obviously have more effect on aerodynamic characteristics of the airplane than would the rime ice or glaze-rime ice.

To determine the feasibility of eliminating ice protection for the empennage of Aircraft D, it would be necessary to conduct flight tests with wooden mockups of these estimated ice shapes attached to the leading edges of the horizontal stabilizer and vertical fin. From such flight tests, it can be determined whether aircraft performance and handling characteristics would be adversely affected by icing. In tests on a current aircraft with simulated ice shapes on the tail, the only significant effect was a one per cent loss of climb gradient. Because the climb gradient was far enough above the minimum requirements, the system has been removed. Some other aircraft have reported significant effects of empennage icing on handling characteristics, particularly with flaps down. For each new aircraft, tests would be needed to ascertain the need for empennage protection.

Deletion of airframe ice protection equipment raises the question of what effects, if any, will result from ice falling from leading edges as the aircraft descends to warmer air.

There have, in fact, been a number of reports of large masses of ice having fallen from the sky in recent years. An article in the June 1960 issue of Weatherwise (Ref. 4.2-5) lists a number of reported ice-falls occurring from February 1953 to November 1959. The origin of some of these ice-falls was undetermined, but there was evidence that a large number of them actually fell from airplanes. Because ice-falls of anywhere from 10 to 100 lb. were reported, it was concluded in Ref. 4.2-5 that it is not likely that they originated from aircraft de-icing systems. By the same token it is not likely that chunks of ice shedding

from unprotected airframe components could account for ice-falls as large as those reported.

Ref. 4.2-5 reports evidence that many of these ice-falls can be attributed to the external disposal of waste water by certain commercial transports (based on chemical analysis of ice samples both in this country and in England). There are certain aircraft which externally dispose of waste water from the cabin and galley washbowls in flight. It has been theorized that the washbowl exhaust water freezes and builds up behind the exit port (while flying in below-freezing temperatures) and then later breaks loose, possibly after descent to warmer air. This theory seems to be supported by the high alkalinity and high solids content discovered by chemical analysis of some ice-fall samples. The British found some ice samples to be strongly perfumed, and they also detected the presence of milk, sugar, and tea leaves.

Another interesting observation made in Ref. 4.2-5 was that the geographical locations of the reported ice-falls were not altogether random. About two-thirds of the ice-falls reported occurred in a band about 200 miles long from southeastern Pennsylvania to Long Island. It could be that this area is the let-down area for transcontinental flights terminating in New York City, and long-distance flights of transports carrying a large number of passengers would most likely yield the largest waste-water accumulations.

Aircraft of current design either collect all waste water, or discharge it through strut drains well away from the fuselage. Thus, the problem of ice-falls should be alleviated as the older aircraft are retired or retro-fitted.

REFERENCES

4.2-1. NACA RM E53C27, "Comparison of Several Methods of Cyclic De-Icing of a Gas-Heated Airfoil," by V. H. Gray and D. T. Bowden.

4.2-2. "Vickers Viking Fluid De-Icing Trials," Project Development of British European Airways.

4.2-3. "Fluid De-Icing," D. C. Tanner, paper presented at Aircraft Ice Protection Conference, 1961, D. Napier & Son, Ltd.

4.2-4. "Design and Development of the Ice Protection Systems for the Lockheed Electra," B. L. Messinger, and J. B. Werner, paper presented at 1959 Aircraft Ice Protection Conference, D. Napier & Son, Ltd. Also published in December 1959 issue of Space/Aeronautics.

4.2-5. "The Ice Fall Problem," J. E. McDonald, published in June 1960 issue of Weatherwise magazine.

120 Ft.
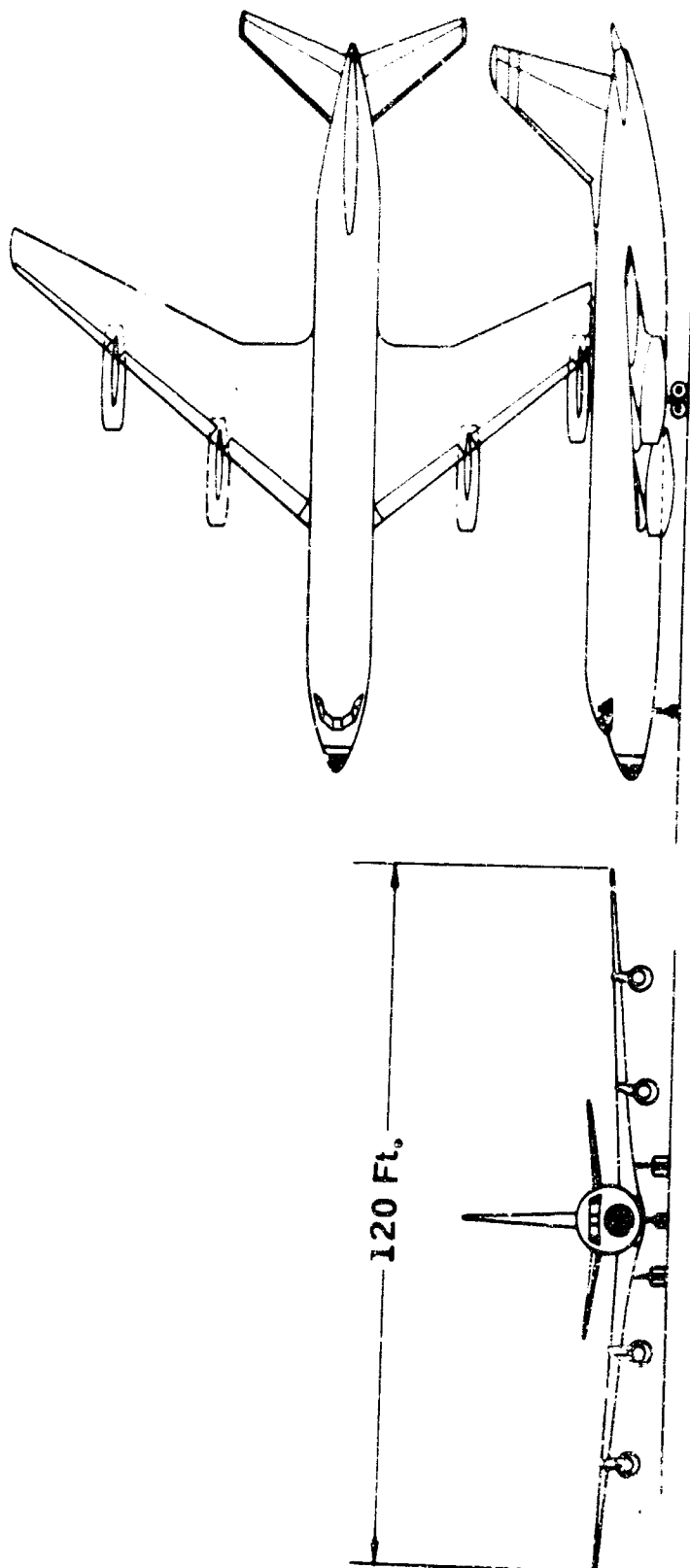
Typical CAR-4b Jet Transport (Aircraft D)

Figure 4.2-1

Windshield Rain
Removal Shutoff

Ground High Pressure
Air Connection

To Radome System

Bleed Air
Emergency Wing
Isolation

Air Conditioning

Main Bleed Air Manifold

Windshield
Rain Removal

Inlet Duct
Lip Valve

Main Bleed
Air Regulator

Wing Leading Edge

Wing Anti-Icing Valves

To Engine Inlet
Duct Lip
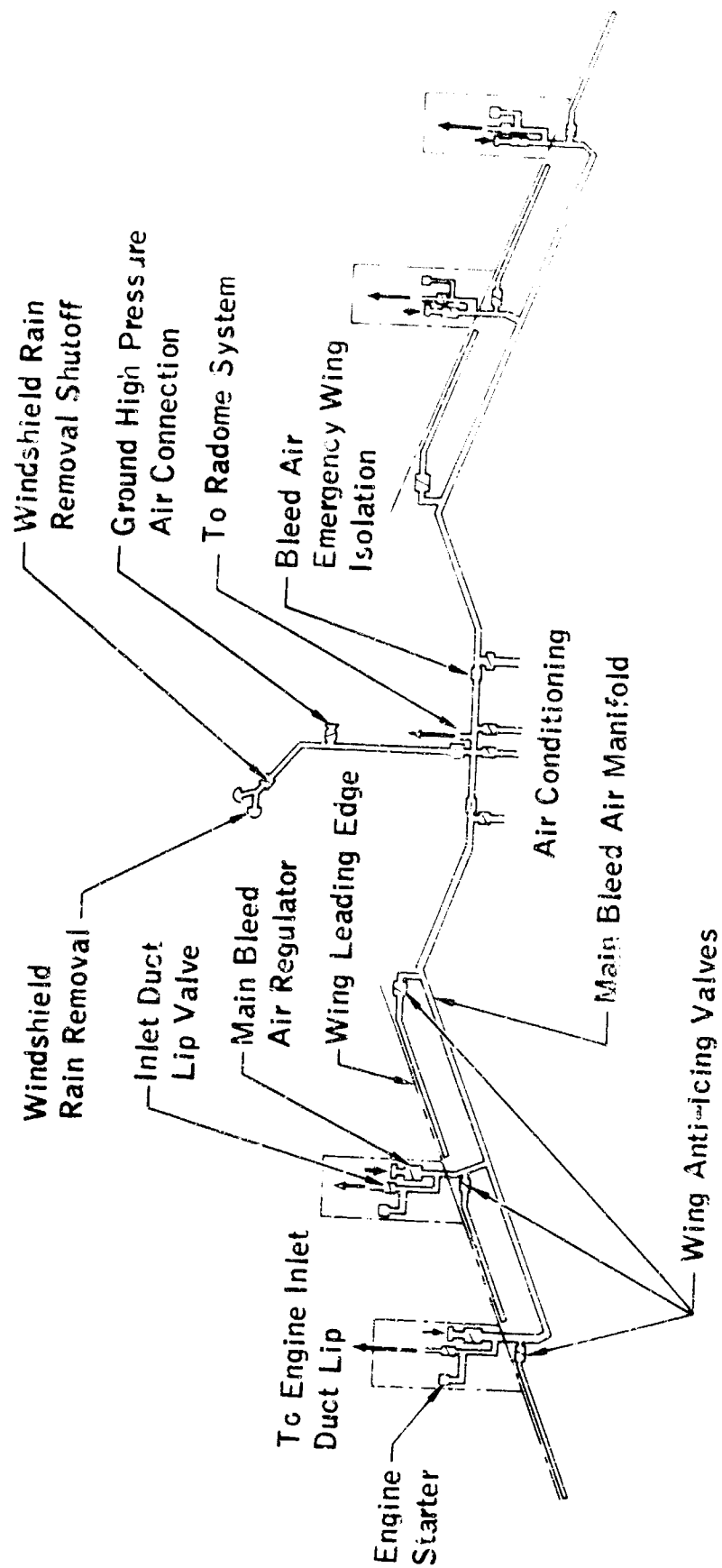
Engine
Starter

Typical Hot-Air Anti-Icing System
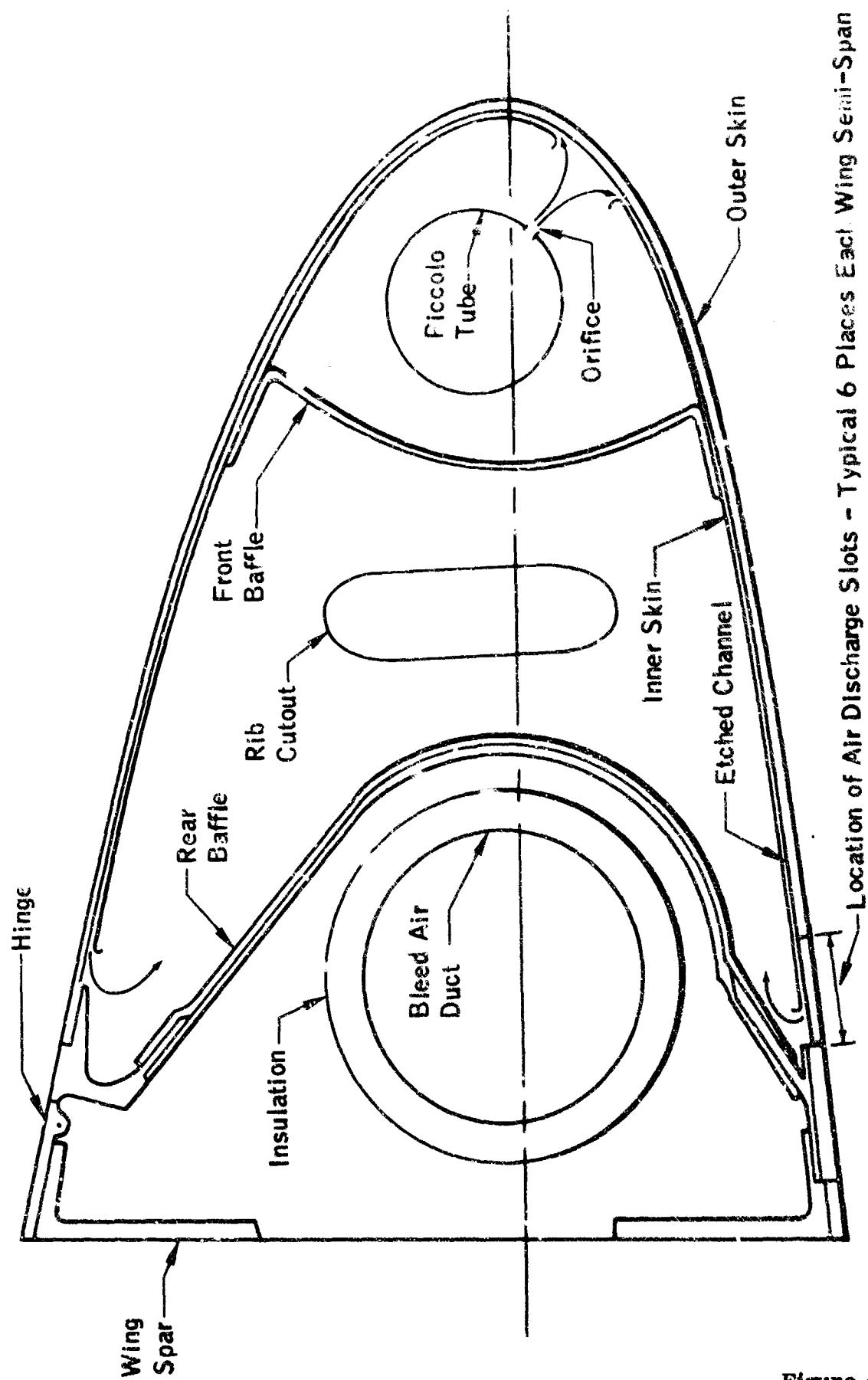
Figure 4.2-2

Typical Hot-Air Anti-Iced Wing Leading Edge

Figure 4.2-3

Outer Skin

Piccolo Tube

Orifice

Front Baffle

Rear Baffle

Rib Cutout

Hinge

Inner Skin

Etched Channel

Location of Air Discharge Slots - Typical 6 Places Each Wing Semi-Span

Insulation

Bleed Air Duct

Wing Spar
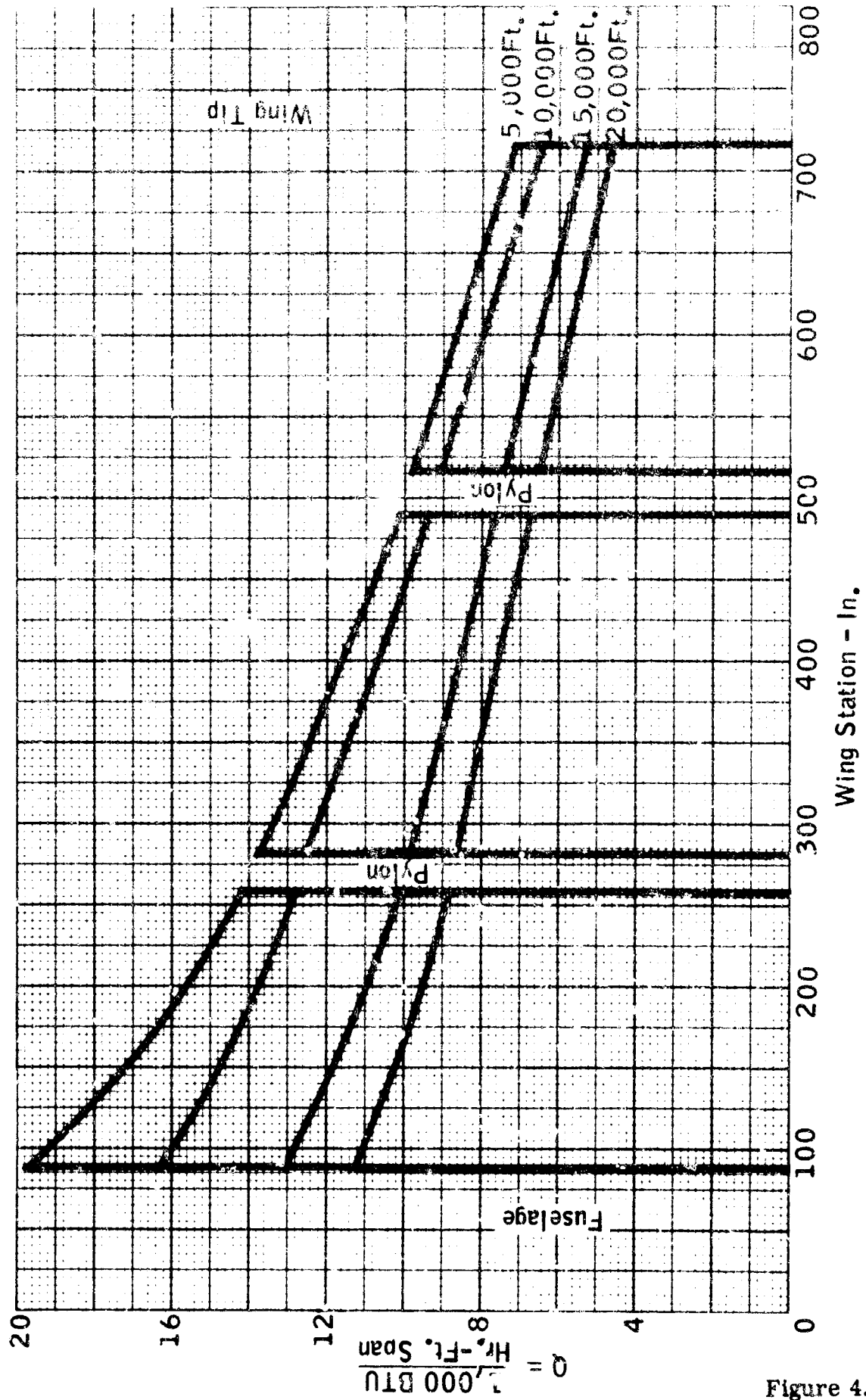
Anti-Icing Heat Requirement Vs. Wing Station, Hold Condition

Figure 4.2-4

Air Flow Rates for Wing Anti-Icing, Hold Condition
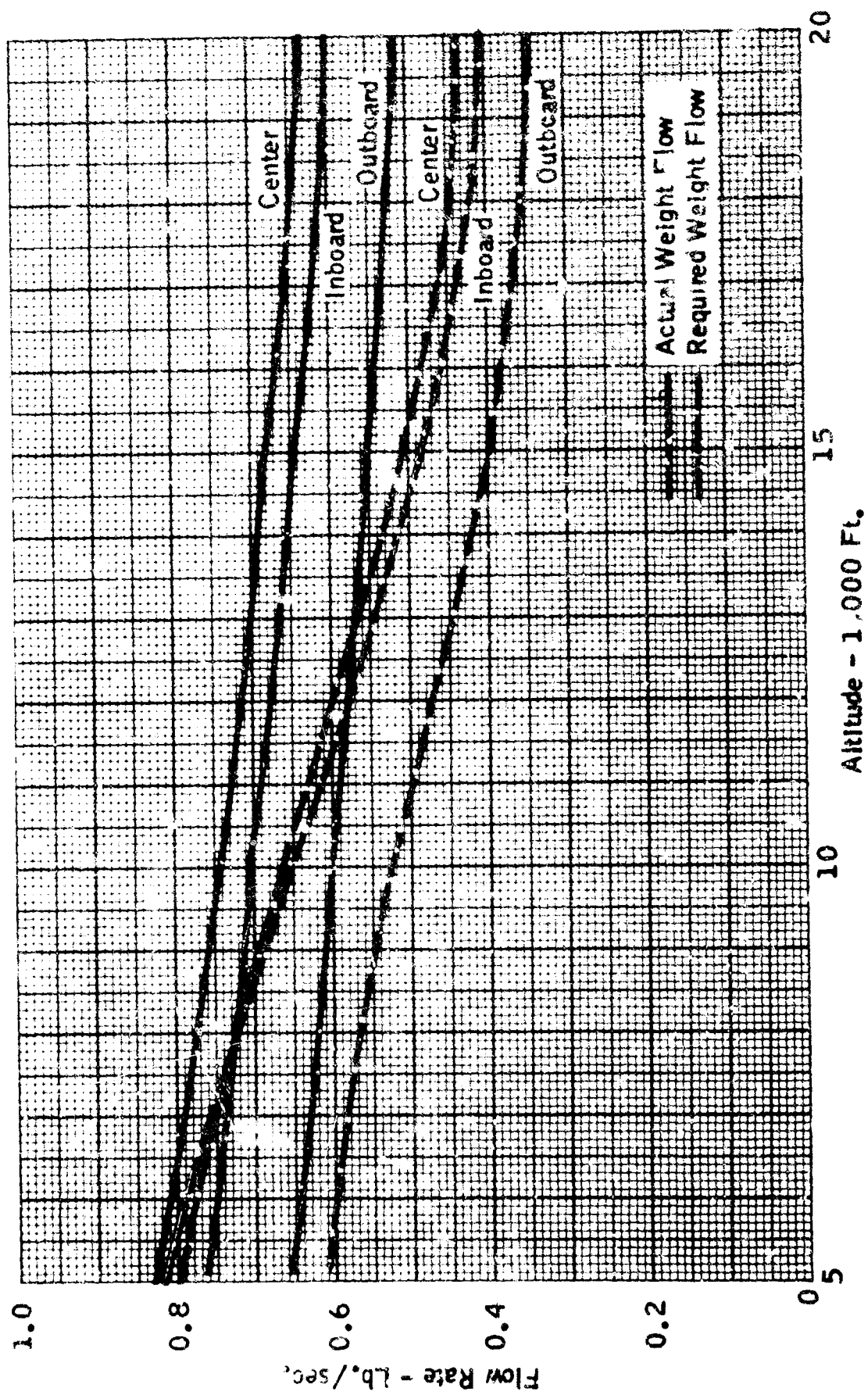
Figure 4.2-5

⊗ Engine Bleed Valve (Pressure Regulating/Shutoff)
✕ De-Icing Valve (Pressure Regulating/Shutoff)
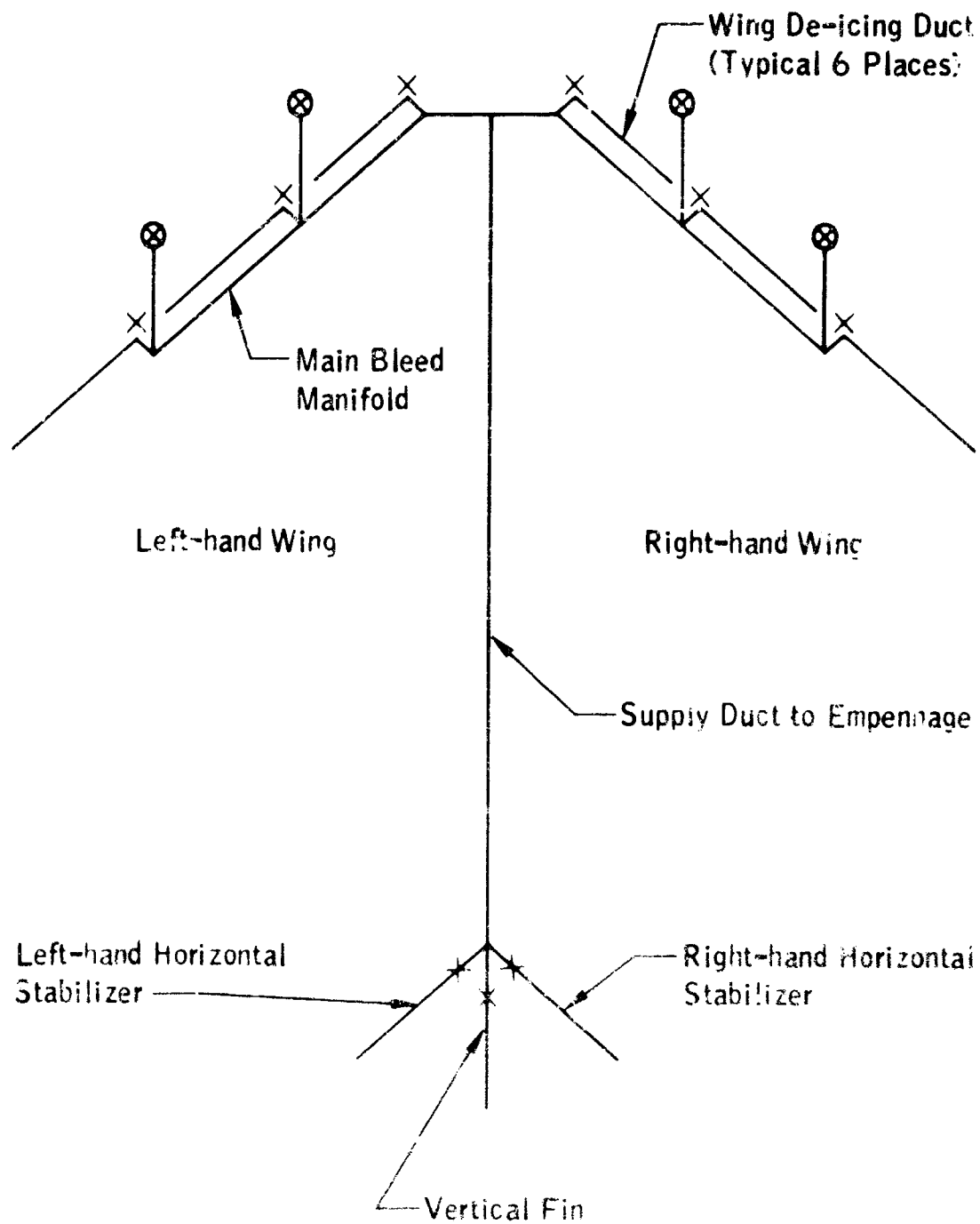
Figure 4.2-6. Typical Hot-Gas De-Icing System for Four-Engine Transport
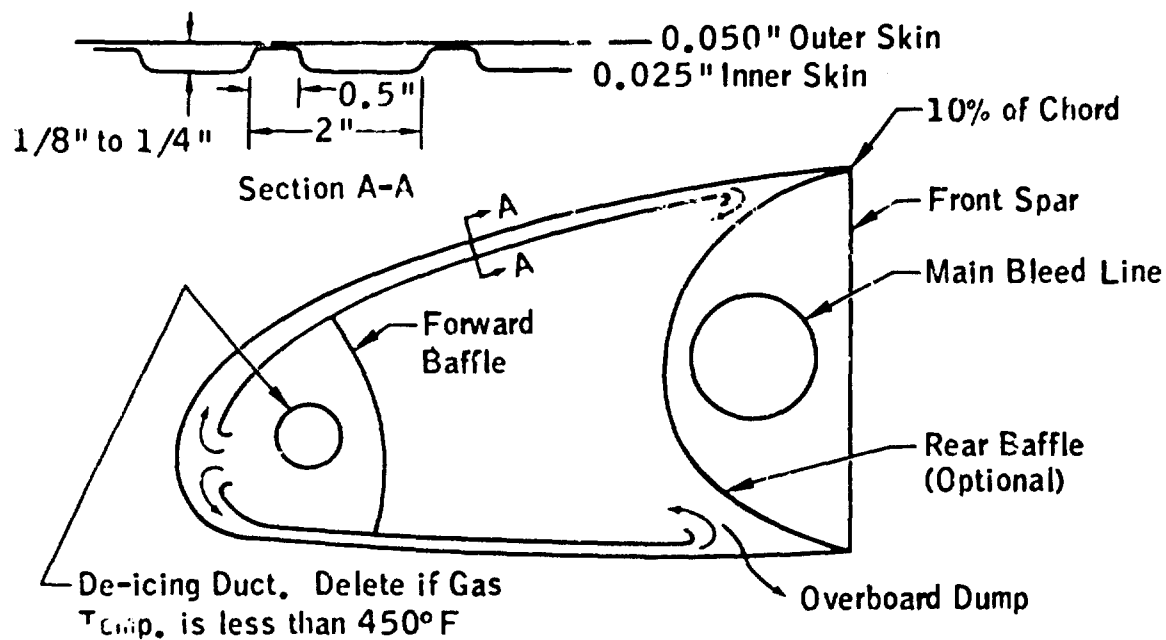
(a) Design for Swept-wing (over 30° sweep)

0.050" Outer Skin
0.025" Inner Skin
10% of Chord
Front Spar
Main Bleed Line
Rear Baffle (Optional)
Overboard Dump
Forward Baffle
De-icing Duct. Delete if Gas Temp. is less than 450°F
1/8" to 1/4"
0.5"
2"
Section A-A
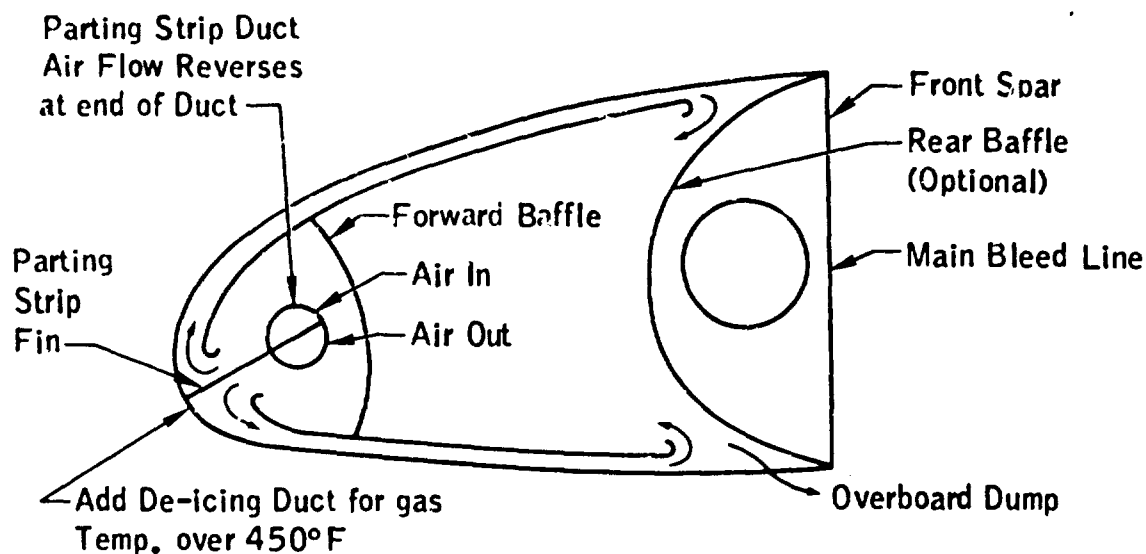
(b) Design for Non-swept Wing (less than 30° sweep)

Parting Strip Duct Air Flow Reverses at end of Duct
Parting Strip Fin
Forward Baffle
Air In
Air Out
Front Spar
Rear Baffle (Optional)
Main Bleed Line
Overboard Dump
Add De-icing Duct for gas Temp. over 450°F

Figure 4.2-7.   Typical Wing Leading Edge Cross Section
for Two Types of Hot-Gas De-Icing Systems
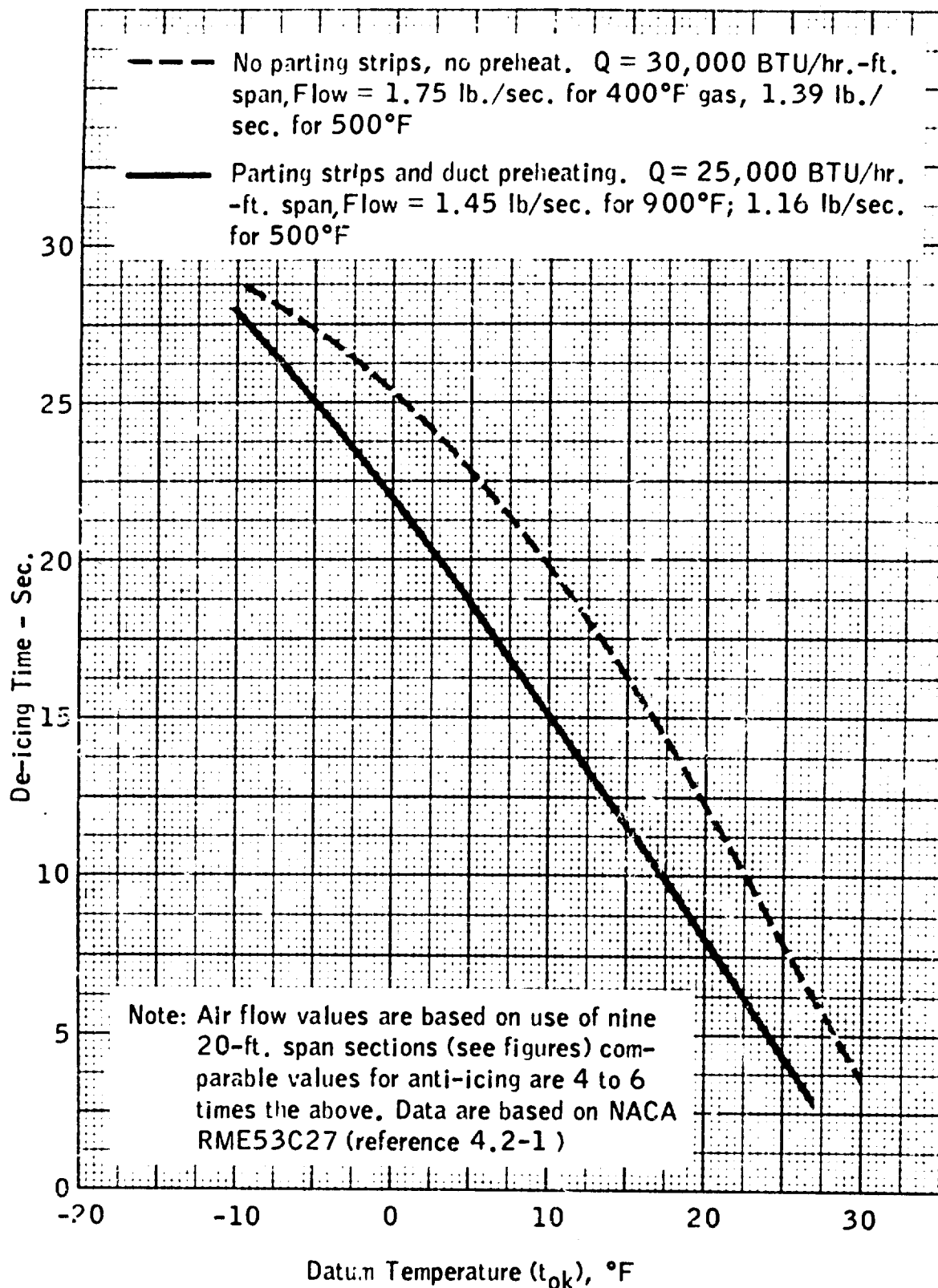
Figure 4.2-8. De-Icing Time Vs. Datum Temperature (t_{ok}) for Two Typical Hot-Gas De-Icing Systems
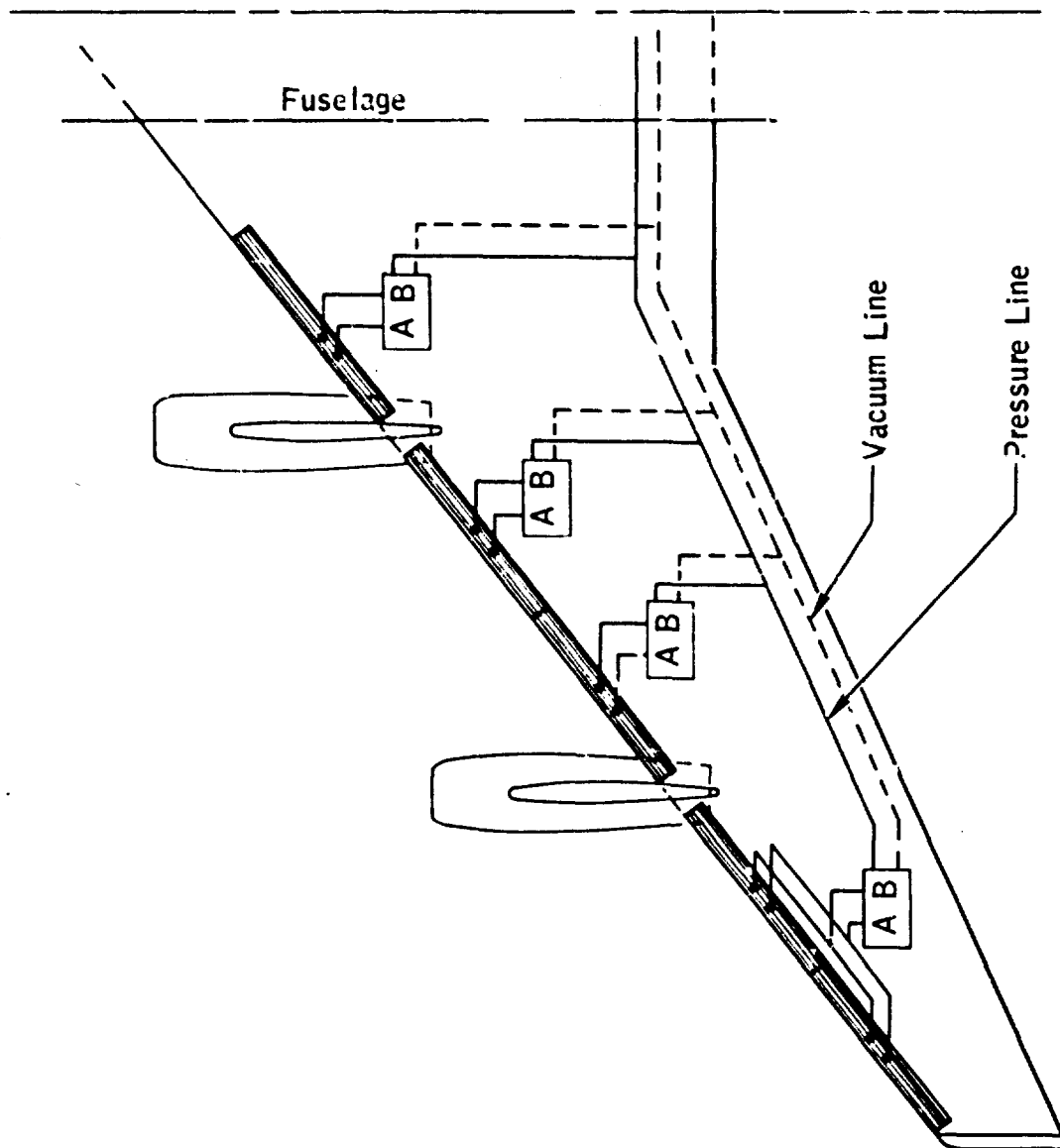
Figure 4.2-9   Wing Pneumatic Boot De-Icing System

Pressure Line

Vacuum Line

Vertical Stabilizer

Pressure Line
Vacuum Line

Horizontal Stabilizer
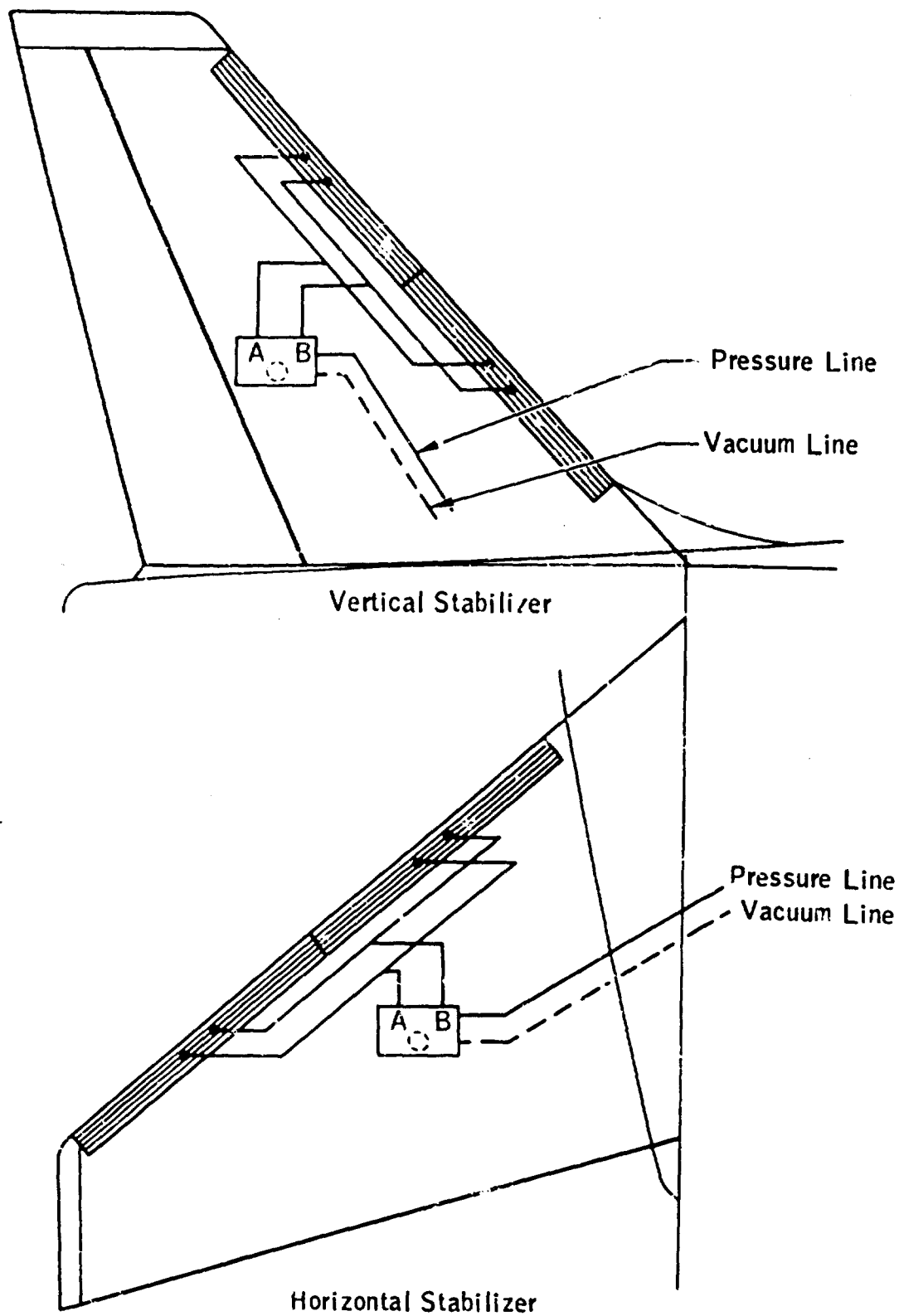
Figure 4.2-10. Empennage Pneumatic Boot System

Continuously Heated
Chordwise Parting Strips
(Typical 15 Places)

Cycled Shedding Zones
(Typical 12 Places)

Fuselage

Wing Station 725.4
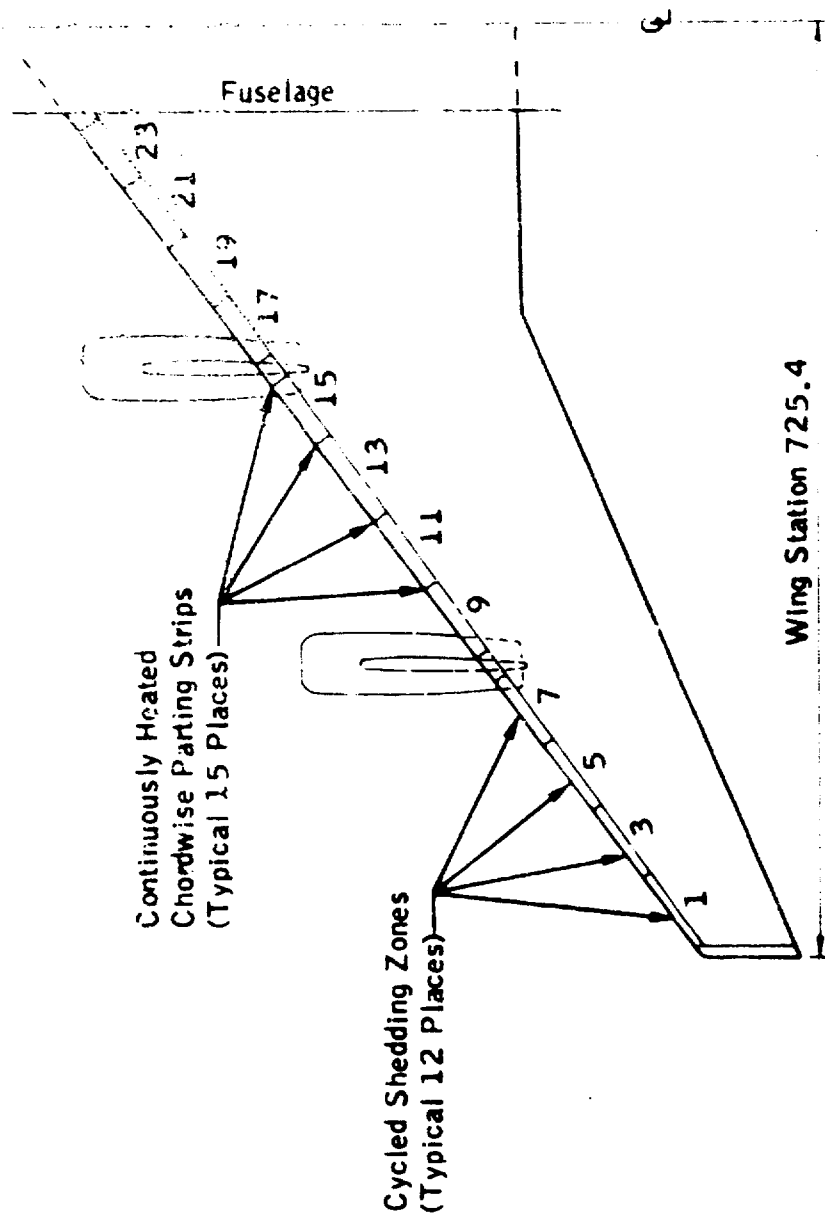
Cyclic Electric Wing De-Icing System

Figure 4.2-11

4.2-42
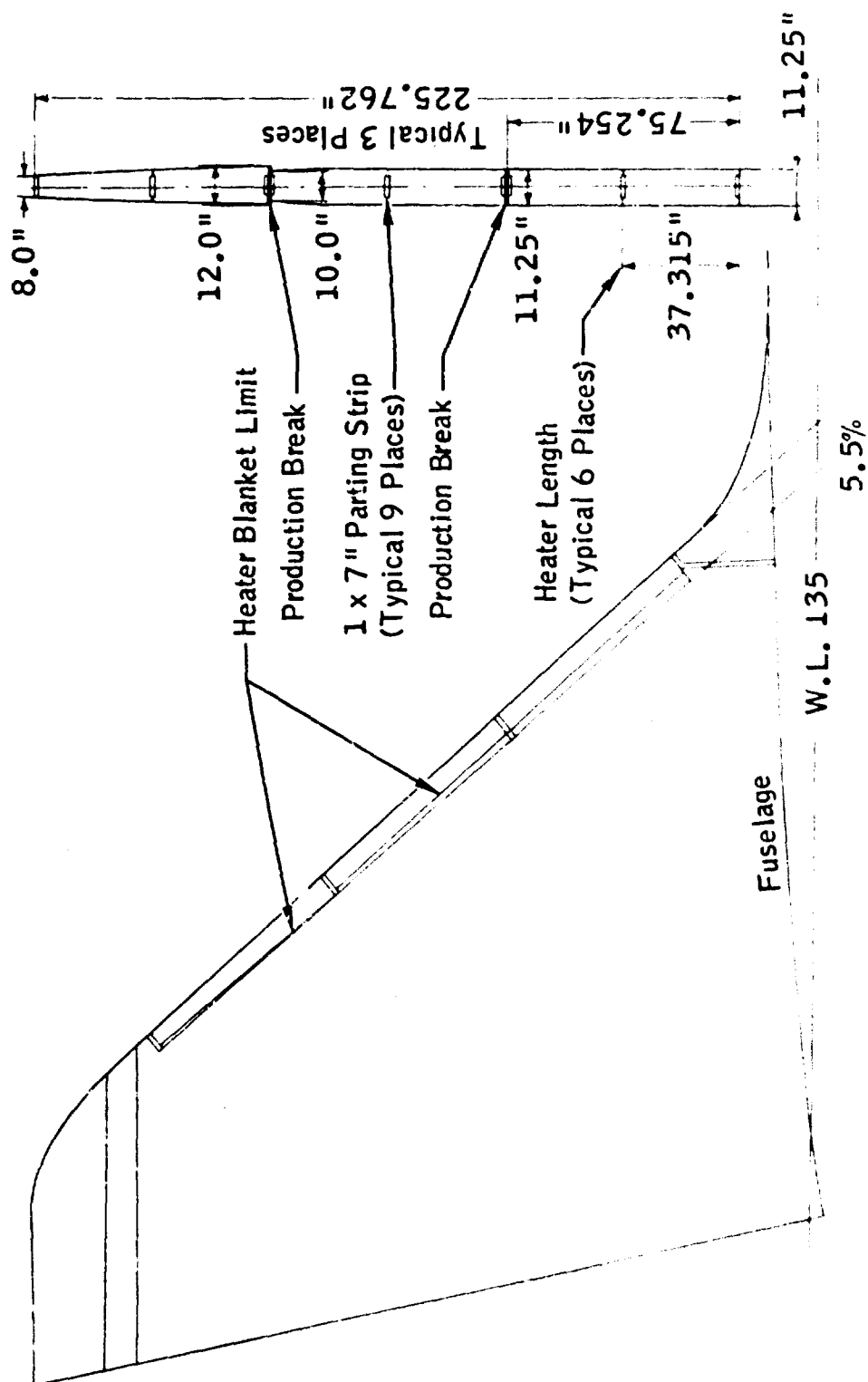
Cyclic Electric System, Vertical Fin of Aircraft D

Figure 4.2-12

Upper Surface

7.0"

10.5"

10.75"

Production Break

1 x 7" Parting Strip
(Typical 9 Places)

4.0"

Typical 3 Places

234"

Production Break

6.0"

Heater Length
(Typical 6 Places)

38.84"

78.0"

10.75"

Lower
Surface

Lower Blanket Limit

Upper Blanket Limit

Front Spar

10%
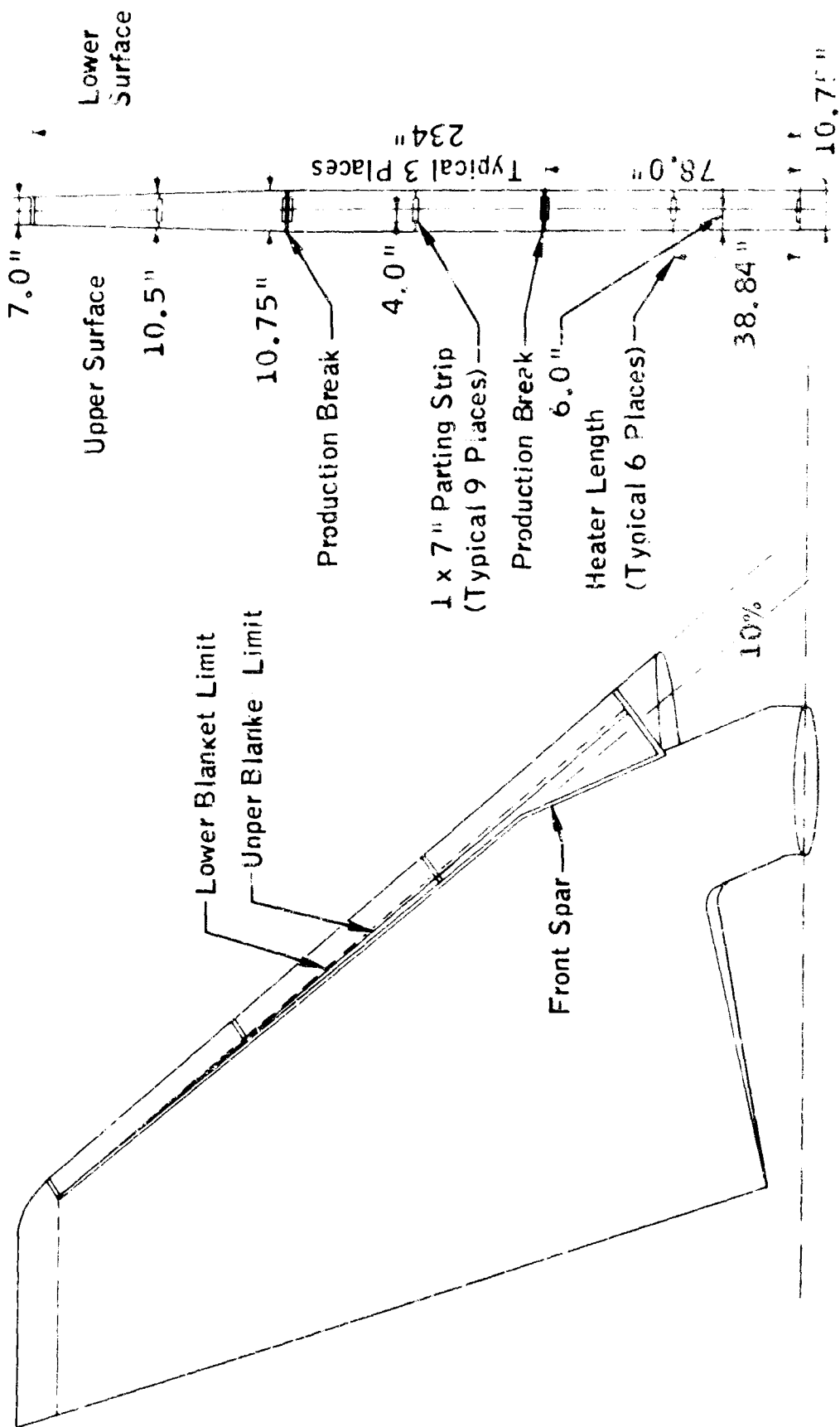
Cyclic Electric System, Horizontal Stabilizer

Figure 4.2-13

4.2-44

Cruise Condition – 20,000 Ft.
Chord – 10.83 Ft.
Thickness – 8.54%

20 Micron Droplet Size

40 Micron Droplet Size

Heater Limit

Heater Limit

Surface Distance in Inches Measured Parallel to Free Air Stream

Local Water Impingement Rate vs. Surface Distance From Zero Chord for Vertical Fin

Water Impingement Rate – Lb/Hr. Ft.^{2}

Figure 4.2-14

4.2-45

Fixed L.E. Rear Baffle

Fixed L.E. Rear Plenum

Slat Rear Plenum

Etched Gas Passage

Slat Piccolo Tube

Slat Spar

Slat Front Plenum

Fixed L.E. Front Plenum

Fixed L.E. Piccolo Tube

Etched Gas Passage

Fixed L.E. Front Baffle

Main Bleed Duct

Typical Wing Leading Edge With Slat

Figure 4.2-15

Typical Wing Leading Edge Flap

Figure 4.2-16

Approach Condition
V_o = 150 Knots
30 Min. Duration
Maximum Continuous Icing
Conditions

Air Direction

Ice
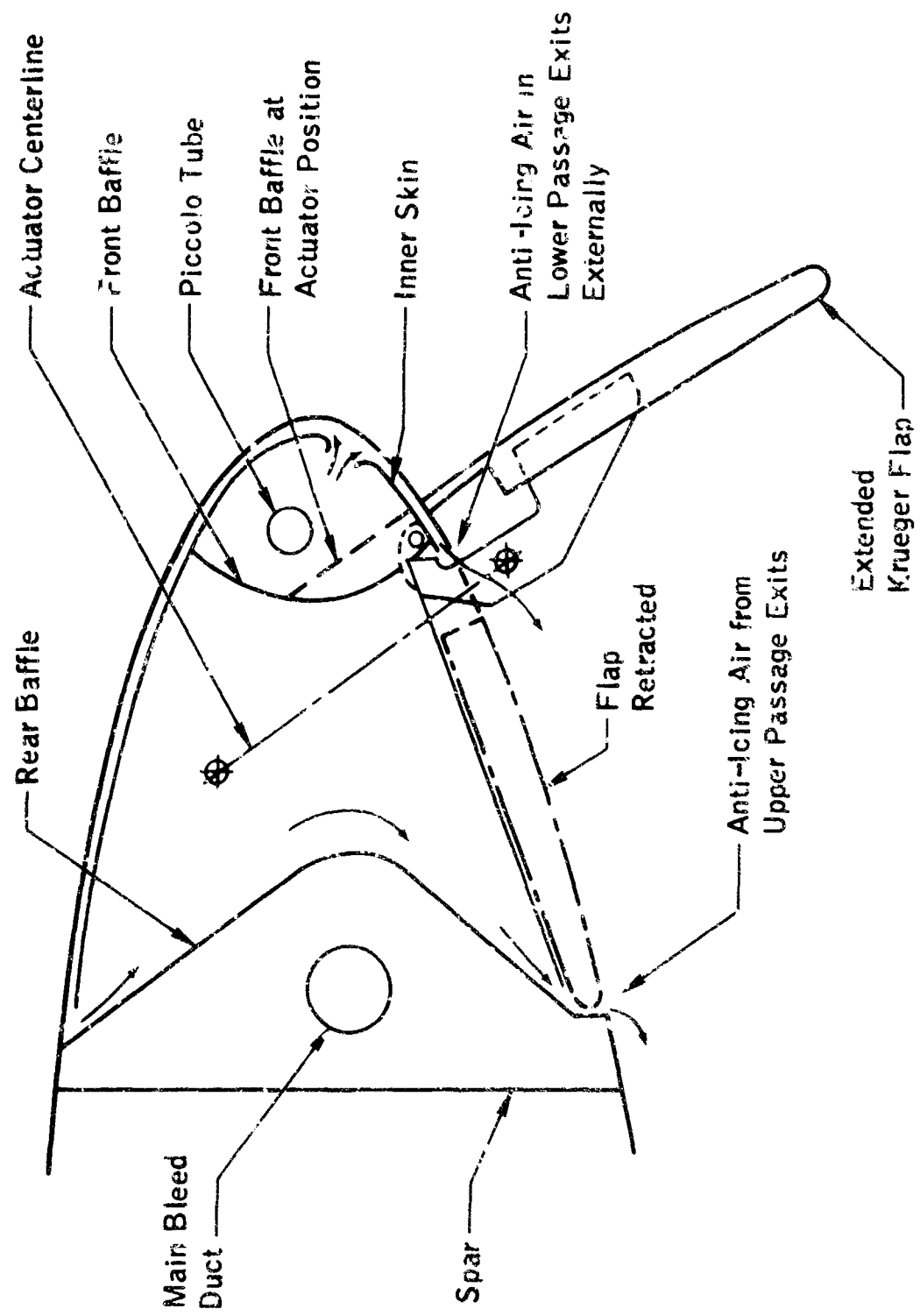
Extended Leading
Edge Flap
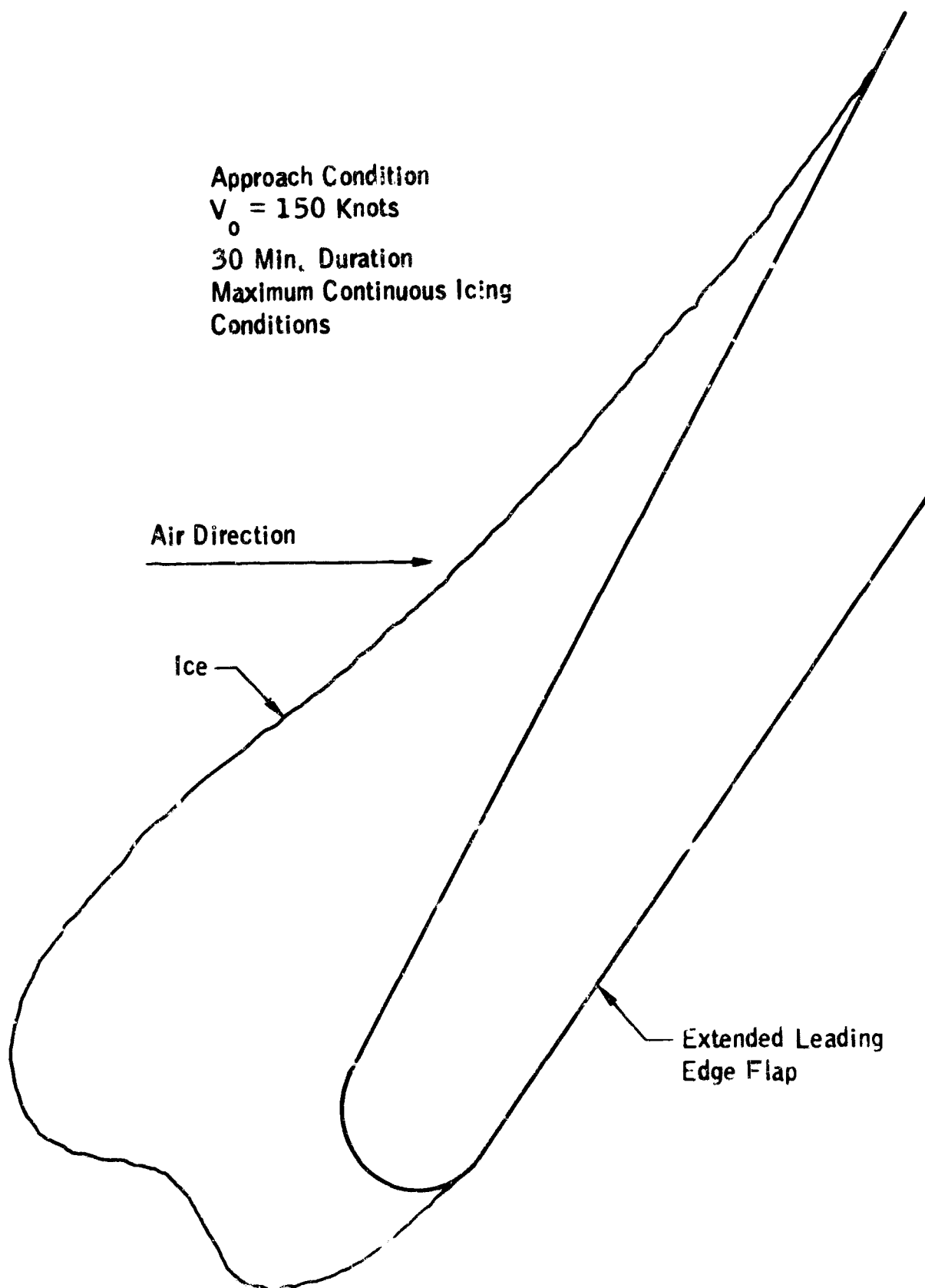
Figure 4.2-17. Ice Accretion on Unprotected Extended Leading Edge Flap
for Maximum Continuous Icing Conditions

4.2-48

1/2-in. Dia. Slugs on Inner Skin
After 0.040 Etching Operation

1/4-in. Dia. Holes
On 1/2-In. Centers

"D" Duct

Section A - A
Typical Double Skin
Arrangement

Piccolo
Tube

Exhaust Plenum
Overboard or to
Engine Inlet

Section A - A
Typical Single Skin
Arrangement

A

① Location of Six Anti-icing
Discharge Ports

Anti-Icing Air Inlet

Looking Aft
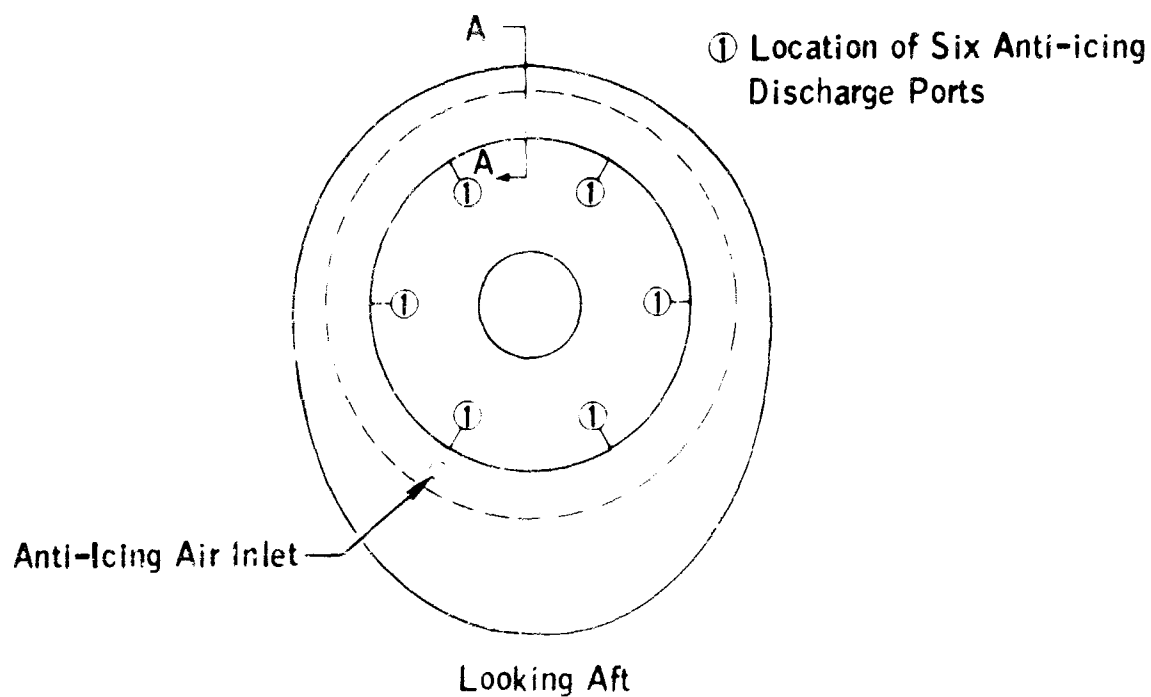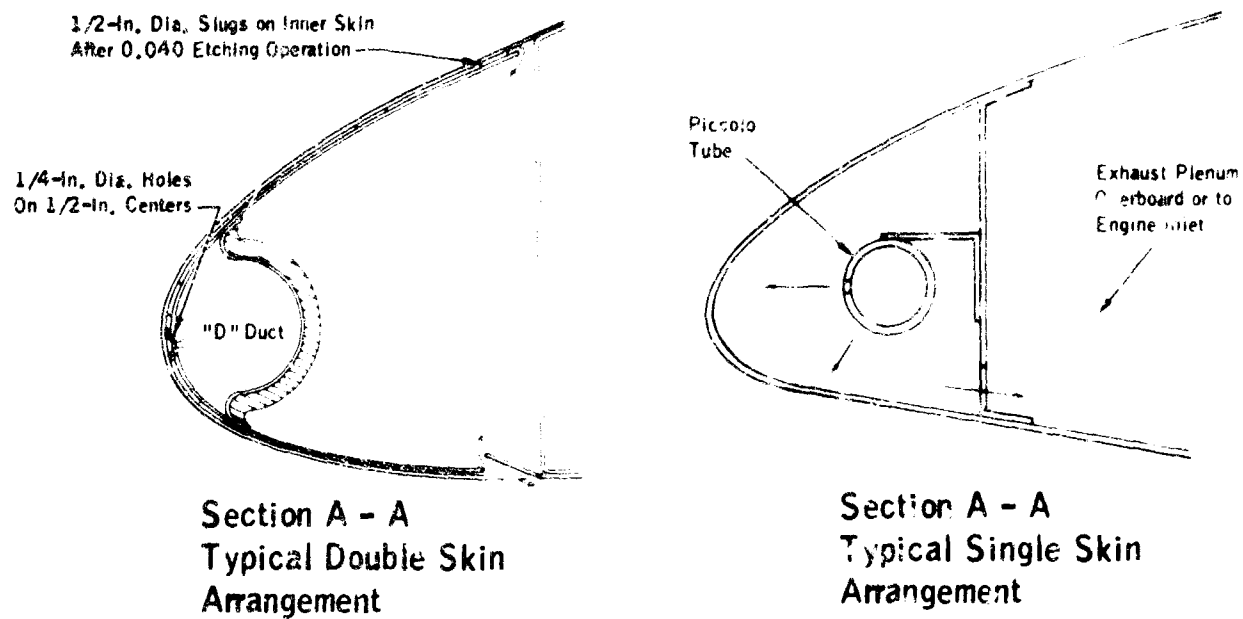
Figure 4.2-18. Typical Engine Inlet Lip Anti-Icing System
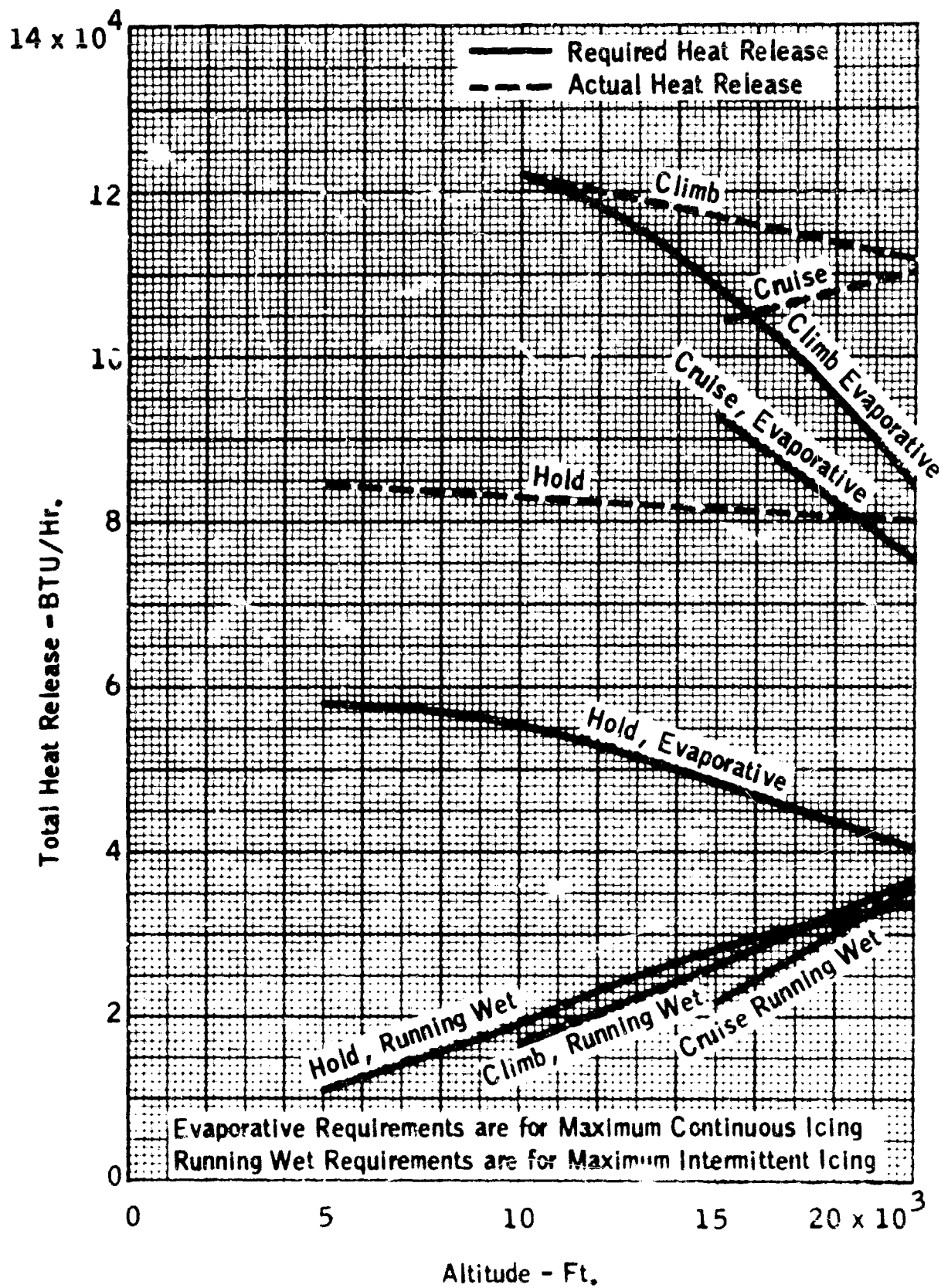
Figure 4.2-19. Typical Engine Inlet Lip Anti-Icing Heat Release Vs. Altitude

4.2-50
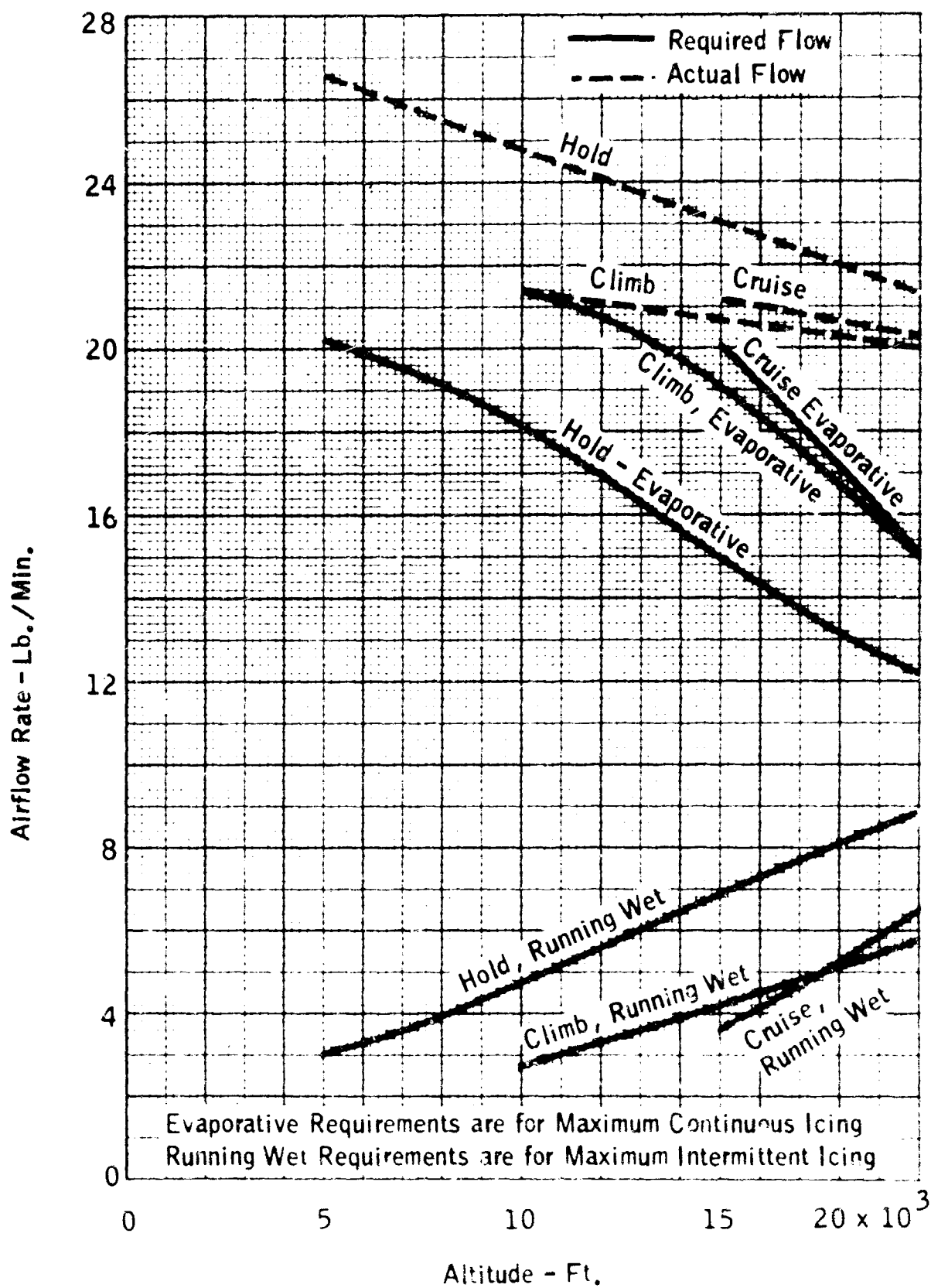
Figure 4.2-20. Typical Engine Inlet Lip Anti-icing Air Flow Requirements Vs. Altitude

Cross Section of Compressor Nose Cone Anti-Icing System
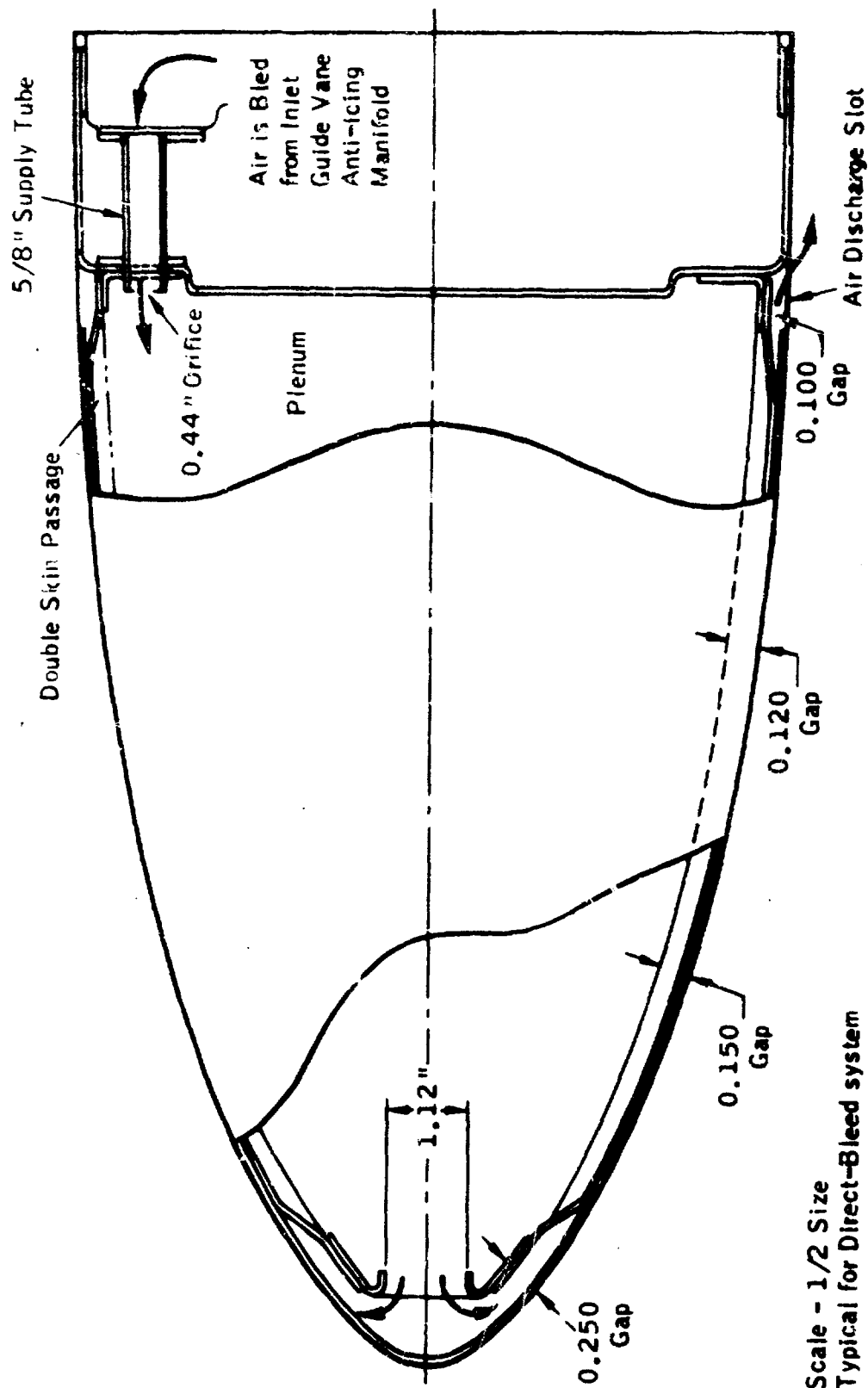
Scale – 1/2 Size
Typical for Direct-Bleed system

Figure 4.2-21
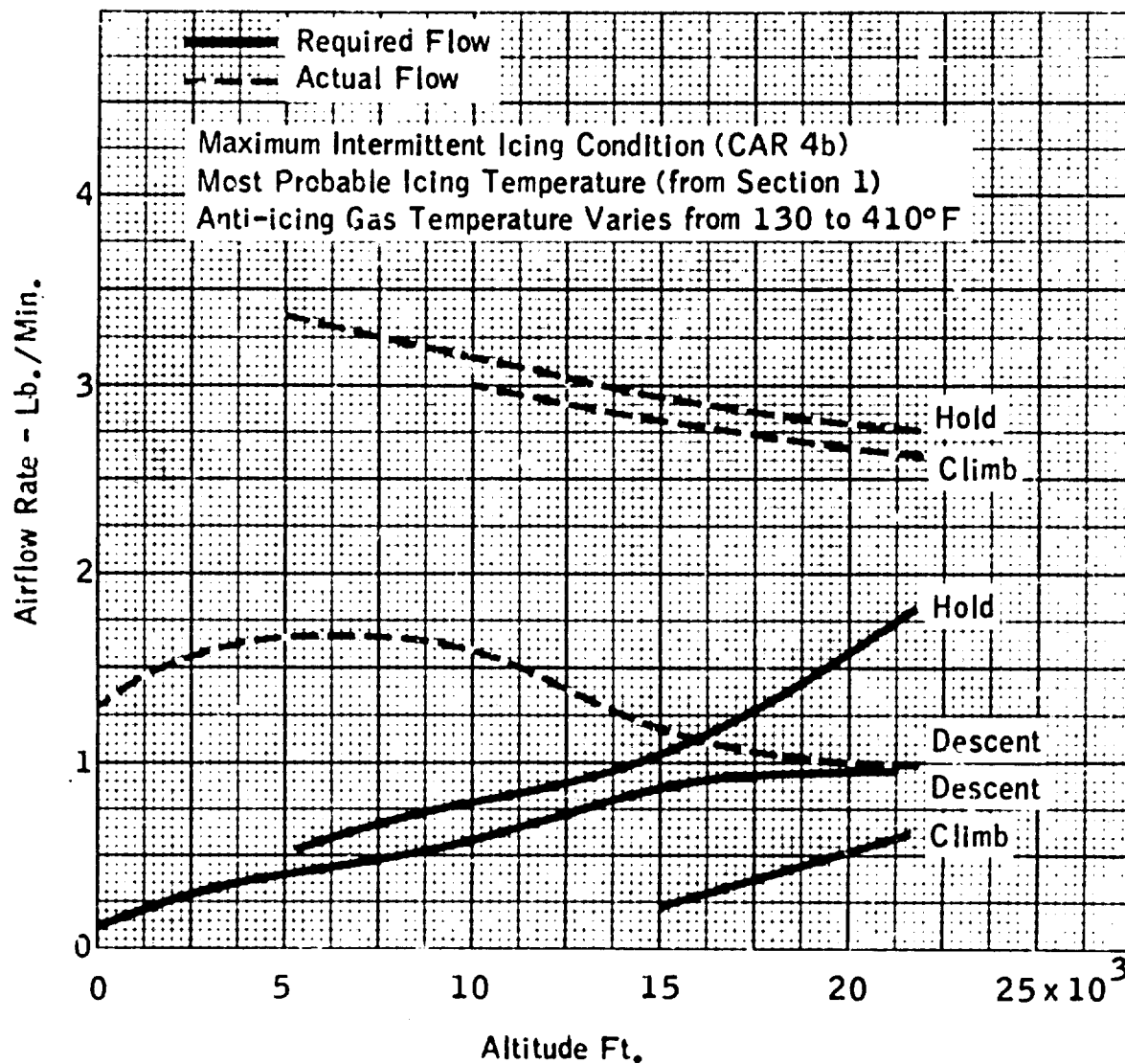
Figure 4.2-22.   Typical Air Flows for Compressor Nose Cone Anti-Icing System, Direct-Bleed Type

4.2-53

(a) Discharge at Rear

Compressor Face

Air from Inlet Guide Vane Discharge

(b) Discharge at Nose

Air from Inlet Guide Vane Discharge
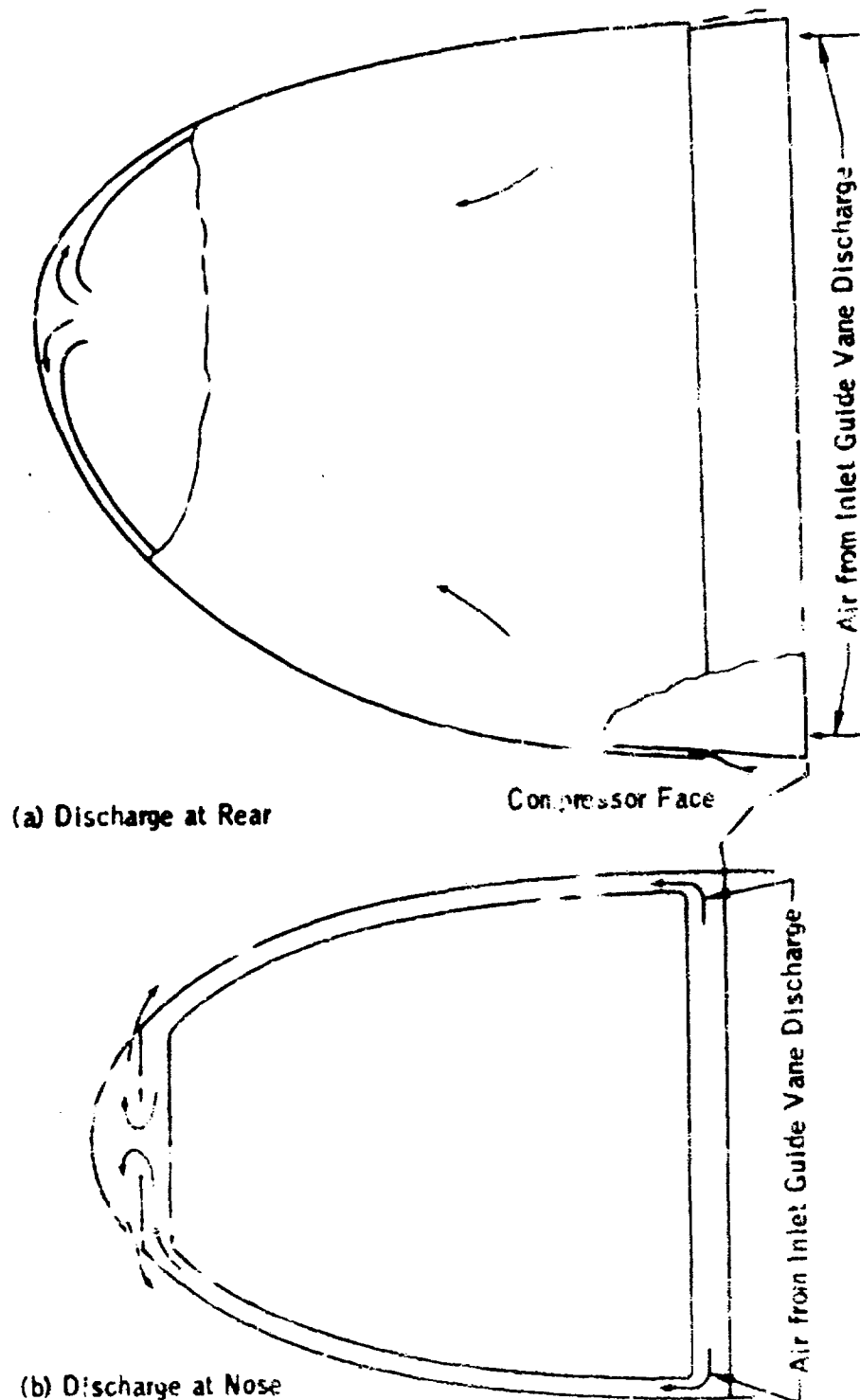
Figure 4.2-23. Two Flow Arrangements for Compressor Nose Cone Anti-Icing

4.2-54
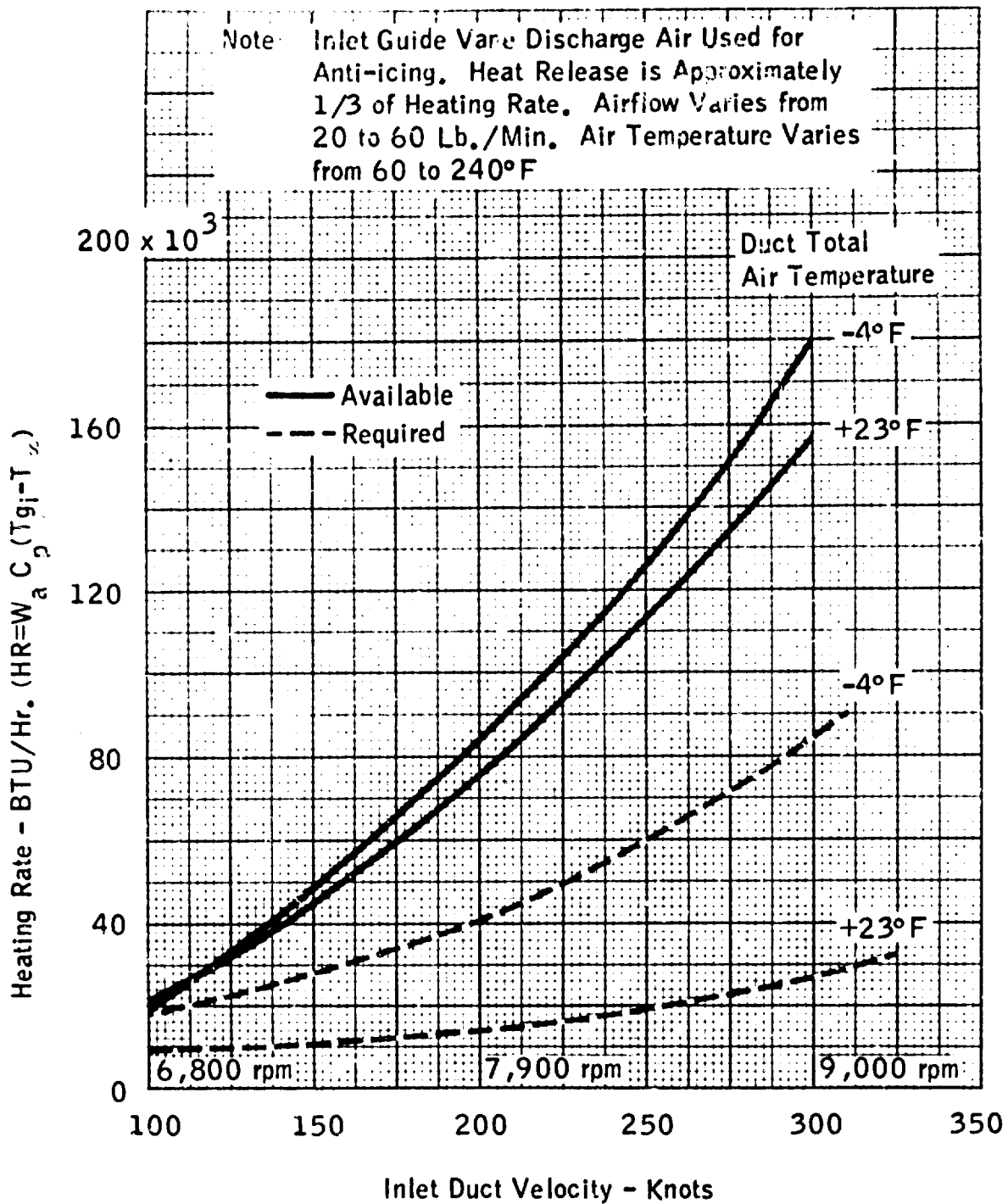
Figure 4.2-24. Typical Heating Rate Required and Available for Compressor Nose Cone

4.2-55
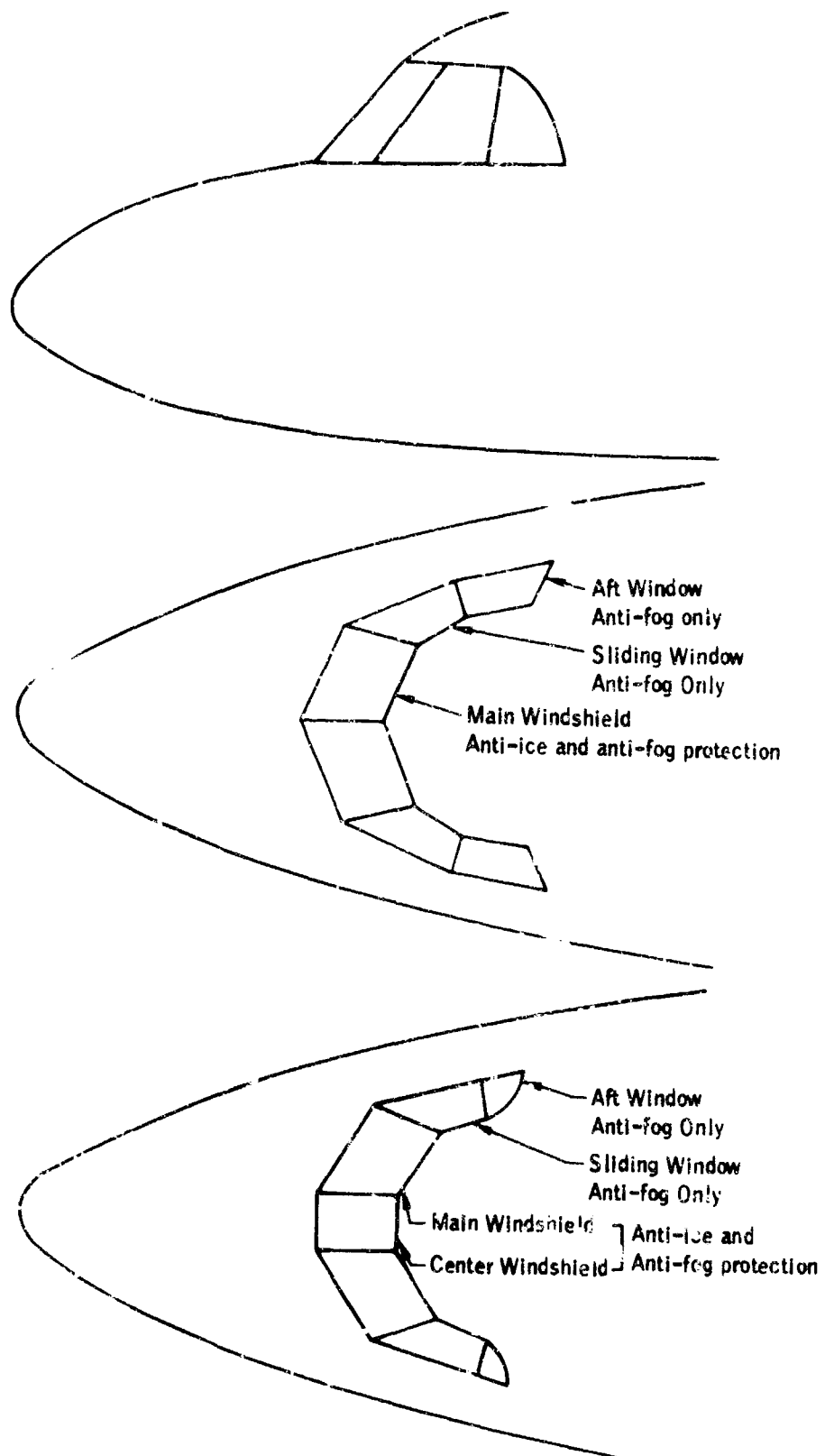
Figure 4.2-25. Typical Windshield Areas to be Protected for Two
Windshield Arrangements on Multi-Engine Transport

Bus Bar

Limits of Anti-ice
Coating Heated Area

Bus Bar
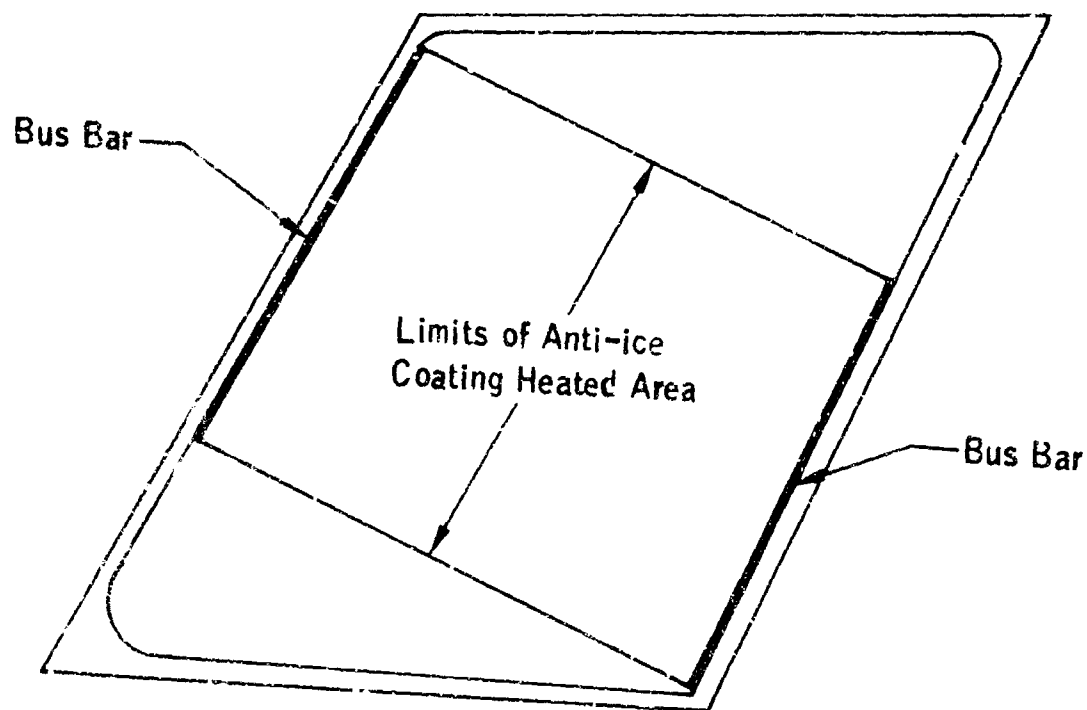
Note: Entire area of panel
protected by anti-fog
coating. Center wind-
shield similar, except
entire area had anti-ice
and anti-fog protection.
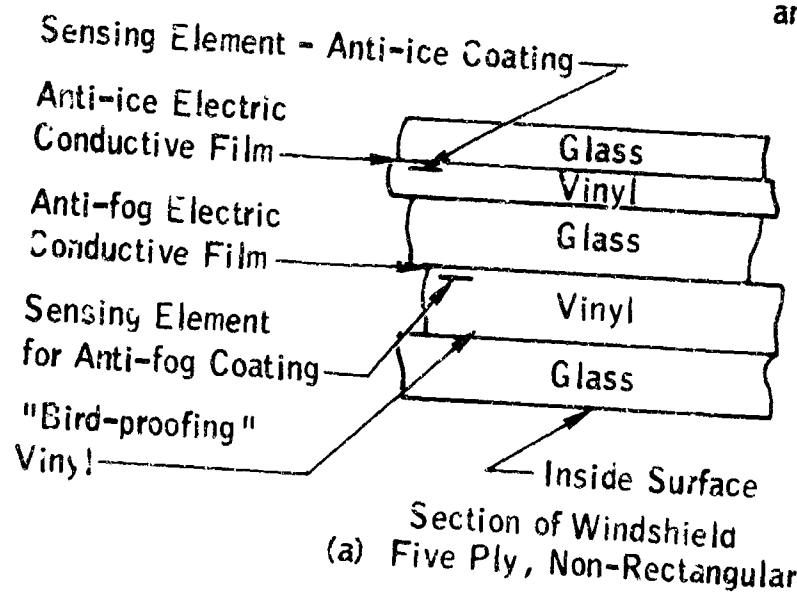
Sensing Element - Anti-ice Coating

Anti-ice Electric
Conductive Film

Anti-fog Electric
Conductive Film

Sensing Element
for Anti-fog Coating

"Bird-proofing"
Vinyl

Glass
Vinyl
Glass
Vinyl
Glass

Inside Surface

Section of Windshield
(a) Five Ply, Non-Rectangular

Figure 4.2-26. Typical Main Windshield Showing Construction and
Location of Conductive Films and Sensing Elements

Full Anti-ice Coverage

Bus Bar

Sensing Element
Anti-ice Heating Medium

Anti-ice surface

Glass

Vinyl

Glass

Inside Surface

(b) Three Ply, Nearly Rectangular

Figure 4.2-26. Typical Main Windshield Showing Construction and
Location of Conductive Films and Sensing Elements

Full Anti-ice and Anti-fog Coverage

Bus Bar

Sensing Element
Anti-Ice Heating Medium

Anti-ice Surface

Glass

Vinyl

Glass

Sensing Element
Anti-Fog Heating
Medium

Vinyl

Glass

Inside Surface

Anti-Fog Surface
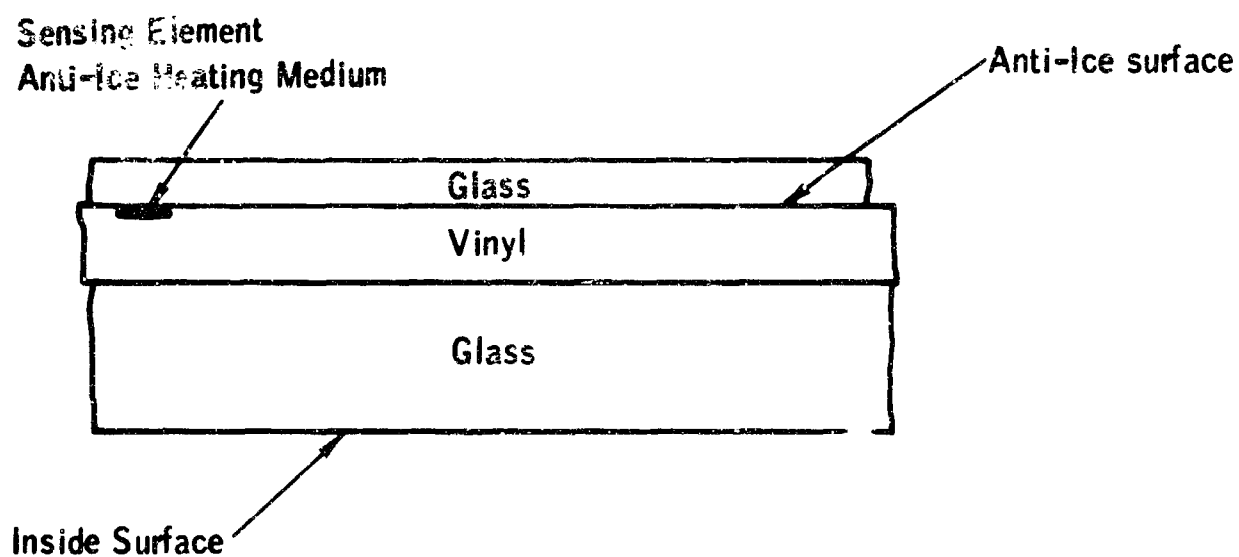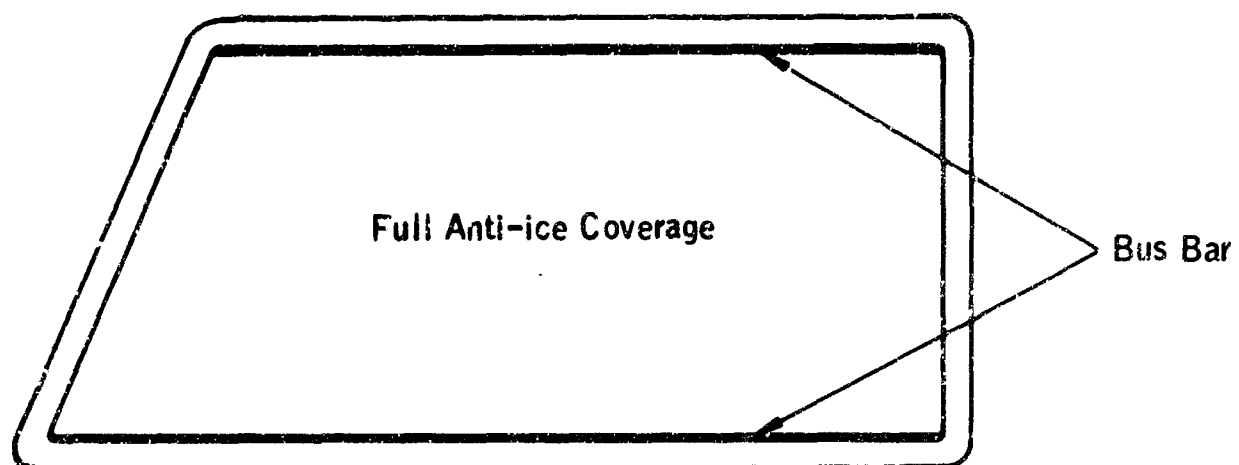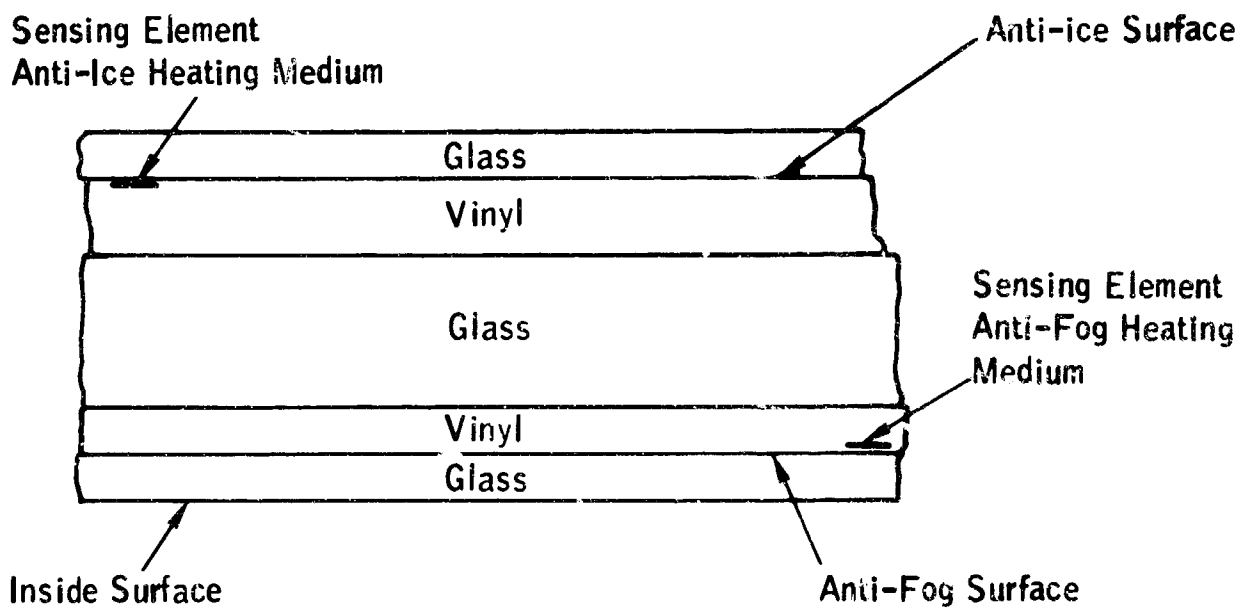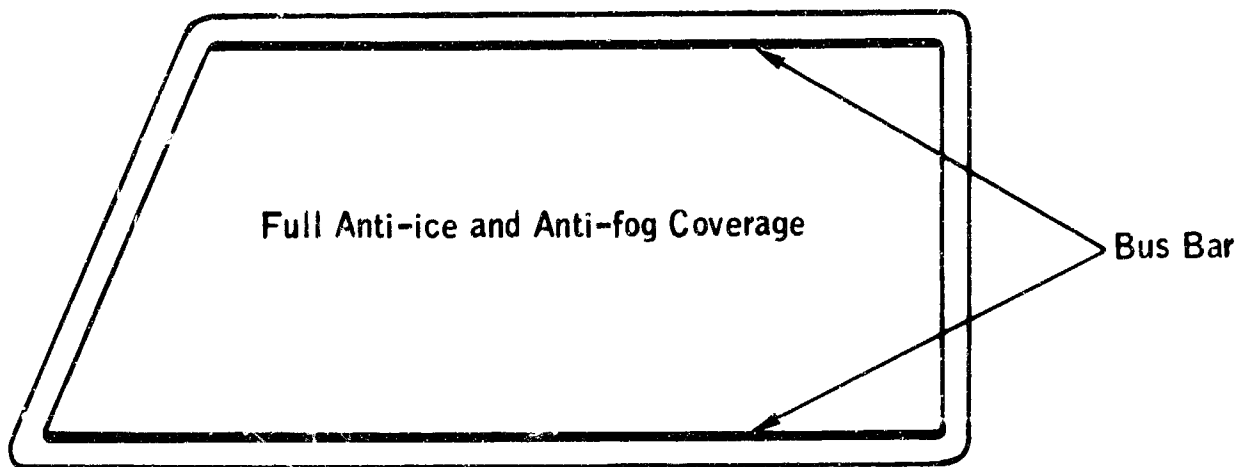
(c) Five Ply, Nearly Rectangular

Figure 4.2.26. Typical Main Windshield Showing Construction and
Location of Conductive Films and Sensing Elements
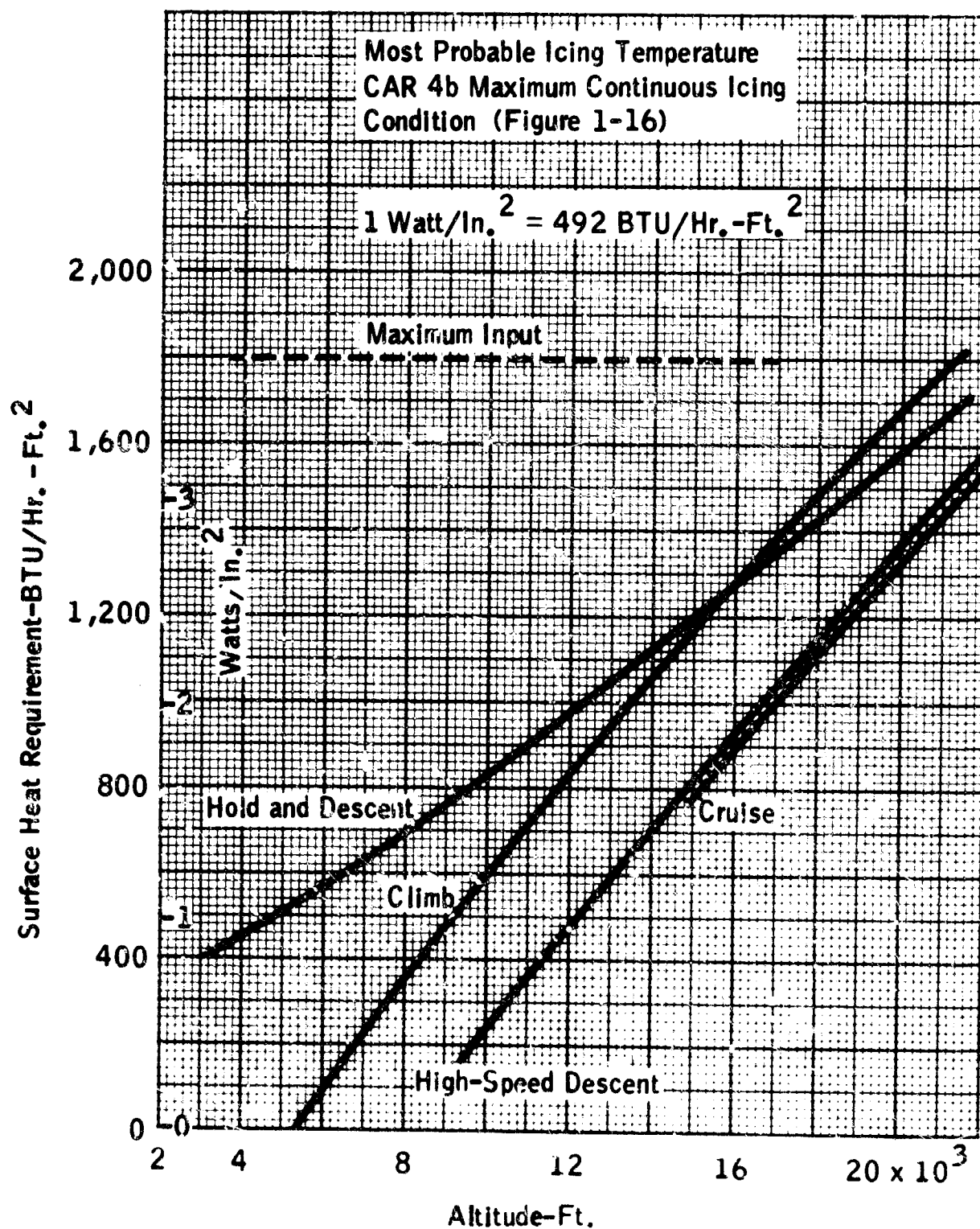
Figure 4.2-27. Typical Anti-Icing Heat Requirements Vs. Altitude for Center Windshield Panel

Number	Description
1	Check Valve
2	Regulator and Relief Valve
3.	Timer
4	Selector Valve
5	Suction Relief Valve
6	Ejector Nozzle
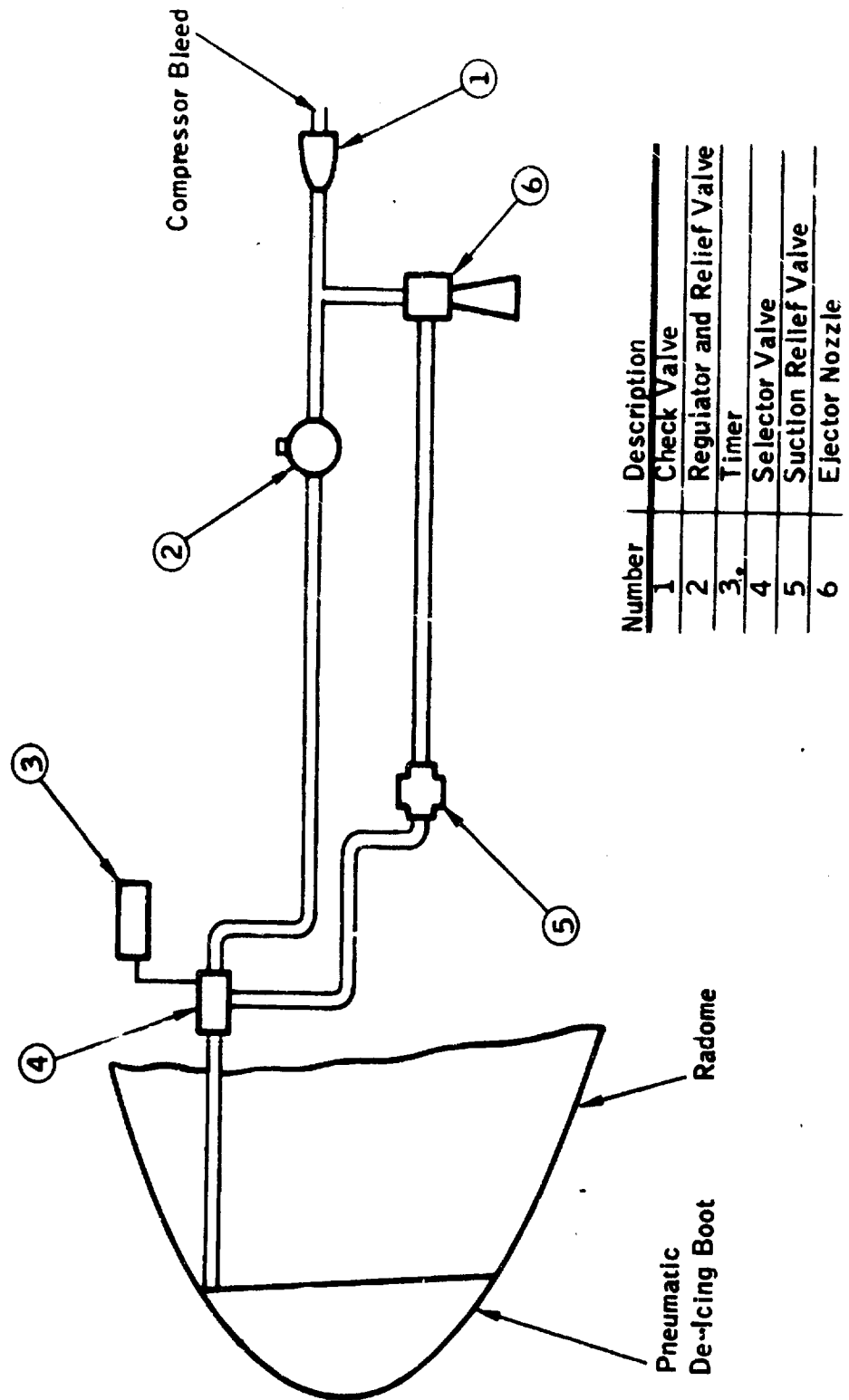
Pneumatic Boot De-Icing System for Nose Radome (Simultaneous Inflation)

Figure 4.2-28

4.2-61

Section A-A

Trim Line

End of Tube

24 In.

24 In.

Nominal Thickness
0.100 ± 0.010 In.

Nominal Thickness
0.200 ± 0.020 In.

Section B-B

A

A

B

B

Manifold Tube

W. L. 43.76

This Area Filled with 1-In. Tubes

Typical Nose Radome De-Icing Boot for Simultaneous Inflation

Figure 4. 2-29

4. 2-62

Overboard Dump

Outlet Manifold

Inlet Manifold

Ambient or Discharge Air

Valve

Bleed Air

1/2-in. Typical

Side View

Section A-A

Front View

Figure 4.2-30. Typical Hot-Air Anti-Icing System for Nose Radome
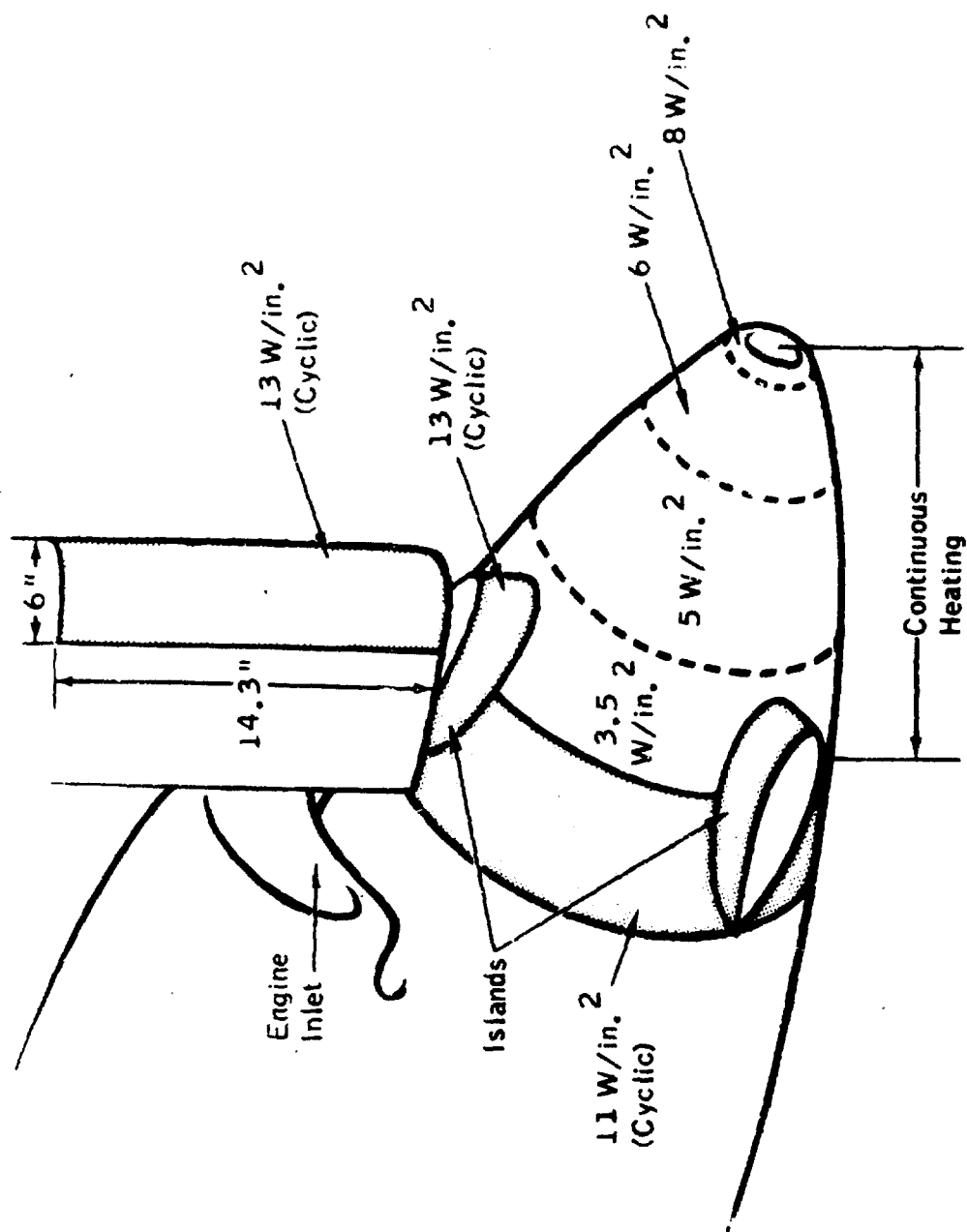
Typical Propeller and Spinner Ice Protection System for Turboprop Aircraft

13 W/in.^{2} (Cyclic)

13 W/in.^{2} (Cyclic)

6 W/in.^{2}

8 W/in.^{2}

5 W/in.^{2}

Continuous Heating

6"

14.3"

3.5 W/in.^{2}

Engine Inlet

Islands

11 W/in.^{2} (Cyclic)

Figure 4.2-31

45-Min. Hold At 5,000-Ft. Altitude

5.4 Sq. In.
Cross-Sectional
Area

2.5 In.

2.7 In.

2.7 In.

Vertical Fin
(At Mid Span)

4.8 Sq. In.
Cross-Sectional
Area

2.9 In.

1.3 In.

0.7 In.

Horizontal Stabilizer
(At Mid Span)
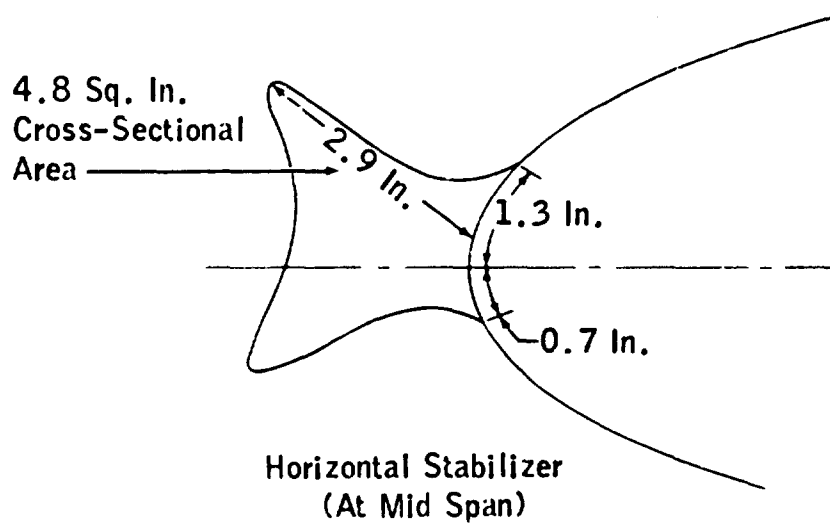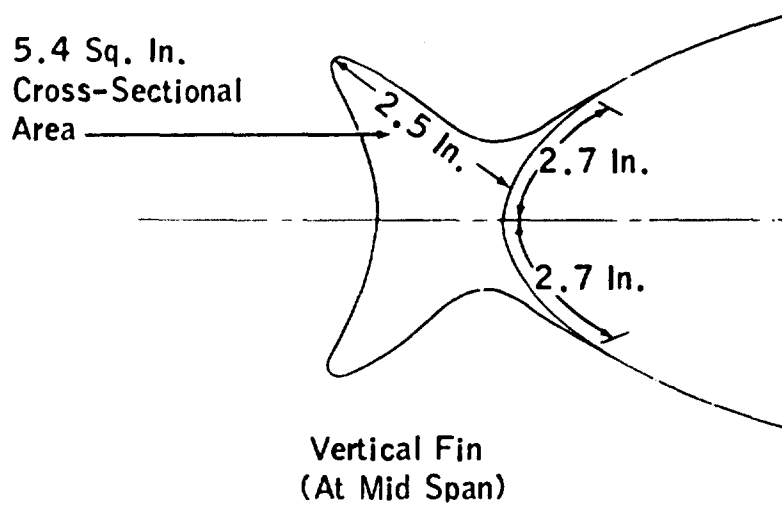
Figure 4.2-32. Typical Ice Shapes for Unprotected Tail of Aircraft D

4.3 APPLICATION TO HELICOPTERS

CONTENTS

LIST OF FIGURES

NOMENCLATURE

A Airfoil area, sq. ft.

C Airfoil chord length, ft.

C_L Coefficient of lift, dimensionless

D_d Droplet diameter, microns

F_M Collection efficiency, dimensionless

G	Per cent depressant in depressant-impinging water mixture
h	Airfoil projected height, ft.
h_a	Average heat transfer coefficient, BTU/hr.-ft.^{2}-°F
K	Inertia parameter, dimensionless
K_W	Surface wetness fraction, dimensionless
K_o	Modified inertia parameter, dimensionless
L	Lift, lb.
LWC	Liquid water content, gm/m^3
M_{ev}	Rate of evaporation of water, lb./hr.-ft.^{2}
M_W	Rate of water impingement, lb./hr.-ft.^{2}
n	Number of rotor blades
q	Heat transfer rate, LFU/hr.-ft.^{2}
r	Rotor station radius, ft.
Re,d	Droplet Reynolds number, dimensionless
S_U	Impingement limit on upper surface, ratio to chord length
S_L	Impingement limit on lower surface, ratio to chord length
t_o	Undisturbed free stream temperature, °F
t_s	Surface temperature, °F
U	Velocity, mph
V_o	Velocity, fps
W	Helicopter gross weight, lb.

W_β	Local water collection rate, lb./hr.-ft. span
W_F	Weight flow of freezing point depressant fluid, lb./hr.-ft.^{2}
W_M	Water catch rate, lb./hr.-ft. span
α	Angle of attack, deg.
β	Local collection efficiency, dimensionless
λ/λ_s	Droplet range ratio, dimensionless
μ	Air viscosity, slugs/ft.-sec.
ρ	Air density, slugs/ft.^{3}
Σ	Summation
τ_1 through τ_5	Temperature terms (NACA TN 2799), °F
ω	Rotational velocity, radians/sec.

4.3.1 SUMMARY

Ice accretion in relatively small quantities may create severe hazards to a helicopter. These hazards may be from excessive vibration caused by unsymmetrical self-shedding of ice from the main and tail rotors, from ice impact damage when self-shedding occurs or from the increase in airfoil drag when self-shedding does not occur. Methods of calculating rotor airfoil ice accretion rates are presented in this subsection, along with some referenced experimental data.

Two ice protection systems that have been developed and tested for helicopter rotors are described. The systems requirements and the results of the test programs are presented. Other rotor ice protection systems that have been investigated are described and the limitations of the systems discussed.

Additional areas of ice protection, such as windshield, engine inlets, essential instruments and rotor head mechanisms, are described and data presented.

4.3.2 INTRODUCTION

Helicopters with all-weather capabilities have been a development of recent years. The delay in all-weather development probably resulted from a lack of all-weather requirements for the helicopter. Improvements in weight-to-power ratios and increased use of the helicopter in the fields of search and rescue, passenger service, military operations, mail delivery, utility inspection and repair, and traffic control have created the all-weather requirements.

At first it was thought that vibration and centrifugal forces would prevent appreciable ice accretion on helicopter rotors. This was not the case--ice does accrete and the increased drag causes an increase in the power requirements of the helicopter. On small helicopters, the increase in airfoil drag may be sufficient to force the aircraft to land, while on larger helicopters the power increments may or may not be acceptable. When self-shedding does occur, it is usually asymmetrical, and this causes an unbalance that may result in severe vibration.

4.3-5

4.3.3 AREAS OF PROTECTION

The helicopter shown in Figure 4.3-1 is considered typical and will be used throughout this subsection to illustrate areas that may require protection.

The rotor on a helicopter is essentially a small-scale airfoil. Ice accretion on an airfoil will result in adverse aerodynamic effects caused by the distortion to the airfoil geometry. The magnitude of these effects will be greater on a small-scale airfoil because of a given thickness of ice represents a proportionally greater distortion to the geometry; further, the small-scale airfoil has a greater catch efficiency. Because of these considerations, the rotor blades on a helicopter will be far more critical than the wings of an airplane with respect to loss of efficiency due to the presence of ice.

Ice collection on the main rotor airfoils follows the usual airfoil collection patterns. From observation, it has been found that ice collection on the airfoil is confined to approximately 9 per cent of chord on the upper surface and approximately 22 per cent of chord on the lower surface (Ref. 4.3-1). This is illustrated in Figure 4.3-2; typical ice collection shapes are shown in Figure 4.3-3. In a spanwise direction, the ice protection system should begin at the inboard station where ice accululation is significant and extend to the point at which self-shedding will occur. Typical systems may extend from the root to 75 per cent span, or from 25 per cent span to tip; depending on rotor design, rotor rpm, and design icing conditions. Spanwise variation of ice accretion for a typical rotor is illustrated in Figure 4.3-3.

The tail rotor is similar to a light aircraft propeller in size and rotational speed. Its prime function is to counteract torque created by the main rotor; therefore, drag or loss of efficiency is not critical. The tail rotor may require ice protection to prevent large ice accumulations from self shedding and creating hazards to other components through severe vibration and flying ice particles.

Another area that normally will require ice protection is the windshield. Windshield ice accretion rates will vary with the mode of flight, windshield location, windshield shape and many other factors that make generalizations impossible. A windshield ice protection system should be designed for the most critical condition for the particular installation. An example of windshield icing during hover in freezing rain (with no protection system) is shown in Figure 4.3-4.

Other areas of a helicopter that may require ice protection are the rotor head mechanism, air inlets and essential instruments.

The rotor head mechanism is not likely to freeze up during flight or malfunction if the mechanism is actuated frequently. But, if icing is a hazard to the mechanism, then a simple windscreen or some de-icing system may be necessary. An example of rotor head icing is presented in Figure 4.3-5.

Propulsion system ice protection may consist of inlet screen anti-icing and turbine engine inlet anti-icing. On one flight test program involving a light, turbine-powered helicopter, the inlet screen iced in a waffle pattern and caused approximately 15 per cent air blockage. The total open area of the inlet screen was twice the engine inlet area; consequently the ice blockage did not affect the engine performance. This area ratio may not always be the case, and icing on an inlet screen may cause sufficient blockage to affect engine performance. Other inlet screens for compartment cooling, carburetor inlets, etc., may require ice protection.

Essential instruments which require air flow past a sensor will be affected by ice accretion and should be ice-protected. Static pressure ports should be located in an area free of ice accretion.

The degree of ice protection given any component will depend upon the available power and the critical nature of potential ice accretion.

4.3.4 ICE ACCRETION

The main rotor of a helicopter may be compared to the wing of a fixed-wing aircraft; it differs chiefly in that the air velocity across the rotor blade varies with the distance from the hub. In hover, the velocity varies from zero at the hub to a maximum at the tip. In forward flight, the tangential velocity near the hub on the retreating blade may be less than the forward flight velocity, resulting in a negative relative velocity on that portion of the blade. On the advancing blade, the relative velocity will be a summation of tangential velocity and forward flight velocity. Under these conditions, ice accretion — which is a function of velocity — will vary from the hub to the rotor tip (Ref. 4.3-1).

Ice accretion calculations are presented for the hover condition since it is the more critical. During hover, the rotor blade is nearly at its highest angle of attack and hover power requirements are exceeded only by vertical ascent requirements. To calculate the impingement limits and water catch, the following conditions are assumed. (These calculation techniques should be typical for helicopters of any size.)

Airfoil:	NACA 0015 (assumed constant from root to tip).
Chord (C):	12 in. (assumed constant from root to tip).
Rotor radius (r):	18.6 ft.
RPM at hover:	333 rpm.
Area of one rotor blade (A):	18.6 sq. ft.
Number of blades (n):	2
Helicopter gross weight (W):	2,300 lb.
Altitude	Sea level.
Ambient Temperature:	17° F (most probable icing temperature at sea level is 26° F. At 26° F much of the outer portion of span would be ice-free. See Figure 4.3-3.)

Droplet diameter

(D_d):   20 and 40 microns

LWC: 0.46 gm/m^3 (Figure 1-26; 20-micron droplet).

Air density (ρ):   0.00259 slug /cu. ft.

Air viscosity (μ): 0.350×10^{-6} slug/ft.-sec.

The 20-micron droplet diameter is assumed for water catch calculations; the 40-micron droplet diameter is assumed for impingement limit calculation.

The first calculations are for determining the lift of the rotor so that rotor angle of attack and airfoil projected frontal height may be determined:

$$L = W = 1/2 \rho V^2 C_L A n$$

The tangential velocity is a function of the rotor span station. To determine the lift, it will be necessary to integrate the expression with respect to span station (radius) from the rotor hub to the blade tip.

$$\partial L = 1/2 \rho V^2 C_L \partial A n$$

Converting velocity and area into terms of radius and rotational velocity

$$\partial L = 1/2 \rho (\omega r)^2 C_L (\partial r) C n$$

Rearranging terms:

$$\partial L = \left| n\ 1/2 \rho \omega^2 C_L C \right| r^2 \partial r$$

$$\Sigma \partial L = \Sigma \left| n\ 1/2 \rho \omega^2 C_L C \right| r^2 \partial r$$

$$L = \left| n\ 1/2 \rho \omega^2 C_L C \right| \int_o^r r^2\, dr$$

$$L = \left| n\ 1/2 \rho \omega^2 C_L C \right| r^3/3$$

Substituting in numbers and solving for C_L

$$C_L = \frac{(3)(2300)}{(0.00259)(0.1047 \times 333)^2 (1)(18.6)^3}$$

$$C_L = 0.340$$

Therefore, the angle of attack, α, is 5 deg. (from NACA Report No. 669 Ref. 4.3-2).

In practice, a helicopter rotor will probably not have a constant airfoil shape from the hub to the tip. In addition, there is twist to the blade that causes a change in angle of attack from the hub to tip. For purposes of illustration, however, the remainder of the calculations in this subsection will assume constant airfoil shape and angle of attack. These variables will ordinarily be considered in the calculations.

Droplet Reynolds number is determined by

$$Re,d = \frac{4.81\,(D_d)\,(\rho)\,(U)\,(10^{-6})}{\mu}$$

$$= \frac{4.81\,(40\ \text{microns})(0.00259\ \text{slug/cu. ft.})(U\ \text{mph})(10^{-6})}{0.350 \times 10^{-6}\ \text{slug/ft.-sec.}}$$

$$= 1.42\ U$$

Calculations of Reynolds numbers (etc.) on the rotor airfoil will be from a station 25 per cent of span to the rotor tip. Rotor tangential velocity vs span station is shown in Figure 4.3-6a. A plot of Reynolds number versus span station is presented in Figure 4.3-6b for the 20 and 40-micron droplets.

From the Reynolds number, the droplet range ratio, λ/λ_s, may be obtained from Section 2, Figure 2-6.

Inertia Parameter

$$K = \frac{1.705 \times 10^{-12}\,(D_d)^2(U)}{\mu\,(C)}$$

$$K = \frac{1.705 \times 10^{-12}\,(40\ \text{microns})^2(U)}{(0.350 \times 10^{-6})(1.0)}$$

$$K = 0.0078U$$

A plot of the inertia parameter versus velocity is presented in Figure 4.3-6c for the 20 and 40-micron droplets.

The modified inertia parameter is expressed as

$$K_o = K(\lambda/\lambda_s)$$

This parameter is plotted in Figure 4.3-6d.

Using a 15 per cent Joukowski airfoil, the limits of impingement for the upper and lower surface can be found from Figure 11 of NACA TN 3839 (Ref. 4.3-3) or from Section 2 of this report. The results are plotted in Figure 4.3-7.

The ratio of projected airfoil height to chord obtained from NACA TN 3839 (or Fig. 2-3) for a 15 per cent Joukowski airfoil at a 5.0° angle of attack is

$$h/C = 0.162$$

The collection efficiency can be estimated from Section 2 of this report. As collection efficiency, E_M, is a function of the modified inertia parameter, K_o, it will vary with span station. The results for this example are presented in Figure 4.3-8a.

Water catch is a function of velocity and collection efficiency, and is expressed as

$$W_M = 0.329 \ (U)(LWC)(h/C) \ (C) \ (E_M)$$

For this calculation, an LWC of 0.46 gm/m^3 will be used. This is determined from Section 1, Figure 1-26 for a 20-micron droplet diameter and 17°F temperature.

$$W_M = 0.0245 \ (U)(E_M) \ lb./hr.-ft. \ span.$$

A curve of water catch versus span station is presented as Figure 4.3-8b.

The determination of local water collection rate, W_β, along the line of β_{max} is illustrated by the following calculation using the previously given conditions.

4.3-11

Using the modified inertia parameters from Figure 4.3-6d, the local collection efficiency, β, is obtained from an extrapolation of Figure 9 of NACA TN 3839. The local water collection rate for β_{max}, therefore, is

$$W_{\beta_{max}} = 0.329\, \beta_{max}(U)(LWC)$$

$$W_{\beta_{max}} = 0.329\, \beta_{max}(U)(0.46\ gm/m^3)$$

The results of this calculation versus span station are from 11 lb./hr.-sq. ft. at span station 4.65 to 50.3 lb./hr.-sq. ft. at the tip.

Values of local collection rate can also be found for different chordwise locations on the airfoil and plotted versus distance from zero chord at each span station for the various droplet sizes. These curves will assist the designer in determining the chordwise extent to which ice protection is desired at each span station. As ice accretion is detrimental to helicopter performance, the ice protection will probably extend to approximately the 40-micron droplet impingement limits. These limits extend from 7 to 9.5 per cent of chord on the upper surface and from 29 to 35 per cent of chord on the lower surface, as illustrated in Figure 4.3-7.

The above calculations determine the rate and limits of water impingement on the rotor blade and as such are of value in determining the anti-icing requirements. However, because of kinetic heating effects, not all of this water catch is necessarily turned into ice. This heating, being a function of velocity, increases with span station and may, depending on ambient temperature, liquid water content, etc., result in some of the water catch flowing away from its immediate area of impingement and freezing to either side of the line of β_{max}, or may even result in some or all of the water catch being blown off the rotor blade before freezing (see ice formation at -2.5° C in Figure 4.3-3). Thus at temperatures higher than about -8° C no ice forms at the blade tip, and the spanwise extent of ice progressively decreases as the temperature increases

above this limiting value. Consequently, it is found that the rate of ice accretion (and hence ice thickness) at the line of β_{max} and the ice shape varies with span station in the manner shown in Figure 4.3-9, the curves of which were calculated for an equivalent cylinder having the same β_{max} as an NACA 0012 airfoil section of 16.4 in. chord. In practice, it has been found that the chordwise extent of icing on both the top and bottom of the blade actually diminishes rather than increases toward the blade tip, as shown in Figure 4.3-7; thus it is regarded that the anti-icing requirements based on the calculated extents, as in Sections 4.3.5 and 4.3.6 are conservative.

4.3.5 THERMAL ANTI-ICING PROTECTION REQUIREMENTS

To calculate the heat required for anti-icing the rotor airfoil, it will be assumed that ice protection will extend from 9 per cent chord on the upper surface to 35 per cent chord on the lower. The results will give a conservative figure in that the rotor does not have a constant angle of attack for full span and other factors will affect the ice accretion. Based on these figures, the wrap-around on the upper surface will be 1.08 in. and 4.20 in. on the lower surface — a total wrap-around of 5.28 in. This gives a protected area of 0.44 sq. ft. per foot of span.

Using the method described in Paragraph 3.5.2, the heat transfer coefficients for the airfoil may be calculated for several spanwise stations. An average value may then be selected for each span station, and a plot of the average heat transfer coefficient, h_a, versus span station can be made. Next, the water impingement rate, M_w, is calculated by dividing the water catch, W_M (Figure 4.3-8b) by the heated area per foot of span (0.44 sq. ft. per ft. of span).

These values for various span stations are used to enter Figures 3-18a and 3-18b to determine the anti-icing heat requirements.

An example for span station 12 would be:

Span Sta.	W_M	M_W	h_a	M_W/h_a	τ_4
12	3.33	7.57	80	0.095	8.5

$$\tau_3 = 1066 \, (M_W/h_a) + \tau_4 \qquad (M_W = M_{ev} \text{ for an evaporative system)}$$

$$\tau_3 = 109.8° \text{ F}$$

therefore $t_s = 84.3°$ F, from Figure 3-18b

$$t_s - t_o = 67.3° \text{F}$$

$$\tau_1 = 73.0° \text{F, from Figure 3-18a}$$

$$\tau_2 = 14.0° \text{F, from Figure 3-18a and velocity for span sta. 12}$$

$$\tau_5 = 0° \text{F (assuming local static pressure is equal to freestream pressure) Figure 3-18b}$$

$$\tau_4 = 8.5° \text{F}$$

The heat transfer rate is

$$q = h_a \left[\left(\tau_1 - \tau_2 \right) + K_W \left(\tau_3 - \tau_4 \right) + \tau_5 \right]$$

(K_W is assumed to equal 1.0 in the impingement area.)

$$q = (80 \text{ BTU/hr.-sq. ft.} ° \text{F})(73.0 - 14.0 + 109.8 - 8.5)$$

$$q = 12,824 \text{ BTU/hr.-sq. ft.}$$

or 5,645 BTU/hr. per foot of span.

The results for the full span are presented in Figure 4.3-8c.

From Figure 4.3-8c it can be seen that several difficulties may encountered in designing a hot gas anti-icing system for helicopter rotors. One difficulty lies in supplying the heat requirement of the rotor tip. Meeting the tip heat requirements may cause the gas temperatures at the rotor hub to be excessive. Corrosion may also be a serious problem if the use of exhaust gases is contemplated.

The heat requirements of Figure 4.3-8c also apply to an electro-thermal system. Ideally, an electro-thermal heating mat would have the power densities vary with the requirements. From a manufacturing standpoint, this may be impractical. An alternative is to divide the blade into sections of nearly equal total power requirements. Each section then would have a power density equal to the maximum power density required for any part of that section. For example, if each blade were divided into three sections each requiring the same total power, then the divisions might be:

a. From span station 4.65 to 10.7 with the power density requirements of station 10.7 uniform throughout. Total power requirements for this section then would be 31,000 BTU/hr.

b. From span station 10.7 to 15.1 with the power densities of station 15.1 uniform throughout for a 31,000-BTU/hr. total.

c. From span station 15.1 to 18.6 with the power density of station 18.6 uniform throughout for a total of 31,000 BTU/hr.

The power density for each section would then be:

a. Station 4.65 to 10.7 — 23.7 watts/sq. in.

b. Station 10.7 to 15.1 — 32.6 watts/sq. in.

c. Station 15.1 to 18.6 — 41.0 watts/sq. in.

The total for both blades would then be 54.5 kw. Also, the power density of each section may cause excessive temperatures at the inboard part of the section. Increasing the number of sections would (1) reduce the total power

required by bringing the stepwise power input curve closer to the power required curve, and (2) would reduce the possibilities of overheating. However, this would complicate the design and manufacture of the heaters and the power required would still be excessive.

4.3.6 FLUID ANTI-ICING PROTECTION REQUIREMENTS

An approximation of the amount of fluid required for anti-icing a rotor blade can be found from Equation 3.4.1 of Paragraph 3.4.2. This equation assumes perfect fluid distribution and if used with ambient temperature rather than datum temperature (see Figure 3-9) does not take into account the kinetic heating and evaporative effects, which will be quite prominent on the outer portions of the blades. But it can be used as shown in the following analysis to give a useful first estimate of the fluid requirements for a system designed to 0°F ambient temperature. The freezing point depressant fluid found best for use on rotor blades and commonly used on helicopters in the U. S. and the USSR is a mixture of 90% (by volume) of denatured ethyl alcohol and 10% glycerine. Using this fluid as an example, Figure 3-9 shows that the mixture of impinging water and anti-icing fluid that will depress the freezing point to 0°F is 30.5% (by weight) of the fluid mixture. The equation then becomes

$$W_F = \frac{30.5 \; M_W}{100-30.5} = 0.44 \; M_W$$

(This equation is based on 0°F ambient temperature, neglecting kinetic temperature rise and evaporation, and assuming ideal fluid distribution).

Since M_W is a function of span station, the fluid requirements also vary with span as shown in Figure 4.3-8d. Summing up the flow along the blade from 4.6-ft. radius to the tip and doubling the value for both blade requirements gives a total flow of about 39 lb./hr.

4.3.7 DESCRIPTION OF SYSTEMS

4.3.7.1 Anti-Icing Systems — The only anti-icing systems that have been developed for helicopters are fluid systems. References 4.3-1 and 4.3-4 give descriptions of some of these.

A typical fluid ice protection system schematic is presented in Figure 4.3-10. The components and weight of the system are comparable to that required for a light airplane. See Paragraph 4.1.4.1, Section 4. The main rotor may be divided into sections with each section having a supply tube connected to the main rotor slinger ring. Tube sizing or restrictions within the tubes may be used to control and balance the flow to each section. Figure 4.3-19 shows the effect of supply tube sizing in one test program.

When a fluid is distributed to a main rotor ice protection system, several forces are acting. One is centrifugal force which causes the fluid to flow from the slinger ring toward the rotor tip. Since the supply tubes are forward of the rotor axis, the centifugal force acting on the fluid in the tubes will have a chordwise component tending to force the fluid toward the leading edge. This component may be considered essentially constant for the full span.

Another force acting upon the fluid as it flows toward the tip is a Coriolis force. This is the force that accelerates the fluid tangentially as it moves radially out the blade. The more rapid the radial movement, the greater the Coriolis force. This effect is illustrated in Figure 4.3-11.

The variation in fluid flow rates shown in Figure 4.3-11 for the various tube sizes can be explained as follows: With a small tube, the flow is restricted and the fluid is expended from the first few inboard holes. As the tube size increases, the various forces are balanced in a manner as to give even distribution along the span. With the larger tube, some of the fluid will flow from the inboard holes. As the rest of the fluid is accelerated radially, the Coriolis

force exceeds the chordwise component of centrifugal force and no fluid will flow out of the leading edge. At the tip, where the fluid is decelerated radially, it again will flow toward the leading edge and out through the holes.

Ideally, the freezing point depressant fluid should wet the entire protected area. With a hole distribution system this is impractical (even with equal distribution of fluid through the holes), while it may be feasible with the porous metal distributor.

Using a hole distribution system, a multiple row of spanwise holes are necessary to accommodate the changes in rotor angle of attack. Spacing of the rows of holes should be kept to a minimum to reduce the ice formation between the rows, yet wide enough to span the variations in stagnation line. Figure 4.3-12 illustrates the variation of stagnation line on a typical helicopter and a suitable chordwise location of the distribution holes. Spanwise spacing of the holes should also be close enough to prevent ice formation between holes. Results reported in Ref. 4.3-1 indicate that a hole spacing of 1-3/16 in. gives satisfactory results. Closer spacing did not improve performance appreciably.

In these systems the fluid can be flowed continuously or it can be cycled. In the cyclic method the fluid is turned off for short periods (no more than 30 seconds) during the icing encounter to conserve fluid. During the time the fluid is off, the residual fluid left on the blade from the previous "on" cycle prevents ice from building up on the blade, both by depressing the freezing point and by preventing any ice that does form from adhering solidly to the to the blade. The system in Reference 4.3-1 uses a cycle of 30 sec. fluid on - 30 sec. off. This method is used instead of a continuous lower flow rate because good distribution of the fluid along the blade cannot be maintained at low flow rates.

4.3-18

Because of the slow reaction of a fluid system and the critical nature of ice accretion, certain operating techniques are recommended. Before entering icing conditions, the system should be turned on to wet the protected surfaces. This acts as an adhesion and freezing point depressant. Each succeeding "on" cycle should begin with the first sign of ice accretion. It has been recommended (Ref. 4.3-1 and 4.3-4) that two different flow rates be provided; one for initial wetting or light icing conditions and the other for severe icing. For a continuous fluid flow system a low and a high flow rate can be used. For a cyclic system either two different flow rates can be used or the system can be cycled on and off for light icing and run continuously at the same flow rate for severe icing.

Fluid (the alcohol-glycerine mixture previous mentioned) flow rates for the cyclic system tested in Reference 4.3-1 are 0.0503 lb./min.-ft. span for intermittent flow (30 sec. on 30 sec. off). For a 35-ft. span the intermittent flow rate would be about 1.75 lb./min. or a total of 53 lb./hr. For continuous flow the rate would be 106 lb./hr. Rates quoted in Reference 4.3-4 are 2.66 lb./min. (0.044 lb./min.-ft. span) preliminary flow and 3.9 lb./min. (0.065 lb./min.-ft. span) high flow for heavy icing conditions. This latter system was not cycled on and off.

4.3.7.2 DE-ICING SYSTEMS — Two types of de-icing system have been proposed for helicopter application: thermal and fluid freezing point depressant. Both systems to function effectively would allow a limited amount of ice accretion, then rapidly remove the ice with minimum runback ice formation.

With a thermal system, activating the de-icing cycle with too little ice accretion causes runback ice formation. Excessive ice accretion before de-icing increases the hazards of drag increase and vibration. With the fluid system, runback is not likely to form, but excessive use of fluid with very little ice accretion would be uneconomical. Permitting excessive ice formation before activation of the de-icing cycle causes the same hazards as the thermal system.

Because of its importance the Thermal De-icing System is described separately in Section 4.3.7.3.

A fluid de-icing system would function by applying a freezing point depressant fluid to the ice-airfoil interface, thus weakening the ice bond to the surface to permit aerodynamic or centrifugal forces to remove the ice. Fluid can be supplied to the blade surface by using a porous metal distributor (Ref. 4.3-5) or closely spaced holes along the stagnation line. However, it has been found on several helicopters that the hole distribution system is not effective in removing ice once an appreciable amount has built up on the blade. The fluid just makes narrow passages in the ice deposit and runs out through them while the other parts of the surface remain still covered with ice. A porous metal distributor should be more promising for de-icing applications because of its more uniform fluid distribution, but there are no test program results except for a note in Reference 4.3-4 that a porous metal distributor became clogged very rapidly.

Experimental investigations of thermal de-icing systems indicate that, depending on the particular helicopter, approximately 1/8 to 1/4-in. ice accretion at the midpoint on the rotor is the optimum thickness for shedding As it is impossible to observe ice build-up on the rotor, a remote icing indicator is desirable. Several such devices have been tested and are discussed in Section 5 of this report.

Several problems have been encountered in selecting a location for ice detection on a helicopter. The ice accretion rate on the rotors is more rapid than on other parts of a helicopter because of the rotor speed and shape. Mounting an ice detector on the fuselage would require a very sensitive instrument capable of detecting conditions that would cause rotor icing. Mounting a detector on the rotor where less sensitivity is required presents the problem of signal transmission through the rotor hub. The spanwise location of the detector on the

rotor blade is also a problem. Icing rates and ice shapes will vary with span on the rotor, depending upon the ambient temperature and LWC. This is illustrated in Figures 4.3-3, 4.3-9a and 4.3-9b. The midpoint of the rotor is usually selected as a compromise location for detector mounting since icing occurs there under nearly all icing conditions.

4.3.7.3 Thermal De-Icing System — Of the two sources of thermal energy — hot air and electricity — only electricity is currently in use for helicopter de-icing systems. Hot air has been considered and some development work has been performed, but, as yet, the system has not been put to use.

Electrical de-icing heating elements for helicopter application are similar to those described in Paragraph 3.6.1.1 of Section 3. The elements are either bonded to or built into the airfoil leading edge. The protected surfaces of the airfoil are divided into several shedding zones, which may be oriented either spanwise or chordwise as illustrated in Figures 4.3-13 and 4.3-14. No parting strips are necessary for rotor de-icing since centrifugal forces will normally remove the ice once the surface bond is broken. Only the spanwise system is currently in use.

Comparative tests of spanwise and chordwise elements were conducted by the National Research Council of Canada. Results are reported in Ref. 4.3-6. Both systems were reported to be effective in removing ice. A direct comparison of specific energy requirements of each zone orientation is presented in Figure 4.3-15. From the standpoint of power, there is a distinct advantage in chord-wise orientation, particularly at lower temperatures. From the standpoint of design simplicity and control, the spanwise zone orientation has the advantage. Consequently, zone orientation may be left to the discretion of the designer.

Several test programs have been conducted with electro-thermal de-icing systems. Ref. 4.3-7, 4.3-6 and 4.3-1 are typical of these programs. Some

of the results of these tests are presented in Figures 4.3-15 through 4.3-17. There is some variation in these results caused primarily by the differences in heater construction. Additional results appear in Figures 4.3-18 through 4.3-20.

Some conclusions and recommendations resulting from the test programs were: That a power density of 25 to 30 watts per sq. in. be used for the heating elements and that close control of both accretion time and heat-on time be exercised.

To illustrate the power requirements of a de-icing system, the helicopter of previous examples will be again used. The same total area will be considered protected using spanwise elements as shown in Figure 4.3-13. If the blade is divided into four spanwise elements with power densities of 30 watts per sq. in., then each element will require approximately 6.75 kw of power. For symmetrical shedding, the power requirements of the two blades will be 13.5 kw. The total power requirement of the helicopter will, therefore, be approximately 16 kv (2.5 kw windshield anti-ice requirement).

4.3.8 MISCELLANEOUS ROTOR ICE PROTECTION SYSTEMS

A pneumatic boot ice protection system has been proposed for helicopter application, but to date has not been used; consequently, its effectiveness is unknown. Each blade was to be divided into two or more spanwise shedding zones with the shedding to be accomplished in a symmetrical manner. Spanwise tubes would be used because the small radius of the rotor leading edge would render chordwise tubes ineffective.

From the standpoint of weight and power requirements, a pneumatic de-icing system appears attractive; however, several difficulties may oe encountered in use. Ice accretions on a fixed-wing aircraft with a pneumatic system should be permitted to reach approximately 1/4 to 3/8 in. for clean, effective

shedding. On a helicopter, the maximum desirable ice accretion before shedding may be 1/8 to 1/4 in., depending on sensitivity of the rotor to ice accretion. The effectiveness of a pneumatic system with such light accretion is questionable. Pneumatic boots on a helicopter rotor would be much more vulnerable to erosion from dust. rain, etc. than on a conventional aircraft, particularly the outer part of the span; accordingly, repairs and replacement would be more frequent. The performance of the airfoil with tubes inflated should be investigated to ensure that the tubes do not create a greater performance loss than the accreted ice.

Another method of protecting rotors that has been attempted without success is covering the rotor leading edge with a water repellent material such as certain fluorocarbon plastics. Although the ice bond to these materials is less than with conventional rotor materials, ice does accrete and self-shedding occurs, usually unsymmetrically, and causes vibration. These materials are also more vulnerable to erosion.

As noted previously in section 2.8.1 silicone base ice adhesion depressant coatings have been found useful (but for limited time periods) for aircraft propellers, and may prove useful for rotors also. If centrifugal forces are great enough, shedding may be satisfactory. Air and rain erosion of the coating severely limit its useful life. Current aircraft standards call for renewing such coatings every 48 hours, or every 8 hours when rain is encountered.

4.3.9 PROTECTION OF WINDSHIELDS AND MISCELLANEOUS COMPONENTS

As stated previously, the wide variety of flight modes and variations in windshield sizes, shapes and installations make generalization of windshield ice protection requirements virtually impossible. A helicopter with a cruise speed of 150 mph would require a windshield power density of 3.15 watts/sq. in. according to MIL-T-5842A (Ref. 3 9). The MIL-T-5842A requirements are usually conservative for most applications. Fluid systems may also be used and would be similar to the systems described in Section 4.1.4.2 and Section 3.4.

If the most critical flight mode is known and the approximate air velocity across the windshield can be determined, then MIL-T-5842A may be used to determine the required power density. The power density requirements may also be determined by using the technique illustrated in Paragraph 4.1.4.2, Section 4.

Tail rotor ice protection is essential to prevent ice accretion and self-shedding that may result in dangerous vibration or damage from flying ice particles. The tail rotor is very similar in size and rpm to a CAR-3 airplane propeller. Protection may be provided using either thermal or fluid ice protection. Ice adhesion depressant coatings may also be considered, if the maintenance aspect is not objectionable. De-icing is adequate if the ice is shed frequently and symmetrically. Frequent shedding is required because of the high water collection efficiency or ice collection efficiency of the tail rotor and the greater tendency to self-shed. Calculations of propeller de-icing requirements are presented in Paragraph 4.1.4. These calculations are also applicable to the tail rotor.

Engine inlet screens, as well as other air inlet screens, on a helicopter prevent debris ingestion during low-level and ground operations. The inlets are normally large enough that air flow through the screens will be a low velocity. With the air flow velocity and direction of relative wind known, preliminary calculations may be made of ice protection requirements. These requirements should be verified by testing, as other factors may influence ice accretion on the screens.

For turbine-powered helicopters, the engine inlet ice protection requirements may be calculated using the meteorological conditions at the inlet. Each installation may have additional factors affecting the icing potential — curved ducts, screens, cavities, etc. The effects of such factors on the air before it

reaches the engine must be determined before calculations can be made of ice protection requirements. Refer to Paragraphs 4.1 and 4.2 for inlet anti-icing.

REFERENCES

4.3-1. Bell Helicopter Company Report No. 529-099-001, Ice Protection Systems for Helicopter Rotors," J. F. Van Wyckhouse, August 1961.

4.3-2. NACA Report No. 669, "Airfoil Section Data as Affected by Support Interference and other Corrections.

4.3-3. NACA TN 3839, "Experimental Droplet Impingement on Several Two-Dimensional Airfoils With Thickness Ratios of 6 to 16 Per Cent," Gelder, T. F., Smyers, W. H. Jr., and Von Glahn, U. Dec. 1956.

4.3-4. "Some Problems of Aircraft and Helicopter Ice Protection," O. K. Trunov and R. H. Teneshev (paper presented at 1961 Aircraft Ice Protection Conference, D. Napier & So. Ltd.), May 1961.

4.3-5. "Fluid De Icing," D. C. Tanner (paper presented at 1961 Aircraft Ice Protection Conference, D. Napier & Son Ltd.), May 1961.

4.3-6. NRC (National Research Council of Canada) Report No. LR-270, "A Comparison Between the Spanwise and Chordwise Shedding Methods of Helicopter Rotor Blade De-Icing," J. R. Stallabrass and G. A. Gibbard, January 1960.

4.3-7. NRC (National Research Council of Canada) Report No. LR-263, "Flight Tests of an Experimental Helicopter Rotor Blade Electrical De-Icer," J. R. Stallabrass, November 1959.

4.3-8. "Canadian Research in the Field of Helicopter Icing," J. R. Stallabrass (paper presented to the Helicopter Association of Great Britain), August 1961.

Figure 4.3-1   Typical Helicopter

	Upper Surface	Lower Surface
Total Ice Impingement	9%C	22%C
Main Body of Ice	7%C	10%C
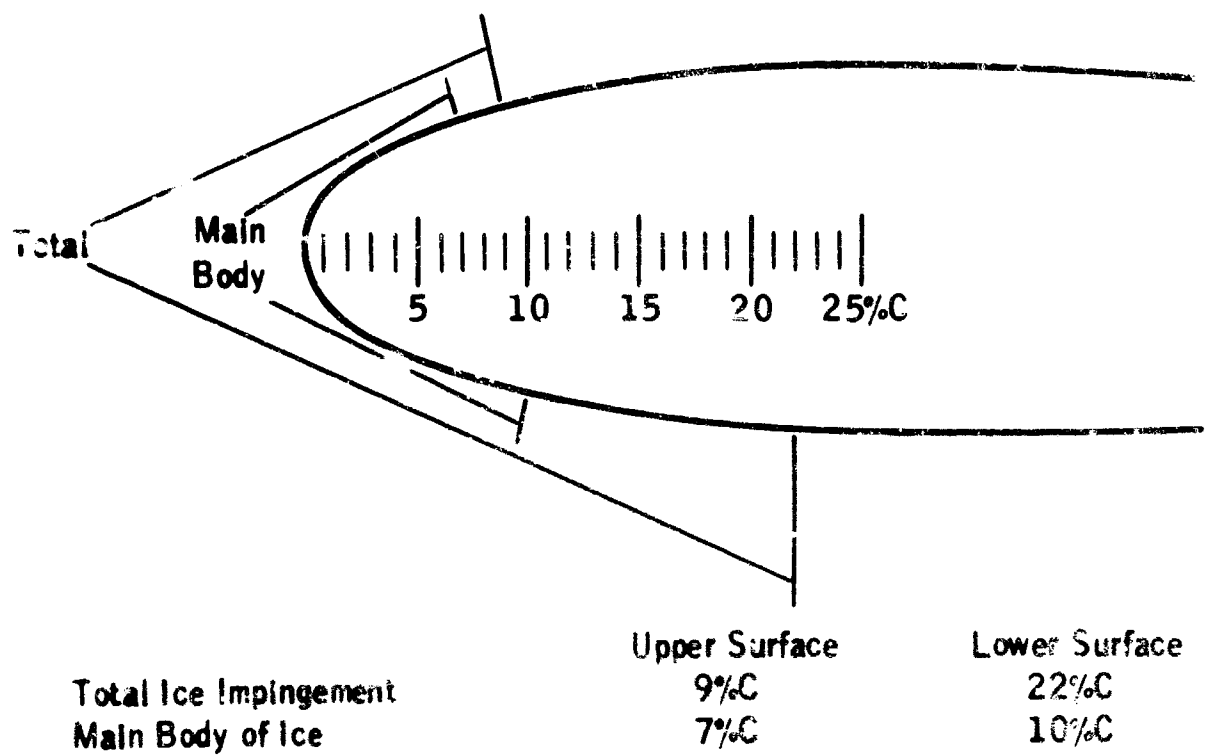
Figure 4.3-2.   Chordwise Extent of Icing on Main Rotor Blade (Ref. 4.3-1).
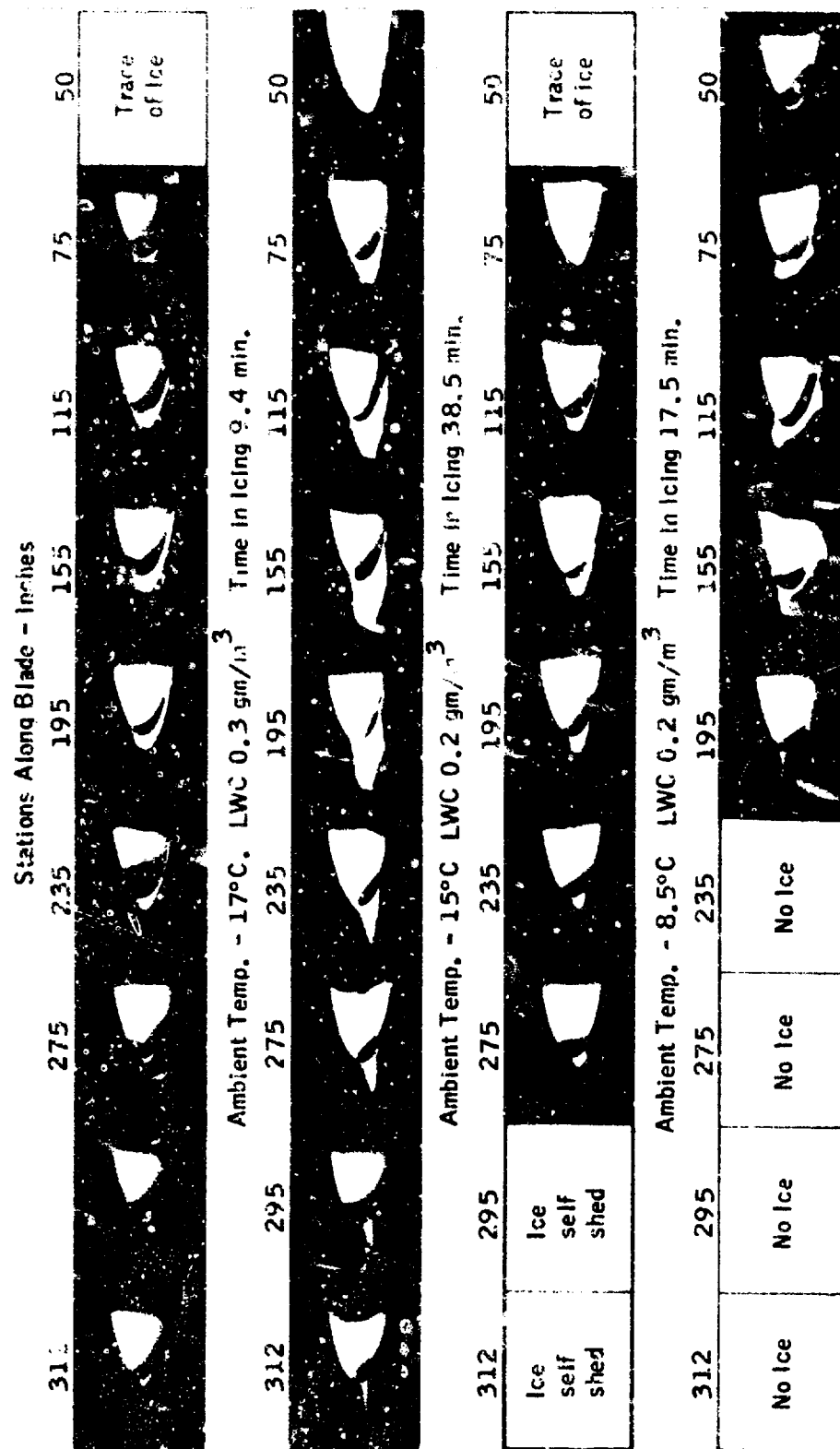
Rotor Blade Ice Formation at Various Temperatures.

Figure 4.3-3

Figure 4.3-4. Windshield Ice Accretion.

Figure 4.3-5. Rotor Head Ice Accretion.

4.3-28
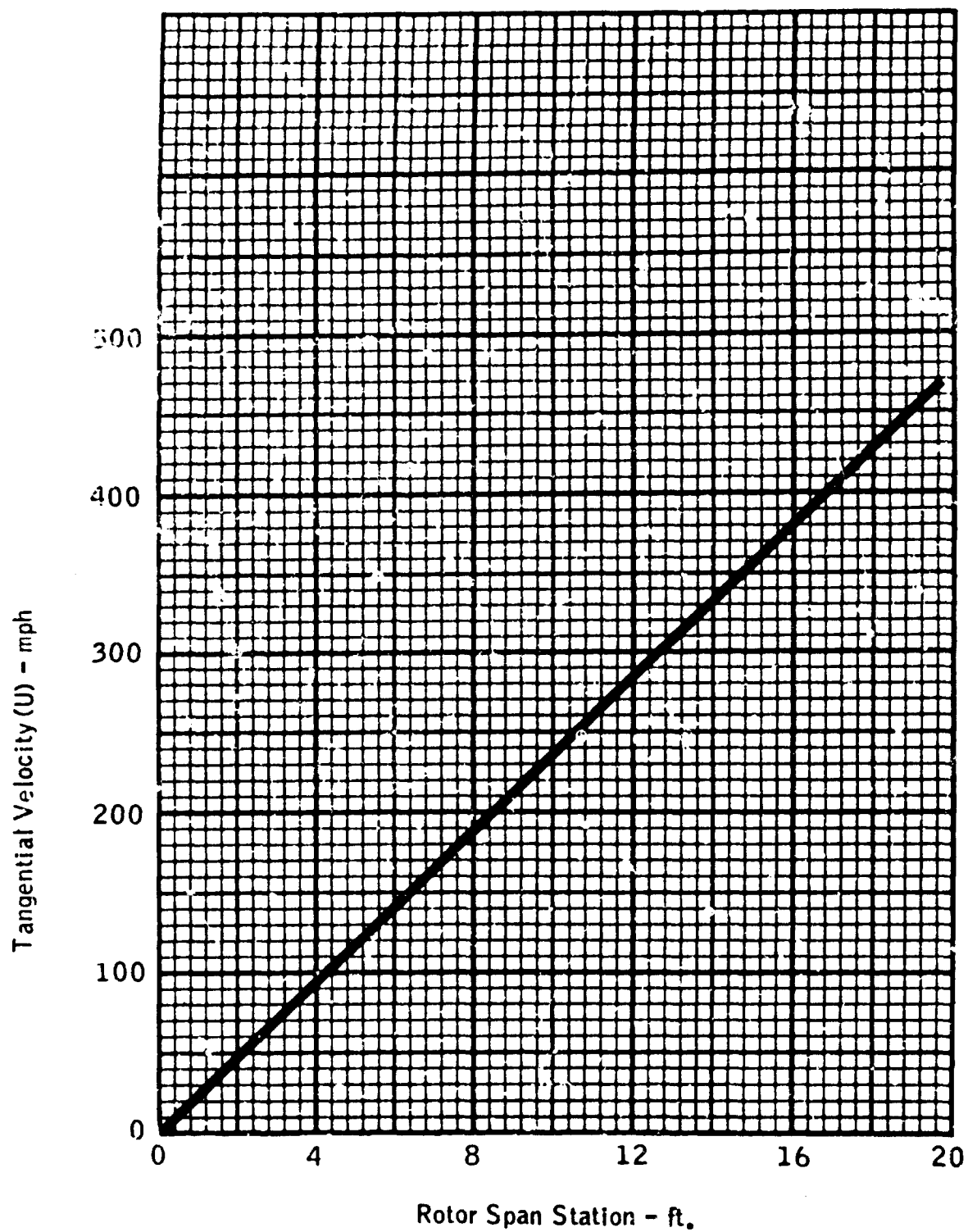
Figure 4.3-6a.   Rotor Tangential Velocity Versus Span Station.
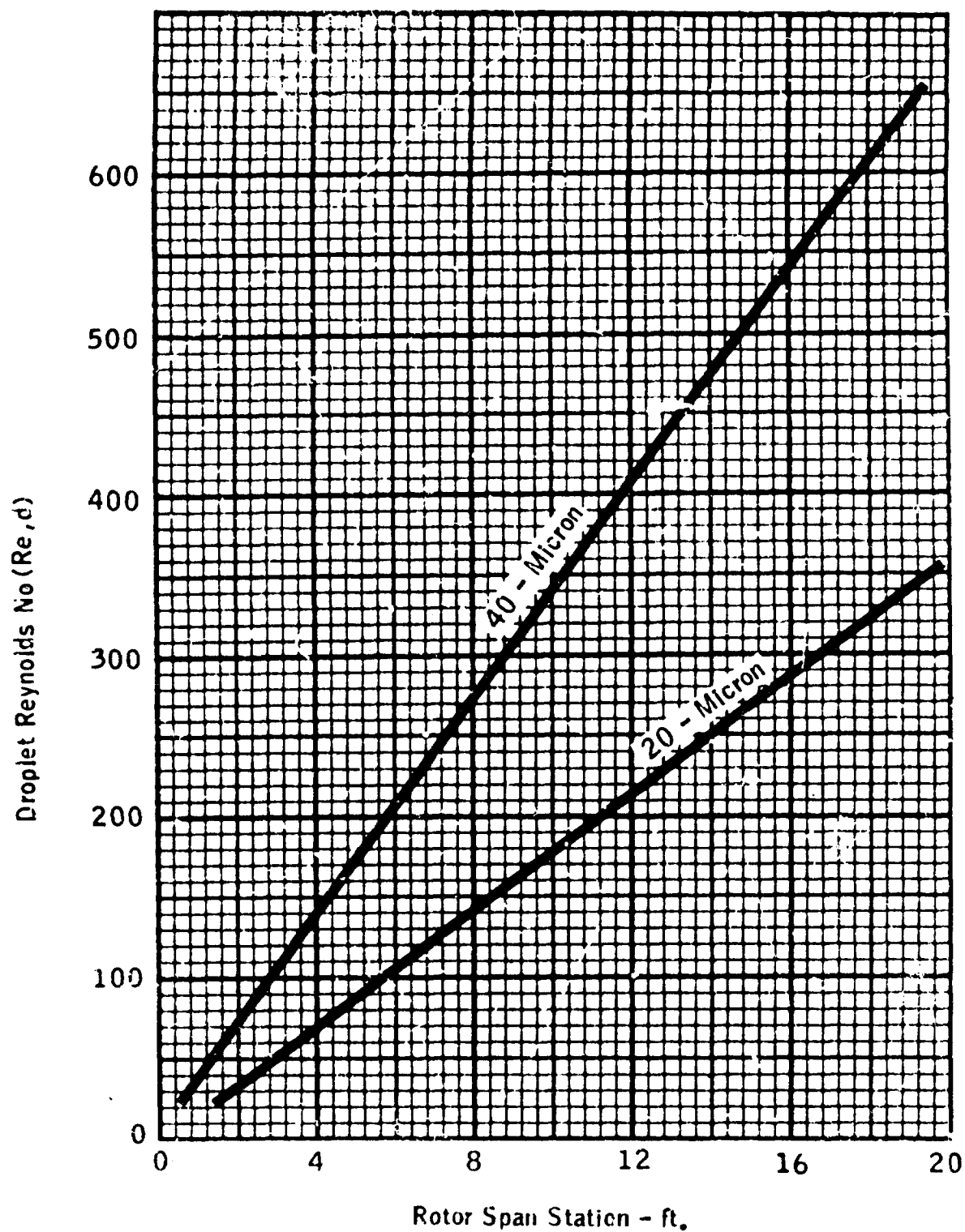
Figure 4.3-6b.   Droplet Reynold's Number Versus Rotor Span Station
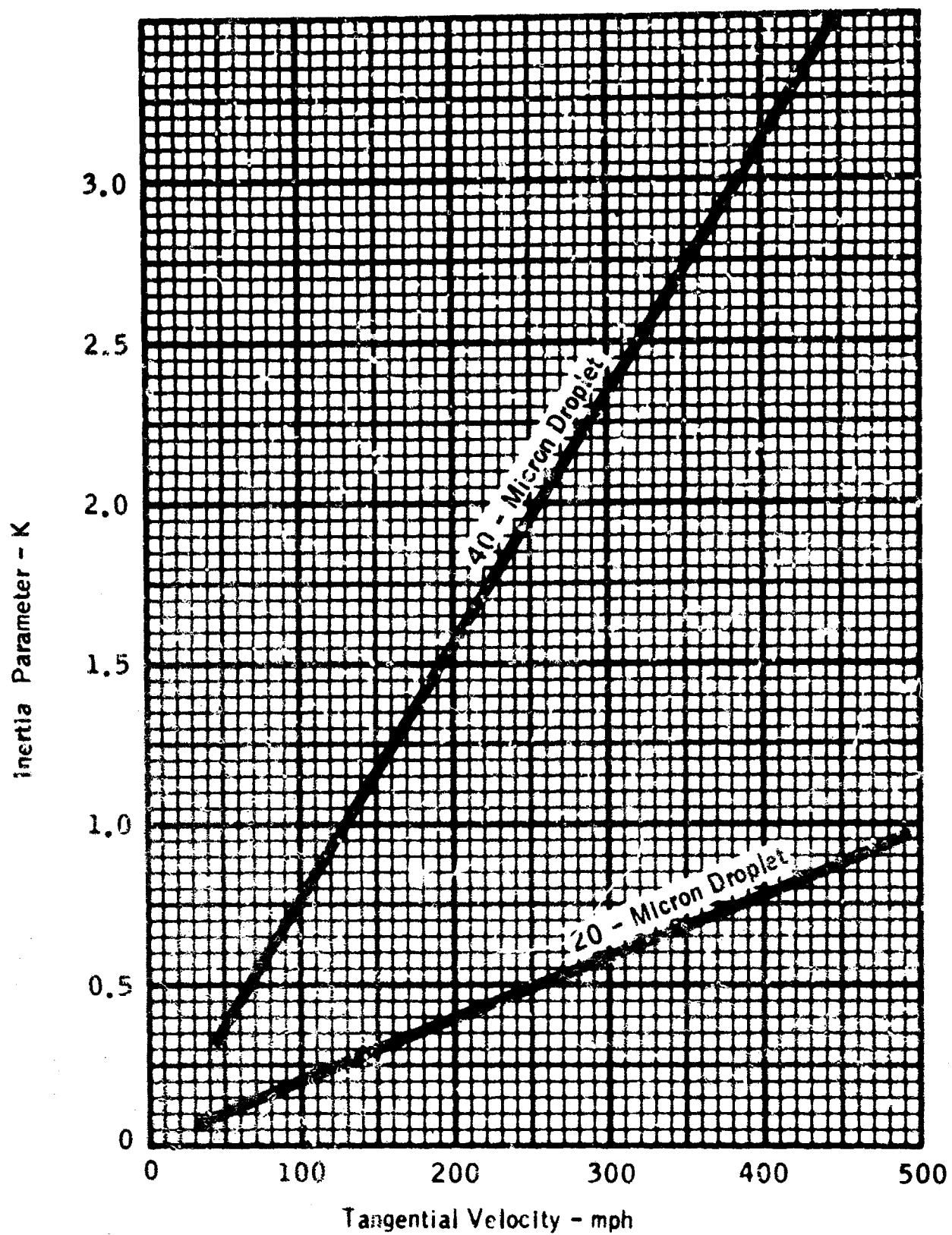
Figure 4.3-8c. Inertia Parameter Versus Rotor Span Station.
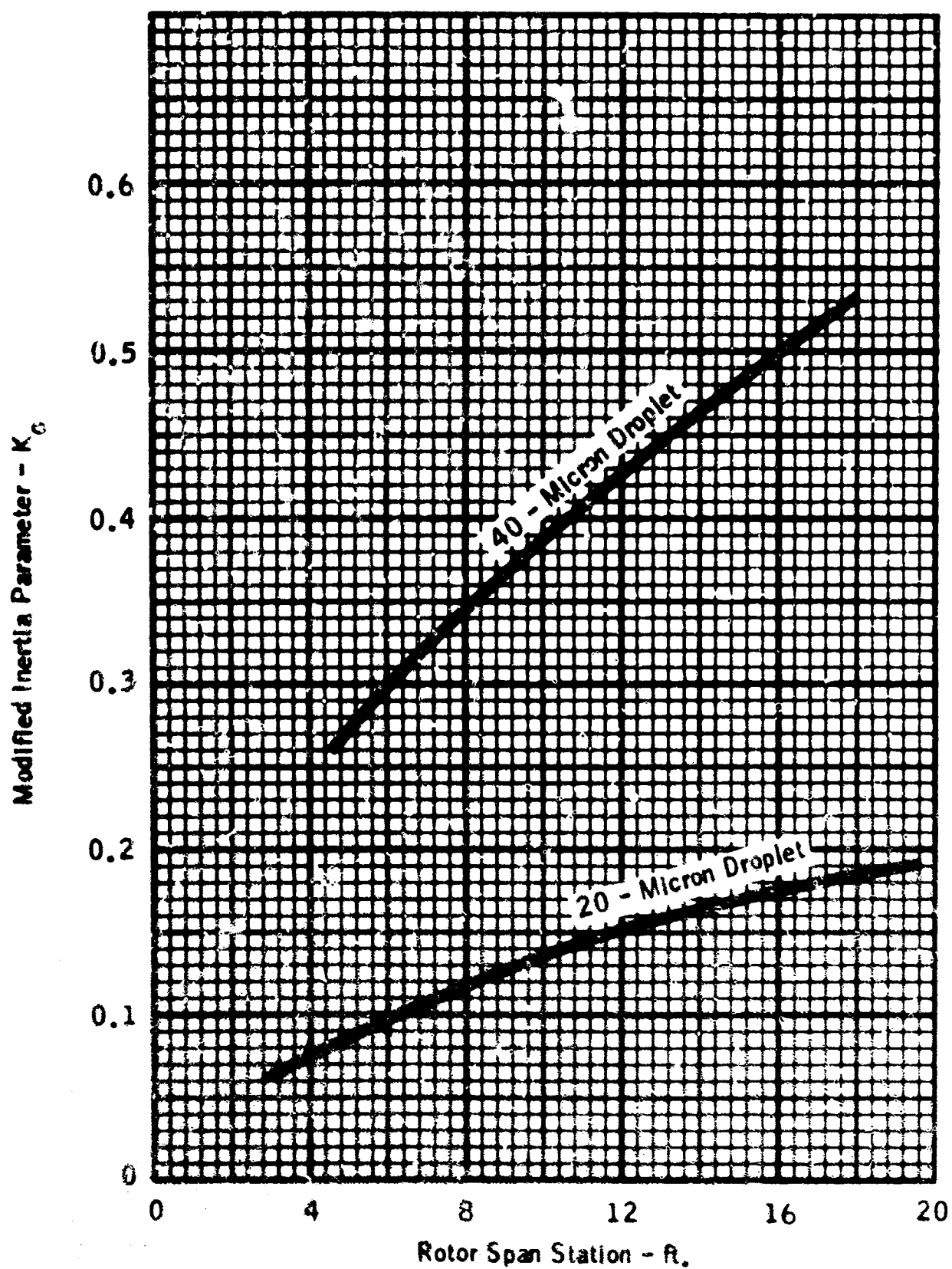
Figure 4.3-6d. Modified Inertia Parameter Versus Rotor Span Station.
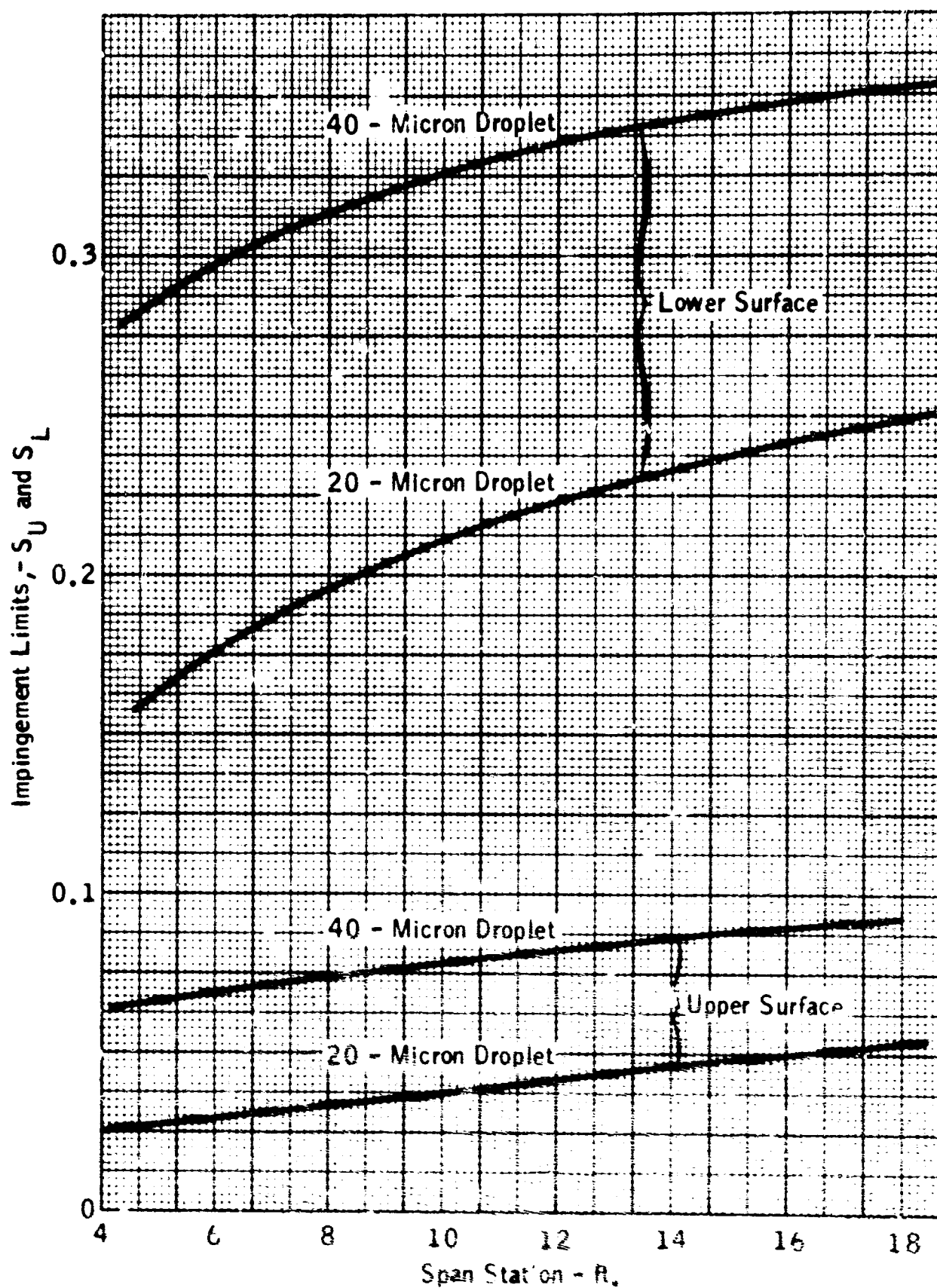
Figure 4.3-7.   Droplet Impingement Limits for 20 and 40-Micron
Drop Sizes.
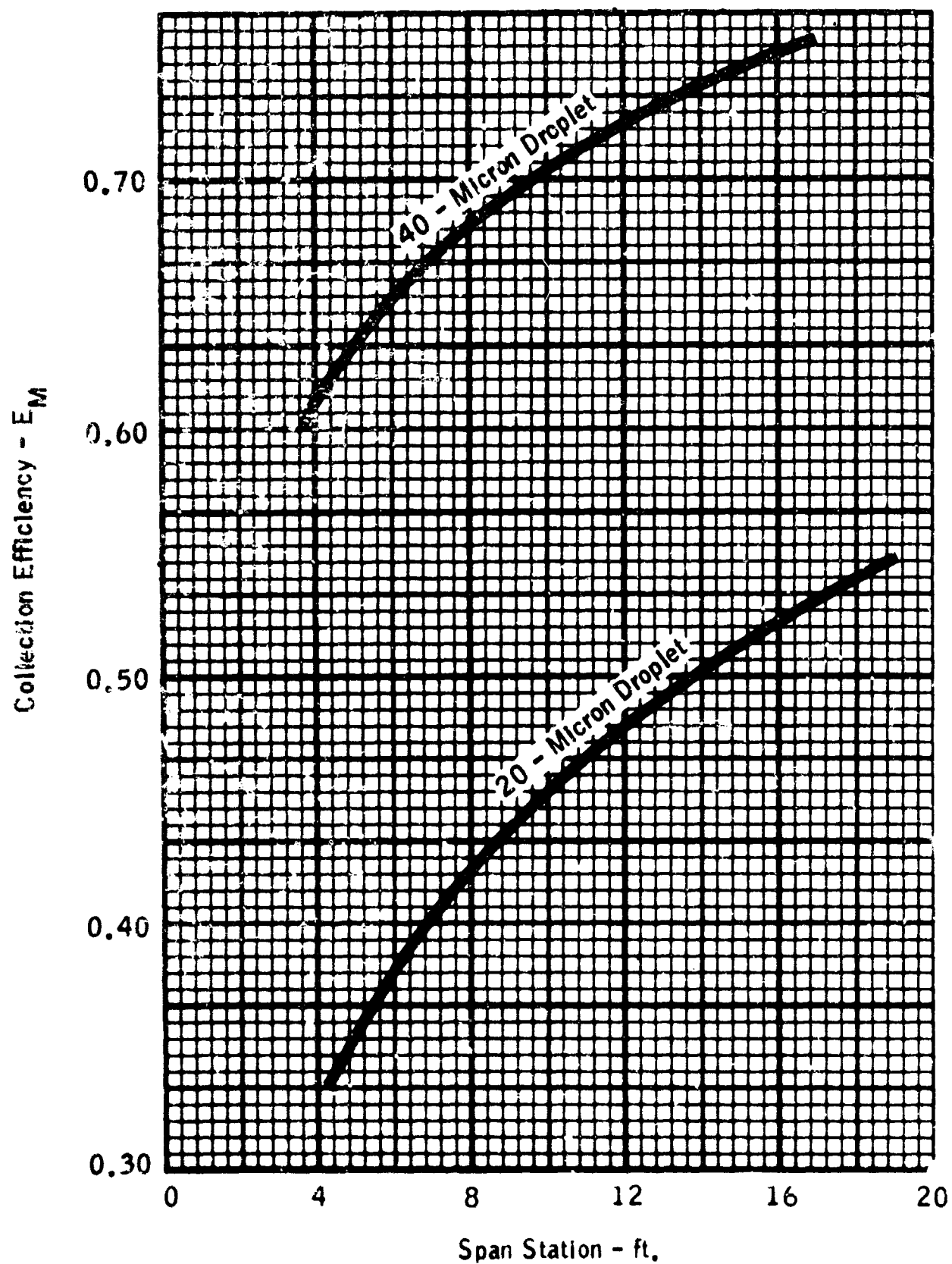
Figure 4.3-8a. Collection Efficiency Versus Rotor Span Station.
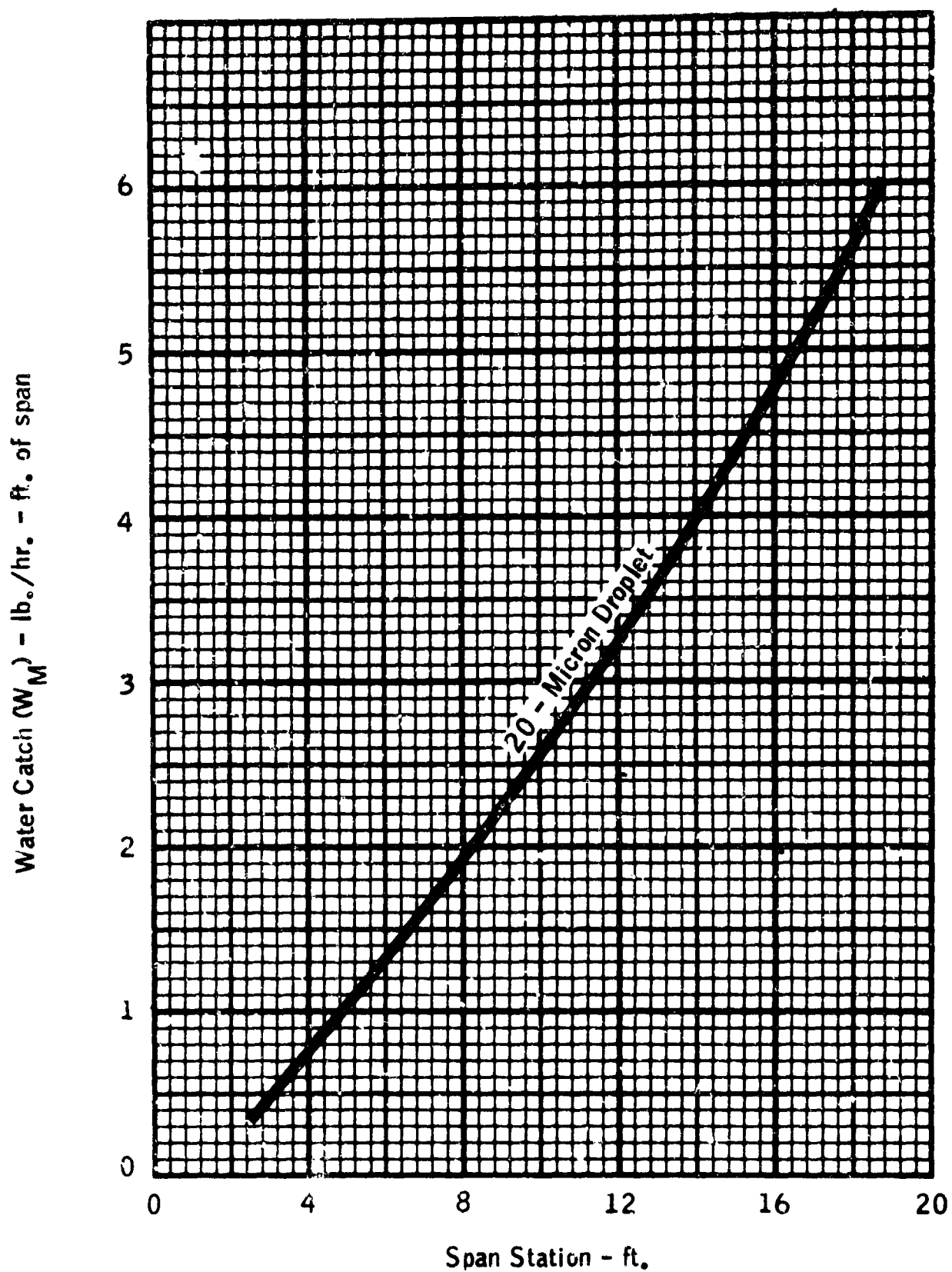
Figure 4.3-8b.   Water Catch Versus Rotor Span Station.
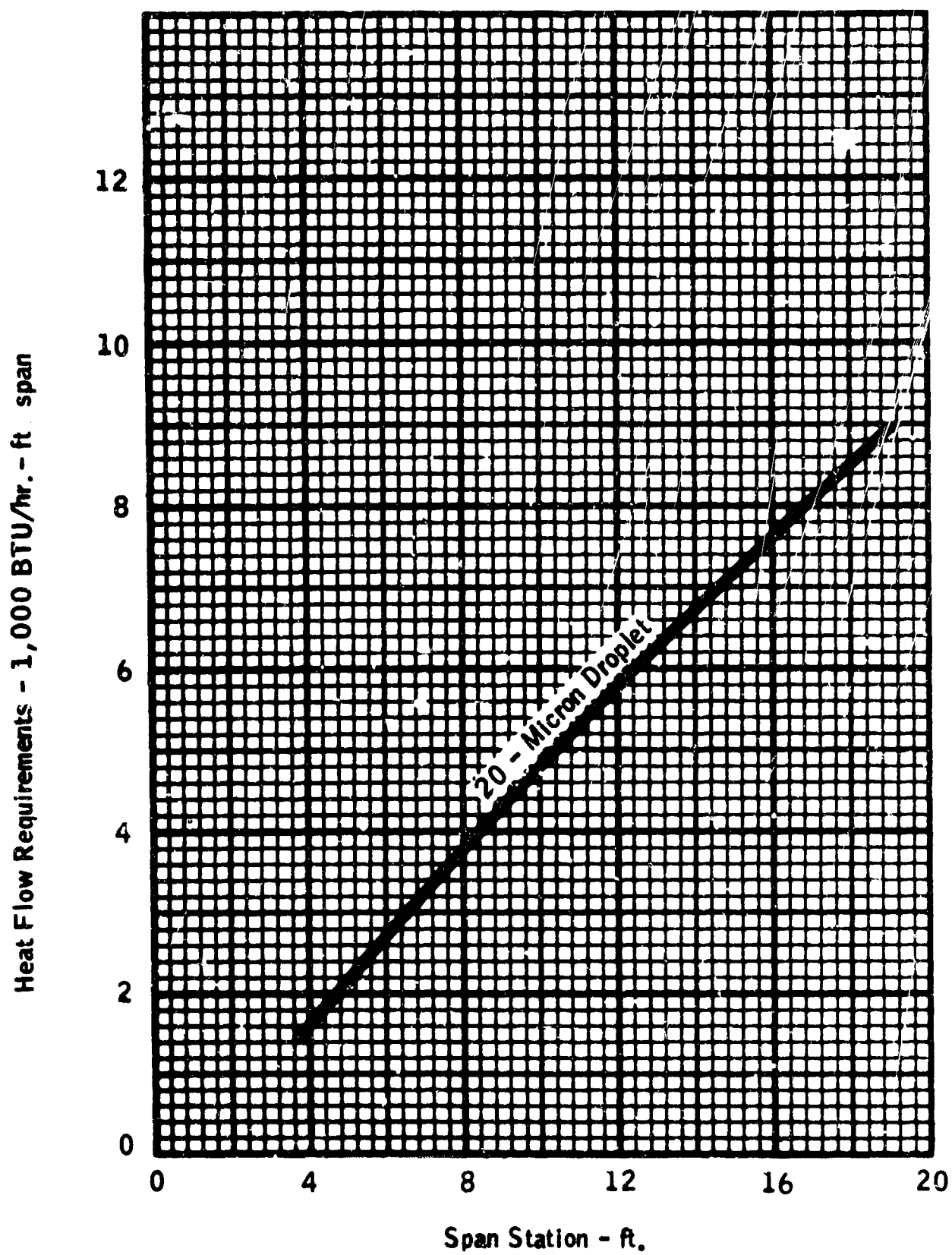
Figure 4.3-8c. Anti-Icing Heat Requirements Versus Rotor Span Station.

4.3-36
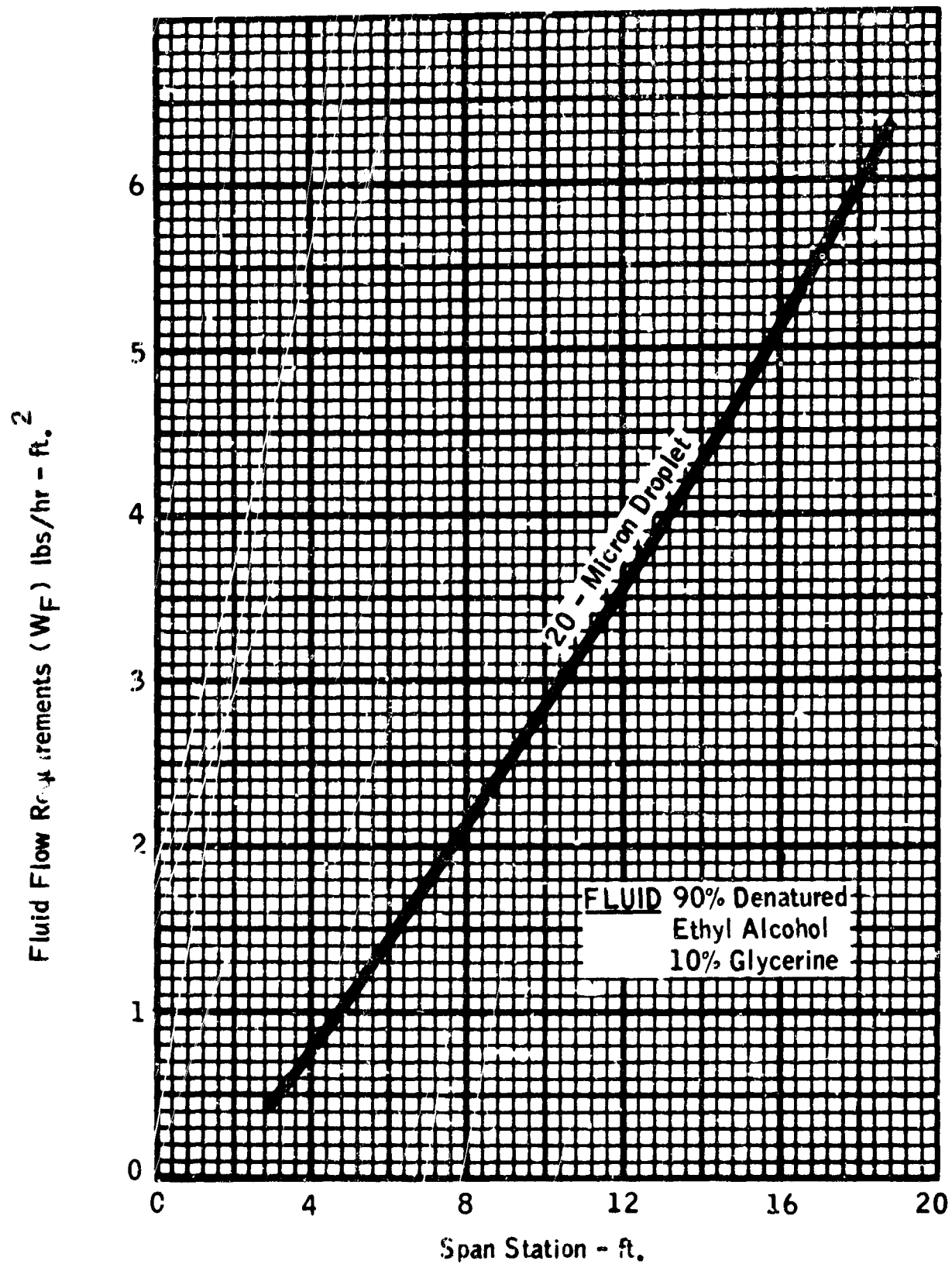
Figure 4.3-8d.   Fluid Anti-Icing Flow Requirements
Versus Rotor Span Station.
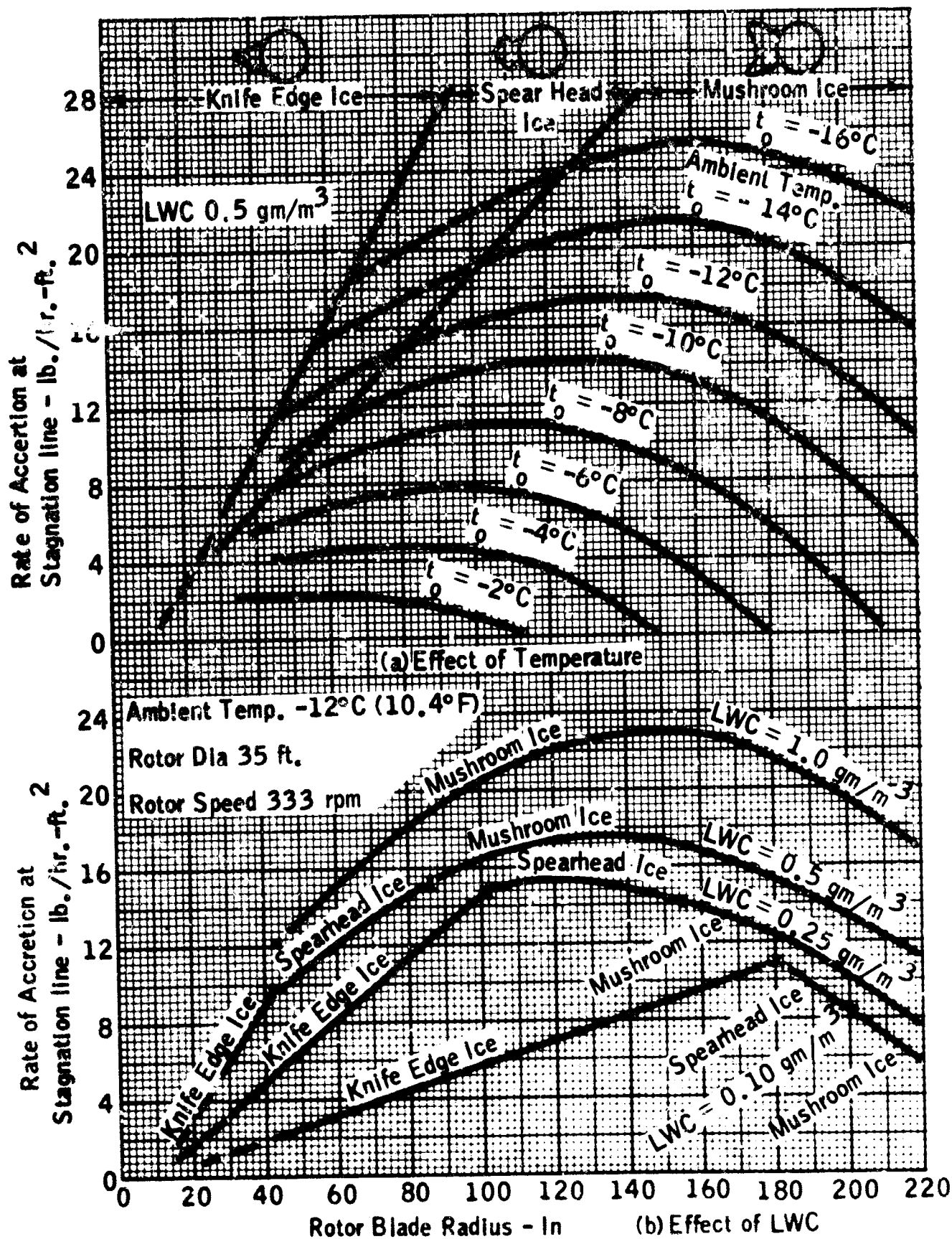
Figure 4. 3-9. Effects of (a) Ambient Temperature and (b) LWC Upon Rate of Accretion and Ice Type (D_d 30-Micron, Ref. 4.3-8)
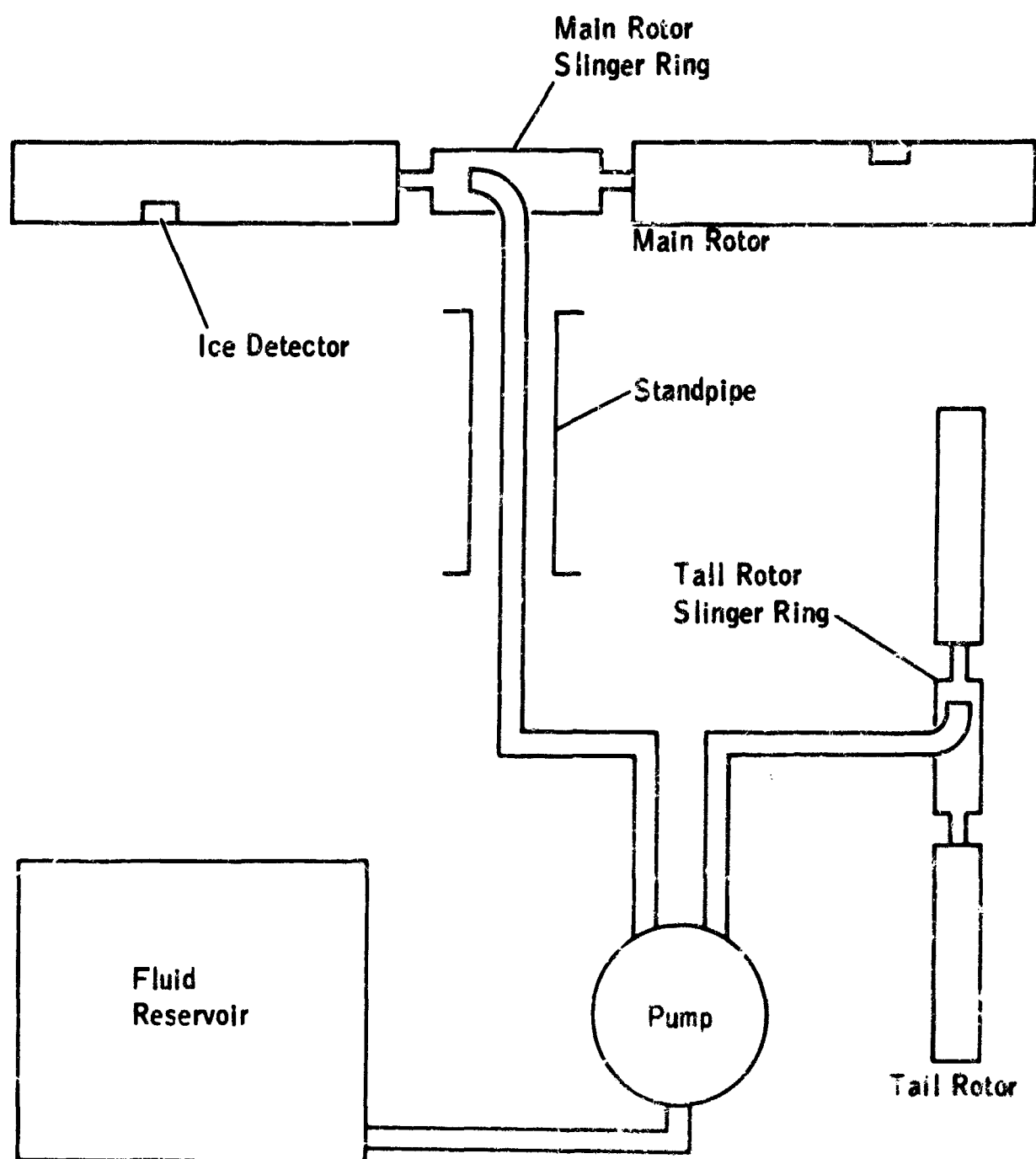
Figure 4. 3-10. Typical Fluid Ice Protection System Schematic (Ref. 4. 3-1).
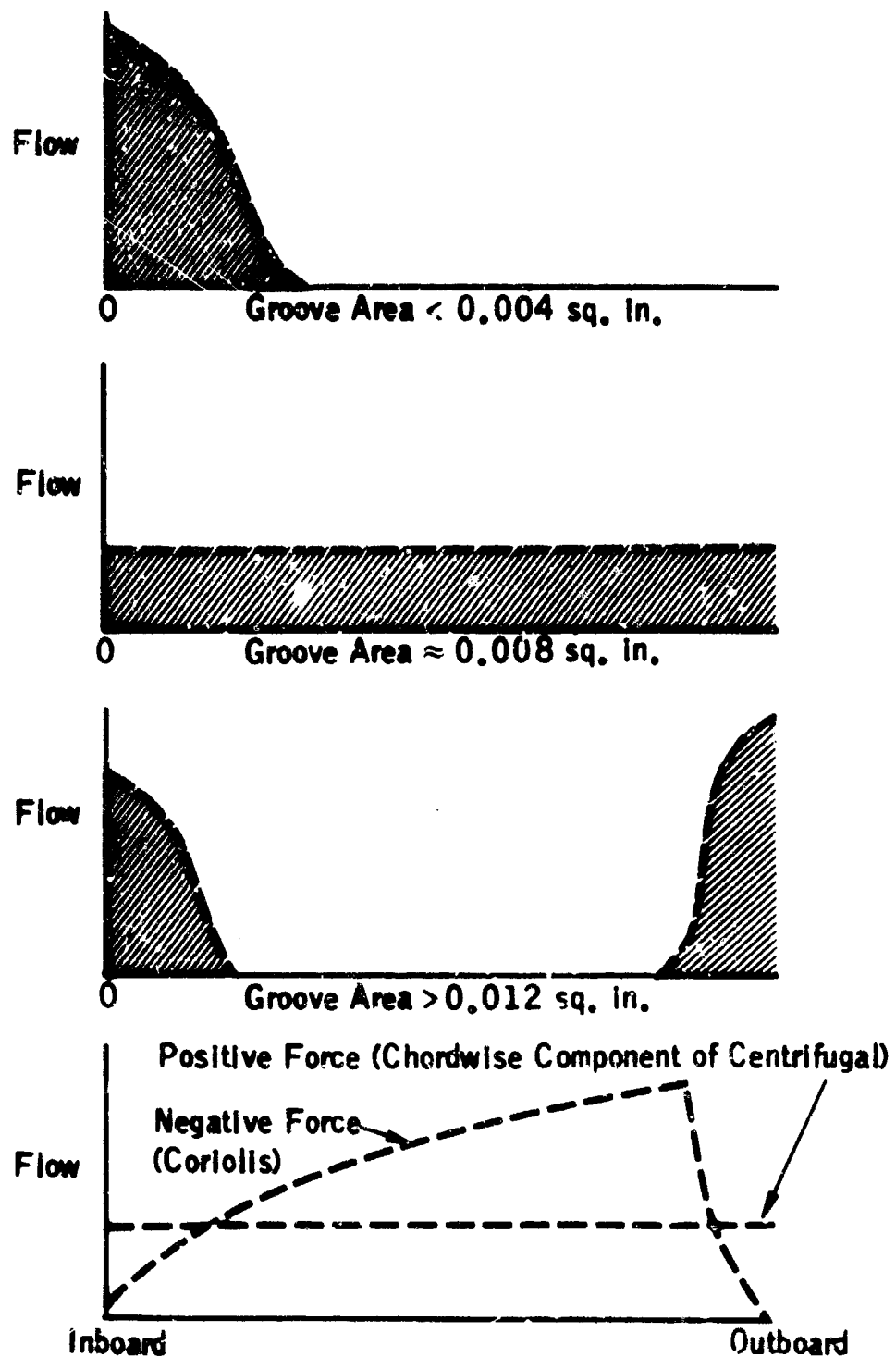
Figure 4.3-11.   Flow Pattern Along Blade Span (Ref. 4.3-1).
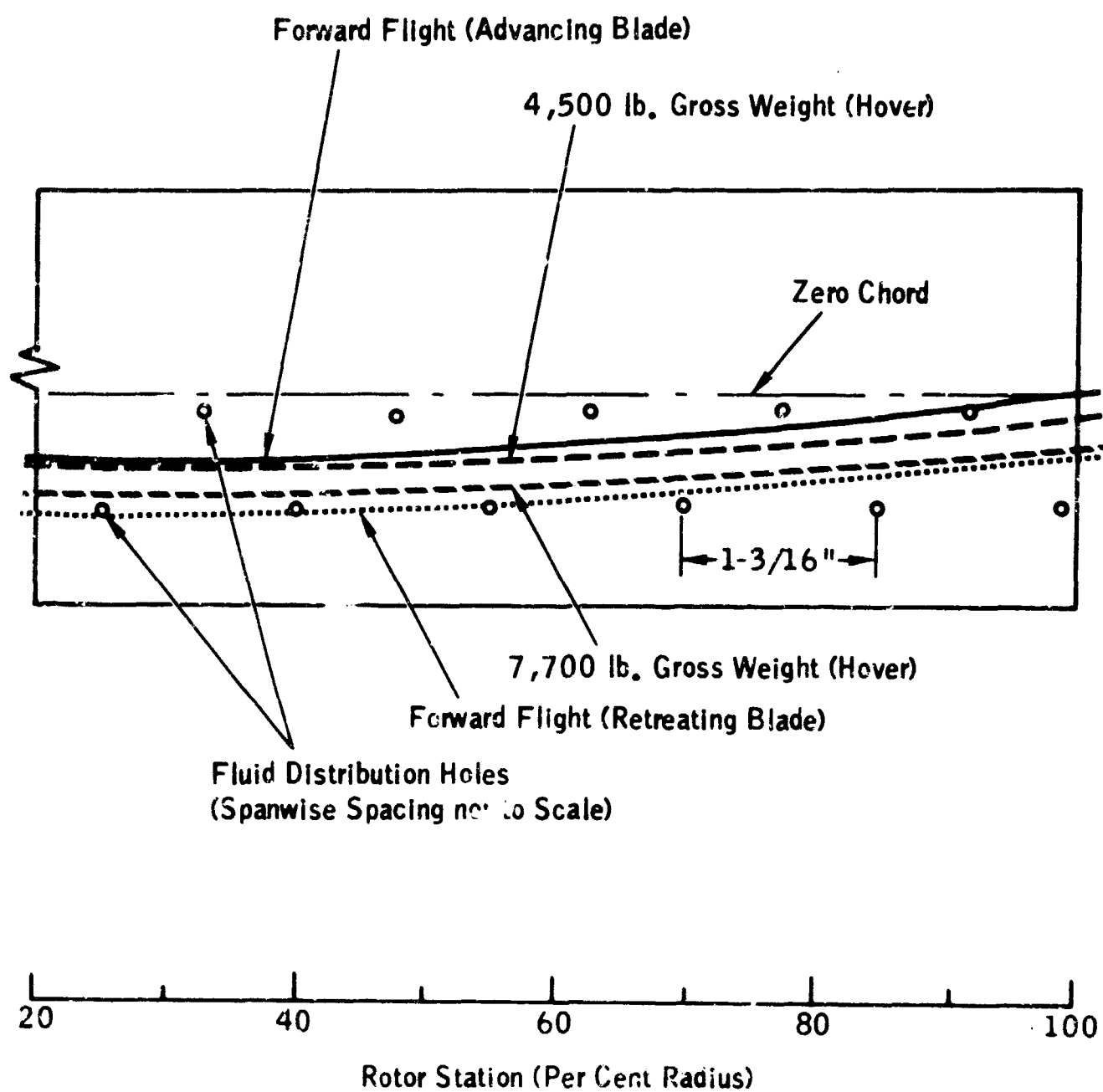
Figure 4.3-12.   Stagnation Point Location for Typical Main Rotor
(Ref. 4.3-1).

4.3-41

(Numbers on individual sections of the heaters indicate order of shedding)
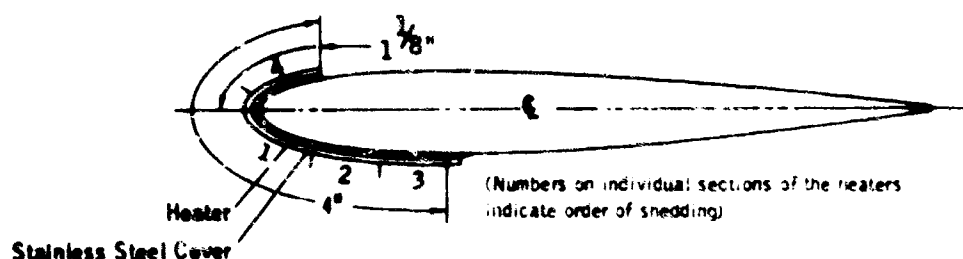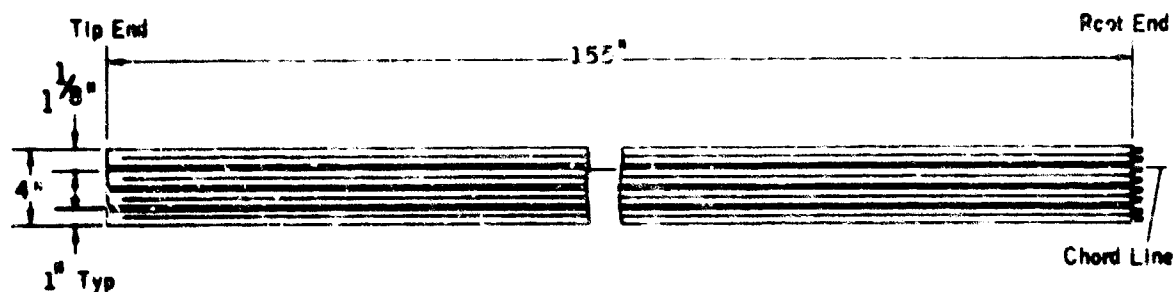
Figure 4.3-13. Spanwise Elements for Chordwise Shedding (Ref. 4.3-4)

(Numbers on individual sections of the heaters indicate order of shedding)
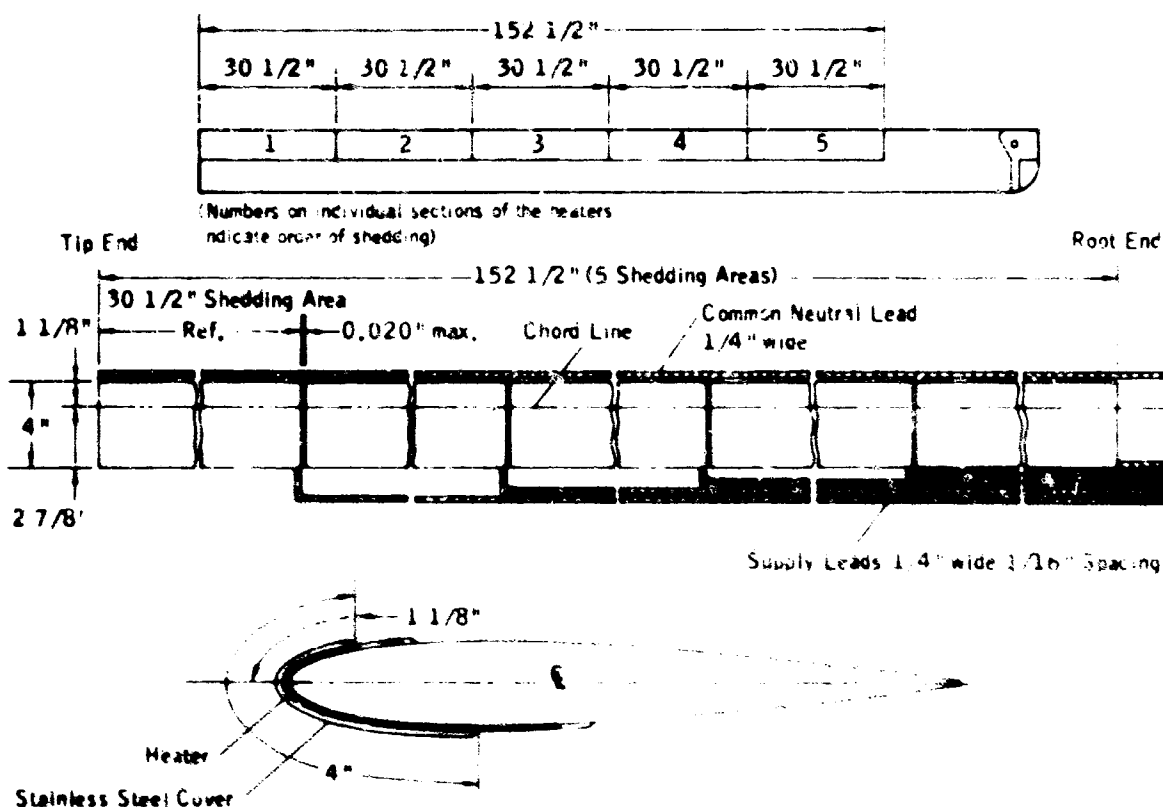
Figure 4.3-14. Chordwise Elements for Spanwise Shedding (Ref. 4.3-4)

4.3-42
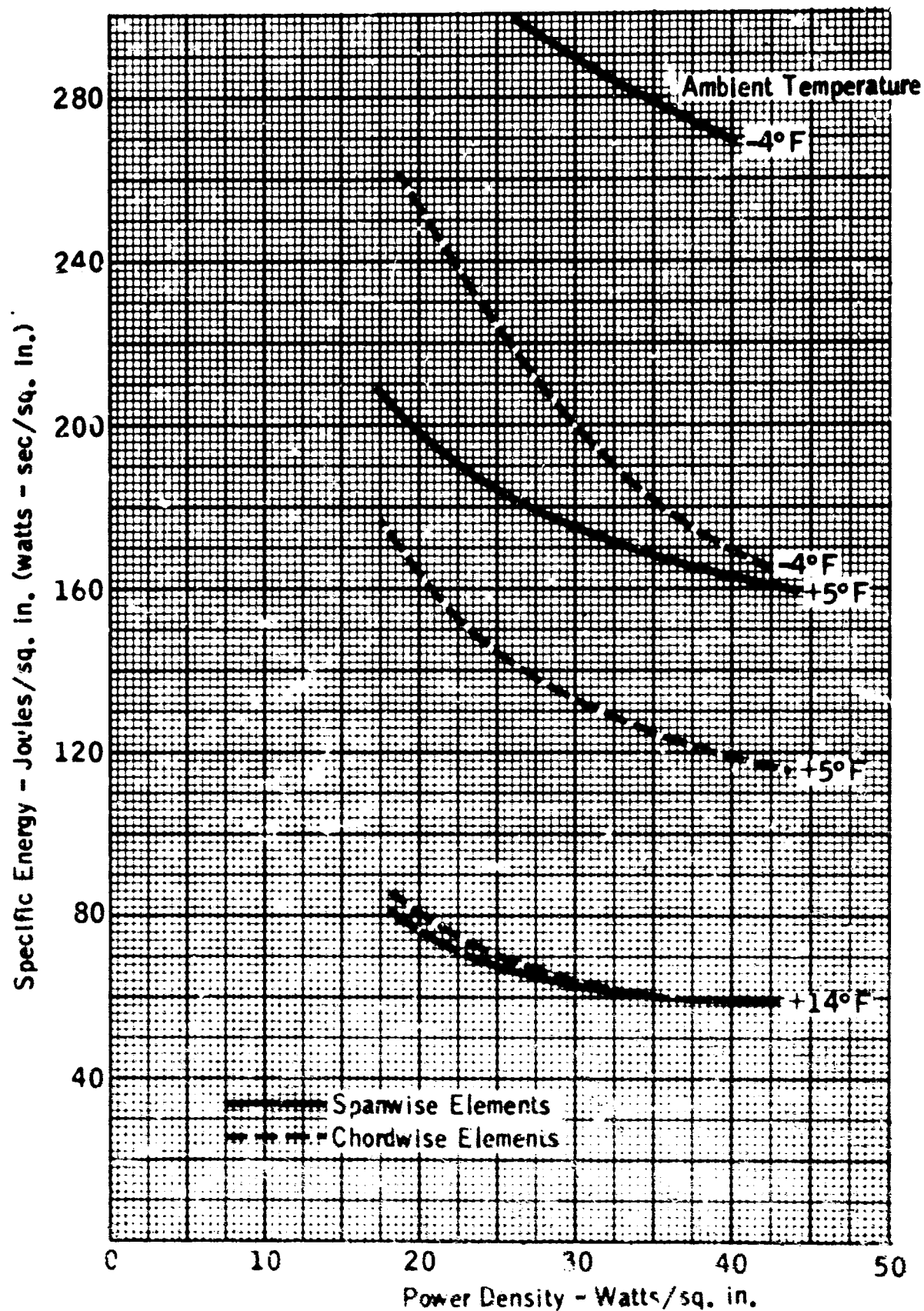
Figure 4.3-15. Specific Energy Required for Shedding to 5-ft. Radius, Spanwise and Chordwise Elements (Ref. 4.3-4).
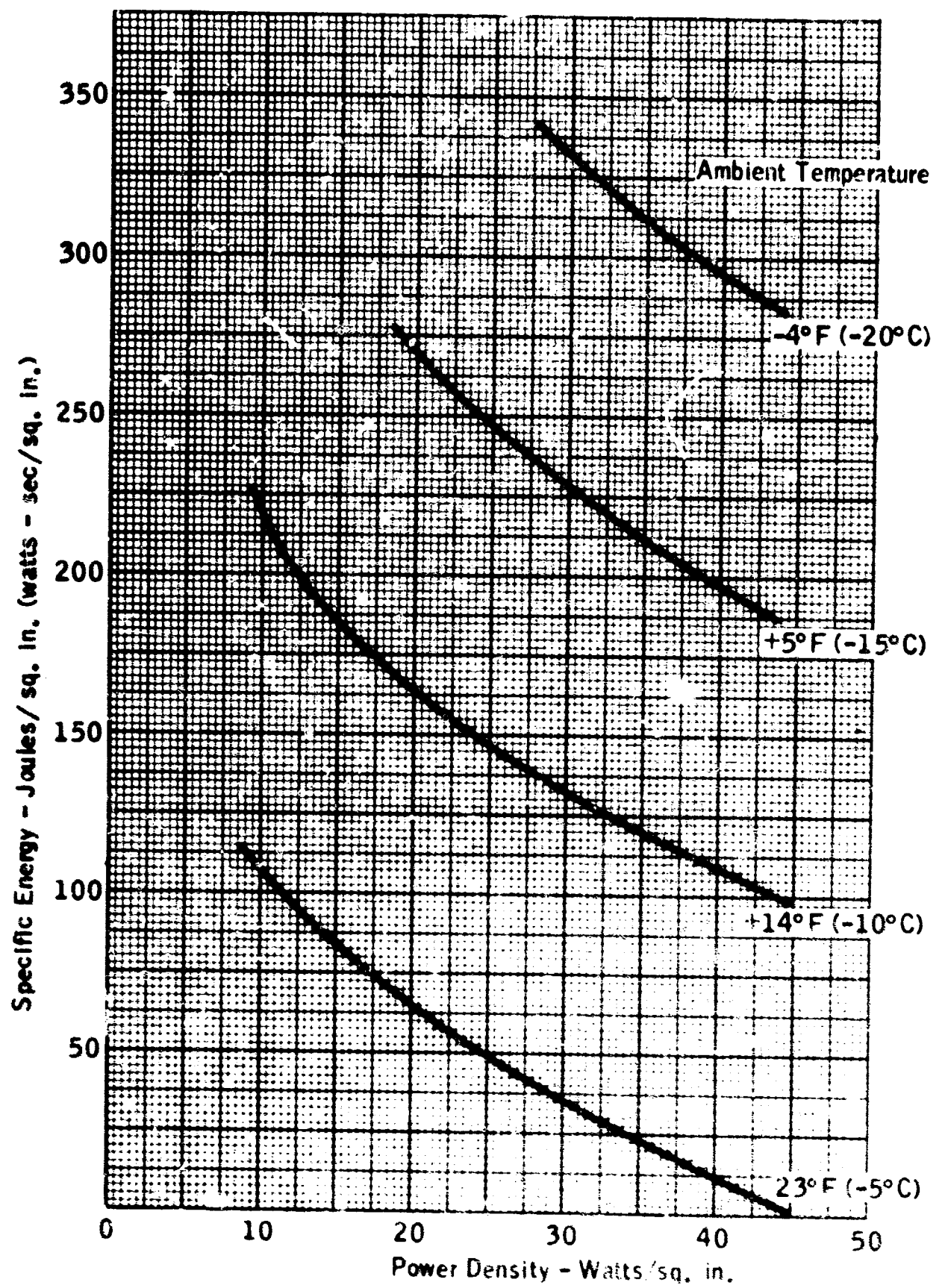
Figure 4.3-16. Specific Energy Required for Shedding to 5-ft. Radius.
Chordwise Elements (Ref. 4.3-5).
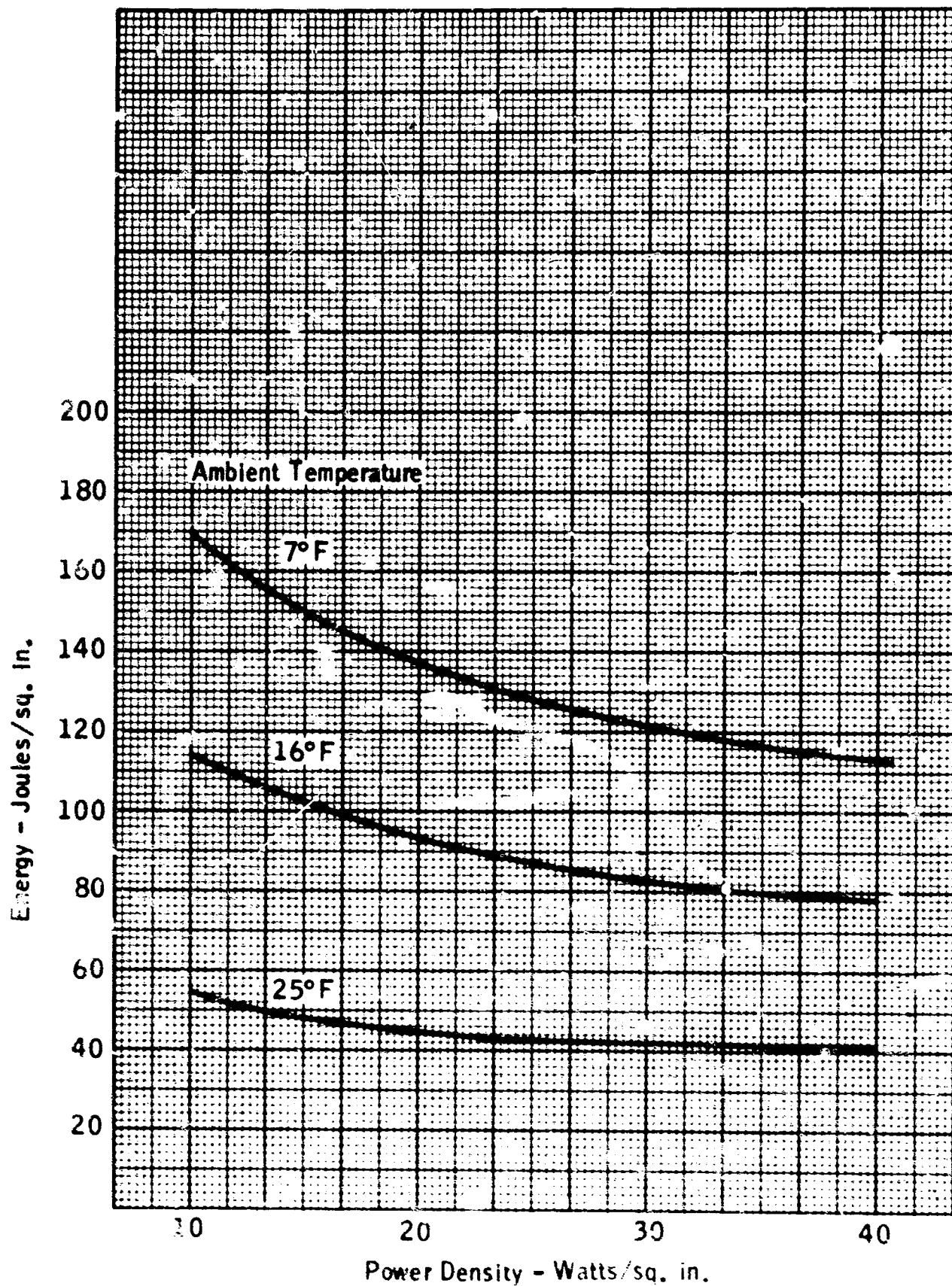
Figure 4.3-17. Energy Versus Power Density for Successful De-Icing, Spanwise Elements (Ref. 4.3-1).
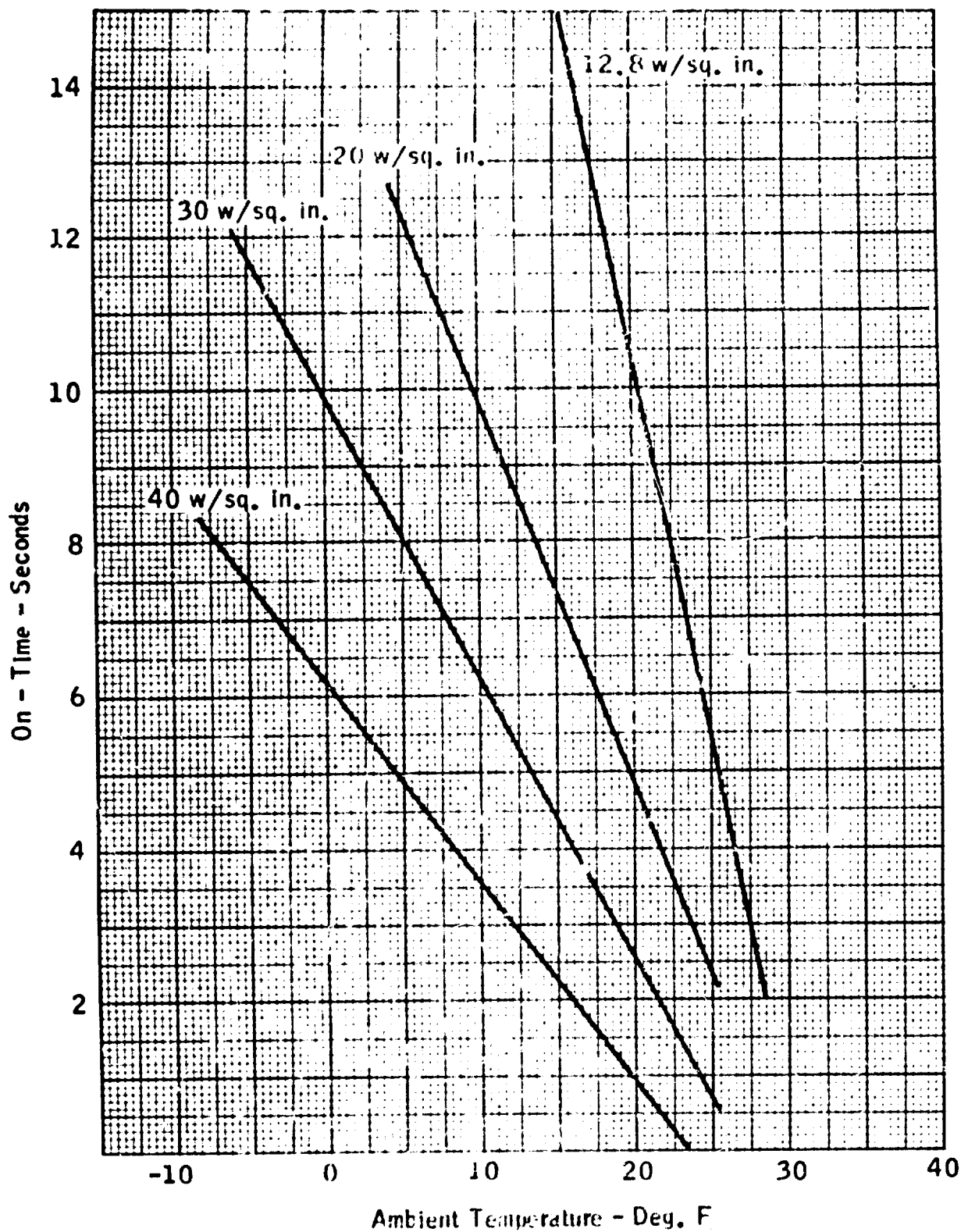
Figure 4.3-18. Power On-Time Required for Shedding to 5-ft. Radius, Chordwise Elements (Ref. 4.3-5).
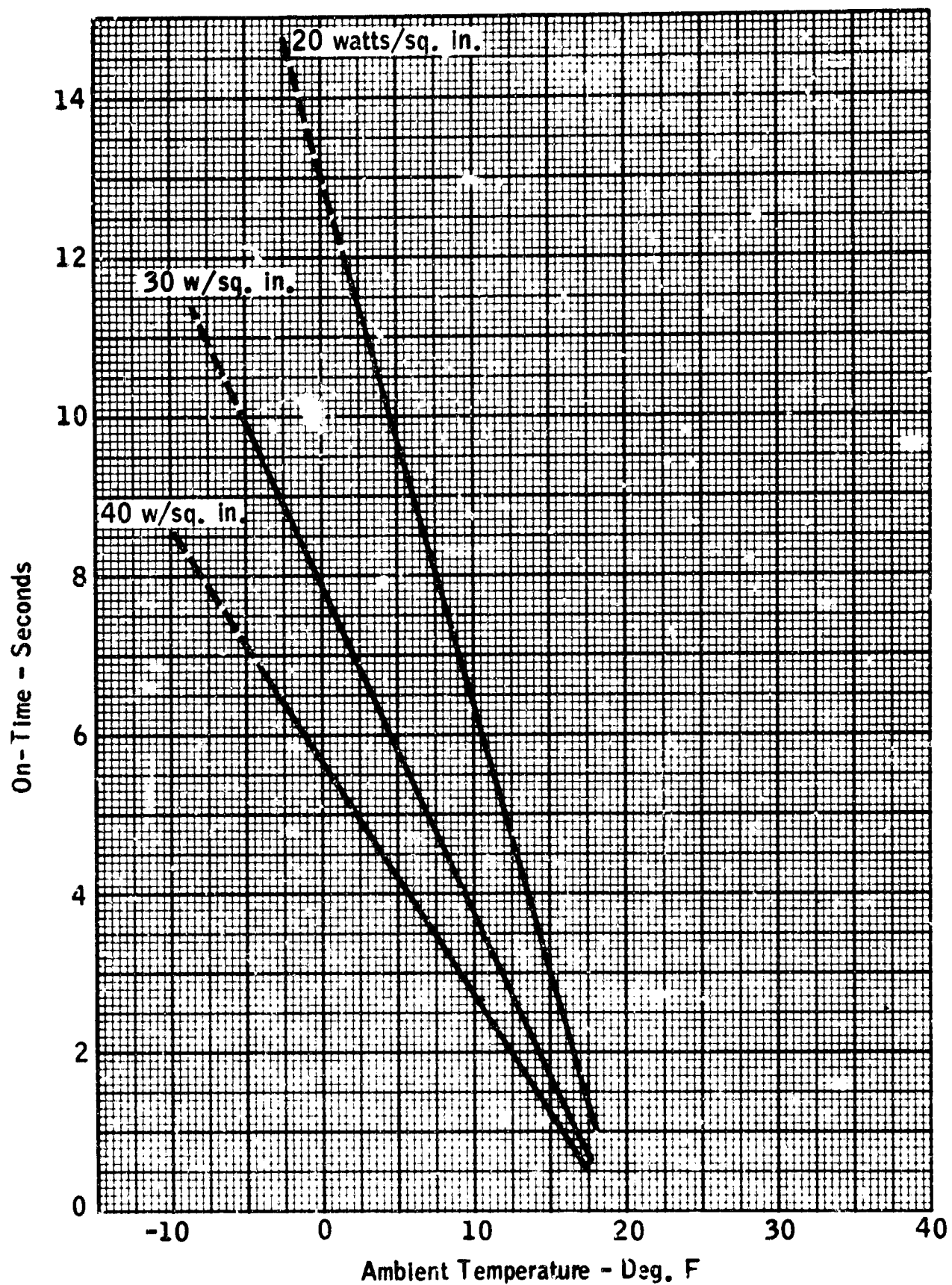
Figure 4.3-19.   Power On-Time Required for Shedding to 5-ft. Radius, Spanwise Elements (Ref. 4.3-4).
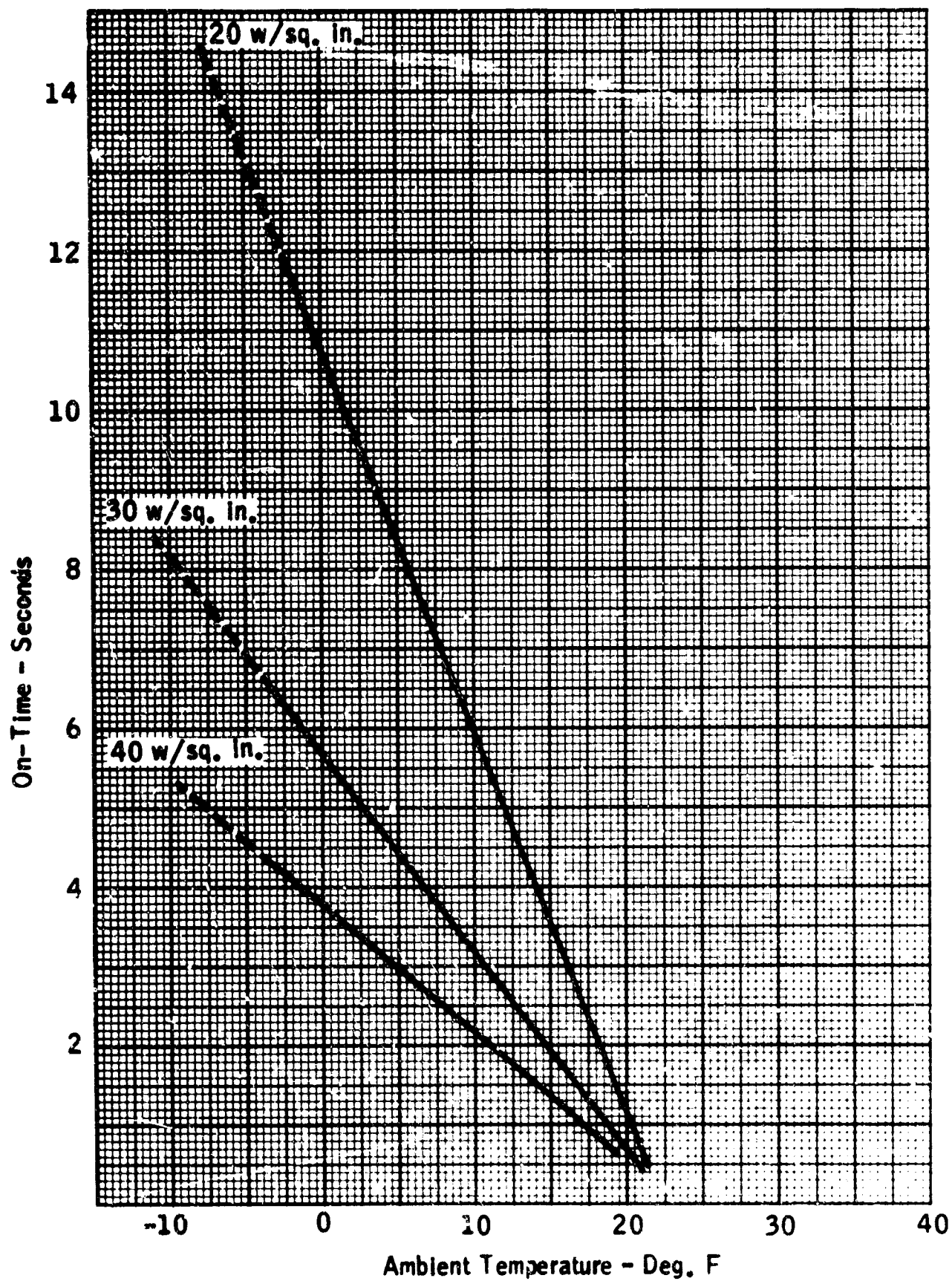
Figure 4.3-20. Power On-Time Required for Shedding to 5-ft. Radius, Chordwise Elements (Ref. 4.3-4).

5 | ICE DETECTORS AND ICE PROTECTION SYSTEM INSTRUMENTS AND CONTROLS

CONTENTS

ICE DETECTORS AND ICE PROTECTION SYSTEM INSTRUMENTS AND CONTROLS

LIST OF FIGURES

5.1 SUMMARY

Ice and icing conditions may be detected in flight either visually or with an ice detector. This section of the report discusses both the methods of detecting icing visually and the principles of operation and characteristics of various types of ice detectors. Comments are also included on methods of detecting icing conditions that would exceed the design capabilities of a particular aircraft and its ice protection systems.

A discussion is also included of general control requirements (and system indication) for the ice protection systems discussed in previous sections of this report.

5.2 ICE DETECTION METHODS

5.2.1 VISUAL ICE DETECTION - A good indication of the possibility of icing can be obtained by observing the types of cloud formations and the outside air temperature. If the outside air temperature is between 20° and 32° F while flying through cumuliform or stratiform clouds, the probability of icing is about 40 per cent. At lower temperatures the probability is lower, becoming negligible at about -35° F (Ref. Figure 1-17). The overall probability of encountering icing conditions is much lower than 40 per cent; it is in the order of two to three per cent as shown in Figure 1-24. However, flight through clouds at temperatures near freezing greatly increases the probability of icing.

Flight through cumulus clouds should be avoided because of the probability of high liquid water contents at the center of the cloud, as well as the presence of severe turbulence and hail. Flight through icing conditions in stratus clouds can often be avoided by climbing over the cloud layer (maximum depth will be less than 6,500 ft.) or changing direction to fly around the cloud bank.

It is possible, of course, for the pilot to visually detect the formation of ice on unheated parts of the windshield or windshield wipers and on the wing leading edges. Wing leading edges are not always easily observed, particularly

on swept-wing aircraft and during night flights. A simple and effective method of improving visual ice detection would be to mount a four to six-in. fixed rod of 1/8 to 1/4-in. diameter on the fuselage in a position where the pilot can easily observe ice formation. (The rod should be long enough to extend outside the air and water droplet boundary layer.) This type of detector may be the most practical solution for light aircraft ice detection because of the relatively high cost and service problems of most other ice detectors.

5.2.2 ICE DETECTOR TYPES — Many methods of detecting ice have been proposed, and a number put into practice. Some of the different types of ice detectors and their current applications are listed in the table below followed by a brief description of each type. Recent information on ice detectors is also contained in the NRC (National Research Council of Canada) Aeronautical Report LR-334 (Ref. 5-1) and in a paper presented at the 1961 Aircraft Ice Protection Conference (Ref. 5-2).

Ice Detector Type	Current Application
Differential Pressure	Commercial transports, various military aircraft and helicopters
Electrical Conductivity	Several military aircraft
Beta Radiation Detector	Helicopters, VTOL, and conventional aircraft
Rotating or Reciprocating Cylinder	Commercial transports (European)
Mass Balance	Helicopters
Electro-Thermal (Resistance)	Measurement of liquid water content in icing tunnels
Heated Rod	Commercial transports (European)
Vibrating Rod	None
Electro-Chemical	None

The differential pressure or pressure probe ice detectors are probably the most widely used for commercial transports and military aircraft. These instruments detect icing by sensing a difference in pressure between a heated

(reference) and an unheated (detector) probe when forward-facing holes in the unheated probe become blocked with ice, or by sensing a change in pressure when holes in the forward face of a single probe become blocked with ice while the aft facing holes remain free of ice. Examples of this type ice detector are shown in Figure 5-1.

An icing signal is relayed to the pilot by means of an indicator light. A one-minute time delay is usually included so that a continuous icing signal is indicated as long as the detector signals icing at least once per minute. An electrical heating circuit is normally included to de-ice the detector probe after each icing signal. Air velocities of about 80 kt. or higher are required to obtain satisfactory ice detection. (This is dictated by the pressure switch setting.)

Despite the wide use of the pressure type ice detector, it has not been completely satisfactory in service because of various limitations. The small probe holes needed to obtain rapid response to icing clog easily from dust, dirt, insects, etc., and are difficult to clean. Finding a suitable location for the detector may also be a problem. Vibration is often a problem with engine-mounted probes; fuselage-mounted probes are subject to damage by maintenance personnel and ground handling equipment. For these reasons, most of the pressure type ice detectors installed for commercial use have been removed, and reliance has been placed on visual detection of ice.

A variation of the pressure type detector for helicopter application makes use of a pressure differential sensed at the leading and trailing edges of the blade. When this differential is destroyed by ice on the forward hole, a pressure switch is actuated. The switch can turn on a warning lamp and, if desired, actuate the blade de-icing system.

An example of the electrical conductivity type ice detector is shown in Figure 5-2. The sensing element of this detector consists of two electrodes separated by a small insulating gap, with an electrical potential applied to the

electrodes. The impingement of water droplets on the sensing element allows current flow across the insulating gap and operates a warning system.

The probe is heated to prevent formation of ice. As the detector is basically a liquid water detector, an air temperature probe is included. An icing signal is produced by the control box when the presence of liquid water is detected at air temperatures below freezing.

A variation of the conductivity type ice detector is shown in Figure 5-3. This type detector has two airfoil-shaped probes separated by an air gap. Icing is detected when the air gap is bridged with ice. A time delay minimizes spurious signals caused by flying through fog, clouds, etc. This form of conductivity detector has the advantage of not requiring an air temperature probe.

An example of a radiation type ice detector is shown in Figure 5-4. The instrument shown is designed so that accreted ice will block off or weaken the flow of beta particle radiation between two points. Strontium 90 is used as the source of beta particle radiation. The primary advantage of the radiation detector is that it is not dependent on air flow for actuation and will work at low velocities. There is considerable interest in development of this type of ice detector for helicopter and VTOL aircraft applications, as well as for conventional aircraft.

An example of a rotating cylinder type of ice detector is shown in Figure 5-5. In this detector, a cylinder exposed to the airstream rotates slowly past a scraper. Ice accreting on the cylinder is shaved off by the scraper; the torque required to remove the ice actuates a warning system. An alternative form of cylinder-type ice detector is a cylinder that extends and retracts. The retraction force increase resulting from ice on the cylinder actuates a warning lamp.

An example of mass balance type ice detector is shown in Figure 5-6. This detector is driven by an electric motor and detects icing by heating one of the rotating arms and sensing the resultant mass unbalance when ice accretes

on the unheated arm. An instrument of this type has been tried on a helicopter.

An electro-thermal ice detector is shown in Figure 5-7. This type detector senses a change in resistance when water droplets impinge on an electrically heated wire. Two wires are used: one at right angles to the airflow, the other parallel to the airflow. The parallel wire (which is sheltered from impingement) gives a reference resistance, whereas the other wire changes temperature (and resistance) when struck by water droplets. Ambient temperature sensing is needed to determine whether a particular condition could cause icing. Because of its fragility, this detector has been used primarily for research work in flight and in icing tunnels.

An alternative form of the electro-thermal ice detector uses heated cylinders; otherwise, the principle of operation is the same. This type would have greater service life expectancy than the thin-wire type.

A simple, visual type ice detector (Figure 5-8) is commercially available for aircraft. This so-called "hot rod" detector is designed to be located in the air stream so that ice forming on the rod can be easily observed by the pilot. A heater can be manually switched on to de-ice the rod, and thus a periodical check for ice-free conditions can be made. This detector is also furnished with a lamp which illuminates the rod during night flying conditions.

There have been a variety of other types of ice detectors proposed that have not been put into production. A vibrating rod ice detector has been proposed which detects a change in frequency when ice buildup occurs. An electro-chemical type ice detector has been shown to be promising, but has not been put into production. This detector uses an electrolyte such as lithium chloride which, when wetted, allows a current to flow between two electrodes; thus detecting impingement of water droplets. An ambient temperature sensor is necessary to determine whether the droplets are supercooled.

In spite of the great amount of work that has been done in the development of ice detectors, a simple, low-cost, dependable ice detector has not yet been

produced. The need for dependability results from the low frequency (about two per cent) of aircraft flight in icing. To detect ice reliably, the detector must have a frequency of failure that is at least an order of magnitude less than the frequency of encountering ice. To date, no such instrument has been produced. The ice detector that most nearly meets all the above requirements is a simple, fixed rod mounted in an area where ice will accumulate and easily be visible to the pilot.

5.3 RECOGNIZING ICING THAT EXCEEDS AIRCRAFT AND ICE PROTECTION SYSTEMS CAPACITY

Aircraft ice protection systems are designed to meet particular operational needs of an aircraft. For commercial aircraft, the icing design requirements (Section 1) are relatively severe, and the probability of exceeding the design conditions is remote. However, many civil and military aircraft are not designed for continuous flight through icing and have either minimum or no ice protection equipment. The probability of exceeding the aircraft and ice protection systems capabilities in this case may be quite high. This portion of the report discusses the types of limitations that may be involved for aircraft and ice protection systems, and means of recognizing that their limits have been exceeded.

Most running wet anti-icing systems and thermal de-icing systems are designed to a minimum ambient temperature of 0° F. Statistical data (Section 1) shows that more than 90 per cent of all encounters occur between 0° and 32° F. As aircraft are normally equipped with ambient temperature indicators, it should be relatively simple to avoid flight through icing at the lower temperatures. Should icing be encountered at temperatures below 0° F, the de-icing systems designed for 0° F may not shed ice, and fluid anti-icing and thermal anti-icing systems will allow accretion of ice on the protected areas. Changes in aircraft speed and handling characteristics may also be noted.

Thermal anti-icing evaporative type systems are usually designed for about 0.5 gm/m^3 liquid water content. At higher liquid water contents, some water will freeze aft of the heated area. A moderate amount of runback icing can be tolerated by most aircraft, provided that it does not become large enough to present an ice accretion shape. It is also possible to determine liquid water content by an instrument such as the NACA icing rate meter; however, no such instrument is commercially available.

Excessive droplet sizes (as in freezing rain) can cause poor performance of ice protection systems, as well as affecting air speed indication by icing of static ports. Excessive chordwise extent of ice on the wing and tail leading edges would be the primary means of identifying this condition. If the surfaces are heated, excessive runback might be noted because of the high catch efficiency of large droplets. Cyclic de-icing systems may not function at large drop size if ice accumulates beyond the normally protected area.

Rapid drop off in air speed or erratic engine operation are two other indications that excessive icing has been encountered. In this case, evasive action must be taken immediately — by climbing over the icing cloud, descending to warmer air, or by flying around the clouds.

When encountering ice crystals and snow in dry clouds, it is not necessary to turn on the ice protection system. However, when ice crystals mixed with liquid water are encountered, it is possible for the capacity of the ice protection system to be exceeded. With the ice protection system in operation at these conditions, the runback may be severe (for thermal systems) and evasive action may be necessary. (See Paragraph 1.4.7 for a further discussion of ice crystals.)

5.4 ICE PROTECTION SYSTEM CONTROLS AND INDICATORS

Certain general comments can be made concerning controls and indicators for the various types of ice protection systems. These comments are made to

assist proper selection of control systems. Specific examples are not included because of the myriad of switches, valves, indicators, timers, etc. available, as well as the rapid advances continually being made in this field. Once the control function has been established for a particular system, vendors of control and indicating equipment can supply current data on the specific items needed.

Ice detectors — either mounted on the fuselage or in turbine engine intakes — are often used to warn the pilot of icing conditions. Indication is usually by a warning light on the control panel. On some turbine engine aircraft, an automatic feature has been incorporated to turn on engine and inlet anti-icing whenever icing is detected. The low reliability of available detectors has made this approach questionable for commercial service; however, it is in use on several military aircraft.

Control systems for pneumatic boot de-icing systems are relatively simple, requiring only a timer and the associated pneumatic valves. The timer controls periodic inflation of the several pneumatic de-icers in a predetermined sequence. Inflation time is normally a constant value of about five seconds, depending on the particular boot design. The period between inflations can be fixed at, say, three minutes or made variable (by pilot selection) to allow more frequent inflation in heavy icing. Solenoid-actuated pneumatic valves control the airflow for inflation. These valves are normally dual purpose, and will also control the vacuum pressure to deflate the de-icers. Pressure and vacuum gages could be provided to monitor system performance; however, this is normally done by simply observing inflation and deflation of the de-icers.

Fluid anti-icing systems are usually controlled by a simple switch-operated solenoid valve (for a pressurized tank system) or by a switch-operated pump. Gages for monitoring system pressure and the amount of fluid remaining are optional, but usually found unnecessary.

Thermal anti-icing systems can be discussed in two categories: electrical and hot air. The electrical system may be only a switch-controlled resistance

heater. In many cases, overheat protection is included (by means of a thermo-switch, thermistor, or positive resistance coefficient wire sensor) to prevent excessive temperatures during low speed or ground operation. Electrical over-load protection is usually furnished by fuses or circuit breakers. In the case of windshields, a pilot relay may be used to operate a power contactor, with a variable-voltage transformer to compensate for aging of the electrical resistance film. Two heat settings are often used: a high setting and an intermediate (1/2 to 2/3 power) setting, with power cycled on and off to maintain a predeter-mined temperature setting. An approach that can be beneficial to windshield life is to use the recently developed static switching and modulating controls that vary power in proportion to the demand, rather than switching power on intermittently.

Hot air anti-icing systems are normally controlled by solenoid-operated pneumatic valves. (Motor-operated valves can also be used.) Overheat pro-tection and/or warning can be provided by means of thermoswitches, thermis-tors, or wire-wound resistance sensors, plus an associated bridge circuit. In the case of engine and inlet anti-icing, it may be required (as on commer-cial aircraft) to have a means of indicating proper system functioning. A pressure switch is commonly used, connected to a warning light to warn of inadequate pressure (and thus inadequate anti-icing) to the system. A valve position indicator or the temperature of a critical anti-icing surface may also be used to indicate proper system operation. Many commercial aircraft tur-bine engines have used pressure switches or valve position indicators for reasons of cost and reliability.

Thermal de-icing systems may also be discussed in two parts electrical and hot air. The cyclic electric systems require a timer and switching device to apply power intermittently to the various heated areas. To minimize run-back icing, it is often desirable to limit surface temperature by a surface temperature cutoff device, or to sense air temperature and decrease heat-on

time as the temperature approaches 32° F. For low power applications (up to 5kw), a switching relay can be used with a motor-driven selector. Power contactors may be needed at higher power. Static switching devices are feasible for larger aircraft, and are currently in use on some transport aircraft. Protection against operation on the ground is usually provided by a landing gear switch. The parting strips (continuously heated strips) also require protection as discussed previously. Protection against overload is provided by circuit breakers and/or fuses. System indication is usually provided by observing electrical loads as the system cycles power from one area to another. Time between cycles can be either fixed or variable, but most systems are currently using fixed time for simplicity.

Hot gas de-icing systems normally use solenoid-actuated pneumatic valves to allow rapid opening and closing. A timer is needed to control the various valves. A fixed cycle may be used, however a variable heat on time (varying with total air temperature) is more common. Time between cycles can also be made variable if desired. This time is usually three to four minutes; however, longer periods may be tolerated in moderate icing conditions. One approach that has been used is to provide normal heat-on (15 to 20 seconds) and heat-off (three to four minutes) periods, with longer heating periods every fourth or fifth cycle. The additional heat period removes runback that may have accumulated during the previous cycles. An overtemperature warning or control (similar to hot air anti-icing) is also desirable.

All hot air systems may or may not contain control of the basic air source. Bleed air systems usually are controlled by pressure regulating valves. In addition, maximum bleed air temperature may be limited by several methods. One is by mixing outside air or exhaust air from the gas passages using an ejector mixing system. Another is mixing low-temperature air from the low-pressure rotor of a dual-rotor compressor with high-temperature bleed air from the high-pressure rotor. Ram air cooled heat exchangers may also be used, although with penalties on weight, thermal efficiency and aircraft drag.

Another method in use on turbine engine anti-icing systems that could be adapted to airframe use is a temperature-modulating valve that reduces air flow as bleed air temperature increases. A coiled thermostatic spring and vane assembly is used to restrict flow at high temperatures. Overheat of the inlet guide vanes and front frame is avoided by use of this type of valve. An on-off type pneumatic control valve is usually in series with the modulating valve.

The final consideration for all control systems is that any single failure should not result in a hazard to the safe operation of the aircraft.

REFERENCES

5-1   NRC (National Research Council of Canada) Aeronautical Report LR-334, "Review of Icing Detection For Helicopters," J. R. Stallabrass, March 1962.

5-2   "Ice Detectors," D. P. Howlett (paper presented at 1961 Aircraft Ice Protection Conference, D. Napier & Son, Ltd.).
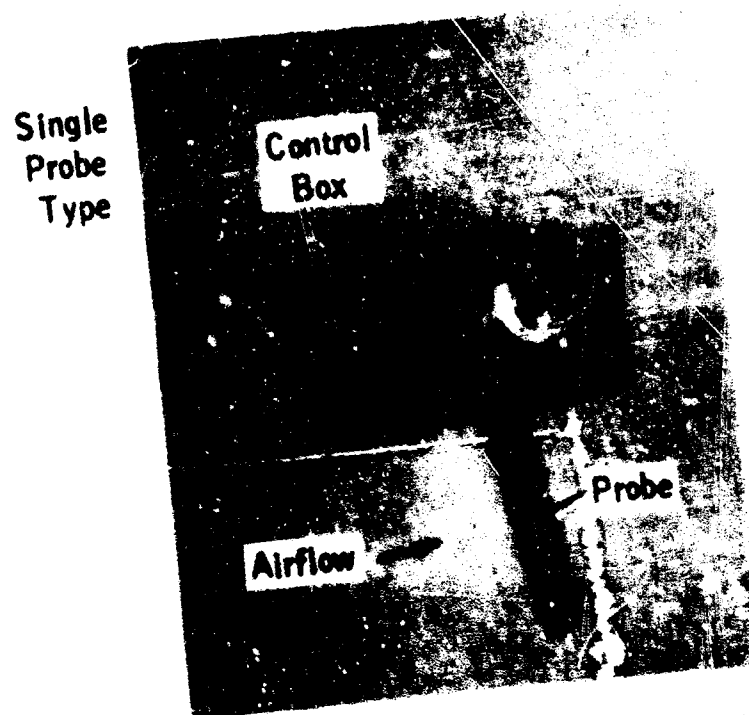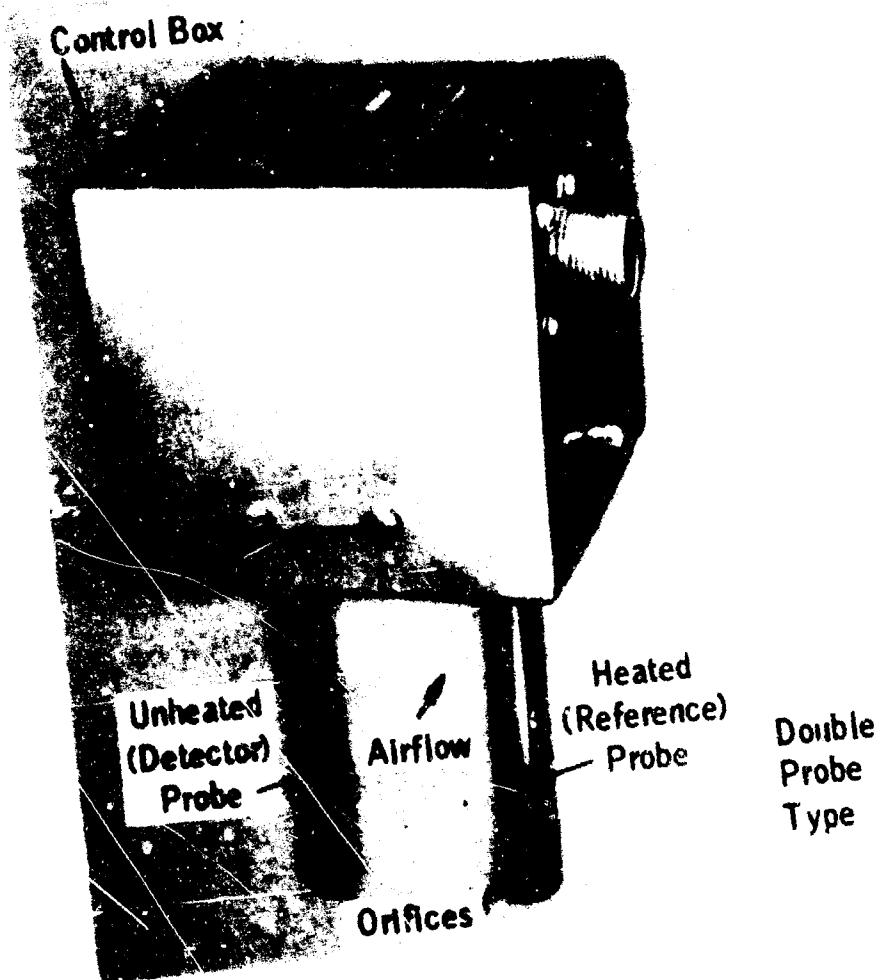
Figure 5-1. Differential Pressure Ice Detectors.
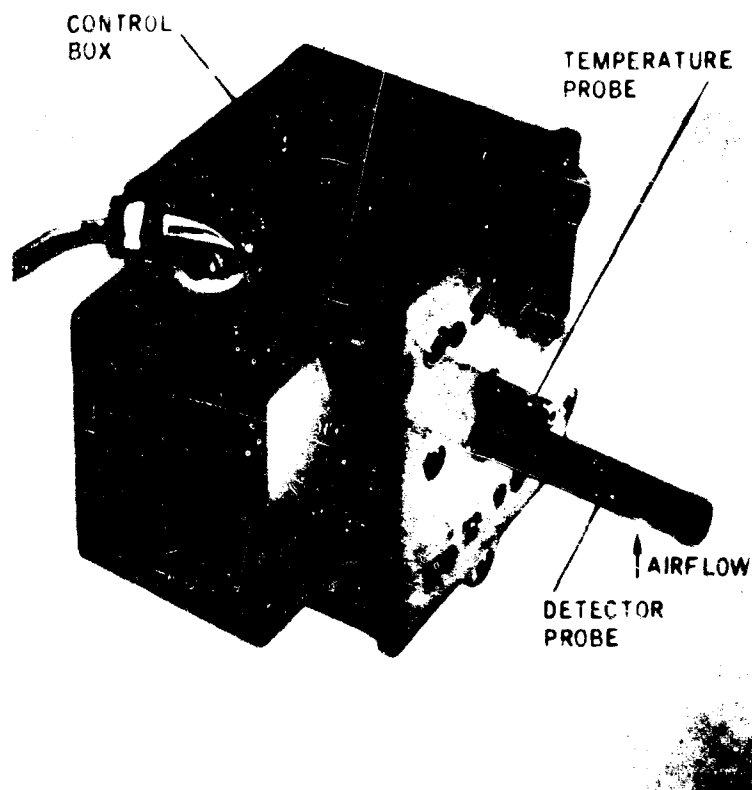
Figure 5-2. Electrical Conductivity Ice Detector (Insulated Gap Type).
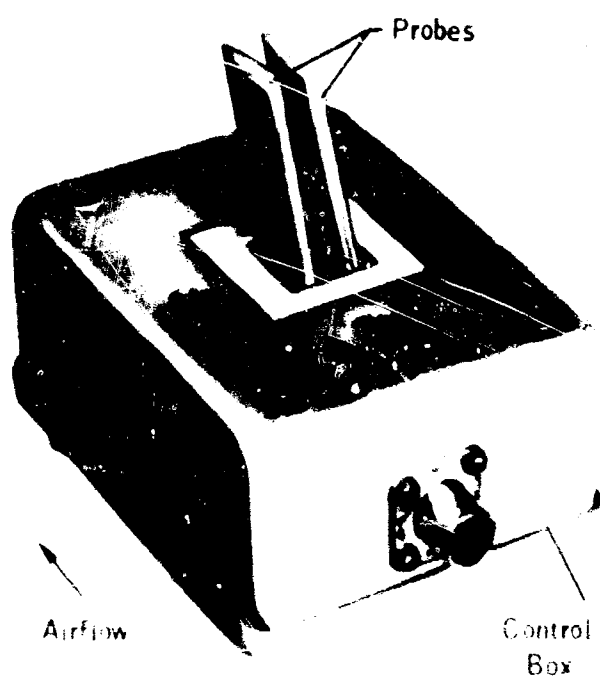
Figure 5-3. Electrical Conductivity Ice Detector (Air Gap Type).
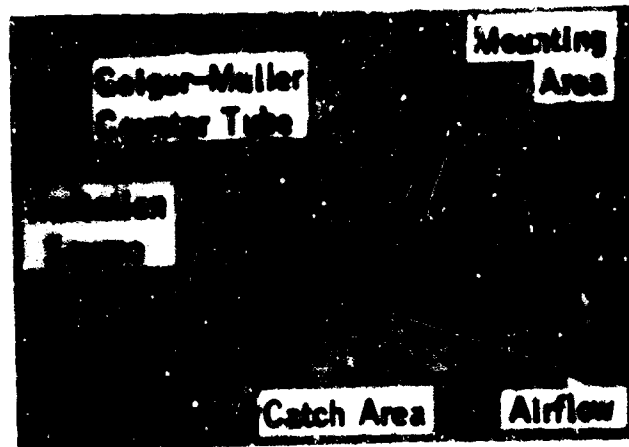
Figure 5-4. Beta Radiation Ice Detector.
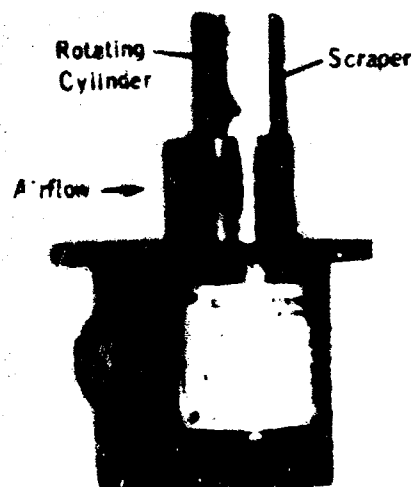
Figure 5-5. Rotating Cylinder Ice Detector.
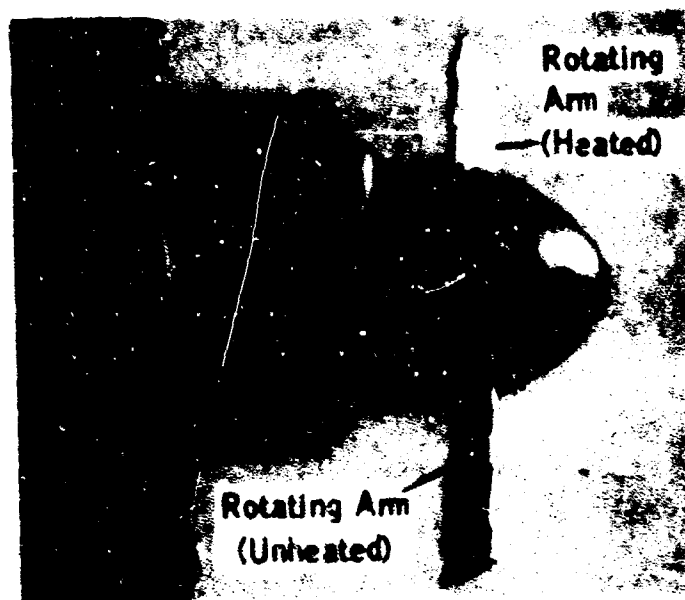
Figure 5-6. Mass Balance Ice Detector.
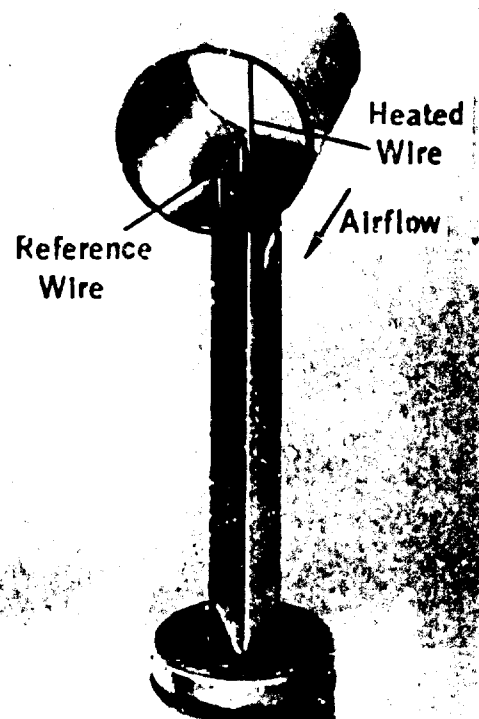
Figure 5-7.   Electro-Thermal Ice Detector.
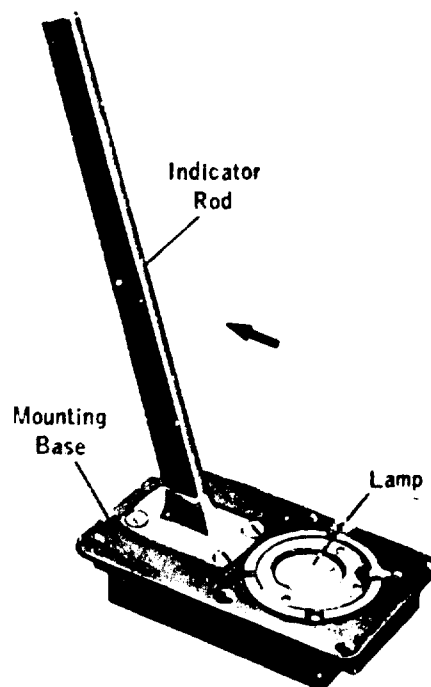
Figure 5-8.   Heated Rod Ice Detector.

6 | TESTING AIRCRAFT AND ICE PROTECTION SYSTEMS

CONTENTS

TESTING AIRCRAFT AND ICE PROTECTION SYSTEMS

LIST OF FIGURES

6.1 SUMMARY

After the design of a new aircraft and its ice protection systems has been completed, or whenever a new ice protection system is designed for an existing aircraft, tests will be required to demonstrate that the system or systems are effective and that the aircraft involved can be flown through icing safely. The method and extent of testing to be performed will vary greatly depending upon previous experience with similar systems and applications and with the degree of ice protection provided.

In this section of the report, test objectives are defined for various types of systems and the types of measurements to be made in assessing system performance are described. Aircraft performance data needed to determine the effect of residual or primary ice formation is also represented.

The methods of testing (icing tunnel, clear air flight, natural icing flight and simulated icing flight) are described, and detailed data on the various test methods is presented. Description and critical sizes are shown for four icing tunnels. Methods of conducting flight tests in clear air and natural icing are shown. Data on use of the aerial tanker to create simulated icing in flight is included, along with the means of interpreting the test data obtained, because the simulation has certain limitations.

Study of the information contained in this section will assist in determining the type of test and test objectives for qualifying a particular system or aircraft, and will help to identify the most appropriate facility for these tests. The types of instrumentation to be used for various systems are also identified. Detailed planning of a specific test, however, must be accomplished individually for each new application.

6.2 INTRODUCTION

After the analysis and design of a particular aircraft and its ice protection systems have been completed, tests will normally be required to demonstrate that

the ice protection systems are adequate and that the aircraft can fly through natural icing conditions safely. The required tests will vary widely, depending upon the type of system, the amount of previous experience, and the mission and operational requirements of the aircraft. This section of the report describes the test requirements or objectives for the various types of systems and aircraft, and presents data on the various methods of accomplishing these test objectives. This section does not present the detailed information necessary for a complete icing test program, but does include information on the types of tests that may be required and the sources to contact for further information. Instrumentation needed for these tests is also discussed.

These test methods include icing wind tunnel tests, flight tests in clear air, and flight tests in either natural or simulated icing. Specific data is included on the capabilities of the various icing tunnels available to the industry. Spray calibration data is shown for the aerial tanker used by the U.S. Air Force for inflight simulation of icing conditions, together with comments on interpretation of data derived from tanker tests. Methods of predicting "wet air" performance from clear air tests are also discussed.

Another subject of ever-increasing importance is the effect of ice accretion on aircraft performance and handling characteristics, as these are the factors that determine the need for ice protection of specific portions of the airframe. Comments on testing with actual and simulated ice accretions are included.

6.3 TEST OBJECTIVES

6.3.1 DATA REQUIRED — Test programs for an aircraft and its ice protection systems have one primary obj t: demonstration of safe flight through natural icing conditions. This objective can be met by conducting tests to show that the systems function properly and that the required performance has been met or exceeded. In cases where ice protection is not provided for all parts of an aircraft, the effect of ice on aircraft performance and handling characteristics must be determined.

6-4

This paragraph describes the test objectives to be considered in wind tunnel and flight testing of aircraft and the associated ice protection systems. For each type of system, certain parameters are important in showing that the system has met design requirements. This discussion covers the parameters to be measured for the various types of systems presented in Section 3, Methods of Protection. A discussion is also included on the types of instrumentation that may be used. A discussion of the methods of testing (icing tunnel, dry air flight, natural icing flight, and simulated flight icing) is contained in Paragraph 6.4.

The pneumatic boot de-icing system has been used extensively and normally would require a minimum of testing. A functional test to determine inflation and deflation time and to check inflation pressure and vacuum pressure is required. The effect of the de-icing boots on aircraft performance and handling characteristics should be determined, both with the boots deflated and with the various sections inflated. The drag effects (if any) of installing the boots can be determined if previous flight test data is available showing the relationship of drag to lift. The ability of the boot to remove ice should also be determined for new de-icing boot/airplane configurations — this can be done in natural or simulated icing. The effects of leading edge radius and de-icing tube diameter upon ice removal characteristics must be determined if previous data is not available. The effect of residual ice (ice remaining on the boot after inflation) should also be determined; normally this would cause a slight increase in drag, but no other effects.

Fluid anti-icing or de-icing systems will require general functional tests, determination of fluid flow rates and distribution, and finally tests in either natural or simulated icing. Fluid distribution can be determined in dry air using visual aids — chalk on the protected surface or dyed fluid to show flow patterns. Final assessment of system performance is dependent on icing tests, as prediction of fluid flow rate requirements (see Section 3) are at best only

approximations. In the case of fluid de-icing systems, the effect of periodic ice accumulation on lift, drag and aircraft handling characteristics should be evaluated.

Electro-thermal anti-icing and de-icing systems normally require only a minimum of testing because of the relatively large amount of background data on such systems. Electrical power delivered to the various heated areas should be determined and compared with design requirements. Surface (inner and outer) temperatures can be measured to check overall heat distribution and to determine internal heat losses. An icing test will usually be required to verify overall performance, to determine any local cold spots, and to evaluate effects of runback icing on lift, drag and aircraft handling characteristics.

The hot gas anti-icing and de-icing systems often require more extensive testing than electrical systems, as the hot gas systems tend to be unique for each new type of aircraft. The hot gas systems are more integrated with the airframe than other types of systems. Tests of anti-icing systems will include measurement of air flow rates, gas temperature (and duct temperature and pressure losses) as well as spanwise and chordwise temperature distribution. Thermal efficiency of the system may also be determined. If the system is not designed for complete evaporation, the effects of runback icing on aerodynamics of the surface or aircraft involved should be evaluated.

Tests of hot gas de-icing systems will require similar tests, plus the measurement of surface and gas temperatures versus time to assess system heating and cooling characteristics. Icing tests will usually be required to determine the optimum combination of heat-on versus heat-off times, to assess possible cold spots, and to determine the amount of runback ice formation.

In the case where no icing protection is used on an aircraft intended for flight through icing, it will be necessary to determine the effects of the maximum likely amount of ice on aircraft performance in terms of increased drag, decreased maximum lift coefficient, increased stall speed, possible damage to

6-6

components and engines, and general effects on aircraft handling qualities. Many military aircraft with relatively high power to weight ratios are flying in icing without airframe protection. Where power to weight ratio is low, however, airframe ice effects may be intolerable (see Sect'on 4).

6.3.2 INSTRUMENTATION — Specific instrumentation and data recording methods used for tests of ice protection systems will vary widely, depending upon the type and size of the aircraft and upon the nature of intended operation in icing. A general discussion of instrumentation is contained in this paragraph; however, the number and specific types of thermocouples, pressure taps, ammeter, etc., must be selected for each specific project.

Evaluation of aircraft flight performance in icing requires measurement of air speed, altitude, ambient temperature, time, angle of attack, and engine performance. Measurement of icing intensity may be required, as described in Paragraph 6.4. Handling qualities may be determined by pilot evaluation plus any special instrumentation deemed necessary.

The hot air thermal systems will require measurement of air flow rates and gas and skin temperatures. Air flow rates can be measured by use of calibrated duct sections having static pressure, total pressure and gas temperature pickups. Thermocouples may be used for temperature measurements. Typical thermocouple installations are shown in Figure 6-1. An excellent discussion of thermocouple installations is contained in the SAE Aero-Space Applied Thermodynamics Manual, Section C, Part G (Ref. 6-8).

Pressures may be measured directly by gages, or may be recorded electrically using pressure transducers. Where transient effects are important — as with the hot gas de-icing system — continuous multi-channel recorders may be required.

For electrical systems, power may be determined by measuring voltage and current, or where element resistance is not variable with temperature, current measurement will be sufficient. Surface and internal temperatures can be measured and recorded by the methods discussed previously.

6-7

Fluid ice protection systems will require measurement of fluid flow rate and tank or pump pressure. Flow rate can be determined by time duration to empty the tank, by an orifice or venturi meter, or by any of several other methods such as a rotameter or a commercially available turbine flow meter.

In any icing test, either wind tunnel or flight, photographic coverage is essential to document test results. The presence of an icing cloud makes good pictures particularly difficult to obtain. One solution is to photograph the ice formations in clear air by climbing out of the icing cloud (in the case of flight testing), by shutting off the spray cloud in icing tunnels, or by operating in clear air when testing with a tanker. Time correlation of photographs with other data is essential.

6.4 METHODS OF TESTING

Four methods of testing ice protection systems can be used to determine effectiveness and airworthiness. These are icing tunnel tests, dry air flight tests, natural icing flight tests, and simulated icing flight tests. The method of testing will vary, depending on the aircraft or components under consideration, the design requirements, and the amount of previous data available on the particular aircraft or component. Perhaps one of the methods or more commonly a combination of methods may be used to demonstrate effectiveness and airworthiness.

6.4.1 ICING TUNNEL TESTING — The icing wind tunnel has an advantage in that it permits direct, quick comparisons of the influence of various design features at a modest cost. On-the-spot modifications can often be made and tested with minimum delay. Wind tunnel tests on specially constructed test models can be made while an aircraft is in the design stage, thus avoiding costly modifications after the aircraft is in production. Satisfactory operation with minimum energy requirements (bleed air, electrical, fluid or other) is the design objective of most ice protection

systems, and can often be determined most accurately by icing tunnel tests.

In the U.S., two icing tunnels are in use for testing of aircraft ice protection systems. The largest is the six by nine-foot icing research tunnel at the NASA Lewis Research Center, Cleveland, Ohio. The Lockheed icing research wind tunnel at Burbank, California, has two throats: one 2.5 by 4-ft., and one 2.5-ft. square. In Canada, icing tunnels of 4.5 by 4.5 ft. and 12 by 12 in. are located at the Low Temperature Laboratory of the Canadian National Research Council in Ottawa.

6.4.1.1 NASA Icing Tunnel — The maximum airspeed in the NASA icing tunnel under icing conditions with a large test model is 240 kt. The tunnel was designed to operate at temperatures to -40° F; however, operation is currently limited to -10° F total air temperature. A plan view of the tunnel is presented in Figure 6-2. This schematic shows the drive fan, ventilating towers, refrigeration coils, spray system, heat exchanger and test section. A 4,160-hp motor drives a fan, consisting of twelve 25-ft. dia. wooden blades. The ventilating tower provides additional cooling load and a location for mixing tunnel air with outside air. The heat exchanger provides a capacity of 5,000,000 BTU/hr., for regulating tunnel air temperature. The refrigeration system is located in a nearby building and has a 7,700-ton capacity. The spray system is located just upstream of the test section. Water for the spray system is demineralized at the rate of 500 gal. per hour and kept in a 750 - gal. storage tank. Filtered, heated air for the air - water - spray system is provided at 120 psi with a capacity of six pounds per second. The test section has a turntable which can be used to rotate test models during testing. Sidewall trunnion mounts are also available. Large models can be lowered into the tunnel through a 48 by 40-in. hatch in the roof of the test section. Three heated observation windows are located on each side of the tunnel and some observations can be made through the glass port on the roof, although this is used primarily for supplying light for photography.

Heated air for model ice protection systems is supplied by three heat exchangers, each with a 1,000 pound per hour capacity with pressure regulation up to 120 psi.

AC and dc electrical power for icing protection is available; the dc systems are 28 volts/100 amp. and 12 volts/50 amp.; the ac systems are 29 volts 50 amp., 110 volts/single phase, and 208 volts/three-phase/50 amp.

Installation of a typical airfoil model is shown in Figure 6-3.

Current policy on operation of the tunnel is that the test facility is available for industry use, provided that a government agency will sponsor and recommend that the test be performed, and that no other commercial facility is adequate for the required tests. Users must provide their own test models, engineers and mechanics; a tunnel operator is provided by NASA to operate the tunnel and spray system. Prospective users should contact:

> Director
> NASA Lewis Research Center
> 21000 Brookpark Road
> Cleveland, Ohio
> Attn: Mr. Joseph O' Herien

6.4.1.2 Lockheed Icing Tunnel — The Lockheed icing tunnel airspeed range under icing conditions is about 50 to 185 kt. in the main throat (2.5 by 4-ft.) and about 50 to 210 kt. in the alternate (2.5 by 2.5 ft.) throat. Lower speeds are possible in the alternate throat but experience is limited.

The 70-ton refrigeration system can provide minimum total tunnel air temperature of -5° F over the above velocity ranges. Figure 6-4 presents a schematic of the Lockheed icing research tunnel with the main throat. The alternative throat is shown in Figure 6-5 as it would be installed within the main throat.

The 200-hp motor drives the seven-foot, variable pitch, four-blade fan. The refrigeration coils are about 15 ft. upstream of the spray system and about

35 ft. upstream of the test section. The spray system provides water droplets from 7 to 35 microns (volume median droplet diameter) at liquid water cor-tents from 0.7 to 4.0 gm/m^3 as shown in Figure 6-6.

An example of tests conducted by the Lockheed company is shown in Figure 6-7.

The tunnel is available for rental to industry. Charge is made for man-power services only (no charge for occupancy and running time). For further data and operating costs, contact:

Lockheed - California Company
Box 551
Burbank, California
Attn: Mr. G. Sim, Dept. Mgr., Wind Tunnels
Bldg. 201, Plant 2, Rye Canyon

6.4.1.3 NRC Icing Tunnel, Ottawa. Canada — The National Research Council of Canada operates a 4.5-foot square icing tunnel as part of the Low Tempera-ture Laboratory. The general arrangement of the closed circuit tunnel is shown in Figure 6-8. The working section is 4.5 ft. square and 11 ft. long. The maximum velocity in the working section is 200 mph. The tunnel is driven by a fan with eight wooden blades operated by a 1,000-hp synchronous motor which permits variable speed operation over the range oi 100 to 1,200 rpm. Airstream cooling is accomplished by passing the air over banks of liquid ammonia-refrigerated pipes. Throttling the liquid ammonia regulates the air-stream temperature. Capacity of the system is sufficient to permit continuous operation at full speed at an air temperature of -25° C (-13° F). Lower air temperatures can be obtained for short intervals of 15 to 30 minutes at full speed or for longer periods at reduced speeds.

The cloud water droplets are produced by an array of air-atomizing water spray nozzles located at the upstream end of the contraction leading to the working section. Control of the drop size is obtained by varying the air pres-sure and water flow to the nozzle in accordance with calibration data. Water

6- 1

content up to 3 gm/m^3 and median droplet diameters down to 15 microns can be obtained at the maximum tunnel velocity.

To provide a higher speed stream for basic research and for testing small components such as guide vanes and icing detectors, an auxiliary tunnel has been built alongside the main tunnel to take air from the downstream side of the refrigeration coils and return it to the upstream side. The position of the auxiliary tunnel is shown in Figure 6-8. The tunnel is constructed of plywood and is built in sections that can be removed and replaced with others of different shapes. In this way, various component configurations may be studied. The current configuration gives a working section of 40 sq. in. and a velocity of 500 mph. The tunnel is driven by a 50-hp centrifugal blower on the upstream side of the spray nozzles. The blower operates at a constant speed. Air velocities in the tunnel are controlled by variable shutters on the blower intake. The air stream temperature is controlled by regulation of the same liquid ammonia refrigeration tubes of the main tunnel.

The National Research Council also has a simulated variable density, high-speed icing tunnel as shown in Figure 6-9. This tunnel is capable of airspeeds up to Mach 0.9 and altitudes up to 30,000 ft. Air temperatures down to -40° C automatically controlled to ±0.5° C are obtained by circulating cold trichloro-ethylene in a finned-tube heat exchanger located in the vertical leg of the tunnel before the contraction. The trichloroethylene is cooled in a heat exchanger system employing the Low Temperature Laboratory's ammonia refrigeration system. The tunnel is powered by a 750-hp dc motor driving a two-stage axial fan through a 3:1 speed increaser. This tunnel, wh'h has a test section 12 in. by 12 in., is intended primarily for basic research into high-speed icing problems and for the test and development of small components such as ice detectors and measuring instruments.

The NRC tunnels normally are used only for government-sponsored research, or for tests of systems that would fulfill research objectives of the

National Research Council. For further information, contact:

The National Research Council of Canada
Division of Mechanical Engineering
Low Temperature Laboratory
Ottawa, Canada
Attn: Mr. J. J. Samolewicz

6.4.2 DRY AIR FLIGHT TESTS — Flight tests of a new aircraft and/or ice protection system are normally made in clear air before the aircraft is committed to actual flight in icing conditions. These tests check the function and performance of the systems to ensure that the requirements established in the initial design have been met. The evaluation should include the full range of power and speed to determine limiting conditions where systems may not furnish adequate protection. The operation of the system can be compared with either results of dry-air icing tunnel tests or with analytical values established during design (with appropriate consideration of the "dry air" condition).

Dry air flight testing of the mechanical pneumatic boot would determine the installation effects, if any, upon aircraft drag performance. These effects are a function of previous conditions of the airframe and the type of boot installation, and thus are difficult to predict (see Section 3). During these tests the functioning of the system may also be demonstrated, as well as any effects upon lift and drag of inflating the boots. General handling characteristics should be checked with the boots deflated and inflated.

The fluid coverage and fluid flow rate tests of the fluid freezing point depressant system may be conducted in dry air. Items to be observed during the tests are fluid consumption rate, proper fluid distribution and adequate coverage of the surface to be protected. Dyed fluid and/or chalk rubbed on the surfaces may be used to aid in observation of fluid distribution.

Dry air flight testing of the electro-thermal ice protection system would establish whether the system function and performance are in accordance with design requirements. Power delivered to the various circuits should be

measured. Surface temperatures should be measured at critical areas and compared with either dry air wind tunnel test data or analytical predictions. General function of the system, including controls and overheat protection, should be determined.

Dry air flight testing of the hot gas anti-icing and de-icing system serves the same purpose as in the electro-thermal system. Of concern in the hot gas system is the availability of hot gas (from either bleed air or an exhaust gas heat exchanger) during periods of reduced power; e.g., during descent or hold. A combustion heater should provide a constant quantity of hot gas independent of flight conditions. During the dry air flight testing, further refinement of the flow distribution may be made, if necessary. Detailed measurements of bleed flow are normally made for the complete range of flight conditions in order to assure that engine bleed limits have not been violated and to establish effects on aircraft performance.

6.4.3 NATURAL ICING FLIGHT TESTS -- Aircraft intended for use in commercial transport are usually flight tested in natural icing before receiving certification. The extent of testing needed will depend on the amount of prior analysis, testing and flight experience with the particular aircraft and its ice protection systems. Because of the high cost of conducting natural icing tests and the fact that the design icing conditions are difficult — if not impossible — to find, the usual procedure is to find icing conditions of whatever severity available and to use previous analytical and test data to extrapolate the natural icing test data to the design extremes.

Current operating costs for jet aircraft are $5,000 to $10,000 per hour, and a typical icing search will involve 30 to 60 hours of flight to obtain one to two hours of actual icing experience, resulting in costs of perhaps $150,000 to $600,000.

The flight test aircraft must have instrumentation to determine liquid water content and droplet size, or a means of determining ice accretion rate and

extent of impingement from which these parameters can be established. Rotating multi-cylinders are the standard instruments, but are inconvenient to use on pressurized aircraft. The NACA icing rate meter or any calibrated ice detector can be used to determine liquid water content; whereas drop size can be approximated from extent of impingement on any shape with known impingement characteristics.

The flight tests in natural icing fall into two categories: functional and performance tests of the ice protection systems, and tests of aircraft and engine operating characteristics for the full range of power and flight conditions to determine system adequacy or limitations. At least minimum instrumentation is needed to measure performance of the ice protection systems. Thermocouples on critical surfaces are usually needed for thermal anti-icing and de-icing systems. A means of observing and photographing ice accretion is also needed.

After icing has been encountered, operation of the aircraft and ice protection systems should be observed long enough to obtain data and to observe any deficiencies in systems operation or loss in aircraft performance and handling characteristics. Following this, ice should be allowed to form on any critical surfaces (such as wings, empennage, and engine inlets) where ice would form as a result of either a single system failure or the pilot's failure to recognize icing immediately. Typical intervals might be two or three minutes in icing with the engine and engine inlet systems off, and 15 to 30 minutes with wing or tail ice protection off (if a single failure would cause the system to be inoperative). After the effects of ice have been noted, the systems can be turned on again to determine their recovery characteristics.

Final evaluation of natural icing test results is dependent on a detailed comparison of extrapolated test results with original design requirements.

6.4.4 NATURAL ICING SIMULATION IN FLIGHT — Because of the difficulty in finding suitable natural icing conditions for development testing and the

limited size of the icing wind tunnels, test methods have been developed to create artificial icing conditions for testing large components and complete ice protection systems inflight. These methods have been quite useful although there are certain inherent limitations, as described below.

One method that has been used extensively for tests of airfoil ice protection is to equip an aircraft as a flying laboratory. The test airfoil is mounted vertically on the upper surface of the fuselage behind a water spray rig in a setup similar to icing tunnel techniques. The aircraft is then flown at an altitude where the desired icing temperatures exist and water is sprayed from the nozzles over the test section. Figure 6-10 illustrates this technique.

A similar system has been used to test propeller and jet engine icing protection. A spray rig is mounted ahead of the test engine or propeller, and water (carried internally in the aircraft) is sprayed to form an icing cloud. A propeller icing test is shown in Figure 6-11.

These methods have the advantage of allowing control over the icing conditions and, in addition, do not involve the hazard of subjecting the entire aircraft to icing. The disadvantage is the cost and complexity of mounting a spray rig and test instrumentation on an aircraft, as well as the high costs associated with flight testing. In addition there is difficulty in measuring the icing conditions.

The two methods just described are adequate for testing components only, but not the complete aircraft. The third method uses a tanker aircraft with a spray nozzle boom extending downward and aft (see Figure 6-12). The spray nozzles create an artificial cloud into which an aircraft is flown to expose various parts of the aircraft to icing. The cloud may not be large enough to envelope the complete aircraft. Several spray nozzle rigs are being used currently to simulate different icing conditions. A "T-bar" water nozzle (Figure 6-13) is used for low-altitude heavy rain and high-altitude ice crystal tests where there is no ice accumulation, although a very high liquid water content (LWC) is required. The T-bar is also used for icing tests where either

accumulation of ice or rate of accumulation is an important test requirement. The plugs at the ends of the T-bar can be exchanged to decrease or increase the LWC of the spray. No attempt to control water droplet size has been made with the T-bar.

A 40-in. diameter spray ring (Figure 6-14) consists of two concentric rings containing 66 spray nozzles. This arrangement is normally used for icing tests at ambient temperatures of from 0° to -25° C. Fuel injection nozzles are used to break up the water into small droplets. The water droplet size from the 40-in. diameter spray rake has been examined by collection on oil slides. The mean effective droplet diameter is in the order of 80 to 100 micron: .nd is nearly constant from 500 to 1,500 ft. from the rake. As the c   d from the rake disperses and increases in size, the LWC per unit are will decrease. Figure 6-15 shows the cloud dispersion rate as a function of distance behind the tanker.

To obtain specific icing conditions on an aircraft or aircraft component, the distance behind the tanker must be maintained at a reasonably constant value. The tanker observer usually controls this condition using some ranging device. The test aircraft is flown parallel to the cloud until it reaches the right range. Upon receiving a signal from the tanker, the aircraft or component is then flown into the icing cloud for a predetermined time. The time between takeoff of the tanker and test should be kept at a minimum to prevent the water from freezing in the nozzles.

At present, complete reliance on use of the tanker to qualify aircraft for flight in icing is a questionable and controversial subject. The excessive drop sizes may show many ice protection systems to be inadequate, whereas in natural icing the systems would be adequate. At the same time, tests involving ice accretion on unprotected components have not to date been capable of producing the double-peaked glaze ice shape that is so damaging to the aerodynamic characteristics of an aircraft. Further work is in progress at increasing cloud

size and improving the droplet size to more nearly conform to natural icing. Although the present simulation is not ideal, the tanker can be a useful tool in evaluating aircraft and ice protection systems in icing, if proper allowance is made for the excessive drop size and for the type of ice shape produced on unprotected surfaces.

An example of light plane simulated icing is shown in Figures 6-16 and 6-17.

6.4.5 TESTING UNPROTECTED AIRCRAFT -- There may be occasions when it is desirable to test an airframe for performance with ice accretions on all or part of the areas normally ice-protected. This testing may be for certification of an aircraft with large power reserves for operation in icing with no ice protection, or to determine whether ice protection may be removed from a component.

The criterion for determining whether ice protection is necessary is aircraft performance with ice accretion. Performance factors considered in this respect are flutter, stall, general handling characteristics, effect upon approach and climb, and effect upon range.

One method of conducting such tests is to seek natural icing and perform all necessary maneuvers and speed changes to determine aircraft performance. This technique involves several difficulties: the first lies in finding natural icing conditions of the severity desired for the tests; the second is the problem of retaining the ice intact while executing the necessary maneuvers. Should some of the ice shed it may be necessary to re-enter the icing conditions and re-accrete the required icing.

An alternative method of icing test may be conducted at any time of year and practically anywhere; this involves simulating the icing on the area in question by artificial means. The weight and shape of the anticipated ice accretion can be formed from some material (e.g., wood) and attached to the aircraft surface. Flights may then be made to determine aircraft performance with the ice accretions.

The criteria for the artificial ice shapes will depend upon the aircraft type and mission. For light aircraft, the flight conditions might be cruise and/or hold. For turbojet transports, the criterion is for 45 minutes hold — 15 minutes departure hold and 30 minutes hold at destination. Examples of the ice shapes and the calculations used to derive them are presented in Paragraphs 4.1.3 and 4.2.11.

6.4.6 HELICOPTER TESTING

Several test facilities have been used to test helicopters in icing conditions and to test helicopter ice protection systems. Two of these facilities have discontinued these tests. One was the Eglin AFB climatic hangar where tests were conducted by tethering a helicopter under a water spray rig within a hangar. This test setup had the advantage of being independent of weather for ambient temperatures, but the icing conditions could not be controlled or determined because of recirculation and ice crystal formation. Too, the tests simulated only the hover mode of flight.

The other facility was located atop Mount Washington in New Hampshire. There, the helicopter was tethered and operated in natural icing conditions. The wind velocity assisted in simulating forward flight, but the temperatures and liquid water content were dependent upon natural conditions.

A facility currently in use is the helicopter spray rig at the National Research Council Low Temperature Laboratory at Ottawa, Canada. An artificial cloud is created by the spray rig shown in Figure 6-18; the temperature is dependent upon natural conditions. This facility is operated in wind velocities from approximately 5 to 30 mph. The 5-mph minimum velocity stems from the air movement necessary to move the artificial cloud out over the helicopter; the maximum velocity, 30 mph, is the structural limitation of the spray rig.

Certain wind directions restrict use of the rig because surrounding structures prohibit maneuvering larger helicopters. Snow and blowing snow also

restrict use of the rig by obscuring visibility. The spray rig can supply cloud conditions with liquid water contents up to 0.9 gm m^3 and droplet size of 30 to 60 microns (median volume diameter). Light freezing rain can also be simulated under suitable ambient conditions. The facility can create a cloud size suitable for testing rotors up to approximately 55 ft. in diameter. A helicopter undergoing tests in the spray rig is shown in Figure 6-19. A tanker aircraft, using boundary layer control for slow flight, is being developed for helicopter testing by WADC. This airplane will permit helicopter tests in flight regimes previously possible only in natural icing. In this manner, components as well as blades may be exposed to severe icing conditions under controlled conditions. It is expected that this facility will be available sometime in 1964.

Much of the testing of a helicopter ice protection system may be accomplished in a whirling arm rig. This type of facility is well suited to testing a fluid system's distribution characteristics, because all forces acting upon the fluid may be simulated. However, icing simulation on a whirling arm rig is not too feasible because of the same difficulties experienced at Eglin — air recirculation within the closed chamber. Electro-thermal systems may be tested in dry air to measure the heat transfer characteristics. The erosion characteristics of ice protection system materials may also be determined in the whirling arm rig.

REFERENCES

6-1 "The Icing Problem: Current Status of NACA Techniques and Research,"
     Uwe H. von Glahn, (paper presented at Ottawa AGARD Conference,
     June 1955).

6-2 WADC Technical Memorandum WCT-TM-59-3, "Technical and Practical
     Aspects of Systems for Simulating Clouds for Flight Test Evaluations,"
     J. K. Thompson, September 1959.

6-3 AGARDograph 16. "Icing Problems and Recommended Solutions," E. A.
     Brun, November 1957.

6-4   "Icing Wind Tunnels," B. D. Lazelle, (paper presented in May 1962 at Aircraft Ice Protection Conference, D. Napier and Son, Ltd.).

6-5   "Simulated Flight Icing Tests with a Tanker Aircraft," P. Schumacher, (paper presented in May, 1962 at Aircraft Ice Protection Conference, D. Napier and Son, Ltd.).

6-6   "The Icing Research Aircraft," B. F. Cheverton, (paper presented in May, 1960 at Aircraft Ice Protection Conference, D. Napier and Son, Ltd.).

6-7   "Icing Standard and Methods Used to Determine the Suitability of Aircraft to Fly in Icing Conditions," H. E. Le Sueur, (paper presented in June, 1958 at Aircraft Ice Protection Conference, D. Napier and Son Ltd.).

6-8   SAE Aero-Space Applied Thermodynamics Manual.

50 Wire Diameters
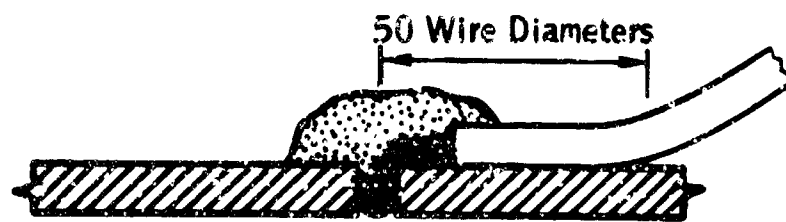
Surface Thermocouple
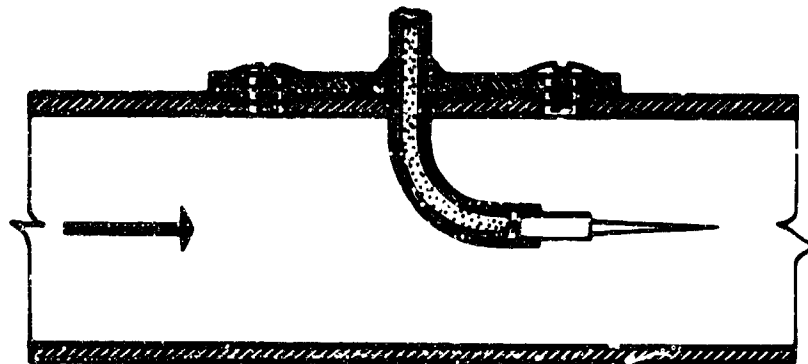
Thermocouple In a Duct

Thermocouple Junction
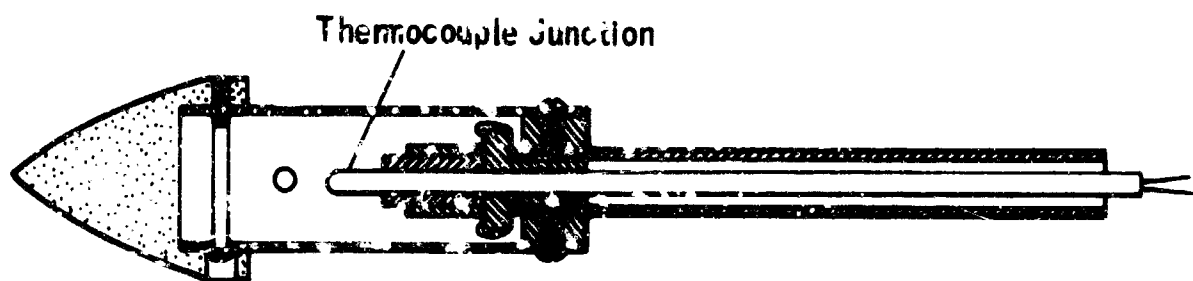
Shielded Thermocouple

Figure 6-1. Thermocouple Installations
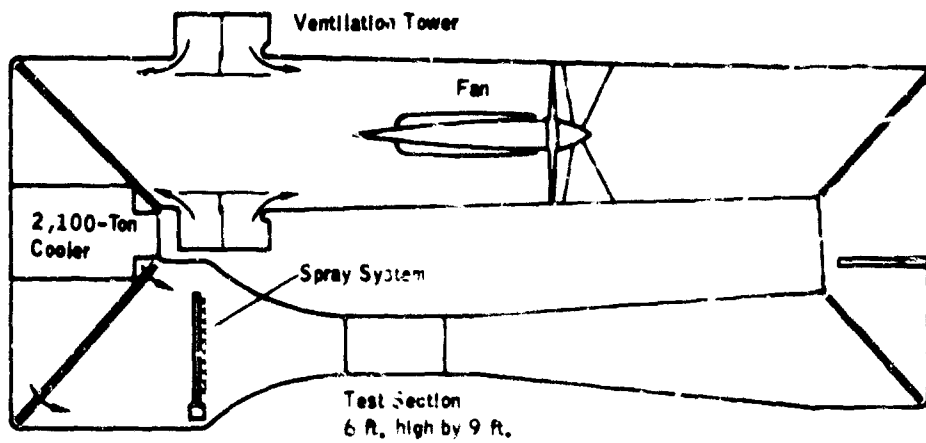
Figure 6-2.   NASA Icing Tunnel Circuit
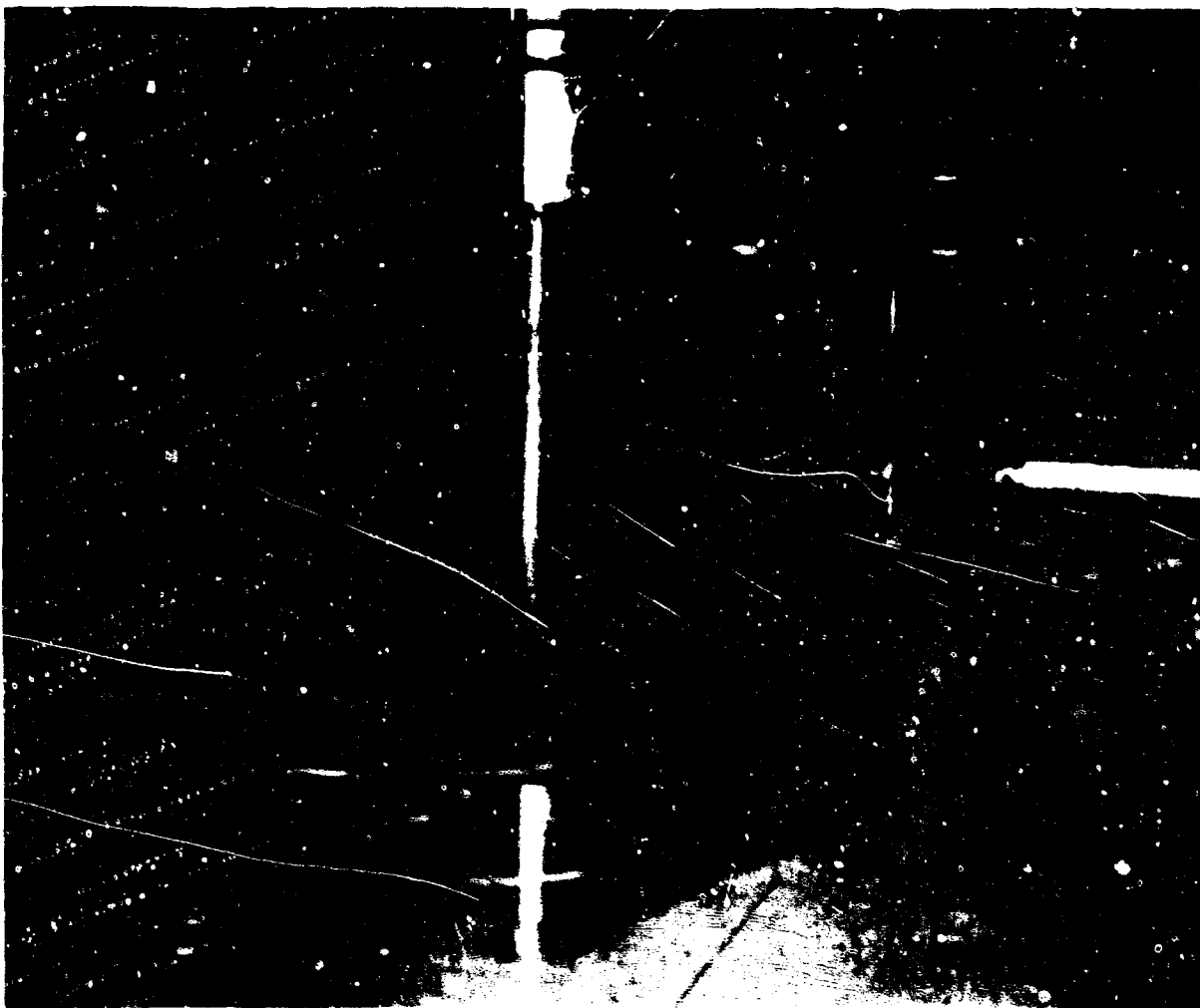
Figure 6-3.   Typical Test Setup in NASA Icing Tunnel
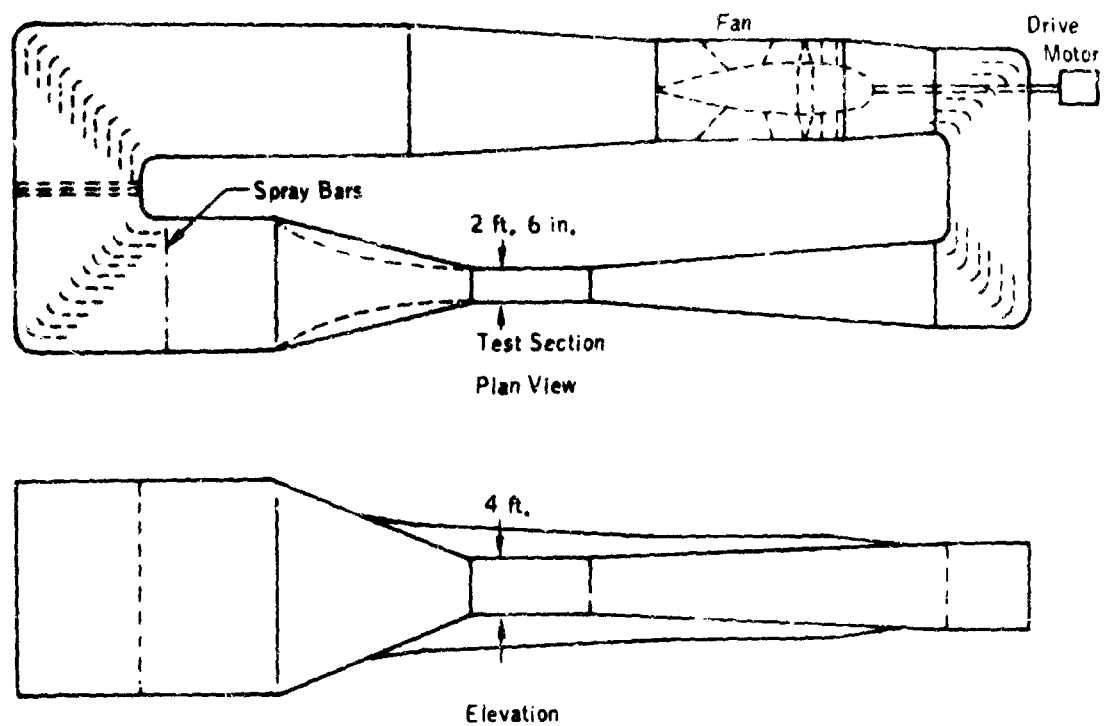
Figure 6-4. Lockheed Icing Research Tunnel Circuit
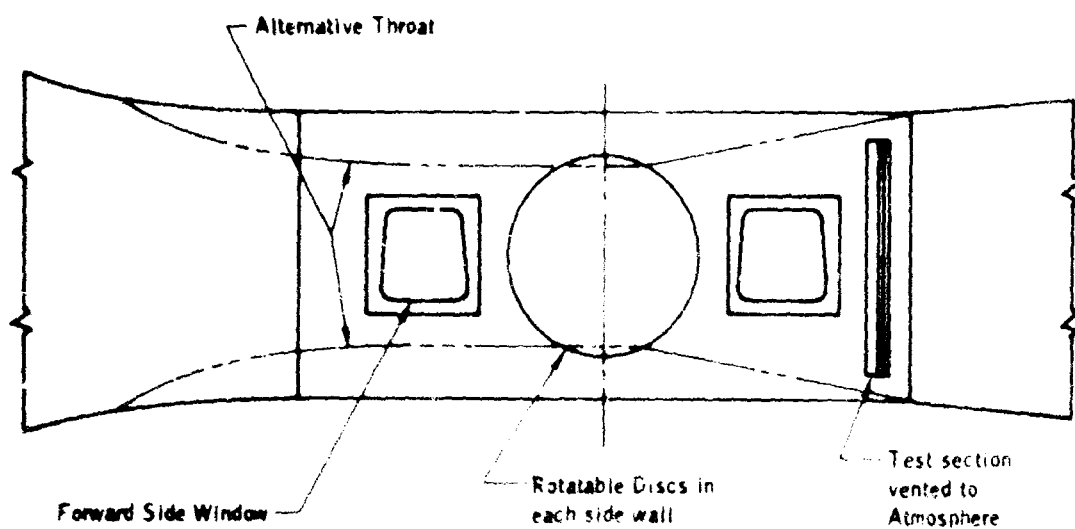
Figure 6-5. Lockheed Icing Tunnel Test Section
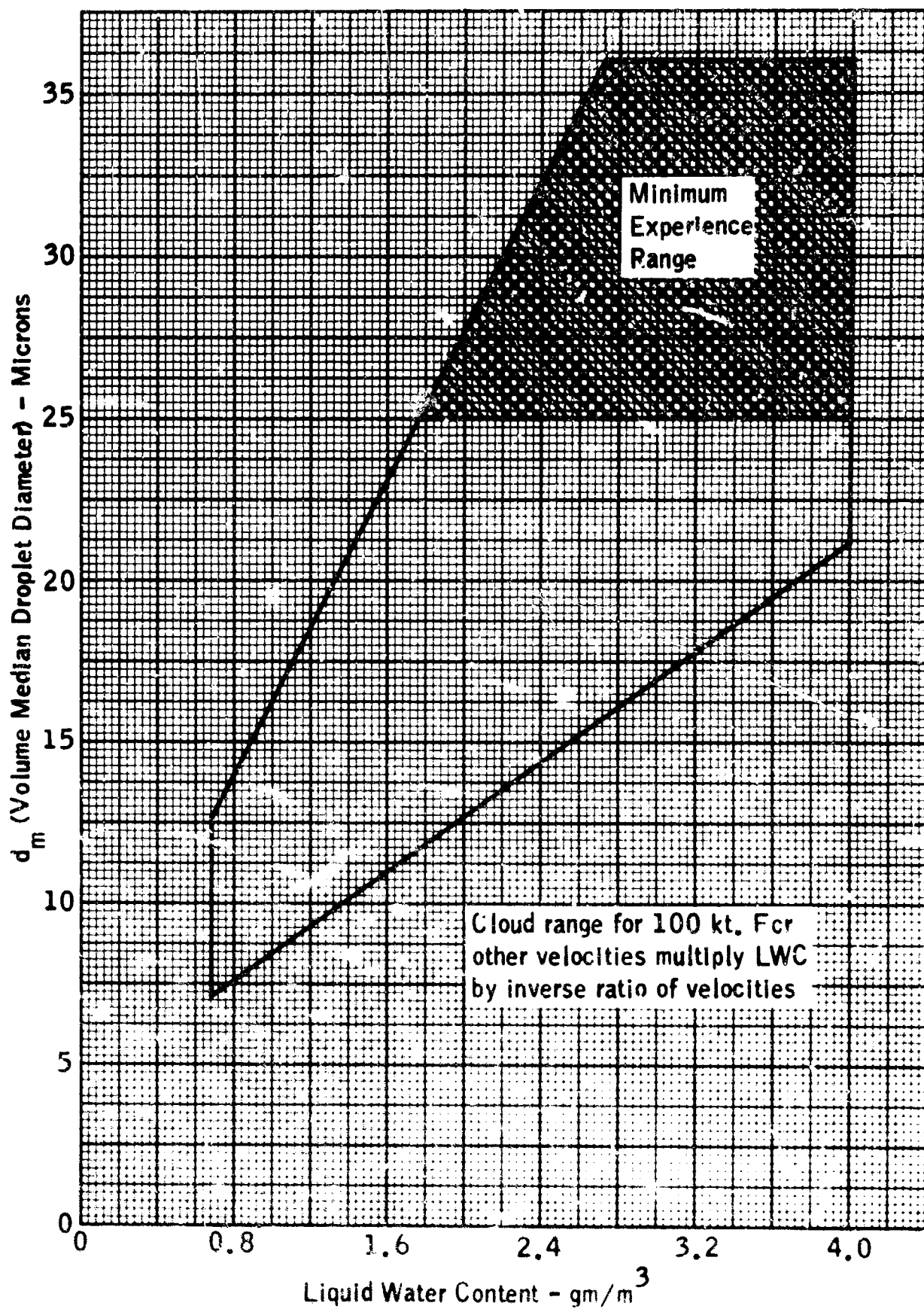
Figure 6-6. Normal Range of Cloud Conditions in Lockheed Icing Tunnel
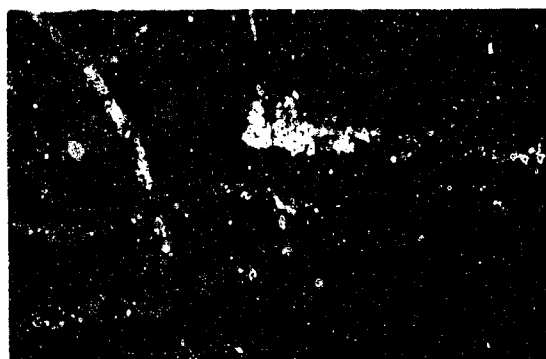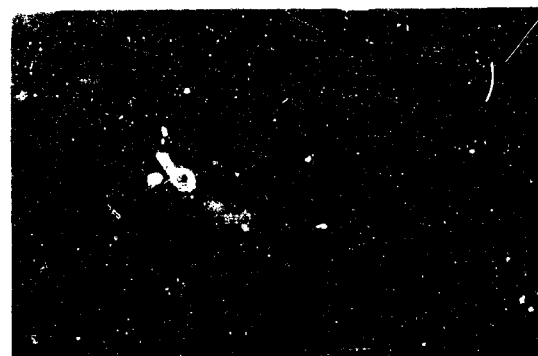
Zero Time Ice Cap   46 Sec After De-Icing Start

$$T_s = -2°F$$
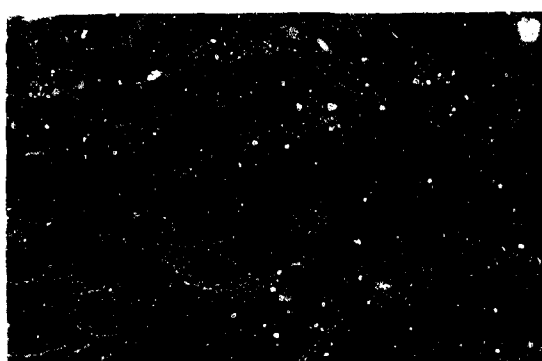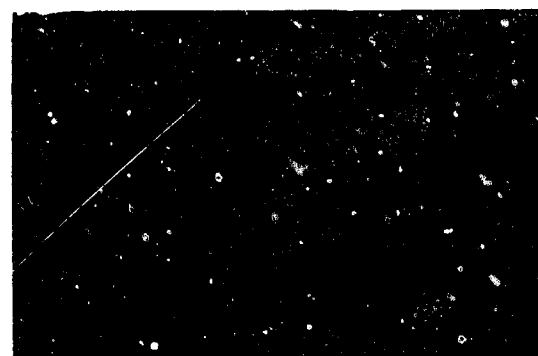
Zero Time Ice Cap   25 Sec After De-Icing Start

$$T_s = 10°F$$
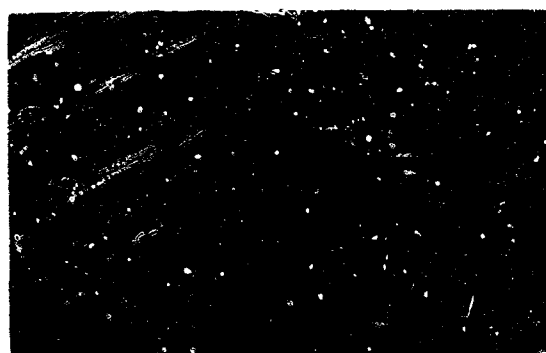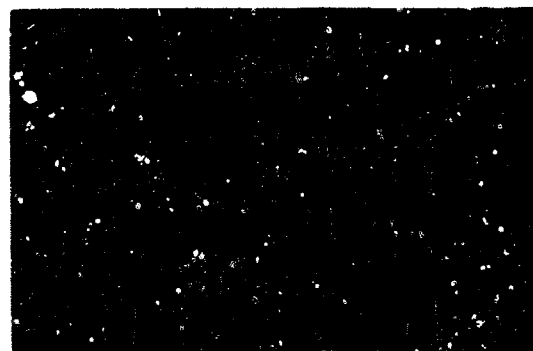
Zero Time Ice Cap   22 Sec After De-Icing Start

$$T_s = 20°F$$

Figure 6-7.   Pitot Tube De-Icing Tests in Lockheed Icing Tunnel
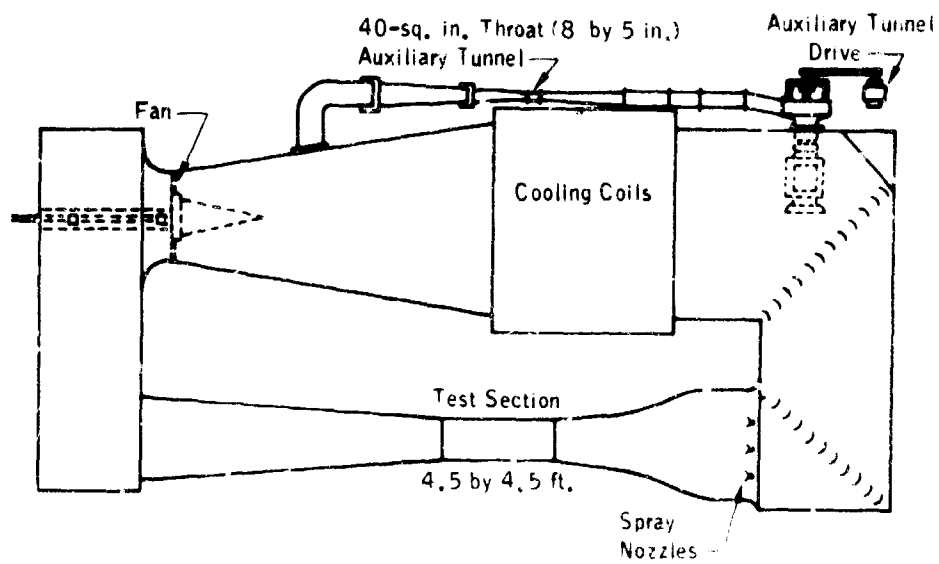
Figure 6-8. NRC Icing Tunnel Circuit
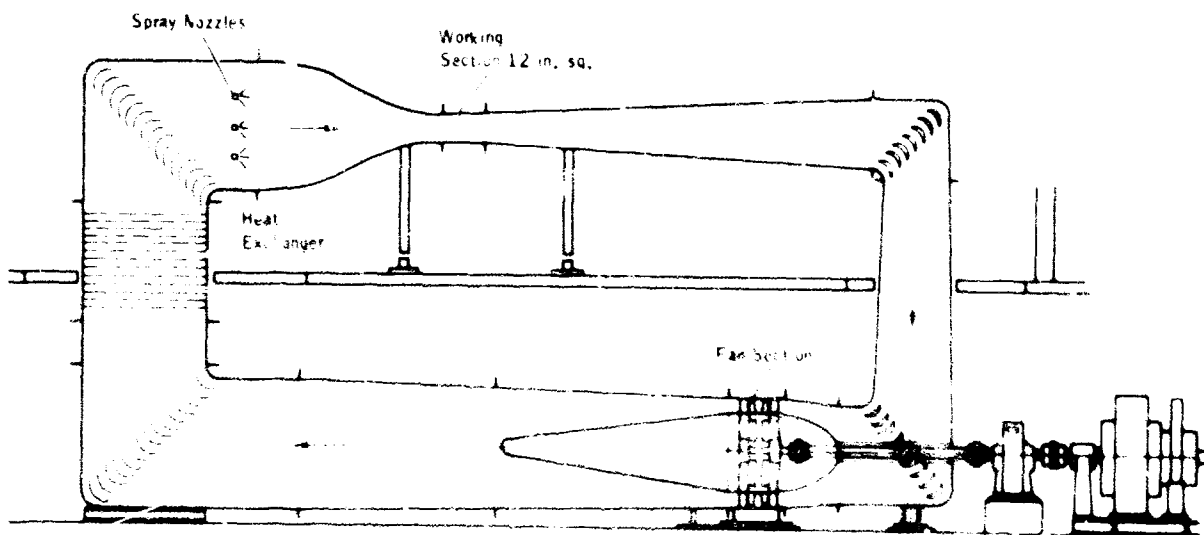
Figure 6-9. NRC High-Speed Icing Tunnel Circuit

Figure 6-10. Airborne Icing Test Bed Laboratory
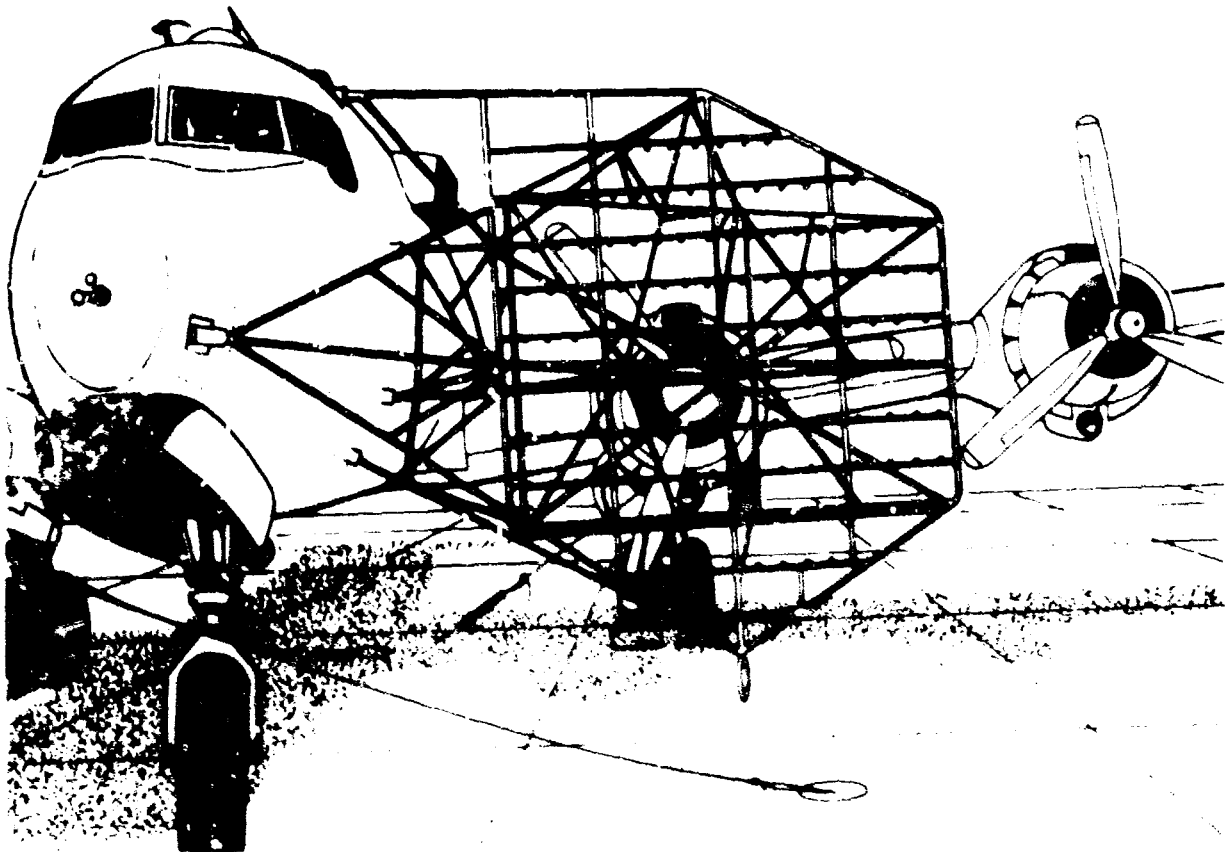
Figu . . . Airborne Icing Tests of Aircraft Components

Figure 6-12.   Spray Pattern From 40-in. Spray Ring
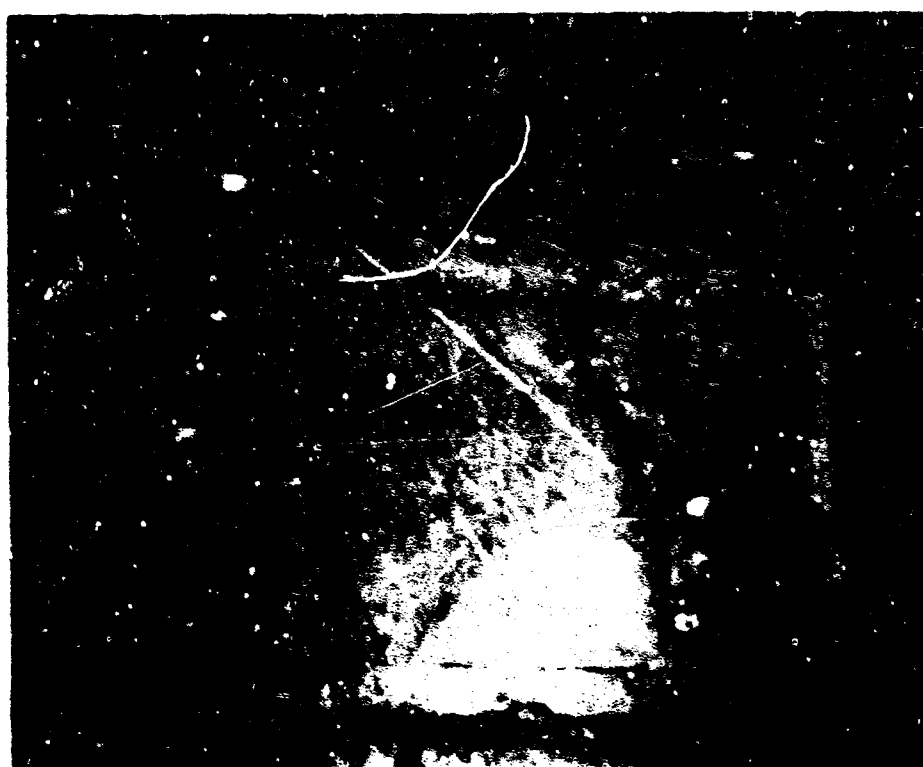
Figure 6-13.   Tanker Spray T-Bar Water Nozzle

Figure 6-14. Forty-Inch Spray Ring
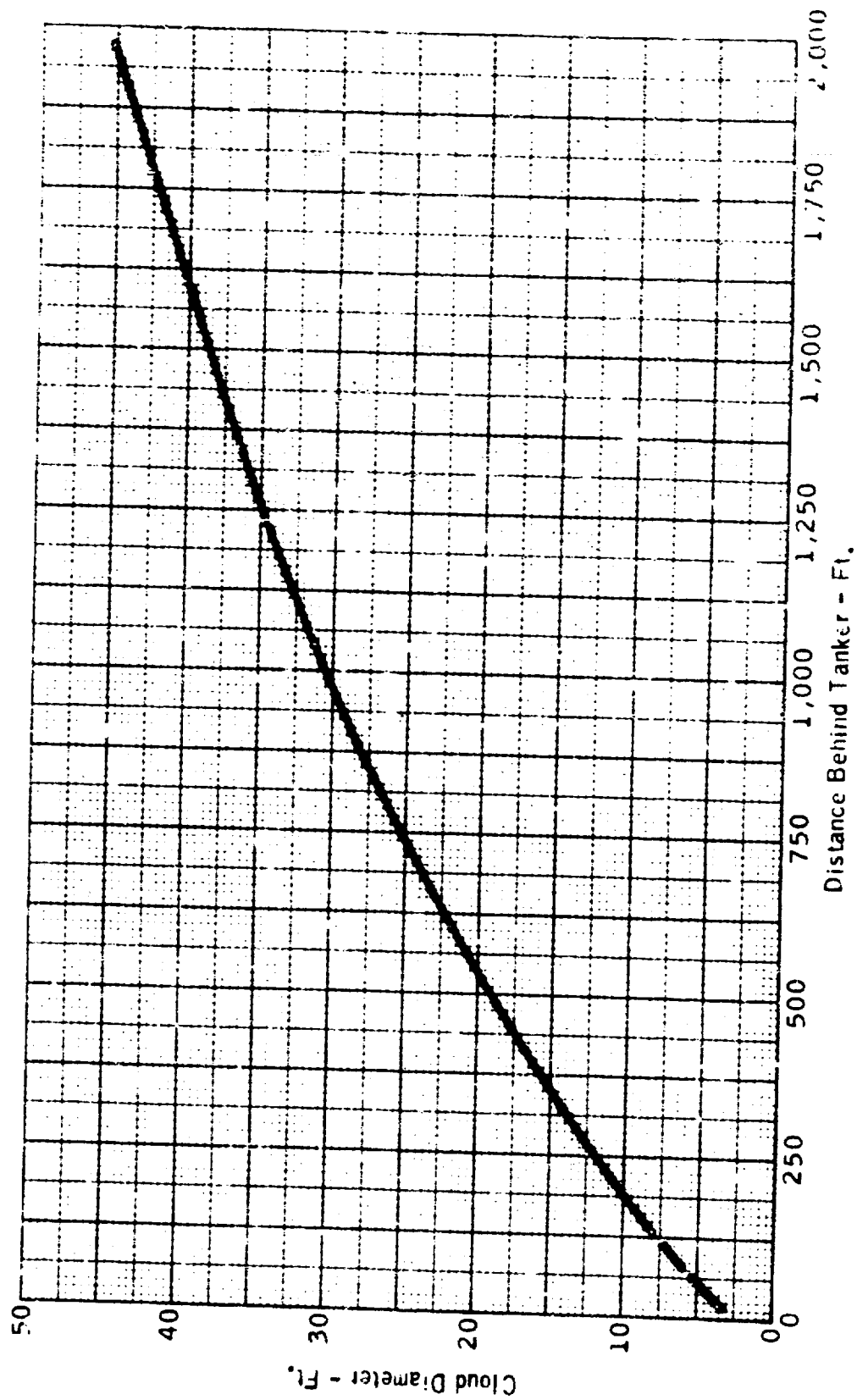
Tanker 40-in. Diameter Spray Ring Dispersion Rate.

Distance Behind Tanker - Ft.

Cloud Diameter - Ft.

Figure 6-15

6-31
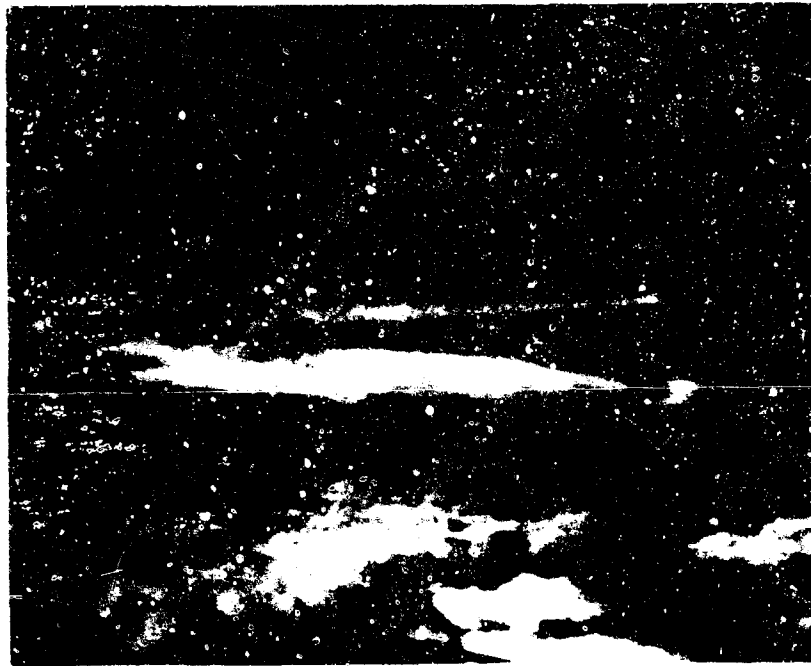
Figure 6-16.   Light Aircraft During Icing Simulation
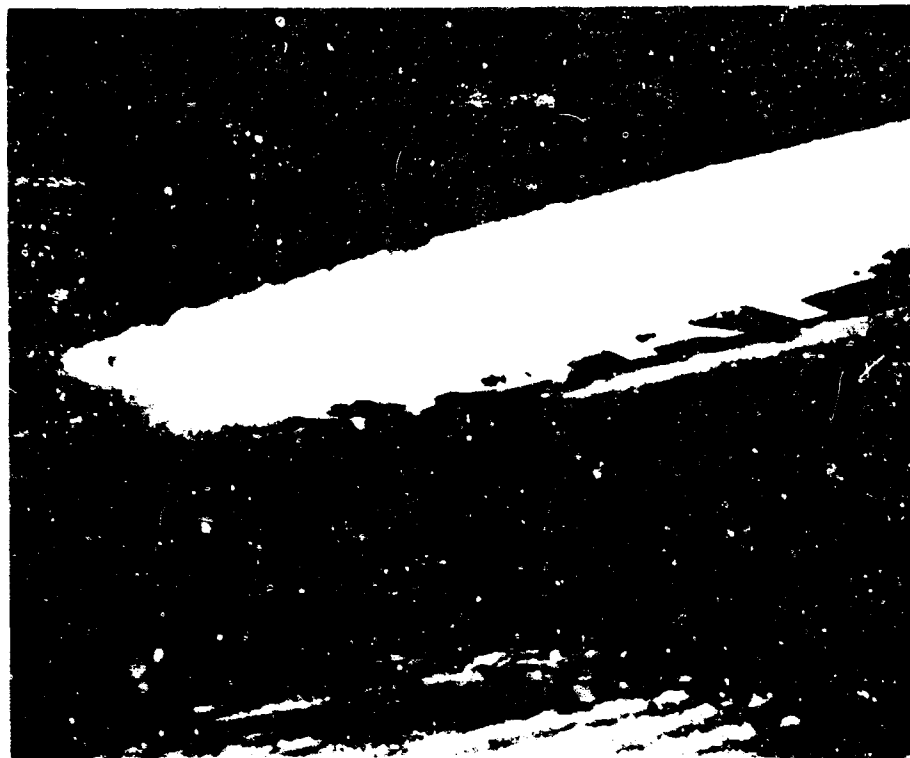
Figure 6-17.   Results of Simulated Icing Tests
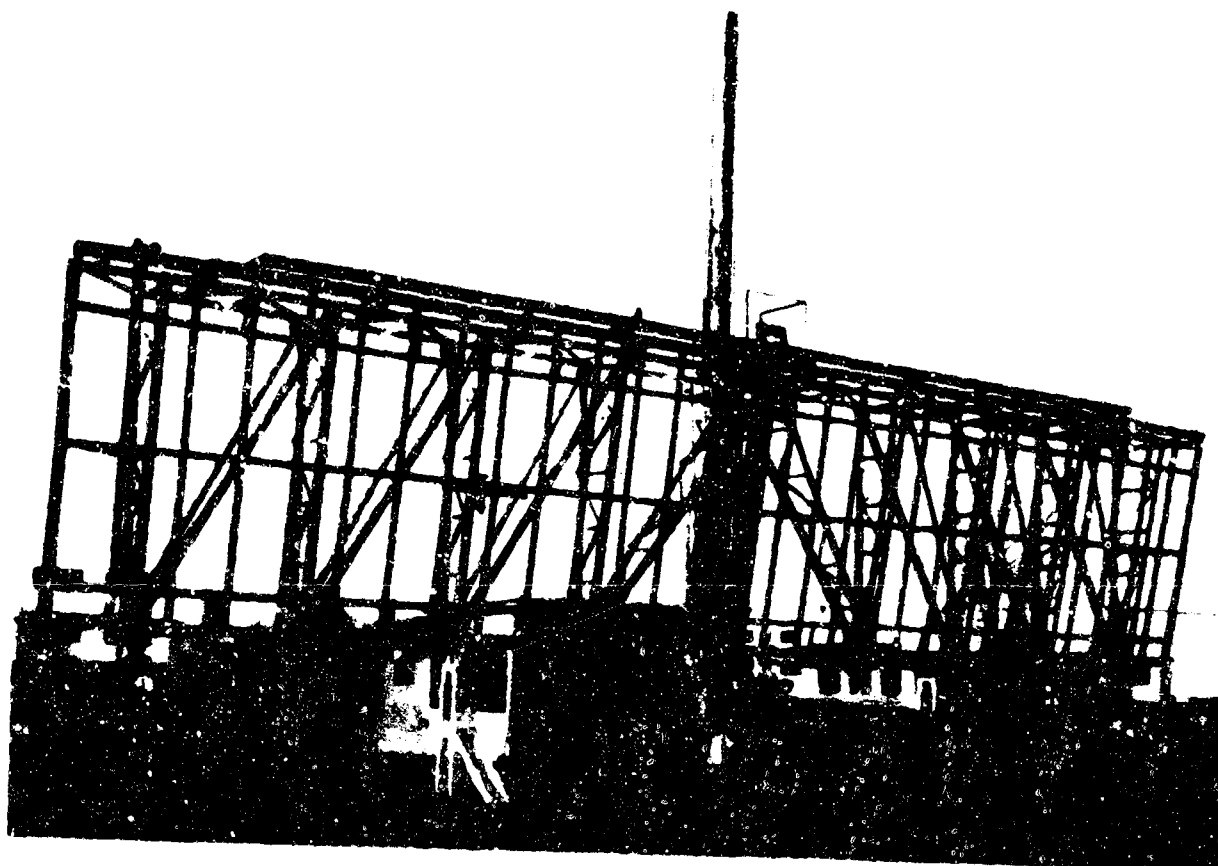
Figure 6-18. NRC Helicopter Spray Rig Framework

Figure 6-19. Helicopter Undergoing Test at NRC Test Site

ACKNOWLEDGMENTS

COMPANIES AND GOVERNMENT AGENCIES

Aerospace Operations
Allison Division of General Motors
650 N. Sepulveda Blvd.
El Segundo, Calif.

Bell Helicopter Co.
P.O. Box 482
Fort Worth, Tex.

The Bendix Corp., Utical Division
117 E. Providencia Ave.
Burbank, Calif.

The Boeing Co., Vertol Division
Norton, Pa.

Cessna Aircraft Co.
Wichita, Kan.

Cook Electric Co
2700 N. Southport Ave.
Chicago 14, Ill.

De Havilland Aircraft of Canada
Malton, Ontario

The Garrett Corp.
AiResearch Manufacturing Division
Phoenix, Ariz.

B. F. Goodrich Aerospace
and Defense Products
500 S. Main St.
Akron 18, Ohio

Goodyear Tire and Rubber Co.
Aviation Products Division
Akron 16, Ohio

Lear Jet Corp.
P.O. Box 1280
Wichita 1, Kan.

Libby-Owens-Ford Glass Co.
3450 Wilshire Blvd.
Los Angeles 5, Calif.

Lockheed-California Co.
Burbank, Calif.

D. Napier and Son, Ltd.
Luton, Bedsfordshire, England

North American Aviation
Los Angeles Division

National Aeronautics and Space
Administration
Lewis Research Center
Cleveland, Ohio

National Research Council of Canada
Ottawa, Canada

Piper Aircraft Corp.
Lock Haven, Pa.

Pittsburgh Plate Glass Co.
One Gateway Center
Pittsburgh 22, Pa.

Servomechanisms, Inc.
200 N. Aviation Blvd.
El Segundo, Calif.

The Sierracin Corp.
903 N. Victory Blvd.
Burbank, Calif.

Sikorsky Aircraft Division
Stratford, Conn.

Swedlow, Inc.
6986 Bandini Blvd.
Los Angeles 22, Calif.

Mr. Robert S. Taylor
2906 Cedarview Drive
Austin 4, Tex.

T. K. S. (Aircraft De-Icing) Ltd.
Drayton House
Gordon Street
London, W. C. I.

United Control Corp.
P. O. Box 3104
Seattle 14, Wash.

GLOSSARY

Adiabatic lifting theory — Method of calculating liquid water content by the adiabatic cooling process (and associated condensation of water droplets) as a mass of air rises.

Angle of attack — Angle between airfoil chord and line of flight.

Anti-icing — The prevention of ice formation on airframe surfaces.

CAR-3 — Civil Air Regulations, Part 3 (aircraft under 12,500 lb.).

CAR-4b — Civil Air Regulations, Part 4b (aircraft over 12,500 lb.).

Collection efficiency — The ratio of actual water collection rate to the water catch rate when water droplet paths are straight lines.

Continuous maximum icing — Icing category from CAR-4b, commonly used for design of wing, empennage, and windshield ice protection on transport aircraft.

Cumulus clouds — Massy, piled-up clouds with a flat base.

Cycled area — In a thermal de-icing system, a section of the protected area which is heated periodically to remove ice.

Datum temperature — Wet air boundary layer temperature for a body traversing a cloud containing free moisture.

De-icing — The removal of ice that has formed on airframe surfaces.

Droplet range ratio — The ratio of the true range of a droplet as a projectile injected into still air to the range of a droplet as a projectile following Stokes' law.

Droplet Reynolds number — The Reynolds number of a droplet in the air stream, usually based on droplet diameter and free stream velocity.

Droplet-trajectory — The path of a water droplet with respect to an airfoil.

Equilibrium surface temperature — Temperature of a surface exposed to
water droplet impingement.

Exceedance probability — The probability that a given parameter will be
equalled or exceeded.

Freezing fraction — That part of the water catch that freezes.

Freezing rain — Rain at temperature slightly below freezing and characterized
by relatively large water droplets that may freeze in contact with airframe
surfaces.

Glaze ice — Clear ice with rapid growth rate and characteristic "double horn"
or "mushroom" formation. (This term is also used by pilots to describe a
smooth film of ice covering leading edges at temperatures just below
freezing.)

Heat release — In thermal ice protection systems, the amount of heat trans-
ferred to the surface to be used for anti-icing or de-icing.

Hold conditions — Low-speed, high-angle-of-attack flight conditions at a
constant altitude (circling one geographical point).

Ice accretion — A growth or buildup of ice, an ice formation.

Ice cap — An ice accretion.

IFR — Instrument flight rules.

Impingement limits — Distance from stagnation to the end of the water
impingement region on both upper and lower surfaces of an airfoil.

Inertia parameter — Dimensionless parameter used to correlate water droplet
impingement data.

Inlet guide vanes — Vanes that guide the inlet airflow in a turbine engine,
located at the front face of the compressor.

Intermittent maximum icing — Icing category from CAR-4b based on cumuliform
clouds having high liquid water content for short times.

Knife edge ice — Ice formed at low temperatures by water droplets freezing
on impact in the shape of a wedge; also called rime ice.

Liquid water content — Water contained as free moisture in a volume of air (does not include water in vapor form).

Local collection rate — Weight of impinging water per unit time and per unit area at a given location.

Loiter — Low-speed, high-angle-of-attack flight conditions.

Mean effective droplet diameter — Half the volume of water in a given sample of air is contained in larger drops, half in smaller drops.

Micron — One millionth of a meter.

Most probable icing temperature — Temperature at which icing is most likely to occur, based on probability.

Mushroom ice — Clear ice with rapid growth rate and characteristic "double horn" formation, also known as "glaze ice."

Parting strips — In a cyclic-electrical de-icing system, continuously heated areas about 1 in. wide (either spanwise or chordwise) which divide the ice into discrete portions.

Piccolo tube — Tube with small, regularly spaced holes for distribution of anti-icing air to leading edges.

Power density - Electrical power per unit area.

Prandtl number — Dimensionless group of gas property values used in heat-transfer correlations.

Projected height — The airfoil height projected along the line of flight.

Rime ice — Milky white, low-density ice formed at low temperatures with a relatively streamlined shape; also referred to as spearhead and knife-edge ice.

Rotating multi-cylinders — Series of rotating cylinders of varying size used to collect ice for the purpose of determining cloud liquid water content and droplet size.

Runback ice — Ice accumulated aft of the protected region, resulting from the water running back and freezing (may be found with partially evaporative anti-icing systems and with de-icing systems).

Running wet — A condition at which an airframe surface is maintained above 32° F (by an anti-icing system) so that impinging water droplets will not freeze.

Spearhead ice — Term used to describe both rime and intermediate rime-glaze types of ice formations.

Stagnation — The point on an airfoil at which velocity is zero.

Stratus clouds — Layer-type clouds, usually at low altitudes.

Super-cooled water droplets — Very small water drops suspended in the air at temperatures below freezing

Surface wetness fraction — The fraction of the surface that is wetted; equal to 1.0 in the impingement region and about 0.25 aft of the impingement area.

Total air temperature — Static air temperature plus kinetic temperature rise.

Volume median droplet diameter — Droplet diameter defined by the condition that half the volume of water in a given sample of air is contained in large drops, half in small drops.

Water catch — The weight of water impinging on an airframe surface (per unit length of span and per unit time for an airfoil).

SUBJECT INDEX

C2925